

# The Synthesis and Optimisation of Toll-Like Receptor Agonists as Potential Immunomodulatory Agents

Thesis submitted to the University of Strathclyde  
Department of Pure and Applied Chemistry  
for the degree of Doctor of Philosophy

by

Daniel Terence Tape

March 2016



## Declaration of Authenticity and Author's Rights.

‘This thesis is the result of the author’s original research. It has been composed by the author and has not been previously submitted for examination which has led to the award of a degree.’

‘The copyright of this thesis belongs to the author under the terms of the United Kingdom Copyright Acts as qualified by University of Strathclyde Regulation 3.50. Due acknowledgement must always be made of the use of any material contained in, or derived from, this thesis.’

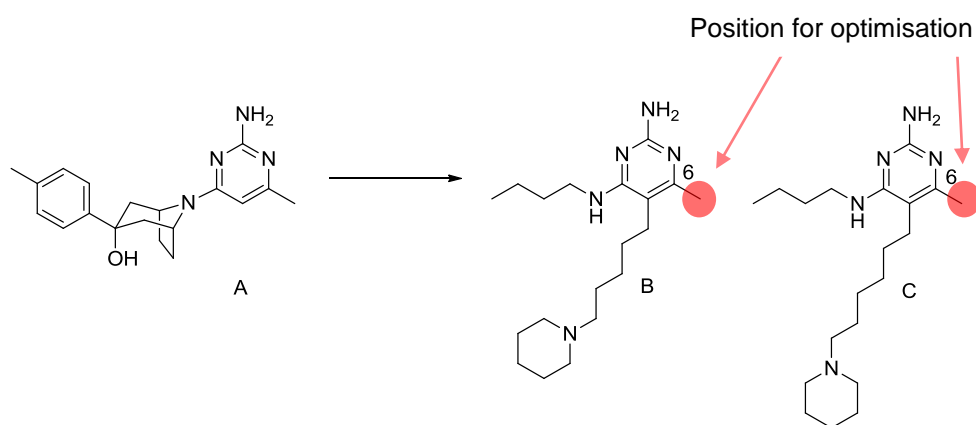
Signed:

Date:

## Abstract.

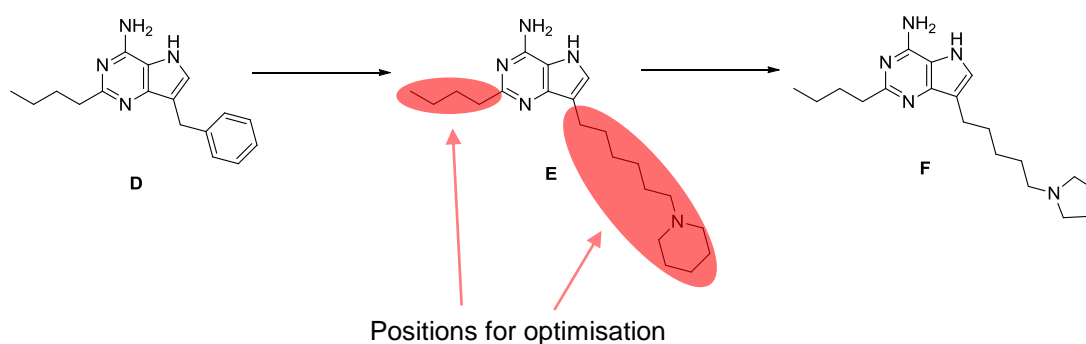
Toll like receptors (TLRs) detect pathogenic compounds and trigger the innate immune defences. In addition, the activation of TLRs can have profound effects on the immune system. The activation of TLR7 in plasmacytoid dendritic cells leads to the production of the cytokine interferon- $\alpha$  (IFN $\alpha$ ). Through a variety of mechanisms, this cytokine polarises the adaptive immune system, enhancing the body's ability to kill the invading organism. Historically, small molecule agonists of TLR7 have been shown to exert an antiviral effect. However, the research presented in this thesis focuses on the potential of such a small molecule TLR7 agonist to treat allergic diseases. Allergic diseases are characterised by an inappropriate response by the immune system to otherwise benign substances called allergens (e.g. pollen, cat dander etc). This response is driven by the so called T<sub>H</sub>2 component of the adaptive component of the immune system. It is proposed that such allergic responses can be reduced in both the short and long term by administration of a small molecule TLR7 agonist, through its ability to rebalance the immune system. This should lead to a cessation of symptoms and potential long term therapeutic benefit.

Two chemical series have been investigated: 2-aminopyrimidines and 9-deazaadenines. The initial 2-aminopyrimidine hit **A** was identified following a high throughput screen and converted to lead compounds **B** and **C**.



Employing molecular modelling tools, the 6-position was identified as a potential point for further optimisation. Subsequent synthesis and biological profiling has enabled the molecular model to be evaluated.

The second series of compounds is based on a 9-deazaadenine core. Hit compound **D** was modified to furnish lead compound **E**. The SAR at the two and seven-positions has been investigated resulting in the optimised compound, a potential clinical candidate **F**. The biological and preclinical toxicological profile of compound **F** is described in detail. The deazaadenine series of compounds has also been optimised for potential use in the treatment of Actinic Keratosis.



### **Animal Studies Statement.**

All animal studies were ethically reviewed and carried out in accordance with U.K. Animals (Scientific Procedures) Act 1986 as amended 2012 and the GSK Policy on the Care, Welfare and Treatment of Laboratory Animals.

### **Human Biological Samples Statement.**

The human biological samples were sourced ethically and their research use was in accord with the terms of the informed consents.

### **Permissions to Reprint or Modify Diagrams.**

In all cases where a diagram has been reprinted or modified from a copyright protected source for use in this thesis the appropriate permission has been obtained. Each figure or table from a copyright protected source is accompanied by the appropriate accreditation text as defined in the legal licence for use. The accreditation text format is different for each copyright holder.

## Acknowledgements.

I would like to thank my supervisor, and TLR7 program leader Dr. Diane Coe for her supervision over the last few years, for helping me to develop, and for managing and assigning programme responsibilities such that I have been able to produce this thesis.

Thanks also to my academic supervisor, Dr. Craig Jamieson for his support and the many useful discussions, both scientific and editorial.

I should also like to thank the following GSK scientists: Dr. Keith Biggadike, Debbie Needham, Aurélie Champigny and industrial placement students Vincent Courtet, Sam Stewart and Jude Nithelan Arokianathar (the TLR7 chemistry team), for synthesising target compounds and medicinal chemistry discussions; Dr. Diana Quint, for help understanding immunology; Jo Hessey, Justine Lau and Fiona Priest for running the *in vitro* biology assays; Doug Ball, for running the necessary *in vivo* biology experiments; Chris Edwards, Dave Mallett, Emma Sherriff and Simon Teague (DMPK support); Shenaz Nunhuck (Physchem advocate); Steve Richards and Sean Lynn (NMR support); Dr. Colin Edge (Computational Chemistry); Bob Gibbon (Pharmaceutical development); Mark Price and Rachel Brown (Safety Assessment) and finally Lionel Trottet (Dermatology DMPK).

Finally I would like to thank Prof. Harry Kelly and Prof. William Kerr, without whom the MPhil / PhD collaboration between GSK and the University of Strathclyde would not exist.

## Abbreviations.

9-BBN	9-Borabicyclo[3.3.1]nonane
ADME	Absorption, Distribution, Metabolism, Excretion
AHR	Airway Hyper-Responsiveness
AO	Aldehyde Oxidase
APCs	Antigen Presenting Cells
BAL	Broncho-Alveolar Lavage
BINAP	2,2'- <i>Bis</i> (diphenylphosphino)-1,1'-binaphthyl
Bn	Benzyl group
BOM-Cl	Chloromethyl phenylmethyl ether
BMDCs	Bone Marrow derived Dendritic Cells
CCPA	2-Chloro- <i>N</i> -6-cyclopentyladenosine
CD-40	Cluster of Differentiation 40
cLogP	Calculated Log P
cysLT	Cysteinyl leukotriene
DABCO	1,4-Diazabicyclo[2.2.2]octane
DAST	<i>N,N</i> -Diethylaminosulfur trifluoride
DBN	1, 5-Diazabicyclo[4.3.0]non-5-ene
DCs	Dendritic Cells (Subtypes c = conventional, p = plasmacytoid, m= myeloid and Mo = monocyte derived)
DCM	Dichloromethane
DEPT	Distortionless Enhancement by Polarization Transfer
DIPEA	<i>N,N</i> -Diisopropylethyl amine
DNA	Deoxyribonucleic acid
DMF	<i>N,N</i> -Dimethylformamide

DMS	Dimethylsulfide
DMSO	Dimethylsulfoxide
dppf	1,1'- <i>Bis</i> (diphenylphosphino)ferrocene
ELISA	Enzyme-Linked Immuno Sorbent Assay
eXp	Expanded cross screening panel (a panel of assays used to assess any off target activity)
hERG	Human <i>Ether-à-go-go</i> related gene
Hermann's Palladacycle	<i>Trans</i> -di( $\mu$ -acetato) <i>bis</i> [ <i>o</i> -(di- <i>o</i> -tolylphosphino)benzyl]-dipalladium(II)
HLM	Human Liver Microsomes
HMBC	Heteronuclear multiple-bond connectivity spectroscopy
HRMS	High Resolution Mass Spectrometry
HSA	Human Serum Albumin
HSP	Heat-Shock Protein (subtypes 60 and 70)
HSQC	Heteronuclear Single-Quantum Coherence spectroscopy
HTS	High Throughput Screening
HWB	Human Whole Blood
IB-MECA	<i>N</i> 6-(3-Iodobenzyl)adenosine-5 $\mu$ - <i>N</i> -methyluronamide
IBX	2-Iodoxybenzoic acid
ICS	Inhaled Corticosteroid
IFN	Interferon (subtypes $\alpha$ and $\gamma$ )
IgE	Immunoglobulin E
IL	Interleukin (subtypes 1 - 22)
IPA	Isopropyl alcohol
IRF	Interferon Regulatory Factor (subtypes 3 and 7)



IVC	<i>In Vitro</i> Clearance
LBF	Liver Blood Flow
LCMS	Liquid Chromatography Mass Spectrometry
LPS	Lipopolysaccharide
Log D <sub>7.4</sub>	Log partition coefficient at pH 7.4
Log P	Log partition coefficient of compound between water and octanol
LRR	Leucine Rich Repeat
LT	Leukotriene (subtypes A <sub>4</sub> , B <sub>4</sub> , C <sub>4</sub> and D <sub>4</sub> )
LTA	Lipoteichoic acid
mCPBA	<i>meta</i> Chloroperbenzoic acid
MDAP	Mass Directed Automated Preparation
MDCK	Madin-Darby Canine Kidney
MHC	Major Histocompatibility Complex
MLA	Mouse Lymphoma Assay
Mol. Wt.	Molecular Weight
MyD88	Myeloid Differentiation Factor 88
NECA	5'- <i>N</i> -Ethylcarboxamido adenosine
NFκB	Nuclear Factor κB
NIS	<i>N</i> -Iodosuccinimide
NK Cells	Natural Killer Cells
NLR	NOD Like Receptor
NMO	<i>N</i> -Methylmorpholine <i>N</i> -oxide
NMR	Nuclear Magnetic Resonance
NOD	Nucleotide-binding Oligomerization Domain
NOESY	Nuclear Overhauser Effect Spectroscopy

OHC	Occupational Hazard Category
ODN	Oligodeoxynucleotide
OxLDL	Oxidised low-density lipoprotein
PAMP	Pathogen Associated Molecular Patterns
Pam <sub>3</sub> CSK <sub>4</sub>	Synthetic bacterial lipopeptide Pam <sub>3</sub> -Cys-Ser-Lys <sub>4</sub>
PBMCs	Peripheral Blood Mononuclear Cells
PD	Pharmacodynamic
PDE	Phosphodiesterase
pEC <sub>50</sub>	-Log <sub>10</sub> half maximal effective concentration (EC <sub>50</sub> )
PFI	Property Forecast Index
PK	Pharmacokinetics
pKa	-Log <sub>10</sub> Acid dissociation constant
PolyA:U	Polyadenylic acid-polyuridylic acid
PolyI:C	Polyinosinic-polycytidylic acid
PSA	Polar Surface Area
RLR	RIG-1 Like Receptor
ROESY	Rotating frame nuclear Overhauser Effect Spectroscopy
RLM	Rat Liver Microsomes
RNA	Ribonucleic acid (single stranded; ss and double stranded; ds)
RT	Room Temperature
RuPhos	2-Dicyclohexylphosphino-2',6'-di- <i>iso</i> -propoxy-1,1'-biphenyl
RSV	Respiratory Syncytial Virus
SAR	Structure Activity Relationship
SEM	2-(Trimethylsilyl)ethoxymethyl
SFI	Solubility Forecast Index

SIT	Allergen specific immunotherapy
S <sub>N</sub> Ar	Nucleophilic aromatic substitution
TBME	<i>Tert</i> -butylmethyl ether
TGFβ	Transforming Growth Factor β
tGPI-mucins	<i>Trypanosoma cruzi</i> glycosylphosphatidylinosito-anchored mucin-like glycoprotein
Tf	Triflate (Trifluoromethylsulfonate)
TFA	Trifluoroacetic acid
T <sub>H</sub> Cell	T-Helper Cell (Subsets 0, 1, 2 and 17)
THF	Tetrahydrofuran
TIR	Toll-interleukin-1 receptor homology domain
TIRAP	Toll-interleukin 1 receptor domain containing adaptor protein
TLR	Toll-Like Receptor
TNF	Tumour Necrosis Factor (Subtypes α and β)
TOM	Tri- <i>iso</i> -propylsilyloxymethyl
TPAP	Tetra- <i>N</i> -propylammonium perruthenate
T <sub>Reg</sub>	Regulatory T-Cell
TWA	Time weighted average
UV	Ultraviolet
μwave	Microwave heating
VSV	Vesicular stomatitis virus
XPhos	2-Dicyclohexylphosphino-2',4',6'-triisopropylbiphenyl
WHO	World Health Organisation

## Contents:

1	Introduction.	1
1.1	Introduction to asthma.	1
1.2	Introduction to the immune system and the pathogenesis of asthma.	2
1.3	Current medications for allergic asthma.	5
1.3.1	$\beta_2$ -Adrenoceptor agonists as bronchodilators for asthma.	5
1.3.2	Inhaled corticosteroids as anti-inflammatory agents for the treatment of asthma.	8
1.3.3	Cysteinyl leukotriene antagonists as orally administered anti-inflammatory agents for asthma therapy.	11
1.3.4	Recombinant monoclonal antibodies as anti-inflammatory agents.	13
1.3.5	Limitations of current asthma therapies and the concept of remission.	14
1.4	Remission through immunomodulation.	14
1.4.1	Specific immunotherapy (SIT).	15
1.4.2	Potential use of small molecules to achieve immunomodulation.	16
1.4.3	Toll Like Receptors.	17
1.4.4	TLR ligands as potential medicines.	18
1.4.5	Endosomal TLR signalling and cytokine induction.	19
1.5	Direct and indirect biological effects of IFN $\alpha$ .	21
1.6	Direct effects of TLR7 agonists on B-cells and T-cells.	22
1.7	Summary of the potential effects of a TLR7 agonist on allergic asthma and possible long term immunomodulation.	23
1.8	Direct effects of TLR7 and TLR9 on the airways.	24
1.9	Known small molecule agonists of TLR7 / inducers of IFN $\alpha$ .	24
1.9.1	Imidazoquinolines and related compounds.	25
1.9.2	Purines and related compounds.	33
1.9.3	8-Oxoadenines.	34
1.9.4	Imidazopyridinones.	40
1.9.5	Pteridinones.	42
1.9.6	Imidazopyridines.	44

1.9.7	2-Aminopyrimidines.	45
1.9.8	Review of the known TLR7 agonist chemotypes.	46
1.10	Aims for a new TLR7 based treatment for allergic respiratory conditions.	46
1.10.1	Consideration of any potential side effects and defining the route of administration.	47
1.10.2	Physicochemical requirements for an inhaled/intranasally administered TLR7 agonist.	48
1.10.3	Dose and activity requirements for an inhaled/intranasally administered TLR7 agonist.	49
2	<b>Results and Discussion Part 1: 2-aminopyrimidines as inducers of IFN<math>\alpha</math>.</b>	<b>52</b>
2.1	Discovery of the Lead compound.	52
2.2	Medicinal chemistry strategy.	55
2.3	Synthetic strategies for the synthesis of tetrasubstituted pyrimidines targets.	58
2.3.1	Synthesis of intermediates <b>70k</b> and <b>71k</b> .	59
2.3.2	Nucleophilic substitution approaches for the functionalisation of <b>70k</b> and <b>71k</b> .	67
2.3.3	Transition metal mediated approaches for the functionalisation of <b>70k</b> and <b>71k</b> .	69
2.3.4	Synthesis of Intermediate <b>71l</b> .	71
2.3.5	Synthesis of <b>71e</b> and <b>71f</b> using a modified strategy.	75
2.3.6	Introduction of an ethyl group into the 6-position.	77
2.4	2-Aminopyrimidines: biological results.	78
2.5	Revisiting the original medicinal chemistry hypothesis.	83
2.6	Summary of 2-aminopyrimidines as potential inducers of IFN $\alpha$ .	86
3	<b>Results and Discussion Part 2: 9-deazaadenines (5H-pyrrolo [3,2-<i>d</i>]pyrimidine-4-amines) as inducers of IFN<math>\alpha</math>.</b>	<b>90</b>
3.1	Discovery of a new lead series.	90

3.1.1	Synthesis of lead compound <b>124a</b> .	93
3.2	Medicinal chemistry strategy 1: investigation of the 2-position.	94
3.2.1	Investigation of the 2-position: synthesis.	97
3.2.2	Investigation of the 2-position: biological results.	115
3.3	Medicinal chemistry strategy 2: investigation of the 7-position.	119
3.3.1	Investigation of the 7-position: varying the chain length.	119
3.3.2	Investigation of the 7-position: varying the terminal group.	120
3.3.3	Investigation of the 7-position: synthesis.	122
3.3.4	Investigation of the 7-position: <i>In vitro</i> biological results.	127
3.4	Revisiting compounds with an ether in the 2-position.	136
3.5	Investigation of the 6-position.	137
3.6	Selection of a compound for further biological/toxicology studies.	142
3.7	Large scale synthesis of compound <b>211b</b> .	143
3.7.1	Investigation into alternatives to the BOM protecting group.	143
3.7.2	Optimisation of Method B to prepare <b>211b</b> .	145
3.8	Further <i>in vitro</i> biological assessment of <b>211b</b> : the functional PBMC assay.	146
3.9	Early toxicological assessment of compound <b>211b</b> .	148
3.10	<i>In vivo</i> biological assessment of compound <b>211b</b> .	158
3.11	Design of TLR7 agonists for dermatological applications.	164
3.11.1	Revisiting 6-methyl-deazaadenines as potent TLR7 agonists.	166
3.12	Conclusions and further work.	170
4	Experimental.	177
4.1	General experimental methods.	177
4.2	Experimental conditions.	181
5	Appendix	318
5.1	Spectral analysis of compound <b>211b</b> .	318
5.1.1	NMR of compound <b>211b</b> .	318
5.1.2	HRMS of compound <b>211b</b> .	319
6	References.	320

## 1 Introduction.

### 1.1 Introduction to Asthma.

Asthma is a common chronic inflammatory condition affecting the respiratory system. Its name derives from the Greek *ἀσθμα*, *asthma*, “panting” in response to the commonly observed symptoms of wheezing, coughing, chest tightness and shortness of breath.<sup>1</sup> These symptoms occur as a result of the smooth muscle tissue lining the bronchiole contracting, in addition mucus is secreted, further restricting airflow (Figure 1). The overall result of this physiological state is to reduce oxygen absorption, in severe cases this can cause asphyxia, resulting in death.<sup>2</sup>

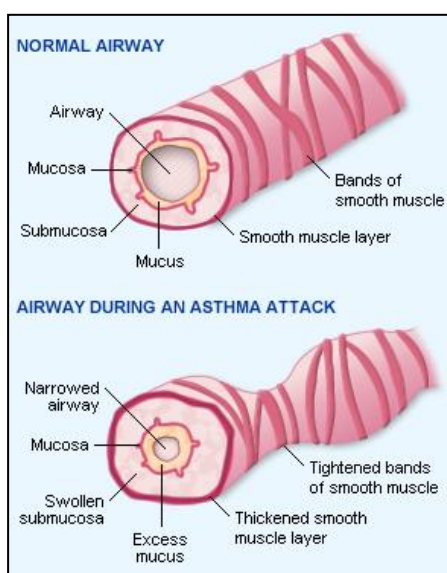


Figure 1: Effect of asthma on the respiratory tract. Figure reproduced from reference 3.

According to the World Health Organisation (WHO) 235-300 million people world wide suffer from asthma, with the prevalence rates varying by country.<sup>4</sup> The disease is most common in the western world with approximately 8.4% of Americans and 9% of British people receiving treatment for asthma.<sup>5</sup> Despite the numerous treatment options available, deaths due to asthma are still relatively common, for example in 2009 there were 1131 deaths from asthma in the UK alone.<sup>6</sup> There is also a significant financial burden associated with asthma, that includes hospitalisation costs, medication costs and loss of income due to absenteeism. These

costs can total many billions of dollars (US) depending on population size and disease prevalence.<sup>7</sup>

Historically asthma was classified according to a number of factors including the frequency of symptoms, the severity of these symptoms and how the patient responded to various treatment regimes.<sup>8</sup> Advances in animal models and cellular biology have led to a more complex phenotypic picture. These various phenotypes have been reviewed by many researchers.<sup>9</sup> The most common phenotype is that of allergic asthma,<sup>10</sup> where the adaptive component of the immune system responds inappropriately to benign airborne antigens called allergens, leading to inflammation, airway hyperresponsiveness (AHR), and the onset of symptoms. In order to understand how the current treatment options for allergic asthma work and to identify new treatment possibilities, it is necessary to examine the biological mechanisms involved in more detail.

## 1.2 Introduction to the immune system and the pathogenesis of asthma.

The immune system is extremely complex but its role is simple: to protect the host organism against invading organisms. The immune system consists of two components the innate and adaptive responses. The innate response occurs immediately following infection with the key effector cells being antigen presenting cells (APCs): the dendritic cells (DCs) and macrophages. These cells sample the surrounding environment using receptors on their surface and by enveloping material in a process called phagocytosis. The enveloped material is then chemically and enzymatically degraded. If the sampled material is from an invading organism, the cells become activated (the mechanisms of activation will be discussed further in Section 1.4.2). Once activated, the APCs produce a number of signalling proteins such as cytokines and chemokines that recruit other cells including neutrophils and natural killer cells to destroy the invading organism. It should be noted that this response does not depend on the nature of the invading organism.



The role of the adaptive immune response is to provide a targeted response depending on the nature of the infection and to remember this response such that re-infection can be dealt with quickly and efficiently. The key effector cells of the adaptive immune response are T-cells and B-cells so called because they originate from the thymus and bone marrow, respectively. These cells harbour randomly generated receptor functionality that can recognise virtually all foreign proteins and polysaccharides, and are therefore capable of responding to any possible infection. The role of B-cells is to produce immunoglobulin antibodies (IgM, IgA, IgG and IgE) that bind to the invading organism and target it for destruction. The nature of the antibody generated is specific to the nature of the invading organism and the location of the infection.<sup>11</sup>

Patients with allergic conditions such as allergic asthma possess long lived memory B-cells that produce immunoglobulin E (IgE) antibodies that are specific to a normally benign substance such as pollen, thus making it an allergen. In the first phase of the allergic response these antibodies bind to receptors on the surface of mast cells. In the presence of the allergen, crosslinking occurs leading to the mast cell degranulating, releasing a range of highly inflammatory compounds that result in the onset of the characteristic asthma symptoms (Figure 2). In addition, IgE and mast cells are also implicated in the long term pathological changes and tissue damage that occur in patients with chronic allergic asthma.<sup>12</sup>

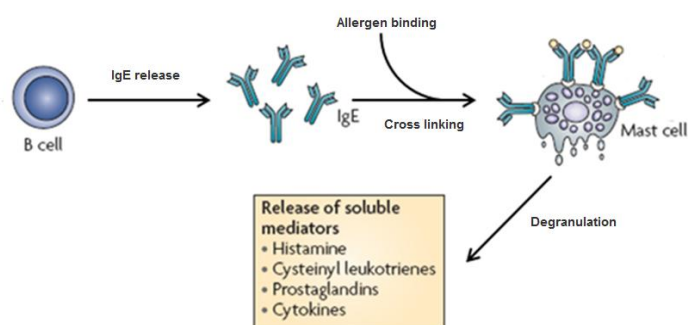


Figure 2: Summary of the B-cell mediated allergic inflammatory process. Figure modified with permission from Macmillan Publishers Ltd: Nature Reviews Immunology (*Nat. Rev. Immunol.* **2008**, 8, 218-230), copyright 2008.<sup>13</sup>

The second phase of the allergic response involves immune cell recruitment and activation; this is initiated by dendritic cells. Once a dendritic cell has phagocytosed foreign material it is trafficked to the lymph nodes *via* the lymphatic system. Here it can present the processed fragments of the antigen/allergen to T-cells, comprising naïve T helper cells (termed  $T_H0$ ), cytotoxic T-cells, and memory T-cells. Those T-cells that have receptors that recognise the presented compound are activated. The activated  $T_H0$  cells can differentiate into several mature T cell subsets, and this differentiation is influenced by the exact composition of the cytokine milieu present.<sup>14</sup> In patients with allergic asthma there is biased differentiation to a mature T-helper cell subset termed  $T_H2$  cells. The inflammatory processes associated with a  $T_H2$  allergic phenotype are summarised in Figure 3.

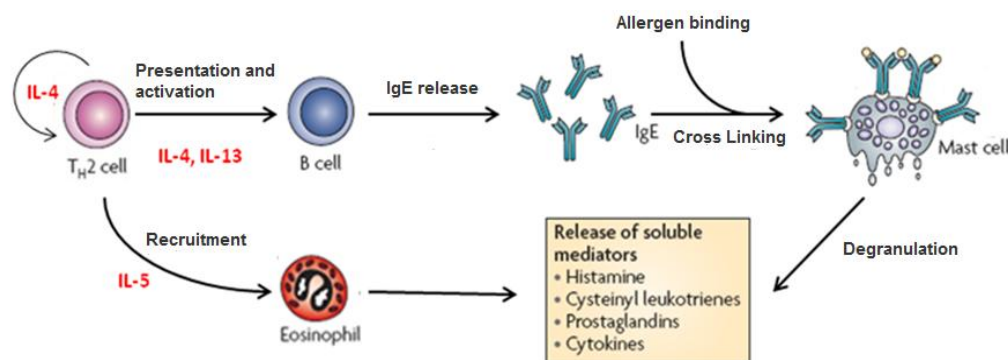


Figure 3: Summary of the  $T_H2$  mediated inflammatory processes involved in allergic inflammation.

Figure modified with permission from Macmillan Publishers Ltd: Nature Reviews Immunology  
(*Nat. Rev. Immunol.* **2008**, 8, 218-230), copyright 2008.<sup>13</sup>

$T_H2$  cells secrete a number of cytokines including the interleukins IL-4, IL-5, and IL-13 (termed  $T_H2$  cytokines). IL-4 has an autocrine action that leads to an increasingly large population of mature  $T_H2$  cells specific to the antigen that initiated the allergic response. IL-5 is responsible for recruiting eosinophils to the lung and activating them to release a multitude of cytokines and pro-inflammatory compounds. B-cells that recognise the allergen are activated by  $T_H2$  cells through complex processes involving the presentation of antigen, IL-4 and IL-13, resulting in the conversion of the B-cell into a plasma cell, generating large quantities of IgE specific for the allergen. Alternatively the B-cell can become a memory B-cell

which generates low levels of the specific IgE but provides a quick response to re-exposure as described above. Some of the activated T<sub>H</sub>2 cells will become memory T-cells that upon reactivation can produce IL-4 thus further enhancing the differentiation of T<sub>H</sub>0 cells into T<sub>H</sub>2 cells.

### 1.3 Current medications for allergic asthma.

To date, all the medications licensed for asthma treat the symptoms resulting from the inflammatory processes involved. These drugs can be broadly separated into two categories: those that act as bronchodilators ('relievers') and those that act as anti-inflammatory agents ('controllers'). In general terms bronchodilators act on receptors present on the smooth muscle tissue to counteract the constriction resulting from the allergic response, whereas anti-inflammatories act by either reducing the levels of inflammatory mediators or by preventing them interacting with receptors associated with further inflammatory events. The subsequent sections briefly discuss the drug classes most widely used to treat allergic asthmatic patients, before reviewing their effectiveness and limitations as asthma treatments.

#### 1.3.1 $\beta_2$ -Adrenoceptor agonists as bronchodilators for asthma.

The history of  $\beta_2$ -adrenoceptor agonists, their development and their use in asthma has been comprehensively covered by Waldeck,<sup>15</sup> with further developments being discussed by Glossop and Price in 2006,<sup>16</sup> and by Cazzola and co-workers in 2011.<sup>17</sup> This section is intended to provide an overview of the area, highlighting the marketed drugs.

The adrenoceptors are G-Protein Coupled Receptors (GPCRs) consisting of seven transmembrane (7TM) domains, and are classified as  $\alpha$  and  $\beta$  subtypes. The adrenoceptors perform crucial roles in the sympathetic arm of the autonomic nervous system,<sup>18</sup> and have numerous biological functions depending on the receptor type and tissue.<sup>19</sup> In all cases the adrenergic binding site is located within the lipid membrane of the cell.

The natural ligand adrenaline **1** (Table 1) is an agonist compound with activity at all the adrenoceptors, and was one of the first compounds successfully used to treat the bronchoconstriction associated with asthma following subcutaneous injection.<sup>20</sup> Its bronchodilatory effect is driven by agonism of the  $\beta_2$ -adrenoceptors present on bronchial smooth muscle. Adrenaline is rapidly inactivated through metabolism thus limiting the duration of action to approximately one hour.<sup>21</sup>

All of the compounds reported as selective  $\beta_2$ -adrenoceptor agonists retain the same basic pharmacophore as adrenaline, that is an aromatic ring with two hydrogen bond donors and an ethanolamine motif. The key molecules that act *via*  $\beta_2$ -agonism and have progressed to become marketed drugs for asthma are depicted in Table 1 (adrenaline is included for comparison) along with human *in vivo* duration of action data for each compound.

The first selective  $\beta_2$ -agonists to be marketed for asthma were salbutamol **2** and terbutaline **3**, both show an extended duration of action with respect to adrenaline, but only provide relief for four to six hours. Salmeterol **4** and formoterol **5** were developed to provide longer term relief (> 12 hours) from bronchoconstriction and overcome nocturnal asthma symptoms. All these compounds are generally administered as inhaled formulations enabling direct delivery to the lungs; however, some drug does reach the systemic circulation either by direct pulmonary absorption or through absorption of the swallowed portion of the inhaled dose, typically 80% of the available dose.<sup>22</sup> Vilanterol **6** was designed to reduce systemic exposure by using a so called soft drug<sup>23</sup> or antedrug<sup>24</sup> approach to minimise the effects from any drug that reaches the systemic circulation either by pulmonary absorption or oral absorption of the swallowed dose. In this case, the compound has been designed to be degraded by hepatic metabolism. This occurs *via* oxidation alpha to the dichlorobenzene ring and subsequent spontaneous acetal hydrolysis which removes the dichlorobenzaldehyde fragment. The resulting compound has significantly reduced potency and reduced duration of action at  $\beta_2$ -receptors, possibly because it can no longer interact with an exosite in the  $\beta_2$ -receptor,<sup>25</sup> Furthermore, in

accordance with current best practices across the pharmaceutical industry vilanterol is administered as a single enantiomer (of the alcohol) rather than as a racemic mixture.

Formoterol and salmeterol can be given as stand alone medications, however these medicines do not address any of the inflammatory processes involved in allergic asthma. A further development in the treatment of asthma was the combination of the compounds with an inhaled corticosteroid (ICS, *vide infra*) in a single device allowing simultaneous delivery of both bronchodilator and anti-inflammatory compounds.

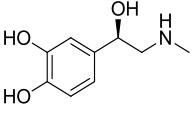
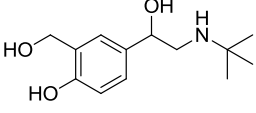
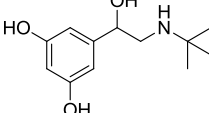
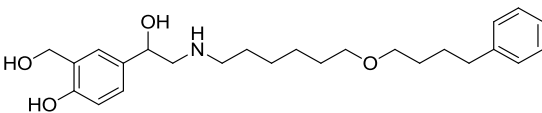
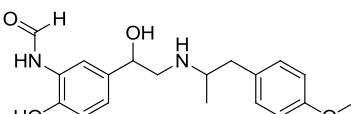
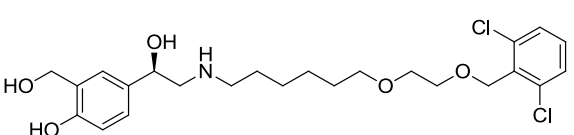
Compound	Structure	Generic name	Human duration of action	Refs.
1		Adrenaline	1 h	20
2		Salbutamol	3-6 h	26
3		Terbutaline	3-6 h	27
4		Salmeterol	> 12 h	28
5		Formoterol	> 12 h	29
6		Vilanterol	> 24 h	30

Table 1: Structures and generic names of marketed  $\beta_2$ -agonists for the treatment of asthma.

### 1.3.2 Inhaled corticosteroids as anti-inflammatory agents for the treatment of asthma.

The use of corticosteroids in asthma treatment has been extensively covered in the literature by Gupta<sup>31</sup> and by Barnes.<sup>32</sup> Those compounds resulting from research in the area that are currently used for asthma therapy are shown in Table 2 along with cortisone (an endogenous corticosteroid).

Natural corticosteroids are a class of steroidal hormones produced in the adrenal glands of vertebrate animals as a result of biochemical modifications to cholesterol. One particular sub-class of corticosteroids are the glucocorticosteroids which exert their actions through the glucocorticosteroid receptor (GR). GR is a nuclear receptor, so called as it is present within the cell nucleus. GR is expressed in almost every cell in the body and regulates genes controlling development, metabolism, and the immune response. Agonism of GRs leads to a broad spectrum of anti-inflammatory activities driven in the most part by the repression of inflammatory genes that code for the various cytokines key to inflammatory processes. This broad ranging repression of inflammatory responses has proven useful in the treatment of chronic inflammatory conditions such as asthma. It should also be noted that activation (agonism) of the glucocorticosteroid receptor also leads to an upregulation of  $\beta_2$ -receptors, thereby making bronchodilators that act by this mechanism more efficacious.<sup>31</sup>

Amongst the first corticosteroids to be prescribed for asthma were cortisone and prednisone. These compounds are prodrugs, a compound that is itself biologically inert but is activated by enzymes *in vivo*, in this case by reduction of the 11-keto function. The compounds are dosed orally, however it has been discovered that systemic corticosteroid exposure is associated with a number of side effects. These side effects include Cushing's syndrome whose symptoms include rapid weight gain; particularly to the face and abdomen, skin thinning, acne, osteoporosis and can lead

to diabetes.<sup>33</sup> In addition, of particular concern is that overuse of glucocorticosteroids has been shown to cause growth retardation in paediatric patients.<sup>34</sup>

A switch to inhaled delivery was the first step in reducing such side effects; by delivering the compound directly to the target organ a lower dose is required to achieve the biologically relevant concentration in the target tissue.

Significant improvements to the side effect profile were made with the development of the inhaled prodrug beclomethasone dipropionate **9**, which is activated by hydrolysis of the 21-ester revealing the active 21-hydroxy derivative.

Despite the switch to inhaled delivery some systemic corticosteroid exposure from a combination of oral and pulmonary absorption is still observed. This has been addressed in a number of ways: budesonide **10**, fluticasone propionate **11**, and fluticasone furoate **13**, were all designed using the soft or antedrug approaches. In addition, these drugs are also significantly retained within the lung tissue resulting in extended durations of action *in vivo* of approximately 12 h (for **10** and **11**) and 24 h (for **12** and **13**). Ciclesonide **14** was designed using a prodrug approach with the 21-ester being essentially devoid of oral bioavailability; lung enzymes hydrolyse this group revealing the active compound.

The marketed products Advair<sup>TM</sup> and Symbicort<sup>TM</sup> (combinations of salmeterol with fluticasone propionate and formoterol with budesonide, respectively) represent the current gold standard for treatment of moderate to severe asthma with Relvar/Breo<sup>TM</sup> (a combination of vilanterol and fluticasone furoate) expected to succeed them in the future.

**GSK CONFIDENTIAL – Property Of GSK – Copying Not Permitted**  
 The Synthesis and Optimisation of Toll-like Receptor Agonists as Potential Immunomodulatory Agents.

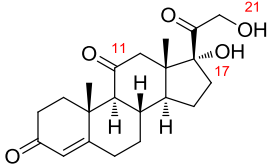
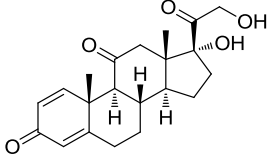
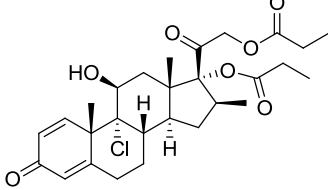
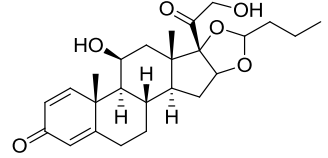
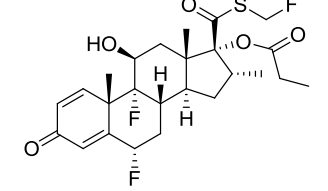
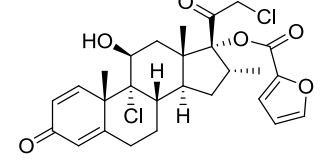
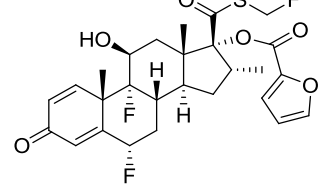
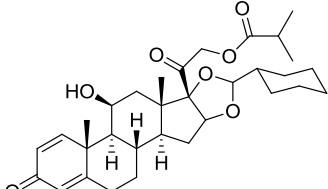
Compound	Structure	Generic name	Refs.
7		<b>Cortisone</b>	<b>35</b>
8		<b>Prednisone</b>	<b>36</b>
9		<b>Beclomethasone dipropionate</b>	<b>37</b>
10		<b>Budesonide</b>	<b>38</b>
11		<b>Fluticasone propionate</b>	<b>39</b>
12		<b>Mometasone furoate</b>	<b>40</b>
13		<b>Fluticasone furoate</b>	<b>41</b>
14		<b>Ciclesonide</b>	<b>42</b>

Table 2: Structures and generic names of corticosteroids that are marketed as asthma treatments.



### 1.3.3 Cysteinyl leukotriene antagonists as orally administered anti-inflammatory agents for asthma therapy.

Aside from the ICS class of compound, despite numerous years of research into a variety of target classes, the only other class of small molecule drugs to be licensed as anti-inflammatory medications for asthma are the leukotriene antagonists. The role of leukotrienes in asthma has been well reviewed in the literature, for example by Singh<sup>43</sup> and by Hallstrand.<sup>44</sup>

The leukotrienes (LTs) are bioactive molecules derived from the ubiquitous membrane constituent arachidonic acid that act principally on a sub-family of GPCRs. The cysteinyl leukotrienes (cysLT) sub class are bronchoconstrictors that are produced by the mast cells,<sup>45</sup> and the eosinophils,<sup>46</sup> and are a critical component of allergic asthma. The cysteinyl leukotrienes LTC<sub>4</sub>, LTD<sub>4</sub> and LTE<sub>4</sub> transduce their effects by binding to the CysLT<sub>1</sub> receptor,<sup>47</sup> making this receptor a favourable target for pharmacological intervention.

The goal for research groups in the pharmaceutical sector was to develop an oral CysLT<sub>1</sub> antagonist compound capable of blocking the effects of the cysteinyl leukotrienes. It was anticipated that antagonising a single class of mediators would result in a better side effect profile than the conventional ICS compounds allowing oral dosing with its advantages in patient acceptability and compliance. These research efforts yielded three orally administered drug molecules (Table 3, note the leukotriene LTC<sub>4</sub> is included for comparison).

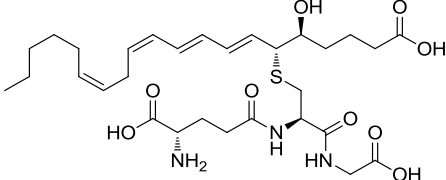
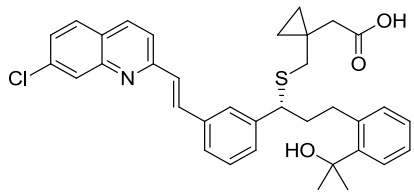
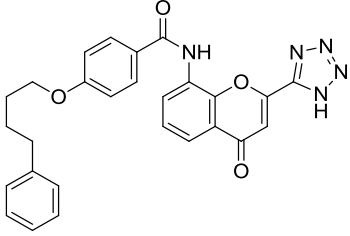
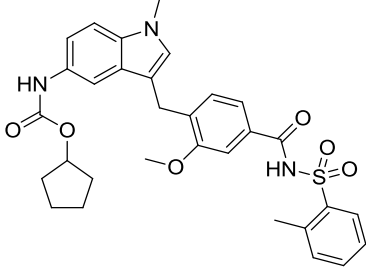
Compound	Structure	Generic Name	Refs.
15		LTC <sub>4</sub>	-
16		Montelukast	48
17		Pranlukast	49
18		Zirflukast	50

Table 3: Structures and generic names for marketed LTD<sub>4</sub> antagonists.

Montelukast is dosed once daily, whereas pranlukast and zirflukast are dosed twice daily. The medicinal chemistry leading to the development of these compounds has been well reviewed by Bernstein<sup>51</sup> and by Montuschi.<sup>52</sup> All three licensed leukotriene antagonists result in a 25-30% improvement in asthmatic symptoms and decreased the number of times a  $\beta_2$ -agonist medication was required. In addition, it has been demonstrated that adding a cysteinyl leukotriene agonist to ICS therapy is as effective in reducing symptoms as doubling the dose of ICS used, without the risk of side effects through the use of more steroid based therapies.<sup>53</sup>

### 1.3.4 Recombinant monoclonal antibodies as anti-inflammatory agents.

In addition to small molecule medicines, the other class of therapeutic agent that has been the subject of significant research efforts are biologics, specifically monoclonal antibodies (mAbs) with to date, one compound, omalizumab (Xolair<sup>TM</sup>), being licensed for asthma therapy.<sup>54</sup> Omalizumab is an anti-IgE monoclonal antibody consisting of 95% human and 5% murine amino acid sequences (Figure 4).

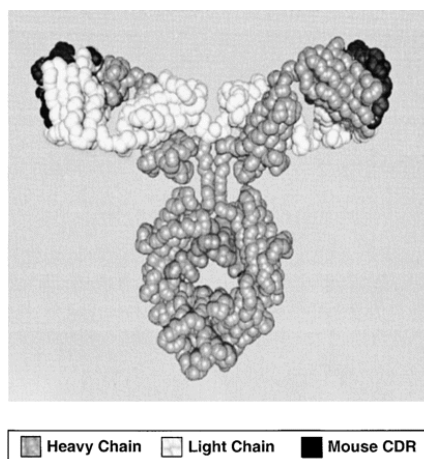


Figure 4: Structure of omalizumab, a monoclonal anti-IgE antibody. Reprinted from The Journal of Allergy and Clinical Immunology, Volume 108. Boushey, H. A. Experiences with monoclonal antibody therapy for allergic asthma, pages, s77-s83 Copyright (2001), with permission from Elsevier.<sup>55</sup>

Omalizumab binds to IgE thereby preventing it from binding to various receptors on mast cells and undergoing cross linking. Accordingly the release of the inflammatory compounds responsible for the symptoms of asthma is reduced. Despite the fact that there are minimal side effects from the treatment, there are factors that limit the use of omalizumab to the treatment of cases of severe allergic asthma where other methods have proven ineffective. These include the high treatment cost and the fact that the drug is administered by monthly subcutaneous injection, resulting in some patient compliance issues.

### 1.3.5 Limitations of current asthma therapies and the concept of remission.

As described above, to date all the medications licensed for asthma only treat the symptoms resulting from the inflammatory processes involved. Whilst they are employed in successful treatment paradigms, these drugs do not have any effect on the pathogenesis of asthma, with patients often requiring treatment for the rest of their lives. A potentially transformational concept for patients is that of remission, whereby the progress of the disease is halted and symptoms reduce significantly, allowing the reduction or cessation of treatment with anti-inflammatory and bronchodilator drugs.

### 1.4 Remission through immunomodulation.

In order to achieve remission, the responses to allergen controlled by the immune system need to be permanently modified. As stated previously, given that in most asthma patients there is biased differentiation of  $T_H0$  cells into  $T_H2$  cells, one potential immunodulatory approach would be to interfere with this process such that the  $T_H0$  cells mature into other T-cell subsets in response to allergen, particularly  $T_H1$  or regulatory T-cells ( $T_{Regs}$ ).  $T_H1$  cells are produced in response to infection and are involved in the cytotoxic processes employed to kill the invading organism. As part of this process  $T_H1$  cells secrete the cytokines IL-2, tumour necrosis factor beta ( $TNF\beta$ ) and interferon gamma ( $IFN\gamma$ ). Together, these cytokines activate macrophages, stimulate cytotoxic T-cells and have an inhibitory effect on  $T_H2$  cells. Regulatory T-cells are known to have a suppressive impact on effector T-cells that is mediated by IL-10 and transforming growth factor beta ( $TGF\beta$ ), and thus have been implicated in regulating  $T_H2$  functions in asthma.<sup>56</sup>  $T_{Reg}$  cells also down regulate the expression of antigen presentation peptides within APCs and can induce IL-10 production within bystander T-cells, all of which contribute to their immunosuppressive effect.<sup>57</sup> If this rebalancing of the adaptive immune response

can be achieved, the T<sub>H</sub>1 and T<sub>Reg</sub> cells produced could become memory T-cells. Consequently, upon future allergen exposure these memory cells could aid in the direction of the adaptive immune response away from the allergic T<sub>H</sub>2 phenotype and provide a long term therapeutic benefit.

### 1.4.1 Specific immunotherapy (SIT)

The changes in T-cell maturation and T-cell responses described above are observed in patients that have undergone allergen specific immunotherapy (SIT) for allergic rhinitis. In such cases patients are exposed to increasing amounts of allergen and gradually, over time (often years), achieve a state of allergen tolerance through long term immunomodulation. The levels of immune cells and corresponding immune biomarkers have been assessed in these patients. In addition to the T-cell changes, B-cells are also affected, producing less IgE and generating blocking antibodies such as IgG (that prevent crosslinking on mast cells). As a result of these changes, the number of mast cells and eosinophils present is also decreased (Figure 5).

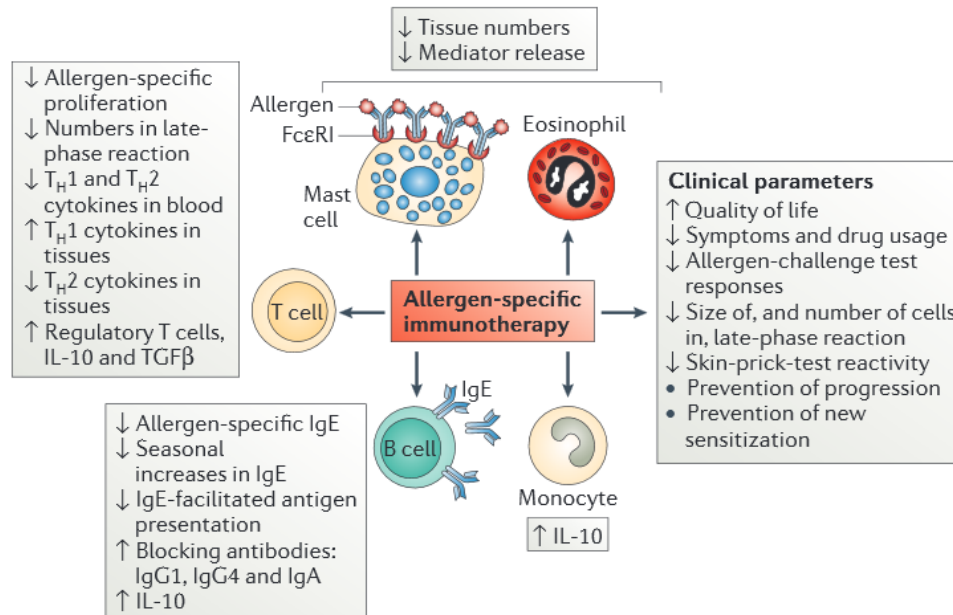


Figure 5: Effects of allergen specific immunotherapy (SIT) on immune and clinical parameters.

Reprinted by permission from Macmillan Publishers Ltd: Nature Reviews Immunology

(*Nat. Rev. Immunol.* **2006**, *6*, 761-771), copyright (2006).<sup>58</sup>

Despite increased interest in SIT as a potential method to treat other allergic diseases including asthma, the exact mechanisms involved in the process are not well understood.<sup>59</sup> Furthermore, application of SIT to asthma patients is often not viable as large numbers of asthmatic patients are polysensitised, that is allergic to a range of allergens.<sup>60</sup>

#### 1.4.2 Potential use of small molecules to achieve immunomodulation.

An advantage of using a small molecule to direct  $T_{H0}$  cells to mature into  $T_{H1}$  and  $T_{Reg}$  cells upon encountering an allergen would be that the compound could be used to induce tolerance in patients against a variety of different allergens. In order to ascertain the biological target for a small molecule immunomodulatory agent it is essential to examine the processes by which the maturation of  $T_{H0}$  cells is controlled. As stated in Section 1.2, it is the nature of the cytokines present during maturation that determine the outcome.

A significant proportion of these cytokines are produced by the activated APCs that encountered the antigen and initiated the immune response. In order to become activated the APC needs to be able to recognise molecules that originate from foreign sources. This is achieved by way of pattern recognition receptors (PRRs) that bind specific pathogen associated molecular patterns (PAMPs). Examples of PAMPs include molecules from bacterial cell walls and viral oligonucleotides. There are a number of different subsets of PRRs including the Toll Like Receptors (TLRs), NOD-like receptors (NLRs) and RIG-1-like receptors (RLRs).<sup>61</sup> These receptors are present on the surface of, or inside the APCs: the dendritic cells (DCs) and macrophages. Binding of a PAMP to its cognate PRR initiates a complex signalling cascade that results in the APC synthesising and secreting various cytokines and chemokines. This is an integral part of the innate immune response, causing vasodilation, fluid exudation, an increase in vascular permeability, and recruitment of neutrophils to envelop and destroy the invading organism. In addition, the cytokines secreted by the APCs direct the maturation of  $T_{H0}$  cells and in doing so direct the wider adaptive immune response to effectively combat the type

of organism infecting the host. The TLRs have been proven to be particularly important in this respect, providing a mechanism by which the innate immune response can link to the adaptive immune response.<sup>62</sup>

On the basis of the above, it may be possible to use to a small molecule agonist compound that targets a specific TLR, causing the production of cytokines necessary to bias maturation of T<sub>H</sub>0 cells to T<sub>H</sub>1 and T<sub>Reg</sub> cells and rebalance the immune response to allergen. Indeed, there is growing body of preclinical and clinical evidence to suggest that pharmaceutical intervention at the TLRs can have beneficial effects in patients with allergic respiratory disease.<sup>63</sup>

### 1.4.3 Toll Like Receptors (TLRs).

In 1985 Christiane Nüsslein-Volhard discovered a receptor and its coding gene that was crucial for driving the immune response in *Drosophila* and declared "Das ist ja toll!" which translates from German as "This is great!" Accordingly, the receptor and gene became known as the toll gene and toll receptor.<sup>64</sup> TLRs are so named because of the shared homology with the toll gene and toll receptor (Figure 6). TLRs are membrane glycoproteins consisting of an internal signalling domain and an external antigen sensing domain consisting of a number of leucine rich repeats (LRR) which impart a solenoid or horse shoe shape to this domain.<sup>65</sup>

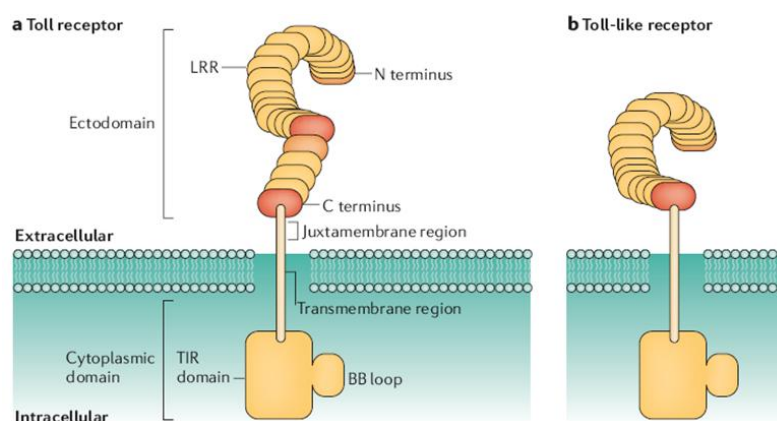


Figure 6: Schematic representation of the basic architecture of Toll and Toll-like receptors. Reprinted by permission from Macmillan Publishers Ltd: Nature Reviews Immunology (*Nat. Rev. Immunol.* **2006**, *6*, 693-698), copyright (2006).<sup>66</sup> . LRR; Leucine rich repeat, TIR; Toll/interleukin-1 signalling domain. BB loop; proline-glycine containing loop.

To date, ten human TLRs have been identified, six of which are located on the plasma membrane and four within the endosome.<sup>67</sup> The locations of each TLR and its known endogenous ligands are summarised in Table 4.

TLR (s)	Subcellular location	Physiological ligands	References
TLR1-TLR2	Plasma membrane	Triacylated lipopeptides	68
TLR2	Plasma membrane	Peptidoglycan, tGPI-mucins, HMGB1, phospholipomannan, porins, haemagglutinin, lipoarabinomannan, glucuronoxlyomannan.	69
TLR2-TLR6	Plasma membrane	Diacylated lipopeptides, LTA, Zymosan.	70
TLR3	Endosome	dsRNA	71
TLR4	Plasma membrane	LPS, VSV glycoprotein G, RSV fusion protein, mannan, fibrinogen, HSP60, HSP70, glucuronoxlyomannan, HMGB1.	72
TLR4-TLR6	Plasma membrane	OxLDL, amyloid- $\beta$ fibrils	73
TLR5	Plasma membrane	Flagellin	74
TLR7	Endosome	ssRNA	75
TLR8	Endosome	ssRNA	76
TLR9	Endosome	DNA, Haemozoin	77
TLR10	Plasma membrane	ND	78

Table 4: Summary of the human TLRs and their respective ligands. Table adapted with permission from Macmillan Publishers Ltd: The Journal of Immunology (*J. Immunol.* **2005**, *174*, 2942-2950), copyright (2012).<sup>79</sup> Summary of abbreviations: tGPI-mucins; *Trypanosoma cruzi* glycosyl phosphatidylinosito-anchored mucin-like glycoprotein, HMGB1; high-mobility group box 1 protein, LTA: lipoteichoic acid, LPS; lipopolysaccharide, VSV; vesicular stomatitis virus, RSV; respiratory syncytial virus, HSP: heat-shock protein, OxLDL; oxidised low density lipoprotein, ND; not determined.

TLRs exist as an equilibrium between the monomeric state and a dimeric complex, in most cases a homodimer. TLR signalling is initiated by either ligand induced rearrangement of such a pre-existing TLR dimer or ligand induced dimerisation. In addition to the endogenous ligands, a wide variety of small molecule ligands have been identified for various members of the TLR family, particularly TLRs 7 and 8.<sup>80</sup>

#### 1.4.4 TLR ligands as potential medicines.

With the role TLRs play in the innate immune system, they make attractive targets for the treatment of a number of diseases. Aside from the treatment of allergic diseases, there is significant potential for TLR ligands in the treatment of microbial



disease states, either by enhancing the hosts defence mechanisms or by blocking inflammation caused by an invading organism. The ability of TLR agonists to potentiate immune responses has led to interest in such therapeutics as vaccine adjuvants.<sup>81</sup> TLR ligand therapy has also shown potential in the treatment of certain cancers<sup>82</sup> and auto-immune disease.<sup>83</sup> The status of TLR based therapies has been extensively reviewed,<sup>84</sup> and continues to garner interest from academic and industrial researchers alike.<sup>85</sup>

Of the therapies being developed for allergic respiratory diseases it is the endosomal TLRs that have shown the most promise. The reasons for this are multifactorial; including the nature of the cytokines induced in the APCs, direct actions on the effectors cells of the immune system and on the airways themselves. Many of these actions also make the endosomal TLRs promising targets in the fields of virology and cancer therapy. Each of these aspects of endosomal TLR biology is discussed in the following sections.

#### 1.4.5 Endosomal TLR signalling and cytokine induction.

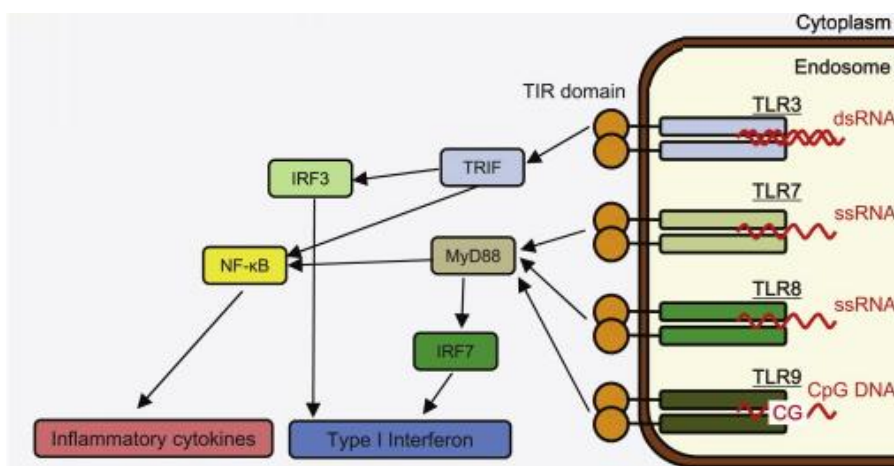


Figure 7: Schematic representation of the signal transduction pathways of the endosomal TLR receptors. Figure modified from *Microbes and Infection*, Volume 16, Ohto, U.; Tanji, H. and Shimizui, T. Structure and function of toll-like receptor 8, Pages No. 273-282, Copyright (2014), with permission from Elsevier.<sup>86</sup> Summary of abbreviations: MyD88; myeloid differentiation factor 88, TRIF; TIR-domain-containing adapter-inducing interferon- $\beta$ , IRF3, and 7; interferon regulatory factor 3, and 7, NF $\kappa$ B; nuclear factor kappa-light-chain-enhancer of activated B cells.

Once an endosomal TLR has bound its cognate agonist ligand a complex signalling process transmits this signal to the cell nucleus and initiates the synthesis and secretion of cytokines and chemokines. This cascade is summarised in Figure 7, and discussed further in detailed reviews by Moynagh<sup>87</sup> and Kužnik.<sup>88</sup> An important feature of the signalling cascade is its bifurcating nature, with ligand binding and signal transduction able to proceed by IRF 3 or 7 and cause the induction of type 1 interferons (IFNs) such as IFN $\alpha$  (depicted in blue in Figure 7). IFN $\alpha$  is a highly T<sub>H</sub>1 polarising cytokine, also possessing potent antiviral and anticancer activities (described in more detail in section 1.5). Alternatively the signalling cascade can proceed by the NF $\kappa$ B pathway and cause the induction of proinflammatory cytokines such as the highly inflammatory tumour necrosis factor (TNF)- $\alpha$ . In order for a TLR agonist compound to be of benefit in allergic conditions, we require the activity of T<sub>H</sub>1 polarising cytokines to significantly outweigh any proinflammatory effects caused by cytokines such as TNF $\alpha$ .

In order to ascertain the identity of the endosomal TLR(s) with the most potential as an immunomodulatory target(s) for allergic asthma, it is important to examine the distribution of the TLRs between the cells of the immune system in more detail. The expression levels of the nucleic acid sensing TLRs (TLRs 3 and 7-9) varies significantly between innate immune cell lines.

Considering first the dendritic cells (DCs); the myeloid DCs (mDCs) and monocyte derived DCs (Mo-DCs) both express TLRs 3, 7 and 8, whereas the plasmacytoid DCs (pDCs) significantly express TLRs 7 and 9 and do not respond to agonists of TLRs 8 or 3.<sup>89</sup> When the pDCs are stimulated with either a TLR7 or a TLR9 agonist, the response is highly selective for the IFN $\alpha$  inducing arm of the cascade, in fact so much IFN $\alpha$  is produced, as much as 3-10 pg/cell in response to viral infection, that pDCs are also known as natural or professional interferon producing cells.<sup>90</sup> In contrast, agonism of TLRs 3, 7, 8 and 9 within mDCs and Mo-DCs are more selective for the proinflammatory pathway and produce significant amounts of

TNF $\alpha$ . In addition TLR3 agonism leads to the induction of IL-12 which is also a T<sub>H</sub>1 polarising cytokine.<sup>91</sup>

Macrophages also express the nucleic acid sensing TLRs 7, 8 and 9 but do not express TLR3.<sup>92</sup> Agonism of the available endosomal TLRs in this cell type does not lead to the induction of IFN $\alpha$ , indicating selectivity for the NF $\kappa$ B arm of the pathway.<sup>93</sup>

Despite the range of cellular responses to TLR7 and 9 agonists, it has been demonstrated that the IFN $\alpha$  upregulation initiated by pDCs is so powerful that the net result of TLR7/9 activation in human peripheral blood mononuclear cells (PBMCs) is strongly biased towards production of IFN $\alpha$ , thus meeting our requirement for T<sub>H</sub>1 biasing cytokines with minimal induction of inflammatory cytokines. In contrast, TLR8 agonism of PBMCs results a cytokine induction profile dominated by TNF $\alpha$ <sup>89</sup> and therefore it is a less attractive target for the treatment of allergic diseases where inflammation is already an issue. Whilst TLR3 agonism does lead to the induction of T<sub>H</sub>1 biasing cytokines, the levels are not as significant as those resulting from TLR7/9 activation. In addition, TLR3 expression is limited to DCs and so potentially beneficial effects on other cells of the adaptive immune system cannot be realised.

## 1.5 Direct and indirect biological effects of IFN $\alpha$ .

The most significant biochemical effect of a TLR7/9 agonist is, as has been described above, the induction of IFN $\alpha$ . This cytokine has a wide range of pronounced effects on the cells of the immune system, both the number and function thereof. IFN $\alpha$  has also been shown to cause human naïve T<sub>H</sub>0 cells to favour differentiation to IFN $\gamma$  secreting T<sub>H</sub>1 like cells.<sup>94</sup> IFN $\alpha$  has also been shown to enhance the ability of Natural Killer (NK) cells to destroy their targets and to produce IFN $\gamma$ ,<sup>95</sup> which further stimulates the differentiation of T<sub>H</sub>0 cells into T<sub>H</sub>1 like cells, thus potentiating this immune response. As a result of this T<sub>H</sub>1 biased

response, there is a concomitant reduction in the differentiation of T<sub>H</sub>0 cells into T<sub>H</sub>2 cells which are involved in the propagation of allergic inflammatory responses.

The effects of IFN $\alpha$  are not limited to T<sub>H</sub>0 cells, as IFN $\alpha$  has multiple effects on cDCs, altering aspects of their differentiation, maturation and migration. IFN $\alpha$  also causes pDCs to lose their ability to produce more IFN $\alpha$ , instead the pDCs acquire enhanced antigen presentation characteristics, thus being more able to present the antigen that triggered activation, to naïve T<sub>H</sub>0 cells.<sup>96</sup> IFN $\alpha$  also stimulates the differentiation of monocytes into DCs and cDCs matured in the presence of IFN $\alpha$  show upregulation of the various antigen presentation apparatus and co-factors.<sup>97</sup> In some cases this has been shown to lead to the induction of IL-10 producing T<sub>Reg</sub> cells,<sup>98</sup> thus providing another mechanism by which T<sub>H</sub>2 mediated allergic responses can be reduced.

In addition, IFN $\alpha$  induces an array of proteins that regulate viral and cellular growth cycles, it also upregulates the expression of antigen and cellular adhesion molecules enabling recognition of infected cells by the circulating leukocytes.<sup>99</sup> As well as affecting the growth cycle of infected cells, IFN $\alpha$  directly inhibits the proliferation of both normal and tumour cells. IFN $\alpha$  exhibits other direct effects on tumour cells, including down regulation of oncogene expression and in common with infected cells, the expression of antigens for immune recognition.<sup>100</sup> The biological effects described above also provide a compelling case for the development of TLR7/9 agonists as potential medicines for the treatment of viral infections and cancer.

## 1.6 Direct effects of endosomal TLR agonists on B-cells and T-cells.

Activation of B-cells by TLR7 in the presence of pDCs triggers differentiation toward plasma cells, predominantly producing the blocking antibodies IgG and IgM. IgG is capable of fixing to mast cells and cross linking with IgE and antigen causing inactivation of the mast cell thus preventing release of the inflammatory compounds contained therein.

It has also been demonstrated that there is a subset of B-cells capable of regulatory roles, through the induction of IL-10. Recently it has been demonstrated that ligation of TLR7 in regulatory B-cells leads to induction of IL-10 and can suppress allergic lung inflammation in mice *via* the actions of regulatory T-cells.<sup>101</sup>

TLR7 has been proven to be expressed on a number of subtypes of T-cells, including T-helper cells, regulatory T-cells and on cytotoxic T-cells.<sup>102</sup> The consequences of TLR7 activation on these cells and the role in disease is not well understood, but TLR7 has been implicated in autoimmune disease.<sup>100,103</sup> Stimulation of T<sub>Reg</sub> cells with a TLR4/9 agonist leads to an increased proliferation of T<sub>Reg</sub> cells,<sup>104</sup> whereas TLR8 stimulation results in a suppression of T<sub>Reg</sub> function.<sup>105</sup> Investigations into the effect of a TLR7 agonist on T<sub>Reg</sub> cells have yet to be reported, thus it is unclear whether suppression or activation would be observed.

### 1.7 Summary of the potential effects of a TLR7/9 agonists on the immune responses in allergic asthma.

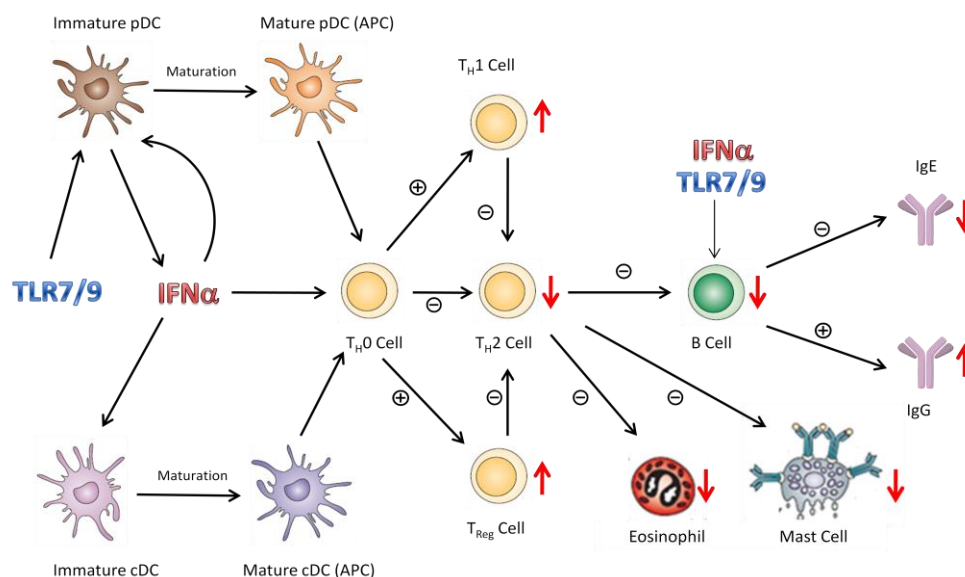


Figure 8: Schematic representation of the direct and indirect effects of a TLR7 agonist on the immune system with respect to allergic asthma. Figure modified with permission from Macmillan Publishers Ltd: Nature Reviews Immunology (*Nat. Rev. Immunol.* **2008**, 8, 218-230), copyright 2008.<sup>13</sup>

The diverse range of effects that a TLR7 or 9 agonist can elicit on cells of the immune system is summarised in Figure 8. The combination of the above described effects has proven to be compelling<sup>106</sup> and the reduction in allergic inflammation has been demonstrated for both TLR7 and TLR9 in preclinical animal models of asthma.<sup>107</sup> As such examples of both TLR7 and TLR9 agonists have been progressed to the clinic for the treatment of asthma.<sup>108,109</sup>

### 1.8 Direct effects of TLR7 and TLR9 on the airways.

As stated in Section 1.1 one of the important symptoms of allergic asthma is airway hyperresponsiveness (AHR). It has been proven that administration of a TLR7 agonist can reduce AHR in mice suffering from allergic inflammation, whereas airway responses were increased upon administration of a TLR9 agonist.<sup>108</sup> It has also been demonstrated that TLR7 agonists can induce a rapid relaxation of smooth muscle in human airways, an effect with obvious benefit to asthma sufferers.<sup>109</sup> In this area it appears that there is a clear advantage associated with the use of a TLR7 compared to a TLR9 agonist.

In addition, at the time of writing the only compounds proven to be TLR9 agonists are synthetic oligonucleotides, whereas numerous small molecule chemotypes have been described as TLR7 agonists (Section 1.9). There are numerous practical and developability challenges associated with oligonucleotide therapies, such as various synthetic challenges and toxicological concerns.<sup>110</sup> Considering these issues along with the airway effects described above, it was decided to pursue a synthetic small molecule TLR7 agonist as a potential immunomodulatory agent for the treatment of allergic asthma.

### 1.9 Known small molecule agonists of TLR7 / inducers of IFN $\alpha$ .

Each known chemical series of potential TLR7 agonists will be reviewed, and the SAR information where available will be discussed in the following sections.

### 1.9.1 Imidazoquinolines and related compounds.

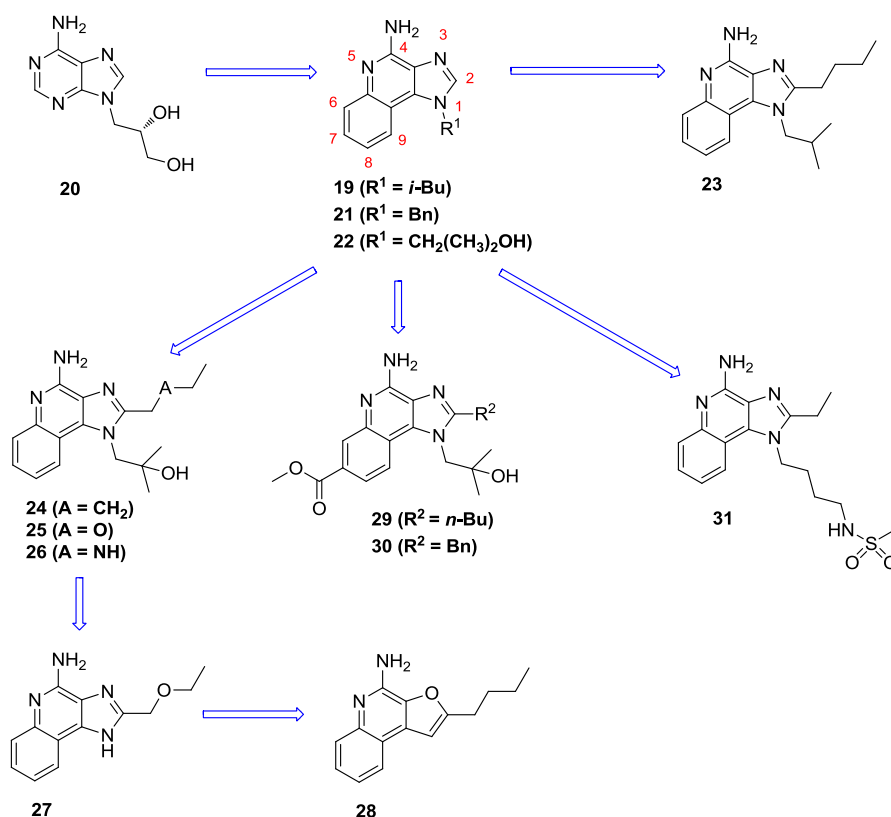


Figure 9: A graphical summary of some of the key imidazoquinoline based compounds and the original lead molecule **20**.

The first small molecule drug to be proven to elicit its biological response *via* TLR7 agonism was the imidazoquinoline based compound, imiquimod **19**,<sup>111</sup> which was approved for use as an antiviral compound in 1997. Imiquimod **19** was developed from the lead compound (S)-2,3-dihydroxypropyladenine **20**. Compound **20** was chosen as the lead compound for this research as it was proven to exhibit weak antiviral activity *in vitro* against herpes simplex virus-1 (HSV-1).<sup>112</sup> Early research centred around the modification of the N-1 position of the imidazoquinoline core and used a human peripheral blood mononuclear cell (PBMC) as a phenotypic assay to measure induction of the cytokine IFN $\alpha$  which can be used as a biomarker of antiviral activity.<sup>113</sup> It was discovered that a wide range of alkyl groups was tolerated in this position, each demonstrating a similar efficacy of 0.5  $\mu$ g/mL for the

minimum effective concentration (MEC) for IFN $\alpha$  induction in the PBMC assay. Incorporation of a benzyl group at the *N*-1 position (compound **21**) led to a 5-fold increase in potency, with the compound exhibiting an MEC of 0.1  $\mu$ g/mL. Also noteworthy is the fact that the carbon atom attached to the ring nitrogen must be primary for the compound to induce IFN $\alpha$ .<sup>114</sup> From this research the *iso*-butyl compound, imiquimod **19** was found to be the most active in a guinea pig *in vivo* model of HSV-1<sup>115</sup> and as such was progressed to the clinic. Further studies with imiquimod revealed that it is metabolised by hydroxylation of the *iso*-butyl group beta to the imidazoquinoline ring to give the similarly potent compound **22** which may explain the enhanced *in vivo* profile of imiquimod **19**, relative to the other compounds with similar MECs in the human PBMC assay.<sup>114</sup> The hydroxylated *iso*-butyl *N*-1 functional group has been subsequently employed in a number of imidazoquinoline analogues including resiquimod **25** and gardiquimod **26**. Imiquimod **19** has subsequently been approved by the FDA as the active constituent in the topical medicine Aldara<sup>TM</sup> for the treatment of external genital warts caused by papilloma viruses. It has also been approved for the treatment of basal cell carcinoma and actinic keratosis (two cancerous skin conditions). Furthermore imiquimod/Aldara has been used to treat other skin conditions, the full scope of which has been reviewed by Ryu<sup>116</sup> and Alomar.<sup>117</sup> Imiquimod has also been proven to induce systemic IFN $\alpha$  after oral dosing in a variety of animal species, and as such was also investigated clinically as an oral IFN $\alpha$  inducer for the treatment of cancer. Imiquimod was not progressed as an oral medication as a result of fatigue and pronounced flu-like symptoms experienced by the patients in these trials.<sup>118,119</sup> These side effects are consistent with significant systemic levels of IFN $\alpha$ , which is in accord with the anticipated mechanism of action following activation of the TLR7 receptor. The occurrence of these side effects presents a significant challenge to the development of further TLR7 agonist therapies.

Extensive investigations into the SAR at the 2-position of the imidazoquinoline template have been carried out.<sup>114,120</sup> These studies have shown that primary alkyl groups increase the IFN $\alpha$  induction potency with respect to imiquimod. An *n*-butyl



group (compound **23**) was found to be optimal, being approximately 50 times more potent than imiquimod in the human PBMC assay. Aromatic, alkoxy and trifluoromethyl groups were not tolerated in the C-2 position. Following the confirmation that imiquimod acts through TLR7 some research groups now employ a TLR7 reporter assay to directly measure activity.<sup>121</sup> This assay measures activation of the NF $\kappa$ B (TNF $\alpha$  inducing) arm of the TLR7 signalling cascade (Figure 7). It should be noted that this assay may not give a true indication of potency as only one pathway is measured and molecules that are selective for the IFN $\alpha$  inducing pathway may appear less potent in this assay. Furthermore the activity of compounds assessed using this assay cannot be directly compared to those compounds assessed using a phenotypic assay such as the human PBMC assay. A number of combinations of potency enhancing N-1 and C-2 were evaluated with compound **24** proving to be the most potent imidazoquinoline TLR7 agonist reported with an EC<sub>50</sub> of 8.6 nM. Incorporation of heteroatoms into the beta position of the C-2 chain is tolerated but reduces TLR7 agonist activity as measured by the reporter assay. Two such compounds, resiquimod **25** and gardiquimod **26** have been extensively studied.<sup>122</sup>

Resiquimod **25** has been evaluated in numerous preclinical models of asthma.<sup>123</sup> In all of these studies there is a clear reduction in the T<sub>H</sub>2 cytokine levels IL-4, IL-5 and IL-13 observed. Furthermore, where measured, TLR7 stimulation led to a reduction in the numbers of eosinophils. In several experiments TLR7 activation was also shown to reduce levels of IgE, this effect has also been demonstrated in PBMCs collected from both allergic and non-allergic human donors, with resiquimod reducing the levels of IgE produced after anti-CD40+IL-4 stimulation.<sup>124</sup> These observations are in line with the biological rationale summarised in Section 1.7.

In addition to acting as TLR7 agonists, resiquimod and a related compound **27** also act as agonists of TLR8.<sup>125</sup> The crystal structure of the TLR8 extracellular region has been acquired by Tanji and co-workers.<sup>126</sup> Crystal structures were obtained for the

performed dimer in the absence of a ligand (Figure 10) and with compounds **25** and **27** bound (Figures 10 and 11).

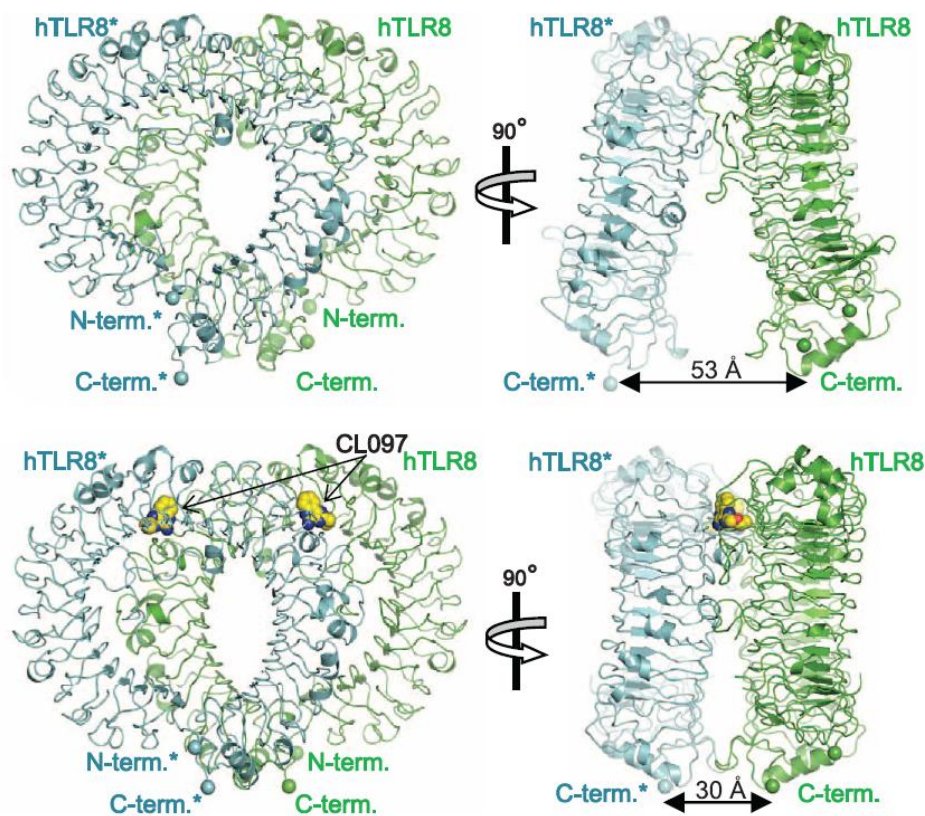


Figure 10: X-ray crystal structures of the preformed TLR8 dimer and that of the structurally rearranged TLR8 dimer in the presence of agonist compound **27** (known in the literature as CL097).

From *Science* **2013**, 339, 1426-1429. Reprinted with permission from AAAS.<sup>130</sup>

Considering first the unliganded dimer, the dimerisation interface occurs in a region between LRRs 8 and 18 and consists of several inter-toll hydrogen bonds: specifically between LRRs 8, 14-15 and 18. In this unliganded state the C-termini of the respective TLR8 monomers are 53 Å apart (Figure 10). In common with TLR7, TLR8 recognises ssRNA and has been shown to also recognise small molecules such as the imidazoquinolines,<sup>127,132</sup> which were crystallised with TLR8 forming a 2:2 ligand:TLR8 complex. In this active state, the C-terminal domains are brought into closer proximity (30 Å) presumably allowing dimerisation of the TIR domains and subsequent adaptor recruitment and signalling. As stated previously the authors

successfully generated crystal structures with compounds **27** and resiquimod **25** (known in the literature as R848). Both molecules induce the conformational change in TLR8 in the same manner, occupying analogous conformations at the same location within the TLR8-TLR8 binding interface (Figure 11).

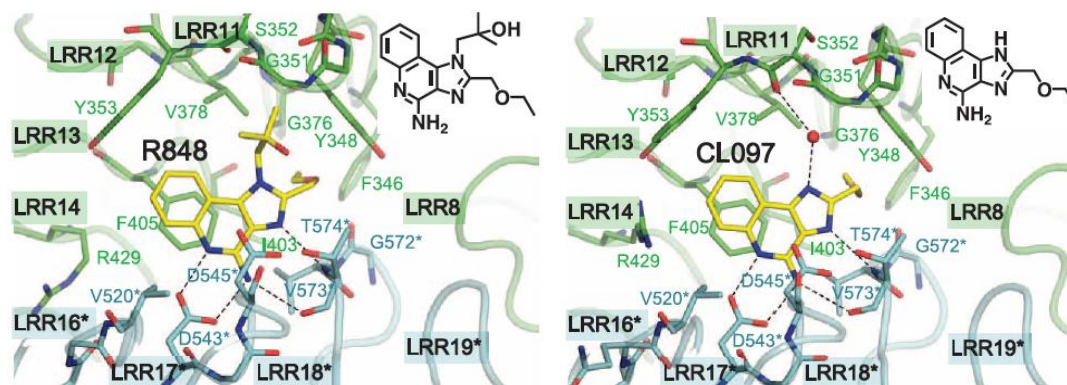


Figure 11: Crystal structures of the agonist compounds resiquimod **25** (R848) and compound **27** (CL097) bound at the dimerisation interface of TLR8, the chemical structure of the ligand is depicted in the top right of each diagram, LRR = leucine rich repeat. From *Science* **2013**, 339, 1426-1429.

Reprinted with permission from AAAS.<sup>130</sup>

Notable interactions include a  $\pi$ -stacking interaction between the benzene part of the isoquinoline ring and with the phenylalanine F405 present in one TLR8 monomer, a salt bridge between the agonist molecule and aspartic acid D543 (stated in the literature as a key binding residue)<sup>128</sup> and two hydrogen bonds to threonine T574 in the other TLR8 monomer. In order to ascertain if the small molecule activators bound to the same site as the natural ssRNA ligands, site directed mutagenesis studies have been performed. Mutations to F405, D543 and T574 (exchanged in turn for an alanine residue) abolished or reduced the agonist activity of the small molecules and also completely abolished any activity arising from ssRNA, indicating that the small molecules are binding to a site that is also crucial for recognition of ssRNA. There is a high degree of homology between TLRs 7 and 8 and the key binding residues are present in TLR7, leading the authors to suggest that the same binding pocket exists in TLR7 and that resiquimod **25** binds to TLR7 through these same residues.

David and co-workers have subsequently used the crystal structure of resiquimod **25** bound to TLR8 to design a series of compounds structurally similar to the imidazoquinolines with varying selectivities between TLR7 and 8.<sup>129</sup> Compound **28** was the most potent TLR8 agonist identified from this research. Using mutagenesis studies the salt bridge interaction with aspartic acid D543 was found to be the most important binding interaction for TLR8 activity. Given the homology between TLR7 and 8 it is not surprising that for the imidazoquinoline series to retain TLR7 activity, replacing or functionalising the amine at the C-4 position of the imidazoquinolines is not tolerated.<sup>114,124</sup>

Further examination of the imidazoquinoline series revealed that substitution of the fused benzene ring (positions 6-9) is only tolerated at the C-7 position in order to retain cytokine induction.<sup>116</sup> Ferguson and co-workers have introduced a methyl ester into this position and generated a range of compounds with varying levels of TLR7 and TLR8 activities.<sup>130</sup> Concurring with previously reported SAR, a butyl group in the C-2 position (compound **27**) was the most active TLR7 agonist. In this subset of compounds incorporation of a benzyl group (compound **28**) into the C-2 position resulted in a potent TLR7 agonist with no reported activity at TLR8.

The latest molecule from the imidazoquinoline series to undergo clinical trials is compound **31** (also known in the literature as '852, PF-4878691 and 3M-001). This compound is reported as having a EC<sub>50</sub> of approximately 100 nM (pEC<sub>50</sub> = 7) in a human PBMC IFN $\alpha$  induction assay.<sup>131</sup> Compound **31** was designed to be an orally or subcutaneously administered TLR7 agonist for the treatment of hepatitis C virus infection. During a phase 1 clinical study, following sub-cutaneous dosing the subjects did experience dose dependent side effects; including injection site irritation, chills and headache.<sup>132</sup> It should be noted that all of these side effects are considered as not severe. In a subsequent study following oral administration, a dose dependent increase in biomarker induction consistent with the desired antiviral effects of a TLR7 agonist was observed. At the highest administered dose, two patients had serious adverse reactions, resulting in flu-like symptoms and

hypotension, leading to the discontinuation of the study. There was another unexpected observation reported in this study: TLR7 expression was upregulated in a dose dependent fashion (Figure 12), thus leading to increased cytokine induction.<sup>133</sup> This positive feedback loop or sensitisation means that there is a very low therapeutic index (TI). The therapeutic index is a comparison of the amount of a therapeutic agent that causes the therapeutic effect to the amount that causes toxicity (in human studies), in this case for antiviral activity over systemic side effects.

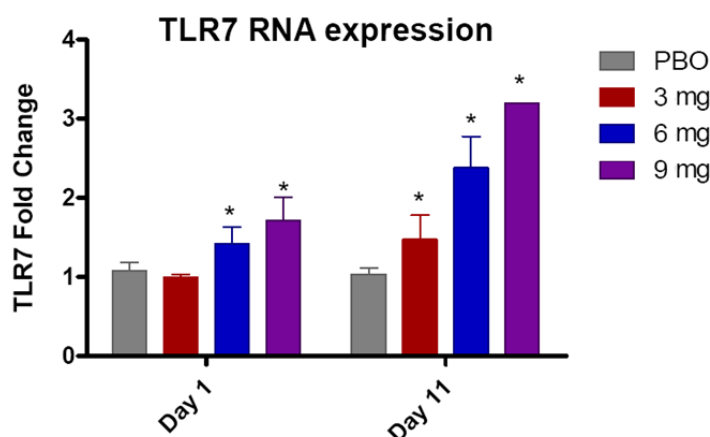


Figure 12: Bar chart indicating the dose dependant upregulation of TLR7 over time upon dosing of compound **31**, analysis of variance \* $p \leq 0.05$ , PBO = placebo. Reprinted from, The innate immune response, clinical outcomes and *ex vivo* HCV antiviral activity of a TLR7 agonist (PF-4878691), Fidock, M. D. *et al.* Journal of Clinical Pharmacology and Therapeutics, Volume 89. Copyright (c) [2011], Wiley & Sons.<sup>139</sup>.

Before examining the other chemotypes proven to agonise TLR7, it is worth discussing the important mechanistic features about TLR8 activation by ssRNA that have been more recently elucidated by Tanji and co-workers,<sup>134</sup> as this information may prove relevant to the understanding of TLR7 activation. They have shown that TLR8 does not actually bind to ssRNA, instead it binds to and is activated by degradation products of ssRNA, a combination of uridine mononucleoside and dinucleotide containing uridine and guanosine (Figure 13).

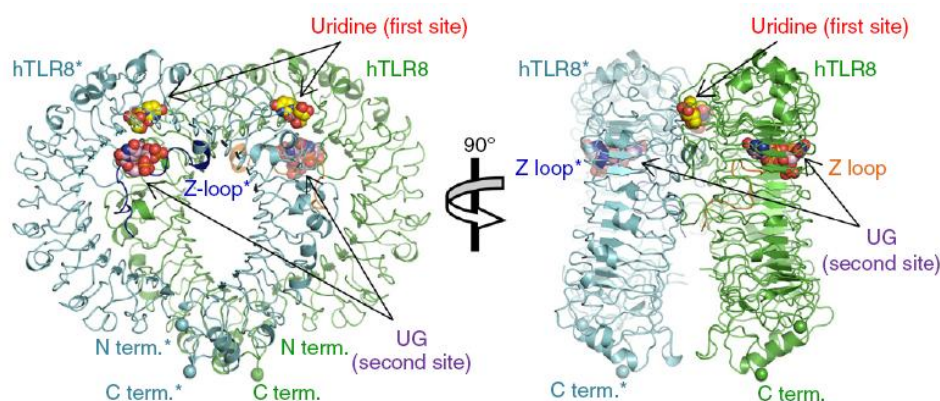


Figure 13: X-ray crystal structures of TLR8 dimer bound to uridine mononucleoside and uridine-guanosine dinucleotide. Reprinted by permission from Macmillan Publishers Ltd: [Nature Structural and Molecular Biology] (*Nat. Struct. Mol. Biol.* **2015**, 22, 109-115), copyright (2015).<sup>140</sup>

Uridine mononucleoside was found to bind in the same binding site as resiquimod **23** (Figure 14). As discussed previously, mutations to the protein in this region prevent activation by small molecules and by ssRNA. Uridine mononucleoside alone only weakly activates TLR8. The presence of the dinucleotide is thought to support the Z-loop and stabilise the active dimer. The dinucleotide was found to bind at a second, previously undescribed binding site (Figure 14). Binding to this site alone cannot activate TLR8 as the site is not located at a dimerisation interface and so cannot induce rearrangement and activation.

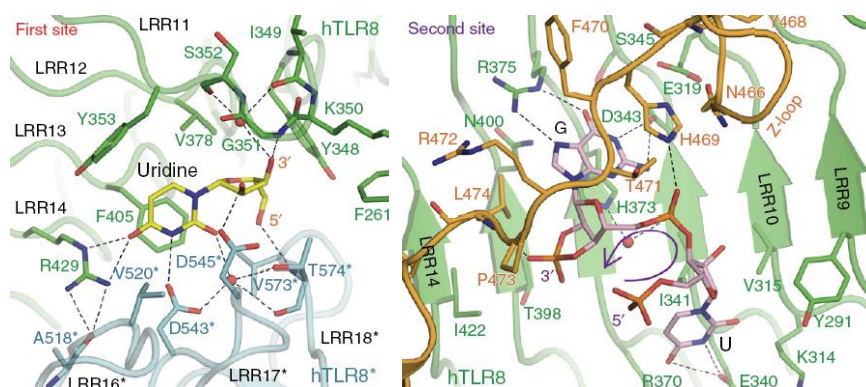


Figure 14: X-ray crystal structures of uridine mononucleoside bound to TLR8 in the first binding site and UG bound in the second binding site. The purple arrow indicates the ability of the uridine nucleotide to rotate and bind in two differing conformations. Reprinted by permission from Macmillan Publishers Ltd: [Nature Structural and Molecular Biology] (*Nat. Struct. Mol. Biol.* **2015**, 22, 109-115), copyright (2015).<sup>140</sup>

This two binding site mode of activation may also apply to TLR7, which in common with TLR8 is activated by ssRNA that is rich in uridine and guanosine.<sup>135</sup> This supposition should be considered when comparing SAR across different TLR7 agonist chemotypes that could potentially bind to and activate TLR7 by differing mechanisms.

### 1.9.2 Purines nucleosides and related compounds.

Guanosine analogues such as 7-thia-8-oxoguanosine (TOG, **32**) and loxoribine **33** (Figure 15) are able to act as antiviral compounds, exerting their action through cytokine induction as a result of TLR7 agonism.<sup>136</sup>

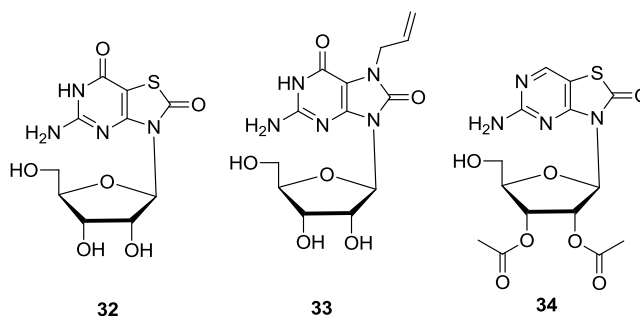


Figure 15: Structures of TLR7 agonists TOG **32**, Loxoribine **33**, and TOG prodrug ANA-975 **34**.

TOG (also called isatoritibe) has been evaluated in clinical trials for the treatment of HCV-1 infection, and proved effective in reducing viral load when dosed once or twice daily.<sup>137</sup> There was however significant concern over potential gastrointestinal side effects, therefore a masked pro-drug of TOG (ANA-975 compound **34**) was developed that reveals the active TOG upon metabolic activation.<sup>138</sup> The development of this drug was suspended following animal toxicology results which did not support further development.<sup>139</sup> Another pro-dug of TOG, ANA-773 (structure not disclosed) is being developed as an oral medicine for the treatment of HCV-1.<sup>140</sup> In the initial clinical study ANA-773 caused a dose dependent decrease in HCV-1 viral load with a concomitant increase in IFN $\alpha$  biomarkers. Those patients receiving large doses of ANA-773 experienced side effects associated with systemic IFN $\alpha$ , including pyrexia, chills, myalgia, headache, nausea and malais.

There were, however, no serious adverse events and no patients discontinued treatment.<sup>141</sup>

### 1.9.3 8-Oxoadenines.

Another purine based series that has been the focus of considerable research efforts has been 8-oxoadenines, with both academic and industrial groups disclosing SAR data, and progressing molecules into the clinic.

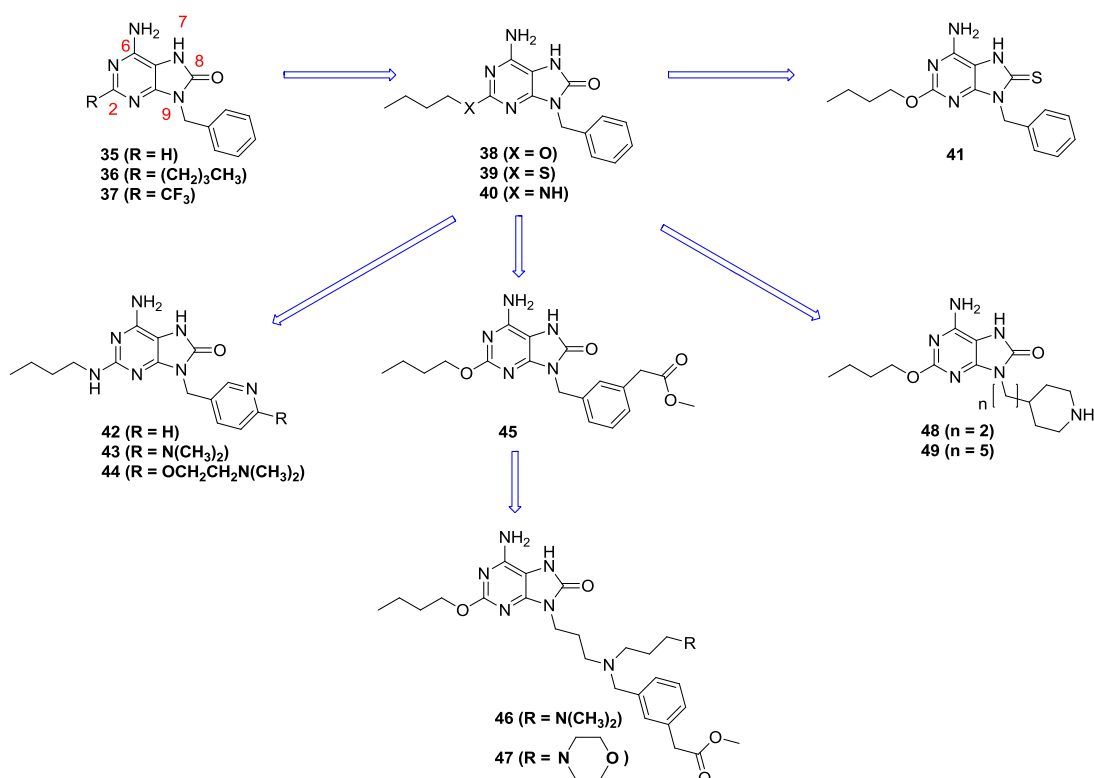


Figure 16: A graphical summary of some of the key 8-oxoadenine based compounds.

Isobe *et al.* at Dainippon Sumitomo Pharma have examined the effect of various 2-alkyl substituents on a 9-benzyl-8-oxoadenine core with a view to developing an orally administered drug for HCV-1 treatment.<sup>142</sup> The activity of the compounds was assessed using mouse splenocytes. In this assay, the compounds of interest were cultured in this cell line and the resultant levels of induced IFN measured and expressed as IFN IU/mL in terms of the international mouse IFN standard obtained



from the National Institutes of Health, Bethesda. Given that only IFN induction data is presented, one cannot be certain at this stage that these compounds are TLR7 agonists. In addition, no data for TNF induction are presented, therefore one cannot analyse SAR with respect to selectivity for the two TLR7/8 signalling pathways (NF $\kappa$ B vs. IRF7, Figure 7) or indeed TLR7 versus TLR8 selectivity.

The initial lead 8-oxoadenine compound **35** was found to induce IFN $\alpha$  with an increased pEC<sub>50</sub> with respect to imiquimod **19**. Introduction of alkyl groups onto the C-2 position increased potency with an *n*-butyl chain (compound **36**) proving optimal for IFN $\alpha$  induction, being approximately 1000 fold more potent than compound **35**. Incorporation of a trifluoromethyl group (compound **37**) indicated that an electron withdrawing group could be introduced in this position. Both *n*-butyl and trifluoromethyl analogues **36** and **37** showed cytokine induction *in vivo* after oral dosing to mice indicating both are orally bioavailable. A further increase in potency was obtained when a heteroatom linker was introduced into the C-2 position, with sulfur and oxygen (compounds **38** and **39**) proving to be more potent than an amine link (compound **40**) in the splenocyte assay.<sup>143</sup> Many heteroatom linked alkyl analogues were synthesised and in the case of oxygen and sulfur linked compounds, the *n*-butyl compounds **38** and **39** were the most potent in the splenocyte assay. Branched alkyl groups were tolerated, as was the introduction of further ether linkages into the chain. It might at first seem surprising that the heteroatom linked *n*-butyl analogues are again the most potent given that they have one more atom in the chain than the carbon linked *n*-butyl compound **36**. This can however be explained if one considers the dihedral angle between the 8-oxoadenine core and the bond between the first and second atoms in the chain and the effect this has on the chain as a whole. When the linking atom is carbon, the chain preferably sits approximately perpendicular to the core (Figure 17). This happens to minimise steric repulsion between the extended alkyl chain in the C-2 position and the large aromatic ring system.

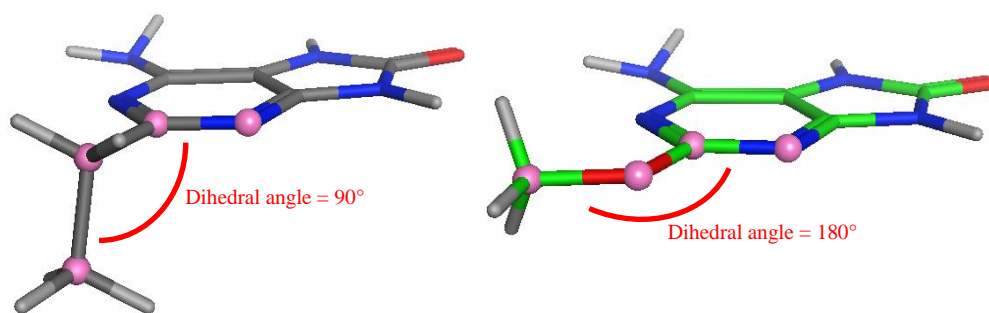


Figure 17: Truncated three dimensional representations of compounds **36** (grey) and **38** (green) to illustrate the differences in the dihedral angle of the C-2 side chain with respect to the 8-oxoadenine core.

When the linking atom is a heteroatom (oxygen, sulfur or nitrogen) the chain lies coplanar with the core as the positive interaction between the heteroatom lone pairs and the aromatic  $\pi$ -cloud overcomes the steric repulsion. Therefore, given this conformational preference, it is entirely feasible that an extra methylene spacer is required for the heteroatom linked alkyl chain to reach the same terminal position as the entirely carbon chain.

Compounds **38** and **39** were evaluated *in vivo* after oral dosing to mice, with the oxygen linked compound **38** proving to be a significantly more potent inducer of IFN $\alpha$  in this instance. A plausible explanation for this is that the sulfur containing compound **39** has a lower oral bioavailability, possibly due to rapid oxidation of the sulfide link in compound **39**. Amine linked analogues exhibited the same general SAR as observed for the sulfur and oxygen analogues but were less potent in all cases in the mouse splenocyte assay.<sup>144</sup> However, when tested *in vivo* amino analogue **40** was observed to have similar potency to compound **38** potentially indicating a higher level of oral bioavailability.

In addition to 8-oxoadenines, both 8-thioxoadenines and 8-aminoadenines have also been shown to induce IFN $\alpha$  and exhibit antiviral activity. Hirota and co-workers have examined replacements for the 8-oxo substituent, and in doing so, discovered that thioxoadenines such as compound **41** are similarly potent IFN $\alpha$  inducers when

compared to their 8-oxoadenine counterparts.<sup>145</sup> The authors also demonstrated that further substitution on the oxygen or sulfur, generating compounds such as methoxy analogue **50** was not tolerated. A potential explanation for this SAR is that the tautomer with a carbonyl or thiocarbonyl group and the adjacent ketoamide NH is required for activity (Figure 18). The analogous 8-aminoadenines exhibit the same general SAR as their 8-oxoadenine counterparts but are less active in all cases.<sup>146</sup>

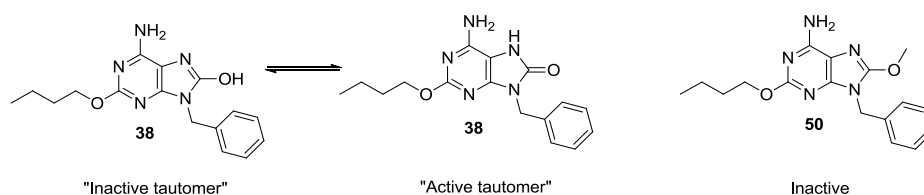


Figure 18: Compound **38** can exist as two tautomers, whereas compound **50** can only exist in one form which may explain its lack of potency.

Despite compounds **38** to **40** being far more potent inducers of IFN $\alpha$  than imiquimod **19**, they were not as potent as resiquimod **25** when profiled *in vitro* in the splenocyte assay or when profiled *in vivo*. With a view to creating compounds that were more potent than resiquimod **25**, 2-*n*-butyl-8-oxoadenines with modified 9-position benzyl groups were investigated.<sup>147</sup>

The potency breakthrough was made when the benzene ring was replaced by a pyridine ring with the 3-linked pyridine (compound **42**). This compound was approximately 30 fold more potent than compound **40** and was as potent *in vitro* as resiquimod **25**. Substitution of the pyridine ring in the 6-position with a dimethylamine (compound **43**) gave a further increase in potency of approximately 10 fold. Unfortunately this potency increase did not translate to an increase in activity when tested *in vivo* after oral dosing to mice or to monkeys. Despite the lack of oral activity of compound **43**, it does have an enhanced solubility profile, most likely due to the enhanced basicity. Therefore, analogues of this type containing a basic amine in the 9-position have been investigated with a view to designing an intravenously administered medicine for treatment of cancer.<sup>148</sup> This research led to the discovery of compound **44** which had the best balance of activity

and solubility. Accordingly, compound **44** was tested in comparison with imidazoquinoline compound **31** in a tumour metastasis model in which compound **44** proved to be approximately 100 fold more active in terms of metastasis inhibition. Furthermore, compound **44** was also found to potentiate the effects of ionizing radiation in murine solid tumour models, thus the study authors recommended that clinical evaluation is warranted.<sup>149</sup>

Researchers at AstraZeneca in conjunction with Dainippon Sumitomo have combined a 2-*O*-butyl-8-oxoadenine with a 9-benzyl group substituted with a plasma labile ester function (compound **45**) as a potential inhaled/intranasal medicine for allergic respiratory conditions.<sup>150</sup> By doing so the compounds are now antedrugs,<sup>23</sup> they are rapidly inactivated by esterases in the systemic circulation, thus minimising systemic exposure. The rationale for making antedrug TLR7 agonists is to minimise or indeed ablate the side effects observed in previous clinical trials of TLR7 agonists that were the result of systemic IFN $\alpha$ .

Direct attachment of a methyl ester to the aromatic ring did not lead to plasma labile compounds when installed in the *meta* and *para* positions, but retained TLR7 activity (as assessed using a TLR7 reporter assay measuring the NF $\kappa$ B pathway). When an extra methylene spacer was introduced the *meta* substituted compound **45** was found to be very rapidly inactivated in plasma with a half life of only 2.6 mins. Therefore, compound **45** is unlikely to activate TLR7 in the systemic circulation.

Compound **45** has been profiled further in functional *in vitro* experiments along with another antedrug, AZ12441970 (compound **46**) that has a TLR7 pEC<sub>50</sub> in the reporter assay of 6.8.<sup>151</sup> Both compounds exhibit no activity in a TLR8 reporter assay and both compounds induced IFN $\alpha$  production in human PBMCs and mouse splenocytes. Compound **46** was found to be a better antedrug in mouse assays, compared with compound **45**, with the primary metabolite, the carboxylic acid, displaying virtually no activity. The compounds were further evaluated in a mouse model of allergic respiratory disease.<sup>157</sup> Both compounds were shown to induce IFN $\alpha$  and a concomitant reduction in the T<sub>H</sub>2 cytokine IL-5 was observed leading to

a reduction in the recruitment of eosinophils. An interesting observation from this study was that in the cellular assays TLR7 gene expression was not upregulated (*c.f.* the clinical data associated with compound **31**, Figure 12). A potential explanation for this is that TLR7 upregulation requires prolonged TLR7 activation, and as these compounds are antedrugs this cannot occur.

Another antedrug AZD8848 (compound **47**) that is similar in chemical structure to compound **46** has progressed to human clinical trials for the treatment of allergic respiratory diseases.<sup>152</sup> In the first study, microgram doses of compound **47** were administered intranasally to patients with allergic rhinitis (another T<sub>H</sub>2 driven allergic respiratory condition). Following dosing the total lymphocyte numbers were reduced and an increase in IL-1Ra (a downstream measure of IFN $\alpha$  induction) was observed. Compound **47** was also found to induce dose dependent flu-like symptoms. However, no parent antedrug was detected in plasma, confirming the rapid hydrolysis of the ester function *in vivo*. Given these observations; the flu like symptoms are most likely to be the result of cytokines induced locally in the nose, being absorbed by the nasal tissue and reaching the systemic circulation.

In the second study compound **47** was dosed intranasally on a weekly basis for 4 weeks with IL-1Ra being measured after each dose. IL-1Ra was found to increase after dosing with a maximum concentration reached after 1 h. Following cessation of dosing, some patients were subjected to a daily nasal allergen challenge. After three days the patients exhibited a reduction in total nasal symptom score compared to the placebo group suggesting a re-balancing of T-cell responses. Given the results seen with compounds **45** and **46** in animal models of asthma (see above), where intranasal dosing was seen to affect the lung, it is postulated that compound **47** may display efficacy in human asthma.

Another clinical study has been conducted with allergic asthmatic patients. In this study patients were dosed intranasally with 60  $\mu$ g of compound **47**, once a week for eight weeks before being challenged with allergen after a further one and four weeks. When assessed after one week the patients did exhibit a reduction in symptoms.

However, no reduction in asthmatic symptoms was observed following an allergen challenge four weeks after the final dose of compound **47**. These observations have been attributed to the fact that the patients were atopic and memory T-cell populations have a life span of several years, instead the reduction in symptoms is attributed to a reduction in responses mediated by this memory T-cell population. Despite the lack of immunomodulation after 4 weeks, the study does indicate that diseases of the lower respiratory tract can be treated *via* intranasal dosing. The study authors do suggest that an increase in dosing frequency and duration of dosing may increase the likelihood of a long term anti-allergic effect.

Researchers elsewhere in our laboratories have examined a series of 8-oxoadenines with C-linked piperidines in the 9-position.<sup>153</sup> They found non-linear relationships between the length of the alkyl chain linking the 8-oxoadenine core with the piperidine and the compounds activity in TLR7 and TLR8 reporter assays. This non linear relationship also translated when induction of the cytokines IFN $\alpha$  and TNF $\alpha$  were assessed in human PBMCs. A two atom linker, compound **48** proved to be the most selective both in the reporter assay (TLR7 vs. TLR8) and in the PBMC assay (IFN $\alpha$  vs. TNF $\alpha$ ). Compound **49** with a five atom spacer was the most potent in terms of TLR7 activation ( $EC_{50} = 100$  nM,  $pEC_{50} = 7$ ) and IFN $\alpha$  induction.

#### 1.9.4 Imidazopyridinones.

Researchers at Pfizer have examined a number of non-purine templates in order to discover a new series of TLR7 agonists for HCV-1 treatment.<sup>154</sup> Each of the four nitrogen groups in the 8-oxoadenine core of compound **51** was systematically replaced with a carbon group and each resulting tri-aza analogue was tested *in vitro*. Of the four compounds tested, the only template that showed any activity was compound **52** where the 7-position nitrogen was replaced by carbon (Figure 19). This study suggests that the other nitrogen atoms present in the 8-oxoadenine core are key for the activity of this series. Compound **52** was however less potent than the 8-oxoadenine compound **51**. In addition, a number of analogues were made to

assess the SAR in the 6-position. The trifluoromethyl containing compound **53** proved to be more active than the methyl analogue (compound **52**). Longer alkyl chains were installed into the 6-position but proved to be less active suggesting some differences in SAR between this series and the progenitor 8-oxoadenine template.

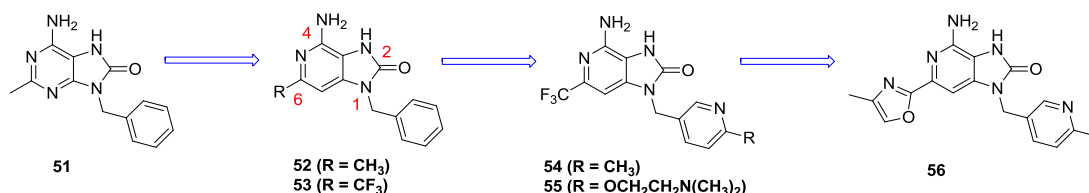


Figure 19: A graphical summary of some of the key imidazo[4,5-*c*]pyridin-2(3*H*)-one based compounds.

As with the 8-oxoadenine series it was possible to replace the pendant benzene ring with a 3-linked pyridine moiety and incorporate substituents at the pyridine 6-position. Both compounds **54** and **55** were shown to be more potent than compound **52** in an assay where the compound is incubated with PBMCs, the supernatant removed and tested for its ability to inhibit HCV replication. Compound **55** and other compounds containing a basic amine were all more potent relative to the parent compound **54**. The authors postulated that the increase in potency is due to accumulation of the basic compounds within the acidic endosomal compartment, although they conceded there is no obvious relationship between pKa and TLR7 potency in their data set. Unfortunately, compounds **54** and **55** proved to be rapidly cleared *in vivo* (rat) with clearance exceeding liver blood flow, indicating the involvement of non-hepatic clearance mechanisms. The compounds were subsequently identified as substrates for aldehyde oxidase (AO) which is oxidising the pyridine ring in the 2-position (Figure 20).<sup>155</sup>

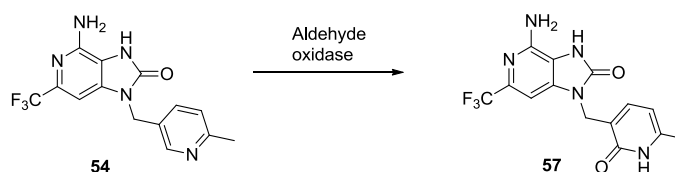


Figure 20: Oxidation of the pyridine ring 2-position in compound **54** by aldehyde oxidase.

Further SAR analysis revealed that the aldehyde oxidase activity could be ablated by modification of not only the pyridine ring, but also the functional group at the 6,5-ring system 6-position. For example compound **56** was stable in rat cytosol over the 1000 minute test period. Molecular models of the 6-trifluoromethyl compounds bound to AO revealed that large 6-position groups prevented access of the compounds to the AO active site.<sup>156</sup> No further studies with these compounds have been reported at the time of writing.

### 1.9.5 Pteridinones

Continuing with this general chemotype, Gilead Pharmaceuticals have reported a monoaromatic pteridinone core template that conveys TLR7 activity.<sup>157</sup>

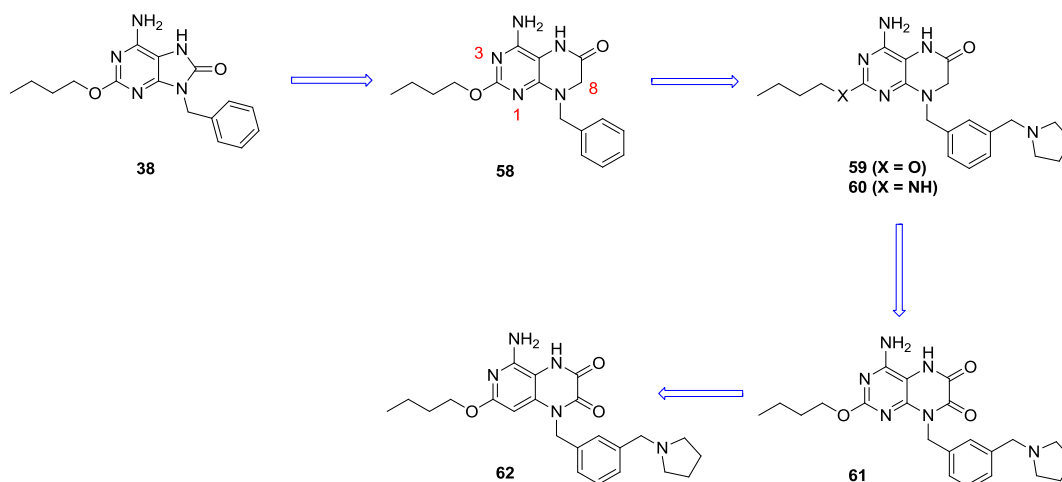


Figure 21: A graphical summary of some of the key pteridinone based compounds and the Lead compound from the 8-oxoadenine series.

The goal of this research was to identify a novel series of compounds with improved potency and selectivity with respect to the existing TLR7 agonist chemotypes described in sections 1.9.2 to 1.9.4, with the aim of developing an orally bioavailable compound for the treatment of viral hepatitis. Expansion of the five membered imidazolone ring present in lead compound **38** resulted in compound **58** which was potent and selective in a human PBMC assay where induction of IFN $\alpha$  and TNF $\alpha$  were measured. Compound **58** has a IFN $\alpha$  induction pEC<sub>50</sub> = 6 and selectivity



IFN $\alpha$ /TNF $\alpha$  of 0.3. Functionalisation of the benzyl group with amines universally increased potency with a *meta*-methylpyrrolidine (compound **59**) exhibiting the highest potency and selectivity for IFN $\alpha$  induction over TNF $\alpha$  induction (pEC<sub>50</sub> = 8.5, IFN $\alpha$ /TNF $\alpha$  = 100). It should be noted that for the *meta*-substituted compounds steric space appears to be at a premium with larger amines being significantly less potent. Much larger groups were however tolerated in the *para*-position but none of these analogues were as selective as compound **59**. It is interesting to note that the amine in compound **59** is five atoms away from the core, the same distance as proved optimal for selectivity in the 8-oxoadenine piperidine series (compound **48**).<sup>159</sup> Changing the C-2 linker from an ether to an amine (compound **60**) was tolerated with only a three fold reduction in potency. SAR with respect to chain length in this area mirrored that described for the 8-oxoadenine series, however, the effects of branching were varied with the size of the branching group appearing to be significant. Introduction of an extra carbonyl group, compound **61** did result in a small increase (less than 10 fold) in the *in vitro* potency. Unfortunately, this modification led to reduced oral absorption. It was found that removal of the N-1 nitrogen still gave active compounds (compound **62**) but did result in an approximately 10-fold reduction in potency compared to compound **61**.

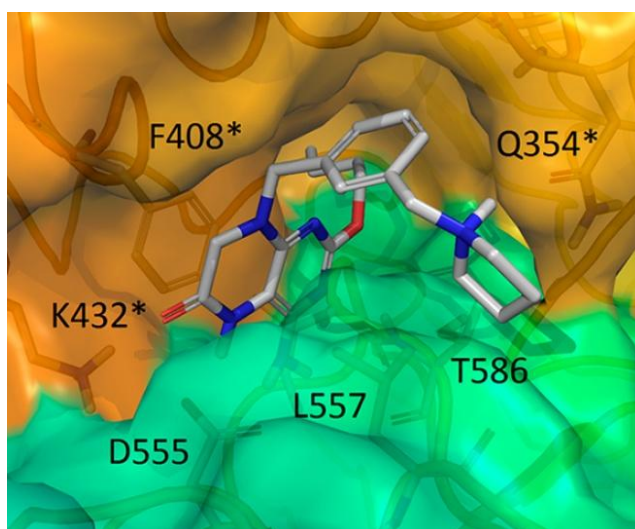


Figure 22: Compound **59** docked into a TLR7 homology model generated using the available TLR8 crystal structure. Reprinted with permission from (The Journal of Medicinal Chemistry, Volume 56, pages 7324-7333). Copyright(2013) American Chemical Society.<sup>163</sup>

Using the available TLR8 crystal structure the authors have generated a TLR7 homology model and docked compound **59** into this construct (Figure 22). The authors suggest that the pteridinone is making hydrogen bonds to D555 and T586 in the same way resiquimod **25** does in the TLR8 active site. It is also suggested that the pyrrolidine may be forming a hydrogen bond with Q354 (not present in TLR8) which may contribute to the compounds potency and selectivity.

Compound **59** was found to have the best overall profile in terms of *in vitro* potency and *in vivo* absorption and has been shown to produce prolonged suppression of the hepatitis B virus in chimpanzees even after cessation of treatment.<sup>158</sup> Accordingly, compound **59** has been progressed into clinical trials for the treatment of hepatitis B infection. In a phase 1 human safety study, gene induction for various cytokines was seen following low (2 mg) doses of compound **59** indicating a potential therapeutic benefit with no observed flu-like symptoms being reported. Patients in the higher dose groups (6 and 12 mg) had detectable levels of serum IFN $\alpha$  and in some cases experienced flu-like symptoms. This demonstrates that there is a therapeutic window (3 fold) between the antiviral effects resulting from cytokine induction and the side effects caused by systemic IFN $\alpha$ .<sup>159</sup>

### 1.9.6 Imidazopyridines.

The most recent chemical series to be reported as TLR7 agonists are the imidazopyridines discovered by David and co-workers.<sup>160</sup>

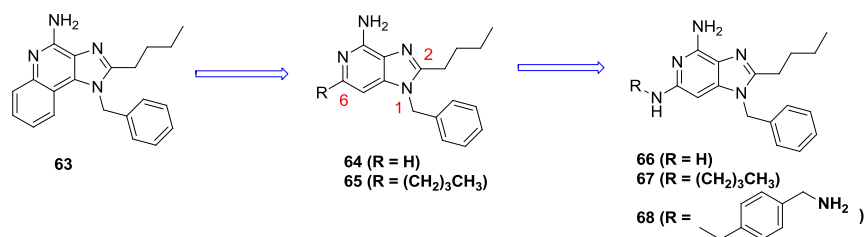


Figure 23: A graphical summary of some of the key imidazopyridine based compounds and the Lead compound from the imidazoquinoline series.

Removing one aromatic ring from the potent imidazoquinoline molecule **63** yielded compound **64**, which was still active in a TLR7 reporter assay albeit less potent (~ 25 fold) than compound **63**. Introduction of a *n*-butyl chain (compound **65**) restored some of the lost activity, now being only approximately 5 fold less potent than compound **63**.

It was found that an amine could be introduced into the 6-position (compound **66**) being approximately as potent as compound **64**. Again, extension to include an *n*-butyl group (compound **67**) improved potency. The SAR with respect to chain length and branching groups is not described in this particular study. The authors do, however, describe a series of functionalised benzylamines in the 6-position. Of particular note is compound **68**, this analogue was no more active than compound **67** in the TLR7 reporter assay but significantly more potent in a PBMC assay measuring IFN $\alpha$  induction. This observation confirms that the TLR7 reporter assay does not necessarily reflect the true activity with respect to functional activity from the point of view of cytokine induction.

### 1.9.7 2-Aminopyrimidines.

Researchers at Dainippon Sumitomo and AstraZeneca have filed a number of patent applications describing 2-aminopyrimidine based compounds as TLR7 agonists.<sup>161</sup> A summary of the structural features covered in these patent applications is shown in Figure 24.

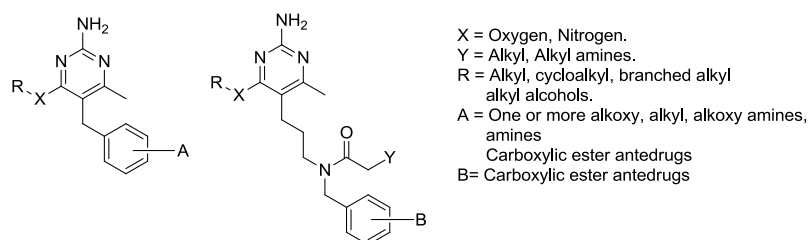


Figure 24: Summary of 2-aminopyrimidines exemplified in AstraZeneca/Dainippon Sumitomo patent applications.

It is interesting to note that the functional groups incorporated into the pyrimidine 5-position are very similar structurally to those incorporated into the 9-position in the

8-oxoadenine series (Section 1.9.3). This suggests that these groups may bind to the same region of the TLR7 receptor.

### 1.9.8 Review of the known TLR7 agonist chemotypes.

All the chemotypes described above do appear to share some common features that possibly form part of the pharmacophore for TLR7 agonist activity. The most important of these appear to be an unsubstituted hetero-aromatic amino group in close proximity to an alkyl chain typically four or five atoms in length. The major challenge with respect to clinical development has been that side effects, sometimes severe in nature, have been experienced by patients in clinical trials. These side effects appear to be mechanism related, that is, due to the induction of cytokines. The nature of the target disease has enabled some researchers to pursue topical delivery and thus minimise the systemic cytokine exposure. However, as described above other researchers have demonstrated that there is a therapeutic window between the induction of clinically beneficial amounts of cytokines and the level of induction that causes side effects. Consideration of the therapeutic index (TI), the ratio of the amount of a therapeutic agent that causes the therapeutic effect to the amount that causes toxicity (in human studies) is therefore, a key parameter to be considered in any future research focused on the development of a TLR7 agonist for clinical use. For comparison the TI for compound **47** is approximately 3 fold<sup>158</sup> and for compound **59** the TI is approximately 4 fold.<sup>164</sup> The survey of the literature presented above supports the view that there is certainly latitude for the development of a novel series of TLR7 agonists with an improved TI.

### 1.10 Aims for a new TLR7 based treatment for allergic respiratory conditions.

There are a number of factors that need to be considered in order to define a target candidate profile that is likely to deliver an efficacious clinical compound. The potential side effects, the route of administration, the physicochemical profile, the pre-clinical *in vitro* and *in vivo* biological profile, and how the compound is

differentiated from any previously reported drugs or clinical compounds. In this instance researchers at AstraZeneca have already developed a clinical candidate for the same indication.<sup>158</sup>

#### 1.10.1 Consideration of any potential side effects and defining the route of administration.

There are a number of known and potential side effects that result from systemic IFN $\alpha$ . In pre-clinical models subcutaneous administration of imiquimod has resulted in fever, increased body temperature and sickness behaviour in rats.<sup>162</sup> Furthermore, and as discussed earlier, it has been demonstrated that raised systemic IFN $\alpha$  levels can result in flu-like symptoms (Section 1.9.1). Another potential concern with raised IFN $\alpha$  levels, is the possibility for the development of autoimmunity (reviewed by Kreig and Vollmer).<sup>163</sup> Autoimmunity is unlikely to be an issue as it is believed that patients will not be dosed chronically with any compound resulting from this research effort. Recently TLR7 has been implicated in neurodegeneration, as a result of interactions with micro RNA (small oligoribonucleotides involved in signalling and regulatory processes).<sup>164</sup> In addition, the clinical data recorded for the imidazoquinoline **31** appears to indicate that repeated TLR7 agonist exposure leads to upregulation of TLR7 and thus could result in hypersensitivity to further TLR7 agonism. Considering the observations stated above, it would be advantageous to design a TLR7 agonist that has poor systemic availability, with exposure limited to the respiratory organs. The first step to achieve this goal is to opt for the route of administration as being topical (either inhaled or intranasal). Adopting this approach should lead to a increased clinical TI for desired over undesired effects when compared to an orally administered TLR7 agonist.

The researchers at AstraZeneca decided to dose topically and to adopt an antedrug approach in order to minimise systemic exposure.<sup>158</sup> The fact that the compound is so rapidly inactivated may, however, have contributed to the lack of long term immunomodulatory effects. Therefore, it is possible that a longer duration of action

is required in order to deliver immunomodulation. Accordingly, it is proposed to limit systemic cytokine exposure not by the antedrug approach, but by designing a molecule that has limited oral bioavailability through negligible oral absorption and/or maximising hepatic clearance. Through the use of this approach it should, in theory, be possible to observe a demonstrable TI following dosing in the clinic.

As explained in Section 1.4.5, TLR7 agonism can lead to the induction of pro-inflammatory cytokines such as TNF $\alpha$  as well as the immunomodulatory cytokine IFN $\alpha$ . It is therefore necessary to endeavour to design a molecule that selectively signals *via* the IRF7 pathway. In order to further reduce the risk of inducing TNF $\alpha$ , the molecule designed needs to be selective for TLR7 over TLR8. This is because, TLR8 agonism primarily leads to the release of TNF $\alpha$ .<sup>89</sup>

#### 1.10.2 Physicochemical requirements for an inhaled/intranasally administered TLR7 agonist.

It has been known for some time that the physicochemical properties of a compound can have a profound effect on its Absorption, Distribution, Metabolism and Excretion (ADME) profile, and a set of guidelines for this (the ‘Rule of Five’) was defined in the seminal work by Lipinski and co-workers.<sup>165</sup> In summary, in order to achieve good oral absorption and permeability the molecule should have a Mol. Wt. < 500, a lipophilicity as predicted by cLogP < 5, Hydrogen bond donors < 5 and acceptors < 10. These rules have received much scrutiny and have been refined by Gleeson, with a reduction in the cLogP limit to 4 and reduction in Mol. Wt. to 400.<sup>166</sup> It has also been noted that during lead optimisation the physicochemical properties tend to increase from lead to candidate, and this puts more emphasis on minimising these properties at lead identification stage.<sup>167</sup>

It is important to remember however, that the guidelines stated above are designed to yield orally bioavailable drug molecules. As we wish to administer our drug *via* the intranasal or inhaled route, we seek to limit the oral bioavailability and so these criteria do not necessarily apply to this research. We do however, need the

compounds to have reasonable permeability to access the desired intracellular target, and to have good solubility such that they can be formulated appropriately. Within our laboratories, Hill and Young have made an important addition to the pantheon of physicochemical rules, by introducing the concept of the solubility forecast index (SFI) which states that for a compound to have good aqueous solubility, the lipophilicity of the compound measured by  $\log D_{7.4}$  added to the number of aromatic rings present in its structure should be less than six.<sup>168</sup> In addition to having a crucial impact on ADME parameters such as clearance and bioavailability, the lipophilicity of a compound has been linked to its promiscuity: defined in this case by a compounds' activity at other targets.<sup>169</sup> This promiscuity is driven by the hydrophobic effect<sup>170</sup> whereby non-polar substances aggregate in aqueous media (in this case drug molecules can associate with and bind to other non-target receptors) and can lead to adverse toxicological outcomes *in vivo*. Blagg and co-workers have gone on to quantify this relationship, and have shown that risk the risk of such toxicity increases 2.5 times when  $c\text{LogP} > 3$  and polar surface area (PSA)  $< 75$ .<sup>171</sup> Hill, Young and co-workers have quantified a link between the SFI of a given compound and its promiscuity, in this publication the same summation that gives SFI is also defined as the property forecast index (PFI), with  $\text{PFI} \leq 7$  and ideally  $\leq 6$  in order to avoid developability concerns, such as poor solubility and toxicity.<sup>172</sup>

### 1.10.3 Dose and activity requirements for an inhaled/intranasally administered TLR7 agonist.

In order to decide what level of activity a clinical compound should have we need to take into account the desired dose. Researchers elsewhere in our laboratories have significant experience in the topical delivery of microgram quantities of drug substance to the airways using various specialised delivery devices. Based upon their experience, a clinical dose of between 1 and 300  $\mu\text{g}$  of compound is optimal for intranasal delivery.<sup>173</sup> Using biological data from the 8-oxoadenine compounds previously discovered in our laboratories and the clinical information from the 8-oxoadenine compound **47**<sup>158</sup> the likely activity required in a human whole blood

assay of IFN $\alpha$  would be a pEC<sub>50</sub> = 7. Compounds with greater activity (pEC<sub>50</sub> > 7.3) would likely lead to nanogram doses which could be challenging to administer. The candidate compound should also demonstrate a reduction in the levels of T<sub>H</sub>2 cytokines in a functional PBMC assay. Finally the compound should be able to induce IFN $\alpha$  *in vivo* following administration in an appropriate animal model.

In summary a potential candidate quality molecule should ideally have the following properties:

- ***In vitro* potency:** IFN $\alpha$  induction in human whole blood pEC<sub>50</sub> 7  $\pm$  0.3, such that the newly designed molecule will have a predicted dose in the microgram range and therefore be suitable for reliable topical delivery.
- ***In vitro* selectivity:** Selective for IFN $\alpha$  induction over TNF $\alpha$  induction ( $\geq$  100-fold). There should be at least a 100 fold concentration difference between the predicted human *in vivo* C<sub>Max</sub> and the EC<sub>50</sub> for activity at targets represented in the extended cross screening (eXp) selectivity panel available in our laboratories.<sup>174</sup> This panel contains many common receptors and enzymes including those that can lead to unwanted outcomes, such as cardiovascular and hepatic toxicities.
- ***In vitro/In vivo* functional activity:** A reduction in measurable T<sub>H</sub>2 cytokines in human PBMCs from allergic individuals after allergen challenge and compound dosing. Induction of IFN $\alpha$  after intranasal dosing in rodents.
- **Drug Metabolism and Pharmacokinetics:** The molecule should have a low oral bioavailability.
- **Chemical and physicochemical properties:** The molecule should be from a series that is structurally distinct from the 8-oxoadenines investigated in our laboratories, so as to derisk any undesirable properties potentially associated with this template. The measured solubility should be greater than



1 mg/mL to enable solution dosing. The compound should have acceptable physicochemical properties such that  $cLogP < 5$  and the  $PFI \leq 6$ .

- ***In vitro/ex vivo* toxicology:** Negative in mini Ames and mouse lymphoma (MLA) genotoxicity assays. There should also be, as a minimum, a 100 fold concentration difference between the predicted human *in vivo*  $C_{Max}$  and the concentration which has no effect in the rabbit ventricular wedge assay. These assays will be defined and discussed further upon data presentation (Discussed in Section 3.9).

## 2 Results and Discussion Part 1: 2-aminopyrimidines as inducers of IFN $\alpha$ .

### 2.1 Discovery of the lead compound.

In order to identify a novel chemical class of compounds with the potential to meet our desired target candidate profile, a high throughput screening (HTS) campaign was undertaken. This campaign yielded a series of pyrimidines as inducers of IFN $\alpha$  in human PBMCs shown in Figure 25. This assay is a phenotypic functional assay where the PBMCs are separated from human blood and incubated with the compound of interest at varying concentrations and the resulting IFN $\alpha$  induction measured.<sup>175</sup> This assay cannot confirm that the IFN $\alpha$  secretion is a result of TLR7 agonism.

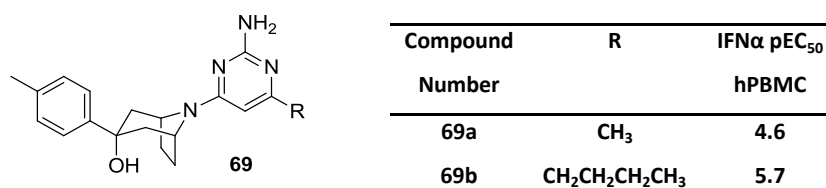


Figure 25: Structure of HTS derived lead compounds and data for their induction of IFN $\alpha$  in PBMCs.

Initial investigations (Hatley, R. J. unpublished work) indicated that changing the 6-methyl group in compound **69a** for a longer alkyl chain was beneficial for activity, with *n*-butyl being optimal. The most active compound discovered from this work, **69b** was shown to induce IFN $\alpha$  with a pEC<sub>50</sub> of 5.7 in human PBMCs.

As described in section 1.9.3, previous work within our laboratories has shown that linking a basic centre to a core scaffold with a five or six atom linker can result in potent, selective TLR7 agonists such as compound **48**.<sup>159</sup> Through application of this knowledge two new pyrimidine compounds were designed: **70a** and **71a**. In addition to introduction of an alkyl chain bearing a basic centre the bicyclic amine present in compound **69** has been replaced with a *n*-butyl function (Champigny, A. C. unpublished work, Figure 26). Both compounds **70a** and **71a** have been shown to

induce IFN $\alpha$  in human whole blood (HWB) (Lau, J.; Hessey, J. unpublished work, Table 5). This assay is again a phenotypic functional assay and was chosen as it potentially gives a better indication of the *in vivo* effects of the compound. These changes have increased the agonist potency, and have simplified the molecular scaffold compared to compound **69a**, and so from an activity perspective, represent attractive leads.

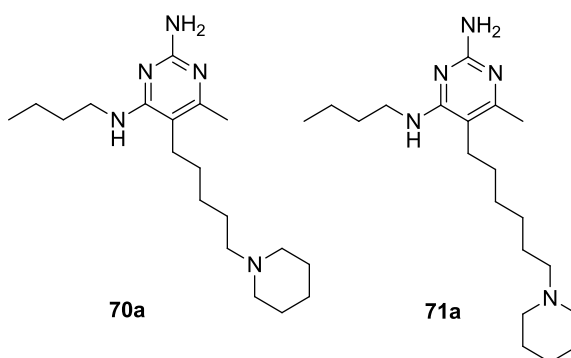


Figure 26: Structures of the two lead compounds

Compound Number	Resiquimod	70a	71a
	<b>25</b>		
IFN $\alpha$ pEC <sub>50</sub> HWB	<b>6.2</b>	<b>6.6</b>	<b>6.6</b>
TNF $\alpha$ pEC <sub>50</sub> HWB	<b>5.4</b>	<b>5.0</b>	<b>4.8</b>
Mol Wt.	<b>314</b>	<b>333</b>	<b>347</b>
PSA	<b>86</b>	<b>67</b>	<b>67</b>
cLogP	<b>2.4</b>	<b>5.3</b>	<b>5.8</b>
cLogD <sub>7.4</sub>	<b>1.8</b>	<b>2.8</b>	<b>2.8</b>

Table 5: Summary of cytokine induction data for potential TLR agonists in HWB, standard deviation = 0.3, PSA calculated using the Ertl method,<sup>176</sup> cLogP calculated using BioByte software,<sup>177</sup> cLogD<sub>7.4</sub> calculated using algorithms available in our laboratories.

Examples of the dose response curves for these compounds in HWB are shown in Figure 27. As can be seen, both compounds have similar activity in terms of IFN $\alpha$  induction to resiquimod **25**. It is also apparent that there is a window of selectivity over induction of TNF $\alpha$  greater than that observed with resiquimod **25**. Resiquimod

has been chosen as the standard for this assay given the wealth of preclinical data in models of asthma as described in section 1.9.1. It can be observed that the IFN $\alpha$  induction curves for **70a** and **71a** do not follow the classical dose response curve shape, instead showing a bell shape, with higher compound concentrations resulting in reduced cytokine induction (relative to the maximum). There are a number of potential explanations for this: it is conceivable that the compounds suffer from poor solubility or are cytotoxic at very high concentrations. Other possible reasons include that such high concentrations cause desensitisation, or that there is a negative feedback component at high concentrations. This potential negative feedback has been examined by Forsbach and co-workers who believe that this is caused by inhibition of STAT-2 phosphorylation.<sup>178</sup> The STAT-2 protein is involved in the upregulation of type 1 interferons following binding of IFN $\alpha$  to the IFN $\alpha$  receptor. Therefore, inhibiting the activation (by phosphorylation) will reduce the total amount of IFN $\alpha$  induction. Similar bell shaped dose response curves have been reported for a number of the 8-oxoadenine compounds and the pteridinone compounds described in Sections 1.9.3. and 1.9.5 suggesting that this non-sigmoidal IFN $\alpha$  induction dose response is perhaps a characteristic feature of TLR7 agonism.<sup>148-155,163</sup>

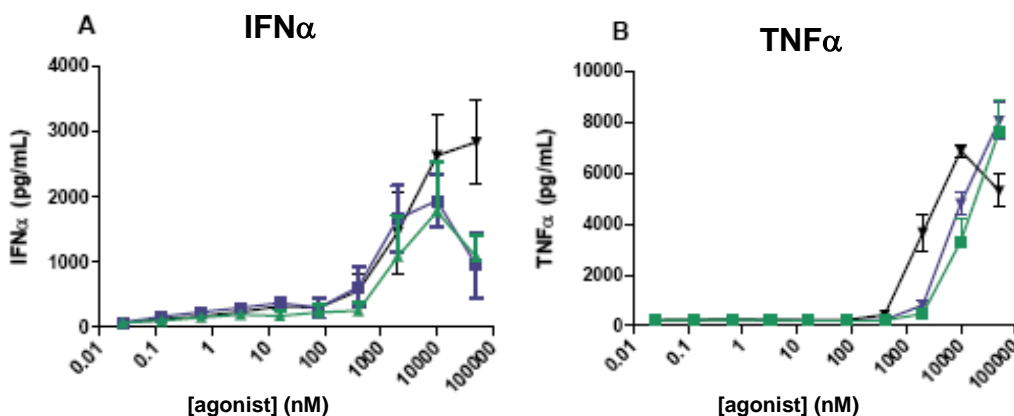


Figure 27: Example dose response curves for IFN $\alpha$  and TNF $\alpha$  induction for **70a** and **71a** in HWB (The green line represents compound **70a**, the blue line compound **71a** and the black line represents the assay standard resiquimod **25**). Note this data is from one single experiment. The average pEC<sub>50</sub> data for the compounds is shown in Table 5.

These two compounds induce IFN $\alpha$  with a pEC<sub>50</sub> slightly below the desired activity range in HWB, and the selectivity over TNF $\alpha$  is below the minimum desired level. Accordingly, the immediate medicinal chemistry goals were to increase the IFN $\alpha$  induction potency, improve the TNF $\alpha$  induction selectivity, and to reduce the intrinsic lipophilicity as assessed by cLogP.

## 2.2 Medicinal chemistry strategy.

At the time this research effort was initiated there was no structural information available for TLR7/8 or for TLR7/8:ligand complexes nor were the TLR7 pharmacophore models of Wang and co-workers<sup>179</sup> available to guide drug design. It was therefore decided to use an exemplar from the 8-oxoadenine series (compound **48**) to guide the design of new analogues. Using the molecular operating environment (MOE 2014 version) software from the Chemical Computing Group (CCG)<sup>180</sup> it is possible to overlay compounds **70a** and **71a** with compound **48**. The biological target, TLR7 lies within the acidic environment of the endosome, with a pH of 6-6.5 existing within the early endosomal compartment and a pH of 5-5.5 in the late endosomal compartment.<sup>181</sup> Accordingly, the molecules are subjected to the modelling experiment in the protonation state predicted by software from Chemaxon<sup>182</sup> to exist at these pH levels. It should be noted that the protonation state of compounds **48** and **70a** is predicted to remain constant between a pH range of 5 to 6.5 with the pyrimidine in compound **70a** being protonated and the 8-oxoadenine core of compound **48** not being protonated.

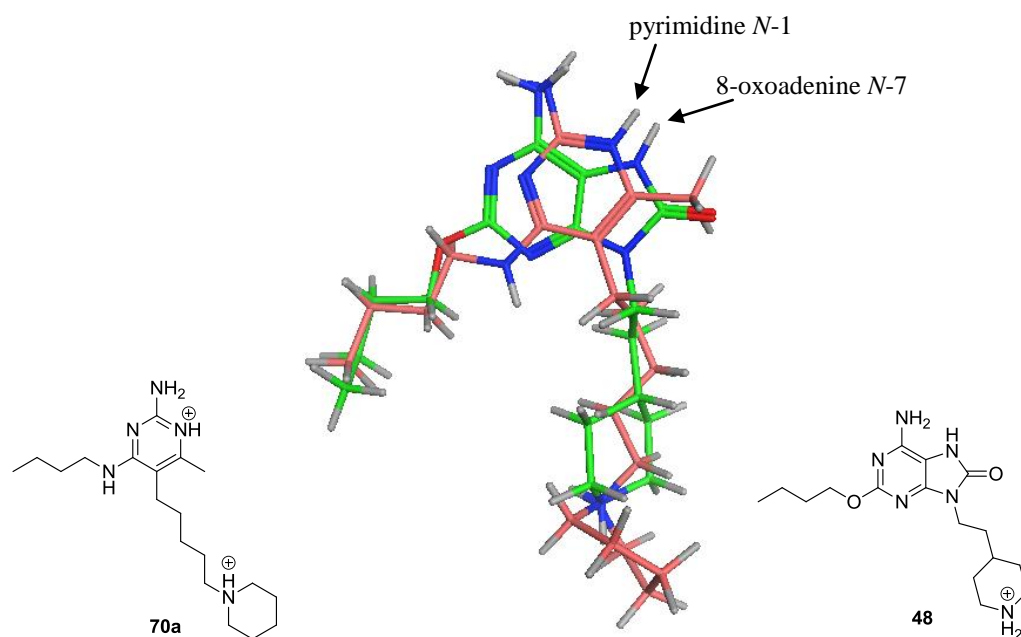


Figure 28: Molecular modelling overlay of compound **70a** (shown in pink) and compound **48** (shown in green).

The most favoured overlay of compounds **70a** and compound **48** is shown in Figure 28. Of particular note is that at an acidic pH in the range 5-6.5 the *N*-1 pyrimidine nitrogen is protonated and so can potentially mimic the *N*-7 function present in the 8-oxoadenine compound **48**. In addition, it is possible to examine the electrostatic fields around these molecules. From consideration of these data, one design hypothesis is that it should be possible to increase the activity and selectivity of cytokine induction selectivity in the pyrimidine series by adjusting the functional groups attached to the pyrimidine core such that resulting electrostatic fields match the 8-oxoadenine series more closely. The areas of matching and contrasting fields are shown in Figure 29.

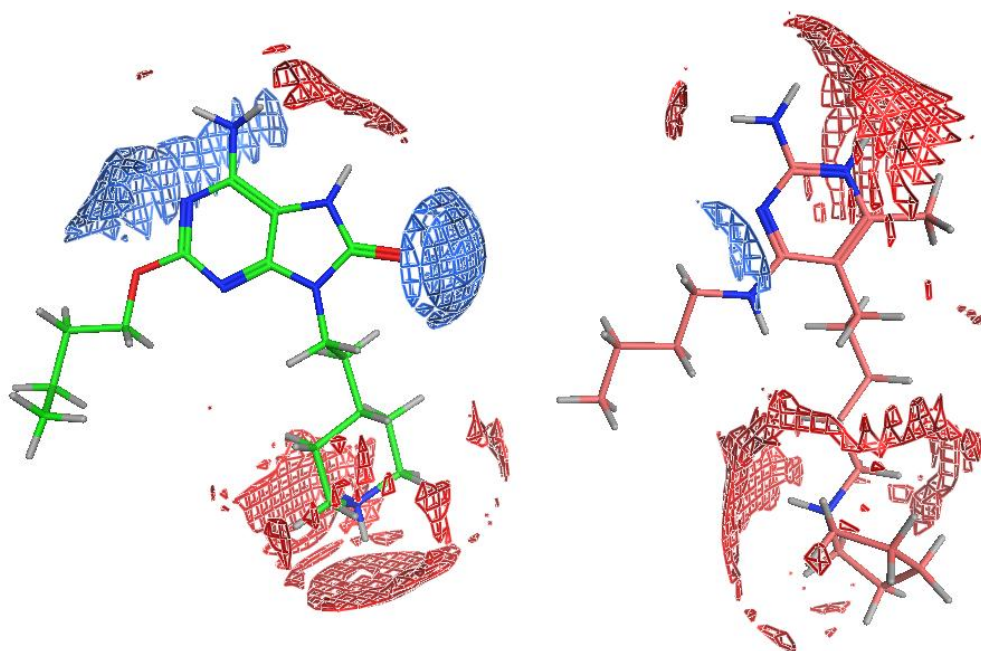
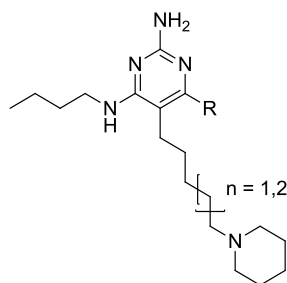


Figure 29: Electrostatic fields for compound **70a** (shown in pink) and compound **48** (shown in green).  
 Negative field surfaces are shown in blue, positive field surfaces in red.

From examining the surfaces, one possible way to improve the field match between the two series is to replace the methyl group in **70a** and **71a** with a polar functional group, which would also reduce cLogP as desired. In order to evaluate this hypothesis and explore SAR at this position a list of targets was proposed (Table 6). The non-polar butyl and phenyl groups were proposed by colleagues within the chemistry team, based on the data for compounds **69a** and **69b**.



R	Compound No.	
	n = 1	n = 2
OCH <sub>3</sub>	70b	71b
NHCH <sub>3</sub>	70c	71c
OH	70d	71d
CH <sub>2</sub> OH	70e	71e
CH <sub>2</sub> F	70f	71f
Ph	70g	71g
CH <sub>2</sub> CH <sub>3</sub>	70h	71h
CF <sub>3</sub>	70i	71i
CH <sub>2</sub> CH <sub>2</sub> CH <sub>2</sub> CH <sub>3</sub>	70j	71j

Table 6: List of groups to be introduced in place of the methyl function in **70a** and **71a**.

### 2.3 Synthetic strategy for the synthesis of tetrasubstituted pyrimidines targets.

With a list of potential targets to improve biological activity in hand, attention then turned to preparation of the analogues of interest. A preferred synthetic strategy is to introduce the diversity as late as possible in the synthetic sequence, thereby reducing the overall number of transformations required to prepare molecules for biological testing. Many of the initial desired targets were reasoned to be accessible from four key intermediates (Figure 30).

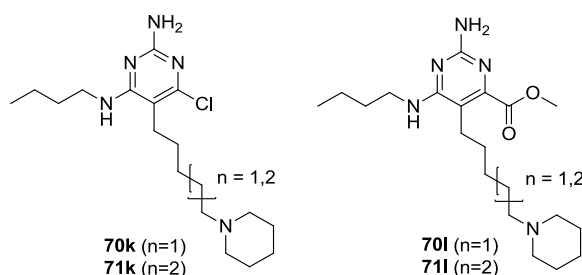


Figure 30: Intermediates targeted for access to modified lead compounds.

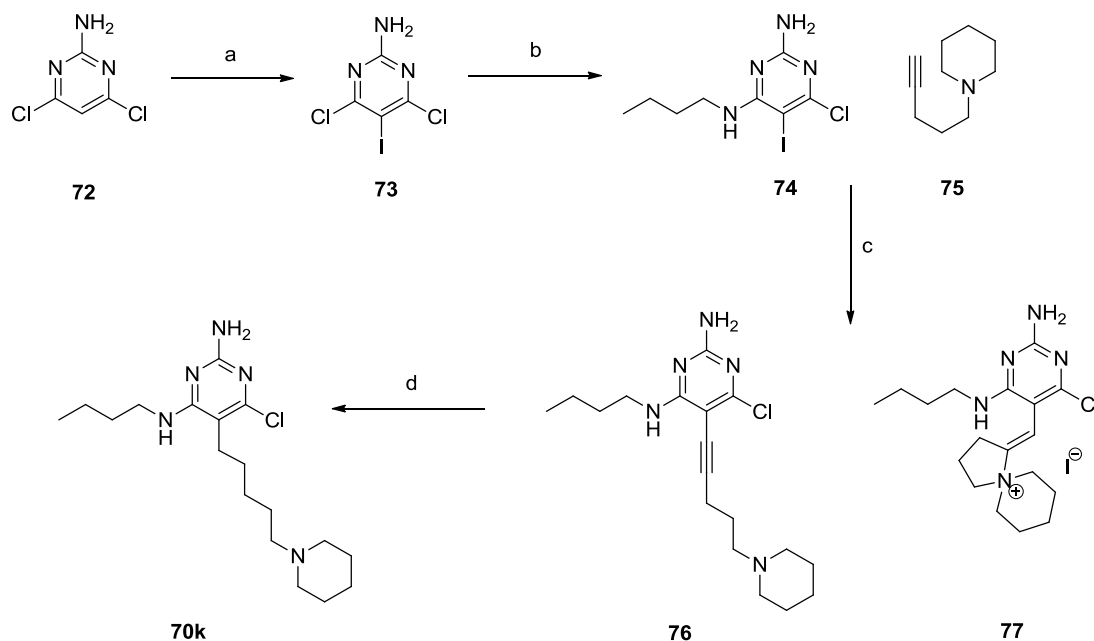
It should be possible to displace the chlorine atom with nucleophiles, or to use transition metal mediated cross couplings to introduce appropriate functionality. It also should be feasible to interconvert the ester to give the alcohol. The monofluoro methyl compound should be accessible from the alcohol. Compounds with the ethyl (70h and 71h), trifluoromethyl (70i and 71i) or the *n*-butyl group (70j and 71j) were made by an alternative route (see Section 2.3.6 for synthesis of the ethyl substituted compounds 70h and 71h by this method). These analogues could also be accessed from intermediates 70k and 71k, for example the *n*-butyl group could be introduced *via* alkyl Suzuki-Miyaura couplings,<sup>183</sup> or iron catalysed Grignard couplings,<sup>184</sup> and the trifluoromethyl group introduced using copper mediated trifluoromethylation,<sup>185,186</sup> or using palladium catalysed methods.<sup>187</sup> Furthermore, it may be possible to access compounds 70k and 71i directly from the chloro derivatives *via* organometallic methodologies (Section 2.3.4).



### 2.3.1 Synthesis of intermediates **70k** and **71k**.

The synthetic approach adopted for the synthesis of intermediate **61k** is outlined in Scheme 1.

Scheme 1



Reagents and Conditions: a) ICl, AcOH, 50%; b) *n*-BuNH<sub>2</sub>, Et<sub>3</sub>N, EtOH, 80°C, 90%; c) CuI,  $(PPh_3)_4Pd$ , Et<sub>3</sub>N, DMF, 60°C, **76** (9-34%), **77**, (11%), d) EtOH, Pd/C Catcart 30 H-Cube™ Full H<sub>2</sub> 25°C, 74%.

Conversion of commercially available pyrimidine **72** to iodide **73** was successfully achieved on tens of gram scale using ICl in acetic acid according to the procedure of Njoroge and co-workers<sup>188</sup> in a moderate yield of 50% which was comparable to the literature yield. Subsequent  $S_NAr$  substitution with *n*-butylamine and  $Et_3N$  in EtOH proceeded in excellent yield to give compound **74**. Modification of a Sonogashira cross coupling reaction, again by Njoroge and co-workers using alkyne **75** (prepared according to the procedure of Gelin and Hablot,<sup>189</sup> from reaction of the alkyl chloride and piperidine) did result in isolation of target alkyne **76** albeit in low yield (9%). In addition, a poorly soluble substance was also isolated in similar quantity (11%)

following precipitation upon work-up. This material had a different retention time by LCMS but an identical m/z mass spectra ionisation signal to **76**.  $^{13}\text{C}$  NMR of the side product gave the first indications of the possible structure of **77**. There were no signals for an alkyne connected to an aromatic ring at 70-90 ppm, instead there were signals at 114 ppm and 152 ppm indicative of a highly polarised alkene such as an enol or enamine (Figure 31). Analysis of the resonances observed in the HMBC spectra confirmed the cyclic nature of the compound, in particular the downfield alkene carbon 15 is able to interact with the protons on three alkyl carbons (16-18). If the molecule was not cyclic in nature the interactions between carbon 15 and the protons on carbon 18 would not be observed (Figure 32).

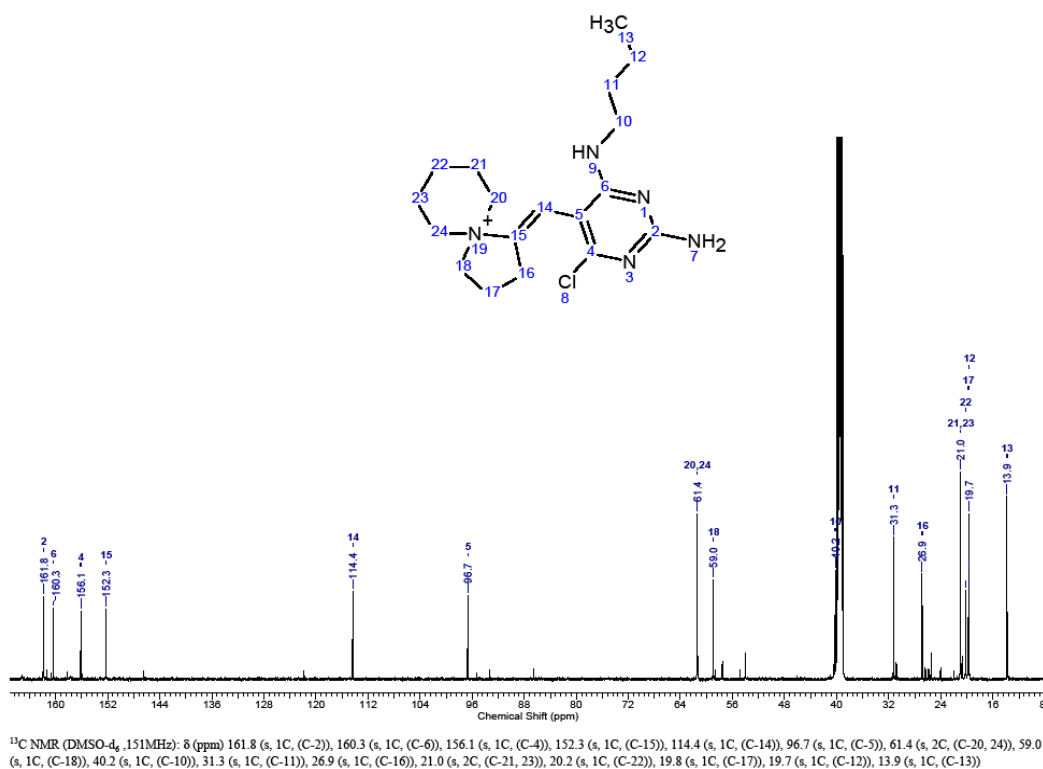


Figure 31:  $^{13}\text{C}$  NMR of cyclised material **77**.

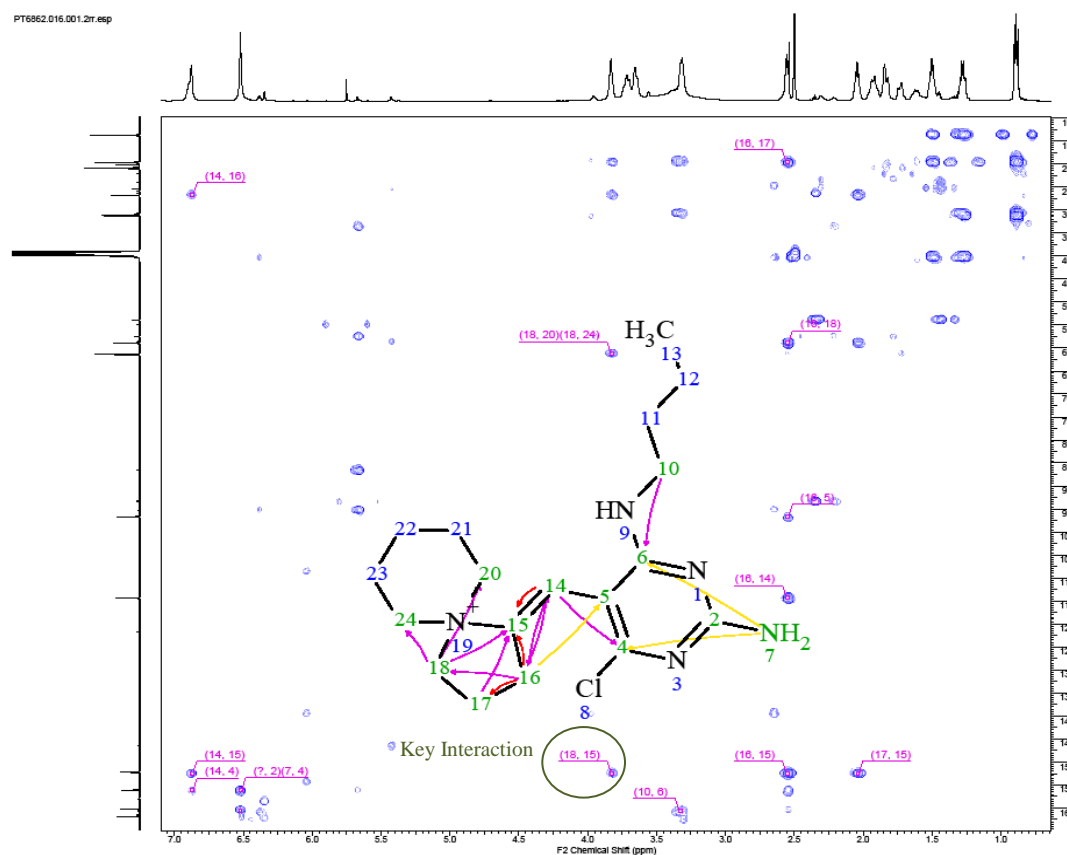
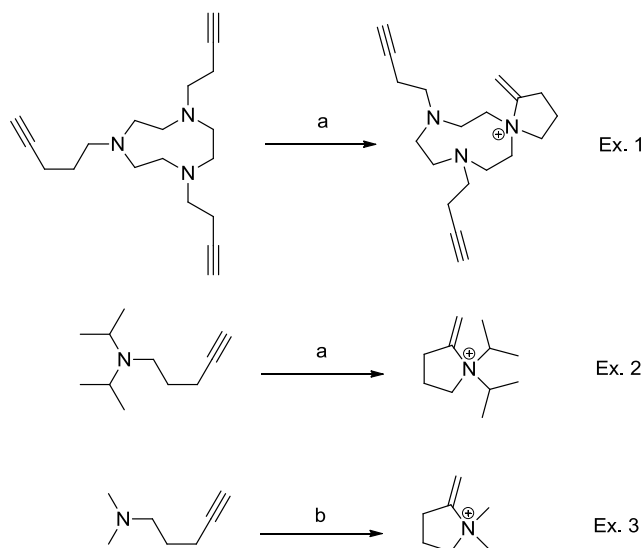


Figure 32: HMBC spectrum of cyclised material **77**.

This cyclisation is favoured according to Baldwin's Rules<sup>190</sup> and would be classified as 5-*exo*-dig hence explaining the propensity for alkene **77** to form. The Sonogashira reaction was repeated at ambient temperature with an amended work up protocol: the reaction was concentrated as before and the residue triturated with EtOAc (rather than partitioning), with the filtrate being dried and concentrated before normal phase purification on silica. These modifications led to an enhancement in yield, isolating **76** in a yield of 34%. It is assumed the counterion for compound **77** is an iodide given the nature of the reaction conditions.

Further examination of the literature also supports the structure of **77** with several similar cyclisations being previously reported (Scheme 2).<sup>191</sup>

Scheme 2 Some reported examples of similar cyclisations.



Reagents and Conditions: a) MeOH, b) H<sub>2</sub>O, HCl.

Common to all these cyclisations is the use of Brønsted acidic conditions, albeit very weakly protic in Examples 1 and 2. These reported observations suggest the starting alkyne **75** may be intrinsically unstable. A change in the physical appearance of **75** upon storage at room temperature from a homogeneous liquid to a fine heterogeneous suspension has been observed, suggesting that this may indeed be the case. Storage of alkyne **75** in the freezer appears to have arrested any change in physical form by visible inspection.

A focused set of reactions was next performed in an attempt to significantly improve the ratio of desired product to cyclised impurity. The results are summarised in Table 7 accompanied by the two isolated reactions 1 and 2 as reference. As is evident from the data in Table 7, reaction 3 did not proceed to the same extent as reaction 2 indicating the alkyne **75** may indeed have decomposed to reduce the amount of alkyne available. It is important to note that the amount of cyclised material increases upon work up (particularly concentration *in vacuo*) accounting for the ratio difference between the ratios of **76:77** in reactions 2 and 3 by LCMS analysis of the reaction mixture and the final isolated ratio (for experiment 2) of 3:4.

**GSK CONFIDENTIAL – Property Of GSK – Copying Not Permitted**  
 The Synthesis and Optimisation of Toll-like Receptor Agonists as Potential Immunomodulatory Agents.

Reaction	Catalyst	Catalyst Loading	CuI Loading	Alkyne Eq.	Temp/Time	Ratio by LCMS 76:77	Conversion by LCMS 76+77
1*	(PPh <sub>3</sub> ) <sub>4</sub> Pd	10 mol %	20 mol %	2	60 °C/4 h	1:1	100%
2*	(PPh <sub>3</sub> ) <sub>4</sub> Pd	10 mol %	20 mol %	2	RT/24 h	>10:1	100%
3	(PPh <sub>3</sub> ) <sub>4</sub> Pd	10 mol %	20 mol %	2	RT/24 h	>10:1	55%
4	(PPh <sub>3</sub> ) <sub>4</sub> Pd	5 mol %	10 mol %	2	RT/24 h	>10:1	15%
5	(PPh <sub>3</sub> ) <sub>2</sub> PdCl <sub>2</sub>	10 mol %	20 mol %	2	RT/24 h	<1:10	100%
6	(PPh <sub>3</sub> ) <sub>2</sub> PdCl <sub>2</sub>	5 mol %	10 mol %	2	RT/24 h	<1:10	100%
7	(PPh <sub>3</sub> ) <sub>4</sub> Pd	10 mol %	20 mol %	3	RT/24 h	7:1	70%
8	(PPh <sub>3</sub> ) <sub>4</sub> Pd	10 mol %	20 mol %	1.2	RT/24 h	>10:1	40%

\* Reference reactions where products were isolated, described in text. In all other cases products were not isolated.

Table 7: Summary of optimisation experiments (Note. the first two cases are from the first two attempts at this reaction described above).

This set of reactions does however show that the amount of alkyne present (reactions 3, 7 and 8) has only a small effect on the reaction profile in terms of the ratio of products. Two to three equivalents of alkyne appear to be optimal in terms of reaction progression after 24 h. Reducing the amount of catalyst does significantly retard the reaction (reaction 4). The most marked effect however is seen when Pd(PPh<sub>3</sub>)<sub>4</sub> is replaced with (PPh<sub>3</sub>)<sub>2</sub>PdCl<sub>2</sub> (reactions 5 and 6) with the latter leading to almost complete cyclisation of any product molecule formed *in situ*. This suggests that the nature of the input (pre)catalyst plays a key role in the mechanism of the cyclisation.

A potential mechanism for the formation of the observed by-product involves the palladium acting as a Lewis acid with the product alkyne co-ordinated to a vacant site on the palladium. The only significant difference between the catalysts evaluated is the number of phosphine ligands able to compete with the alkyne for the vacant sites. It appears that when more ligand is present there is less of the reactive Pd<sup>(0)</sup>L<sub>2</sub> (where L is PPh<sub>3</sub>) species available to undergo oxidative addition and

co-ordinate to the alkyne and hence go on to cyclise (potential mechanistic features are shown in Figure 29).

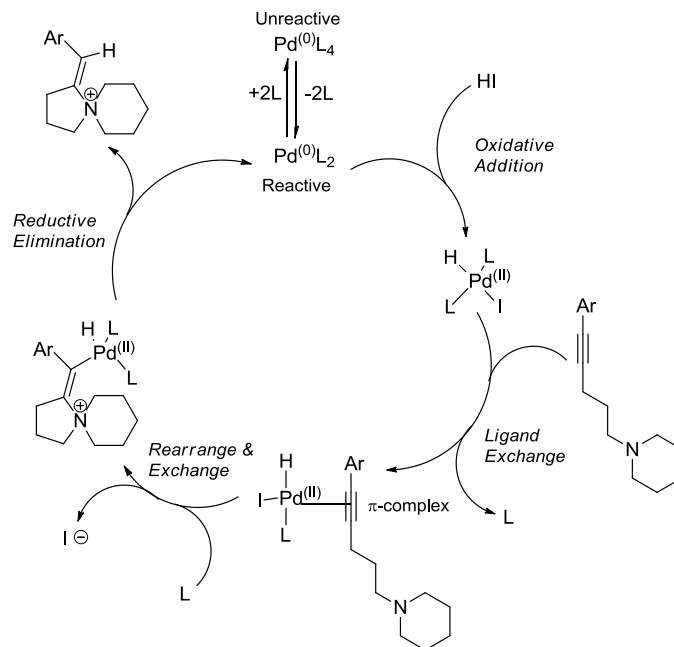


Figure 33: Potential mechanism for the unwanted palladium catalysed 5-*exo-dig* cyclisation.

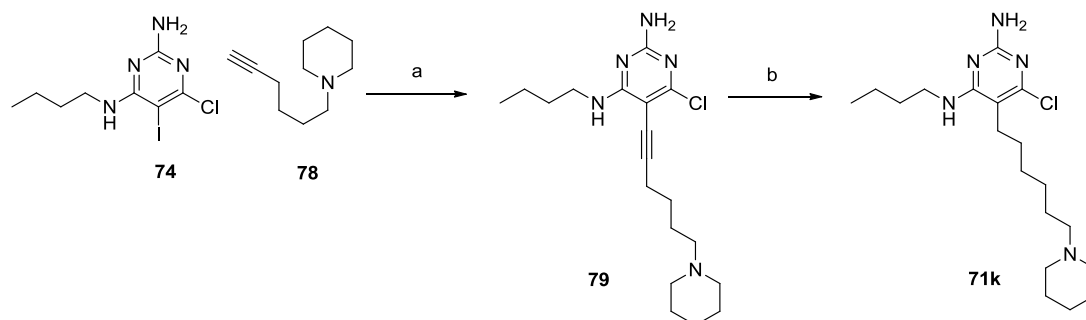
The Sonogashira reaction was also attempted with Pd(dppf)Cl<sub>2</sub> as catalyst, however the reaction failed to proceed. Sonogashira cross coupling reactions using an alkyne without a nucleophilic amine have been investigated and will be discussed later (Scheme 4) as a means of circumventing this side reaction.

Attempts to hydrogenate **76** using Pd/C at atmospheric pressure failed to yield any product or intermediate alkene (Scheme 1). Pleasingly, when the transformation was attempted under pressure (approximately 10 bar) using a Thales H-Cube<sup>TM</sup>, the hydrogenation proceeded to completion without reducing the aromatic chloride required for further transformations. The biological evaluation of compound **70k** is reported in section 2.4.

The chemistry defined in Scheme 1 substituting alkyne **75** with alkyne **78** (prepared according to the procedure of Meier and co-workers<sup>192</sup>) proceeded in similar fashion to yield compound **79**, (Scheme 3). The poor yield observed for the Sonogashira

cross coupling is most likely due to the formation of a significant quantity of an impurity (by LCMS), from analysis of the  $m/z$  ionisation in the LCMS spectra the identity of which is likely to be a compound similar to **77**, formed by a 6-*exo*-dig cyclisation, which is also favoured according to Baldwin's rules.

Scheme 3

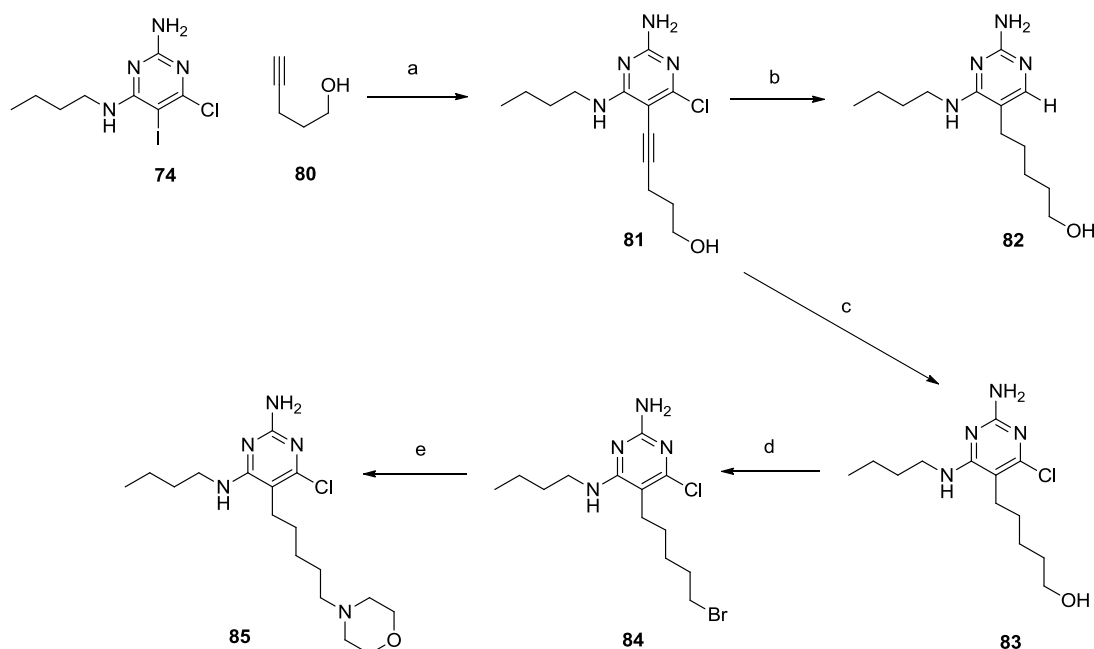


Reagents and Conditions: a) CuI, (PPh<sub>3</sub>)<sub>4</sub>Pd, Et<sub>3</sub>N, DMF, 20 °C, 21%; b) EtOH, Pd/C Catcart 30 H-Cube<sup>TM</sup>, 10 bar H<sub>2</sub>, 20 °C, 75%.

As stated above, a potential means of avoiding the problem of intramolecular cyclisation would be to conduct the Sonogashira chemistry without a nucleophilic amine present. This was investigated using alkyne **80** (Scheme 4), and the reaction proceeded to give a much improved yield of 56% with no cyclisation observed. Hydrogenation using the previously successful conditions (H-Cube<sup>TM</sup>) or at atmospheric pressure reduced the alkyne as required but also resulted in dechlorination of the pyrimidine ring to give **82**. There is literature precedent to suggest that rhodium can be used to reduce alkynes in the presence of chloropyrimidines.<sup>193</sup> Therefore, this procedure was attempted in the H-Cube<sup>TM</sup> using rhodium as the catalyst, however no hydrogenation was observed. The only difference between the conversion of alkyne **81** to alkane **82** and the conversion of alkyne **76** to alkane **70k** (or indeed alkyne **79** to alkane **71k**) is the presence of a basic centre. It is postulated therefore that the amine is tuning the activity of the palladium catalyst by acting as a strong  $\sigma$ -donating ligand. There is literature evidence to support this hypothesis, with several reported examples of reduction of alkynes in the presence of (het)aryl chlorides using amines as additives.<sup>194</sup> Based on

this, it was decided to attempt a hydrogenation on alkyne derivative **81** with one equivalent of an amine added to the reaction mixture.

Scheme 4



Reagents and Conditions: a) CuI, (PPh<sub>3</sub>)<sub>4</sub>Pd, Et<sub>3</sub>N, DMF, 20 °C, 56%; b) EtOH, Pd/C Catcart 30 H-Cube<sup>TM</sup> Full H<sub>2</sub>, 25 °C, 91%; c) EtOH, *N*-methylpiperidine, Pd/C Catcart 30 H-Cube<sup>TM</sup> Full H<sub>2</sub>, 25 °C, 50%; d) CBr<sub>4</sub>, PPh<sub>3</sub>, DCM, 53%; e) Morpholine, Et<sub>3</sub>N, MeCN, 20 °C, 70%.

*N*-Methylpiperidine was chosen as it best represents the pK<sub>a</sub> and nucleophilicity of the amine in compounds **76** and **79**. At atmospheric pressure the hydrogenation now failed to proceed, therefore the H-Cube<sup>TM</sup> instrument was employed for further experimentation. Using one equivalent of *N*-methylpiperidine led to two materials being observed: the desired chloropyrimidine **83** and the over reduced compound **82** in a ratio of approximately 1:1. It was possible to isolate **83** from this reaction in 25% yield and confirm its identity. Increasing the amount of amine to two equivalents improved the ratio of compound **83**:**82** to approximately 2:1. Using these conditions and column chromatography it was possible to isolate alcohol **83** in 46% yield. Further hydrogenation and purification of mixed fractions containing product and partially hydrogenated intermediate furnished a second batch of alcohol



**83** in 4% yield. The alcohol **83** was of suitable purity for further chemical transformations. Bromination with CBr<sub>4</sub> and PPh<sub>3</sub> (the Appel reaction),<sup>195</sup> followed by subsequent displacement proceeded in satisfactory yield to furnish the morpholino compound **85**. On balance this route does not provide a suitable alternative to that in Scheme 1 or 3; replacing a two step procedure with a four step process that also contains some low to moderate yielding steps. The Appel reaction used in this synthesis could potentially be improved using the recent developments in both catalytic methods<sup>196</sup> and optimised work-up protocols.<sup>197</sup>

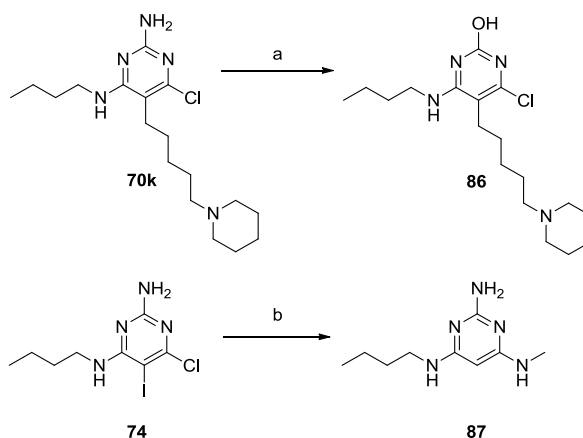
### 2.3.2 Nucleophilic substitution approaches for the functionalisation of **70k** and **71k**.

A number of S<sub>N</sub>Ar reactions have been attempted on the chloropyrimidine systems **70k**, **74** and **76**, all of which proved unsuccessful, even in the presence of various additives. Acids can be utilised in order to protonate the pyrimidine ring thus making it more electrophilic and more reactive to nucleophiles. When the reaction was attempted using hydrochloric acid and water (as the nucleophile) the 2-amino function was displaced in preference to the chlorine to give **86**. These investigations are summarised in Table 8 with selected examples shown in Scheme 5.

Starting Material	Nucleophile	Conditions	Outcome (by LCMS analysis of reaction mixture)
<b>70k</b>	NaOH	1,4-dioxane, 170 °C, $\mu$ wave	No displacement
<b>70k</b>	HCl, H <sub>2</sub> O	1,4-dioxane, 150 °C, $\mu$ wave	Displacement of 2-Amino group to give compound <b>86</b>
<b>70k</b>	MeNH <sub>2</sub>	EtOH, 150 °C, $\mu$ wave	No displacement
<b>70k</b>	MeNH <sub>2</sub>	EtOH, 150 °C, 18-crown-6 (1 Eq), KF (1 Eq), $\mu$ wave	No displacement
<b>76</b>	<i>n</i> -BuNH <sub>2</sub>	1,4-dioxane, 170 °C, $\mu$ wave	No displacement
<b>74</b>	MeNH <sub>2</sub>	EtOH, 150 °C, 18-crown-6 (1 Eq), KF(1 Eq), $\mu$ wave	Conversion to des-iodo compound <b>87</b>
<b>74</b>	MeNH <sub>2</sub>	EtOH, 100 °C, 18-crown-6 (1 Eq), KF(1 Eq), $\mu$ wave	Starting material remaining with some conversion to give compound <b>87</b>

Table 8: Attempted S<sub>N</sub>Ar reactions

Scheme 5 Some example reactions from Table 8. Note the compounds were not isolated with the structures being derived from LCMS analysis alone.



Reagents and Condition: a)  $\text{HCl}_{(\text{aq})}$ , 1,4-dioxane, 150 °C,  $\mu\text{wave}$ , b)  $\text{MeNH}_2$ , KF, 18-crown-6, EtOH, 150 °C,  $\mu\text{wave}$ .

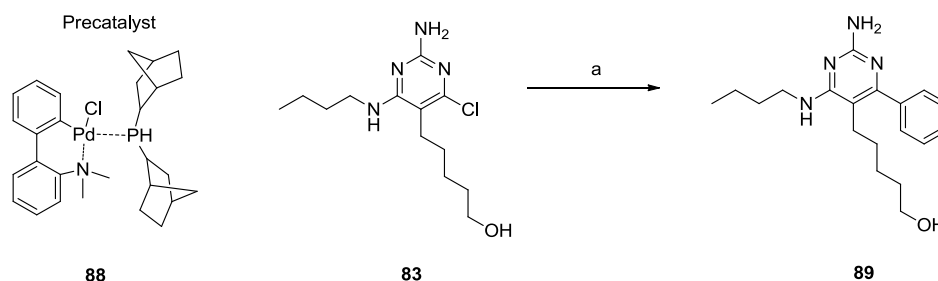
Given the volatile nature of methylamine, an  $\text{S}_{\text{N}}\text{Ar}$  reaction was attempted with *n*-butylamine allowing a higher temperature to be employed in the microwave without danger of over pressurisation. Again, no displacement was observed, therefore attempts were made to introduce the polar functionality prior to the Sonogashira reaction by attempting  $\text{S}_{\text{N}}\text{Ar}$  reactions on the iodide **74**.

Compound **74** is less electron rich than **70k/76** and so should be a better substrate for  $\text{S}_{\text{N}}\text{Ar}$  reactions despite the introduction of the sterically large iodine. This approach showed some promise, however de-iodination of the desired product to give **87** was observed in all cases (Scheme 5). This de-iodination could potentially be the result of a thermally initiated radical decomposition. It appears that the pyrimidine ring in compounds **70k** and **71k** (or **76** with alkyne still in place) is too electron rich for nucleophilic displacement to take place.

### 2.3.3 Transition metal mediated approaches for the functionalisation of **70k** and **71k**.

Given the lack of success with  $S_NAr$  approaches, it was decided to investigate the use of transition metal (palladium or copper) mediated methodologies to generate the desired target molecules. An initial Suzuki-Miyaura cross coupling with phenylboronic acid using chloro(di-2-norbornylphosphino)-(2'-dimethylamino-1,1'-biphenyl-2-yl) palladium(II)<sup>198</sup> **88** as the precatalyst, was examined using compound **83**. This particular reaction was chosen for several reasons: firstly by using compound **83** if the chemistry was not successful we conserve supplies of **70k/71k** which were at a premium. Secondly, Suzuki-Miyaura cross coupling reactions are amongst the most reliable and robust cross couplings; therefore it was reasoned that if this reaction was not successful more elaborate transition metal mediated processes would also be likely to fail. Finally, the introduction of a phenyl group is one of the desired methyl group replacements as defined in Table 6.

Scheme 6 Trial Suzuki-Miyaura reaction.

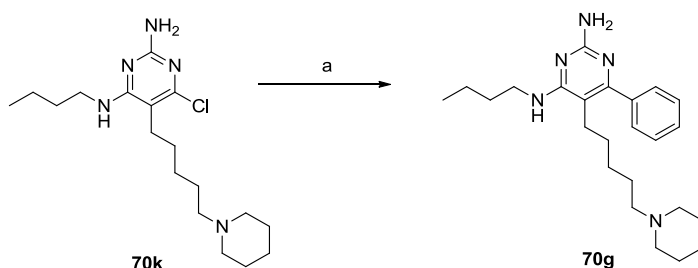


Reagents and Conditions: a)  $\text{PhB(OH)}_2$ , 4:1 1,4-dioxane:water,  $\text{K}_2\text{CO}_3$ , **88**,  $\mu\text{wave}$  150 °C, 28%.

This initial cross coupling reaction proved successful, yielding compound **89** (Scheme 6) and so further chemistry using aryl chloride intermediate **70k** as the precursor of choice was carried out. Using the same Suzuki-Miyaura cross coupling conditions that had yielded the alcohol **89**, the amine derivative **70g** was successfully synthesised again in modest yield after mass directed automated preparation (MDAP). It is important to note that all final compounds that are to be evaluated in

biological assays should be at least 95% pure by UV. MDAP is a convenient purification method for delivering compounds at this purity and unless stated, all final compounds are purified using this method. Unfortunately the utilisation of MDAP as a method for purification often results in a reduction in overall yield. This is due to losses of compound either due to solubility in the MDAP solvents (water and MeCN) or due to the sacrifice of compound containing minor impurities.

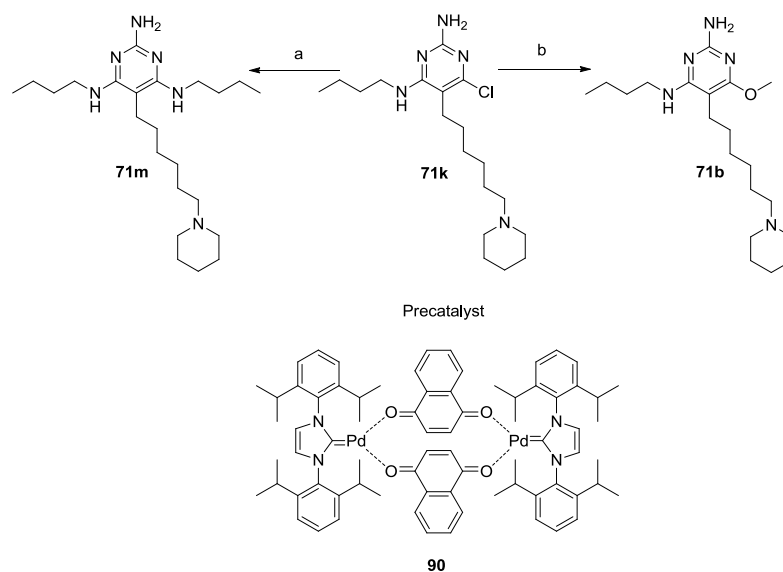
Scheme 7



Reagents and Conditions: a) PhB(OH)<sub>2</sub>, 4:1 1,4-dioxane:water, K<sub>2</sub>CO<sub>3</sub>, **88**, μwave 150 °C, 33%.

Given the success of the Suzuki-Miyaura coupling, attention was then focused on the amine derivatives. By adapting the Buchwald-Hartwig coupling procedure of Hanan and co-workers<sup>199</sup> using a different palladium *N*-heterocyclic carbene precatalyst, (1,3-*bis*(2,6-diisopropylphenyl)imidazol-2-ylidene(1,4-naphthoquinone)palladium(0) dimer **90** and using *n*-butylamine as the coupling partner compound **71m** was generated (Scheme 8). The synthesis of compound **71c** (containing an NMe group) was not attempted using this methodology in light of biological data which is discussed later (Section 2.4). Using the procedure of Morgentin and co-workers<sup>200</sup> and performing the reaction in a Reactival<sup>TM</sup> with copper ‘Ullman’ type catalysis, the methoxy group was successfully introduced to give **71b**. Attempts to demethylate the methyl ether and generate pyrimidinone compound **71d** using either BBr<sub>3</sub><sup>201</sup> or sulfuric acid failed.<sup>202</sup> Compounds **70g**, **71b** and **71m**, were all submitted for biological testing (discussed in Section 2.4). Given the cytokine induction data generated for these compounds synthesis of pyrimidinone compounds **70d** and **71d** was not pursued further.

Scheme 8

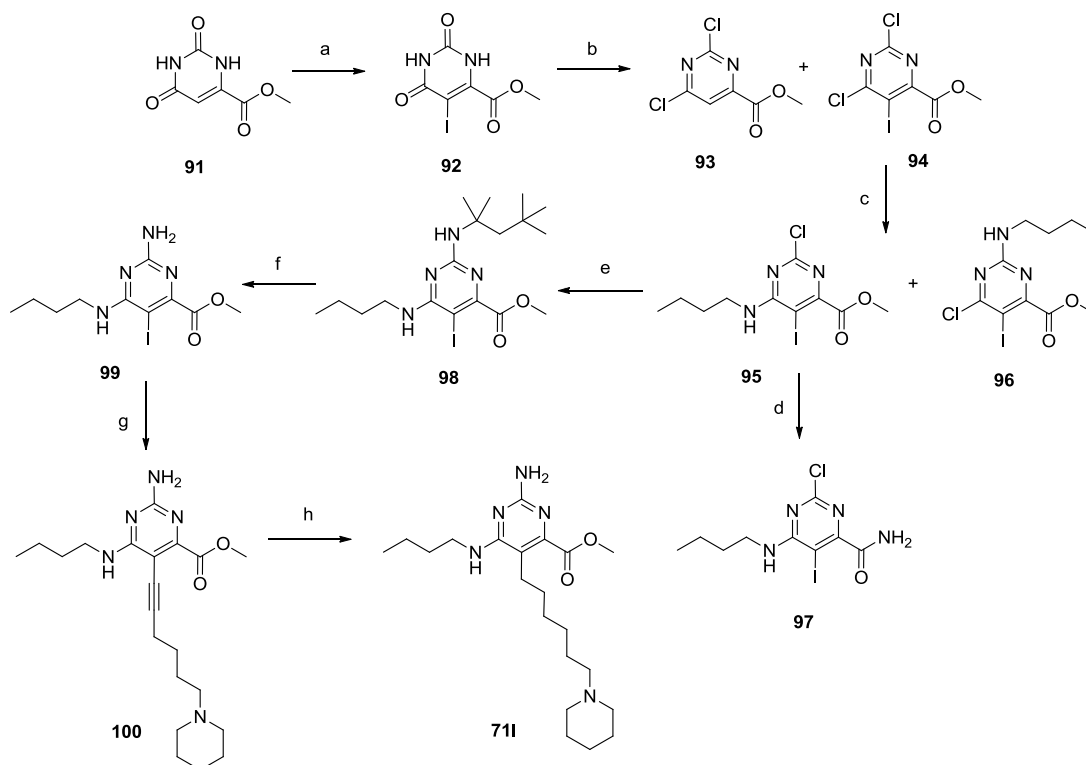


Reagents and Conditions: a) *n*-BuNH<sub>2</sub>, toluene, NaO<sup>t</sup>Bu, **90**,  $\mu$ wave 150 °C, 41%; b) MeOH, NaO<sup>t</sup>Bu, Cu, Reactival<sup>TM</sup> 140-150 °C, 39%.

#### 2.3.4 Synthesis of Intermediate **71l**.

Having successfully prepared the amino, alkoxy and phenyl analogues of **70** and **71**, attention was then turned to the analogues that require the ester intermediate **71l** for synthesis to be accomplished (Scheme 9). Iodination of methyl orotate **91** was achieved in 66% yield according to the procedure of Epp and co-workers<sup>203</sup> using iodine and periodic acid in MeOH. Subsequent reaction of compound **92** with POCl<sub>3</sub> and catalytic DMF proceeded to give two compounds, which after separation by chromatography gave compound **94** in 47% yield and the des-iodo compound **93** in 25% yield. Nucleophilic substitution of dichloride **94** with *n*-butylamine gave two products that following chromatography were isolated separately to give the expected 4-isomer **95** in 73% and the 2-isomer **96** in 9% yield. The identity of the isomer **95** was confirmed by HMBC NMR, where a three bond interaction between the butylamine NH and the aromatic C5 is observed (Figure 34). It would not be possible to observe this interaction in compound **96**.

Scheme 9



Reagents and Conditions: a) MeOH, I<sub>2</sub>, periodic acid, 70 °C, 66%; b) POCl<sub>3</sub>, DMF, 120 °C; **94** (47%), **93** (25%); c) EtOH, *n*-BuNH<sub>2</sub>, Et<sub>3</sub>N, **95** (73%), **96** (9%); d) NH<sub>3</sub>, MeOH, μwave 100 °C, 58%; e) MeCN, 18-crown-6, KF, *tert*-octylamine, DIPEA, μwave 150 °C, 19%; f) TFA, 70 °C, 86%; g) CuI, (PPh<sub>3</sub>)<sub>4</sub>Pd, Et<sub>3</sub>N, DMF, 1-(pent-4-yn-1-yl)piperidine (**78**), 20%; h) EtOH, Pd/C Catcart 30 H-Cube™ 10 bar H<sub>2</sub>, 40 °C, 46%. Nucleophilic substitution of the 2-Cl in compound **95** was attempted using NH<sub>3</sub> in MeOH, however the reaction yielded the primary carboxamide **97** from aminolysis of the methyl ester instead of the desired product. Based on the formation of the carboxamide **97** when using ammonia, it was decided to attempt the displacement using a less nucleophilic ammonia precursor (*tert*-octylamine).<sup>204</sup> Initially thermal or microwave heating in MeCN did not produce any of the desired compound, however addition of stoichiometric KF and 18-crown-6 and continued microwave heating did give the desired aryl amine **98** but in a disappointing yield of 19% with extensive decomposition (mainly de-carboxylation and de-iodination) observed. It is believed that the additives aid the nucleophilic displacement in the following ways: it is well known that in the case of S<sub>N</sub>Ar

reactions fluoride is a better leaving group than chloride. Additionally, the 18-crown-6 complexes the potassium counterion allowing the fluoride to displace the chloride, thereby enhancing the reactivity towards the intended amine nucleophile. Changing the solvent to 1,4-dioxane had no beneficial effect on yield or reaction profile. Buchwald-Hartwig cross coupling conditions<sup>205</sup> were also investigated using compound **95** as the substrate but failed to yield the desired product.

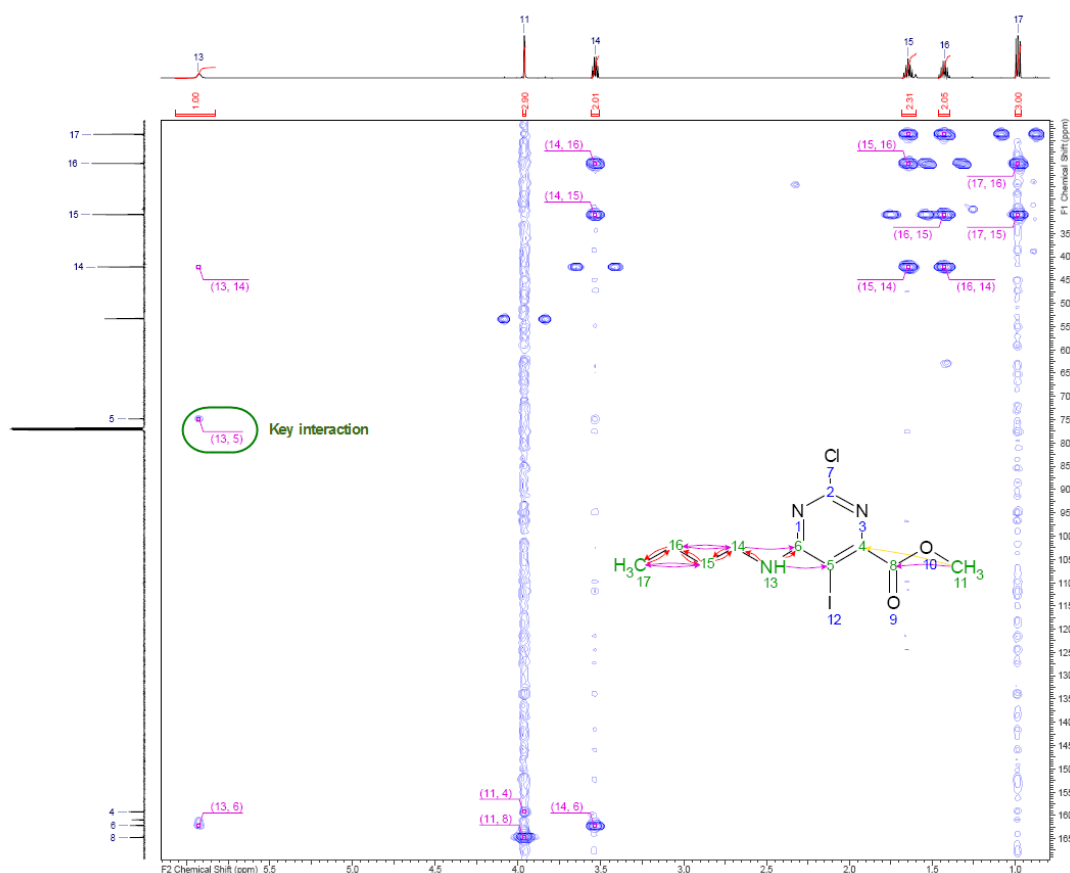


Figure 34: HMBC NMR of compound **95** showing the three bond interaction between *NH*13 and *C*5.

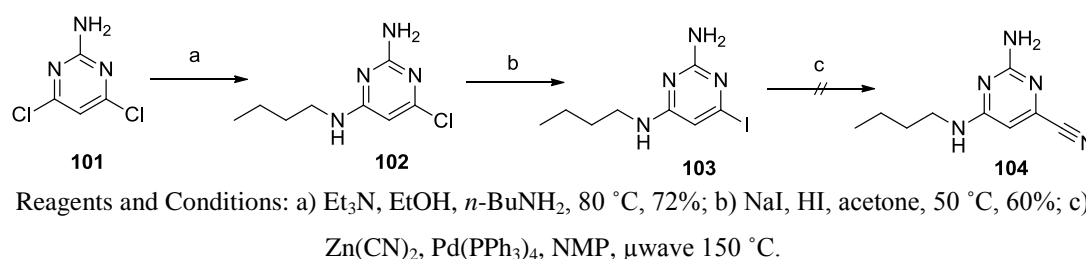
Following the  $S_NAr$  reaction to give compound **98**, the *tert*-octyl group was removed in good yield using refluxing TFA. Using the same Sonogashira cross coupling conditions previously employed yielded alkyne **100** (again putative cyclisation of the product was observed by LCMS with approximately 30% of cyclic product present). Subsequent hydrogenation using the H-Cube<sup>TM</sup> gave the ester

analogue **71l** in 46% yield (Scheme 17). This compound was submitted for biological evaluation (see Section 2.4 for results). Unfortunately, the amount of **71l** available was very limited and so further derivatisation at this stage was not possible. Accordingly, alternative approaches to **71l** were then investigated.

Utilising the chloropyrimidine **71k** as the substrate a number of transition metal mediated approaches to introduce the desired ester function were investigated. Generation of the ester directly using Hermann's Palladacycle,  $\text{Mo}(\text{CO})_6$  and *n*-butanol<sup>206</sup> failed as did attempts to introduce a nitrile at this position using Negishi cross coupling conditions and  $\text{Zn}(\text{CN})_2$ <sup>207</sup> with a view to subsequent conversion to the desired ester containing compound **71l**. The reasons for the failure are unclear given the relative success of other transition metal mediated reactions undertaken with compound **71k** as the substrate (Schemes 7 and 8).

An alternative synthetic sequence with a view to introducing the nitrile earlier was also investigated (Scheme 10). Following an initial  $\text{S}_{\text{N}}\text{Ar}$  reaction on the dichloropyrimidine **101** with *n*-butylamine, halogen exchange (iodine for chlorine) was successfully achieved on **102** using the protocol of Doláková and co-workers.<sup>208</sup>

Scheme 10



The Negishi cross coupling with  $\text{Zn}(\text{CN})_2$  failed to yield any of the desired compound. The lack of success could possibly be due to the presence of weakly acidic protons in the 2 and 4 positions of the pyrimidine system.<sup>209</sup> Another potential reason for the lack of success in performing the required aryl cyanation could be catalyst poisoning by excess cyanide.<sup>210</sup> No further investigations into transition metal mediated carbonylations or cyanations on compounds **70k/71k** were

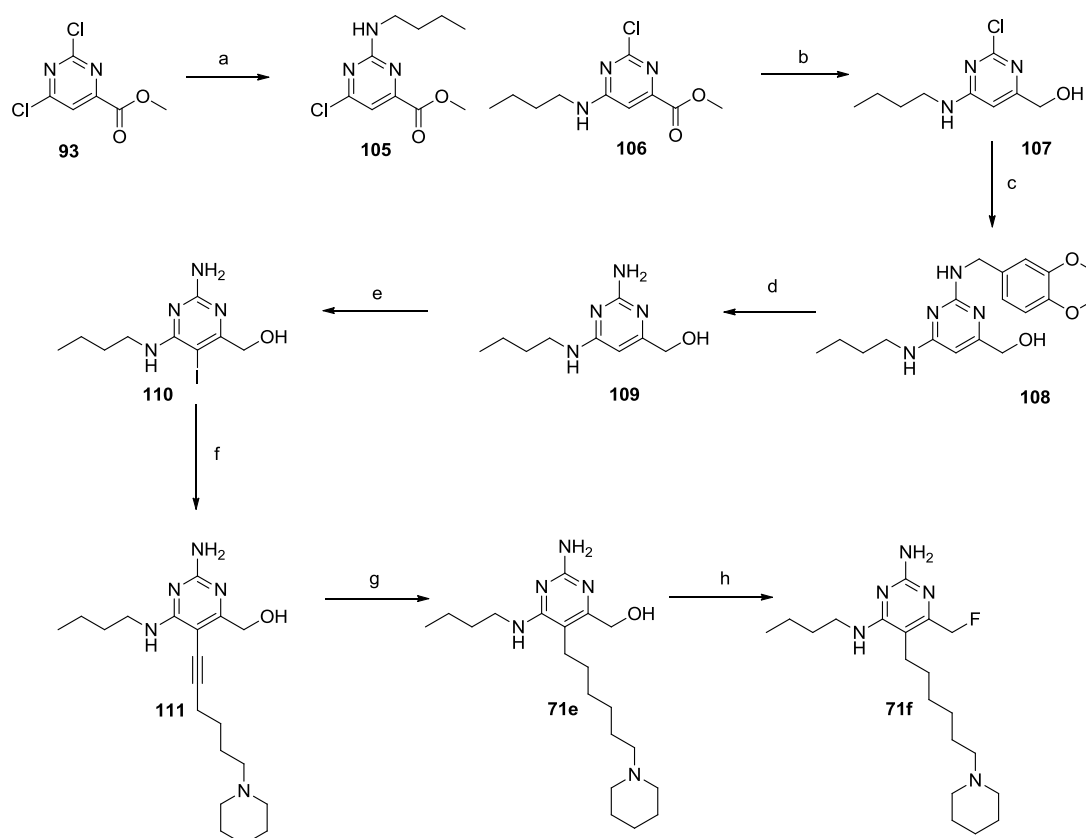


undertaken. The hydroxymethyl derivatives **70e/71e** were synthesised by a different approach in which the order of introduction of the pyrimidine substituents is changed (Section 2.3.5).

### 2.3.5 Synthesis of **71e** and **71f** using a modified strategy.

Originally it was planned to generate hydroxymethyl compound **71e** from reduction of the precursor ester **71i**. However, and as described earlier, there were issues with the synthesis of **71i**, and in particular there were difficulties in introducing the 2-amino function whilst retaining the ester and iodide.

Scheme 11



Reagents and Conditions: a) *n*-BuNH<sub>2</sub>, Et<sub>3</sub>N, MeCN, **106** (54%), **105** (15%); b) LiAlH<sub>4</sub>, THF, 0 °C, 55%; c) 3,4-dimethoxybenzylamine, *n*-BuOH,  $\mu$ wave 150 °C, 81%; d) TFA, anisole,  $\mu$ wave 100 °C, 93%; e) NIS, AcOH, 45%; f) 1-(pent-4-yn-1-yl)piperidine (**78**), CuI, Pd(PPh<sub>3</sub>)<sub>4</sub>, Et<sub>3</sub>N, DMF, 39%; g) EtOH, Pd/C Catcart 30 H-Cube™ Full H<sub>2</sub>, 40 °C, 82%; h) XtalFluor-E™, -78 °C  $\rightarrow$  rt, 14%.

Based on this, an alternative strategy to furnish alcohol **71e** and the derived fluoromethyl compound **71f** is detailed in Scheme 11. Using the commercially available dichloropyrimidyl ester **93**, it was possible to perform an  $S_NAr$  reaction with *n*-butylamine with some preference for the desired 4-isomer (compound **106**) over the unwanted 2-isomer (compound **105**). The compounds were separated by chromatography and isolated in yields of 54% and 15%, respectively. The identity of compound **106** was confirmed by ROESY NMR spectroscopy: through space interactions between the *C*-5 aryl proton and the methylene protons in the butyl chain were detected for compound **106** (Figure 35). These interactions would not be possible with isomer **105**.

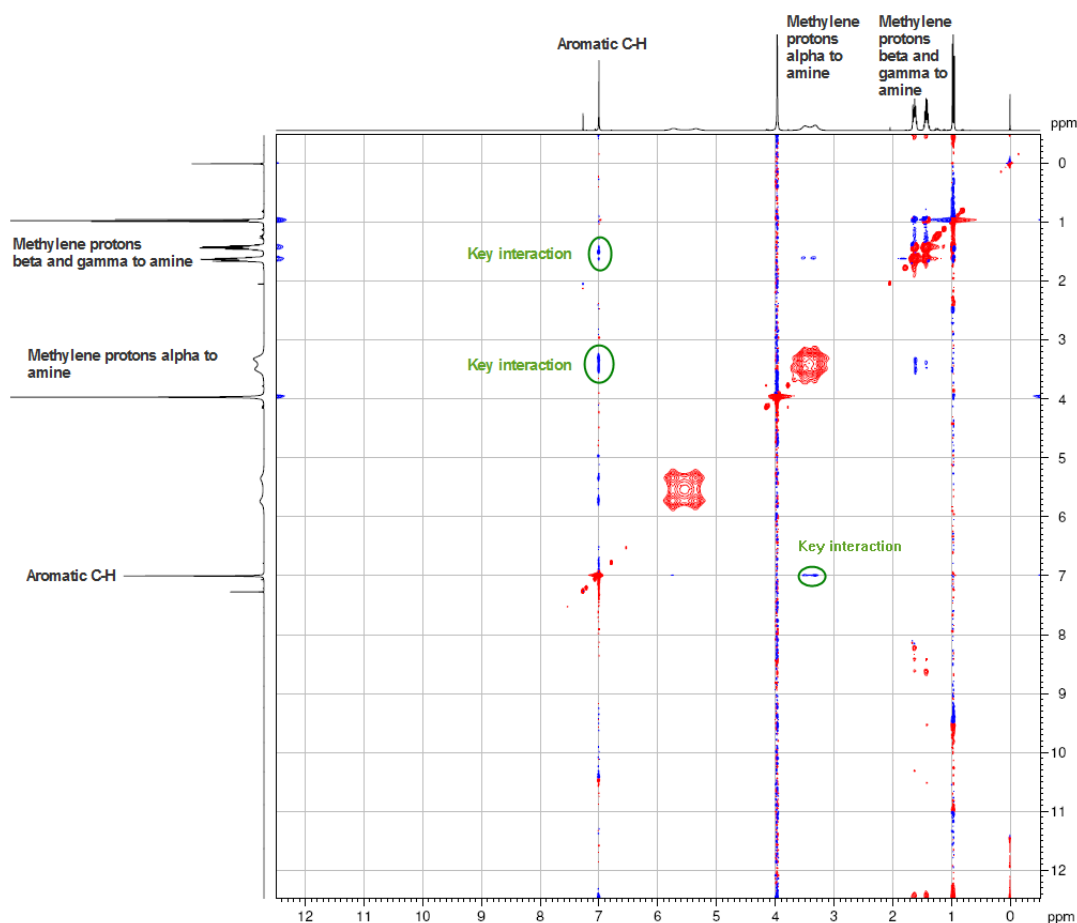


Figure 35: ROESY NMR spectra clearing showing through space interactions between the aryl proton and methylene groups in the *n*-butyl chain present in compound **106**.

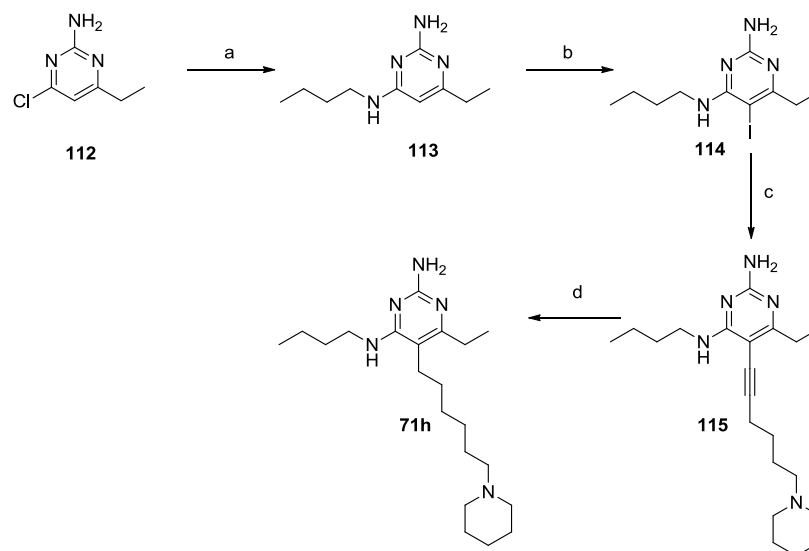
The ester group was then reduced with  $\text{LiAlH}_4$  in moderate yield. Subsequently it was decided to attempt to perform the difficult 2-chloro displacement on this intermediate as it does not bear the ester or the iodide moieties that were not compatible with the displacement conditions previously attempted. Given the absence of these functionalities, a more nucleophilic ammonia equivalent than *tert*-octylamine could be used. In this case 3,4-dimethoxybenzylamine was chosen as it is still relatively labile in strong acid. Using this approach the amine was introduced in good yield using *n*-butanol as the solvent. Microwave heating in TFA with anisole as a scavenger (to trap the highly electrophilic benzyl carbocation) removed the dimethoxybenzyl group, furnishing the desired 2-amino compound **109** in excellent yield. Subsequent iodination was achieved using *N*-iodosuccinimide furnishing intermediate iodide **110**. The Sonogashira cross coupling with alkyne **78** proceeded in a reasonable yield of 39%, and subsequent hydrogenation furnished **71e** in 82% yield. Deoxofluorination of the alcohol **71e** to furnish **71f** was carried out using the tetrafluoroborate salt of DAST (named XtalFluor-E<sup>TM</sup> by Omega Chemicals).<sup>211</sup> This particular reagent was used as it has been shown to be more stable than DAST and has the added advantage of being a crystalline solid, making it easy to handle.<sup>212</sup> Using XtalFluor-E<sup>TM</sup> the deoxofluorination furnished **71f**, albeit in a disappointing yield of 14% after MDAP purification. Following isolation, compounds **71e** and **71f** were submitted for biological evaluation.

### 2.3.6 Introduction of an ethyl group into the 6-position.

Compound **71h** was made according to the route shown in Scheme 12. In order to synthesise this target compound it was decided to use a commercially available pyrimidine with an ethyl group already incorporated (compound **112**) as the starting material. The *n*-butylamine side chain is introduced *via* an  $\text{S}_{\text{N}}\text{Ar}$  reaction, furnishing **113** in excellent yield. This was followed by iodination and subsequent Sonogashira reaction with alkyne **78**. The Sonogashira cross coupling was again low yielding due to competing cyclisation as previously described. Finally, hydrogenation using the H-cube<sup>TM</sup> furnished **71h** in satisfactory yield. A synthetic sequence analogous

to that described in Scheme 12 was utilised by other members of our laboratory to synthesise **70a**, **71a**, **71i**, and **71j**.

Scheme 12

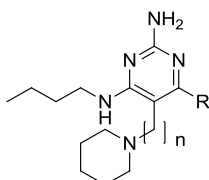


Reagents and conditions: a) *n*-BuNH<sub>2</sub>, *n*-BuOH,  $\mu$ wave 150 °C, 90%; b) ICl, AcOH, 20 °C, 41%; c) CuI, (PPh<sub>3</sub>)<sub>4</sub>Pd, Et<sub>3</sub>N, DMF, 1-(pent-4-yn-1-yl)piperidine (**78**), 20 °C, 23%; d) EtOH, Pd/C Catcart 30 H-Cube<sup>TM</sup> Full H<sub>2</sub>, 40 °C, 70%.

## 2.4 2-Aminopyrimidines: biological results.

The compounds selected for biological evaluation including those synthesised as outlined above and a number generated by colleagues (Champigny, A. C.; Courtet, V. unpublished work), were evaluated in the HWB assay available in our laboratories (Lau, J.; Hessey, J. unpublished work). In this assay the compounds are incubated with HWB for 24 h, and the resulting mixture is centrifuged. The levels of induction of the cytokines IFN $\alpha$  and TNF $\alpha$  present in the supernatant are measured using MSD technology<sup>180</sup> which is based on a enzyme-linked immunosorbent (ELISA) assay and a pEC<sub>50</sub> is generated and standardised using resiquimod **25** (present in every experiment). The standard deviation for the cytokine induction data is 0.3 log units.

To recap, molecular modelling suggested that it may be possible to increase the activity and/or cytokine induction selectivity by replacing the methyl group in **70a** or **71a** with a polar group. In addition, there was some evidence from the initial HTS lead compounds **69a** and **69b** that replacing the methyl group with a larger alkyl group would increase activity.



Compound No.	R	n	Induction of IFN $\alpha$ pEC50	Induction of TNF $\alpha$ pEC50	cLogP	cLogD <sub>7.4</sub>	Pyrimidine predicted pKa
25	N/A	N/A	6.2	5.4	1.8	2.1	N/A
*70a	CH <sub>3</sub>	5	6.6	5.0	5.3	2.8	7.8
70g	Ph	5	<4.3	<4.3	6.6	4.5	6.7
70k	Cl	5	<4.3	<4.3	5.6	4.2	4.8
*71a	CH <sub>3</sub>	6	6.6	4.8	5.8	2.8	7.8
71b	OCH <sub>3</sub>	6	<4.3	<4.3	6.3	3.9	6.8
71e	CH <sub>2</sub> OH	6	<4.3	4.6	4.3	2.3	6.7
71f	CH <sub>2</sub> F	6	<5.6	4.8	5.4	3.9	5.7
71h	CH <sub>2</sub> CH <sub>3</sub>	6	<5.7	5.1	6.4	3.5	7.6
<sup>+</sup> 71i	CF <sub>3</sub>	6	<4.3	<4.3	6.3	4.7	4.3
*71j	CH <sub>2</sub> CH <sub>2</sub> CH <sub>2</sub> CH <sub>3</sub>	6	<4.3	<4.3	7.4	3.6	7.6
71k	Cl	6	<4.3	<4.3	6.1	4.2	4.8
71l	CO <sub>2</sub> CH <sub>3</sub>	6	<4.3	<4.3	5.0	3.5	4.4
71m	NHCH <sub>2</sub> CH <sub>2</sub> CH <sub>2</sub> CH <sub>3</sub>	6	<4.3	<4.3	7.8	3.5	6.7

Table 9: Summary of cytokine induction data for potential TLR agonists in HWB, standard deviation = 0.3 \* compounds synthesised by Champigny, A. C. <sup>+</sup> compound synthesised by Courtet, V. C. cLogP calculated using BioByte software,<sup>183</sup> cLogD<sub>7.4</sub> calculated using algorithms available in our laboratories. pKa predicted using ChemAxon software.<sup>188</sup>

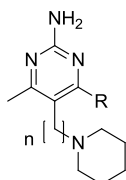
Examining the polar methyl replacements, it appears that this region of the molecule is very sensitive with respect to the introduction of polar functions and the sterics of the polar group. The inactivity of the chloro, trifluoromethyl and ester containing compounds (**70k**, **71k**, **71i** and **71l**) can potentially be rationalised by the effect these substituents have on the pKa of the pyrimidine core. These substituents reduce the predicted pKa and so the pyrimidine may no longer be fully protonated at the pH levels present in the endosome, thus a potentially key binding function may no

longer be present. The substituents present in compounds **71b**, **71e** and **71f** do not alter the protonation state of the pyrimidine at pH values in the range 5-6.5. Examination of the original molecular model would suggest that both the hydroxyl group present in compound **71e** or the methoxy group present in compound **71b** should mimic the 8-oxo group present in compound **48** and could act as a hydrogen bond acceptor if required. Compound **71f** containing a fluoromethyl group may also be able to act as a hydrogen bond acceptor, however the ability of covalently bonded fluorine to make hydrogen bonds between proteins and ligands remains a topic of some debate.<sup>213</sup> The inactivity of compounds **71b**, **71e** and **71f** could be attributed to the position of the potential hydrogen bond acceptor functionality not being optimal. In addition, compounds **71b** and **71e** are both larger than the parent methyl compound **71a**. If there is restricted space in the active site, a larger ligand may not be able to bind optimally to the receptor resulting in reduced activity. Another potential explanation for the observed SAR is that the molecular modelling undertaken does not accurately reflect the binding modes of the two different chemical series, as this assumes commonality in their respective interactions with the receptor.

The cytokine induction data generated for the original HTS lead molecules **69a** and **69b** (Figure 25) demonstrated that replacement of the methyl group with a larger alkyl group was not only tolerated but led to a significant increase in the potency of cytokine induction. Replacement of the methyl group (compound **71a**) with a butyl group (compound **71j**) results in no detectable cytokine induction being measured. When the methyl is replaced with an ethyl group (compound **71h**) some cytokines are detected in the assay but at a significantly reduced level, particularly in the case of IFN $\alpha$ , where not only is the pEC<sub>50</sub> reduced but also the maximum level of cytokine induction, suggesting the compound is less efficacious as well as less potent. Furthermore, the other pyrimidine derivatives featuring large substituents, **70g** (phenyl) and **71m** (butylamino) did not induce any detectable levels of cytokines. Considering the entire data set, it appears that the steric size of the

functional groups present on the pyrimidine template plays a key role in the ability of the compound to bind TLR7 and induce cytokines.

It is interesting to note that the only aminopyrimidine compounds that show good cytokine induction are those where the R-group (Table 9) is a methyl (compounds **70a** and **71a**). The series of aminopyrimidines reported by researchers at AstraZeneca (Section 1.9.7) all have a methyl group in the analogous position to the series described here. The SAR investigations described above may help explain the compound scope defined in the AstraZeneca patent applications, which was limited at this position.



Compound Number	R	n	Induction of IFN $\alpha$ pEC50	Induction of TNF $\alpha$ pEC50	cLogP	cLogD <sub>7,4</sub>
25	N/A	N/A	6.2	5.4	1.8	2.1
70a*	NH(CH <sub>2</sub> ) <sub>3</sub> CH <sub>3</sub>	5	6.6	5.0	5.3	2.8
116 <sup>+</sup>	O(CH <sub>2</sub> ) <sub>3</sub> CH <sub>3</sub>	5	5.4	6.0	5.4	3.4
117*	N(CH <sub>3</sub> )(CH <sub>2</sub> ) <sub>3</sub> CH <sub>3</sub>	5	<4.3	<4.3	5.4	3.8
118a*		5	<4.3	<4.3	6.1	2.4
118b*		5	6.8	5.2	6.1	2.4
71a*	NH(CH <sub>2</sub> ) <sub>3</sub> CH <sub>3</sub>	6	6.6	4.8	5.8	2.8
119 <sup>+</sup>	CH <sub>2</sub> (CH <sub>2</sub> ) <sub>3</sub> CH <sub>3</sub>	6	<4.3	<4.7	6.0	2.8
120a*		6	<5.5	<4.7	5.2	1.4
120b*		6	6.8	4.7	5.2	1.4

Table 10: Summary of cytokine induction data for potential TLR agonists in HWB, standard deviation = 0.3, \* compounds synthesised by Champigny, A. C. <sup>+</sup> compound synthesised by Courtet, V. C.

Replacing the *n*-butylamino group in molecules **70a** and **71a** has also been the subject of investigations elsewhere in our laboratories (Champigny, A.C. and Courtet, V. unpublished work), with key results summarised in Table 10. One particularly interesting observation from the data presented above is that replacing the *N*-butyl for an *O*-butyl (**70a** to **116**) reduces the ability to induce IFN $\alpha$  and increases the induction of TNF $\alpha$ . A possible explanation for this selectivity switch is that changing the heteroatom linker alters the pK<sub>a</sub> of the pyrimidine ring system. The predicted pK<sub>a</sub> of the ring system in compound **70a** is 7.6 whereas the predicted pK<sub>a</sub> of the pyrimidine ring in ether linked compound **116** is only 5.4. Given that the pH of the endosome, where TLR7 is located ranges from 5-6.5, a significant portion of compound **116** will be unprotonated, potentially accounting for the reduction in IFN $\alpha$ . This however, does not adequately explain the rise in TNF $\alpha$  induction. It is possible that replacing the amine with an ether has altered the selectivity of TLR7 signalling between the IRF7 and NF $\kappa$ B downstream pathways or resulted in compound **116** being a TLR8 agonist. These changes could be a result of different hydrogen bonding interactions, with the amine acting as a hydrogen bond donor and the ether as an acceptor.

The data in Table 10 also indicates that a heteroatom linker between the aminopyrimidine and butyl functions is required given the lack of observed cytokine induction for the carbon linked compound **119**. The data from compound **117** suggests that tertiary amine linkers are not tolerated and so this nitrogen atom cannot be used to introduce a branching group. Branching is however tolerated from the carbon alpha to the heteroatom but only one enantiomer results in significant IFN $\alpha$  induction.

Compound **120b** is the first compound synthesised in this series that meets the required *in vitro* cytokine induction selectivity profile. Compound **120b** is also expected to be more soluble than the lead compound **71a** because of the solubilising alcohol group, however the compound still has an intrinsic lipophilicity (cLogP) of greater than five. It is anticipated that combination of the branched amine group



present in compound **120b** with a less lipophilic *C*-5 alkyl amine may give rise to compounds that meet all of the desired physicochemical properties and maintain the desired cytokine induction activity and selectivity. These combinations were not ultimately investigated due to the discovery of a second series of novel compounds described in Section 3.

In conclusion, these initial results suggest that the molecular modelling hypothesis may not be valid. In addition, these tetrasubstituted pyrimidines do not follow the same SAR as found for the HTS lead compounds **69a** and **69b**.

## 2.5 Revisiting the original medicinal chemistry hypothesis.

Our original medicinal chemistry strategy was based in part on the molecular overlay of the 2-aminopyrimidine **70a** with the active and selective 8-oxoadenine compound **48** discovered in our laboratories. As stated above, the biological results obtained for a series of 2-aminopyrimidine compounds designed to better mimic the 8-oxoadenine series does not appear to support this molecular overlay.

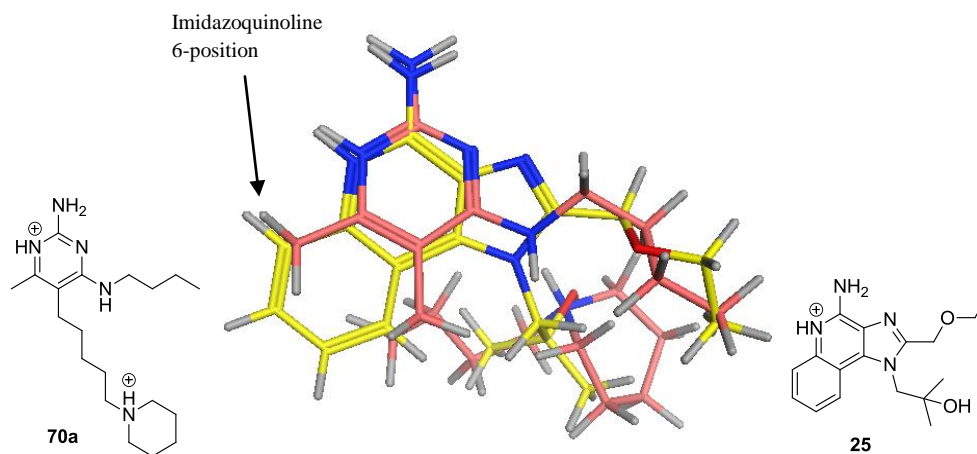


Figure 36: Molecular modelling overlay of compound **70a** (shown in pink) and resiquimod **25** (shown in yellow). The arrow marks the 6-position of the imidazoquinoline ring.

In an effort to better understand the observed SAR, molecular overlays of compound **70a** and examples of TLR7 agonist compounds from other chemical series were generated. The molecular overlay of compound **70a** with resiquimod **25** is

particularly interesting, with good overlap of potential pharmacophoric features (Figure 36) and electrostatic fields (Figure 37). It is interesting to note that in this conformation, the electrostatic field for compound **70a** is now different from that generated in Section 2.2 (Figure 29). A possible explanation for this, is that the protonated terminal amine is now in closer proximity to the pyrimidine core.

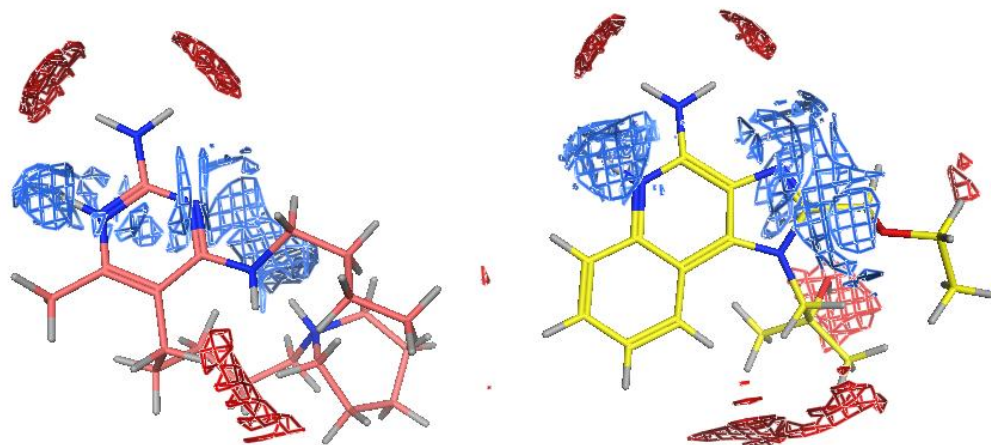


Figure 37: Predicted electrostatic fields for compound **70a** (shown in pink) and resiquimod **25** (shown in green). Negative field surfaces are shown in blue, positive field surfaces in red.

This overlay may be able to explain the data observed when the methyl group is replaced (compounds **70a – 70m**). The methyl group in compound **70a** occupies a near identical region of space as the imidazoquinoline 6-position in this overlay. David and co-workers have examined adding functional groups onto the 6-position of imidazoquinolines and found that substitution from this position was not tolerated with respect to IFN $\alpha$  induction (Section 1.9.1).<sup>116</sup> If the molecular overlay (Figure 36) is a true representation of the binding mode of these two chemotypes then it is possible to rationalise the inactivity of several compounds discussed above in Section 2.4. This general overlay can also explain why compounds with an alcohol bearing branched amine in are tolerated (Figure 38). As is evident from the overlay, the alcohol in compound **120b** can reach the same space and adopt a similar vector to the tertiary alcohol in resiquimod **25** and so potentially interact with the receptor in the same way.

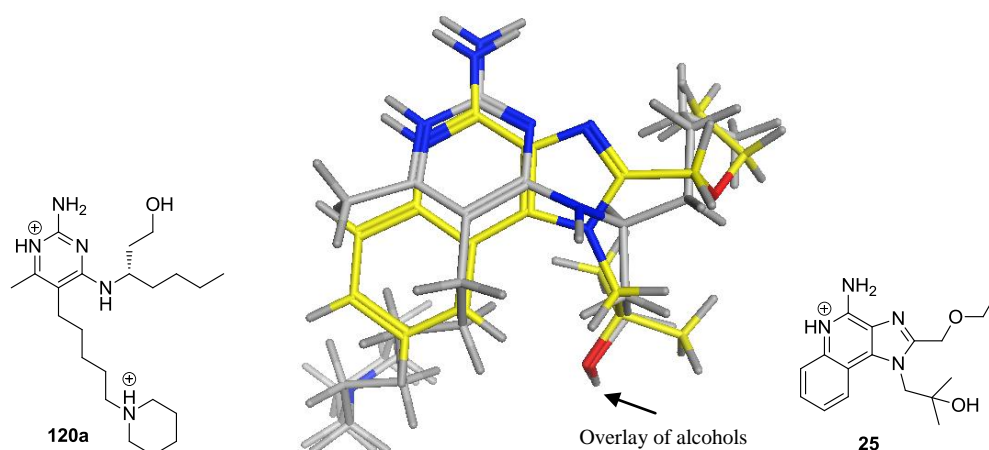


Figure 38: Molecular modelling overlay of compound **120a** (shown in grey) and resiquimod **25** (shown in yellow).

From consideration of these modelling results it appears that the SAR of the 2-aminopyrimidine series more closely mirrors that of the imidazoquinoline series as opposed to the 8-oxoadenine series.

David *et al.* have suggested that the series of imidazopyridines they have reported bind to TLR7 in the same way as the imidazoquinolines (Section 1.9.6).<sup>166</sup> Considering the molecular modelling overlay of compound **70a** with resiquimod **25** and that the *N*-butyl imidazopyridine compound **67** shows good activity, one might expect compound **71m** to be active as well. Indeed, a molecular overlay of the two compounds suggests a good alignment of functionality (Figure 39).

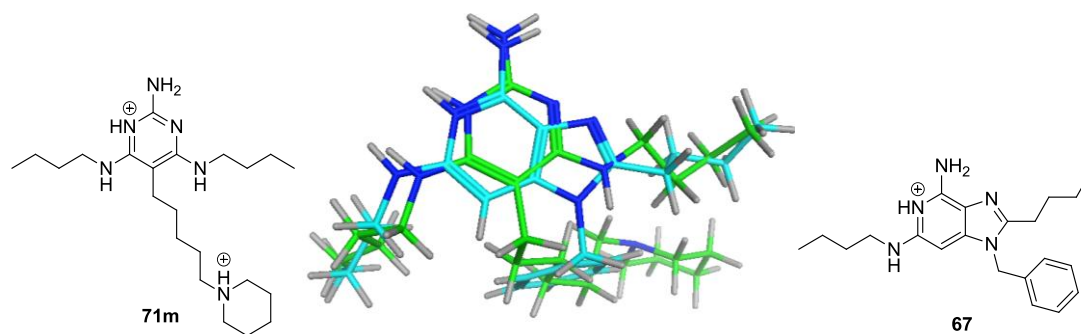


Figure 39: Molecular modelling overlay of compound **71m** (shown in green) and imidazopyridine **67** (shown in cyan).

This potentially suggests that the imidazoquinolines and imidazopyridines bind to TLR7 in different ways.

The modelling results overlaying the 2-aminopyrimidine compounds with known TLR7 agonist chemotypes and the biological data presented suggests that there may be at least two different binding sites or binding modes within the same active site, or that there are potentially multiple mechanisms of TLR7 activation. Until TLR7-ligand X-ray crystal structures are obtained this hypothesis cannot be conclusively proven.

Further investigations into the 2-aminopyrimidine series were not undertaken due to the emergence of a new lead series in our laboratories based on a heteroaromatic core structure not previously described as a TLR7 agonist or inducer of IFN $\alpha$ . Nevertheless, the SAR observed and the chemistry explored for the 2-aminopyrimidines should however aid both medicinal and synthetic chemistry design in the new series. This new series and subsequent research is described in Section 3 of this thesis.

## 2.6 Summary of 2-aminopyrimidines as potential inducers of IFN $\alpha$ and potential further work.

Following an HTS campaign, a 2-aminopyrimidine based compound **69a** was identified as a hit. Simplification of the 4-position amine group and introduction of an alkyl chain with a basic terminus into the 5-position resulted in lead compounds **70a** and **71a**. These compounds induced IFN $\alpha$  in HWB and displayed a level of selectivity over induction of the pro-inflammatory cytokine TNF $\alpha$  approaching the desired 100-fold level. Through molecular modelling overlays with 8-oxoadenine compound **48** (a potent and selective TLR7 agonist) the 6-position (substituted with a methyl group in the lead compounds) was identified as an area of the molecule which through modification had the potential to increase potency, selectivity and further improve the physicochemical properties.

**GSK CONFIDENTIAL – Property Of GSK – Copying Not Permitted**  
 The Synthesis and Optimisation of Toll-like Receptor Agonists as Potential Immunomodulatory Agents.

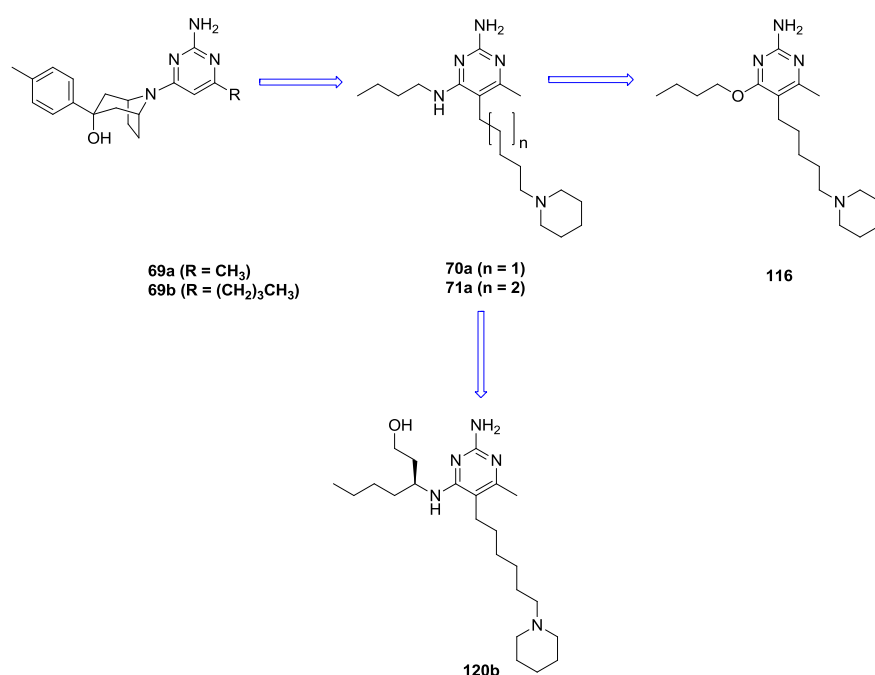


Figure 40: Graphical summary of the key compounds from the 2-aminopyrimidine series.

Compound Number	HWB Induction of IFN $\alpha$ pEC50	HWB Induction of TNF $\alpha$ pEC50	PBMC Induction of IFN $\alpha$ pEC50	cLogP	cLogD <sub>7.4</sub>	cPFI
69a	-	-	4.6	2.3	2.4	4.4
69b	-	-	5.7	4.5	5.2	7.2
70a	6.6	5.0	-	5.3	2.8	3.8
71a	6.6	4.8	-	5.8	2.8	3.8
116	5.4	6.0	-	5.4	3.4	4.4
120b	6.8	4.7	-	5.2	1.4	2.4

Table 11: Summary of cytokine induction data for potential TLR agonists, standard deviation = 0.3

A variety of synthetic strategies were required to furnish 13 different methyl replacements. During these synthetic investigations a novel cyclised compound **77** was identified and the structure confirmed by NMR studies. An X-ray crystal structure of this novel compound would complement the NMR studies. To obtain such a structure, further work would be required to identify a crystallisation system possibly involving exchanging the anion to obtain a stable crystalline form.<sup>214</sup> The formation of the cyclic compound appears to be catalysed by the presence of palladium (II) species. In order to probe the mechanistic features of this cyclisation

one could envisage attempting to react the desired uncyclised alkyne with a number of palladium sources and a range of additives. Such studies may also provide insight into the optimisation of the Sonogashira cross coupling conditions such that the formation of the cyclic compound is minimised.

The most significant synthetic challenges centred around the difficulty in performing nucleophilic aromatic substitution reactions on highly substituted electron rich pyrimidines. These challenges were overcome in two ways: either by strategic use of various protected ammonia equivalents or by the employment of Buchwald-Hartwig cross coupling reactions using *N*-heterocyclic carbene ligands. At the time of writing no previous examples of the use of *tert*-octylamine to introduce a 2-amino group onto a pyrimidine has been reported.

Examination of the cytokine induction data for the 6-methyl replacements indicated that this area of the molecule is extremely sensitive to changes in steric size and electrostatic properties. These observations led to a re-examination of the original modelling approach and support the possibility of multiple modes of activation of TLR7 by chemically distinct classes of molecule.

Further SAR investigations carried out in our laboratories show that a branching point can be introduced in the 4-position and that polar functionality can be incorporated onto this branch. The resulting compound **120b** meets the desired *in vitro* cytokine induction potency and selectivity criteria. In addition, this compound has better physicochemical properties than the lead compounds being less lipophilic and also having a known solubilising group. Compound **120b** was not profiled further due to a change in focus to another more promising chemical series (Section 3). Also of particular note is that altering the linking atom from nitrogen to oxygen alters the selectivity of cytokine induction to favour TNF $\alpha$ . Such a change in profile has not been reported for any of the other known TLR7 agonist chemotypes. The oxygen linked compound **116** may in fact be a TLR8 or mixed TLR7/8 agonist. TLR8 agonism could potentially be assessed using a TLR8 reporter assay and if activity was demonstrated this compound could provide an important starting point

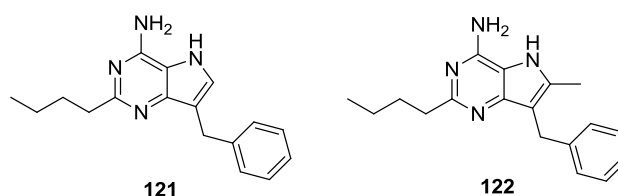
for a TLR8 drug discovery programme. Within this template there is considerable scope for further investigations of the 4-position. For example, the length of the alkyl chain has not been specifically examined nor has the introduction of ethers into this chain.

Finally, to date the 5-position group of the pyrimidine scaffold has not been investigated. There are numerous possibilities in this area including examining the position and pKa of the amine group. It is possible that further investigations on this 2-aminopyrimidine template could yield a potential candidate compound that would meet all our desired criteria, including delivering a molecule with improved physicochemical properties.

### 3 Results and Discussion Part 2: 9-deazaadenines (5*H*-pyrrolo[3,2-*d*]pyrimidine-4-amines) as inducers of IFN $\alpha$ .

#### 3.1 Discovery of a new lead series

During the development of the 8-oxoadenine series within our laboratories investigations were undertaken to identify other analogous aromatic core scaffolds that could induce IFN $\alpha$  (Smith, S. A. and co-workers unpublished work). From these efforts, it was shown that a 9-deazaadenine (5*H*-pyrrolo[3,2-*d*]pyrimidin-4-amine) core displayed induction of IFN $\alpha$  and TNF $\alpha$  in hPBMCs (Figure 41).

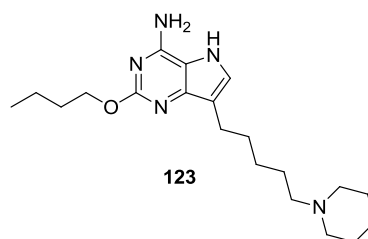


Compound Number	PBMC Induction of IFN $\alpha$ pEC50	PBMC Induction of TNF $\alpha$ pEC50
121	6.0	6.6
122	5.1	6.7

Figure 41: Structure and PBMC cytokine induction data for two 9-deazaadenines, standard deviation = 0.3.

Given the structural similarities between these compounds and the 8-oxoadenine series it was believed that changes could be made that would result in reversing the cytokine induction selectivity to favour IFN $\alpha$  induction. Changing the butyl function to an *O*-butyl and changing the benzyl to an alkyl chain bearing a piperidine with the basic centre 5-atoms from the core resulted in compound **123** (Mitchell, C. J. unpublished work). When tested *in vitro* compound **123** did show some modest selectivity for IFN $\alpha$  induction (Figure 42). However, the compound did not show a significant increase in potency similar to that observed in the 8-oxoadenine series (Section 1.9.3, compound **36** vs. compound **38**).

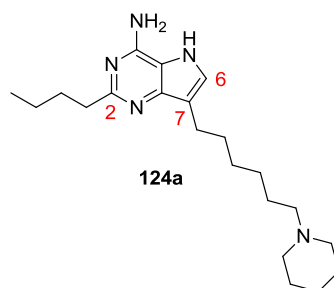




Compound Number	PBMC Induction of IFN $\alpha$ pEC50	PBMC Induction of TNF $\alpha$ pEC50
<b>123</b>	<b>5.8</b>	<b>4.9</b>

Figure 42: Structure and PBMC cytokine induction data for a modified 9-deazaadenine intended to better resemble the 8-oxoadenine series, standard deviation = 0.3.

Removal of the oxygen linker in the 2-position whilst retaining the butyl chain and C-7 substituent compound **124a** (diformate salt, Needham, D. unpublished work) exhibited good potency in HWB similar to that of compound **120b** with a comparable selectivity for IFN $\alpha$  induction over TNF $\alpha$  induction. *In vitro* cytokine induction data, dose response curves and developability assay results are summarised in Figures 43, 44 and Table 12.



Compound Number	HWB Induction of IFN $\alpha$ pEC50	HWB Induction of TNF $\alpha$ pEC50	Mol. Wt.	cLogP	Chrom. LogD <sub>7.4</sub> (PFI)	HSA Binding	Solubility Saline (mg/mL)	MDCK Permeability (nm/s)
<b>124a</b>	<b>6.8</b>	<b>&lt;4.8</b>	<b>449</b>	<b>6.0</b>	<b>1.8 (3.8)</b>	<b>91%</b>	<b>2.8</b>	<b>26</b>

Figure 43: Structure, *in vitro* activity and developability data for **124a**, standard deviation = 0.3, cLogP calculated using BioByte software,<sup>183</sup>

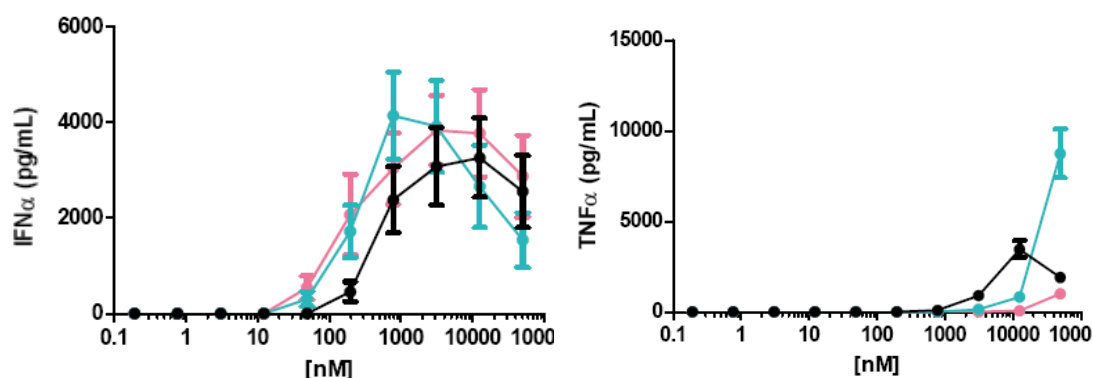


Figure 44: Dose response curves for IFN $\alpha$  and TNF $\alpha$  induction for **120b**, **124a** and **25** in HWB (The pink line represents compound **120b**, the blue line compound **124a** and the black line represents the assay standard resiquimod **25**). Note this data is from one single experiment.

Species	Rat	Human
Turnover of <b>124a</b> in microsomes mL/min/g of tissue	8.8	1.2
Turnover of <b>124a</b> scaled as % LBF	80%	62%

Table 12: *In vitro* clearance (IVC) data for **124a** in liver microsomes. IVC data scaled using the “well stirred model” to give a percentage of liver blood flow (LBF) assessment.<sup>215</sup>

Compound **124a** induces IFN $\alpha$  with a pEC<sub>50</sub> of 6.8, and TNF $\alpha$  with a pEC<sub>50</sub> of <4.8, a >2 log unit difference (*cf.* >1.9 log units for compound **120b**). Examining the dose response curves in a head to head assay it appears that compound **124a** has much better selectivity than both resiquimod **25** and **120b** (Figure 44). Furthermore the molecule has an excellent measured solubility of 2.8 mg/mL in saline (Gibbon, B. unpublished work), which would be suitable for a solution formulation. Further profiling indicated that the compound shows moderately permeability in Madin-Darby canine kidney (MDCK) cells. Good permeability is required for activity as the TLR7 receptor is intracellular in nature. Compound **124a** (Table 12) was shown to be rapidly cleared in rat liver microsomes (RLM) and moderately cleared in human liver microsomes (HLM). The molecule exhibits relatively low plasma protein binding, thereby ensuring a large free fraction available to be cleared from the body. Additionally the synthetic chemistry of 9-deazaadenines is well described in the literature and has proven tractable in our laboratory. Based on the

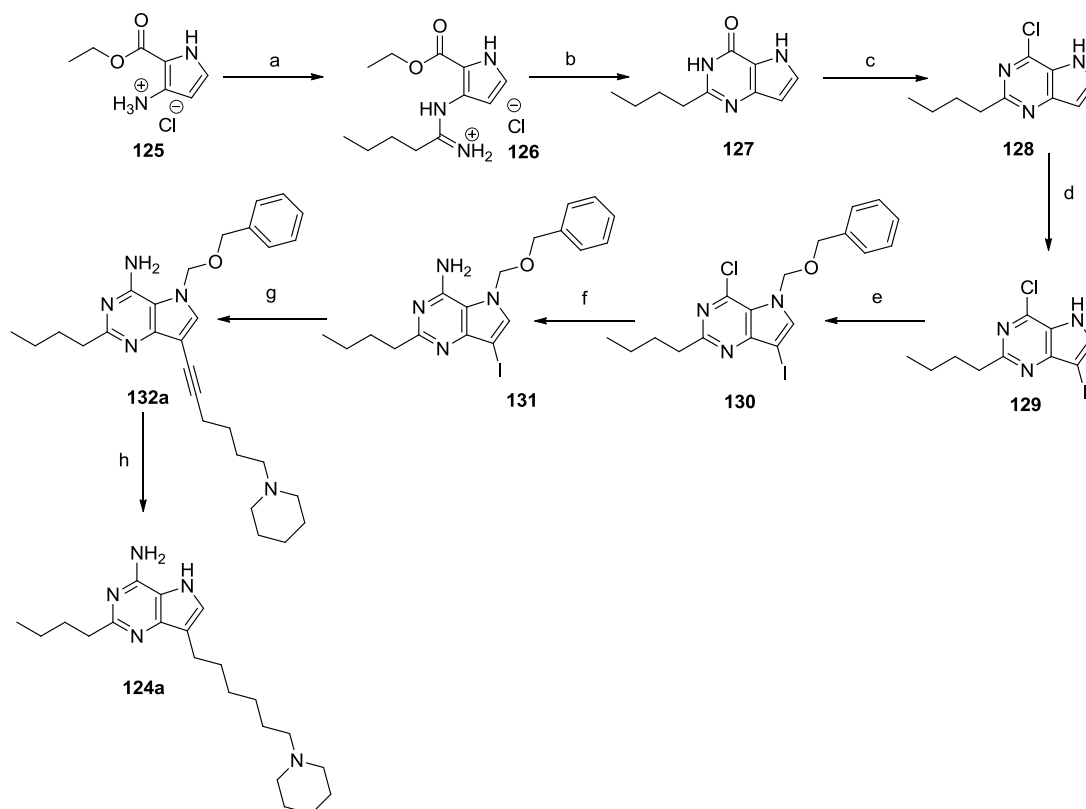
profile presented above compound **124a** represents a very good starting point for lead optimisation.

The focus of the initial lead optimisation was to maintain the potency of IFN $\alpha$  induction at a pEC<sub>50</sub> of approximately 7, to increase the selectivity window over TNF $\alpha$  induction significantly to over 100-fold and to increase the clearance in human liver microsomes to ensure minimal systemic exposure *in vivo*. Once these objectives have been achieved, the resulting compound can be assessed in further biological and toxicological assays and additional optimisation performed as required.

### 3.1.1 Synthesis of lead compound **124a**.

The synthesis executed to deliver compound **124a** is shown in Scheme 13 and described below (Needham, D. and Coe, D. M. unpublished work). Using the commercially available aminopyrazole ester **125** the deazaadenine ring system is constructed by adopting the synthetic strategy employed by Norman and co-workers, with addition of the pyrrole onto a nitrile to give compound **126** and subsequent base mediated cyclisation.<sup>216</sup> The pyrrolopyrimidinone is converted into chloropyrrolopyrimidine **128** using POCl<sub>3</sub> in excellent yield. Following the procedures defined by Otmar and co-workers the compound is iodinated, the indole-like nitrogen is protected with a BOM group, and the resulting compound **130** is reacted with ammonia to displace the chloride and yield compound **131**.<sup>217</sup> Otmar and co-workers demonstrated that if the protection step was performed before the iodination the overall yield was severely affected with the iodination performing very poorly and in some cases (depending on the 4-position group) not proceeding at all. The pendant amine functionality is introduced in the same manner as described for the aminopyrimidine series, through a Sonogashira cross coupling with alkyne **78**. Finally, the protecting group is removed and the alkyne reduced by hydrogenation over palladium on carbon in the H-Cube apparatus to give **124a** as an amorphous solid.

Scheme 13

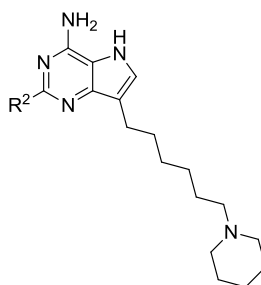


Reagents and conditions: a) *n*-BuCN, HCl, 1,4-dioxane, 50 °C, 84%; b) NaOH, EtOH, reflux, 98%; c) POCl<sub>3</sub>, reflux, 96%; d) NIS, THF, 20 °C, 85%; e) NaH, BOM-Cl, THF, 0 °C, 62%; f) NH<sub>3</sub>, IPA,  $\mu$ wave, 150 °C, 90%; g) Pd(PPh<sub>3</sub>)<sub>2</sub>Cl<sub>2</sub>, CuI, 1-(pent-4-yn-1-yl)piperidine (**78**), Et<sub>3</sub>N, DMF, 55 °C, 68%; h) EtOH, Pd/C Catcart 30 H-Cube<sup>TM</sup> Full H<sub>2</sub>, 60 °C, 44%.

### 3.2 Medicinal chemistry strategy 1: investigation of the 2-position.

Given the lack of success in the use of molecular modelling tools in designing new 2-aminopyrimidines, and the possibility of multiple binding sites, these tools were not employed in the design of new 9-deazaadenine compounds. Compound **124a** has a relatively large *n*-butyl chain in the 2-position, therefore it is anticipated that many other functional groups of similar or smaller steric size could be incorporated into this position. In several of the previously described TLR7 agonist series (sections 1.9 and 2.4) introduction of a branching group onto the alkyl chain can

result in altered cytokine induction profiles. Therefore the investigation of branching groups in the 2-position of the deazaadenines is also of interest. The proposed 2-position modifications are shown in Table 13 and further discussed below. The a suffix is given to the compound numbers to indicate the presence of a piperidine as the terminus of the 7-position group. As stated previously (Section 1.10.1), the reduction of both the intrinsic lipophilicity of the neutral uncharged compound (LogP) and the lipophilicity of the compound at physiological pH (LogD<sub>7.4</sub>) can reduce potential off target activities and increase solubility. Therefore, where possible the predicted lipophilicity of the new target compound is reduced with respect to the lead compound **124a**.



Compound number	R <sup>2</sup>	cLogP	cLogD <sub>7.4</sub>
133a	NH(CH <sub>2</sub> ) <sub>3</sub> CH <sub>3</sub>	6.3	2.5
134a	CH <sub>3</sub>	4.4	0.2
135a	CH <sub>2</sub> CH <sub>3</sub>	4.9	0.5
136a	CH <sub>2</sub> CH <sub>2</sub> CH <sub>3</sub>	5.5	0.8
137a	CH <sub>2</sub> (CH <sub>2</sub> ) <sub>3</sub> CH <sub>3</sub>	6.5	1.8
138a	CH(CH <sub>3</sub> ) <sub>2</sub>	5.3	1.6
139a	CH <sub>2</sub> CH(CH <sub>3</sub> ) <sub>2</sub>	5.9	1.6
140a	CH <sub>2</sub> CH <sub>2</sub> CH(CH <sub>3</sub> ) <sub>2</sub>	6.4	1.7
141a	CH <sub>2</sub> CH <sub>2</sub> OCH <sub>3</sub>	3.8	0.1
142a	CH <sub>2</sub> OCH <sub>2</sub> CH <sub>3</sub>	4.1	0.8
143a	OCH <sub>2</sub> CH <sub>2</sub> CH <sub>3</sub>	5.9	2.1
144a	CF <sub>3</sub>	4.9	2.0
145a	Ph	6.0	3.1
146a	CH <sub>2</sub> NHCH <sub>2</sub> CH <sub>3</sub>	3.7	-0.5

Table 13: List of target 2-groups and the calculated lipophilicities<sup>183</sup> for the resulting final compounds.

For all compounds, it was planned to incorporate a six carbon linked piperidine as this was present in the lead compound thereby allowing comparison of substituents at the 2-position. In the 8-oxoadenine series, replacing a directly linked butyl chain with an nitrogen linked butyl chain was favourable therefore compound **133a** was proposed. It was also decided to determine if the length of the alkyl chain in the 2-position could be reduced (compounds **134a**, **135a** and **136a**) without loss of activity or selectivity, as if successful there is an obvious benefit in terms of lipophilicity. In order to investigate branching groups isopropyl, isobutyl and isopentyl (compounds **138a**, **139a** and **140a**) were proposed. These specific analogues were chosen as in each case the unsubstituted *n*-alkyl compound will be available for direct pair-wise comparison, for example isopropyl compound **138a** vs. ethyl compound **135a**. It was also decided to introduce an ether link into various positions of the alkyl chain in this series (compounds **141a**, **142a** and **143a**) as such a substitution will also result in a decrease in lipophilicity. To further expand assessment of potential SAR the trifluoromethyl analogue **144a** was proposed as this group was tolerated in several previously reported series (8-oxoadenine compound **37** and imidazopyrimidinones **54** and **55**). In order to assess the potential for the introduction of aromaticity in this region a phenyl substituted analogue (compound **145a**) was targeted.

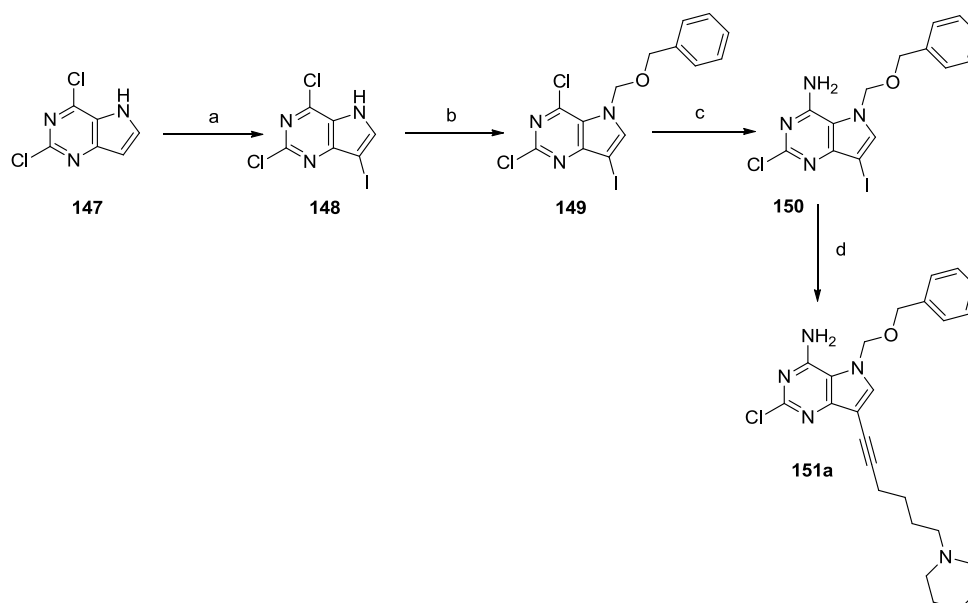
The amine in the 7-position is believed to convey two benefits to the compounds properties: to improve solubility and to enable accumulation of the compound in the acidic endosomal compartments, as proposed by researchers at Pfizer (Section 1.9.4).<sup>160</sup> Incorporation of an amine in the 2-position may result in similar benefits therefore it was decided to investigate if an amine can be tolerated within 2-position alkyl chain (compound **146a**). By incorporating an amine in the 2-position we may be able to dispense with the amine (and associated extended lipophilic linker) in the 7-position. In general the 9-deazadenine core has a predicted pKa of ~ 4 so will not be fully protonated in the endosome. Therefore a basic amine elsewhere in the compound may be required to enable endosomal accumulation. The amine in compound **146a** has a predicted pKa of 7.6 which is lower than the piperidine in

compound **124a** (predicted pKa =10), but should still be completely protonated at the pHs that exist in the endosome (pH 5-6.5).

### 3.2.1 Investigation of the 2-position: synthesis.

It was rationalised that all the desired 2-position analogues described above might be accessed from a common intermediate **151a** where a chlorine is present in the 2-position of the deazadenine core. This compound was synthesised from the commercially available dichloro compound **147** using the procedures of Otmar and co-workers (Scheme 14).<sup>225</sup> The iodination, BOM protection and amination reactions to furnish compounds **148**, **149** and **150** proceeded, as expected, in good to excellent yields. Initially, the Sonogashira cross coupling of compound **150** with the piperidine functionalised alkyne **78** was attempted using Pd(PPh<sub>3</sub>)<sub>4</sub> as the catalyst, resulting in poor conversion to the desired product. Using Pd(PPh<sub>3</sub>)<sub>2</sub>Cl<sub>2</sub>, however, led to isolation of the desired alkyne **151a** in a moderate yield of 52%.

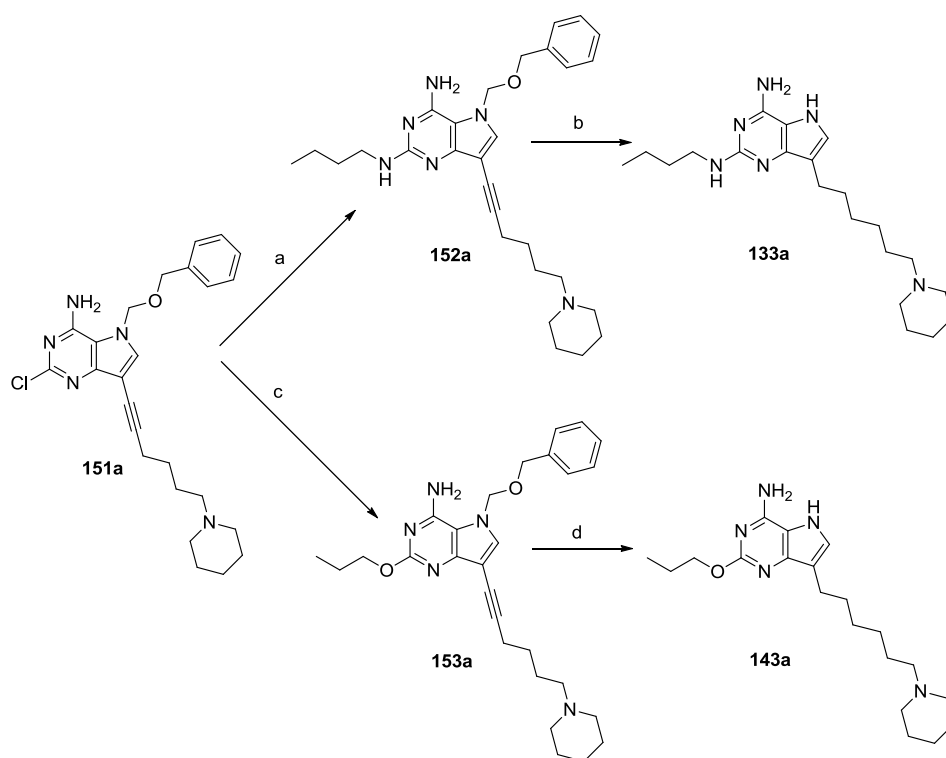
Scheme 14



Reagents and conditions: a) NIS, THF, 20 °C, 96%; b) NaH, BOM-Cl, THF, 0 °C, 76%; c) NH<sub>3</sub>, IPA,  $\mu$ wave, 120 °C, 73%; d) Pd(PPh<sub>3</sub>)<sub>2</sub>Cl<sub>2</sub>, CuI, 1-(pent-4-yn-1-yl)piperidine (**78**), Et<sub>3</sub>N, DMF, 20 °C, 52%.

When alkyne **78** was employed in Sonogashira cross coupling reactions with an aminopyrimidine iodide (Section 2.3.1) an intramolecular 6-*exo*-dig cyclisation was observed. There was no evidence for a similar cyclisation occurring in this instance. A potential explanation for this is that the aromatic coupling partner in this case is more electron rich and so does not polarise the resulting alkyne to act as an electrophile and thus promote the cyclisation reaction. The chlorine atom in **151a** can be displaced in S<sub>N</sub>Ar reactions, and this strategy was employed in the synthesis of butylamino compound **133a** and propoxy compound **143a** (Scheme 15, Courtet, V. unpublished work).

Scheme 15



Reagents and conditions: a) *n*-BuNH<sub>2</sub>,  $\mu$ wave, 200 °C, 86%; b) EtOH, Pd/C Catcart 30 H-Cube<sup>TM</sup> Full H<sub>2</sub>, 40 °C, 22%; c) NaO<sup>t</sup>Bu, *n*-PrOH,  $\mu$ wave, 150 °C, 16%; d) EtOH, Pd/C Catcart 30 H-Cube<sup>TM</sup> Full H<sub>2</sub>, 60 °C, 29%.

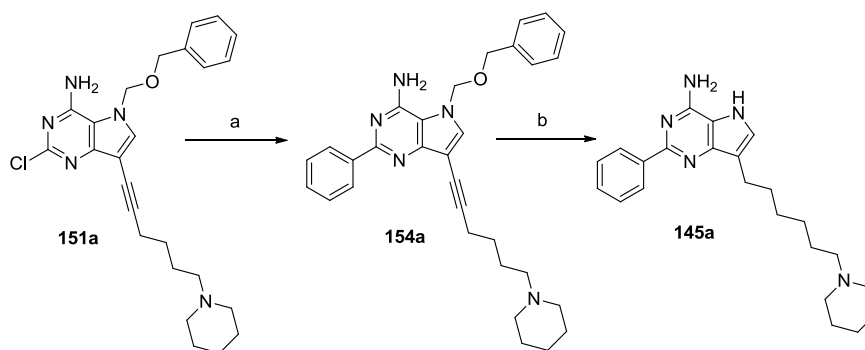
The S<sub>N</sub>Ar reaction of **151a** with *n*-butyl amine required very forcing conditions to proceed. Catalytic hydrogenation using the H-cube<sup>TM</sup> required high temperature and



did not proceed to completion. It was found that although the alkyne was fully reduced, the removal of the BOM protection was incomplete. In order to remove the remaining BOM group it was necessary to replace the palladium containing cartridge (the Catcart) and to cycle the solution through the H-cube™ instrument a second time. This led to significant loss of compound due to increased manual handling and loss of compound within the carbon filled Catcart prior to the required MDAP purification, explaining the low observed yield of 22%. Ether **153a** was synthesised using S<sub>N</sub>Ar chemistry in an analogous way to that of **152a**. In this case a by-product believed to be the result of water (present in the *n*-propanol) acting as the nucleophile was observed by LCMS, thereby resulting in a reduced isolated yield of compound **153a**. Reduction/deprotection as before gave compound **143a** in 29% yield.

Phenyl substituted compound **145a** was synthesised using a Suzuki-Miyaura cross coupling reaction with **151a** and phenylboronic acid using Pd(PPh<sub>3</sub>)<sub>4</sub> as the catalyst, proceeding in good yield to furnish **154a**. Catalytic hydrogenation (again two cycles needed) and purification by MDAP gave **145a** in 17% yield (Scheme 16).

Scheme 16

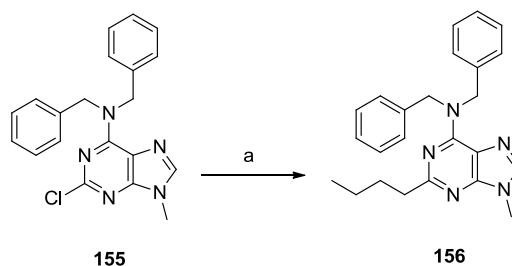


Reagents and conditions: a) PhB(OH)<sub>2</sub>, K<sub>2</sub>CO<sub>3</sub>, Pd(PPh<sub>3</sub>)<sub>4</sub>, 4:1 1,4-dioxane:H<sub>2</sub>O,  $\mu$ wave, 150 °C, 70%; b) EtOH, Pd/C Catcart 30 H-Cube™ Full H<sub>2</sub>, 60 °C, 17%.

Given the success of the palladium mediated cross-coupling on **151a** it was decided to attempt to introduce the desired 2-alkyl groups *via* an sp<sup>3</sup>-sp<sup>2</sup> Suzuki-Miyaura cross coupling. Bartoccini and co-workers have introduced an *n*-butyl group (and an

ethyl group) onto a structurally similar 2-halopurine using such methodology (Scheme 17).<sup>218</sup>

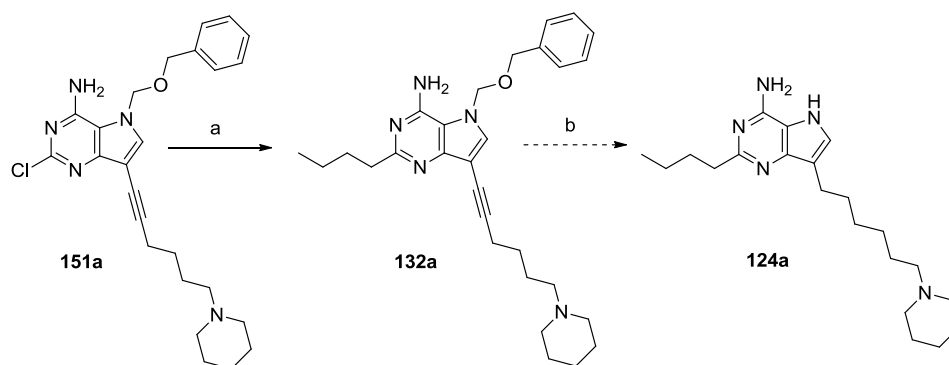
Scheme 17



Reagents and conditions: a)  $\text{Bu}_3\text{B}$ ,  $\text{Pd}(\text{dppf})\text{Cl}_2$ ,  $\text{Cs}_2\text{CO}_3$ , THF, 60 °C, 85%.<sup>227</sup>

It was anticipated that this methodology could be utilised to introduce some of the alkyl chain analogues of **124a**. The number of trialkyl boranes that are commercially available is limited and does not include many of the alkyl groups we wished to incorporate into the 2-position. It should be possible, however, to prepare 9-BBN derivatives with the alkyl group of choice in place and utilise these compounds as cross coupling partners. The only significant issue with such alkyl-9-BBN derivatives is that they are known to be unstable in air,<sup>219</sup> hence they need to be generated *in situ* and coupled immediately. The most frequently used catalysts for this type of Suzuki-Miyaura coupling are  $\text{Pd}(\text{PPh}_3)_4$  or  $\text{Pd}(\text{dppf})\text{Cl}_2$ .<sup>220</sup>

Scheme 18



Reagents and conditions: a)  $\text{Bu}_3\text{B}$ , THF, DMF,  $\text{Pd}(\text{dppf})\text{Cl}_2$ ,  $\text{Cs}_2\text{CO}_3$ , see Table 14 for conditions and yields; b) EtOH, Pd/C Catcart 30 H-Cube<sup>TM</sup> Full  $\text{H}_2$ , 60 °C.

Before investigating couplings with alkyl-9-BBN derivatives, re-synthesis of **124a** was attempted using Bu<sub>3</sub>B (as a solution in THF) to establish the viability of such sp<sup>3</sup>-sp<sup>2</sup> Suzuki-Miyaura cross coupling reactions with chloro compound **151a**. The reactions were performed using Pd(dppf)Cl<sub>2</sub> as the catalyst, Cs<sub>2</sub>CO<sub>3</sub> as the base, either THF or DMF as the bulk reaction solvent, with the reactions conducted at a range of temperatures and using a variety of work-up protocols (Scheme 18 and Table 14).

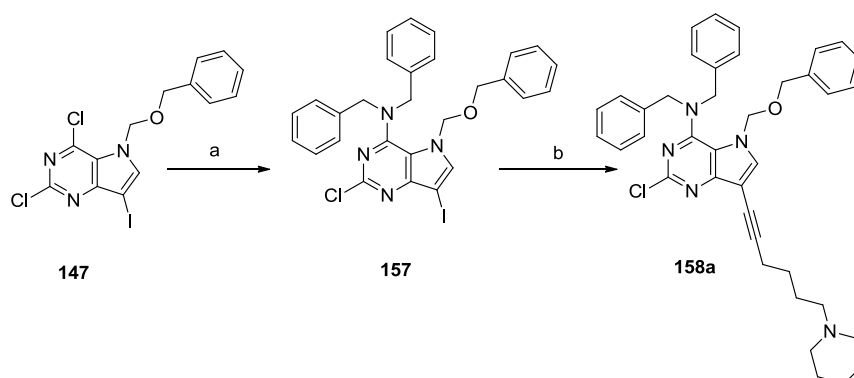
Reaction	Solvent	Temperature/Time	Work-up protocol	Yield of 132a
1	DMF	reflux / 16 h then 150 °C / 5 h	None	5%
2	DMF	120 °C / 2 h	Neutral Aqueous	8%
3	THF	100 °C / 1 h then 120 °C / 1 h	Aqueous NaOH	14%
4	THF	120 °C / 2 h	Aqueous NaOH	13%
5	THF	120 °C / 2 h	AcOH	6%

Table 14: Attempted sp<sup>3</sup>-sp<sup>2</sup> Suzuki-Miyaura cross coupling using Bu<sub>3</sub>B, THF, DMF, and Pd(dppf)Cl<sub>2</sub>. Temperatures greater than 70 °C refer to microwave heating.

Conducting the reaction at reflux did not result in significant product formation by LCMS therefore microwave heating was employed resulting in increased conversion to the desired compound. There was, however, still some starting material remaining and a significant quantity of material that had undergone proto-dehalogenation. Purification by MDAP did furnish the desired product **132a** in 5% yield. In order to improve the impurity profile the reaction temperature was decreased to 120 °C (reaction 2) and an aqueous work up was used resulting in a minimal improvement in yield to 8%. It was reasoned that the impurity profile of the reaction might be further improved by reducing the reaction temperature. Another area for optimisation is the work up, with poor isolation attributed to numerous boron-amine complexes that do not break up to release product. Reducing the temperature to 100 °C did not result in improved conversion of **151a** into product by LCMS analysis (reaction 3) however the inclusion of a wash with aqueous NaOH in the work up stage did result in an improvement in the isolated yield (reactions 3 and 4). An acetic acid quench did not improve product isolation (reaction 5).

From consideration of the literature substrate in Scheme 17 it was decided to investigate the reaction with the amino function protected with two benzyl functions. Therefore compound **158a** was synthesised (Scheme 19).

Scheme 19



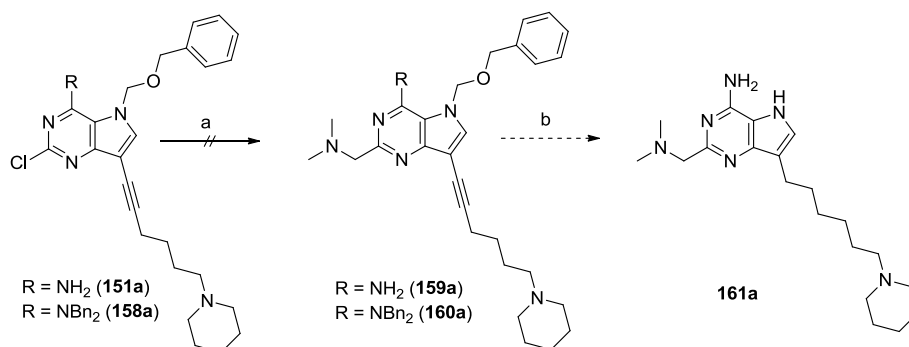
Reagents and conditions: a) EtOH,  $\text{Bn}_2\text{NH}$ , reflux, 87%; b)  $\text{Pd}(\text{PPh}_3)_2\text{Cl}_2$ , CuI, 1-(pent-4-yn-1-yl)piperidine (**78**),  $\text{Et}_3\text{N}$ , DMF, 20 °C, 34%.

Unfortunately attempts to perform the Suzuki-Miyaura reaction with  $\text{Bu}_3\text{B}$  on compound **158a** did not result in improved product formation by LCMS. The reasons for the lack of reaction of either compound **151a** or **158a** with  $\text{Bu}_3\text{B}$  are at present unclear, however the most likely factors are the presence of the alkyne or the pendant basic amine, which could interact with the catalyst either preventing the transmetalation of the alkyl function from boron or promoting  $\beta$ -hydride elimination once transmetalation has occurred. These chemical features are not present in the structure of compound **155** reported in the literature.

In parallel with the investigations described above, the synthesis of amine target **146a** from intermediate **151a** was also investigated. It was decided to exploit some of the chemistry reported by Molander and co-workers, who have described Suzuki-Miyaura type couplings to yield amino-methyl compounds using organotrifluoroborates as coupling partners.<sup>221</sup> The desired amine trifluoroborate required to make compound **146a** was not commercially available, therefore  $(\text{CH}_3)_2\text{NCH}_2\text{BF}_3\text{K}$  was used as a surrogate to establish the methodology. Both

chloropyrimidine intermediates **151a** and **158a** were evaluated as coupling partners (Scheme 20).

Scheme 20



Reagents and conditions: a) (CH<sub>3</sub>)<sub>2</sub>NCH<sub>2</sub>BF<sub>3</sub>K, THF, H<sub>2</sub>O, Cs<sub>2</sub>CO<sub>3</sub>, for catalyst, temperature and outcome see Table 15; b) EtOH, Pd/C Catcart 30 H-Cube<sup>TM</sup> Full H<sub>2</sub>, 60 °C.

Four different catalytic systems were evaluated at reflux and with microwave heating at 150 °C. The catalyst systems evaluated were: Pd(OAc)<sub>2</sub>/XPhos as described in the original Molander publications and two palladacycles that incorporate XPhos: one described by Buchwald for Suzuki-Miyaura cross couplings (**162**),<sup>222</sup> one described by Wu and co-workers that has been used for the coupling of organotrifluoroborates with aryl bromides and chlorides (**163**),<sup>223</sup> and finally Pd(OAc)<sub>2</sub>/RuPhos as described by Molander and co-workers for the Suzuki-Miyaura coupling of alkyl trifluoroborates to aryl chlorides.<sup>224</sup> The palladacycle precatalysts are shown in Figure 38, with precatalyst **163** prepared according to the procedure of Wu and co-workers.<sup>225</sup>

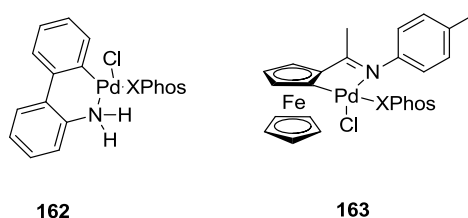


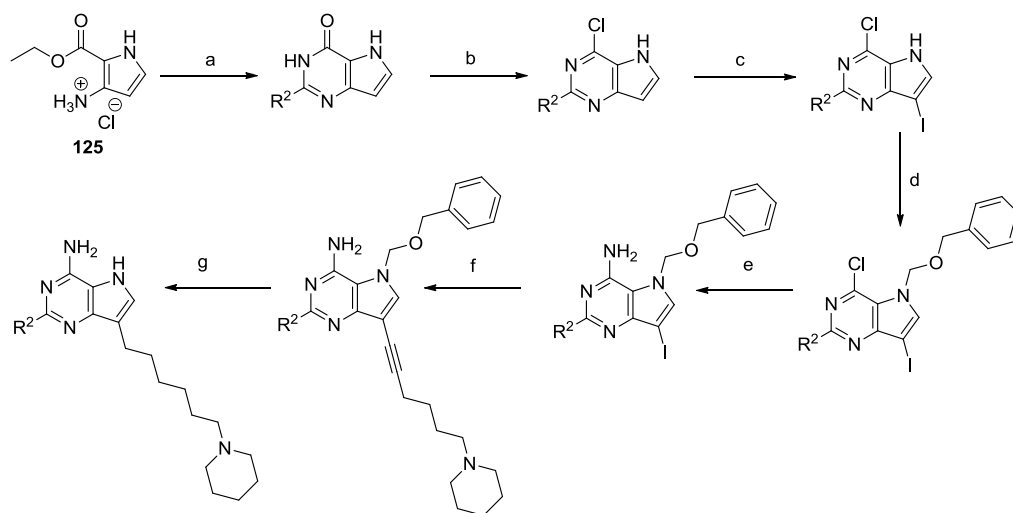
Figure 45: Structures of two palladacycles used as precatalysts in the aminomethylation reaction.

Coupling Partner	Catalyst system	Temperature/Time	Outcome
151a	Pd(OAc) <sub>2</sub> /XPhos	80 °C / 16 h	No reaction by LCMS
158a	Pd(OAc) <sub>2</sub> /XPhos	80 °C / 16 h	No reaction by LCMS
151a	162	80 °C / 16 h	No reaction by LCMS
158a	162	80 °C / 16 h	No reaction by LCMS
151a	Pd(OAc) <sub>2</sub> /XPhos	120 °C / 1 h	No reaction by LCMS
151a	163	80 °C / 16 h	No reaction by LCMS
158a	163	80 °C / 16 h	No reaction by LCMS
151a	Pd(OAc) <sub>2</sub> /RuPhos	80 °C / 16 h	No reaction by LCMS

Table 15: Attempted palladium mediated aminomethylations. All reactions use Cs<sub>2</sub>CO<sub>3</sub> (3 Eq), Catalyst 5 mol%, 10:1 THF:H<sub>2</sub>O 0.12 M, (CH<sub>3</sub>)<sub>2</sub>NCH<sub>2</sub>BF<sub>3</sub>K (1.5 Eq).

Various attempts at cross-coupling reactions with (CH<sub>3</sub>)<sub>2</sub>NCH<sub>2</sub>BF<sub>3</sub>K failed to proceed (Table 15), with unchanged starting material evident by LCMS analysis in all cases. This could be due to lack of transmetallation or perhaps instability of the borate salt being used. Given the lack of success conducting any palladium mediated cross couplings other than a sp<sup>2</sup>-sp<sup>2</sup> Suzuki-Miyaura cross coupling alternative routes to give the remaining desired 2-position analogues were investigated.

Scheme 21: Method A. For yields and compound numbers see Table 16.



Reagents and conditions: a) i) R<sup>2</sup>CN, HCl, 1,4-dioxane, 50 °C; ii) NaOH, EtOH, reflux; Or: R<sup>2</sup>(C=NH)NH<sub>2</sub>, *o*-xylene, 160 °C; b) POCl<sub>3</sub>, reflux; c) NIS, THF, 20 °C; d) NaH, BOM-Cl, THF, 0 °C; e) NH<sub>3</sub>, IPA, μwave, 150 °C; f) Pd(PPh<sub>3</sub>)<sub>2</sub>Cl<sub>2</sub>, CuI, 1-(pent-4-yn-1-yl)piperidine (**78**), Et<sub>3</sub>N, DMF, 55 °C; g) EtOH, AcOH, Pd/C Catcart 30 H-Cube<sup>TM</sup> Full H<sub>2</sub>, 60 °C.

In order to generate the desired 2-position analogues the synthetic route that delivered lead compound **124a** (Scheme 13) was revisited. The ethyl (**135a**), pentyl (**137a**), isopropyl (**138a**) and isopentyl (**140a**) analogues were synthesised from the corresponding nitriles, (Scheme 21) with the yield for each step being presented in Table 16. The related methyl (**134a**), propyl (**136a**), isobutyl (**139a**) and ethoxymethyl (**141a**) analogues were also synthesised from the corresponding nitriles (Champigny, A. Courtet, V. unpublished work).

R <sub>2</sub>	Yield (Compound Number)						
	Step						
	a	b	c	d	e	f	g
CH <sub>2</sub> CH <sub>3</sub>	32% (164)	81% (165)	84% (166)	71% (167)	86% (168)	30% (169a)	32% (135a)
CH <sub>2</sub> (CH <sub>2</sub> ) <sub>3</sub> CH <sub>3</sub>	58% (170)	51% (171)	78% (172)	87% (173)	73% (174)	42% (175a)	32% (137a)
CH(CH <sub>3</sub> ) <sub>2</sub>	67% (176)	73% (177)	95% (178)	89% (179)	85% (180)	51% (181a)	11% (138a)
CH <sub>2</sub> CH <sub>2</sub> CH(CH <sub>3</sub> ) <sub>2</sub>	68% (182)	83% (183)	90% (184)	90% (185)	82% (186)	47% (187a)	27% (140a)
CF <sub>3</sub>	66%* (188)	100% (189)	54% (190)	56% (191)	87% (192)	38% (193a)	12% (144a)

Table 16: Yields and corresponding compound numbers for each step shown in Scheme 21.

\* synthesised from CF<sub>3</sub>(C=NH)NH<sub>2</sub>

Two modifications have been made to the synthetic sequence from that shown in Scheme 13: the catalyst loading in the Sonogashira step has been reduced from 20 mol % in copper and 10 mol % in palladium, to 12 mol % in copper and 6 mol% in palladium. This reduction is a result of optimisation studies described in Section 3.3.3. The second change is that acetic acid has been added to the final deprotection step. This has been found elsewhere in our laboratories to improve the yield of the removal of the BOM protecting group under palladium mediated hydrogenation conditions (using the H-Cube<sup>TM</sup>). This improvement in yield is most likely down to the acetic acid helping to solubilise the starting material, the intermediate alkane and the product amines, thus reducing losses of compound within the palladium cartridge. The trifluoromethyl analogue **144a** was synthesised in a similar manner

except that the trifluoromethyl substituent is introduced *via* the corresponding amidine as opposed to the nitrile according to the procedure of Norman and co-workers<sup>224</sup> The reaction requires the amidine to act as a nucleophile and attack the amine bearing carbon on the pyrrole fragment. This is a particularly difficult  $S_NAr$  reaction resulting in the loss of ammonia, hence the need for a very high boiling solvent (*o*-xylene). The methoxyethyl compound **142a** was also synthesised from the amidine (Champigny, A. unpublished work).

As described earlier, palladium mediated approaches designed to introduce an amine into the 2-position of the ring system proved unsuccessful. The incorporation of an amine was still of considerable interest as inclusion of a 2-position amine may enable the removal of the 7-position amine (and a large lipophilic chain) whilst retaining a highly basic centre to aid solubility and potential endosomal retention. Such a change may also lead to differing selectivity with respect to cytokine induction. However, perhaps more importantly this change introduces another potential site of metabolism. An amine bearing an alkyl unit may be susceptible to *N*-dealkylation, yielding a metabolite of reduced chain length which may be inactive.

There is literature precedent to suggest a chloromethyl group can be chemically incorporated in the 2-position,<sup>226</sup> therefore **146a** could be synthesised *via*  $S_N2$  displacement of the alkyl chloride present in compound **194a** with ethylamine, followed by an  $S_NAr$  reaction with ammonia. This intermediate could then be hydrogenated to yield compound **146a** as summarised in Figure 46.

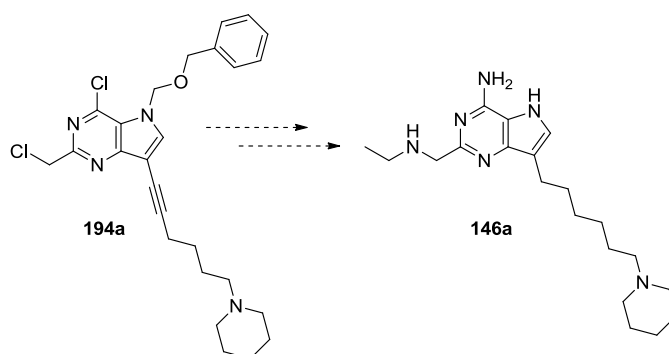
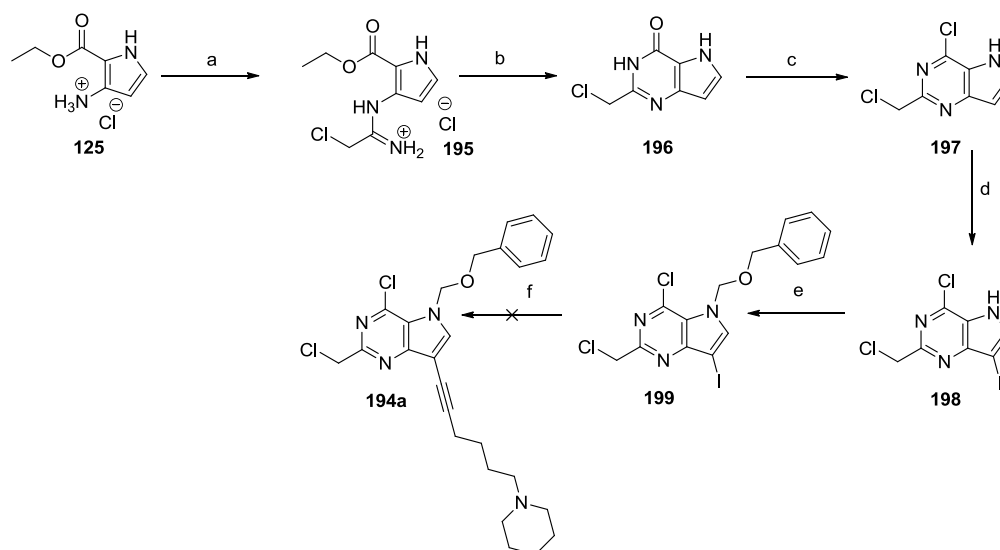


Figure 46: Strategy for the synthesis of **146a**.



The synthesis of intermediate **194a** was attempted using an analogous series of transformations that were used to produce other 2-position variants (Schemes 13 and 21), modifying the first step of the synthesis to use chloroacetonitrile (Scheme 22). The amidine derivative **195** was produced from reaction of **125** with the corresponding nitrile in good yield. In this instance the cyclisation was effected using aqueous ammonia, with cyclisation occurring once the HCl salt has reacted with ammonia and the pH is above 7. Chlorination and iodination proceeded as expected in excellent yields with no chromatography required. In order to protect the pyrrole-like nitrogen it was deprotonated using sodium hydride. It was uncertain whether the nitrogen anion would attack the BOM-Cl as desired or displace the pseudo benzylic chloride leading to self coupling. Pleasingly, the anion reacted with the BOM-Cl furnishing **199** in good yield. Chromatography is usually required at this stage, in this case however the product could be isolated in very high purity by simple trituration of the crude material.

Scheme 22.



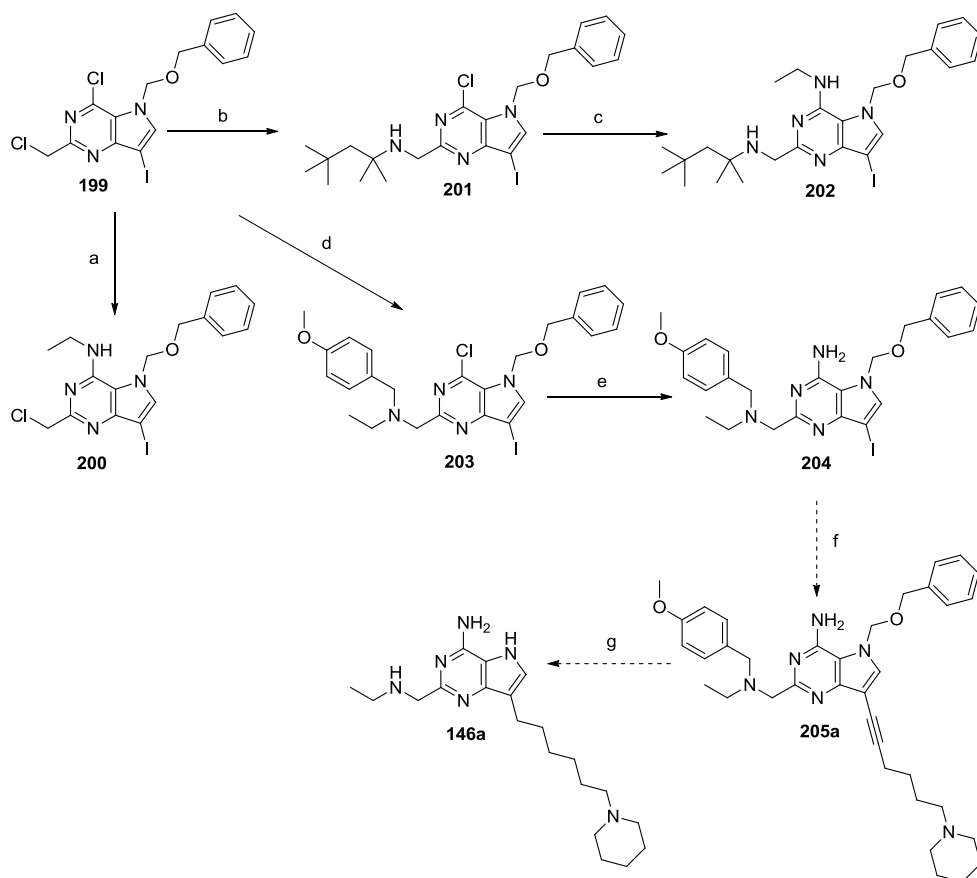
Reagents and conditions: a) HCl, 1,4-dioxane, ClCH<sub>2</sub>CN, 80 °C, 81%; b) NH<sub>3</sub>, H<sub>2</sub>O, 20 °C, 72%; c) POCl<sub>3</sub>, reflux, 86%; d) NIS, THF, 20 °C, 100%; e) BOM-Cl, NaH, THF, 0 °C, 77%; f) Pd(PPh<sub>3</sub>)<sub>2</sub>Cl<sub>2</sub>, CuI, DMF, Et<sub>3</sub>N, 1-(pent-4-yn-1-yl)piperidine (**78**), 20 °C.

The Sonogashira cross coupling of **199** with alkyne **78** was attempted using Pd(PPh<sub>3</sub>)<sub>2</sub>Cl<sub>2</sub> as the catalyst. Analysis of the reaction mixture by LCMS indicated the desired product **194a** had been formed, however, a significant quantity of a by-product was present. During the work-up procedure the desired compound **194a** was converted into the by-product and therefore compound **194a** was not isolated. The by-product shows the same m/z ionisation signal in the LCMS and therefore it is believed that a cyclisation reaction similar to that observed with the 2-aminopyrimidines may have occurred.

The Sonogashira cross coupling reaction was also attempted using Pd(PPh<sub>3</sub>)<sub>4</sub> as the catalyst using DMF as solvent. In this case, there was an improvement in the reaction profile by LCMS, but this did not provide an improved isolated yield. One possible explanation is that further conversion to the putative cyclised material is occurring upon concentration to remove the reaction solvent (DMF). THF is often used as a solvent in Sonogashira reactions and was investigated as the solvent for this reaction. The reaction was carried out at an elevated temperature of 60 °C and led to complete conversion to the putative cyclised by-product by LCMS analysis. In light of this observation the reaction was repeated using THF as solvent but conducting the reaction at ambient temperature over 16 h. Analysis of the reaction by LCMS indicated complete consumption of starting material and a ratio of desired product:by-product of 2:1. As THF was used as solvent the concentration step believed to be responsible for the formation of further by-product was not required, however, even after chromatographic and MDAP purification it was not possible to separate compound **194a** from co-running impurities.

It may be possible to optimise this particular Sonogashira reaction, however it was decided to investigate the introduction of the two required amine functionalities prior to the problematic Sonogashira cross coupling reaction. These investigations are detailed in Scheme 23.

Scheme 23.



Reagents and conditions: a) EtNH<sub>2</sub>, Et<sub>3</sub>N, MeOH, reflux, 34%; b) *tert*-octylamine, Et<sub>3</sub>N, EtOH, reflux, 12%; c) EtNH, Et<sub>3</sub>N, EtOH,  $\mu$ wave, 150 °C, 75%; d) (*p*-methoxybenzyl)ethylamine, Et<sub>3</sub>N, MeCN, reflux, 54%; e) NH<sub>3</sub>, IPA,  $\mu$ wave 150 °C, 84%; f) Sonogashira cross coupling, *vide infra*; g) EtOH, Pd/C Catcart 30 H-Cube<sup>TM</sup> Full H<sub>2</sub>, 60°C;

Compound **199** was reacted with EtNH<sub>2</sub> at reflux in MeOH leading to isolation of a single positional isomer following chromatographic purification. Examination of the HMBC NMR (Figure 47) indicated that the newly introduced CH<sub>2</sub> protons (in the EtNH fragment) correlated to an aryl carbon, and not to a benzylic system.

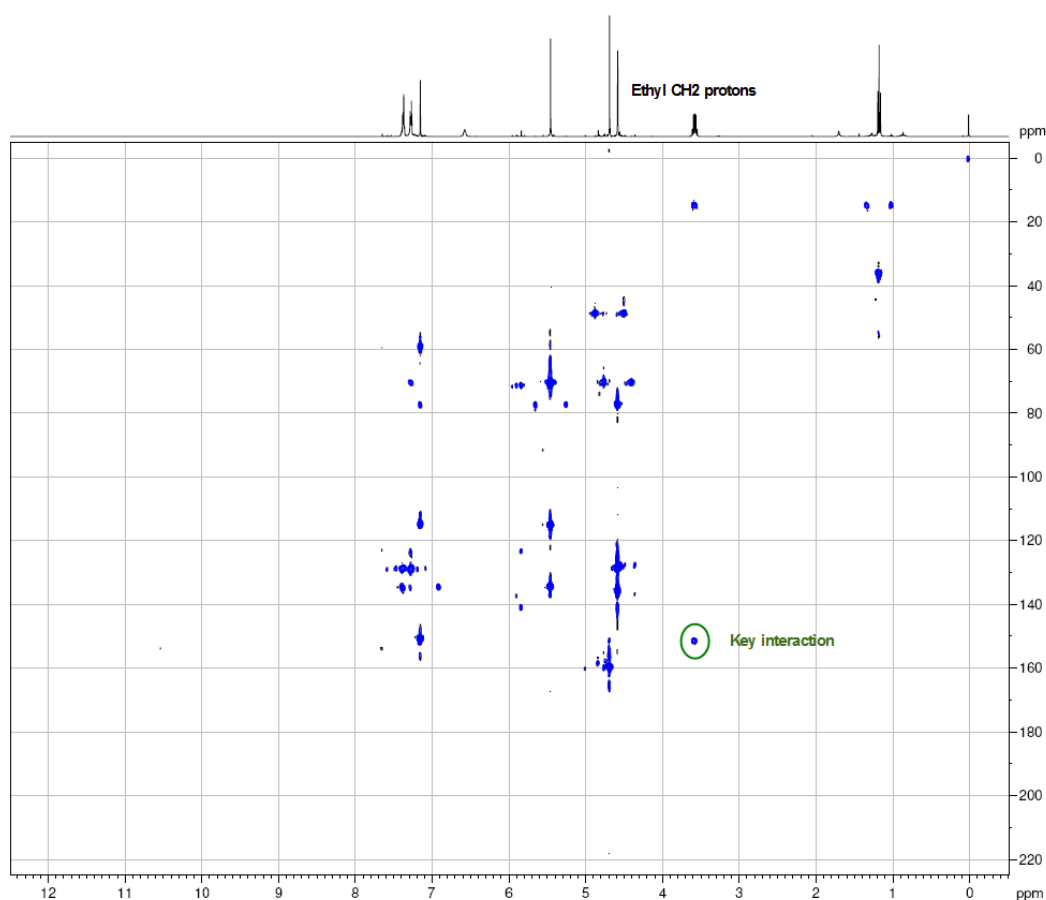


Figure 47: HMBC NMR spectra of compound **200** showing an interaction between the newly introduced CH<sub>2</sub> group and an aromatic carbon atom.

Based on the above, it was determined that EtNH<sub>2</sub> had added to **199** via an S<sub>N</sub>Ar reaction to give **200**, rather than the desired S<sub>N</sub>2 displacement. Given this result it was decided to introduce the aryl amine first. In this case, ammonia was not chosen for this reaction on account of its volatility. Instead, the ammonia equivalent: *tert*-octylamine, was utilised. Again, a single isomer was isolated and this was reacted with EtNH<sub>2</sub>. HMBC NMR utilising the same correlations as previously described was used to confirm the identity of the product molecule as being compound **202** (Figure 48).

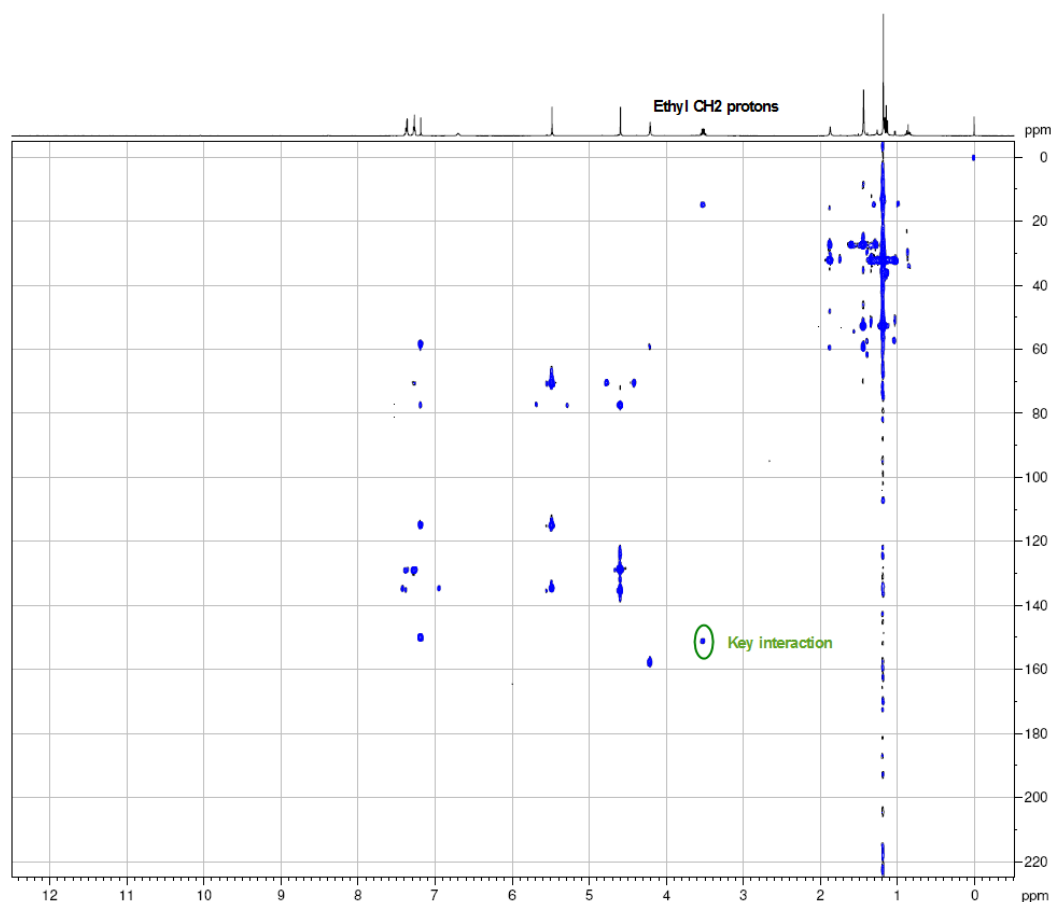


Figure 48: HMBC NMR spectra of compound **202** showing an interaction between the newly introduced CH<sub>2</sub> group and an aromatic carbon atom.

In this instance, it appears that the *tert*-octylamine has switched reactivity and proceeded to add in an S<sub>N</sub>2 fashion to give compound **201**. The difference in reactivity is most likely due to the increased size of this nucleophile with steric clashes with the BOM group disfavouring the desired S<sub>N</sub>Ar reaction.

Given this series of observations a nucleophilic displacement reaction was attempted with (*p*-methoxybenzyl)ethylamine. Being a large nucleophile, one might expect addition to proceed in an S<sub>N</sub>2 fashion, and then it should be possible to remove the 4-methoxybenzyl *via* hydrogenation (most likely concomitantly with the alkyne reduction and BOM removal) to expose the desired 2-position functionality. This strategy was successful with both displacement steps proceeding in satisfactory

yields to furnish compound **204**. Analysis of this compound by  $^1\text{H}$  NMR now shows the characteristic aromatic  $\text{NH}_2$  broad singlet resonance signal at  $\sim 6$  ppm in common with all other BOM protected deazadenine compounds in this series (See Section 4 for examples).

The Sonogashira cross coupling was attempted using the standard conditions ( $\text{PdCl}_2(\text{PPh}_3)_2$ ,  $\text{CuI}$ ,  $\text{Et}_3\text{N}$  in DMF) but failed to show any conversion (by LCMS analysis), indeed it was possible to recover a significant portion of unchanged starting material. This was unexpected as the structure of **204** is very similar to substrates that have successfully undergone Sonogashira cross coupling reactions. A possible explanation for the failure is that molecule **204** contains two similar four atom motifs that could chelate metals (Figure 49). These bidentate motifs are potentially very good metal binders with both a good  $\sigma$ -donor atom and a  $\sigma$ -donor/ $\pi$ -acceptor atom and so could potentially sequester the metal species and prevent cross coupling.

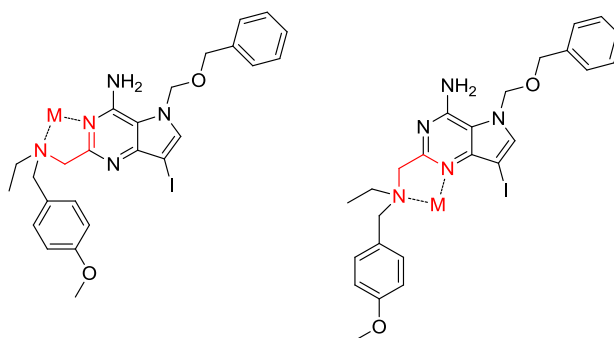


Figure 49: Molecule **204** with possible metal chelation motifs and metal bound shown in red.

If the metal chelated is palladium, one possible solution would be employ a phosphine ligand that is both larger and a more powerful  $\sigma$ -donor than  $\text{PPh}_3$ . Such a ligand may be able to displace the palladium from the *bis*-nitrogen chelator. One such phosphine that has been employed in Sonogashira couplings is  $\text{P}^t\text{Bu}_3$  which is both an extremely good  $\sigma$ -donor as well as exhibiting a cone angle close to  $180^\circ$ .<sup>227</sup> This ligand has been utilised with  $\text{Pd}(\text{PhCN})_2\text{Cl}_2$  as the palladium source in Sonogashira cross couplings.<sup>228</sup> If the metal being chelated is copper then it will be

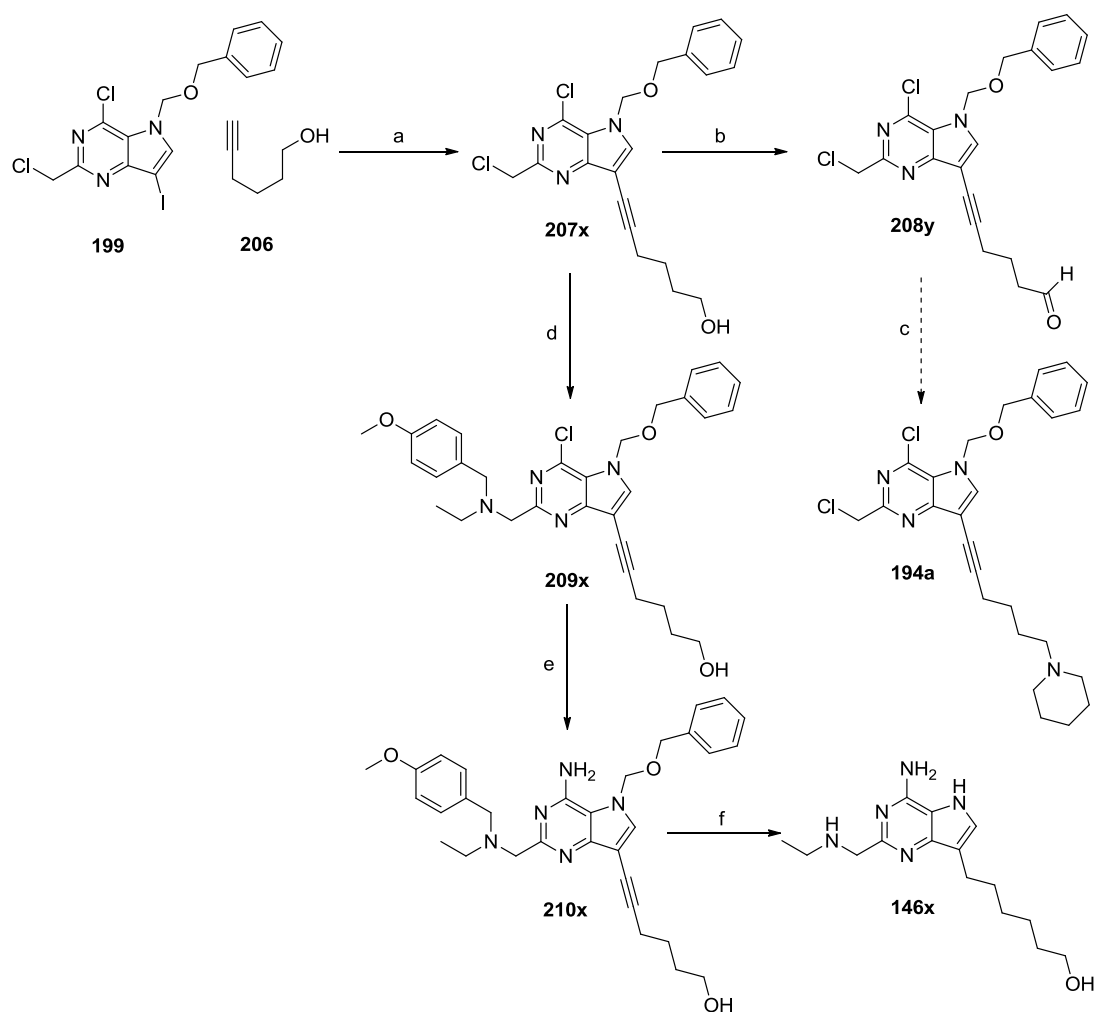
useful to investigate the use of copper free Sonogashira conditions. Conveniently,  $P^tBu_3$  is often used to effect such couplings, for example with  $Pd_2(dba)_3$  and  $Et_3N$ <sup>229</sup> or using  $(allylPdCl)_2$  and  $iPr_2NH$  or DABCO.<sup>230</sup>  $P^tBu_3$  itself is extremely air sensitive and is often substituted for the convenient air stable tetrafluoroborate salt.<sup>231</sup> Therefore the cross coupling was attempted using an amalgamation of the above described conditions namely:  $Pd(PhCN)_2Cl_2$ ,  $HP^tBu_3BF_4$ ,  $iPr_2NH$  and  $CuI$  in DMF. Unfortunately none of these experiments gave the desired compound **205a** in detectable quantities (by LCMS analysis). Given these results it was decided to revisit the chemistry described in Scheme 22 that utilised the dichloro intermediate **199** as the Sonogashira cross coupling partner.

Based on the lack of success in the Sonogashira coupling of **199** with the piperidine functionalised alkyne **78** and the potential cyclization reaction, it was decided to employ methodology analogous to that used for the 2-aminopyrimidines (Scheme 4), that is to use hex-5-yn-1-ol (compound **206**) as the coupling partner and then perform an oxidation to the aldehyde, followed by reductive amination with piperidine to yield compound **194a**. The results of this strategy and further experimentation are detailed in Scheme 24.

Compound **199** successfully underwent a Sonogashira cross coupling with hex-5-yn-1-ol **206**, and it was possible to isolate **207x** in 26% yield. Despite the relatively low yield this method could be used to furnish sufficient quantities of alcohol **207x**. This compound was oxidised to give aldehyde **208y** using TPAP and  $NMO$ <sup>232</sup> albeit again in only a modest yield of 36%. By analysis of the reaction mixture by LCMS the major impurity/side product was determined to be the carboxylic acid, a result of over oxidation. This over oxidation is known to occur if any water is present in the reaction mixture. As the reaction was conducted using 0.115 mmol of alcohol **207x**, only 6.4  $\mu L$  of water is required for complete over oxidation to occur. Therefore, despite the employment of 4 Å molecular sieves to dry the reaction solvent, water that is structurally bound to the glass reaction vessel could account for the over oxidation observed by LCMS. This structurally bound

water could be removed with flame drying, unfortunately this practice is prohibited in our laboratories. Other oxidants have not been investigated as they can lead to significant practical challenges, particularly when employed on a large scale. For example the Swern oxidation leads to the production of toxic and extremely odorous DMS, the use of Dess Martin periodinane or the related IBX pose a significant risk of explosions and the use of chromium reagents is disfavoured for toxicity reasons.

Scheme 24.



Reagents and conditions: a) Pd(PPh<sub>3</sub>)<sub>2</sub>Cl<sub>2</sub>, CuI, DMF, Et<sub>3</sub>N, hex-5-yn-1-ol (**206**), 20 °C, 26%; b) TPAP, NMO, DCM, MeCN, 20 °C, 36%; c) piperidine, NaHB(OAc)<sub>3</sub>, DCM; d) (*p*-methoxybenzyl)ethylamine, Et<sub>3</sub>N, MeCN, reflux, 31%; e) NH<sub>3</sub>, IPA, μwave 150 °C, 87%; f) 1) EtOH, Pd/C Catcart 30 H-Cube™ Full H<sub>2</sub>, 60 °C; 2) TFA, μwave, 150 °C, 22% (2 steps).



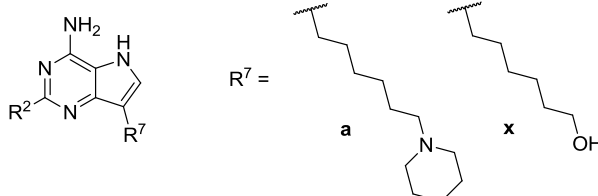
Unfortunately the reductive amination with piperidine did not proceed as desired, some reductive amination did take place to generate **194a** *in situ* but this compound also underwent an S<sub>N</sub>Ar reaction with piperidine displacing the 4-position chloride. It was therefore decided to take alcohol **207x** and introduce the 2-position amine before installing the 7-position pendant piperidine. This was accomplished in an analogous fashion to that previously described in Scheme 23, by performing an S<sub>N</sub>2 displacement with (*p*-methoxybenzyl)ethylamine, followed by an S<sub>N</sub>Ar displacement with ammonia to give compound **210x**. At this stage supplies of alcohol **210x** were extremely limited, and it was therefore decided to perform the hydrogenation and amine deprotections and generate compound **146x**. The hexanol side chain had been proven to convey cytokine induction activity when attached to the lead 2-butyl-deazaadenine core (synthesis discussed in Section 3.3.3). It should therefore still be possible to evaluate the introduction of the 2-position amine as there is at least one active exemplar to form a matched pair for SAR analysis (presented in Section 3.2.2).

### 3.2.2 Investigation of the 2-position: biological results.

The ability of the compounds prepared above to induce IFN $\alpha$  and TNF $\alpha$  was assessed in the human whole blood (HWB) assay available in our laboratories (described above in Section 2.4), with the data presented below in Table 17. The *in vitro* metabolism of compounds of interest was assessed using rat and human liver microsomes, with the IVC data also presented in Table 17 in mL/min/g and scaled again using the “well stirred model” to give a percentage of liver blood flow (LBF) assessment.<sup>224</sup>

Considering the cytokine induction data for compound **123** (2-OBu, Figure 42) which was only weakly active in PBMCs, it is perhaps not surprising that compound **133a** (2-NHBu) does not induce detectable levels of cytokines in HWB. More surprising is the dramatic effect the length of any alkyl chain has at this position. When R<sup>2</sup> is a butyl group (compound **124a**) we observe significant cytokine induction; reducing the length by one methylene group (compound **136a**) leads to a

100 fold reduction in the potency of cytokine induction. A further chain length reduction to an ethyl group (compound **135a**) results in extremely weak cytokine induction, and the methyl compound **134a** did not induce detectable cytokines in the HWB assay.



Compound number	R <sup>2</sup>	Induction of IFN $\alpha$ pEC50	Induction of TNF $\alpha$ pEC50	IVC Rat mL/min/g (% LBF)	IVC Human mL/min/g (% LBF)	cLogP	cLogD <sub>7,4</sub>
124a	CH <sub>2</sub> CH <sub>2</sub> CH <sub>2</sub> CH <sub>3</sub>	6.8	<4.8	8.8 (80%)	1.2 (62%)	6.0	1.6
133a <sup>+</sup>	NH(CH <sub>2</sub> ) <sub>3</sub> CH <sub>3</sub>	<4.3	<4.3	-	-	6.3	2.5
134a*	CH <sub>3</sub>	<4.3	<4.3	-	-	4.4	0.2
135a	CH <sub>2</sub> CH <sub>3</sub>	<4.4	<4.3	-	-	4.9	0.5
136a <sup>+</sup>	CH <sub>2</sub> CH <sub>2</sub> CH <sub>3</sub>	4.9	<4.3	-	-	5.5	0.8
137a	CH <sub>2</sub> (CH <sub>2</sub> ) <sub>3</sub> CH <sub>3</sub>	6.0	4.7	-	-	6.5	1.8
138a	CH(CH <sub>3</sub> ) <sub>2</sub>	<4.3	<4.3	-	-	5.3	1.6
139a <sup>+</sup>	CH <sub>2</sub> CH(CH <sub>3</sub> ) <sub>2</sub>	<4.3	<5.4	-	-	5.9	1.6
140a	CH <sub>2</sub> CH <sub>2</sub> CH(CH <sub>3</sub> ) <sub>2</sub>	5.2	<4.3	-	-	6.4	1.7
141a*	CH <sub>2</sub> CH <sub>2</sub> OCH <sub>3</sub>	6.2	<4.3	5.9 (73%)	<0.5 (<42%)	3.8	0.1
142a*	CH <sub>2</sub> OCH <sub>2</sub> CH <sub>3</sub>	5.9	<5.3	5.9 (73%)	<0.5 (<42%)	4.1	0.8
143a <sup>+</sup>	OCH <sub>2</sub> CH <sub>2</sub> CH <sub>3</sub>	<4.3	<4.8	-	-	5.9	2.1
144a	CF <sub>3</sub>	<4.6	<4.3	-	-	4.9	2.0
145a	Ph	<4.3	<4.3	-	-	6.0	3.1
124x	CH <sub>2</sub> CH <sub>2</sub> CH <sub>2</sub> CH <sub>3</sub>	5.6	4.6	-	-	3.8	1.9
146x	CH <sub>2</sub> NHCH <sub>2</sub> CH <sub>3</sub>	<4.3	<4.3	-	-	1.7	-0.7

Table 17: Summary of cytokine induction data for potential TLR agonists in HWB, \* compounds synthesised by Champigny, A. C. <sup>+</sup> compound synthesised by Courtet, V. C. cLogP calculated using BioByte software,<sup>183</sup> cLogD<sub>7,4</sub> calculated using algorithms available in our laboratories.

This effect is observed in the 8-oxoadenine series (Section 1.9.3) but to a far lesser extent. In the 2-alkyl-8-oxoadenine series the drop in activity when the chain length is reduced from *n*-butyl to methyl was approximately 50 fold<sup>148</sup> and the effect was even less pronounced (approximately 10 fold) in the heteroatom linked series.<sup>149,150</sup> By contrast, the drop in activity in reducing the 2-position *n*-butyl to a methyl in the imidazoquinoline series is only 5 fold (Section 1.9.1).<sup>114,116</sup> When the chain is

extended to *n*-pentyl (compound **137a**) there is a 5-fold reduction in IFN $\alpha$  induction activity and a reduction in cytokine induction selectivity. The reduction in activity observed in the current series broadly matches the SAR of the 8-oxoadenine series (Section 1.9.3). A potential hypothesis that could account for the dramatic reduction in activity with decreasing chain length is that this group is not actively participating in binding to TLR7 but is leading to a conformational change in the target receptor, triggering the agonist response.

Examining the introduction of branching methyl groups onto the alkyl linker (compounds **138a**, **139a** and **140a**) suggests that branching in the alpha, beta and gamma positions results in a reduction in cytokine induction activity of 5-fold or greater. In the 8-oxoadenine series introduction of a branching methyl group in an analogous position was tolerated with no loss in activity (Section 1.9.3). A possible explanation is that the extra steric bulk is preventing the chain or the group in the 2-position accessing the “agonist trigger” point, which could be buried within the receptor active site. An alternative explanation could be that the 9-deazaadenine template is less tolerant of steric bulk in this region as the series may make fewer interactions within the binding site due to the lack of the 8-oxo group.

Further evidence to support this hypothesis is that the phenyl compound **145a** does not act as an agonist and induce cytokines. Aryl groups were successfully incorporated onto an analogous position in the imidazopyridinone agonist series (Section 1.9.4) which also contains an oxo group. Similarly the trifluoromethyl was active in the imidazopyridinone series (Section 1.9.4), and in the 8-oxoadenines (1.9.3) but when incorporated onto the 9-deazaadenine series the resulting analogue (compound **144a**) does not induce detectable levels of cytokines. In this instance, compounds **144a** and **145a** appear to exhibit the same SAR as the imidazoloquinolines series, in which a trifluoromethyl or a phenyl was not tolerated (Section 1.9.1).

Introduction of an ether into the 2-alkyl chain appears to be tolerated, with both **141a** and **142a** showing significant cytokine induction. There is a reduction in the

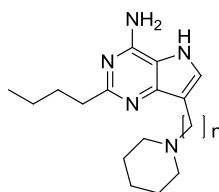
potency of IFN $\alpha$  induction by 0.6 and 0.9 log units, respectively, and the selectivity window is maintained. As expected, an alkyl chain linked to the core by oxygen (**143a**) was not tolerated, confirming that the linking atom is optimally a carbon atom. Both **141a** and **142a** also have significantly reduced lipophilicity (about 100 fold) and as such warranted further investigation. Accordingly, compounds **141a** and **142a** were assessed in rat and human liver microsomes. Both compounds show reduced clearance compared to **124a**. Given the only difference between the molecules is a single point change (carbon exchanged for oxygen), the reduction in clearance is therefore, most likely attributable to the reduction in lipophilicity. Despite this, if clearance can be increased as a result of modification of the 7-position, these 2-position ethers may be revisited.

In conclusion, this 9-deazaadenine series does not appear to completely follow the SAR of either the 8-oxoadenines (Section 1.9.3), imidazoquinolines (Section 1.9.1) or the imidazopyridinone series (Section 1.9.4). In common with both the 8-oxoadenines and the imidazoquinolines, the length of the alkyl chain is optimally four atoms in length but the decrease in activity associated with shorter chains is more pronounced. However, unlike the 8-oxoadenine based series, several structural features are not tolerated. Branching does not appear to be tolerated, whereas this was beneficial in the 8-oxoadenine and 2-aminopyrimidine series. Furthermore, heteroatom linkers, trifluoromethyl groups, and aromatic rings are not tolerated. When heteroatoms are incorporated into the chain the SAR is again divergent compared to previously described series. In the imidazoquinoline series both ether and amine linkers are well tolerated (resiquimod **25** and gardiquimod **26**); in this deazaadenine series ethers are tolerated but amines are not. It is however not completely clear if this effect is related to a difference in permeability for this series or a change from agonist to antagonist behaviour.

### 3.3 Medicinal chemistry strategy 2: investigation of the 7-position.

#### 3.3.1 Investigation of the 7-position: varying the chain length.

The first investigations into the nature of the 7-position substituent focused on varying the length of the alkyl chain connecting the deazaadenine core to the pendant piperidine (Champigny, A. C. unpublished work). The cytokine induction and physicochemical property data for these compounds is shown in Table 18. The compounds shown in Table 18 were synthesised according to method outlined in Scheme 13 using alkynes of differing length in place of piperidine functionalised hexyne **78**.



Compound number	n	Induction of IFN $\alpha$ pEC50	Induction of TNF $\alpha$ pEC50	IVC Rat mL/min/g (% LBF)	IVC Human mL/min/g (% LBF)	cLogP	cLogD <sub>7.4</sub>
<b>124a</b>	6	6.8	<4.8	8.8 (80%)	1.2 (62%)	6.0	1.6
<b>211a</b>	5	6.8	<4.7	30 (93%)	2.0 (73%)	5.5	1.6
<b>212a</b>	4	5.3	<4.8	-	-	4.9	1.4

Table 18: Summary of cytokine induction data for potential TLR agonists in HWB, compounds synthesised by Champigny, A. C.

Considering this small set of compounds it appears that reducing the length of the alkyl chain spacer from hexyl (compound **124a**) to pentyl (compound **211a**) maintains cytokine induction potency and selectivity and importantly from the perspective of topical delivery, this modification increases microsomal clearance in both rat and human liver microsomes. Furthermore, there is the expected reduction in the intrinsic lipophilicity as predicted by cLogP. A further reduction to a butyl linker however reduces cytokine induction and selectivity for IFN $\alpha$  versus TNF $\alpha$  significantly.

### 3.3.2 Investigation of the 7-position: varying the terminal group.

From consideration of the SAR reported for other TLR7 agonist chemotypes (Section 1.9) the nature of the terminal functional group attached to the alkyl linker can convey differing effects on cytokine induction and selectivity. Given that the 5-carbon alkyl linker appears to be optimal in terms of activity and lipophilicity (Table 18) it was chosen as the primary focus for these investigations. It was also postulated that altering the terminal group might have a significant impact of the levels of hepatic clearance. Evidence for this theory was provided by the metabolism prediction software Metasite.<sup>233</sup> This software uses the structural features of the molecule to predict the most likely sites of metabolism. In addition, the software can itself use this information to predict the most likely metabolites. It should be noted however that this software only predicts metabolism by the cytochrome P450 family of enzymes. Compound **211a** was examined using the Metasite tool, and the primary site of metabolism was predicted to be alpha to the tertiary amine. One metabolic process resulting from cytochrome P450 catalysed oxidation alpha to a tertiary amine is *N*-dealkylation.<sup>234</sup> The general mechanism of this process is shown in Figure 50.

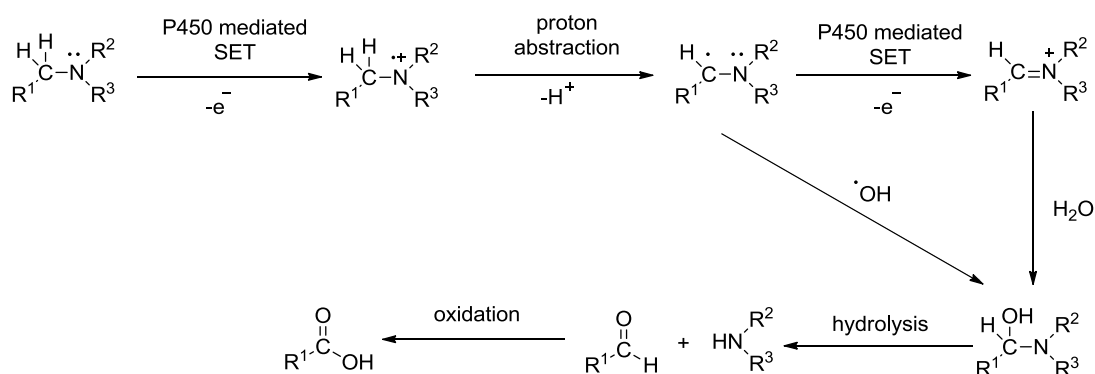
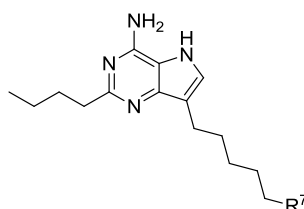


Figure 50: Mechanism of *N*-dealkylation of tertiary amines.

The first step in the mechanism is a P450 mediated single electron transfer (SET) removing an electron from the amine.<sup>235</sup> This is followed by proton abstraction to leave a neutral radical which can either undergo another SET process followed by

reaction with water, or can react with a hydroxy radical.<sup>236</sup> Both processes lead to hydroxylation of the  $\alpha$ -carbon, this intermediate, a hemi-aminal can hydrolyse to give a secondary amine and an aldehyde. The aldehyde is then likely to be further oxidised by any number of hepatic enzymes. For all the different amines evaluated in Metasite, *N*-dealkylation is predicted as the major route of metabolism, giving rise to the carboxylic acid. Given these predictions, the electronic properties of the terminal amine, particularly the pKa may be a crucial determinant in the rate of microsomal clearance, with weakly basic amines promoting the hydrolysis step and highly basic amines being more easily subject to SET processes.



Compound number	R <sup>7</sup>	cLogP	cLogD <sub>7.4</sub>	Predicted amine pKa
211a		5.5	1.6	9.8
211x		3.3	1.9	-
211b		4.9	1.3	10.1
211c		5.2	2.0	9.4
211d		4.9	3.2	8.8
211e		3.3	1.7	5.5
211f		3.9	1.5	7.0
211g		3.3	1.5	9.2
211h		4.3	1.3	9.2

Table 19: Identity and physicochemical predictors of the compounds prioritised for synthesis. Note compound **211b** is included for comparison, pKa predicted using ChemAxon software.<sup>188</sup>

In order to ascertain if this was an area of the deazaadenine that warranted significant attention a small set of eight amine replacements were targeted for synthesis, and these compounds are shown in Table 19. The first of these replacements was an alcohol to investigate if a basic centre is required at all. The other seven replacements were chosen based upon previous experience within our laboratories and inspired by the work of Müller and co-workers<sup>237</sup> in order to cover a wide area of physiochemical property space. It should be noted that all final amine containing compounds amines are tertiary amines. Primary and secondary amines were not included at this stage, as the final compound would contain a highly nucleophilic amine, and as such may be toxic.<sup>238</sup>

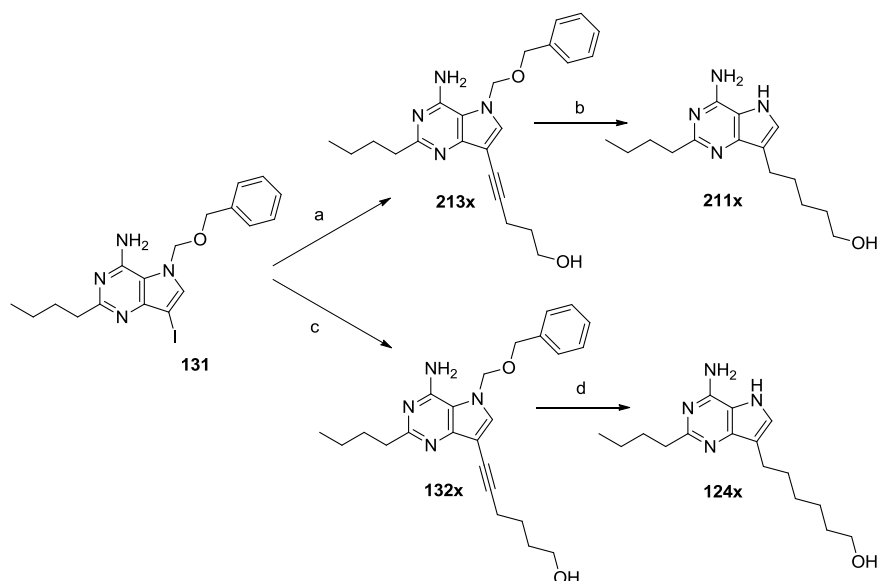
### 3.3.3 Investigation of the 7-position: synthesis.

In order to synthesise the desired compounds (Table 19) it was decided that the existing synthetic route as described in Scheme 21 (herein described as Method A) was no longer appropriate as it would require synthesis of each substituted alkyne individually. It was therefore decided to adapt the methodology developed for synthesis of 2-aminopyrimidines (Scheme 4) i.e. introduction of an alcohol bearing alkyne *via* a Sonogashira cross coupling, followed by subsequent bromination using the Appel reaction.<sup>201</sup>

Alcohol bearing compounds **211x** and the related **124x** (a six atom linked alcohol) were made by the synthetic route shown in Scheme 25 starting with the previously synthesised intermediate **131**. Again, the only synthetic step to cause difficulty was the final removal of the BOM group, with multiple H-cube cycles required to effect complete deprotection.



Scheme 25



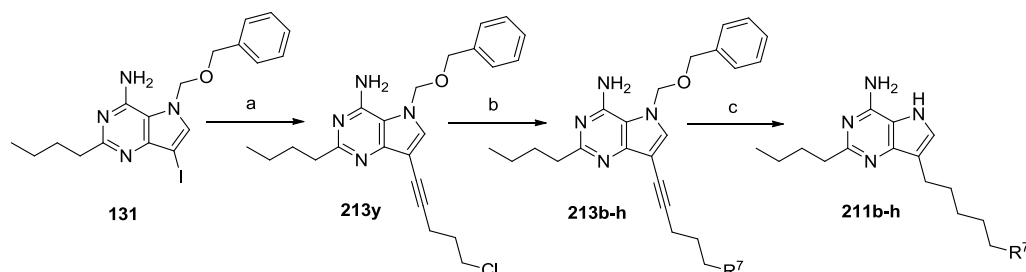
Reagents and conditions: a) Pd(PPh<sub>3</sub>)<sub>2</sub>Cl<sub>2</sub>, CuI, pent-4-yn-1-ol (**80**), Et<sub>3</sub>N, DMF, 20 °C, 59%; b) EtOH, Pd/C Catcart 30 H-Cube<sup>TM</sup> Full H<sub>2</sub>, 60 °C, 28%; c) Pd(PPh<sub>3</sub>)<sub>2</sub>Cl<sub>2</sub>, CuI, hex-5-yn-1-ol (**206**), Et<sub>3</sub>N, DMF, 20 °C, 67%; d) EtOH, Pd/C Catcart 30 H-Cube<sup>TM</sup> Full H<sub>2</sub>, 60 °C, 22%.

Before proceeding with the bromination of **211x** a Sonogashira coupling was attempted using 5-chloropent-1-yne (**214**) as the alkyne coupling partner. Pleasingly the reaction proceeded cleanly to furnish **211y** in 43% yield. Given the reaction with the alcohol functionalised alkyne **80** proceeded in only slightly higher yield (59%, Scheme 25), it was decided to use the chloro compound **211y** as the substrate for the subsequent S<sub>N</sub>2 displacements with the target amines and to optimise this particular Sonogashira cross coupling (Scheme 26: Method B).

Optimisation studies showed that reducing the catalyst loading from 20 mol % in CuI and 10 mol % in Pd(PPh<sub>3</sub>)<sub>2</sub> to 12 and 6 mol %, respectively, accompanied by a reduction in the number of equivalents of 5-chloropent-1-yne **214** from 1.5 to 1.3 gave the best results. When coupled with a purification using aminopropyl functionalised silica chromatography, these improvements resulted in an increased yield of compound **211y** of 79% (Stewart, S. and Coe, D. M. unpublished work). Displacement of the chlorine proved more difficult than expected, requiring three

equivalents of both the desired amine and triethylamine, elevated temperature and long reaction times.

Scheme 26: Method B



Reagents and conditions: a) 6 mol% Pd(PPh<sub>3</sub>)<sub>2</sub>Cl<sub>2</sub>, 12 mol% CuI, 5-chloropent-1-yne (**214**), Et<sub>3</sub>N, DMF, 20 °C, 79%; b) R<sub>1</sub>R<sub>2</sub>NH, Et<sub>3</sub>N; c) H-Cube, Pd/C, H<sub>2</sub>; see Table 20 for yields of steps b and c.

Unfortunately, it was not possible to generate compound **213h** using this methodology. The most likely explanation for this is the volatility of azetidine as other poorly nucleophilic amines did undergo the desired S<sub>N</sub>2 reaction. Once formed intermediates **213b-213g** were subjected to hydrogenation in the H-Cube<sup>TM</sup>, acetic acid was added when possible (all cases except compound **213g**, where esterification is a possibility) in an effort to increase the solubility of the product so maximising recovery. The hydrogenations also proved to be problematic, requiring multiple cycles through the H-cube to achieve complete removal of the BOM group. Following MDAP purification compounds **211b-211g** were isolated in acceptable yields of 21–52% (Table 20).

The biological data for these compounds will be presented in Section 3.3.4, the results of which indicate that modification of the 7-position gives rise to significant differences in the biological profile of 9-dezaadenine compounds.

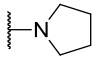
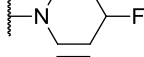
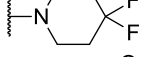
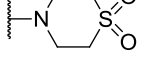
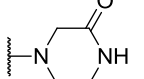
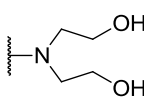
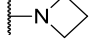
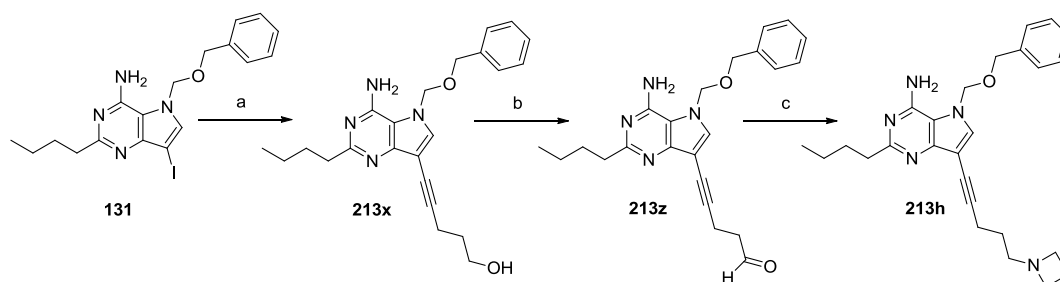
<b>R<sub>7</sub></b>	<b>Step b</b> Compound Number / yield	<b>Step c</b> Compound Number / yield
	<b>213b</b> / 58%	<b>211b</b> / 21 %
	<b>213c</b> / 39%	<b>211c</b> / 45%
	<b>213d</b> / 43%	<b>211d</b> / 33%
	<b>213e</b> / 58%	<b>211e</b> / 38%
	<b>213f</b> / 24%	<b>211f</b> / 52%
	<b>213g</b> / 39%	<b>211g</b> / 48%
	<b>213h</b> / 0%	<b>N/A</b>

Table 20: Summary of the reaction yields observed for steps b and c. An alternative synthetic strategy (Method C) was required to generate azetidine compound **211h** and other compounds derived from volatile amines or amines with reduced nucleophilicity. Given the previously described successful reactions to yield 9-deazaadenines functionalised with terminal alcohols (intermediates **132x** and **213x** Scheme 25), it was decided to investigate the use of these compounds with respect to further functionalisation with amines. One such approach would be to convert the alcohol into the bromide as initially proposed and use this as a substrate in S<sub>N</sub>2 displacements. Despite the enhanced reactivity of bromide with respect to chloride it was anticipated that heat may still be required to effect the displacement and so may still be ineffective in the generation of azetidine compounds **213h** and thus **211h**. It was therefore decided to investigate oxidation of the alcohol to the corresponding aldehyde and use this to perform reductive amination chemistry (Scheme 27).

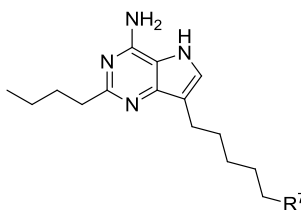
Scheme 27: Method C



Reagents and conditions: a) 10 mol % Pd(PPh<sub>3</sub>)<sub>2</sub>Cl<sub>2</sub>, 20 mol % CuI, pent-4-yn-1-ol (**80**), Et<sub>3</sub>N, DMF, 20 °C, 59%; b) 10 mol % TPAP, NMO, 4 Å sieves, DCM, MeCN, 51%; c) azetidine, Na(OAc)<sub>3</sub>BH, 73%.

Reductive amination reactions usually proceed at ambient temperature, thereby negating problems with either amine volatility or a lack of nucleophilicity. The oxidation of alcohol **213x** was successfully achieved using TPAP/NMO as described by Ley and co-workers<sup>241</sup> to give compound **213z** in a moderate yield of 51%. The reasons for choosing this particular method of oxidation and a potential explanation for the moderate yield have been discussed previously in Section 3.2.1. Pleasingly the reductive amination of aldehyde **213z** with azetidine proceeded smoothly in 73% yield (Champigny, A. C. unpublished work).

Using methods B and C, a wide range of amines have been introduced onto the terminus of the 7-position, separated from the deazaadenine core by either a pentyl or hexyl linker. Those analogues synthesised by the author are described in Table 21 along with the method of synthesis used in each case and the associated yields.



Final compound number	R <sup>7</sup>	Method of synthesis	Yield of intermediate "213"	Yield of final compound "211"
211i		B	63% (213i)	63% (211i)
211j		B	58% (213j)	51% (211j)
211k		B	64% (213k)	38% (211k)
211l		B	45% (213l)	62% (211l)
211m		C	32% (213m)	32% (211m)
211n		C	54% (213n)	44% (211n)

Table 21: Identity, method of synthesis and yields for further 7-position analogues.

### 3.3.4 Investigation of the 7-position: *In vitro* biological results.

To recap, to meet our desired target profile we require the potential candidate to induce IFN $\alpha$  in HWB with a pEC<sub>50</sub> of 7 $\pm$ 0.3 and for there to be at least a 100 fold window between IFN $\alpha$  and TNF $\alpha$  induction. Furthermore, the compound should be rapidly cleared in liver microsomes to try to ensure negligible bioavailability *in vivo*. In addition the compound must have a solubility of > 1 mg/mL at pH 7 and a cLogP < 5.

Given the large number of groups introduced in the 7-position to replace the piperidine present in compound **211a**, the biological data for new analogues is presented in a series of Tables (Tables 22, 23 and 24) where R<sup>7</sup> refers to the functional group at the terminus of the pentyl chain (Figure 51).

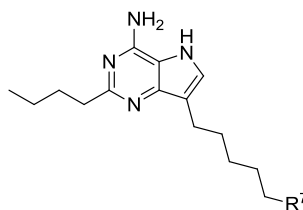


Figure 51: Generic structure of compounds described in Tables 22, 23 and 24

Considering compounds **211a**, **211b**, **211h** and **211i** as a subset where only the ring size of the heterocyclic amine is altered, it is evident that the potencies of IFN $\alpha$  induction when a piperidine or pyrrolidine ring is in place (Compounds **211a** and **211b**) are higher than that for both the smaller and larger ring size compounds. However, it is not simply the ring size that alters between these compounds, as there is a significant increase in cLogP and a slight change in pKa as the ring size increases. Therefore, it is not possible to determine the specific effect the size parameter has on IFN $\alpha$  induction. Considering the IVC data, there does appear to be a correlation between ring size and the level of clearance seen in human liver microsomes. In this set, the larger the ring size, the higher the extent of metabolism observed in human liver microsomes, ranging from a very low predicted *in vivo* clearance of <42% LBF for the azetidine (**211h**) to a high predicted *in vivo* clearance of 77% LBF for the azepane (**211i**). There are several factors that are potentially contributing to this relationship, the size of the ring may be having an effect on binding of the compound to the various metabolising enzymes present in liver microsomes. In addition as the ring size increases there is a concomitant increase in cLogP, which itself will lead to more rapid metabolism. Finally, as explained in Section 3.3.2 pKa of the compounds will affect the rate of metabolism by cytochrome p450s. The azetidine **211b** has the lowest pKa and thus will be the slowest analogue to undergo p450 mediated SET, if this step is rate limiting it may explain the significantly reduced IVC.

Pyrrolidine compound **211b** has a measured aqueous solubility at pH 6 of >3 mg/mL (Gibbon, B. unpublished work) which would be suitable for the desired solution

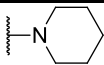
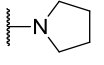
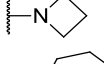
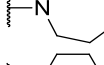
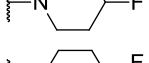
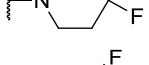
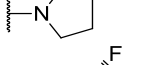
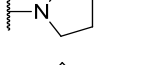
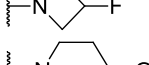
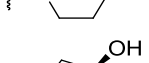
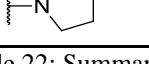
Compound number	R <sup>7</sup>	Induction of IFN $\alpha$ pEC50	Induction of TNF $\alpha$ pEC50	IVC Rat mL/min/g (% LBF)	IVC Human mL/min/g (% LBF)	cLogP	cLogD <sub>7.4</sub>	Predicted amine pKa	Aqueous solubility pH 6 (mg/mL)
*211a		6.8	<4.7	30 (93%)	2.0 (73%)	5.5	1.6	9.8	-
211b		6.7	<4.5	20 (90 %)	1.5 (67 %)	4.9	1.3	10.1	>3
*211h		6.4	<4.3	19 (89 %)	<0.53 (<42 %)	4.3	1.3	9.2	-
211i		6.3	4.7	24 (92 %)	2.4 (77%)	6.0	1.6	10.4	-
211c		7.3	<4.8	16 (88 %)	8.8 (92%)	5.2	2.0	9.4	-
211d		6.1	<4.3	-	-	4.9	3.2	8.8	-
*211o		7.4	4.8	9.7 (82 %)	6.9 (90 %)	4.9	2.2	8.4	-
*211p		7.1	4.7	-	-	4.9	2.2	8.4	-
211n		6.9	4.8	30.5 (93%)	8.7 (92%)	4.6	2.7	6.2	-
#211q		6.1	<4.5	2.6 (54%)	0.58 (44%)	3.4	0.9	9.4	-
*211r		6.0	<4.3	2.8 (56%)	0.85 (54%)	3.7	1.3	9.5	-

Table 22: Summary of *in vitro* biological data for potential TLR agonists in HWB, cytokine induction standard deviation = 0.3

\* compounds synthesised by Champigny, A. C. # compounds synthesised by Stewart, S.

formulation. Given the similarity in pKa over this subset it is likely that the other three compounds would also exhibit significant solubility at this pH.

When a single fluorine atom is added to the piperidine ring (compound **211c**, Table 22) there is a significant increase in the IFN $\alpha$  induction potency of 0.5 log units, with a negligible rise in the TNF $\alpha$  induction potency. Compound **211c** is also less lipophilic than the corresponding unsubstituted piperidine **211a** and yet surprisingly the compound is more rapidly cleared in human liver microsomes. Introduction of a second fluorine atom onto the piperidine ring (compound **211d**) however decreases potency significantly.

Introduction of a fluorine atom onto the pyrrolidine ring (compounds **211o** and **211p** vs. **211b** Table 22) has a similar effect to that seen when introduced onto a piperidine, namely a significant increase in the potency of IFN $\alpha$  induction with only a small rise in the potency of TNF $\alpha$  induction. There appears to be little difference in terms of potency and selectivity between the two enantiomers (assay accuracy is approximately 0.3 units). Substitution of the azetidine with a single fluorine atom (compound **211n**) also leads to an increase in potency of IFN $\alpha$  induction suggestive of a robust structure activity relationship between mono-fluoro substitution and IFN $\alpha$  induction potency.

Compounds **211o** and **211n** were submitted for IVC assessment and again addition of a fluorine onto the ring has significantly increased clearance by human liver microsomes (**211o** vs. **211b** and **211n** vs. **211h**), confirming there is also a relationship between mono fluoro substitution and human metabolism. Compounds **211c**, **211o** and **211n** have the same or reduced cLogP compared to the unsubstituted analogues, it is therefore likely that the pKa difference may be contributing to the increased clearance. The lower pKa of these amines would promote the final hydrolysis step in p450 mediated *N*-dealkylation.

Introduction of an alcohol onto the various cyclic amines might be expected to produce a similar effect to fluorine as these substitutions are often considered isosteric as they are a similar size and electronegativity. Instead, introduction of an



Compound number	R <sup>7</sup>	Induction of IFN $\alpha$ pEC50	Induction of TNF $\alpha$ pEC50	IVC Rat mL/min/g (% LBF)	IVC Human mL/min/g (% LBF)	cLogP	cLogD <sub>7,4</sub>	Predicted amine pKa(s)
#211s		5.4	<4.3	-	-	3.5	0.2	10.5, 8.5
*211t		5.3	<4.3	-	-	3.6	0.1	10.7, 8.0
*211u		4.9	<4.3	-	-	4.2	0.6	10.3, 7.6
#211v		5.9	<4.3	2.9 (57 %)	<0.53 (<42%)	3.1	1.0	9.2
211k		6.9	4.6	-	-	5.4	1.8	10.4
211l		6.8	4.5	-	-	5.4	1.8	10.4
211m		6.7	<4.3	-	-	4.9	3.0	9.3

Table 23: Summary of *in vitro* biological data for potential TLR agonists in HWB, cytokine induction standard deviation = 0.3

\* compounds synthesised by Champigny, A. C. # compounds synthesised by Stewart, S.

alcohol appears to significantly reduce the potency of IFN $\alpha$  induction in all comparable cases (**211q** vs. **211a** and **211r** vs. **211b**). In addition, for those examples where IVC was assessed, the introduction of the hydroxyl results in a significant decrease in IVC in both rat and human liver microsomes. It is possible that this reduction in potency and microsomal clearance is a direct result of the reduced lipophilicity of the hydroxyl substituted amines (Table 22). It should be noted that metabolism in liver hepatocytes has not been assessed and therefore the actual clearance rate of the hydroxyl compounds may be higher than predicted by the microsomal data. This is because liver microsomes do not contain those enzymes responsible for phase 2 metabolic processes such as glycosylation (known to be an important mechanism for clearance of some organic alcohols).

The amine substituted compounds shown in Table 23 were suggested as potential target molecules by another member of our laboratory (Needham, D) as there is literature evidence to suggest that introduction of an amine or acetamide onto a piperidine ring can increase metabolism.<sup>239</sup> Introduction of a basic amine onto the piperidine ring (compounds **211s-211u**) results in a significant decrease in the potency of cytokine induction in all cases. By comparison, introduction of the acetamide (compound **211v**) restored IFN $\alpha$  induction. This compound was assessed in the IVC assay, and proved to be slowly metabolised, which is not consistent with the literature precedent.<sup>247</sup> A possible explanation for this is that all the drug molecules analysed in the literature do indeed contain amino piperidines, however, in all examples the piperidine is directly attached to a (hetero)aromatic rather than separated by an alkyl spacer.

Introduction of an extra methyl group onto the cyclic amines (Table 23) does not result in a significant change in potency. Furthermore, there does not appear to be a significant stereochemical bias (the accuracy of data from the HWB assay is  $\pm 0.3$  log units). Any slight increase in activity is most likely the result of the increased lipophilicity of these compounds.

It was found that the amine could be replaced with a terminal alcohol whilst maintaining a good level of cytokine induction potency and selectivity (compounds

**124x** and **211x**, Table 24). Removal of a basic amine is generally considered to be preferable in terms of limiting off target activity.<sup>176</sup> However the removal of the amine results in a drastically reduced saline solubility of 6 µg/mL (Saklatvala, P. Unpublished work) for compound **124x** (Table 24) as opposed to 2.8 mg/mL for compound **124a** (Figure 43). Based on this, the alcohol **211x** is also likely to have very poor solubility as so cannot not be progressed for solution dosing.

Both thiomorpholine dioxide **211e** and piperizinone **211f** are significantly less lipophilic than lead piperidine **211a** yet still exhibit relatively good IFN $\alpha$  induction potency. Both compounds are also cleared by liver microsomes to a similar extent as the lipophilic amines **211a** and **211b**, and thus are of significant interest. Disappointingly, however, both compounds show reduced aqueous solubility at pH 7.4 (Table 24), almost certainly as a direct result of the reduced amine pKa.

The diethanolamine compound **211g** appears to display the same SAR as observed for hydroxyl substituted cyclic amines in that the compound still exhibits moderate potency but shows low turnover in liver microsomes.

Introduction of a morpholine ring (compound **211j**) results in a highly active compound with respect to IFN $\alpha$  induction with selectivity over TNF $\alpha$  induction of approximately 500 fold. The isosteric spirocyclic oxetane compound **211w**, however, had significantly less IFN $\alpha$  induction and reduced selectivity. The two compounds are very similar in terms of lipophilicity and share the cyclic ether motif but do differ in the pKa of the amine by 0.6 log units (4 fold). Therefore, it is possible that the pKa of the amine does play a significant role in determining the level and nature of cytokine induction. The other key difference in these compounds is the molecular flexibility, with the morpholine being able to adopt a conformation that can place the cyclic ether in a favourable position to pick up a positive interaction or to avoid a negative interaction.

Compound number	R <sup>7</sup>	Induction of IFN $\alpha$ pEC50	Induction of TNF $\alpha$ pEC50	IVC Rat mL/min/g (% LBF)	IVC Human mL/min/g (% LBF)	cLogP	cLogD <sub>7.4</sub>	Predicted amine pKa(s)	Aqueous solubility saline mg/mL
211x		6.4	4.7	-	-	3.3	1.9	-	-
124x		5.6	4.6	-	-	3.8	1.9	-	0.006
211e		6.3	<5.4	9.5 (82 %)	7.5 (90%)	3.3	1.7	5.5	0.021
211f		6.3	<4.6	5.1 (69 %)	2.3 (73 %)	3.9	1.5	7.0	0.074
211g		6.3	<4.8	3.1 (58 %)	<0.53 (<42%)	3.3	1.5	9.2	-
211j		7.1	4.7	-	-	4.3	2.0	7.7	-
*211w		6.0	4.7	-	-	4.1	2.5	8.5	-

Table 24: Summary of *in vitro* biological data for potential TLR agonists in HWB, cytokine induction standard deviation = 0.3,

\* compound synthesised by Champigny, A. C.

Considering all the compounds from Tables 22, 23 and 24, there still do not appear to be any obvious relationships between the physicochemical parameters of pKa, cLogP or size with the biological parameters, cytokine induction and IVC. However, there are some meaningful structure activity relationships that can be discerned. For example, introduction of an alcohol onto any of the cyclic amine systems appears to have a consistent effect; reducing cytokine induction and reducing P450 mediated metabolism in all cases. This reduction is unlikely to be simply the introduction of a highly electronegative atom, as introduction of fluorine appears to increase induction and in some cases metabolism, nor is it likely to be a simple lipophilicity effect or pKa effect, as the sulfone containing compound (**211e**) maintains cytokine induction and is rapidly turned over. It is perhaps more likely that the presence of a hydrogen bond donor is the key chemical feature. This would also explain the diminished cytokine induction seen for amines **211s-211u** which also possess hydrogen bond donors, either present in the parent structure or *via* protonation of the amine within the endosome. In contrast, molecules bearing a strong hydrogen bond acceptor function in the region of the molecule such as a carbonyl or sulfonyl group appear to maintain good IFN $\alpha$  induction, and are in some cases perhaps also slightly more selective for IFN $\alpha$  over TNF $\alpha$  induction. It is possible that the presence of a hydrogen bond donor in the region of the molecule is forming a negative interaction with the enzyme responsible for metabolism. This may retard metabolism attributable to that particular enzyme, possibly to such an extent that a different enzyme becomes the major metaboliser. Compound **211v** features both a hydrogen bond donor and an acceptor which may explain the good cytokine induction profile but significantly reduced metabolism.

There are a number of analogues in this set that either meet or are likely to meet the desired primary *in vitro* and physiochemical criteria for a potential clinical candidate. These include piperidine **211a** and pyrrolidine **211b** both of which are rapidly cleared and have greater than 100 fold selectivity for IFN $\alpha$  induction over TNF $\alpha$  induction and a pEC<sub>50</sub> for IFN $\alpha$  in the desired window. Compound **211b** has a measured solubility of > 3 mg/mL at a pH of 6 and given the pKa of compound **211a** this is likely to be similarly soluble. Of the two molecules **211b** is favoured due its

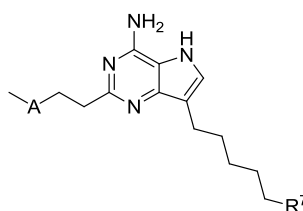
lower lipophilicity. Three fluorinated compounds **211c**, **211o**, and **211p** are also worthy of consideration. They have activity at the top end of the desired window (7-7.3) and show good selectivity and rapid clearance. These fluorinated analogues are less basic than **211b** and so may be slightly less soluble.

### 3.4 Revisiting compounds with an ether in the 2-position.

Previous introduction of an ether into the butyl group in the 2-position has been shown to slightly reduce cytokine induction but significantly reduces metabolism of the compounds in liver microsomes. Through investigation of the 7-position it has been discovered that reduction in ring size from a piperidine to a pyrrolidine with a concomitant reduction in chain length to a five methylene spacer, maintains metabolism (whilst reducing cLogP). Furthermore, introduction of a single fluorine atom onto a cyclic amine can increase cytokine induction and metabolism. It is therefore logical that these chemical motifs be combined in the same molecule and may give rise to compounds with the exact balance of biological properties required to enable selection of a development candidate. Four such molecules were synthesised using method B; *via* a chloro displacement (Stewart, S.; Champigny, A. C. unpublished work). The biological results for these compounds are shown in Table 25, along with compounds described in Section 3.2.2.

In the previous 2-butyl series, substitution of a methyl-piperidine for a pyrrolidine (**124a** versus **211b**) maintained cytokine induction, but in this case a significant decrease in cytokine induction (**141a** vs. **214b**) is observed. Surprisingly, introduction of a fluorine atom onto either a pyrrolidine or piperidine ring did not increase cytokine induction into the desired window. As observed previously (Section 3.2.2, Table 17), for the same amine at the terminus of the 7-position, compounds with an ether in the 2-position are less rapidly cleared than their 2-butyl counterparts (compound **214c** vs. compound **211c**). This is perhaps due to the generally reduced intrinsic lipophilicity of the series, such that the cLogP now falls within the range shown to give rise to lead like oral candidates.<sup>171</sup> It appears the

SAR of the 7-position in this series may be slightly different to the 2-butyl series, with SAR observed separately in the 2 and 7 positions not being additive.



Compound number	R <sup>7</sup>	A	Induction of IFN $\alpha$ pEC50	Induction of TNF $\alpha$ pEC50	IVC Rat mL/min/g (% LBF)	IVC Human mL/min/g (% LBF)	cLogP	cLogD <sub>7,4</sub>
124a		CH <sub>2</sub>	6.8	<4.8	8.8 (80 %)	1.2 (62 %)	6.0	1.8
141a		O	6.3	<5.3	5.9 (73 %)	<0.53 (<42 %)	3.8	0.1
211b		CH <sub>2</sub>	6.7	<4.5	20 (90 %)	1.5 (67 %)	4.9	1.3
211c		CH <sub>2</sub>	7.3	<4.8	16 (88 %)	8.8 (92 %)	5.2	2.0
#214b		O	5.7	<4.3	-	-	2.7	-0.3
#214c		O	6.2	<4.3	6.4 (75 %)	0.61 (45 %)	3.0	0.5
*214o		O	5.6	4.4	-	-	2.7	0.8
*214p		O	5.4	<4.3	-	-	2.7	0.8

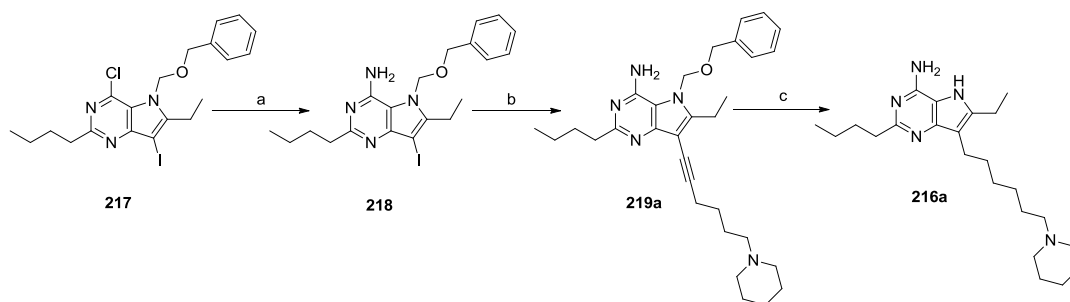
Table 25: Summary of cytokine induction data in HWB, standard deviation = 0.3, associated physicochemical data and measured *in vitro* clearance for potential TLR agonists. \* compound synthesised by Champigny, A. C. # compound synthesised by Stewart, S. cLogP calculated using BioByte software,<sup>183</sup> cLogD<sub>7,4</sub> calculated using algorithms available in our laboratories, pKa predicted using ChemAxon software.<sup>188</sup>

### 3.5 Investigation of the 6-position.

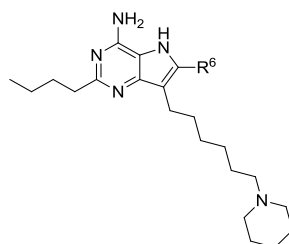
In parallel to the investigations described above some initial investigations into the nature of the 6-position substituent were undertaken, focusing on methyl and ethyl substituents. The synthesis of the ethyl compound **216a** from intermediate chloride **217** (available in our laboratory, synthesised by Champigny, A. C. unpublished work) is shown in Scheme 28. The methyl analogue was synthesised by an analogous

method by another member of our laboratory (Champigny, A. C. unpublished work). The *in vitro* cytokine induction data for these analogues is shown in Table 26.

Scheme 28



Reagents and conditions: a) NH<sub>3</sub>, IPA,  $\mu$ wave 150 °C, 73%; b) Pd(PPh<sub>3</sub>)<sub>2</sub>Cl<sub>2</sub>, CuI, 1-(pent-4-yn-1-yl)piperidine (**78**), Et<sub>3</sub>N, DMF, 20 °C, 24%; c) H-Cube™, Pd/C, H<sub>2</sub>, EtOH, 35%.



Compound number	R <sup>6</sup>	Induction of IFN $\alpha$ pEC50	Induction of TNF $\alpha$ pEC50	cLogP	cLogD <sub>7.4</sub>
*124a	H	6.8	<4.8	6.0	1.6
*215a	CH <sub>3</sub>	7.5	4.9	6.4	2.2
216a	CH <sub>2</sub> CH <sub>3</sub>	5.6	4.7	7.0	2.6

Table 26: Summary of cytokine induction data in HWB, standard deviation = 0.3, and associated physiochemical data. \* compound synthesised by Champigny, A. C.

Introduction of a methyl group into the 6-position leads to a significant increase in the potency of induction of IFN $\alpha$  (to a level above our desired maximum) and also increases selectivity over TNF $\alpha$  induction. Extension to an ethyl group however causes a significant decrease in activity and selectivity. Given this limited data set and the availability of substituted pyrroles, investigations into the 6-position were not continued. Alternative synthetic strategies to directly functionalise the



deazaadenine ring such as C-H activation<sup>240</sup> might provide access to further analogues but has not been pursued at this time.

It has been demonstrated (in Section 3.3.1) that reducing the length of the linker in the 7-position to four carbons reduces the potency of IFN $\alpha$  induction. It was therefore anticipated that combining this structural feature with a 6-methyl substituent might result in IFN $\alpha$  potency in our desired range. Accordingly, compound **220b** (Figure 52) was considered worthy of investigation. The pyrrolidine was chosen to be the terminal amine as when linked through a five carbon linker this group conveyed good cytokine induction and moderate human *in vitro* clearance (Section 3.3.4).

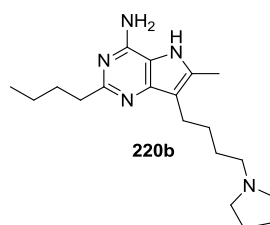
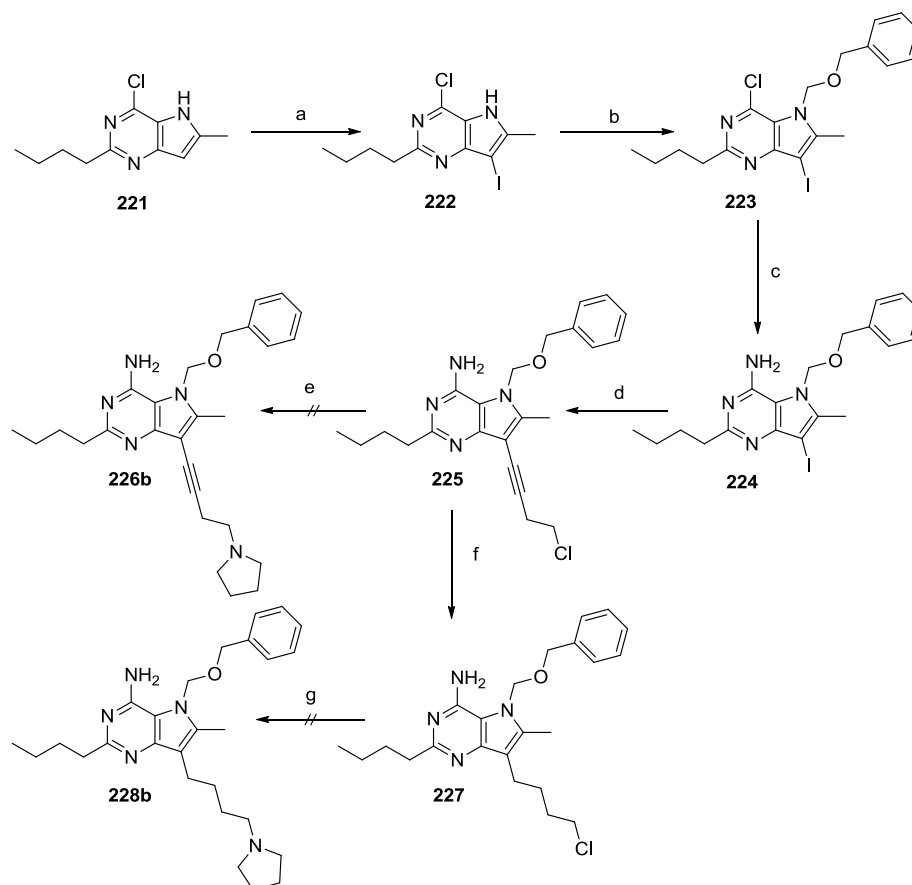


Figure 52: Structure of compound **220b** combining a 6-methyl group with a four carbon linked pyrrolidine.

The synthesis of compound **220b** using Method B (see Scheme 26 for general conditions) did not prove to be straightforward (Scheme 29). Intermediate **221** (available in our laboratory, synthesised by Champigny, A. C. unpublished work) was iodinated using NIS in an excellent yield of 98%. The BOM protection was then introduced through deprotonation of the pyrrole-like nitrogen using NaH, followed by an S<sub>N</sub>2 displacement reaction with BOM-Cl. The amine at the 4-position was introduced by an S<sub>N</sub>Ar reaction of the aryl chloride **223** with ammonia. At this stage a Sonogashira cross coupling reaction was carried out with 4-chlorobut-1-yne as the coupling partner, which proceeded to furnish compound **225** in 49% yield. The desired S<sub>N</sub>2 reaction between compound **225** and pyrrolidine did not proceed as desired, instead appearing (from LCMS analysis) to have undergone an elimination reaction (probably E<sub>2</sub> in nature) to give an alkene. The driving force for this elimination is presumably that a highly conjugated species is

generated. Given this observation it was decided to attempt to hydrogenate the alkyne so removing the possibility of conjugation. To ensure the survival of the BOM group the hydrogenation was carried out at 20 °C in the absence of AcOH. This reaction proceeded as desired, with no BOM deprotection observed by LCMS of the reaction, to give compound **227** in a satisfactory yield of 73%. Unfortunately the displacement reaction using compound **227** still did not proceed as desired, again with elimination observed by LCMS analysis of the reaction mixture. This was surprising as elimination had not been observed in any other displacement reaction where production of a conjugated species was not a possibility.

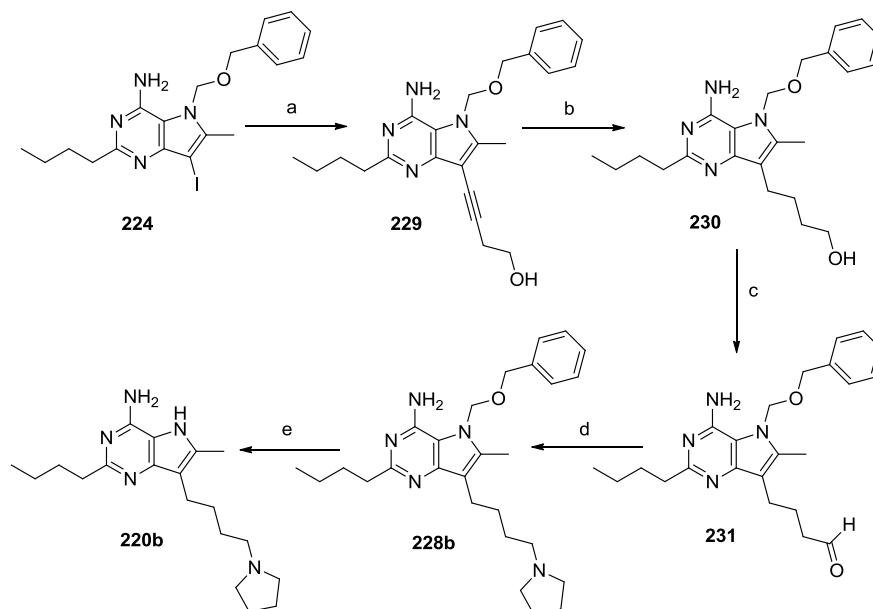
Scheme 29:



Reagents and conditions: a) NIS, THF, 98%; b) BOM-Cl, NaH, THF, 69%; c) NH<sub>3</sub>, IPA,  $\mu$ wave 150 °C, 90%; d) Pd(PPh<sub>3</sub>)<sub>2</sub>Cl<sub>2</sub>, CuI, 4-chlorobut-1-yne, Et<sub>3</sub>N, DMF, 20 °C, 49%; e) pyrrolidine, Et<sub>3</sub>N, MeCN, 60°C; f) H-Cube™, Pd/C, H<sub>2</sub>, EtOH, 73%; g) pyrrolidine, Et<sub>3</sub>N, MeCN, 60°C.

As a result compound **220b** was synthesised by an alternative strategy as outlined in Scheme 30.

Scheme 30:



Reagents and conditions: a) Pd(PPh<sub>3</sub>)<sub>2</sub>Cl<sub>2</sub>, CuI, but-3-yn-1-ol, Et<sub>3</sub>N, DMF, 20 °C, 59%;  
b) H-Cube<sup>TM</sup>, Pd/C, H<sub>2</sub>, EtOH, 63%; c) TPAP, NMO, DCM, MeCN, 50%; d) pyrrolidine,  
Na(OAc)<sub>3</sub>BH, 47%; e) H-Cube<sup>TM</sup>, Pd/C, H<sub>2</sub>, EtOH, AcOH, 53 %.

Given the problems observed with elimination occurring instead of displacement, it was decided to proceed with introduction of the pyrrolidine *via* a reductive amination approach similar to Method C (see Scheme 27 for general conditions). Accordingly, compound **224** was cross coupled with but-3-yn-1-ol in a moderate yield of 59%. It was feared that if oxidation to the aldehyde was undertaken on this compound (**229**) that the oxidised compound would reside exclusively in the enol form, as a result of conjugation, therefore being resistant to reductive amination. In order to prevent this possibility, the alkyne in compound **229** was hydrogenated to give alcohol **230**. Oxidation with TPAP/NMO proceeded in 50% yield to furnish aldehyde **231**. The pyrrolidine was then introduced by reductive amination and converted to compound **220b** by further hydrogenation in the presence of AcOH, thereby removing the BOM

protecting group. Compound **220b** was submitted for activity testing and for IVC assessment (Table 27).

Compound Number	Induction of IFN $\alpha$ pEC50	Induction of TNF $\alpha$ pEC50	IVC Rat mL/min/g (% LBF)	IVC Human mL/min/g (% LBF)	cLogP	cLogD <sub>7,4</sub>
<b>220b</b>	6.2	<4.5	18.6 (90 %)	<0.53 (<42%)	4.8	1.4

Table 27: Summary of cytokine induction data in HWB, standard deviation = 0.3, associated physiochemical data and measured *in vitro* clearance for compound **220b**.

The combination of a 6-methyl function with a reduced chain length 7-position linker has resulted in IFN $\alpha$  induction below our desired potency range. Furthermore, the compound is not appreciably turned over in human liver microsomes. Based on this compound **220b** was not progressed further.

### 3.6 Selection of a compound for further biological/toxicology studies.

From consideration of all potential TLR7 mediated cytokine inducers synthesised to date the most promising compounds remain those described in Section 3.3.4. Of these compounds, pyrrolidine **211b** was chosen as the most promising potential candidate molecule (Figure 53).

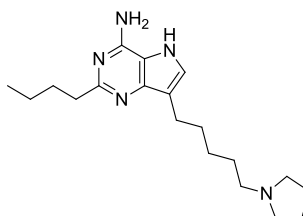


Figure 53: Structure of potential clinical compound **211b** selected for further profiling.

This compound was selected in preference to the fluorinated compounds **211c**, **211o**, and **211p** for two reasons. As compounds **211c** and **211o** are at the high limit of our desired IFN $\alpha$  induction window, there remains the possibility that final clinical doses of these compound may be in the nanogram range, leading to potential formulation challenges. In addition, there is a cost of goods advantage to using pyrrolidine as the terminal base as opposed to a fluorinated amine, particularly a chiral amine such as those present in compounds **211o** and **211p**.

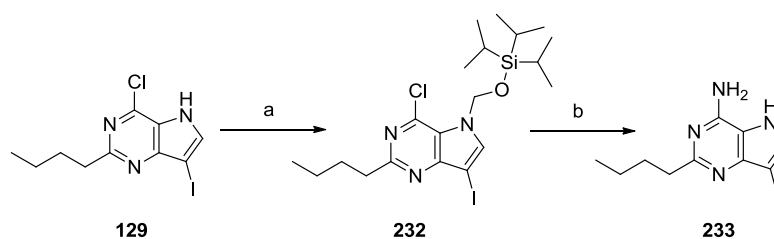
### 3.7 Large scale synthesis of compound **211b**.

Having selected compound **211b** for further profiling, larger quantities of material need to be prepared. Therefore it was decided to attempt to address some of the challenges associated with the current synthetic route, specifically the introduction of the desired amine group at the terminus of the 7-position alkyl chain and the removal of the BOM protecting group.

#### 3.7.1 Investigation into alternatives to the BOM protecting group.

During the synthesis of the above described compounds the removal of the BOM protecting group has often proven to be problematic. Therefore different protecting group strategies were evaluated. A number of groups have been reported in the literature as being incorporated onto 9-deazaadenines to protect the 5-position nitrogen, these include the previously described BOM group and two similar variants the TOM<sup>241</sup> and SEM<sup>242</sup> groups. Both of these groups are removed using fluoride ions and so may provide a suitable alternative to the difficult to remove BOM group. The first alternative to be investigated was the TOM group (Scheme 31, Courtet. V.; unpublished work).

Scheme 31 Evaluation of TOM protection.

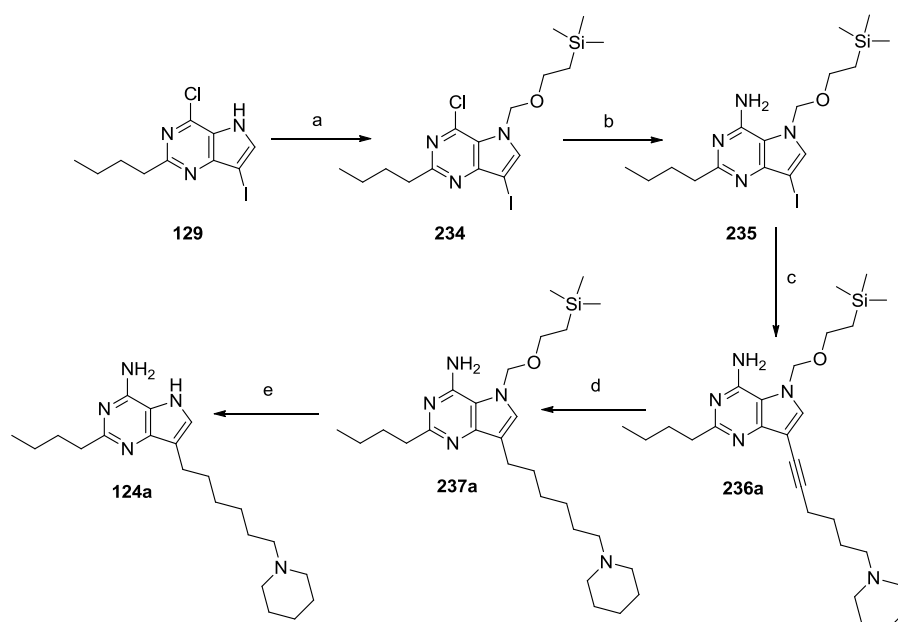


Reagents and conditions: a) NaH, TOM-Cl, THF, 0 °C, 96%; b) NH<sub>3</sub>, IPA,  $\mu$ wave, 150 °C, compound not isolated, structure derived from LCMS analysis.

The TOM moiety was introduced in an analogous manner to BOM, using TOM-Cl and sodium hydride to functionalise **129** in an excellent yield of 96%. Disappointingly, when subjected to the conditions necessary to introduce the

2-amino group, removal of the TOM group was observed according to LCMS analysis.

Scheme 32



Reagents and conditions: a) NaH, SEM-Cl, THF, 0 °C, 90%; b) NH<sub>3</sub>, IPA,  $\mu$ wave, 150 °C, 75%; c) Pd(PPh<sub>3</sub>)<sub>2</sub>Cl<sub>2</sub>, CuI, 1-(pent-4-yn-1-yl)piperidine (**78**), Et<sub>3</sub>N, DMF, 20 °C, 20%; d) EtOH, AcOH, Pd/C Catcart 30 H-Cube™ Full H<sub>2</sub>, 60 °C, 57%; e) THF, ethylene diamine, TBAF, 70 °C, 50%.

The SEM group was introduced using SEM-Cl and sodium hydride in 90% yield, and this group did survive the amination conditions (Scheme 32). In order to evaluate this protecting group further it was decided to resynthesise **124a**. Once the SEM group was introduced a Sonogashira reaction using the piperidine functionalised alkyne **78** as the coupling partner was attempted, although this reaction proceeded in a disappointing yield of 20%. The primary reason for this reduction in yield is that the purification of **236a** proved extremely challenging as there were several very close running impurities when using normal phase purification conditions. Hydrogenation of the alkyne proceeded in a moderate yield of 57%, this yield is lower than expected, but is most likely due to losses of compound within the CatCart being more significant (in yield terms) for small scale reactions. The SEM group was removed using the conditions of Muchowski and co-

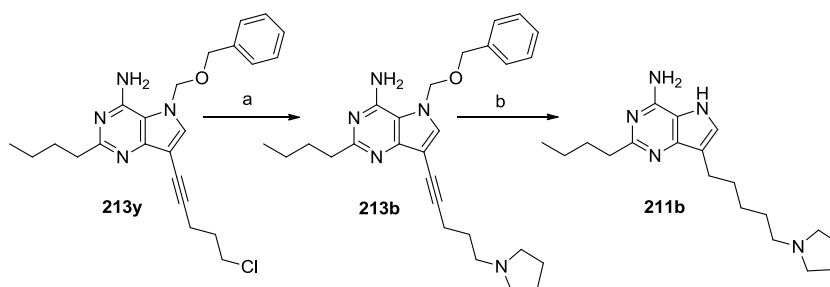
workers,<sup>243</sup> here in addition to TBAF, ethylene diamine is used as a scavenger to remove the formaldehyde generated during the deprotection. The deprotection proceeded in a moderate yield of 50% after purification by MDAP.

In conclusion, use of the SEM protecting group offers no advantage over the previously employed BOM group, in fact using the SEM group presents its own challenges, particularly during the purification of Sonogashira cross coupling reactions. Another protecting group often used for indole-like nitrogens is the tosyl (or the closely related benzene sulfonyl) group. This group however, would not be compatible with the current synthetic strategy. The sulfonamide function would be hydrolysed during the nucleophilic displacement reaction with ammonia (given the forcing conditions required). Therefore, the BOM group was utilised in the large scale synthesis of compound **211b**.

### 3.7.2 Optimisation of Method B to prepare **211b**.

When compound **211b** was first prepared from chloro compound **213y** the initial chloro displacement using three equivalents each of triethylamine and pyrrolidine gave intermediate compound **213b** in 58% yield. The formate salt of **211b** was then isolated in 21% yield following catalytic hydrogenation and purification by MDAP. Through the use of chloro derivative **213y** produced according to the optimised conditions (described in Section 3.3.3, Scheme 26) compound **213b** was prepared in 69% yield (Coe, D. M. Unpublished work).

Scheme 33: Optimised synthesis of **213b** via chloro displacement and conversion to **211b** [Method B]



Reagents and conditions: a) pyrrolidine, Et<sub>3</sub>N, MeCN, 60 °C, 69%; b) H-Cube<sup>TM</sup>, 10 % Pd/C, H<sub>2</sub>, EtOH, AcOH, 61%.

Following hydrogenation using the H-Cube<sup>TM</sup> apparatus and a trituration using hot ethyl acetate (Scheme 33) compound **211b** was isolated in excellent purity (99.2% purity by HPLC and NMR) as a crystalline free base. This method was employed to deliver gram quantities of compound **211b** at a purity level suitable for toxicological assessment.

### 3.8 Further *in vitro* biological assessment of **211b**: the functional PBMC assay.

Having demonstrated that compounds from the deazaadenine series do induce IFN $\alpha$  in human whole blood, the next requirement is to ascertain if this cytokine induction can alter the allergic response following allergen exposure. The purpose of the functional PBMC assay is to assess if a compound of interest can modify the allergic response *in vitro*. The assay employs PBMCs from human volunteers who are allergic to Timothy grass (TG) pollen, or to house dust mites (HDM). The cells are cultured with the allergen and varying concentrations of the compound of interest, after 5-6 days the cells are spun in a centrifuge and the supernatant collected and analysed for the presence of various cytokines. In the absence of the IFN $\alpha$  inducing TLR7 agonist the allergic T<sub>H</sub>2 response would dominate (Section 1.2) and so cytokines associated with this response such as IL5 and IL13 would be present. The cytokine levels observed for compound **211b** from the two such allergen driven PBMC assays for one representative donor are shown in Figures 54 and 55 (Priest, F. Unpublished work).



**GSK CONFIDENTIAL – Property Of GSK – Copying Not Permitted**  
 The Synthesis and Optimisation of Toll-like Receptor Agonists as Potential Immunomodulatory Agents.

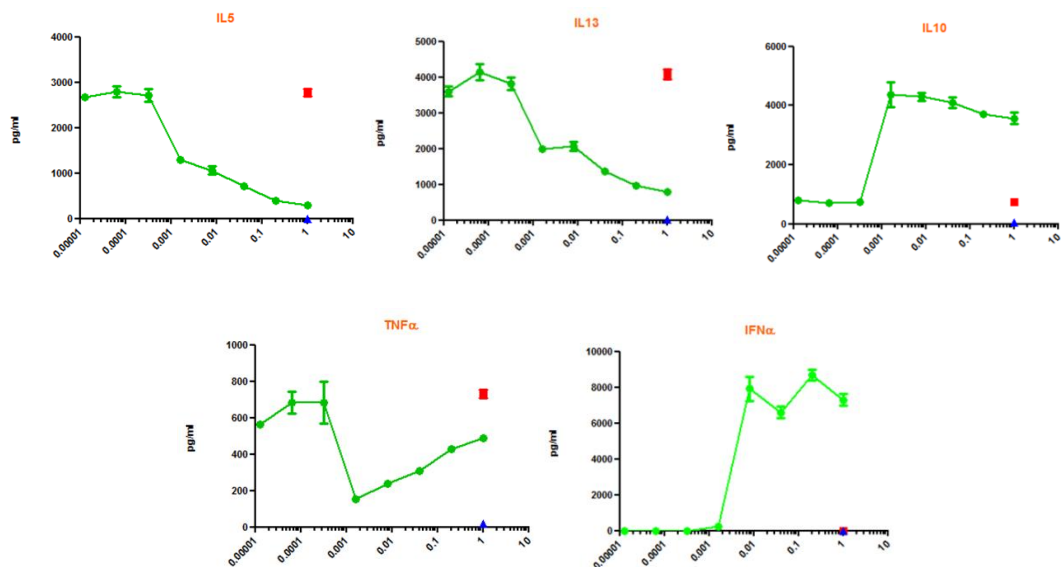


Figure 54: Cytokine production from one representative HDM allergic donor PBMCs when treated with compound and allergen. X-axis is compound concentration (µM), the green line is for compound **211b**, red marker response to allergen only, blue marker no allergen or TLR7 agonist.

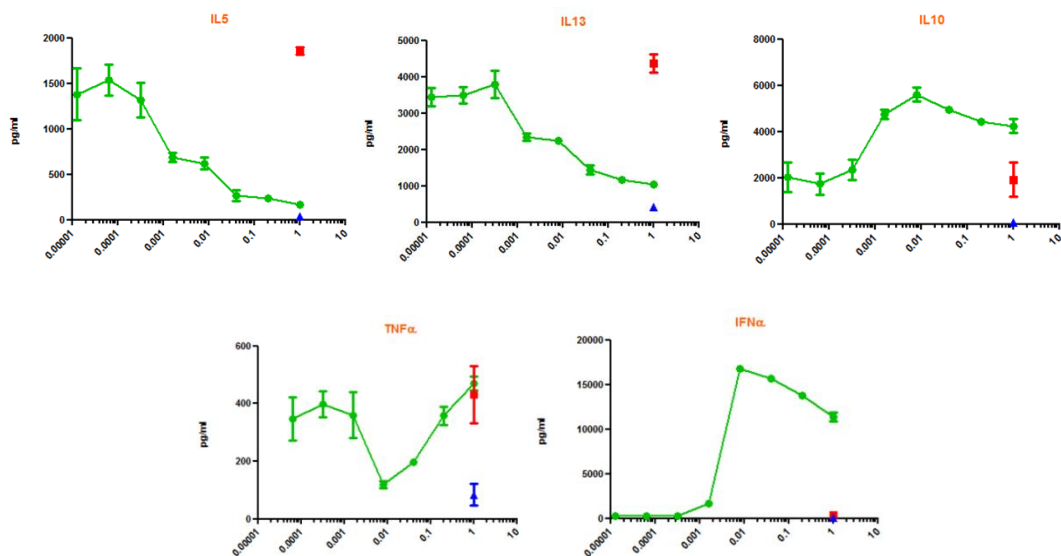


Figure 55: Cytokine production from one representative TG allergic donor PBMCs when treated with compound and allergen. X-axis is compound concentration (µM), the green line is for compound **211b**, red marker response to allergen only, blue marker no allergen or TLR7 agonist.

As can be observed from the above plots following administration of compound **211b** we see the desired dose dependent reduction of the  $T_H2$  cytokines IL5 and IL13. Also observed is a concomitant dose dependent increase in the  $T_H1$  like

cytokine IFN $\alpha$ , and the regulatory cytokine IL10. These observations are exactly in line with the biological rationale and predictions for the effect of dosing a TLR7 agonist at the same time as an allergen. We also observed a reduction in TNF $\alpha$ , despite an unusual dose response curve shape the level of TNF $\alpha$  is generally reduced compared to the control (allergen only) group. A possible explanation for the unusual curve shape could be due to the compound having some TLR8 agonist activity, albeit at a much reduced level to its TLR7 agonist activity. At high concentrations we may be approaching the pEC<sub>50</sub> of this biological effect, thereby leading to a return to the levels of TNF $\alpha$  induced by allergen alone. In conclusion, these data support the progression of compound **211b** as a potential anti-allergy therapy as it is indicative of being able to modulate the immune response in the desired manner.

### 3.9 Early toxicological assessment of compound **211b**.

Compound **211b** was submitted for early genotoxicity assessment in the Mini Ames test<sup>244</sup> and the mouse lymphoma assay;<sup>245</sup> and for cardiotoxicological assessment in the *ex vivo* rabbit ventricular wedge study.<sup>246</sup> In addition, compound **211b** was submitted to wider selectivity profiling in the extended cross screening panel (eXp) available in our laboratories.

The Ames test is a bacterial assay for mutagenicity and is a strong predictor of genotoxic carcinogenicity. The test employs several strains of mutated bacteria (the mini Ames utilises less bacterial strains) that can only survive and replicate on histidine or tryptophan rich media, which is attributable to the mutation preventing histidine or tryptophan production. This mutated area of the bacterial genome acts a hot spot for mutagens that cause DNA damage *via* different mechanisms. When these bacteria are grown in the presence of the compound of interest on agar plates with minimal histidine or tryptophan, only those bacteria that revert/mutate can grow and form colonies. The number of spontaneously revertant colonies is relatively constant per plate, so if the compound of interest induces mutations, the number of colonies increases in a dose dependent manner. In addition, some plates are

subjected to a fraction of rat liver (the S9 fraction, so called as it is the supernatant obtained from centrifuging homogenised liver at 9000 g for 20 min).<sup>247</sup> This provides a source of cytochrome P450s and other metabolic enzymes; thus if the compound of interest forms mutagenic substances upon metabolism, these will also be detected. Compound **211b** proved to be negative in this assay both in the absence or presence of the liver fraction, indicating it is not mutagenic in nature.

The mouse lymphoma assay is a mammalian *in vitro* genotoxicity assay, which utilises mouse lymphoma cells and detects non-lethal gene mutations and structural chromosomal changes in proliferating mammalian cells. These lymphoma cells are sensitive to mutations that lead to altered forms of thymidine kinase. Mutations in this enzyme result in the cells being resistant to the normally cytotoxic trifluorothymidine (TFT). The lymphoma cells are cultured with the compound of interest before being transferred to a medium containing TFT, and only those cells that have been subject to mutations in the gene corresponding to thymidine kinase, and hence resistance, survive and grow. The size of any surviving colonies can give information about the mechanism of genotoxicity. Again, in common with the Ames assay the mouse lymphoma assay can be conducted in the presence of the S9 liver fraction, allowing the presence of any genotoxic metabolites to be detected. Compound **211b** also proved to be inactive in this assay. Together with the Ames data this is extremely promising regarding the progression of compound **211b**. It is also reasonable to assume that the risk of analogues being genotoxic is low, as the core heterocycle associated with the lead series does not appear to react with DNA and cause mutation in this case.

The rabbit ventricular wedge study is an *ex vivo* study to assess the arrhythmogenic potential of compounds. The assay uses part of the rabbit ventricle and is a functional, multiple-ion channel assay in which a segment of rabbit heart is pulsed at 0.5 and 1 Hz whilst being arterially perfused with varying concentrations of the compound of interest, followed by measuring and recording an electrocardiogram (ECG). Using this ECG it is possible to assess parameters such as contractility, action potentials and proarrhythmic potential (including ventricular tachycardia,

ventricular fibrillation and Torsade de Pointes [TdP]). Torsades de Pointes is of particular concern as it can prove fatal and has led to the withdrawal or restriction of several marketed drugs.<sup>248</sup> The term Torsades de Pointes was first used by Dessertenne to describe a distinctive form of ventricular tachycardia, so called because the electrical axis of the ECG trace varies cyclically, resulting in a twisted series of peaks.<sup>249</sup> TdP is associated, clinically with long QT syndrome and is usually the result of drug treatment or genetic mutations of the cardiac ion channels.<sup>250</sup>

In order to analyse the results from the rabbit wedge assay, it is necessary to understand how to read and interpret an ECG. An ECG is essentially a graph plotting time on the x-axis and the polarisation of the heart tissue on the y-axis. A typical ECG consists of several features: a P wave, a QRS complex, and a T wave (Figure 56), the distance (time) between these features can be diagnostic of various cardiac abnormalities.

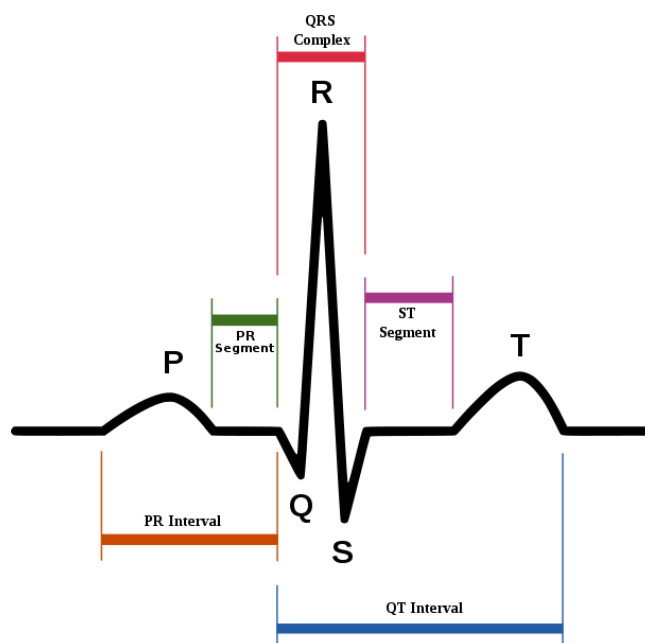


Figure 56: A typical ECG trace showing the P-wave, the QRS complex, the T-wave and several diagnostic time periods.

During a normal heart beat the heart tissue starts off negatively charged. The electrical impulse that leads to polarisation and contraction of heart tissue originates in the sinoatrial node and propagates in the right atrium, travels to the left atrium and on to the atrioventricular node. This electrical impulse causes voltage gated ion channels to open, leading to the influx of positively charged ions, so causing a positive change in charge as observed in the vertical height of the ECG trace. This polarisation of the atria is observed as the P-wave in the ECG. Following atrial polarisation the electrical impulse proceeds from the atrioventricular node to the bundle of His and then to the cardiac purkinje fibres. The ventricles then polarise and contract leading to the QRS complex; this is much bigger than the P-wave, reflecting the size differential between the atria and the ventricles. The T-wave represents the repolarisation of the ventricles back to the resting state. The final parameter of interest is the Tp-e, which is defined as the peak to end time of the T-wave.<sup>251</sup> The ECG produced from the rabbit ventricular wedge study is shown in Figure 57. .

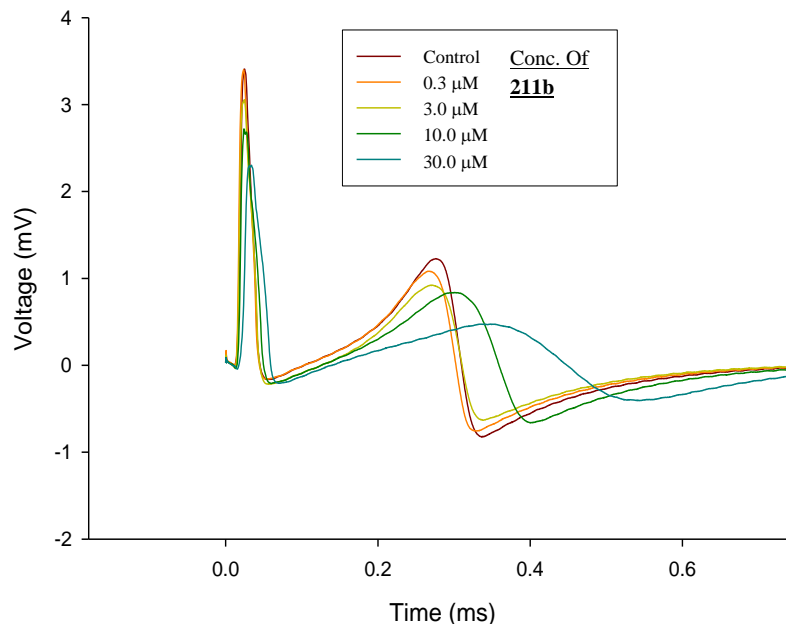


Figure 57: Single wave ECGs recorded from rabbit wedge experiment for varying concentrations of **211b** at 0.5 Hz pulsing rate. (Brown, R. unpublished work).

It should be noted that as the study does not use atrial tissue the P-wave is absent from the ECG. The relationship between QRS, QT, Tp-e and the concentration of compound **211b** are shown in Figure 58.

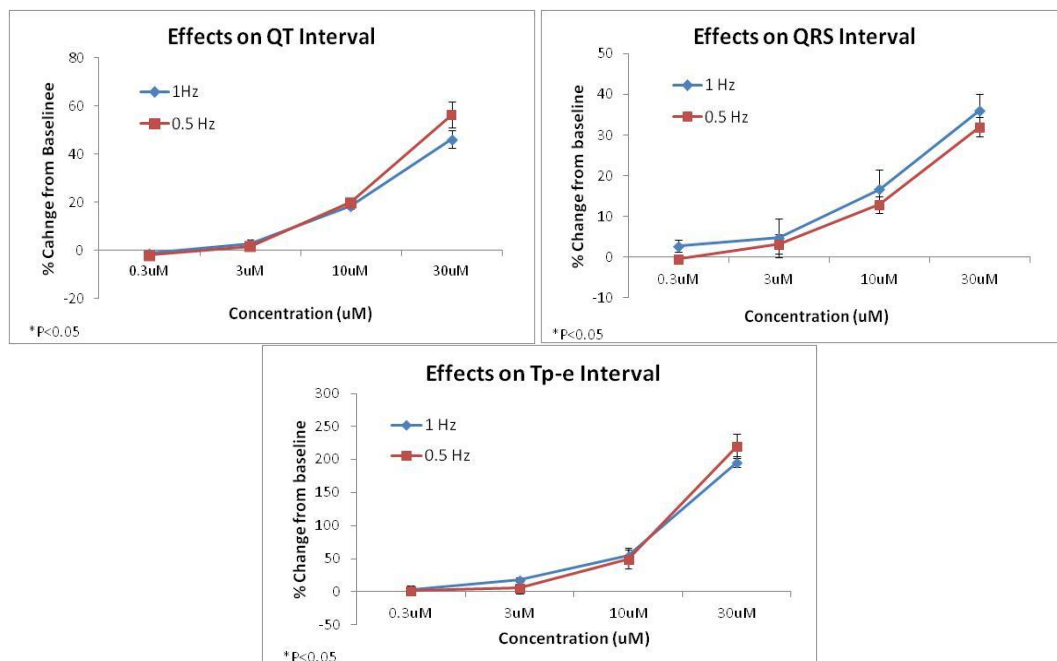


Figure 58: Graphs showing the effect compound **211b** at varying concentrations at two different pulse rates on QT, QRS and Tp-e (Brown, R. unpublished work).

From analysis of these graphs it is evident that compound **211b** produced dose-dependent prolongation of the QT interval, with significant prolongation being observed at high concentrations. In addition, compound **211b** significantly prolonged the QRS interval and Tp-e interval at concentrations of 10  $\mu\text{M}$  and 30  $\mu\text{M}$ . Using these parameters it is possible to generate a TdP score. This score considers the  $\Delta\text{QT}$  the  $\Delta\text{Tp-e}/\text{QT}$  and if any incidence of early after depolarisation observed in the ECG trace. The score assigns a numerical value to the severity of each of the described incidences for a specific compound concentration. It has been shown that compounds with a TdP score above 2.5 are considered to be associated with an increased risk for the development of TdP *in vivo*.<sup>252</sup> For compound **211b** the peak TdP scores were 3.75 at 1 Hz and 3.8 at 0.5 Hz in the presence of 30  $\mu\text{M}$  of the compound.

Using the rabbit wedge data we can define a no effect level (NOEL) for potential cardiac events (including TdP) for compound **211b** of 3  $\mu\text{M}$ . In order for a compound to be developable there should be a therapeutic index (TI) of at least 100 fold for our desired clinical effect over any cardiac side effect. The therapeutic index is a comparison of the amount of a therapeutic agent that causes the therapeutic effect to the amount that causes toxicity (in human studies). Assuming a clinical dose of 1-100  $\mu\text{g}$  (based on previous clinical observations) the following predicted TIs can be generated (Table 28 [Teague, S unpublished work]). In this model it is assumed that all of the dose will be bioavailable after intranasal dosing, that there is no observed systemic clearance, that the blood volume is 5 L, and the plasma protein binding is 82.1 % (measured value). Given these assumptions, which can be considered as a worst case scenario, here even with a 100  $\mu\text{g}$  dose, we still have a 276 fold TI. Given that compound **211b** is moderately cleared (in human liver microsomes) the TI should in fact be larger than this calculated figure.

Dose ( $\mu\text{g}$ )	Mol. Wt.	$C_{\text{MAX}}$ (ng/mL)	$C_{\text{MAX}}$ ( $\mu\text{M}$ )	Human Fu	$[\text{C}_{\text{MAX}}]_{\text{u}}$ ( $\mu\text{M}$ )	Rabbit Wedge NOAEL ( $\mu\text{M}$ )	Cardiac TI
<b>1</b>	329	0.20	0.0006	0.179	0.0001	3	<b>25470</b>
<b>10</b>	329	2.00	0.0061	0.179	0.0011	3	<b>2757</b>
<b>100</b>	329	20.00	0.0607	0.179	0.01088	3	<b>276</b>

Table 28: Calculations of the cardiac TI for three doses of compound **211b**.

Despite the calculation above indicating that there should be a sufficiently large therapeutic index for compound **211b**, it would be useful to ascertain and understand the cause of the observed cardiac effect from the point of view of receptor pharmacology. This information could subsequently be used to design new compounds which do not show potential cardiovascular side effects.

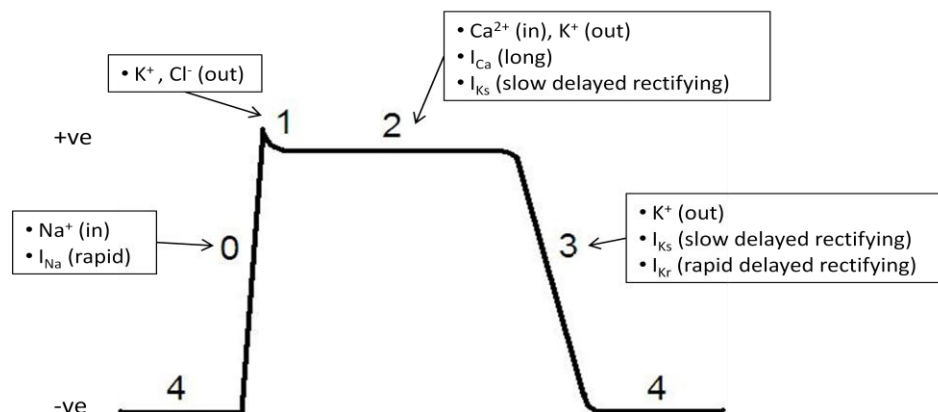


Figure 59: Schematic representation of the phases of the cardiac action potential, annotated the ions and currents.

Elongation of the QT and Tp-e are effects indicative of a change (slowing) of the repolarisation of the ventricular heart tissue. Elongation of the QRS can be caused by either a reduction in the speed of polarisation of, or the depolarisation of the ventricular tissue. These (de)polarisation events make up the cardiac action potential, which is the result of various cardiac ion channels for  $\text{Ca}^{2+}$ ,  $\text{Na}^+$  and  $\text{K}^+$  opening and closing at specific times. The action potential consists of four phases (Figure 59). During phase 0 the sodium channel Nav1.5 opens allowing the rapid entry of sodium ions into the cardiac cells, resulting in depolarisation. Following this depolarisation event the Nav1.5 channel closes and there is a small flux of potassium and sodium ions. During phase 2, the plateau phase, calcium ions enter the cells *via* the L-type calcium channel (Cav1.2). To balance the net charge, potassium ions leave the cells *via* the  $I_{\text{Ks}}$  potassium channel. It should be noted that this channel is also referred to as the KCNQ1/minK channel in reference to  $\alpha$ -subunit proteins that it contains. During phase 3 the cells undergo repolarisation, this is effected by closing of the Cav1.2 channels and opening of the  $I_{\text{Kr}}$  channel. In addition the  $I_{\text{Ks}}$  channels remain open, adding to the influx of potassium ions. The  $I_{\text{Kr}}$  channel is often referred to as the hERG channel,<sup>262</sup> as its sequence is coded by the so-called human *ether-a-go-go* related gene. As one might envisage, interacting with any of these ion channels can have profound effects on the cardiac action potential leading to the manifestation of unwanted cardiac events *in vivo*. For



example blocking the Nav1.5 channel will slow down polarisation, manifesting in an elongated QRS wave in the ECG, thereby contributing to a long QT.<sup>253</sup> Blockade of the I<sub>Kr</sub> (hERG) channel significantly reduces the rate of repolarisation and therefore, most incidences of QT and TdP are attributable to blockade of this channel.<sup>254</sup> Recently it has been demonstrated that blockade of the I<sub>Ks</sub> channel cannot only contribute to prolongation of QT caused by hERG block, but can induce TdP in isolation and so should also be considered when assessing potential cardiac liabilities.<sup>255</sup>

Cardiovascular ion channel target	pIC <sub>50</sub>	IC <sub>50</sub> (µM)
hERG	<4.5	>30.2
KCNQ1/minK	<4.6	>25.1
Kv1.5	<4.3	>50.1
L-type Ca channel Cav1.2	<4.8	>15.8
Nav 1.5	<4.0	>100

Table 29: pIC<sub>50</sub> and IC<sub>50</sub> values for compound **211b** at various ion channels associated with cardiovascular toxicity. Note: these results are from high throughput IonWorks assays<sup>256</sup> and the high throughput Barracuda assay (hERG only).<sup>257</sup>

Many of the ion channels known to be associated with cardiac risk (including those discussed above) are assessed as part of the extended cross screening panel available in our laboratories (eXp). The biological profile of compound **211b** at the cardiac ion channels of interest is shown in Table 29.

The results at the various ion channels from the eXp cross screening assays do not completely explain the origin of the cardiovascular effects seen in the rabbit wedge study as all the IC<sub>50</sub> values are higher than 10 µM where significant effects were seen. These experimental IC<sub>50</sub> values are however generated using high throughput methodologies which can underestimate activity. Therefore the activity of compound **211b** at the hERG, Nav1.5 and Cav1.2 ion channels was investigated in greater detail by QPatch electrophysiology (Table 30).<sup>258</sup>

Cardiovascular ion channel target	pIC <sub>50</sub>
hERG	4.6
Nav 1.5	<4.5
L-type Ca channel Cav1.2	<4.5

Table 30: QPatch results for compound **211b** against hERG, Nav1.5 and Cav1.2

Unfortunately none of the QPatch experiments significantly enhanced our understanding of the cardiac liabilities (risk of TdP) suggested by the rabbit wedge assay. Using the above results we can estimate (from the dose response curves) that at concentrations of **211b** of 10  $\mu\text{M}$  (where significant effects were observed in the rabbit wedge experiment) are only causing approximately 25% inhibition of hERG and less than 25% inhibition of Nav1.5. Neither inhibition alone is significant enough to cause such a dramatic prolongation of QRS, QT and Tp-e as observed in the rabbit wedge experiment. However, it is possible that there is some synergy of effects, particularly between hERG and  $I_{Ks}$  ( $\text{pIC}_{50} = 4.8$ , Table 29), especially considering that the rabbit expresses fewer  $I_{Ks}$  channels than humans.<sup>259</sup>

In addition to cardiovascular ion channels the eXp panel also contains a number of 7-TM receptors known to have cardiovascular effects. The pharmacological profile of compound **211b** against these receptors is reported in Table 31.

Cardiovascular target	Mode	Compound 202b	
		$\text{pXC}_{50}$	$\text{XC}_{50}$ ( $\mu\text{M}$ )
Adenosine 2a	Agonist	<4.5	>31.6
Adrenergic $\alpha 1b$	Antagonist	5.3	5.0
Adrenergic $\alpha 2c$	Agonist	<4.5	>31.6
Adrenergic $\beta 2$	Agonist	<4.5	>31.6
Adrenergic $\beta 2$	Antagonist	<4.5	>31.6
Muscarine 2	Agonist	<4.8	>15.8
Muscarine 2	Antagonist	<4.5	>31.6
Serotonin 1B	Agonist	<4.5	>31.6
Serotonin 1B	Antagonist	<4.5	>31.6
Serotonin 2A	Agonist	<4.4	>39.8
Serotonin 2A	Antagonist	<4.4	>39.8
Vasopressin 1a	Antagonist	<4.3	>50.1

Table 31:  $\text{pIC}_{50}$  and  $\text{IC}_{50}$  values for compound **211b** at various targets associated with cardiovascular toxicity.

Compound **211b** does show some activity at cardiovascular targets, however these activities cannot explain the prolongation of cardiac repolarisation observed in the rabbit ventricular wedge assay. Blockade of  $\alpha 1b$  adrenergic receptors has been shown not to increase QT, but instead can act to slow the sinus rhythm,<sup>260</sup> however, given the rabbit wedge is artificially pulsed this activity does not explain the

observed effects. Muscarine 2 receptor antagonism has no effect on the ventricular muscles.<sup>261</sup> Finally serotonin receptors play a role in cardiac blood flow not in the electrophysiology of the heart beat.<sup>262</sup>

One class of receptors associated with cardiac effects that is not part of the eXp panel is the adenosine receptors. Given the heterocyclic core of the lead molecule is a deazaadenine, and that adenosine itself contains an adenine ring system, it was suspected that our series of molecules may be capable of interacting with this target class. As such compound **211b**, were profiled against the A<sub>1</sub>, A<sub>2A</sub>, A<sub>2B</sub>, and A<sub>3</sub> receptors in both agonist and antagonist modes. The results of this screening are summarised in Table 32.

Cardiovascular target	Mode	Compound 202b % of control agonist response
Adenosine A <sub>1</sub>	Agonist	23
Adenosine A <sub>2A</sub>	Agonist	0
Adenosine A <sub>2B</sub>	Agonist	-2
Adenosine A <sub>3</sub>	Agonist	-10
Adenosine A <sub>1</sub>	Antagonist	Agonist
Adenosine A <sub>2A</sub>	Antagonist	-17
Adenosine A <sub>2B</sub>	Antagonist	-21
Adenosine A <sub>3</sub>	Antagonist	6

Table 32: Agonist and antagonist responses of compound **211b**, (10 µM concentration) at adenosine receptors. Reference agonists: CCPA, NECA and IB-MECA.

From the above tables it is evident that all three compounds are very weak Adenosine A<sub>1</sub> agonists. Adenosine A<sub>1</sub> agonism can slow the heart rate,<sup>263</sup> however the compounds exhibit only minimal agonist activity at 10 µM concentrations and so cannot, on their own, explain the pronounced effects seen at this concentration in the rabbit wedge assay.

In conclusion, the exact cause of the prolongation to the repolarisation of cardiac tissue observed in the rabbit wedge assay has yet to be explained. No single interaction with a target investigated so far can explain the cardiac effects. There are two possible reasons for this: that the target causing the effect has not been

investigated, or that a number of small off target effects are combined in an additive or synergistic manner leading to the effects observed in rabbit cardiac tissue. As stated earlier, at the potential clinical dose, there still should be a minimum TI of approximately 280 fold, thus these unwanted side effects should not pose a barrier to the (pre)clinical development of compound **211b**. Additionally, any cardiovascular risk will need to be discharged prior to the selection of a clinical candidate by an *in vivo* study using a relevant preclinical species.

### 3.10 *In vivo* biological assessment of compound **211b**.

Having profiled our most promising compound **211b** in a range of safety assays attention then turned to understanding its *in vivo* DMPK profile. Presented below are the first round of *in vivo* PK results for compounds **211b** following 1 mg/kg intravenous infusions, as saline solutions to three separate rats, it should be noted that in this case compound **211b** was present as the formate salt.

Compound Number (salt form)	Cl mL/min/kg (% LBF)	V <sub>ss</sub> L/kg	t <sub>1/2</sub> (h)	IVC Rat mL/min/g (% LBF)
<b>211b (formate salt)</b>	<b>84 (98 %)</b>	<b>19.6</b>	<b>3.5</b>	<b>20 (90 %)</b>

Table 33: First round *in vivo* DMPK results for compound **202b**.

From these data it appears that the IVC in rats is predictive of the *in vivo* clearance observed, suggesting the human IVC could be predictive for human *in vivo* clearance. The DMPK of compound **211b** was also assessed following IV dosing as a 1 mg/kg solution of the free base in the cyclodextrin kleptose. The compound now exhibited relatively low clearance (Table 34, entry 2). At this stage it was not certain if the discrepancy was a result of experimental error, or if the changes in salt form and formulation were responsible. Therefore two more experiments were carried out on compound **211b**: a repeat of the original experiment (formate salt in saline) and an experiment where the formate salt was dosed as a kleptose solution (Table 34).

Compound Number (Salt form/Formulation)	Cl mL/min/kg (% LBF)	V <sub>ss</sub> L/kg	t <sub>1/2</sub> (h)
211b (formate/saline)	84 (98 %)	19.6	3.5
211b (free base/kleptose)	22 (26 %)	8.8	6.3
211b (formate/saline) Rpt.	26 (30 %)	13.8	8.8
211b (formate/kleptose)	28 (33 %)	13.3	8.4

Table 34: Further *in vivo* DMPK assessment of compound **211b**.

From these data it is evident that the discrepancy was with the first experiment, as all three repeat experiments yield similar clearance results, with compound **211b** actually being low to moderately cleared and exhibiting reduced clearance with respect to the IVC prediction. One potential explanation for the differences in clearance between the IVC result and the *in vivo* experiment could be a difference in cell permeability. The IVC experiment uses microsomes obtained from liver cells, but not actual whole cells. A poorly permeable compound would have limited access the hepatic cells, resulting in a reduced hepatic clearance. The permeability for the compound **211b** was assessed using MDCK cells and the data is presented in Table 35. Another possible explanation would be if compound **211b** is highly bound to blood/plasma proteins. There would be less of this compound available to enter hepatic cells and thus be cleared. Protein binding for compound **211b** in rat blood was assessed and this data is also presented in Table 35.

Compound	MDCK permeability (nm/s)	Rat blood protein binding
<b>211b</b>	<b>10.3</b>	<b>84%</b>

Table 35: Permeability and protein binding data for compound **211b**.

Compound **211b** is moderately permeable in MDCK cells and has low rat plasma protein binding. These data are, therefore, unable to adequately explain the differences between clearance in liver microsomes and measured *in vivo* clearance.

Despite the *in vivo* clearance of compound **211b** being classed as low the compound was not detectable in blood following administration of a 3 mg/kg oral dose, indicating a very low oral bioavailability in line with the desired target candidate profile. In addition, the intranasal bioavailability of compound **211b** was assessed

following a 0.5 mg/kg intranasal dose. Compound **211b** was detectable in the systemic circulation resulting in a calculated intranasal bioavailability of 39%. Pleasingly, the  $C_{Max}$  following intranasal administration (total or unbound) did not reach the WB IFN potency of compound **211b**. This indicates that the systemic levels of compound from this route of administration should not be an issue as there is unlikely to be a sufficient concentration of compound in the blood to engage with TLR7 and give IFN $\alpha$  induction. Considering the very low oral bioavailability of the compound, any **211b** detected in the systemic circulation must originate from intranasal absorption of the dose rather than as a result of the swallowed portion of the dose. Furthermore the fact that compound **211b** shows negligible oral bioavailability, means the likely therapeutic index over any potential cardiac side effects is, as expected, greater than the 276 fold predicted as a worst case scenario in Table 28.

Having demonstrated that compound **211b** meets the desired profile in terms of *in vitro* activity, selectivity and toxicological outcomes, and that the compound has a DMPK profile suitable for inhaled/intranasal delivery it was then assessed in relevant animal *in vivo* pharmacodynamic experiments. For the compound to meet the required *in vivo* activity profile, it is necessary to demonstrate IFN $\alpha$  induction with a significant window over any observed TNF $\alpha$  induction. Measurement of IFN $\alpha$  levels *in vivo* can be very challenging and based on this, for the initial animal experiments it was decided to measure the levels of IP-10. IP-10 is an IFN-induced cell-secreted chemokine that has been used as a surrogate biomarker for IFN $\alpha$ , and has been shown to provide a more sensitive measure of IFN as opposed to direct measurement.<sup>264</sup>

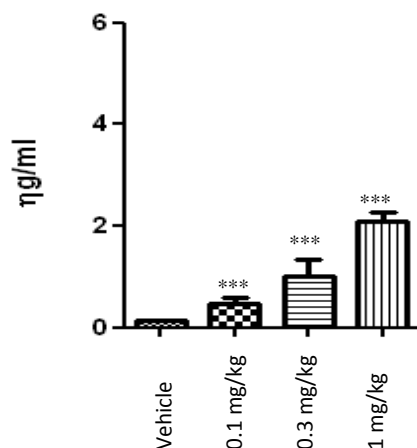


Figure 61: Systemic IP-10 levels 4 hours after intranasal administration of solutions of compound **211b** at doses of 0.1, 0.3 and 1 mg/kg to naïve BALB/c mice.

Pleasingly there is a dose dependent increase in serum IP-10 levels, suggesting the intranasal administration of compound **211b** has led to significant synthesis of IP-10 and hence IFN $\alpha$  *in vivo*.

Following on from this promising result 1 mg/kg solutions compound **211b** were dosed in 5  $\mu$ L (intranasal) and 50  $\mu$ L (inhaled, delivered by the nose) quantities to naïve BALB/c mice. After 4 hours the animals were humanely killed and the levels of cytokines in both the serum and bronchoalveolar lavage (BAL) were measured (Ball, D. I. unpublished work). This data is presented in Figures 62, 63 and 64.

It can be observed that compound **211b** exhibits the desired pharmacodynamic profile, with significant induction of IFN $\alpha$ , IP-10 and very little TNF $\alpha$  by either the inhaled or intranasal dosing route. In addition, from these experiments it appears that intranasal administration may be preferred on account of the lack of measurable TNF $\alpha$  in the BAL.

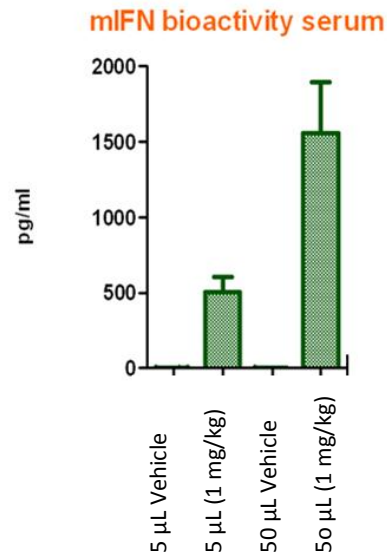


Figure 62: Measured serum levels of murine IFN $\alpha$  following 5  $\mu$ L (intranasal) and 50  $\mu$ L (inhaled) doses of 1 mg/kg **211b**.

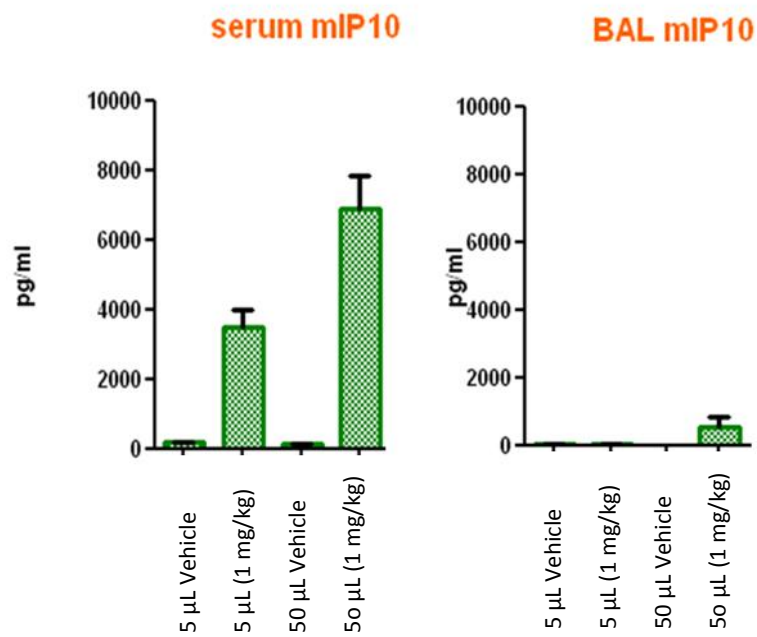


Figure 63: Measured serum and BAL levels of murine IP-10 following 5  $\mu$ L (intranasal) and 50  $\mu$ L (inhaled) doses of doses of 1 mg/kg **211b**.



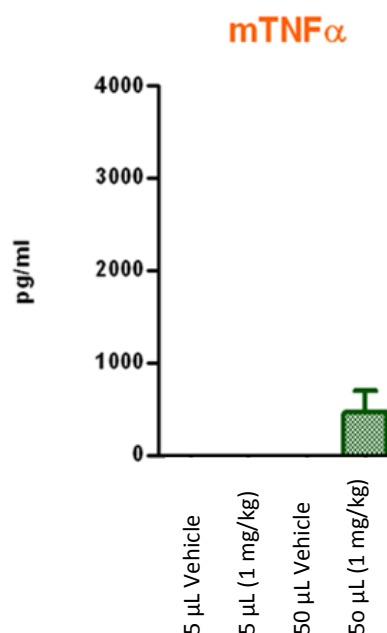


Figure 64: Measured BAL levels of murine TNF $\alpha$  following 5  $\mu$ L (intranasal) and 50  $\mu$ L (inhaled) doses of 1 mg/kg **211b**.

These *in vivo* pharmacodynamic results represent an extremely important milestone in the potential progression of compound **211b** to the clinical setting. Considering that all the *in vivo* and *in vitro* results collected for compound **211b** meet the desired targets, this primary goal of this research has been achieved and compound **211b** can now be considered as a potential clinical candidate following further safety and formulation studies.

Given that the *in vivo* PD results for compound **211b** are extremely encouraging it is anticipated that other compounds from this chemical series could also be potential therapeutic agents that act by inducing IFN $\alpha$  as a result of TLR7 agonism. In order to maximise the possible therapeutic benefit, other potential applications should also be explored. As stated previously another proven application of the immunomodulatory effects of TLR7 agonism is in the treatment of a variety of skin lesions. It has been demonstrated that there are compounds from the dezaadenine series that exhibit a DMPK profile consistent with topical dosing. Therefore, dezaadenine based IFN $\alpha$  inducers could also prove useful in the treatment of skin conditions.

### 3.11 Design of TLR7 agonists for dermatological applications.

The known TLR7 agonist, imiquimod **19**, is marketed as Aldara™ as a 5% by wt. cream for topical application, for the treatment of skin lesions.<sup>265,266</sup> Imiquimod is a weak TLR7 agonist (when evaluated in our laboratories), hence the requirement for the high dose of a 5% by wt. formulation. A more potent TLR7 agonist may lead to an enhanced product profile. Therefore it was decided to investigate our current TLR7 compound set for the possibility of topical dermal applicability and to actively pursue this indication when designing new target molecules.

In order to design better molecules for skin conditions, it is useful to understand the challenges this route of delivery poses and what governs topical efficacy. The natural function of the skin is to prevent external chemicals or microbes from entering the systemic circulation. In general terms the efficacy of a drug can be calculated using the PK/PD approach:

Eq. 1 Generic PK/PD approach:  $\text{Efficacy} = \text{Concentration (free)} / \text{Potency}$

One can apply to same PK/PD model to generate the following equation for topical efficacy:

Eq. 2 Topical PK/PD approach:  $\text{Topical Efficacy} = \text{Skin Concentration (free)} / \text{Potency}$

If we assume that the skin is a single layer acting as a barrier to penetration it is possible to apply Fick's law of diffusion and use this to calculate the percutaneous flux of a compound and hence the free skin concentration of a test compound.<sup>267</sup>

This may initially seem too great a simplification given the complex multi layer structure of the skin, however it has been shown that the outermost layer, the stratum corneum provides the single biggest barrier (rate limiting) to skin absorption.<sup>268</sup>

Thus:

Eq. 3  $\text{Topical Efficacy} = (\text{Percutaneous Flux}/\text{Potency}) \times \text{Constant}$

Where Percutaneous Flux = Skin permeability x Solubility in the vehicle. Potts and Guy went on to relate the physicochemical properties of the penetrant molecule to its skin permeability and so generate the following equation for skin permeability ( $k_p$ ):<sup>269</sup>

$$\text{Eq. 4 } \text{Log } k_p = -2.72 + 0.71\text{LogP} - 0.0061\text{MW}$$

Where  $k_p$  is skin permeability ( $\text{cmh}^{-1}$ ), P is the partition coefficient of the molecule between  $\text{H}_2\text{O}$  and octanol and MW is the molecular weight of the molecule. The vehicle (formulation) used to deliver the molecule to the skin is almost always largely aqueous in nature and so it is possible to use the ACD software calculation for aqueous solubility (S):<sup>270</sup>

$$\text{Eq. 5 } \text{Log } S = 0.796 - 0.854\text{LogP} - 0.00728\text{MW} + \text{correction}$$

From these two equations it is evident that both  $\text{cLogP}$  and MW are the key factors influencing percutaneous flux. Using these calculations without corrections, and a constant  $\text{cLogP}$ , it is possible to ascertain that a change in MW of 35 or 70 results in a decrease in flux by approximately 3 and 9 fold, respectively. Assuming a constant MW an increase in  $\text{cLogP}$  of 0.5 or 1 log units results in a decrease in flux of 1.2 and 1.4 fold, respectively (see Table 36). Based on all of the above, these calculations indicate the main physicochemical factor governing percutaneous flux is the MW of the compound.

MW	cLogP	Log $k_p$	$k_p$	Log S uncorrected	S uncorrected	Flux uncorrected	Flux ratio
350	3	-2.725	0.001884	-4.314	4.85289E-05	9.14113E-08	1.0
385	3	-2.9385	0.001152	-4.5688	2.69898E-05	3.10957E-08	2.93968
420	3	-3.152	0.000705	-4.8236	1.50107E-05	1.05779E-08	8.641716
350	3.5	-2.37	0.004266	-4.741	1.81552E-05	7.74462E-08	1.180321
350	4	-2.015	0.009661	-5.168	6.79204E-06	6.56145E-08	1.393157

Table 36: Calculations to demonstrate the effects of varying MW and  $\text{cLogP}$  on percutaneous flux.

The percutaneous skin flux of imiquimod **19** has been measured and using these data it possible to define a desired molecular weight and activity profile. In order to

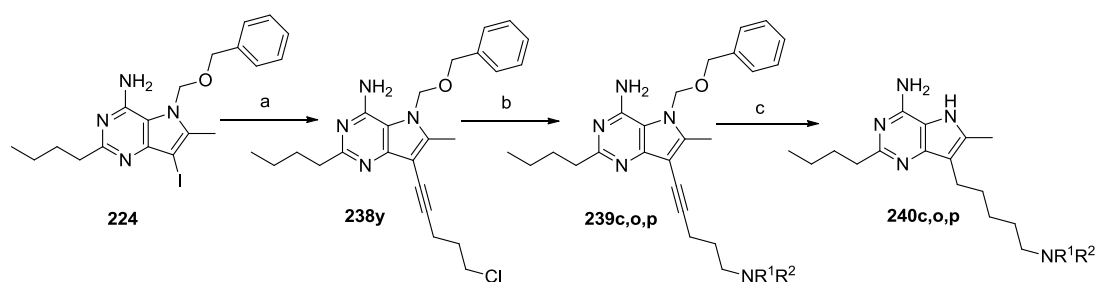
develop a cream for topical use at 0.01% by wt. to 0.001% by wt. the following potency window can be set for a molecule with a MW of 350 (compound **211b** MW = 329): IFN $\alpha$  (HWB) induction pEC<sub>50</sub> 7 to 8 (ideally towards the upper end of this window). The desired topical concentration window was defined by collaborators elsewhere in our laboratories that would ultimately be used to progress a dermatological TLR7 asset to the clinic.

Given this information, it was apparent that there was a requirement to increase the IFN $\alpha$  induction potency of our current series with a minimal increase in molecular weight, whilst maintaining solubility and selectivity over TNF $\alpha$  induction. In addition the molecules should still be rapidly metabolised to minimise systemic exposure for the reasons stated earlier.

### 3.11.1 Revisiting 6-methyl-deazaadenines as potent TLR7 agonists.

It has been shown that introduction of a methyl group at the 6-position led to an increase in potency over the 6-hydrogen analogues of between 0.2 and 1 log units, equating to an increase of between approximately 1.5 and 10 fold for an increase of only 14 mass units (Section 3.5).

Scheme 34: Compounds synthesised by the author.



Reagents and conditions: a) 6 mol % Pd(PPh<sub>3</sub>)<sub>2</sub>Cl<sub>2</sub>, 12 mol % CuI, 5-chloropent-1-yne, Et<sub>3</sub>N, DMF, 20 °C, 44%; b) 4-fluoropyrrolidine, Et<sub>3</sub>N, MeCN, 60 °C, 53% (**239c**), 55% (**239o**) and 46% (**239p**); c) H-Cube<sup>TM</sup>, 10 % Pd/C, H<sub>2</sub>, EtOH, AcOH, 30 % (**240c**), 50% (**240o**) and 45% (**240p**).

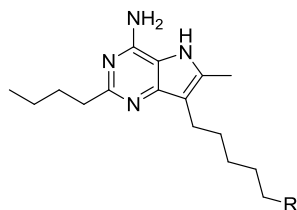
Therefore, it was decided to synthesise additional analogues with this functionality in place with five and six carbon spacers in the 7-position and the more potent amines

at the terminus. This range of compounds was synthesised using previously established methods from available intermediate **224** (Scheme 34).

The cytokine induction results for this set of compounds are summarised in Tables 36 and 37. Compounds of interest from this set were submitted for evaluation of their metabolism in rat and human liver microsomes (data also presented in Tables 36 and 37). Given the dramatic effect that molecular weight can have on skin penetration, it was decided to employ one of the measures of ligand efficiency to aid the comparison and ranking of compounds for further assessment. Of the various available measures of ligand efficiency,<sup>271</sup> the binding efficiency index (BEI) was chosen as this directly links potency and molecular weight. The BEI is only genuinely applicable to binding assay results, but serves as a crude comparator in this situation with substitution of pIC<sub>50</sub> for the measured pEC<sub>50</sub> (cytokine induction) allows us to generate an efficiency index (EI) for our series:

$$\text{Eq. 6 } EI = \text{pEC}_{50} (\text{IFN}\alpha \text{ HWB}) / (\text{MW}/1000)$$

Considering the compounds with a 6-methyl group and a five methylene spacer (Table 37), it is evident that the inclusion of the 6-methyl group leads to an increase in potency, ranging from 0.7 to 1.2 log units over the corresponding unsubstituted analogues. Of particular note are compounds **240o**, **240p** and **240h**; compounds **240o** and **240p** are the most potent inducers of IFN $\alpha$  made so far in this chemical series, maintaining approximately 1000 fold selectivity for IFN $\alpha$  over TNF $\alpha$ . Compound **240h**, whilst being slightly less potent than many of the comparator compounds is very small and so the good levels of activity lead to a very high EI, suggesting this compound has a good chance of achieving topical dermal efficacy, and as such this compound was assessed in human and rat liver microsomes. Compound **240b** was also submitted for IVC assessment, allowing the single point change (6-H to 6-Me) to be evaluated over two pairs (**211b** and **240b** and **240h** and **240h**). In both cases the introduction of a 6-methyl group has decreased the turnover of the compounds in rat liver microsomes, leading also to compounds that show no turnover in human liver microsomes.

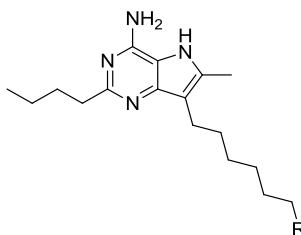


Compound Number	R	Induction of IFN $\alpha$ pEC50	Induction of TNF $\alpha$ pEC50	IVC Rat mL/min/g (% LBF)	IVC Human mL/min/g (% LBF)	MW	EI
240a*		7.8	4.8	-	-	357	21.8
240b#		7.2	4.7	11.7 (84%)	<0.53 (<42%)	343	21.0
240c		7.5	4.8	-	-	375	20.0
240o		7.9	5.0	-	-	361	21.9
240p		7.9	4.9	-	-	361	21.9
240g*		7.8	5.4	-	-	359	21.7
240h#		7.6	4.7	6.7 (76%)	<0.53 (<42%)	329	23.1
240n#		7.1	5.0	16.7 (89%)	3.0 (80%)	347	20.5

Table 37: Summary of cytokine induction data in HWB, standard deviation = 0.3, associated physiochemical data and measured *in vitro* clearance. cLogP calculated using BioByte software,<sup>183</sup> cLogD<sub>7.4</sub> calculated using algorithms available in our laboratories. \* compound synthesised by Champigny, A. C. # compound synthesised by Stewart, S.

This suggests that the 6-methyl substituent is detrimental to hepatic turnover. When analysing the set of four fluorinated analogues there does appear to be some divergent SAR in comparison with the unsubstituted 6-position counterparts (Table 22). In this set the two fluoro substituted pyrrolidines (**240o** and **240p**) are significantly more active than the pyrrolidine **240b** as predicted. However, the introduction of a fluorine onto the piperidine (compound **240c**) or the azetidine (**240n**) results in compounds with reduced potency and selectivity compared to the parent unsubstituted analogues (**240a** and **240h**). At present we are unable to rationalise this observation. The 6-methyl, six methylene spaced compounds (Table 38) have similar activities to their five methylene counterparts and so achieve a reduced EI and increased cLogP.

**GSK CONFIDENTIAL – Property Of GSK – Copying Not Permitted**  
 The Synthesis and Optimisation of Toll-like Receptor Agonists as Potential Immunomodulatory Agents.



Compound Number	R	Induction of IFN $\alpha$ pEC50	Induction of TNF $\alpha$ pEC50	IVC Rat mL/min/g (% LBF)	IVC Human mL/min/g (% LBF)	MW	EI
215a*		7.5	4.9	-	-	371	20.2
215b <sup>#</sup>		7.6	4.8	25.0 (92%)	<0.53 (<42%)	357	21.6
215h <sup>#</sup>		7.7	4.8	27.2 (93%)	<0.53 (<42%)	343	22.4

Table 38: Summary of cytokine induction data in HWB, standard deviation = 0.3, associated physiochemical data and measured *in vitro* clearance. cLogP calculated using BioByte software,<sup>183</sup> cLogD<sub>7.4</sub> calculated using algorithms available in our laboratories. \* compound synthesised by Champigny, A. C. # compound synthesised by Stewart, S.

Potential explanations for the increase in activity observed for 6-methyl compounds are that the methyl group is occupying a small hydrophobic pocket and making favourable interactions. Also the presence of any group in the 6-position is likely to favour conformations of the 7-position alkyl chain that are out of the plane of the heteroaromatic core. Such conformations may be favourable, hence the increase in observed potency of IFN $\alpha$  induction.

In common with the five methylene linker compounds, introduction of the 6-methyl group has reduced human *in vitro* clearance in this sub series also (compounds **215b** and **215h**), thus adding weight to the hypothesis that the 6-methyl group blocks human hepatic turnover. Given that the primary mechanism of clearance is believed to be as a result of *N*-dealkylation, the 6-methyl may be preventing the molecules binding to the hepatic enzyme responsible for this clearance mechanism.

In conclusion, through the combination of the most potent 7-position amines linked to a 6-methyldeazaadenine core, several extremely potent IFN $\alpha$  inducers have been identified. In addition an efficiency index (EI) linked to molecular weight, the key

physicochemical parameter for skin penetration has been calculated for these new compounds. This index will aid the selection of compounds from this set for any future topical profiling and potential progression towards the clinic.

### 3.12 Conclusions and further work.

During the course of the research presented within this thesis a non-selective inducer of IFN $\alpha$  (with respect to TNF $\alpha$  induction) deazaadenine **121** (discovered within our laboratories) was modified to include active functional groups from the 8-oxoadenine series, resulting in compound **123**. The cytokine induction selectivity was improved but surprisingly the potency was not increased as expected. Further modification gave lead compound **124a**, which represents a previously unreported class of molecules able to induce IFN $\alpha$  in human whole blood. Furthermore compound **124a** exhibits a significant selectivity window over TNF $\alpha$  induction (not described for other known TLR7 agonists) and has a pharmacokinetic profile in line with the project aims. Reducing the length of the 7-position linker chain length from hexyl to pentyl gave compound **211a**. This compound exhibited a marginally improved cytokine induction selectivity window, reduced lipophilicity and maintained the desired DMPK profile. Through analysis of potential metabolic pathways, the 7-position amine was identified as the position where modification could tune the DMPK profile further, and was investigated. A pyrrolidine containing compound **211b** was identified that slightly improved the cytokine induction selectivity, reduced lipophilicity further, whilst maintaining a DMPK profile (minimal oral bioavailability) suitable for inhaled/intranasal delivery. Analysis of this compound set using an efficiency index (mass dependent) further highlighted the improvements made during the drug discovery process (Table 39).



**GSK CONFIDENTIAL – Property Of GSK – Copying Not Permitted**  
 The Synthesis and Optimisation of Toll-like Receptor Agonists as Potential Immunomodulatory Agents.

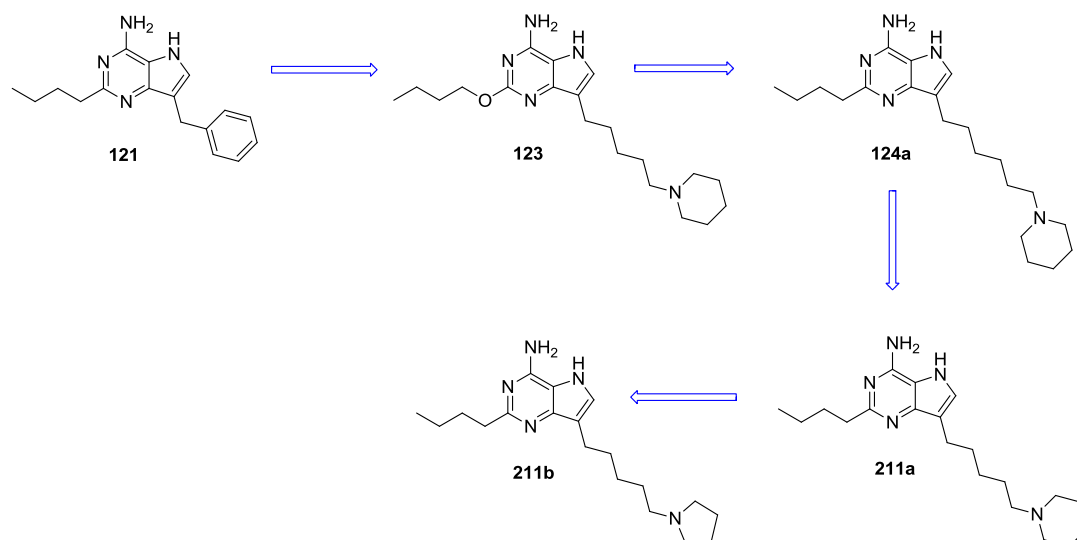


Figure 65: Summary of key compounds in the discovery **211b**.

Compound Number	HWB Induction of IFN $\alpha$ pEC50	HWB Induction of TNF $\alpha$ pEC50	PBMC Induction of IFN $\alpha$ pEC50	PBMC Induction of TNF $\alpha$ pEC50	IVC Rat mL/min/g (% LBF)	IVC Human mL/min/g (% LBF)	cLogP	EI
<b>121</b>	-	-	6.0	6.6	-	-	4.8	-
<b>123</b>	-	-	5.8	4.9	-	-	6.4	-
<b>124a</b>	6.8	<4.8	-	-	8.8 (80%)	1.2 (62%)	6.0	18.7
<b>211a</b>	6.8	<4.7	-	-	30 (93%)	2.0 (73%)	5.5	19.5
<b>211b</b>	6.7	<4.5	-	-	20 (90%)	1.5 (67%)	4.9	20.3

Table 39: Summary of the properties of key compounds in the discovery of **211b**.

Compound **211b** was found to elicit the desired suppression of T<sub>H</sub>2 like pro-inflammatory cytokines in a functional allergen driven PBMC assay. Pharmacokinetic assessment of compound **211b** shows that despite a disconnect between the IVC and the *in vivo* clearance in the rat, the desired PK profile could be realised with compound **211b** showing negligible oral bioavailability. Furthermore, the desired cytokine induction profile was also observed *in vivo* (in mouse). The compound showed no risk of mutagenicity in preclinical toxicity assays and there was at least a 100 fold TI over any potential cardiovascular effects. In this way compound **211b** meets all the criteria defined as project aims for a potential clinical candidate for the treatment of asthma (and other respiratory conditions with an allergic component). In addition, it is anticipated that the observed selectivity for

IFN $\alpha$  induction over TNF $\alpha$  induction may result in a better side effect profile compared to the previously described TLR7 agonists.

Having achieved the goal of identifying a potential clinical candidate for allergic asthma, attention was given to other applications of compounds from the deazaadenine series. Treatment of skin conditions was identified as an area worthy of further research. A series of compounds with enhanced IFN $\alpha$  induction potency and increased efficiency with respect to molecular weight were identified and may prove to be of further interest.

Examination of the SAR for the deazadenine series revealed some similarities with other reported TLR7 agonists particularly in the region of the putative agonist trigger in the C-2 position. In common with the other reported chemotypes, a *n*-butyl or other linear four atom chain appeared to be optimal for agonist activity. However, in contrast to the reported chemotypes, branching substitutions on this chain were not tolerated. In addition, there was a requirement in the deazaadenine series for the atom linking this chain to the heteroaromatic core to be a carbon, whereas in the reported 8-oxoadenine series this atom was optimally a heteroatom (oxygen, nitrogen, or sulfur). Another area of seemingly divergent SAR is the 6-position. Unlike other chemical series based on a modified purine scaffold, the deazadenine series does not require an oxo group to be present in this position to induce cytokines. From the data presented in Table 26, it appears that groups larger than a methyl group are not tolerated in this position. A methyl group in the 6-position increases the potency of cytokine induction and has proved a key feature in the design of compounds for the treatment of skin conditions. Other small functional groups such as CF<sub>3</sub>, CHF<sub>2</sub>, CH<sub>2</sub>F and CH<sub>2</sub>OH should be sterically tolerated and it would be interesting to evaluate the effect that these groups might have on cytokine induction (Figure 66).

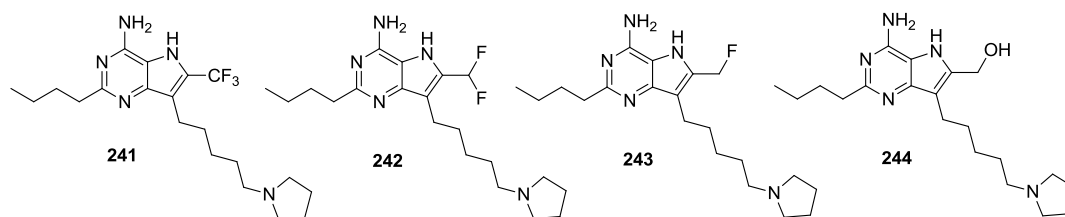


Figure 66: Structures of further 6-position analogues.

In combination with the research reported for the 2-aminopyrimidine series, the observations of divergent SAR between described series of TLR7 agonists is suggestive of multiple binding sites or binding modes, however there is at present no X-ray crystallographic data for TLR7 to support this hypothesis. It may be possible to provide further evidence for this hypothesis by conducting competition experiments where two or more examples from different chemotypes are co-administered to PBMCs or whole blood and the effects on IFN $\alpha$  induction investigated. If the compounds from different chemotypes bind to different binding domains it may be possible to observe a synergistic increase in potency. If, however, two compounds with different levels of potency that bind to the same site are co-administered there will be competition resulting in an activity level in-between the two individual potencies. Such investigations may also allow those compounds from each series that proved to be inactive to be investigated as potential antagonists. At present little has been written about the possibility of multiple modes of activation of TLR7. As such the data presented, and compounds synthesised during this research may prove highly significant in the future understanding of TLR7 activation and signalling.

Given that a TLR7 crystal structure with or without agonist bound has yet not been reported we cannot ascertain with any confidence the binding site that the reported deazaadenines occupy. The science of photoaffinity labelling,<sup>272</sup> may in combination with selective protein degradation provide an answer to this problem. This would require the incorporation of a photoreactive functionality into a deazaadenine molecule, once bound the photoreactive group can be activated resulting in a covalent bond being formed between the ligand and an amino acid

residue present in the binding site. Following this, the protein can be degraded and the portion of the protein bound to the ligand identified. This information would prove extremely useful in both identification of the location of the binding site and would enhance computational modelling of the binding site and subsequent structure based drug design.

From the SAR presented in this thesis it is apparent that the 7-position substituent can be modified to optimise potency but also importantly the physiochemical and DMPK properties. It has been identified that a five or six atom linker capped with an amine appears to provide the a better balance of biological and physiochemical properties compared to a four atom linker. However, longer linking chains have not been investigated, further work in this area may yield further insight into how this substituent effects activity and metabolism. Given the flexibility inherent in the investigated 7-position groups the biological profile may be able to be modified by the introduction of conformational restraints. However without further structural information concerning the conformation this group adopts during binding/activation, the rational design of such constraints will be very challenging.

Also of possible interest, would be to investigate the possibility of forming active dimeric compounds where two deazadenine cores are linked together. There are several potential advantages depending on the length of the linker, and how the molecules are binding to TLR7. If the compounds bind to TLR7 in an analogous way to how resiquimod **25** binds TLR8 (Section 1.9.1),<sup>124,132</sup> a long linker may allow both uridine binding sites to be occupied by the same molecule. A shorter chain might allow the dimer to bind to both the uridine and oligonucleotide binding sites.



Figure 67: Structure of a potential dimeric TLR7 agonist **245n**.

Considering the SAR presented above, the 7-position may provide the ideal linking function. A potential dimeric compound **245n** is shown in Figure 67.

Another potential avenue of further research could be to adopt an antedrug approach where the compound contains an ester that is rapidly hydrolysed by blood esterases resulting in an inactive compound. This approach may further reduce any potential side effects that might result from pulmonary absorption of the molecule. An ester could potentially be introduced in the 2-position where the hydrolysed compound would have a reduced chain length and thus may not be able to act as an agonist (Figure 68). Adopting this approach however, may not deliver long term immunomodulation, as observed with the antedrug compounds developed by AstraZeneca (Section 1.9.3).

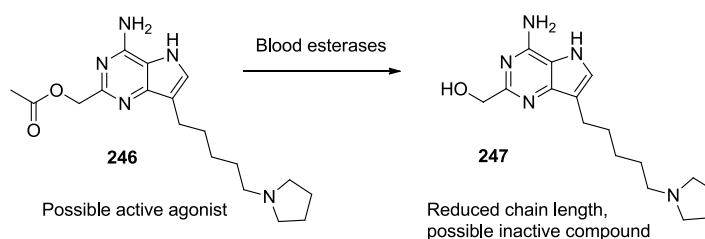


Figure 68: Potential antedrug compound **246** and potentially inactive metabolite **247**.

The research described within this thesis has focused on the design of compounds that act as full agonists. A potential way of increasing therapeutic index is to identify a partial agonist, in this case reducing the peak level of IFN $\alpha$  induction whilst still effecting immunomodulation. It has been shown that incorporation of some groups in the 2-position result in full agonists, whereas other groups lead to inactive compounds. Further investigations in this area might result in a partial agonist.

Finally it should be possible to modify the substituents present on the deazaadenine core to provide an orally bioavailable molecule. For example it has been demonstrated that inclusion of an ether in the 2-position butyl chain retains significant IFN $\alpha$  induction, significant selectivity over TNF $\alpha$  induction and reduces compound clearance in human liver microsomes. Furthermore, addition of hydroxyl groups onto the 7-position amine also reduced IVC. One might expect either of

these motifs, or a combination thereof, for example in compound **248** (Figure 69) might result in an orally bioavailable deazadenine TLR7 agonist.

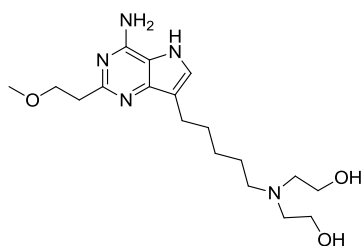


Figure 69: Potentially orally bioavailable IFN $\alpha$  inducing compound **248**.

Such a compound could potentially find use in the treatment of viral conditions such as hepatitis. Careful consideration would need to be given to exact biological properties required to minimise the side effects associated with systemic IFN $\alpha$  whilst still providing therapeutic efficacy.

Given that the natural ligand for the TLR7 receptor is viral RNA it is both surprising and exciting to note the increasing number of small molecule chemotypes being reported as TLR7 agonists (Section 1.9). These molecules allow medicinal chemists to potentially exploit aspects of both the innate and adaptive immune systems and create novel medicines capable of treating a wide variety of diseases either by symptom control or potentially transformational long term immunomodulation. As such research into TLR7 and indeed the other TLRs remains an area of great interest and future potential. Further evaluation of some of the advanced assets identified in this study such as **211b** will also further demonstrate the utility of TLR7 agonists as immunomodulatory agents for the treatment of allergic asthma.

## 4 Experimental

### 4.1 General experimental methods.

TLR7 agonists: The highly potent immunostimulatory TLR7 agonists described herein should be handled with appropriate containment controls particularly when manipulating powder samples which may become easily airborne. The hygiene guide for this class of compounds is  $< 1 \mu\text{g}/\text{m}^3$  [8 h TWA] to prevent exposure certain experimental procedures routinely carried out on the open bench, such as infrared spectroscopy and melting point determination, are strictly prohibited for such compounds.

All reagents were obtained from commercial suppliers and were used without further purification unless otherwise stated.

Anhydrous solvents were obtained from Sigma-Aldrich and transferred from the Sure Seal™ bottles by syringe, under an atmosphere of nitrogen.

Reactions performed under microwave irradiation were carried out in a Biotage Initiator instrument using sealed glass tubes.

All intermediate compounds are at least 90% pure, all final test compounds are greater than 95% pure unless stated otherwise. These purity assessments are made using the UV absorption spectra collected as part of LCMS analysis.

Reaction mixtures and products were analysed by LCMS using either system A or B:

#### System A

Column: 50 mm x 2.1 mm ID, Acquity UPLC BEH C<sub>18</sub> column.

Flow Rate: 1 mL/min

Temp: 40 °C

UV detection range: 210 to 350 nm

Mass spectrum: Recorded on a mass spectrometer using alternate-scan positive and negative mode electrospray ionisation.

Solvents:     A:     0.1 % v/v solution of formic acid in water  
              B:     0.1 % v/v solution of formic acid in acetonitrile

Gradient:	<u>Time (min.)</u>	<u>A %</u>	<u>B %</u>
	0	97	3
	1.5	0	100
	1.9	0	100
	2.0	100	0

### System B

Column:       50 mm x 2.1 mm ID, Acquity UPLC BEH C<sub>18</sub> column.

Flow Rate:    1 mL/min

Temp:         40 °C

UV detection range: 210 to 350 nm

Mass spectrum:       Recorded on a mass spectrometer using alternate-scan positive and negative mode electrospray ionisation.

Solvents:     A:     10 mM solution of ammonium bicarbonate in water  
              B:     acetonitrile

Gradient:	<u>Time (min.)</u>	<u>A %</u>	<u>B %</u>
	0	99	1
	1.5	3	97
	1.9	3	97
	2.0	99	1

Thin layer chromatography was carried out using POLYGRAM<sup>®</sup> SIL G/UV<sub>254</sub> plates with 0.2 mm silica gel and fluorescent indicator UV<sub>254</sub> (available from Macherey-Nagel, Germany). TLC plates were analysed using an Ultra-Violet Products Inc. Chromato-Vue<sup>®</sup> CC20G and developed using potassium permanganate solution or iodine as appropriate.

Chromatographic purification was typically performed using pre-packed silica gel cartridges (2 g to 100 g). The Flashmaster II is an automated multi-user flash



chromatography system, available from Argonaut Technologies Ltd. It provides quaternary on-line solvent mixing to enable gradient methods to be run. Samples are queued using the multi-functional open access software, which manages solvents, flow-rates, gradient profile and collection conditions. The system is equipped with a Knauer variable wavelength UV-detector and Gilson FC204 fraction collectors enabling automated peak-cutting, collection and tracking.

Mass directed autopreparative (MDAP) HPLC was undertaken under the conditions given below. The UV detection was an averaged signal from wavelength of 210 nm to 350 nm and mass spectra were recorded on a mass spectrometer using alternate-scan positive and negative mode electrospray ionisation.

#### Method A

Method A was conducted on an Xbridge C<sub>18</sub> column (typically 150 mm x 19 mm i.d. 5 µm packing diameter) at ambient temperature. The solvents employed were:  
A = 10 mM aqueous ammonium bicarbonate adjusted to pH 10 with ammonia solution.

B = acetonitrile

#### Method B

Method B was conducted on a Sunfire C<sub>18</sub> column (typically 150 mm x 30 mm i.d. 5 µm packing diameter) at ambient temperature. The solvents employed were:

A = 0.1 % v/v solution of formic acid in water

B = 0.1 % v/v solution of formic acid in acetonitrile.

Solvent removal using a stream of nitrogen was performed at 40-50 °C on a GreenHouse Blowdown system available from Radleys™ Discovery Technologies, Saffron Walden, Essex, CB11 3AZ, United Kingdom.

<sup>1</sup>H NMR spectra were recorded in either CDCl<sub>3</sub>, CD<sub>3</sub>OD or DMSO-*d*<sub>6</sub> on either a Bruker AV or DXP 400/500/600 spectrometer working at 400 MHz, 500 MHz and 600 MHz, respectively. Chemical shifts are reported in ppm and coupling constants are reported in Hz and refer to <sup>3</sup>J<sub>H-H</sub> interactions unless otherwise stated. The

internal standard used was either tetramethylsilane or the residual protonated solvent at 7.26 ppm for CDCl<sub>3</sub>, 3.31 ppm for CD<sub>3</sub>OD or 2.50 ppm for DMSO-*d*<sub>6</sub>.

<sup>13</sup>C NMR spectra were recorded in either CDCl<sub>3</sub>, CD<sub>3</sub>OD or DMSO-*d*<sub>6</sub> on either a Bruker AV or DXP 400/500/600 spectrometer working at 101 MHz, 126 MHz and 151 MHz, respectively. Chemical shifts are reported in ppm, the internal standard used was tetramethylsilane.

Infrared spectra were obtained using a Perkin Elmer Spectrum One FT-IR Spectrometer either from solids or by allowing a thin film of compound as a solution in DCM to evaporate.

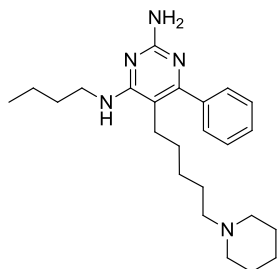
Accurate masses (HRMS) were obtained using a Bruker Apex IV Fourier transform ion cyclotron mass spectrometer (FTICR MS) which provides mass measurements of typically <1 ppm. This system uses a solid phase "trap and purge" method, coupled to an ESI/API interface. In addition to the accuracy of the mass measurement, the Bruker Data Analysis software uses a Molecular Formula Finder routine which further limits possible molecular formulae by employing isotopic pattern matching algorithms.

Melting points were obtained using a Stuart SMP-10 or SMP-40 melting point apparatus available from Bibby Scientific, Staffordshire, ST15 0SA, United Kingdom.

**All compounds synthesised by the author unless specified. Compounds marked\* or # were synthesised by Vincent Courtet or Sam Stewart respectively under the supervision of the author. Compounds marked <sup>Ω</sup> were made by Diane Coe.**

## 4.2 Experimental conditions.

### ***N*-4-butyl-6-phenyl-5-(5-(piperidin-1-yl)pentyl)pyrimidine-2,4-diamine (70g)**



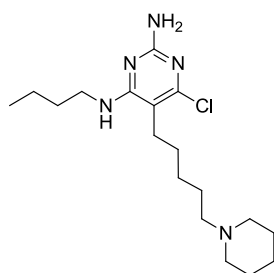
Chemical Formula: C<sub>24</sub>H<sub>37</sub>N<sub>5</sub>  
Molecular Weight: 395.58

To a suspension of phenylboronic acid (20 mg, 0.16 mmol), *N*-4-butyl-6-chloro-5-(5-(piperidin-1-yl)pentyl)pyrimidine-2,4-diamine (38 mg, 0.11 mmol) and potassium carbonate (30 mg, 0.22 mmol) in 1,4-dioxane (1.0 mL) and water (0.25 mL) was added chloro(di-2-norbornylphosphino)-(2'-dimethylamino-1,1'-biphenyl-2-yl) palladium (II) (6 mg, 11 μmol). The reaction vessel was sealed and heated in a Biotage Initiator microwave (using absorption setting high) to 150 °C for 1 h. The reaction mixture was decanted and to this mixture was added further phenylboronic acid (20 mg, 0.16 mmol), potassium carbonate (30 mg, 0.22 mmol) and chloro(di-2-norbornylphosphino)-(2'-dimethylamino-1,1'-biphenyl-2-yl)palladium (II) (6 mg, 11 μmol). The reaction vessel was sealed and heated in a Biotage Initiator microwave (using absorption setting high) to 150 °C for 1 h. The reaction mixture was partitioned between DCM (10 mL) and saturated aqueous sodium bicarbonate (10 mL). The organic phase was separated, dried (hydrophobic frit) and concentrated *in vacuo* before dissolving in 1:1 MeOH:DMSO (1 mL) and being purified by MDAP on an Xbridge column using MeCN-water with an ammonium carbonate modifier. The solvent was removed under a stream of nitrogen in the Radleys<sup>TM</sup> blowdown apparatus to give the title compound as a gum (14 mg, 33 %).

<sup>1</sup>H NMR (400 MHz, CDCl<sub>3</sub>) δ 7.43 - 7.32 (m, 5H), 4.65 (s, 2H), 4.57 (t, *J* = 5.1 Hz, 1H), 3.52 - 3.44 (m, 2H), 2.37 - 2.23 (m, 6H), 2.22 - 2.15 (m, 2H), 1.66 - 1.53 (m, 6H), 1.48 - 1.33 (m, 8H), 1.24 - 1.14 (m, 2H), 0.98 (t, *J* = 7.3 Hz, 3H); <sup>13</sup>C NMR

(101 MHz, CDCl<sub>3</sub>)  $\delta$  163.6, 162.0, 160.5, 140.1, 128.1, 127.8, 105.8, 59.2, 54.6, 40.8, 31.8, 28.7, 27.6, 26.5, 25.9, 24.4, 20.2, 13.9, two quaternary heteroaromatic carbons not observed; LCMS (System B) R<sub>t</sub> 1.17 min, m/z 396 ([M+H]<sup>+</sup>); HRMS Anal. Calcd. For C<sub>24</sub>H<sub>38</sub>N<sub>5</sub> = 396.3127. Found = 396.3129 ([M+H]<sup>+</sup>); IR (cm<sup>-1</sup>) 2930, 1623, 1561.

**N-4-butyl-6-chloro-5-[5-(1-piperidinyl)pentyl]-2,4-pyrimidinediamine (70k)**

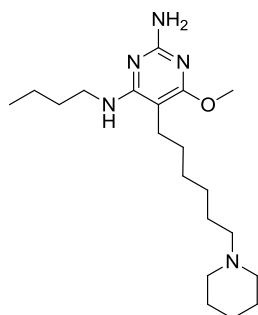


Chemical Formula: C<sub>18</sub>H<sub>32</sub>ClN<sub>5</sub>  
Molecular Weight: 353.93

A solution of *N*-4-butyl-6-chloro-5-[5-(1-piperidinyl)-1-pentyn-1-yl]-2,4-pyrimidinediamine (**76**) (122 mg, 0.35 mmol) in EtOH (35 mL) was filtered and hydrogenated using the H-cube (settings: 25 °C, Full H<sub>2</sub>, 1 mL/min flow rate) and a 10% Pd/C CatCart 30 as the catalyst. The reaction mixture was concentrated *in vacuo* and azeotroped with petroleum ether (40-60) to give the title compound (97 mg, 74%) as a gum.

<sup>1</sup>H NMR (400 MHz, CDCl<sub>3</sub>)  $\delta$  4.97 - 4.90 (m, 1H), 4.71 (br s, 2H), 3.48 - 3.38 (m, 2H), 2.70 - 2.60 (m, 4H), 2.57 - 2.51 (m, 2H), 2.46 (t, *J* = 7.5 Hz, 2H), 1.83 - 1.74 (m, 4H), 1.73 - 1.64 (m, 2H), 1.63 - 1.33 (m, 10H), 0.99 - 0.92 (m, 3H); LCMS (System B) R<sub>t</sub> 1.08 min, m/z 354, 356 ([M+H]<sup>+</sup>).

**N-4-butyl-6-methoxy-5-(6-(piperidin-1-yl)hexyl)pyrimidine-2,4-diamine (71b)**



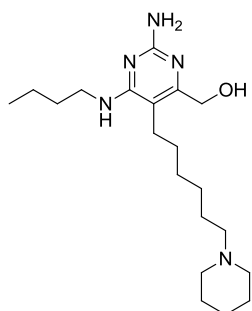
Chemical Formula: C<sub>20</sub>H<sub>37</sub>N<sub>5</sub>O  
Molecular Weight: 363.54

A solution of *N*-4-butyl-6-chloro-5-(6-(piperidin-1-yl)hexyl)pyrimidine-2,4-diamine (**71k**) (78 mg, 0.21 mmol), sodium *tert*-butoxide (62 mg, 0.65 mmol) and copper powder (2 mg, 0.03 mmol) in MeOH (2 mL) was sealed in a Reactival<sup>TM</sup> and heated to 140 °C for 24 h and allowed to cool to ambient temperature. To the reaction mixture was added a further aliquot of copper powder (2 mg, 0.03 mmol) and the reaction mixture was heated to 150 °C for 6 h. The reaction mixture was allowed to cool and further sodium *tert*-butoxide (62 mg, 0.65 mmol) was added and the reaction was sealed and heated to 150 °C for a further 16 h. The reaction mixture was allowed to cool to ambient temperature and was diluted with MeOH (5 mL), filtered through a pad of celite before concentration *in vacuo* to give a pale yellow solid (*ca.* 400 mg). The solid was triturated with EtOAc (10 mL) filtered and the filtrate was concentrated *in vacuo*. The sample was dissolved in 1:1 MeOH:DMSO (1 mL) and purified by MDAP on an Xbridge column using MeCN-water with an ammonium carbonate modifier. The solvent was removed under a stream of nitrogen in the Radleys<sup>TM</sup> blowdown apparatus to give the title compound (30 mg, 39 %) as a gum.

<sup>1</sup>H NMR (400 MHz, CDCl<sub>3</sub>) δ 4.48 (br s, 2H), 4.28 - 4.22 (m, 1H), 3.82 (s, 3H), 3.44 - 3.36 (m, 2H), 2.40 - 2.32 (m, 4H), 2.30 - 2.23 (m, 4H), 1.63 - 1.52 (m, 6H), 1.51 - 1.35 (m, 8H), 1.35 - 1.27 (m, 4H), 0.96 (t, *J* = 7.3 Hz, 3H); <sup>13</sup>C NMR (101 MHz, CDCl<sub>3</sub>) δ 167.3, 162.4, 160.3, 90.5, 59.6, 54.6, 53.1, 41.0, 32.2, 29.5, 28.3, 27.6, 26.8, 25.9, 24.5, 22.3, 20.1, 13.9 two quaternary heteroaromatic carbons not

observed; LCMS (System A)  $R_t$  0.54 min,  $m/z$  364 ( $[M+H]^+$ ); HRMS Anal. Calcd. For  $C_{20}H_{38}N_5O$  = 364.3071. Found = 364.3075 ( $[M+H]^+$ ); IR ( $cm^{-1}$ ) 3335, 2931, 2856, 1575.

**(2-Amino-6-(butylamino)-5-(6-(piperidin-1-yl)hexyl)pyrimidin-4-yl)methanol**  
**(71e)**



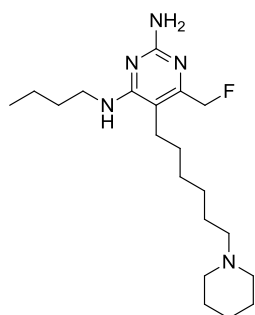
Chemical Formula:  $C_{20}H_{37}N_5O$   
Molecular Weight: 363.54

A solution of (2-amino-6-(butylamino)-5-(6-(piperidin-1-yl)hex-1-yn-1-yl)pyrimidin-4-yl)methanol (**111**) (250 mg, 0.70 mmol) in EtOH (40 mL) was filtered and hydrogenated using the H-cube (settings: 40 °C, Full  $H_2$ , 1 mL/min flow rate) and a 10% Pd/C CatCart 30 as the catalyst. The reaction mixture was concentrated *in vacuo* to give the title compound as a white solid (208 mg, 82%).

$^1H$  NMR (400 MHz,  $CDCl_3$ )  $\delta$  4.63 (br s, 2H), 4.53 - 4.46 (m, 1H), 4.46 (s, 2H), 3.48 - 3.40 (m, 2H), 2.41 (br s, 4H), 2.35 - 2.28 (m, 2H), 2.18 (t,  $J$  = 7.5 Hz, 2H), 1.67 - 1.56 (m, 4H), 1.55 - 1.48 (m, 2H), 1.48 - 1.24 (m, 12H), 0.97 (t,  $J$  = 7.4 Hz, 3H) exchangeable OH not observed;  $^{13}C$  NMR (101 MHz, MeOD)  $\delta$  163.4, 161.8, 160.8, 106.4, 62.1, 60.4, 55.5, 41.6, 32.7, 30.4, 29.9, 28.7, 27.2, 26.4, 25.1, 24.8, 21.2, 14.3; LCMS (System A)  $R_t$  0.47 min,  $m/z$  364 ( $[M+H]^+$ ); HRMS Anal. Calcd. For  $C_{20}H_{38}N_5O$  = 364.3071. Found = 364.3071 ( $[M+H]^+$ ); IR ( $cm^{-1}$ ) 3348, 3153, 2930, 1578; Mpt. 111-113 °C.

**N-4-butyl-6-(fluoromethyl)-5-(6-(piperidin-1-yl)hexyl)pyrimidine-2,4-diamine**

**(71f)**

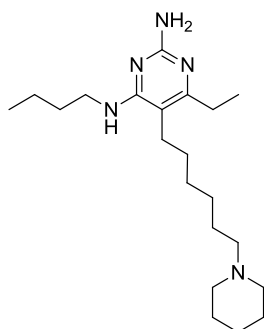


Chemical Formula: C<sub>20</sub>H<sub>36</sub>FN<sub>5</sub>  
Molecular Weight: 365.53

To a stirred solution of (2-amino-6-(butylamino)-5-(6-(piperidin-1-yl)hexyl)pyrimidin-4-yl)methanol (**71e**) (50 mg, 0.14 mmol) in anhydrous DCM (2 mL) at -78 °C under a nitrogen atmosphere was added XtalFluor-E (48 mg, 0.21 mmol). The reaction mixture was stirred at -78 °C for 10 min before allowing the reaction mixture to warm to ambient temperature and stirred at for a further 16 h. To the reaction mixture was added a further aliquot of XtalFluor-E (48 mg, 0.21 mmol) and stirring at ambient temperature continued for 3 h. The reaction mixture was diluted with DCM (10 mL) and washed with saturated aqueous sodium bicarbonate (10 mL). The resultant organic layer was dried (hydrophobic frit) and concentrated *in vacuo*, dissolved in 1:1 MeOH:DMSO (1 mL) and purified by MDAP on an Xbridge column using MeCN-water with an ammonium carbonate modifier. The solvent was removed under a stream of nitrogen in the Radleys<sup>TM</sup> blowdown apparatus to give the title compound (7 mg, 14%).

<sup>1</sup>H NMR (400 MHz, CDCl<sub>3</sub>) δ 5.20 (d, *J* = 47 Hz, 2H), 4.67 - 4.56 (m, 3H), 3.48 - 3.40 (m, 2H), 2.50 - 2.27 (m, 8H), 1.68 - 1.57 (m, 6H), 1.57 - 1.50 (m, 2H), 1.50 - 1.29 (m, 10H), 0.97 (t, *J* = 7.4 Hz, 3H); LCMS (System B) R<sub>t</sub> 1.08 min, m/z 366 ([M+H]<sup>+</sup>).

**N-4-butyl-6-ethyl-5-(6-(piperidin-1-yl)hexyl)pyrimidine-2,4-diamine (71h)**

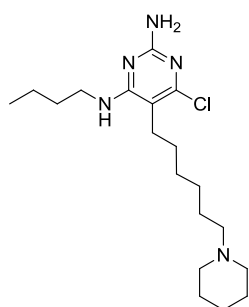


Chemical Formula: C<sub>21</sub>H<sub>39</sub>N<sub>5</sub>  
Molecular Weight: 361.57

A solution of *N*-4-butyl-6-ethyl-5-(6-(piperidin-1-yl)hex-1-yn-1-yl)pyrimidine-2,4-diamine (**115**) (95 mg, 0.27 mmol) in EtOH (15 mL) was filtered and hydrogenated using the H-cube (settings: 40 °C, Full H<sub>2</sub>, 1 mL/min flow rate) and a 10% Pd/C CatCart 30 as the catalyst. The reaction mixture was concentrated *in vacuo* and azeotroped with DCM and petroleum ether (40-60) to give the title compound (67 mg, 70 %) as a beige solid.

<sup>1</sup>H NMR (400 MHz, CDCl<sub>3</sub>) δ 6.41 - 6.25 (m, 1H), 6.24 - 5.90 (m, 2H), 3.56 - 3.45 (m, 2H), 3.03 - 2.81 (m, 4H), 2.81 - 2.71 (m, 2H), 2.60 (q, *J* = 7.5 Hz, 2H), 2.43 - 2.33 (m, 2H), 1.94 (br s, 4H), 1.86 - 1.74 (m, 2H), 1.68 - 1.56 (m, 4H), 1.51 - 1.43 (m, 6H), 1.42-1.34 (m, 2H), 1.34 - 1.28 (m, 3H), 0.95 - 0.92 (m, 3H); LCMS (System B) R<sub>t</sub> 1.29 min, m/z 362 ([M+H]<sup>+</sup>).

**N-4-butyl-6-chloro-5-[6-(1-piperidinyl)hexyl]-2,4-pyrimidinediamine (71k)**



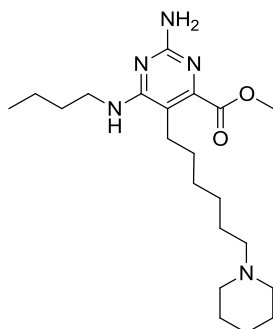
Chemical Formula: C<sub>19</sub>H<sub>34</sub>ClN<sub>5</sub>  
Molecular Weight: 367.96



A solution of *N*-4-butyl-6-chloro-5-[6-(1-piperidiny)-1-hexyn-1-yl]-2,4-pyrimidinediamine (**79**) (100 mg, 0.275 mmol) in EtOH (30 mL) was filtered and hydrogenated using the H-cube (settings: 20 °C, 10 bar, 1 mL/min flow rate) and a 10% Pd/C CatCart 30 as the catalyst. The reaction mixture was concentrated *in vacuo* to give the title compound (**76** mg, 75%) as a colourless gum.

<sup>1</sup>H NMR (400 MHz, CDCl<sub>3</sub>) δ 4.79 - 4.72 (m, 1H), 4.69 (s, 2H), 3.45 - 3.37 (m, 2H), 2.71 (br s, 4H), 2.63 - 2.54 (m, 2H), 2.47 - 2.40 (m, 2H), 1.88 - 1.78 (m, 4H), 1.75 - 1.65 (m, 2H), 1.63 - 1.51 (m, 4H), 1.51 - 1.32 (m, 8H), 0.96 (t, *J* = 7.3 Hz, 3H); <sup>13</sup>C NMR (101 MHz, CDCl<sub>3</sub>) δ 162.2, 160.2, 157.4, 104.8, 58.4, 53.9, 41.1, 31.6, 29.0, 27.5, 27.0, 26.2, 25.2, 24.3, 23.3, 20.1, 13.8; LCMS (System A) R<sub>t</sub> 0.61 min, m/z 368, 370 ([M+H]<sup>+</sup>); HRMS Anal. Calcd. for C<sub>19</sub>H<sub>35</sub>ClN<sub>5</sub> = 368.2576. Found = 368.2576 ([M+H]<sup>+</sup>); IR (cm<sup>-1</sup>) 3315, 2931, 1556.

**Methyl-2-amino-6-(butylamino)-5-(6-(piperidin-1-yl)hexyl)pyrimidine-4-carboxylate (71I)**



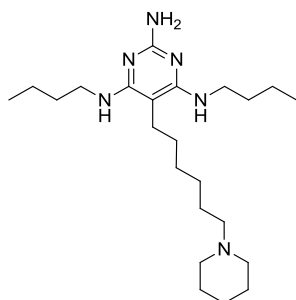
Chemical Formula: C<sub>21</sub>H<sub>37</sub>N<sub>5</sub>O<sub>2</sub>  
Molecular Weight: 391.55

A solution of methyl 2-amino-6-(butylamino)-5-(6-(piperidin-1-yl)hex-1-yn-1-yl)-pyrimidine-4-carboxylate (**100**) (28 mg, 0.07 mmol) in EtOH (8 mL) was filtered and hydrogenated using the H-cube (settings: 40 °C, 10 bar, 1 mL/min flow rate) and a 10% Pd/C CatCart 30 as the catalyst. The reaction mixture was concentrated *in vacuo* and the resulting residue was dissolved in DCM and purified on a silica cartridge (5 g) using a 0-25% MeOH/DCM gradient. The appropriate fractions were

combined and evaporated *in vacuo* to give the title compound (13 mg, 46 %) as a colourless gum.

<sup>1</sup>H NMR (400 MHz, MeOD) 3.87 (s, 2H), 3.43 (t, *J* = 7.3 Hz, 2H), 3.32 - 3.28 (m, 2H), 3.24 - 3.11 (m, 3H), 3.06 - 2.98 (m, 2H), 2.52 - 2.44 (m, 2H), 1.89 - 1.80 (m, 4H), 1.78 - 1.53 (s, 7H), 1.53 - 1.26 (m, 10H), 0.95 (t, *J* = 7.4 Hz, 3H); <sup>13</sup>C NMR (101 MHz, MeOD) δ 167.9, 163.7, 161.8, 151.7, 109.3, 58.5, 54.4, 53.0, 41.7, 32.5, 29.7, 27.5, 25.7, 25.0, 24.4, 22.8, 21.2, 14.3; LCMS (System B) R<sub>t</sub> 1.07 min, m/z 392 ([M+H]<sup>+</sup>); HRMS Anal. Calcd. For C<sub>21</sub>H<sub>38</sub>N<sub>5</sub>O<sub>2</sub> = 392.3026. Found = 392.3035 ([M+H]<sup>+</sup>); IR (cm<sup>-1</sup>) 3347, 2933, 1730, 1575.

**N-4,N-6-dibutyl-5-(6-(piperidin-1-yl)hexyl)pyrimidine-2,4,6-triamine (71m)**



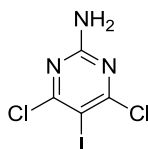
Chemical Formula: C<sub>23</sub>H<sub>44</sub>N<sub>6</sub>  
Molecular Weight: 404.64

To a suspension of *N*-4-butyl-6-chloro-5-(6-(piperidin-1-yl) hexyl) pyrimidine-2,4-diamine (84 mg, 0.23 mmol) (**71k**), 1,3-*bis*(2,6-diisopropylphenyl)-imidazol-2-ylidene-(1,4-naphthoquinone)palladium(0) dimer (30 mg, 0.02 mmol) and sodium *tert*-butoxide (44 mg, 0.46 mmol) in anhydrous toluene (2 mL) was added *n*-butylamine (0.05 mL, 0.48 mmol). The reaction vessel was sealed and heated in a Biotage Initiator microwave (using absorption setting normal) to 150 °C for 1 h. After cooling, the reaction mixture was diluted with MeOH (10 mL) and filtered through a pad of celite before concentration *in vacuo*. The residue was partitioned between EtOAc (30 mL) and water (30 mL). The organic phase was separated and dried (hydrophobic frit) before concentration *in vacuo*. The sample was dissolved in 1:1 MeOH:DMSO (1 mL) and purified by MDAP on an Xbridge column using MeCN-water with an ammonium carbonate modifier. The solvent was removed a

stream of nitrogen in the Radleys™ blowdown apparatus to give the title compound (38 mg, 41 %) as a colourless gum.

<sup>1</sup>H NMR (400 MHz, CDCl<sub>3</sub>) δ 4.37 (s, 2H), 4.04 (t, *J* = 5.3 Hz, 2H), 3.42 - 3.34 (m, 4H), 2.39 - 2.31 (m, 4H), 2.29 - 2.23 (m, 2H), 2.16 - 2.09 (m, 2H), 1.64 - 1.47 (m, 10H), 1.46 - 1.27 (m, 12H), 0.95 (t, *J* = 7.4 Hz, 6H); <sup>13</sup>C NMR (101 MHz, 101 MHz, CDCl<sub>3</sub>) δ 160.6, 86.6, 59.5, 54.7, 40.9, 32.4, 29.8, 27.9, 26.9, 26.0, 24.7, 23.7, 20.2, 13.8 two quaternary heteroaromatic carbons not observed; LCMS (System B) R<sub>t</sub> 1.22 min, m/z 405 ([M+H]<sup>+</sup>); HRMS Anal. Calcd. For C<sub>23</sub>H<sub>45</sub>N<sub>6</sub> = 405.3706. Found = 405.3691 ([M+H]<sup>+</sup>); IR (cm<sup>-1</sup>) 2929, 2856, 1576.

#### **4,6-Dichloro-5-iodo-2-pyrimidinamine (73)**

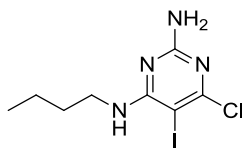


Chemical Formula: C<sub>4</sub>H<sub>2</sub>Cl<sub>2</sub>I N<sub>3</sub>  
Molecular Weight: 289.89

To a stirred solution of 4,6-dichloro-2-pyrimidinamine (30.7 g, 187 mmol) in AcOH (900 mL) was added a solution of iodine monochloride (30.9 mL, 616 mmol) in AcOH (500 mL) dropwise over 90 min. The resulting solution was stirred at ambient temperature for 1 h after which time a suspension formed and was allowed to stand at ambient temperature for 20 h. The precipitate was collected by filtration and washed with AcOH (*ca.* 50 mL) before drying *in vacuo* to give the title compound (22.5 g, 42 %) as a white solid. The filtrate was allowed to stand for a further six days after which time the crystalline precipitate was collected by filtration and dried *in vacuo* to give a further portion of the title compound (4.14 g, 8 %) as a white solid.

<sup>1</sup>H NMR (400 MHz, CDCl<sub>3</sub>) δ 5.31 (br s, 2H); LCMS (System B) t<sub>RET</sub> 0.96 min, m/z 288, 290, 292 ([M-H]<sup>-</sup>).

**N-4-butyl-6-chloro-5-iodo-2,4-pyrimidinediamine (74)**

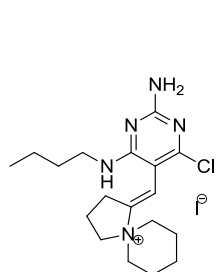


Chemical Formula: C<sub>8</sub>H<sub>12</sub>ClIN<sub>4</sub>  
Molecular Weight: 326.57

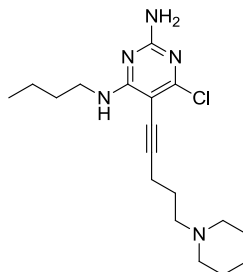
To a stirred mixture of 4,6-dichloro-5-iodo-2-pyrimidinamine (**73**) (5.4 g, 18.6 mmol) and triethylamine (5.71 mL, 41.0 mmol) in EtOH (80 mL) was added *n*-butylamine (2.03 mL, 20.5 mmol) in one charge and the reaction mixture was stirred at ambient temperature for 2 h before heating to reflux for 2.5 h. The reaction mixture was allowed to cool to ambient temperature and was concentrated *in vacuo*. The resulting residue was partitioned between EtOAc (250 mL) and water (250 mL). The organic phase was separated and the aqueous phase back extracted with EtOAc (100 mL). The combined organic extracts were washed with brine (250 mL), dried (MgSO<sub>4</sub>), filtered and concentrated *in vacuo*, before being dissolved in DCM and purified on a silica cartridge (100 g) using a 0-50% EtOAc-cyclohexane gradient over 60 min. The appropriate fractions were combined and evaporated *in vacuo* to give the title compound (5.45 g, 90 %) as a white solid.

<sup>1</sup>H NMR (400 MHz, CDCl<sub>3</sub>) δ 5.42 - 5.35 (m, 1H), 4.88 (br s, 2H), 3.41 (dt, *J* = 7.0, 5.5 Hz, 2H), 1.64 - 1.55 (m, 2H), 1.47 - 1.35 (m, 2H), 0.97 (t, *J* = 7.3 Hz, 3H); LCMS (System A) R<sub>t</sub> 1.05 min, *m/z* 327, 329 ([M+H]<sup>+</sup>); Mpt. 108-112 °C.

**(1E)-1-{[2-amino-4-(butylamino)-6-chloro-5-pyrimidinyl]methylidene}-5-azoniaspiro[4.5]decane iodide (77) and N-4-butyl-6-chloro-5-[5-(1-piperidinyl)-1-pentyn-1-yl]-2,4-pyrimidinediamine (76) Method A**



Chemical Formula: C<sub>18</sub>H<sub>29</sub>ClIN<sub>5</sub>  
Molecular Weight: 477.81



Chemical Formula: C<sub>18</sub>H<sub>28</sub>ClN<sub>5</sub>  
Molecular Weight: 349.90

A degassed stirred mixture of *N*-4-butyl-6-chloro-5-iodo-2,4-pyrimidinediamine (200 mg, 0.61 mmol) (**74**), tetrakis(triphenylphosphine)palladium(0) (71 mg, 0.061 mmol) and copper(I) iodide (23 mg, 0.12 mmol) in anhydrous DMF (8 mL) was heated to 60 °C under a nitrogen atmosphere. To the reaction mixture was added a degassed solution of 1-(4-pentyn-1-yl)piperidine (185 mg, 1.23 mmol) and triethylamine (0.171 mL, 1.23 mmol) in anhydrous DMF (2 mL) dropwise over 2 min. The reaction mixture was stirred at 70 °C for 4 h. The reaction mixture was concentrated *in vacuo* and the residue was partitioned between water (20 mL) and EtOAc (20 mL). The organic phase, now a suspension, was separated and the aqueous phase back extracted with EtOAc (20 mL). The combined organic phases were filtered and the resultant solid dried *in vacuo*. The sample was dissolved in 1:1 MeOH:DMSO (1 mL) and purified by MDAP on an Xbridge column using MeCN/water with an ammonium carbonate modifier. The solvent was evaporated *in vacuo* and azeotroped successively with DCM and petroleum ether (40-60) to give **77** (32 mg, 11 %) as a grey solid.

<sup>1</sup>H NMR (600 MHz, DMSO-d<sub>6</sub>) δ 6.88 (br s, 2H), 6.52 (br s, 2H), 3.83 (br s, 2H), 3.71 (d, *J* = 10.6 Hz, 2H), 3.66 (br s, 2H), 3.32 (d, *J* = 5.3 Hz, 2H), 2.61 - 2.52 (m, 2H), 2.09 - 2.00 (m, 2H), 1.93 (d, *J* = 12.7 Hz, 2H), 1.87 - 1.78 (m, 2H), 1.78 - 1.67 (m, 1H), 1.66 - 1.55 (m, 1H), 1.54 - 1.46 (m, 2H), 1.32 - 1.21 (m, 2H), 0.94 - 0.83 (m, 3H); <sup>13</sup>C NMR (151 MHz, DMSO-d<sub>6</sub>) δ 161.8, 160.3, 156.1, 152.3, 114.4, 96.7,

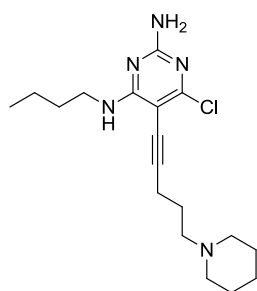
61.4, 59.0, 40.2, 31.3, 26.9, 21.0, 20.2, 19.8, 19.7, 13.9; LCMS (System B)  $R_t$  0.77,  $m/z$  350, 352 ( $[M+H]^+$ ); HRMS Anal. Calcd. For  $C_{18}H_{30}ClN_5$  = 350.2111. Found = 350.2100 ( $[M+H]^+$ ); IR ( $cm^{-1}$ ) 3319, 2935, 1651, 1553; Mpt. 250-254 °C (decomp.).

The original organic mother liquor was dried ( $MgSO_4$ ), filtered and concentrated *in vacuo*. The sample was dissolved in DCM and purified on a silica cartridge (20 g) using a 0-100% EtOAc-cyclohexane + 0-20% MeOH gradient over 40 min. The appropriate fractions were combined and evaporated *in vacuo* to give a beige gum. Trituration with petroleum ether (40-60) give a beige solid that was collected by filtration and dried *in vacuo* to give **76** (20 mg, 9 %) as a yellow solid.

$^1H$  NMR (600 MHz,  $DMSO-d_6$ )  $\delta$  6.66 (br s, 2H), 6.55 (t,  $J$  = 5.8 Hz, 1H), 3.32 (q,  $J$  = 6.8 Hz, 2H), 2.47 (t,  $J$  = 7.0 Hz, 2H), 2.44 (t,  $J$  = 7.2 Hz, 2H), 2.40 (br s, 4H), 1.70 (quin,  $J$  = 7.0 Hz, 2H), 1.54 - 1.46 (m, 6H), 1.42 - 1.35 (m, 2H), 1.32 - 1.24 (m,  $J$  = 7.5 Hz, 2H), 0.89 (t,  $J$  = 7.3 Hz, 3H);  $^{13}C$  NMR (151 MHz,  $DMSO-d_6$ )  $\delta$  163.0, 160.4, 158.4, 99.3, 88.9, 72.4, 57.3, 53.9, 40.1, 31.2, 25.4, 25.3, 23.8, 19.6, 17.4, 13.8; LCMS (System B)  $R_t$  1.20 min,  $m/z$  350, 352 ( $M+H^+$ ).

**N-4-butyl-6-chloro-5-[5-(1-piperidinyl)-1-pentyn-1-yl]-2,4-pyrimidinediamine**

**(76) Method B**



Chemical Formula:  $C_{18}H_{28}ClN_5$   
Molecular Weight: 349.90

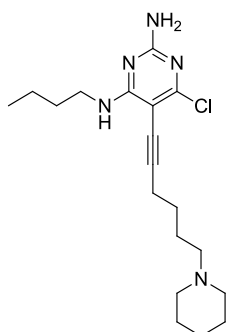
A degassed, stirred mixture of *N*-4-butyl-6-chloro-5-iodo-2,4-pyrimidinediamine (200 mg, 0.61 mmol), tetrakis(triphenylphosphine)palladium(0) (71 mg, 0.061 mmol) and copper(I) iodide (24 mg, 0.13 mmol) in anhydrous DMF (8 mL) was stirred at ambient temperature for 10 min. To the reaction mixture was added a

degassed solution of 1-(4-pentyn-1-yl)piperidine (185 mg, 1.23 mmol) and triethylamine (0.171 mL, 1.23 mmol) in anhydrous DMF (2 mL) dropwise over 30 sec. The reaction mixture was stirred at ambient temperature for 19 h. The reaction mixture was concentrated *in vacuo* and the resultant solid triturated with EtOAc and filtered before the filtrate was concentrated *in vacuo*. The sample was dissolved in DCM and purified on a silica cartridge (20 g) using a 0-25% MeOH-DCM gradient over 30 min. The appropriate fractions were combined and evaporated *in vacuo* to give the title compound (72 mg, 34 %) as a yellow solid. Note: **77** was not isolated

<sup>1</sup>H NMR (400 MHz, DMSO-d<sub>6</sub>) δ 6.66 (br s, 2H), 6.60 - 6.53 (m, 1H), 3.38 - 3.24 (m, 2H), 2.53 - 2.45 (m, 8H), 1.79 - 1.68 (m, 2H), 1.57 - 1.45 (m, 6H), 1.41 (br s, 2H), 1.35 - 1.22 (m, 2H), 0.90 (t, *J* = 7.4 Hz, 3H); LCMS (System B) R<sub>t</sub> 1.21 min, m/z 350, 352 ([M+H]<sup>+</sup>).

**N-4-butyl-6-chloro-5-[6-(1-piperidinyl)-1-hexyn-1-yl]-2,4-pyrimidinediamine**

**(79)**



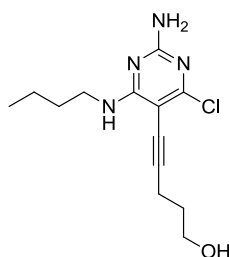
Chemical Formula: C<sub>19</sub>H<sub>30</sub>ClN<sub>5</sub>  
Molecular Weight: 363.93

To a stirred, degassed solution of *N*-4-butyl-6-chloro-5-iodo-2,4-pyrimidinediamine (974 mg, 2.98 mmol) (**76**), copper(I) iodide (0.11 g, 0.60 mmol) and tetrakis(triphenylphosphine)palladium(0) (0.35 g, 0.30 mmol) in anhydrous DMF (40 mL) at ambient temperature was added a solution of 1-(5-hexyn-1-yl)piperidine (1.00 g, 6.05 mmol) and triethylamine (0.83 mL, 6.00 mmol) in anhydrous DMF (40 mL) dropwise over 10 min. The reaction mixture was stirred at ambient temperature under a nitrogen atmosphere for 20 h. The reaction mixture was concentrated *in*

*vacuo* and the resultant black residue was triturated with EtOAc (100 mL), filtered and concentrated *in vacuo*. The sample was dissolved in DCM and purified on silica cartridges (100 g) using a 0-25% MeOH:DCM gradient over 60 min. The appropriate fractions were combined and evaporated *in vacuo*. The appropriate fractions were combined and evaporated *in vacuo* to give the title compound (223 mg, 21%) as a yellow gum.

<sup>1</sup>H NMR (400 MHz, CDCl<sub>3</sub>) δ 5.53 - 5.47 (m, 1H), 4.89 (s, 2H), 3.47 - 3.39 (m, 2H), 2.57 - 2.50 (m, 4H), 1.86 - 1.71 (m, 2H), 1.71 - 1.63 (m, 6H), 1.63 - 1.54 (m, 2H), 1.54 - 1.48 (m, 2H), 1.45 - 1.34 (m, 2H), 0.97 (t, *J* = 7.3 Hz, 3H); <sup>13</sup>C NMR (101 MHz, CDCl<sub>3</sub>) δ 163.4, 160.0, 159.2, 99.9, 91.6, 72.5, 58.2, 54.1, 40.8, 31.6, 26.6, 25.0, 24.9, 23.7, 20.0, 19.7, 13.8; LCMS (System B) R<sub>t</sub> 1.18 min, m/z 364, 366 ([M+H]<sup>+</sup>); HRMS Anal. Calcd. for C<sub>19</sub>H<sub>31</sub>ClN<sub>5</sub> = 364.2268. Found = 364.2266 ([M+H]<sup>+</sup>); IR (cm<sup>-1</sup>) 3293, 2932, 1586, 1556.

**5-[2-Amino-4-(butylamino)-6-chloro-5-pyrimidinyl]-4-pentyn-1-ol (81)**



Chemical Formula: C<sub>13</sub>H<sub>19</sub>ClN<sub>4</sub>O  
Molecular Weight: 282.77

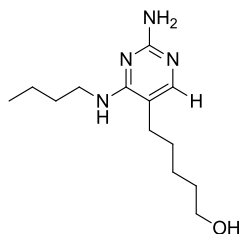
A degassed stirred mixture of *N*-4-butyl-6-chloro-5-iodo-2,4-pyrimidinediamine (**74**) (650 mg, 1.99 mmol), tetrakis(triphenylphosphine)palladium(0) (230 mg, 0.20 mmol) and copper(I) iodide (76 mg, 0.40 mmol) in anhydrous DMF (25 mL) was stirred at ambient temperature for 5 min. To the reaction mixture was added a degassed solution of 4-pentyn-1-ol (0.37 mL, 4.0 mmol) and triethylamine (0.555 mL, 4.0 mmol) in anhydrous DMF (5 mL) dropwise over 30 sec. The reaction mixture was stirred at ambient temperature for 22 h before the reaction was concentrated *in vacuo*. The residue was partitioned between water (100 mL) and EtOAc (80 mL). The organic phase was separated and the aqueous phase back



extracted with EtOAc (40 mL). The combined organic phases were dried (MgSO<sub>4</sub>), filtered and concentrated *in vacuo*. The resulting residue was dissolved in DCM and purified on a silica cartridge (50 g) using a 0-100% EtOAc-DCM gradient over 60 min. The appropriate fractions were combined and evaporated *in vacuo* to give a sticky yellow solid. This was triturated with diethyl ether (*ca.* 5 mL). The resultant off white solid was collected by filtration and dried *in vacuo* to give the title compound (234 mg, 42 %) as a gum. The mother liquor and aqueous layer were analysed by LCMS and found to contain significant amounts of product. The aqueous layer was extracted with DCM (100 mL). The extract and mother liquor were combined and concentrated *in vacuo*. The sample was dissolved in DCM and purified on a silica cartridge (50 g) using a 0-50% EtOAc-DCM gradient over 40 min. The appropriate fractions were combined and evaporated *in vacuo* to give a yellow oil. The sample was dissolved in DCM and further purified on a silica cartridge (20 g) using a 0-50% EtOAc-cyclohexane gradient over 40 min. The appropriate fractions were combined and evaporated *in vacuo* to give a further batch of the title compound (78 mg, 14 %) as a white solid.

<sup>1</sup>H NMR (400 MHz, CDCl<sub>3</sub>) δ 5.64 - 5.56 (m, 1H), 4.91 (br s, 2H), 3.86 (q, *J* = 5.9 Hz, 2H), 3.45 - 3.37 (m, 2H), 2.65 (t, *J* = 6.9 Hz, 2H), 1.93 - 1.84 (m, 2H), 1.64 - 1.53 (m, 3H), 1.45 - 1.34 (m, 2H), 0.96 (t, *J* = 7.4 Hz, 3H); <sup>13</sup>C NMR (126 MHz, CDCl<sub>3</sub>) δ 163.5, 160.0, 159.2, 99.7, 91.6, 72.6, 61.8, 40.8, 31.6, 31.3, 20.0, 16.7, 13.8; LCMS (System B) R<sub>t</sub> 0.91 min, m/z 283, 285 ([M+H]<sup>+</sup>); HRMS Anal. Calcd. For C<sub>13</sub>H<sub>20</sub>ClN<sub>4</sub>O = 283.1320. Found = 283.1317 ([M+H]<sup>+</sup>); IR (cm<sup>-1</sup>) 3320, 3182, 2932, 1652, 1560; Mpt. 103-107 °C.

### **5-[2-Amino-4-(butylamino)-5-pyrimidinyl]-1-pentanol (82)**

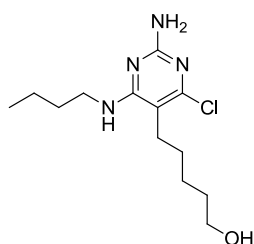


Chemical Formula: C<sub>13</sub>H<sub>24</sub>N<sub>4</sub>O  
Molecular Weight: 252.36

A solution of 5-[2-amino-4-(butylamino)-6-chloro-5-pyrimidinyl]-4-pentyn-1-ol (230 mg, 0.81 mmol) (**81**) in EtOH (40 mL) was filtered and hydrogenated using the H-cube (settings: 25 °C, Full H<sub>2</sub>, 1 mL/min flow rate) and a 10% Pd/C CatCart 30 as the catalyst. The reaction mixture was concentrated *in vacuo* to give the title compound (187 mg, 91 %) as a white solid.

<sup>1</sup>H NMR (400 MHz, MeOD) δ 7.96 - 7.90 (m, 1H), 7.37 (s, 1H), 3.59 - 3.49 (m, 4H), 2.41 - 2.33 (m, 2H), 1.57 (m, 6H), 1.66 - 1.51 (m, 2H), 1.47 - 1.32 (m, 2H), 0.96 (m, 3H), exchangeable protons (NH<sub>2</sub> and OH) not observed; <sup>13</sup>C NMR (101 MHz, MeOD) δ 163.9, 156.2, 138.0, 112.1, 62.9, 42.2, 33.4, 32.3, 28.7, 27.7, 26.7, 21.3, 14.3; LCMS (System B) R<sub>t</sub> 0.79 min, m/z 253 ([M+H]<sup>+</sup>); HRMS Anal. Calcd. For C<sub>13</sub>H<sub>25</sub>N<sub>4</sub>O = 253.2023. Found = 253.2024 ([M+H]<sup>+</sup>); IR (cm<sup>-1</sup>) 3302, 2932, 1650, 1573; Mpt. 159-163 °C.

### **5-[2-Amino-4-(butylamino)-6-chloro-5-pyrimidinyl]-1-pentanol (83)**



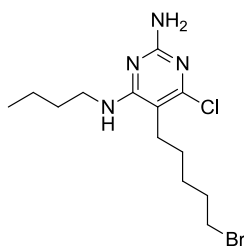
Chemical Formula: C<sub>13</sub>H<sub>23</sub>ClN<sub>4</sub>O  
Molecular Weight: 286.80

To a solution of 5-[2-amino-4-(butylamino)-6-chloro-5-pyrimidinyl]-4-pentyn-1-ol (483 mg, 1.71 mmol) (**81**) in EtOH (100 mL) was added *N*-methylpiperidine (0.42 mL, 3.4 mmol). The resultant solution was hydrogenated using the H-cube (settings: 25 °C, full H<sub>2</sub>, 1 mL/min flow rate) and 10% Pd/C CatCart 30 as the catalyst. The reaction mixture was concentrated *in vacuo* and the resulting residue was dissolved in DCM and purified on a silica cartridge (100 g) using a 0-100% EtOAc-DCM gradient over 60 min. The appropriate fractions were combined and evaporated *in vacuo* to give the title compound (227 mg, 46 %) as a colourless oil which solidified on standing. The remaining fractions containing a mixture of intermediate alkene and desired alkane (by LCMS analysis) were combined and concentrated *in vacuo*.

The sample was dissolved in EtOH (20 mL) treated with *N*-methylpiperidine (0.084 mL) and was hydrogenated using the H-cube (settings: 25° C, 10 bar, 1 mL/min flow rate) and a 10% Pd/C CatCart 30 as the catalyst. The reaction was concentrated *in vacuo* before the sample was dissolved in DCM and purified on silica cartridge (20 g) using a 0-100% EtOAc-DCM gradient over 40 min. The appropriate fractions were combined and evaporated *in vacuo* to give a further batch of the title compound (20 mg, 4%) as a white solid.

<sup>1</sup>H NMR (400 MHz, CDCl<sub>3</sub>) δ 4.74 - 4.64 (m, 3H), 3.72 - 3.64 (m, 2H), 3.43 - 3.37 (m, 2H), 2.50 - 2.43 (m, 2H), 1.69 - 1.44 (m 9H), 1.43 - 1.33 (m, 2H), 0.96 (t, *J* = 7.3 Hz, 3H); LCMS (System A) R<sub>t</sub> 0.65 min, m/z 287, 289 ([M+H]<sup>+</sup>).

#### **5-(5-Bromopentyl)-*N*4-butyl-6-chloro-2,4-pyrimidinediamine (84)**



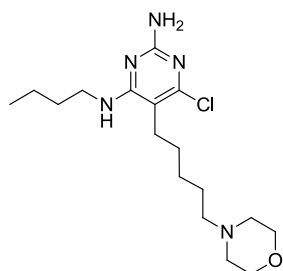
Chemical Formula: C<sub>13</sub>H<sub>22</sub>BrClN<sub>4</sub>  
Molecular Weight: 349.70

To a stirred solution of 5-[2-amino-4-(butylamino)-6-chloro-5-pyrimidinyl]-1-pentanol (**83**) (60 mg, 0.21 mmol) and carbon tetrabromide (83 mg, 0.25 mmol) in DCM (1.5 mL) was added a solution of triphenylphosphine (66 mg, 0.25 mmol) in DCM (1 mL) in a dropwise fashion. The reaction mixture was stirred at ambient temperature for 18 h. After this time further carbon tetrabromide (83 mg, 0.25 mmol) and triphenylphosphine (66 mg, 0.25 mmol) were added and the reaction mixture was stirred at ambient temperature for a further 2 h. The reaction mixture was concentrated *in vacuo* (water bath max temp 20 °C). The sample was dissolved in DCM and purified on a silica cartridge (20 g) using a 0-50% EtOAc-cyclohexane +0-20% MeOH gradient over 40 min. The appropriate fractions were combined and evaporated *in vacuo* to give a yellow oil. The oil was dissolved in DCM purified on silica (Si) 10g using a 0-50% ethyl acetate-cyclohexane gradient over 20 mins. The

appropriate fractions were combined and evaporated *in vacuo* to give the title compound (39 mg, 53%) as a colourless gum.

$^1\text{H}$  NMR (400 MHz,  $\text{CDCl}_3$ )  $\delta$  4.72 (br s, 2H), 4.64 - 4.56 (m, 1H), 3.46 - 3.38 (m, 4H), 2.48 - 2.42 (m, 2H), 1.96 - 1.84 (m, 2H), 1.63 - 1.48 (m, 6H), 1.44 - 1.34 (m, 2H), 0.97 (t,  $J = 7.3$  Hz, 3H); LCMS (System B)  $R_t$  1.25 min,  $m/z$ , 347, 349, 351, 353 ( $[\text{M}+\text{H}]^+$ ).

***N*-4-butyl-6-chloro-5-[5-(4-morpholinyl)pentyl]-2,4-pyrimidinediamine (85)**



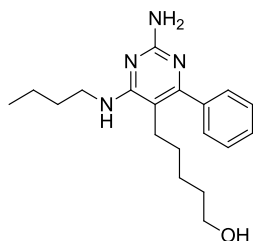
Chemical Formula:  $\text{C}_{17}\text{H}_{30}\text{ClN}_5\text{O}$   
Molecular Weight: 355.91

To a stirred solution of 5-(5-bromopentyl)-*N*-4-butyl-6-chloro-2,4-pyrimidinediamine (38 mg, 0.11 mmol) (**84**) in MeCN (2 mL) was added triethylamine (20  $\mu\text{L}$ , 0.14 mmol) and morpholine (20  $\mu\text{L}$ , 0.23 mmol). The reaction mixture was stirred at ambient temperature for 16 h. To the reaction mixture was added a further aliquot of morpholine (20  $\mu\text{L}$ , 0.23 mmol) and the reaction mixture was warmed to 50  $^\circ\text{C}$  for 3 h. The reaction mixture was allowed to cool to ambient temperature and partitioned between DCM (10 mL) and water (10 mL). The organic phase was separated and dried (hydrophobic frit) before concentration *in vacuo*. The sample was dissolved in DCM and purified on a silica cartridge (5 g) using 10% MeOH in DCM. The appropriate fractions were combined and evaporated *in vacuo* to give the title compound (27 mg, 70 %) as a solid.

$^1\text{H}$  NMR (400 MHz,  $\text{CDCl}_3$ )  $\delta$  4.72 (br s, 2H), 4.64 - 4.56 (m, 1H), 3.75 - 3.68 (m, 4H), 3.45 - 3.38 (m, 2H), 2.49 - 2.40 (m, 6H), 2.37 - 2.30 (m, 2H), 1.63 - 1.45 (m, 6H), 1.44 - 1.32 (m, 4H), 0.96 (t,  $J = 7.3$  Hz, 3H);  $^{13}\text{C}$  NMR (101 MHz,  $\text{CDCl}_3$ )  $\delta$  162.1, 160.3, 157.5, 104.7, 67.0, 59.0, 53.8, 41.1, 31.7, 27.6, 27.3, 26.4, 26.3, 20.1,

13.9; LCMS (System B)  $R_t$  1.00 min,  $m/z$  356, 358 ( $[M+H]^+$ ); HRMS Anal. Calcd. For  $C_{17}H_{31}ClN_5O$  = 356.2212. Found = 356.2211 ( $[M+H]^+$ ); IR ( $cm^{-1}$ ) 3312, 2930, 1561; Mpt. 98-102 °C.

**5-[2-Amino-4-(butylamino)-6-phenyl-5-pyrimidinyl]-1-pentanol (89)**



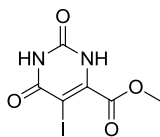
Chemical Formula:  $C_{19}H_{28}N_4O$   
Molecular Weight: 328.45

To a suspension of 5-[2-amino-4-(butylamino)-6-chloro-5-pyrimidinyl]-1-pentanol (**83**) (50 mg, 0.17 mmol), phenylboronic acid (30 mg, 0.25 mmol) and potassium carbonate (36 mg, 0.26 mmol) in 1,4-dioxane (1 mL) and water (0.25 mL) was added chloro(di-2-norbornylphosphino)(2'-dimethylamino-1,1'-biphenyl-2-yl)palladium (II) (10 mg, 0.02 mmol). The reaction vessel was sealed and heated in a Biotage Initiator microwave (using absorption setting high) to 150 °C for 1 h. After cooling, the reaction mixture, further phenylboronic acid (30 mg, 0.25 mmol), potassium carbonate (36 mg, 0.260 mmol) and chloro(di-2-norbornylphosphino)(2'-dimethylamino-1,1'-biphenyl-2-yl) palladium (II) (10 mg, 0.02 mmol) were added. The reaction vessel was sealed and heated in a Biotage Initiator microwave (using absorption setting high) to 150 °C for 1 h. After cooling, the reaction mixture was filtered through celite, the cake washed with  $CHCl_3$  and the filtrate partitioned between 1:1  $CHCl_3$ :EtOAc (10 mL) and water (10 mL). The organic phase was separated and dried (hydrophobic frit) before concentration *in vacuo*. The residue was dissolved in DCM and purified on a silica cartridge (10 g) using 10% MeOH in DCM. The appropriate fractions were combined and concentrated *in vacuo* to give two batches of the title compound: batch 1 (5 mg, 9 %) and batch 2 (11 mg, 19 %).

$^1H$  NMR (400 MHz,  $CDCl_3$ )  $\delta$  7.44 - 7.33 (m, 5H), 5.01 – 4.85 (m, 3H), 3.55 (t,  $J$  = 6.3 Hz, 2H), 3.52 - 3.43 (m, 2H), 2.34 - 2.26 (m, 2H), 1.67 - 1.56 (m, 2H), 1.51 -

1.36 (m, 6H), 1.32 - 1.24 (m, 2H), 0.98 (t,  $J = 7.3$  Hz, 3H) exchangeable proton (OH) not observed; LCMS (System A)  $R_t$  0.77 min,  $m/z$  329 ( $[M+H]^+$ ).

**Methyl 5-iodo-2,6-dioxo-1,2,3,6-tetrahydro-4-pyrimidinecarboxylate (92)**

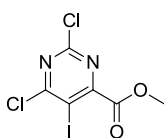


Chemical Formula:  $C_6H_5IN_2O_4$   
Molecular Weight: 296.02

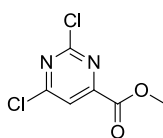
A stirred mixture of methyl orotate (**91**) (20.0 g, 118 mmol), iodine (12.8 g, 50.4 mmol) and periodic acid (4.8 g, 21.1 mmol) in MeOH (400 mL) was heated at reflux for 3 h. The reaction mixture was allowed to cool to ambient temperature. The majority of the volatiles were removed *in vacuo* and the resultant solid was slurried in water (500 mL) and the resulting grey suspension stirred rapidly for 30 min. The suspension was filtered and the solid was dried *in vacuo* for 16 h to give the title compound (22.8 g, 66 %) as a white solid.

$^1H$  NMR (400 MHz, DMSO- $d_6$ )  $\delta$  11.69 (s, 1H), 11.64 (s, 1H), 3.87 (s, 3H); LCMS (System B)  $R_t$  0.42 min,  $m/z$  297 ( $[M+H]^+$ ); Mpt. 267-270 °C (decomp.)

**Methyl 2,6-dichloro-5-iodo-4-pyrimidinecarboxylate (94) and methyl 2,6-dichloro-4-pyrimidinecarboxylate (93)**



Chemical Formula:  $C_6H_3Cl_2IN_2O_2$   
Molecular Weight: 332.91



Chemical Formula:  $C_6H_4Cl_2N_2O_2$   
Molecular Weight: 207.01

To solid methyl 5-iodo-2,6-dioxo-1,2,3,6-tetrahydro-4-pyrimidinecarboxylate (2.00 g, 6.76 mmol) (**92**) was added neat phosphorus(V) oxychloride (10.0 mL, 107 mmol) and DMF (0.20 mL, 2.58 mmol). The reaction mixture was stirred at reflux for 5 h before being concentrated *in vacuo* and the resultant viscous oil poured onto iced water (50 mL). This was extracted with DCM (2 x 40 mL), and the combined organic phases were washed with water (40 mL), dried (hydrophobic frit) and

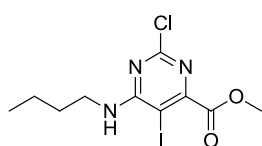
concentrated *in vacuo*. The resulting residue was dissolved in DCM and purified on a silica cartridge (50 g) using a 0-50% EtOAc-cyclohexane gradient over 40 min. The appropriate fractions were combined and concentrated *in vacuo* to give the title compound **85** (1.06 g, 47 %) as a white solid.

<sup>1</sup>H NMR (400 MHz, CDCl<sub>3</sub>) δ 4.03 (s, 3H); LCMS (System B) R<sub>t</sub> 1.08 min, m/z 333, 335, 337 ([M+H]<sup>+</sup>).

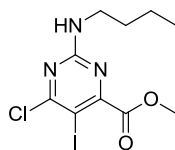
Fractions containing the second compound were combined and concentrated *in vacuo* to give the title compound **93** (353 mg, 25%) as a white solid.

<sup>1</sup>H NMR (400 MHz, CDCl<sub>3</sub>) δ 7.99 (s, 1H), 4.03 (s, 3H); LCMS (System B) R<sub>t</sub> 0.84 min, m/z 207, 209, 211 ([M+H]<sup>+</sup>).

**Methyl 6-(butylamino)-2-chloro-5-iodo-4-pyrimidinecarboxylate (95) and methyl 2-(butylamino)-6-chloro-5-iodo-4-pyrimidinecarboxylate (96)**



Chemical Formula: C<sub>10</sub>H<sub>13</sub>ClIN<sub>3</sub>O<sub>2</sub>  
Molecular Weight: 369.59



Chemical Formula: C<sub>10</sub>H<sub>13</sub>ClIN<sub>3</sub>O<sub>2</sub>  
Molecular Weight: 369.59

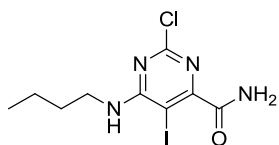
To a stirred solution of methyl 2,6-dichloro-5-iodo-4-pyrimidinecarboxylate (3.0 g, 9.0 mmol) (**94**) in EtOH (45 mL) was added triethylamine (2.64 mL, 18.9 mmol) and *n*-butylamine (0.94 mL, 9.46 mmol). The reaction mixture was stirred at ambient temperature for 5 h before being concentrated *in vacuo* and the residue partitioned between EtOAc (100 mL) and water (100 mL). The organic phase was separated and the aqueous phase back extracted with EtOAc (50 mL). The combined organic extracts were washed with brine (100 mL), dried (MgSO<sub>4</sub>), filtered and concentrated *in vacuo*. The resulting residue was dissolved in DCM and purified on a silica cartridge (100 g) using a 0-25% EtOAc-cyclohexane gradient over 60 min. The appropriate fractions were combined and evaporated *in vacuo* to give the title compound **95** (2.44 g, 73 %) as an orange oil.

$^1\text{H}$  NMR (400 MHz,  $\text{CDCl}_3$ )  $\delta$  5.96 – 5.88 (m, 1H), 3.97 (s, 3H), 3.54 (dt,  $J = 7.0$ , 5.5 Hz, 2H), 1.70 - 1.60 (m, 2H), 1.49 - 1.37 (m, 2H), 0.99 (t,  $J = 7.3$  Hz, 3H);  $^{13}\text{C}$  NMR (101 MHz,  $\text{CDCl}_3$ )  $\delta$  164.8, 162.2, 160.9, 159.3, 74.8, 53.3, 42.2, 30.9, 20.0, 13.7; LCMS (System B)  $R_t$  1.23 min,  $m/z$  370, 372 ( $[\text{M}+\text{H}]^+$ ); HRMS Anal. Calcd. For  $\text{C}_{10}\text{H}_{14}\text{ClIN}_3\text{O}_2 = 369.9814$ . Found = 369.9811 ( $[\text{M}+\text{H}]^+$ ); IR ( $\text{cm}^{-1}$ ) 3383, 2956, 1738, 1570.

Fractions containing the second isomer were combined and concentrated *in vacuo* to give the title compound **96** (290 mg, 9 %) as a yellow oil.

$^1\text{H}$  NMR (400 MHz,  $\text{CDCl}_3$ )  $\delta$  5.31 (s, 1H), 3.98 (s, 3H), 3.44 - 3.37 (m, 2H), 1.62 - 1.52 (m, 2H), 1.46 - 1.33 (m, 2H), 0.95 (t,  $J = 7.3$  Hz, 3H); LCMS (System B)  $R_t$  1.31 min,  $m/z$  370, 372 ( $[\text{M}+\text{H}]^+$ )

#### **6-(Butylamino)-2-chloro-5-iodo-4-pyrimidinecarboxamide (97)**



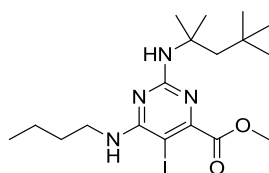
Chemical Formula:  $\text{C}_9\text{H}_{12}\text{ClIN}_4\text{O}$   
Molecular Weight: 354.58

A solution of methyl 6-(butylamino)-2-chloro-5-iodo-4-pyrimidinecarboxylate (**95**) (100 mg, 0.27 mmol) in 7N ammonia in MeOH (2.00 mL, 14.0 mmol) was sealed and heated in a Biotage Initiator microwave (using absorption setting high) to 100 °C for 1 h. After cooling, the reaction mixture was concentrated *in vacuo*. The resulting residue was preabsorbed onto Florosil and purified on a silica cartridge (20 g) using a 0-50% EtOAc-cyclohexane gradient over 40 min. The appropriate fractions were combined and evaporated *in vacuo* to give the title compound (56 mg, 58%) as a white solid.

$^1\text{H}$  NMR (400 MHz,  $\text{CDCl}_3$ )  $\delta$  7.63 (br s, 1H), 6.35 - 6.27 (m, 1H), 5.63 (br s, 1H), 3.54 (dt,  $J = 7.0$ , 5.5 Hz, 2H), 1.72 - 1.61 (m, 2H), 1.50 - 1.39 (m, 2H), 0.99 (t,  $J = 7.3$  Hz, 3H); LCMS (System B)  $R_t$  0.99 min,  $m/z$  355, 357 ( $[\text{M}+\text{H}]^+$ ).



**Methyl 6-(butylamino)-5-iodo-2-[(1,1,3,3-tetramethylbutyl)amino]-4-pyrimidine carboxylate (98)**

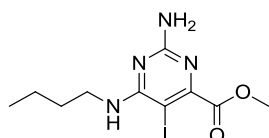


Chemical Formula: C<sub>18</sub>H<sub>31</sub>IN<sub>4</sub>O<sub>2</sub>  
Molecular Weight: 462.37

A stirred mixture of methyl 6-(butylamino)-2-chloro-5-iodo-4-pyrimidinecarboxylate (**95**) (285 mg, 0.77 mmol), *tert*-octylamine (0.257 mL, 1.54 mmol), triethylamine (0.22 mL, 1.54 mmol), potassium fluoride (45 mg, 0.78 mmol) and 18-crown-6 (204 mg, 0.77 mmol) in MeCN (5 mL) was heated to reflux for 3 h. To the reaction mixture was added further *tert*-octylamine (0.257 mL, 1.54 mmol). The reaction vessel was sealed and heated in a Biotage Initiator microwave (using absorption setting normal) to 150 °C for 2 h. The reaction mixture was partitioned between EtOAc (20 mL) and water (20 mL). The organic phase was separated and dried (hydrophobic frit) and concentrated *in vacuo*. The resulting residue was dissolved in DCM and purified on a silica cartridge (20 g) using a 0-25% EtOAc-cyclohexane gradient over 60 min. The appropriate fractions were combined and evaporated *in vacuo* to give the title compound (66 mg, 19 %) as a yellow oil.

<sup>1</sup>H NMR (400 MHz, CDCl<sub>3</sub>) δ 5.52 - 5.45 (m, 1H), 5.00 (br s, 1H), 3.93 (s, 3H), 3.50 - 3.42 (m, 2H), 1.90 (s, 2H), 1.68 - 1.59 (m, 2H), 1.48 - 1.38 (m, 8H), 1.02 - 0.94 (m, 12H); LCMS (System B) R<sub>t</sub> 1.63 min, m/z 463 ([M+H]<sup>+</sup>).

**Methyl 2-amino-6-(butylamino)-5-iodo-4-pyrimidinecarboxylate (99)**

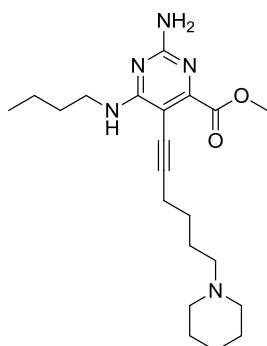


Chemical Formula: C<sub>10</sub>H<sub>15</sub>IN<sub>4</sub>O<sub>2</sub>  
Molecular Weight: 350.16

A solution of methyl 6-(butylamino)-5-iodo-2-[(1,1,3,3-tetramethylbutyl)amino]-4-pyrimidinecarboxylate (**98**) (46 mg, 0.14 mmol) in TFA (1.00 mL, 26.0 mmol) was heated at 70 °C for 16 h. The reaction mixture was concentrated *in vacuo*. The residue was taken up in DCM (10 mL) and washed with saturated aqueous sodium bicarbonate (10 mL). The organic phase was separated and dried (hydrophobic frit) before concentration *in vacuo* to give the title compound (30 mg, 86 %) as a white solid.

<sup>1</sup>H NMR (400 MHz, CDCl<sub>3</sub>) δ 5.57 - 5.51 (m, 1H), 4.88 (br s, 2H), 3.95 (s, 3H), 3.47 - 3.39 (m, 2H), 1.65 - 1.57 (m, 2H), 1.47 - 1.36 (m, 2H), 0.97 (t, *J* = 7.3 Hz, 3H); <sup>13</sup>C NMR (126 MHz, CDCl<sub>3</sub>) δ 166.1, 162.0, 161.2, 158.7, 63.1, 53.0, 41.6, 31.2, 20.1, 13.8; LCMS (System B) R<sub>t</sub> 1.00 min, *m/z* 351 ([M+H]<sup>+</sup>); HRMS Anal. Calcd. For C<sub>10</sub>H<sub>16</sub>IN<sub>4</sub>O<sub>2</sub> = 351.0313. Found = 351.0316 ([M+H]<sup>+</sup>); IR (cm<sup>-1</sup>) 3501, 3414, 3288, 3152, 2959, 1727, 1630, 1549; Mpt. 115-118 °C.

**Methyl 2-amino-6-(butylamino)-5-(6-(piperidin-1-yl)hex-1-yn-1-yl)pyrimidine-4-carboxylate (100)**



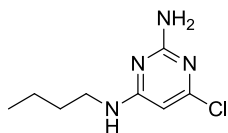
Chemical Formula: C<sub>21</sub>H<sub>33</sub>N<sub>5</sub>O<sub>2</sub>  
Molecular Weight: 387.52

A degassed stirred mixture of methyl 2-amino-6-(butylamino)-5-iodo-4-pyrimidine carboxylate (**99**) (130 mg, 0.37 mmol), tetrakis(triphenylphosphine)palladium(0) (43 mg, 0.04 mmol) and copper(I) iodide (15 mg, 0.08 mmol) in anhydrous DMF (5 mL) was stirred at ambient temperature for 10 min. To the reaction mixture was added a degassed solution of 1-(hex-5-yn-1-yl)piperidine (123 mg, 0.74 mmol) and triethylamine (0.10 mL, 0.74 mmol) in anhydrous DMF (2 mL) in one charge. The

reaction mixture was stirred at ambient temperature for 22 h before the reaction was concentrated *in vacuo*. The resultant gum was triturated with EtOAc (50 mL) filtered and concentrated *in vacuo*, before being dissolved in DCM and purified on a silica cartridge (50 g) using a 0-25% MeOH-DCM gradient over 30 min. The appropriate fractions were combined and evaporated *in vacuo* to give the title compound (28 mg, 20%) as a yellow oil.

$^1\text{H}$  NMR (400 MHz,  $\text{CDCl}_3$ )  $\delta$  5.82 - 5.75 (m, 1H), 4.98 (s, 2H), 3.91 (s, 3H), 3.49 - 3.41 (m, 2H), 3.02 (br s, 4H), 2.95 - 2.78 (m, 2H), 2.58 (t,  $J = 6.7$  Hz, 2H), 2.13 - 2.03 (m, 2H), 2.03 - 1.93 (m, 4H), 1.74 - 1.55 (m, 6H), 1.46 - 1.33 (m, 2H), 0.97 (t,  $J = 7.3$  Hz, 3H); LCMS (System B)  $R_t$  1.10 min,  $m/z$  388 ( $[\text{M}+\text{H}]^+$ ).

#### **N-4-butyl-6-chloropyrimidine-2,4-diamine (102)**



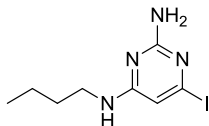
Chemical Formula:  $\text{C}_8\text{H}_{13}\text{ClN}_4$   
Molecular Weight: 200.67

To a suspension of 4,6-dichloropyrimidin-2-amine (5.00 g, 30.5 mmol) in EtOH (70 mL) was added neat triethylamine (9.35 mL, 67.1 mmol) and *n*-butylamine (3.18 mL, 32.0 mmol) and the reaction mixture was heated to reflux for 20 h. The reaction mixture was allowed to cool to ambient temperature and was concentrated *in vacuo*. The resulting residue was partitioned between EtOAc (250 mL) and water (250 mL). The organic phase was separated and the aqueous phase back extracted with EtOAc (100 mL). The combined organic phases were washed with brine (250 mL), dried ( $\text{MgSO}_4$ ), filtered and concentrated *in vacuo* before being dissolved in DCM and purified on a silica cartridge (100 g) using a 0-100% EtOAc-cyclohexane gradient over 60 mins. The appropriate fractions were combined and evaporated *in vacuo* to give the title compound (4.42 g, 72 %) as a white solid.

$^1\text{H}$  NMR (400 MHz,  $\text{CDCl}_3$ )  $\delta$  5.79 (s, 1H), 4.88 (br s, 3H), 3.23 (br s, 2H), 1.62 - 1.52 (m, 2H), 1.47 - 1.34 (m, 2H), 0.95 (t,  $J = 7.3$  Hz, 3H); LCMS (System B)  $R_t$

0.89 min, m/z 201, 203 ([M+H]<sup>+</sup>).

### **N-4-butyl-6-iodopyrimidine-2,4-diamine (103)**

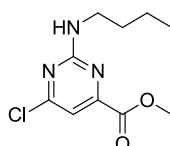


Chemical Formula: C<sub>8</sub>H<sub>13</sub>I<sub>1</sub>N<sub>4</sub>  
Molecular Weight: 292.12

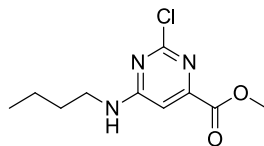
To a stirred suspension of *N*-4-butyl-6-chloropyrimidine-2,4-diamine (**102**) (200 mg, 1.0 mmol) and sodium iodide (448 mg, 2.99 mmol) in acetone (1 mL) was added hydriodic acid 57% solution in water (1.50 mL, 11.4 mmol) in one charge. The reaction mixture was heated to 50 °C for 7 h, then stirred at ambient temperature for 16 h. The reaction mixture was partitioned between 2M aqueous sodium hydroxide (40 mL) and DCM (40 mL). The organic phase was separated and the aqueous phase back extracted with DCM (20 mL). The combined organic phases were dried (hydrophobic frit) and concentrated *in vacuo* before being dissolved in DCM and purified on a silica cartridge (20 g) using a 0-50% EtOAc-cyclohexane gradient over 40 min. The appropriate fractions were combined and evaporated *in vacuo* to give the title compound (175 mg, 60 %) as a colourless oil.

<sup>1</sup>H NMR (400 MHz, CDCl<sub>3</sub>) δ 6.24 (s, 1H), 4.87 (br s, 2H), 4.77 - 4.63 (br s, 2H), 3.22 (br s, 2H), 1.60 - 1.51(m, 2H), 1.45 - 1.33 (m, 2H), 0.95 (t, *J* = 7.3 Hz, 3H);  
LCMS (System B) R<sub>t</sub> 0.95 min, m/z 293 ([M+H]<sup>+</sup>)

### **Methyl 2-(butylamino)-6-chloropyrimidine-4-carboxylate (105) and Methyl 6-(butylamino)-2-chloropyrimidine-4-carboxylate (106)**



Chemical Formula: C<sub>10</sub>H<sub>14</sub>ClN<sub>3</sub>O<sub>2</sub>  
Molecular Weight: 243.69



Chemical Formula: C<sub>10</sub>H<sub>14</sub>ClN<sub>3</sub>O<sub>2</sub>  
Molecular Weight: 243.69

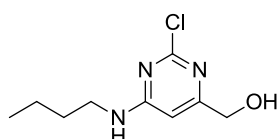
To a stirred solution of methyl 2,6-dichloropyrimidine-4-carboxylate (5.00 g, 24.2 mmol) in MeCN (75 mL) was added triethylamine (7.00 mL, 50.2 mmol) and *n*-butylamine (2.50 mL, 250 mmol). The reaction mixture was stirred at ambient temperature for 30 min before concentration *in vacuo*. The residue was partitioned between EtOAc (500 mL) and water (500 mL), with the organic phase being separated, dried (MgSO<sub>4</sub>), filtered and concentrated *in vacuo* before dissolving in DCM and purification on silica cartridges (2 x 100 g) using a 0-50% EtOAc-cyclohexane gradient over 60 min. The appropriate fractions were combined and evaporated to give the title compound **106** (3.16 g, 54%) as a white solid.

<sup>1</sup>H NMR (400 MHz, CDCl<sub>3</sub>) δ 7.00 (br s, 1H), 5.70 - 5.20 (m, 1H), 3.96 (s, 3H), 3.49 (br s, 1H), 3.33 (br s, 1H), 1.70 - 1.56 (m, 2H), 1.48 - 1.35 (m, 2H), 0.96 (t, *J* = 7.3 Hz, 3H); <sup>13</sup>C NMR (101 MHz, CDCl<sub>3</sub>) δ 164.4, 106.0, 100.9, 53.3, 42.0, 41.0, 31.1, 19.9, 13.7; LCMS (System B) R<sub>t</sub> 1.00 min, m/z 244, 246 ([M+H]<sup>+</sup>); HRMS Anal. Calcd. For C<sub>10</sub>H<sub>15</sub>ClN<sub>3</sub>O<sub>2</sub> = 244.0847. Found = 244.0847 ([M+H]<sup>+</sup>); IR (cm<sup>-1</sup>) 3367, 2956, 1707, 1604; Mpt 115-117 °C.

The fractions containing the second isomer were combined and concentrated *in vacuo* to give title compound **105** (888 mg, 15%) as a yellow oil which solidified over time.

<sup>1</sup>H NMR (400 MHz, CDCl<sub>3</sub>) δ 7.00 (s, 1H), 5.55 (br s, 1H), 3.96 (s, 3H), 3.59 - 3.40 (m, 2H), 1.65 - 1.52 (m, 2H), 1.48 - 1.35 (m, 2H), 1.00 - 0.93 (m, 3H); LCMS (System B) R<sub>t</sub> 1.18 min, m/z 244, 246 ([M+H]<sup>+</sup>).

### **6-(Butylamino)-2-chloropyrimidin-4-yl)methanol (107)**



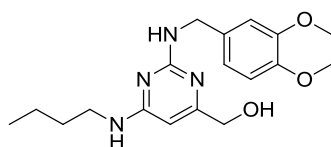
Chemical Formula: C<sub>9</sub>H<sub>14</sub>ClN<sub>3</sub>O  
Molecular Weight: 215.68

To a solution of methyl 6-(butylamino)-2-chloropyrimidine-4-carboxylate (**106**) (1.00 g, 4.10 mmol) in anhydrous THF (20 mL) at 0 °C under a nitrogen atmosphere

was added lithium aluminium hydride 1M in diethyl ether (12.3 mL, 12.3 mmol) in a dropwise fashion over 10 mins. The reaction mixture was stirred at 0 °C for 90 min before allowing to warm to ambient temperature. The reaction was then quenched with aqueous NH<sub>4</sub>Cl (*ca.* 50 mL), water (50 mL) and extracted with EtOAc (2 x 75 mL). The combined extracts were washed with water (100 mL), brine (50 mL), dried (MgSO<sub>4</sub>), filtered and concentrated *in vacuo* to give a yellow oil. The oil was dissolved in DCM and purified on a silica cartridge (100 g) using a 0-25% MeOH-DCM gradient over 40 min. The appropriate fractions were combined and evaporated *in vacuo* to give the title compound (490 mg, 55%) as a orange oil which solidified on standing.

<sup>1</sup>H NMR (400 MHz, CDCl<sub>3</sub>) δ 6.31 (s, 1H), 5.30 (br s, 1H), 4.58 (d, *J* = 4.3 Hz 2H), 3.32 (br s, 2H), 2.80 (br s, 1H), 1.67 - 1.55 (m, 2H), 1.48 - 1.36 (m, 2H), 0.97 (t, *J* = 7.3 Hz, 3H); LCMS (System B) R<sub>t</sub> 0.83 min, m/z 216, 218 ([M+H]<sup>+</sup>); Mpt. 98-100 °C.

**(6-(Butylamino)-2-((3,4-dimethoxybenzyl)amino)pyrimidin-4-yl)methanol (108)**

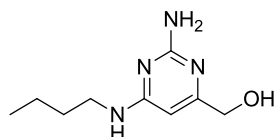


Chemical Formula: C<sub>18</sub>H<sub>26</sub>N<sub>4</sub>O<sub>3</sub>  
Molecular Weight: 346.42

A solution of (6-(butylamino)-2-chloropyrimidin-4-yl)methanol (1.27 g, 5.89 mmol) and (3,4-dimethoxyphenyl)methanamine (**107**) (1.78 mL, 11.8 mmol) in 1-butanol (12 mL) was sealed and heated in a Biotage Initiator microwave (using absorption setting high) to 150 °C for 1 h. After cooling, the reaction mixture was partitioned between EtOAc (250 mL) and water (250 mL). The organic phase was separated and dried (MgSO<sub>4</sub>), filtered and concentrated *in vacuo* before dissolving in DCM and purification on a silica cartridge (100 g) using a 0-10% MeOH-DCM gradient over 60 min. The appropriate fractions were combined and evaporated *in vacuo* to give the title compound (1.66 g, 81%) as an orange oil that solidified on standing.

$^1\text{H}$  NMR (400 MHz,  $\text{CDCl}_3$ )  $\delta$  6.92 - 6.85 (m, 2H), 6.85 - 6.78 (m, 1H), 5.64 (s, 1H), 5.22 (br s, 1H), 4.78 - 4.72 (m, 1H), 4.53 (d,  $J = 6.0$  Hz, 2H), 4.43 (s, 2H), 3.88 - 3.84 (m, 6H), 3.30 - 3.21 (m, 2H), 1.61 - 1.51 (m, 2H), 1.45 - 1.32 (m, 2H), 0.95 (t,  $J = 7.4$  Hz, 3H) exchangeable proton (OH) not observed;  $^{13}\text{C}$  NMR (126 MHz,  $\text{CDCl}_3$ )  $\delta$  163.6, 161.0, 149.1, 148.2, 132.1, 119.7, 111.2, 110.9, 63.0, 55.9, 55.9, 45.3, 41.1, 31.5, 20.1, 13.8; LCMS (System B)  $R_t$  0.97 min,  $m/z$  347 ( $[\text{M}+\text{H}]^+$ ); HRMS Anal. Calcd. For  $\text{C}_{18}\text{H}_{27}\text{N}_4\text{O}_3 = 347.2078$ . Found = 347.2071 ( $[\text{M}+\text{H}]^+$ ); IR ( $\text{cm}^{-1}$ ) 3368, 3266, 2913, 1622, 1587, 1551; Mpt. 96-98 °C.

**(2-Amino-6-(butylamino)pyrimidin-4-yl)methanol (109)**

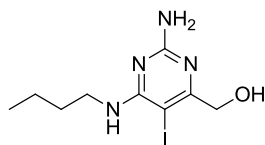


Chemical Formula:  $\text{C}_9\text{H}_{16}\text{N}_4\text{O}$   
Molecular Weight: 196.25

A solution of (6-(butylamino)-2-((3,4-dimethoxybenzyl)amino)pyrimidin-4-yl)methanol (1.63 g, 4.71 mmol) (**108**) and anisole (1.03 mL, 9.41 mmol) in TFA (9.00 mL, 117 mmol) was sealed and heated in a Biotage Initiator microwave (using absorption setting high) to 100 °C for 20 min. After cooling, the reaction mixture was concentrated *in vacuo* before dissolving in DCM and purification on a silica cartridge (100 g) using a 0-25% MeOH-DCM gradient over 60 min. The appropriate fractions were combined and evaporated *in vacuo* to give the title compound (860 mg, 93%) as an off white solid.

$^1\text{H}$  NMR (400 MHz, MeOD)  $\delta$  6.00 (br s, 1H), 4.44 (s, 2H), 3.48 - 3.41 (m, 2H), 1.63 - 1.52 (m, 2H), 1.44 - 1.32 (m, 2H), 0.98 - 0.92 (m, 3H) exchangeable protons (NH,  $\text{NH}_2$ , and OH) not observed; LCMS (System B)  $R_t$  0.64 min,  $m/z$  197 ( $[\text{M}+\text{H}]^+$ ).

**(2-Amino-6-(butylamino)-5-iodopyrimidin-4-yl)methanol (110)**

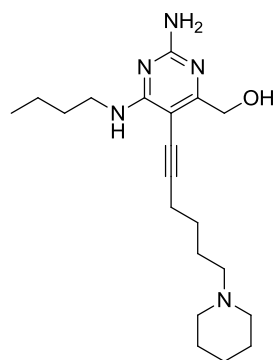


Chemical Formula: C<sub>9</sub>H<sub>15</sub>IN<sub>4</sub>O  
Molecular Weight: 322.15

To a stirred solution of (2-amino-6-(butylamino)pyrimidin-4-yl)methanol (825 mg, 4.20 mmol) (**109**) in AcOH (10 mL) was added *N*-iodosuccinimide (1.04 g, 4.62 mmol). The reaction mixture was stirred at ambient temperature for 2 h. The mixture was cooled to 0 °C and was neutralised with 2M aqueous sodium hydroxide and extracted with DCM (4 x 50 mL). The combined organic phases were washed with saturated aqueous sodium thiosulfate (200 mL). The resultant organic phase was dried (hydrophobic frit) and concentrated *in vacuo* before the sample was dissolved in DCM and purified on a silica cartridge (100 g) using a 0-10% MeOH-DCM gradient over 60 min. The appropriate fractions were combined and evaporated *in vacuo* to give the title compound (603 mg, 45%) as an off white solid.

<sup>1</sup>H NMR (400 MHz, CDCl<sub>3</sub>) δ 5.27 - 5.18 (m, 1H), 4.78 (br s, 2H), 4.38 (s, 2H), 4.26 (br s, 1H), 3.48 - 3.40 (dt, *J* = 7.0, 5.5 Hz, 2H), 1.65 - 1.53 (m, 2H), 1.47 - 1.36 (m, 2H), 0.98 (t, *J* = 7.3 Hz, 3H); LCMS (System B) R<sub>t</sub> 0.94 min, m/z 323 ([M+H]<sup>+</sup>).

**(2-Amino-6-(butylamino)-5-(6-(piperidin-1-yl)hex-1-yn-1-yl)pyrimidin-4-yl)methanol (111)**



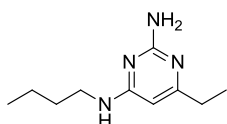
Chemical Formula: C<sub>20</sub>H<sub>33</sub>N<sub>5</sub>O  
Molecular Weight: 359.51



A degassed stirred mixture of (2-amino-6-(butylamino)-5-iodopyrimidin-4-yl)methanol (600 mg, 1.86 mmol) (**110**), tetrakis(triphenylphosphine)palladium(0) (215 mg, 0.19 mmol) and copper(I) iodide (71 mg, 0.37 mmol) in anhydrous DMF (30 mL) was stirred at ambient temperature for 10 min before addition of a degassed solution of 1-(hex-5-yn-1-yl)piperidine (616 mg, 3.73 mmol) and triethylamine (0.52 mL, 3.73 mmol) in anhydrous DMF (10 mL) dropwise over 10 min. The reaction mixture was stirred at ambient temperature for 5.5 h before being concentrated *in vacuo*. The resulting residue was triturated with EtOAc (100 mL), filtered and concentrated *in vacuo* to give a yellow oil which was dissolved in DCM and purified on a silica cartridge (50 g) using a 0-50% MeOH (+1% Et<sub>3</sub>N) -DCM gradient over 40 min. The appropriate fractions were combined and evaporated *in vacuo* to give the title compound (263 mg, 39 %) as a yellow oil.

<sup>1</sup>H NMR (400 MHz, CDCl<sub>3</sub>) δ 5.42 - 5.33 (m, 1H), 4.82 (br s, 2H), 4.55 (s, 2H), 3.47 - 3.40 (m, 2H), 2.50 (t, *J* = 6.7 Hz, 2H), 2.46 - 2.22 (m, 6H), 1.72 - 1.50 (m, 10H), 1.50 - 1.35 (m, 4H), 0.97 (t, *J* = 7.3 Hz, 3H) exchangeable proton (OH) not observed; LCMS (System B) R<sub>t</sub> 1.05 min, m/z 360 ([M+H]<sup>+</sup>).

### **N-4-butyl-6-ethylpyrimidine-2,4-diamine (113)**



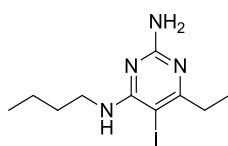
Chemical Formula: C<sub>10</sub>H<sub>18</sub>N<sub>4</sub>  
Molecular Weight: 194.28

A mixture of 4-chloro-6-ethylpyrimidin-2-amine (**112**) (0.50 g, 3.17 mmol) and 1-butylamine (1.00 mL, 10.1 mmol) in 1-butanol (3 mL) was sealed and heated in a Biotage Initiator microwave (absorption setting normal) to 150 °C for 2 h. After cooling, the reaction mixture was diluted with EtOAc (40 mL) and washed with water (50 mL). The organic phase was separated and the aqueous phase back extracted with EtOAc (20 mL). The combined organic extracts were washed further

with water (50 mL) and brine (50 mL) before drying (MgSO<sub>4</sub>), filtering and concentrating *in vacuo* to give the title compound (554 mg, 90 %) as a white solid.

<sup>1</sup>H NMR (400 MHz, CDCl<sub>3</sub>) δ 5.68 - 5.61 (m, 1H), 4.87 (br s, 2H), 4.76 (br s, 1H), 3.30-3.19 (m, 2H), 2.52 - 2.40 (m, 2H), 1.63 - 1.50 (m, 2H), 1.46 - 1.32 (m, 2H), 1.27 - 1.16 (m, 3H), 0.99 - 0.89 (m, 3H); LCMS (System B) R<sub>t</sub> 0.87 min, m/z 195 ([M+H]<sup>+</sup>).

#### **N-4-butyl-6-ethylpyrimidine-2,4-diamine (114)**

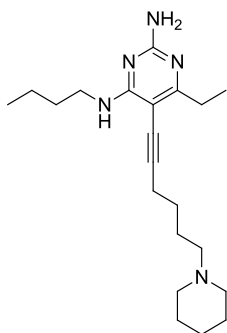


Chemical Formula: C<sub>10</sub>H<sub>17</sub>N<sub>4</sub>  
Molecular Weight: 320.17

To a stirred solution of *N*-4-butyl-6-ethylpyrimidine-2,4-diamine (**113**) (0.55 g, 2.83 mmol) in AcOH (25 mL) at ambient temperature was added a solution of ICl (0.28 mL, 5.7 mmol) in AcOH (10 mL) dropwise over 10 min. The reaction mixture was stirred at ambient temperature for 2 h before being concentrated *in vacuo* and the resulting residue partitioned between water (50 mL) and EtOAc (50 mL). The organic phase was separated and washed with saturated aqueous sodium thiosulfate (50 mL). The resulting organic phase was dried (MgSO<sub>4</sub>), filtered and concentrated *in vacuo* before the sample was dissolved in DCM and purified on a silica cartridge (20 g) using a 0-100% EtOAc-cyclohexane gradient over 40 min. The chromatography failed to yield pure product, so all product containing fractions were combined and concentrated *in vacuo* to give a red oil. The oil was dissolved in EtOAc (100 mL) and washed further with saturated sodium thiosulfate (100 mL) leading to decolourisation. The organic phase was separated and dried (MgSO<sub>4</sub>) filtered and concentrated *in vacuo* to give the title compound (375 mg, 41 %).

$^1\text{H}$  NMR (400 MHz,  $\text{CDCl}_3$ )  $\delta$  5.42 - 5.32 (m, 1H), 4.98 (br s, 2H), 3.45 - 3.35 (m, 2H), 2.75 - 2.65 (m, 2H), 1.65 - 1.53 (m, 2H), 1.47 - 1.36 (m, 2H), 1.25 - 1.17 (m, 3H), 0.97 (t,  $J = 7.8$  Hz, 3H); LCMS (System B)  $R_t$  1.16 min,  $m/z$  321 ( $[\text{M}+\text{H}]^+$ ).

***N*-4-butyl-6-ethyl-5-(6-(piperidin-1-yl)hex-1-yn-1-yl)pyrimidine-2,4-diamine**  
**(115)**

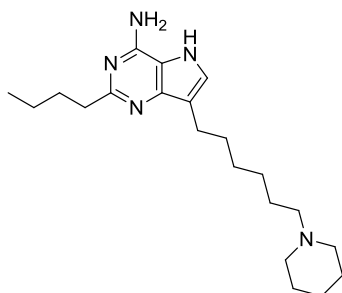


Chemical Formula:  $\text{C}_{21}\text{H}_{35}\text{N}_5$   
Molecular Weight: 357.54

To a degassed stirred suspension of copper(I) iodide (44 mg, 0.23 mmol), tetrakis(triphenylphosphine)palladium(0) (134 mg, 0.12 mmol) and *N*-4-butyl-6-ethyl-5-iodopyrimidine-2,4-diamine (**114**) (370 mg, 1.16 mmol) in anhydrous THF (10 mL) at 50 °C was added a solution of triethylamine (0.32 mL, 2.31 mmol) and 1-(hex-5-yn-1-yl)piperidine (382 mg, 2.31 mmol) in anhydrous THF (3 mL) dropwise over 5 min. The reaction mixture was stirred at 70 °C under a nitrogen atmosphere for 16 h, after cooling, the reaction mixture was diluted with EtOAc (100 mL) and washed with water (100 mL). The aqueous phase was back extracted with EtOAc (50 mL) and the combined extracts were washed with brine (100 mL), dried ( $\text{MgSO}_4$ ), filtered and concentrated *in vacuo*. The resulting residue was dissolved in DCM and purified on a silica cartridge (50 g) using a 0-25% MeOH-DCM gradient over 60 min. The appropriate fractions were combined and evaporated *in vacuo* to give the title compound (95 mg, 23%) as a yellow oil.

$^1\text{H}$  NMR (400 MHz,  $\text{CDCl}_3$ )  $\delta$  5.53 - 5.44 (m, 1H), 4.96 (br s, 2H), 3.47 - 3.38 (m, 2H), 2.79 - 2.59 (m, 8H), 2.55 (t,  $J = 7.0$  Hz, 2H), 1.93 - 1.75 (m, 6H), 1.73 - 1.63 (m, 2H), 1.63 - 1.50 (m, 4H), 1.47 - 1.33 (m, 2H), 1.27 - 1.18 (m, 3H), 0.99 - 0.92 (m, 3H) ; LCMS (System B)  $R_t$  1.24 min,  $m/z$  358 ( $[\text{M}+\text{H}]^+$ ).

**2-Butyl-7-(6-(piperidin-1-yl)hexyl)-5H-pyrrolo[3,2-d]pyrimidin-4-amine, di-formate salt (124a)**

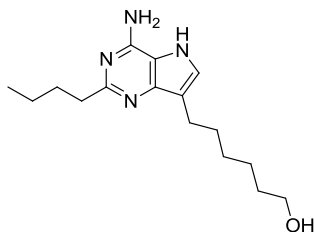


Chemical Formula: C<sub>21</sub>H<sub>35</sub>N<sub>5</sub>  
Molecular Weight: 357.54

A mixture of 2-butyl-7-(6-(piperidin-1-yl)hexyl)-5-((2-(trimethylsilyl) ethoxy) methyl)-5H-pyrrolo[3,2-d]pyrimidin-4-amine (**237a**) (50 mg, 0.10 mmol), ethylenediamine (11  $\mu$ L, 0.16 mmol) and TBAF 1 M in THF (310  $\mu$ L, 0.31 mmol) was sealed and heated to 70 °C for 3.5 h. The reaction mixture was concentrated *in vacuo* and the residue was dissolved in 1:1 MeOH:DMSO (1 mL) and purified by MDAP on a Sunfire C18 column using MeCN-water with a formic acid modifier. The solvent was removed under a stream of nitrogen in the Radleys<sup>TM</sup> blowdown apparatus to give the title compound (23 mg, 50%) as a clear gum.

<sup>1</sup>H NMR (400 MHz, MeOD)  $\delta$  8.55 (br s, 2H), 7.39 (s, 1H), 3.15 (br s, 4H), 3.04 – 2.94 (m, 2H), 2.86 - 2.70 (m, 2H), 2.73 (t,  $J = 7.5$  Hz, 2H), 1.90 - 1.76 (m, 6H), 1.74 - 1.60 (m, 6H), 1.49 - 1.37 (m, 6H), 0.96 (t,  $J = 7.5$  Hz, 3H) exchangeable protons (NH and NH<sub>2</sub>) not observed; LCMS (System B) R<sub>t</sub> 1.03 min, m/z 358 ([M+H]<sup>+</sup>).

**6-(4-Amino-2-butyl-5H-pyrrolo[3,2-d]pyrimidin-7-yl)hexan-1-ol (124x)**



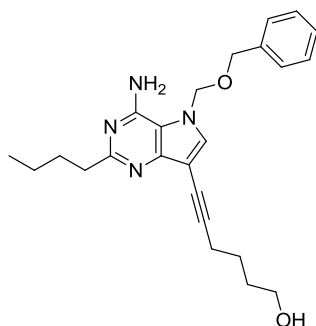
Chemical Formula: C<sub>16</sub>H<sub>26</sub>N<sub>4</sub>O  
Molecular Weight: 290.40

A solution of 6-(4-amino-5-((benzyloxy)methyl)-2-butyl-5H-pyrrolo[3,2-d]

pyrimidin-7-yl)hex-5-yn-1-ol (**132x**) (94 mg, 0.23 mmol) in EtOH (12 mL) was hydrogenated using the H-cube (settings: 60 °C, Full H<sub>2</sub>, 1 mL/min flow rate) and a 10% Pd/C CatCart 30 as the catalyst. The solution was further hydrogenated using the H-cube (settings: 60 °C, Full H<sub>2</sub>, 1 mL/min flow rate) and 10% Pd/C CatCart 30 as the catalyst. The reaction mixture was concentrated and was dissolved in 1:1 MeOH:DMSO (1 mL) and purified by MDAP on an Xbridge column using MeCN-water with an ammonium carbonate modifier. The solvent was removed under a stream of nitrogen in the Radleys™ blowdown apparatus to give the title compound (15 mg, 22 %), as a white solid.

<sup>1</sup>H NMR (400 MHz, MeOD) δ 7.21 (s, 1H), 3.53 (t, *J* = 6.5 Hz, 2H), 3.34 (s, 2H), 2.76 - 2.68 (m, 4H), 1.79 - 1.63 (m, 4H), 1.57 - 1.48 (m, 2H), 1.46 - 1.34 (m, 6H), 0.95 (t, *J* = 7.4 Hz, 3H) two exchangeable protons not observed; LCMS (System B) R<sub>t</sub> 0.83 min, m/z 291 ([M+H]<sup>+</sup>).

**6-(4-Amino-5-((benzyloxy)methyl)-2-butyl-5H-pyrrolo[3,2-d]pyrimidin-7-yl)hex-5-yn-1-ol (132x)**



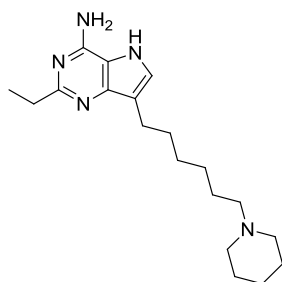
Chemical Formula: C<sub>24</sub>H<sub>30</sub>N<sub>4</sub>O<sub>2</sub>  
Molecular Weight: 406.52

To a degassed suspension of 5-((benzyloxy)methyl)-2-butyl-7-iodo-5H-pyrrolo[3,2-d]pyrimidin-4-amine (**131**) (152 mg, 0.35 mmol), copper(I) iodide (14 mg, 0.07 mmol), and *bis*(triphenylphosphine)palladium(II) dichloride (24 mg, 0.03 mmol) in anhydrous DMF (3 mL) was added a solution of hex-5-yn-1-ol (51 mg, 0.52 mmol) and triethylamine (77 μL, 0.56 mmol) in anhydrous DMF (2 mL) dropwise over 2 min. The reaction mixture was stirred at ambient temperature for 20 h. before being concentrated *in vacuo* and the resulting residue partitioned between EtOAc (50 mL)

and water (50 mL). The organic phase was separated, dried (MgSO<sub>4</sub>), filtered and concentrated *in vacuo* to give a red oil. The oil was dissolved in DCM and purified on a silica cartridge (20 g) using a 0-10% MeOH-DCM gradient over 40 mins. The appropriate fractions were combined and evaporated *in vacuo* to give the title compound (95 mg, 67 %) as an orange oil.

<sup>1</sup>H NMR (400 MHz, CDCl<sub>3</sub>) δ 7.42 - 7.35 (m, 3H), 7.32 - 7.24 (m, 3H), 6.85-6.40 (br s, 1H) 5.47 (s, 2H), 4.59 (s, 2H), 3.82 - 3.77 (m, 2H), 3.68 (t, *J*= 7.2 Hz, 2H), 3.00 - 2.93 (m, 2H), 2.61 - 2.54 (m, 2H), 2.31 (t, *J*= 7.2 Hz, 2H), 1.91 - 1.83 (m, 2H), 1.73 - 1.58 (m, 2H), 1.50 - 1.41 (m, 2H), 0.97 (t, *J* = 7.3 Hz, 3H); LCMS (System B) R<sub>t</sub> 1.09 min, m/z 407 ([M+H]<sup>+</sup>), Note: compound is only 85% pure by UV.

**2-Ethyl-7-(6-(piperidin-1-yl)hexyl)-5H-pyrrolo[3,2-*d*]pyrimidin-4-amine (137a)**



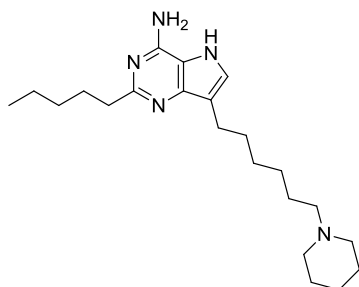
Chemical Formula: C<sub>19</sub>H<sub>31</sub>N<sub>5</sub>  
Molecular Weight: 329.48

A filtered solution of 5-((benzyloxy)methyl)-2-ethyl-7-(6-(piperidin-1-yl)hex-1-yn-1-yl)-5H-pyrrolo[3,2-*d*]pyrimidin-4-amine (**169a**) (98 mg, 0.22 mmol) in EtOH (9 mL) and AcOH (1 mL) was hydrogenated using the H-cube<sup>TM</sup> (settings: 60 °C, Full H<sub>2</sub>, 1 mL/min flow rate) and a 10% Pd/C CatCart 30 as the catalyst. The reaction mixture was concentrated *in vacuo* and the residue was dissolved in 1:1 DMF:DMSO (1 mL) and purified by MDAP on an Xbridge column using MeCN-water with an ammonium carbonate modifier. The solvent was dried under a stream of nitrogen in the Radleys<sup>TM</sup> blowdown apparatus to give the title compound (23 mg, 32 %) as a white solid.

<sup>1</sup>H NMR (400 MHz, MeOD) δ 7.24 (s, 1H), 2.81 - 2.73 (m, 4H), 2.43 (br s, 4H),

2.34 - 2.28 (m, 2H), 1.75 - 1.66 (m, 2H), 1.65 - 1.58 (m, 4H), 1.57 - 1.36 (m, 8H), 1.33 (t,  $J = 7.7$  Hz, 3H) exchangeable protons (NH and NH<sub>2</sub>) not observed; LCMS (System B) R<sub>t</sub> 0.83 min, m/z 330 ([M+H]<sup>+</sup>).

**2-Pentyl-7-(6-(piperidin-1-yl)hexyl)-5H-pyrrolo[3,2-d]pyrimidin-4-amine (136a)**



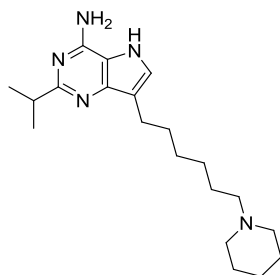
Chemical Formula: C<sub>22</sub>H<sub>37</sub>N<sub>5</sub>  
Molecular Weight: 371.56

A filtered solution of 5-((benzyloxy)methyl)-2-pentyl-7-(6-(piperidin-1-yl)hex-1-yn-1-yl)-5H-pyrrolo[3,2-d]pyrimidin-4-amine (**175a**) (130 mg, 0.27 mmol) in EtOH (9 mL) and AcOH (1 mL) was hydrogenated using the H-cube<sup>TM</sup> (settings: 60 °C, Full H<sub>2</sub>, 1 mL/min flow rate) and a 10% Pd/C CatCart 30 as the catalyst. The reaction mixture was concentrated *in vacuo* and the residue was dissolved in 1:1 MeOH:DMSO (1 mL) and purified by MDAP on an Xbridge column using MeCN-water with an ammonium carbonate modifier. The solvent was evaporated *in vacuo* to give the title compound (32 mg, 32 %) as an off white solid.

<sup>1</sup>H NMR (400 MHz, MeOD) δ 7.24 (s, 1H), 2.79 - 2.72 (m, 4H), 2.43 (br s, 4H), 2.34 - 2.28 (m, 2H), 1.82 - 1.73 (m, 2H), 1.73 - 1.66 (m, 2H), 1.65 - 1.57 (m, 4H), 1.57 - 1.33 (m, 12H), 0.99 - 0.90 (m, 3H) exchangeable protons (NH and NH<sub>2</sub>) not observed; LCMS (System B) t<sub>RET</sub> 1.17 min, m/z 372 ([M+H]<sup>+</sup>).

**2-Isopropyl-7-(6-(piperidin-1-yl)hexyl)-5H-pyrrolo[3,2-d]pyrimidin-4-amine**

**(138a)**



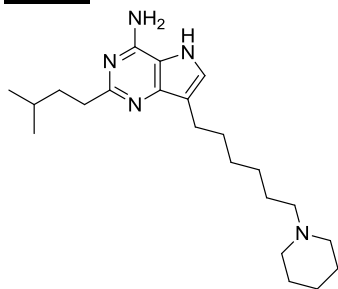
Chemical Formula: C<sub>20</sub>H<sub>33</sub>N<sub>5</sub>  
Molecular Weight: 343.51

A filtered solution of 5-((benzyloxy)methyl)-2-isopropyl-7-(6-(piperidin-1-yl)hex-1-yn-1-yl)-5H-pyrrolo[3,2-d]pyrimidin-4-amine (**181a**) (160 mg, 0.35 mmol) in EtOH (15 mL) and AcOH (2 mL) was hydrogenated using the H-cube<sup>TM</sup> (settings: 60 °C, Full H<sub>2</sub>, 1 mL/min flow rate) and a 10% Pd/C CatCart 30 as the catalyst. The solution was re-hydrogenated using the H-cube<sup>TM</sup> (settings: 60 °C, Full H<sub>2</sub>, 1 mL/min flow rate) and the same 10% Pd/C CatCart 30 as the catalyst. The solution was re-hydrogenated using the H-cube<sup>TM</sup> (settings: 60 °C, Full H<sub>2</sub>, 1 mL/min flow rate) and a new 10% Pd/C CatCart 30 as the catalyst. The solution was concentrated *in vacuo* and was dissolved in 1:1 MeOH:DMSO (1 mL) and purified by MDAP on an Xbridge column using MeCN-water with an ammonium carbonate modifier. The solvent was evaporated *in vacuo* to give the title compound (13.5 mg, 11 %) as a white solid.

<sup>1</sup>H NMR (400 MHz, DMSO-*d*<sub>6</sub>) δ 10.43 (s, 1H), 7.21 (d, *J* = 2.5 Hz, 1H), 6.44 (s, 2H), 2.96 - 2.85 (m, 1H), 2.59 (t, *J* = 7.5 Hz, 2H), 2.30 - 2.23 (m, 4H), 2.21 - 2.16 (m, 2H), 1.69 - 1.60 (m, 2H), 1.50 - 1.43 (m, 4H), 1.42 - 1.28 (m, 8H), 1.22 (d, *J* = 6.9 Hz, 6H); LCMS (System B) R<sub>t</sub> 0.96 min, m/z 344 ([M+H]<sup>+</sup>).



**2-Isopentyl-7-(6-(piperidin-1-yl)hexyl)-5H-pyrrolo[3,2-d]pyrimidin-4-amine (140a)**

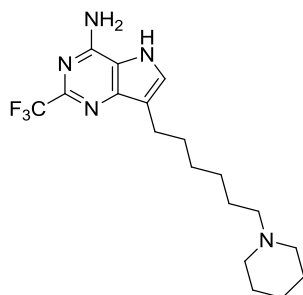


Chemical Formula: C<sub>22</sub>H<sub>37</sub>N<sub>5</sub>  
Molecular Weight: 371.56

A filtered solution of 5-((benzyloxy)methyl)-2-isopentyl-7-(6-(piperidin-1-yl)hex-1-yn-1-yl)-5H-pyrrolo[3,2-d]pyrimidin-4-amine (**187a**) (145 mg, 0.30 mmol) in EtOH (9 mL) and AcOH (1 mL) was hydrogenated using the H-cube<sup>TM</sup> (settings: 60 °C, Full H<sub>2</sub>, 1 mL/min flow rate) and a 10% Pd/C CatCart 30 as the catalyst. The reaction mixture was concentrated *in vacuo* and the residue was dissolved in 1:1 DMF:DMSO (2 x 1 mL) and purified by MDAP on an Xbridge column using MeCN-water with an ammonium carbonate modifier. The solvent was evaporated *in vacuo* to give a white solid (42 mg). The material was triturated with EtOAc (*ca.* 4 mL), filtered and the solid dried *in vacuo* to give the title compound (30 mg, 27 %) as a white solid.

<sup>1</sup>H NMR (400 MHz, MeOD) δ 7.25 - 7.20 (m, 1H), 2.81 - 2.69 (m, 4H), 2.41 (br s, 4H), 2.34 - 2.26 (m, 2H), 1.74 - 1.56 (m, 9H), 1.56 - 1.31 (m, 8H), 1.02 - 0.93 (m, 6H) exchangeable protons (NH and NH<sub>2</sub>) not observed.; LCMS (System B) R<sub>t</sub> 1.04 min, m/z 370 ([M-H]<sup>-</sup>).

**7-(6-(Piperidin-1-yl)hexyl)-2-(trifluoromethyl)-5H-pyrrolo[3,2-d]pyrimidin-4-amine (146a)**



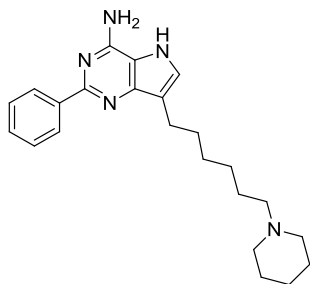
Chemical Formula: C<sub>18</sub>H<sub>26</sub>F<sub>3</sub>N<sub>5</sub>  
Molecular Weight: 369.43

A filtered solution of 5-((benzyloxy)methyl)-7-(6-(piperidin-1-yl)hex-1-yn-1-yl)-2-(trifluoromethyl)-5H-pyrrolo[3,2-d]pyrimidin-4-amine (**193a**) (200 mg, 0.41 mmol) in EtOH (18 mL) and AcOH (2 mL) was hydrogenated three times using the H-cube (settings: 60 °C, Full H<sub>2</sub>, 1 mL/min flow rate) and a 10% Pd/C CatCart 30 as the catalyst, followed by one hydrogenation cycle (settings: 60 °C, Full H<sub>2</sub>, 1 mL/min flow rate) and a 10% Pt/C CatCart 30. The reaction mixture was concentrated *in vacuo* and the residue taken up in TFA (3 mL). The reaction vessel was sealed and the mixture heated at 85 °C for 16 h. The reaction was resealed and heated in a Biotage Initiator microwave (using initial absorption setting very high) to 120 °C for 3 h. After cooling the resultant mixture was concentrated *in vacuo* to give a solid (100 mg). The solid was dissolved in 1:1 MeOH:DMSO (1 mL) and purified by MDAP on Xbridge column using MeCN-water with an ammonium carbonate modifier. The solvent was dried under a stream of nitrogen in the Radleys blowdown apparatus to give the title compound (17.5 mg, 12 %) as a yellow gum.

<sup>1</sup>H NMR (400 MHz, DMSO-d<sub>6</sub>) δ 11.10 (br s, 1H), 7.46 (s, 1H), 7.21 (br s, 2H), 2.64 (t, *J* = 7.5 Hz, 2H), 2.29 (br s, 4H), 2.24 - 2.17 (m, 2H), 1.68 - 1.60 (m, 2H), 1.50 - 1.42 (m, 4H), 1.42 - 1.25 (m, 8H); <sup>13</sup>C NMR (101 MHz, DMSO-d<sub>6</sub>) δ 150.6, 146.8, 144.9 - 145.1 (m), 126.6 - 126.9 (m), 120.7 (q, *J*=275 Hz), 116.1, 113.6, 58.5, 53.9, 29.5, 28.7, 26.7, 26.2, 25.4, 24.0, 23.2; <sup>19</sup>F NMR (376 MHz, DMSO-d<sub>6</sub>) δ -67.20; LCMS (System B) R<sub>t</sub> 1.01 min, m/z 370 ([M+H]<sup>+</sup>); HRMS Anal. Calcd. For

$C_{18}H_{27}F_3N_5 = 370.2213$ . Found = 370.2228 ( $[M+H]^+$ ); IR ( $cm^{-1}$ ) 3166, 2930, 2852, 1665, 1617.

**2-Phenyl-7-(6-(piperidin-1-yl)hexyl)-5H-pyrrolo[3,2-d]pyrimidin-4-amine, Formic acid salt (145a)**



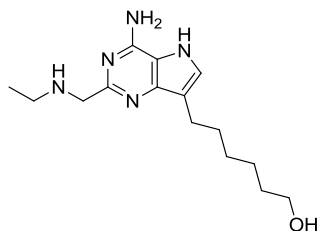
Chemical Formula:  $C_{23}H_{31}N_5$   
Molecular Weight: 377.53

A solution of 5-((benzyloxy)methyl)-2-phenyl-7-(6-(piperidin-1-yl)hex-1-yn-1-yl)-5H-pyrrolo[3,2-d]pyrimidin-4-amine (**154a**) (113 mg, 0.23 mmol) in EtOH (12 mL) was hydrogenated using the H-cube (settings: 60 °C, Full  $H_2$ , 1 mL/min flow rate) and a 10% Pd/C CatCart 30 as the catalyst. The solution was further hydrogenated using the H-cube (settings: 60 °C, Full  $H_2$ , 1 mL/min flow rate) and a new 10% Pd/C CatCart 30 as the catalyst. The reaction was concentrated *in vacuo* and dissolved in 1:1 MeOH:DMSO (1 mL) and purified by MDAP on a Sunfire C18 column using MeCN-water with a formic acid modifier. The solvent was removed under a stream of nitrogen in the Radleys™ blowdown apparatus to give the title compound as the formic acid salt (16.5 mg, 17%).

$^1H$  NMR (400 MHz, MeOD)  $\delta$  8.55 (br s, 1H), 8.23 - 8.15 (m, 2H), 7.46 - 7.36 (m, 3H), 7.27 (s, 1H), 3.06 (br s, 4H), 2.98 - 2.89 (m, 2H), 2.84 (t,  $J = 7.4$  Hz, 2H), 1.87 - 1.72 (m, 6H), 1.71 - 1.64 (m, 2H), 1.64 - 1.55 (m, 2H), 1.52 - 1.40 (m, 4H); exchangeable protons (NH,  $NH_2$ , and OH) not observed.  $^{13}C$  NMR (101 MHz, MeOD)  $\delta$  158.1, 152.1, 147.7, 140.7, 130.2, 129.2, 129.2, 127.9, 117.4, 114.3, 58.3, 54.1, 31.0, 29.6, 27.4, 24.9, 24.5, 24.3, 22.8; LCMS (System B)  $R_t$  1.14 min,  $m/z$  378 ( $[M+H]^+$ ); HRMS Anal. Calcd. For  $C_{23}H_{32}N_5 = 378.2658$ . Found = 378.2651

$[M+H]^+$ ; IR ( $\text{cm}^{-1}$ ) 3175, 2931, 2365, 1585, 1538.

**6-(4-Amino-2-((ethylamino)methyl)-5H-pyrrolo[3,2-d]pyrimidin-7-yl)hexan-1-ol**  
**(146x)**

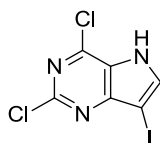


Chemical Formula:  $\text{C}_{15}\text{H}_{25}\text{N}_5\text{O}$   
Molecular Weight: 291.39

A solution of 6-(4-amino-5-((benzyloxy)methyl)-2-((ethyl(4-methoxybenzyl)amino)methyl)-5H-pyrrolo[3,2-d]pyrimidin-7-yl)hex-5-yn-1-ol (**210x**) (67 mg, 0.13 mmol) in EtOH (9 mL) and AcOH (1 mL) was hydrogenated using the H-cube (settings: 60 °C, Full  $\text{H}_2$ , 1 mL/min flow rate) and a 10% Pd/C CatCart 30 as the catalyst. The solution was further hydrogenated using the H-cube (settings: 60 °C, Full  $\text{H}_2$ , 1 mL/min flow rate) and a 10% Pd/C CatCart 30 as the catalyst. The reaction mixture was concentrated *in vacuo* and the residue dissolved in TFA (1 mL, 12.98 mmol). The reaction vessel was sealed and heated in a Biotage Initiator microwave (using initial absorption setting very high) to 150 °C for 1 h. After cooling the reaction mixture was concentrated *in vacuo* to give a brown gum. The gum was dissolved in 1:1 MeOH:DMSO 1 mL and purified by MDAP on an Xbridge column using MeCN-water with an ammonium carbonate modifier. The solvent was dried under a stream of nitrogen in the Radleys blowdown apparatus to give the title compound (8 mg, 22 %) as a gum.

$^1\text{H}$  NMR (400 MHz, MeOD)  $\delta$  8.55 (br s, 1H), 7.31 (s, 1H), 4.21 (s, 2H), 3.55 (t,  $J = 6.6$  Hz, 2H), 3.21 (q,  $J = 7.3$  Hz, 2H), 2.76 (t,  $J = 7.6$  Hz, 2H), 1.78 - 1.69 (m, 2H), 1.58 - 1.52 (m, 2H), 1.46 - 1.36 (m, 7H) exchangeable protons (NH,  $\text{NH}_2$ , and OH) not observed; LCMS (System B)  $R_t$  0.68 min,  $m/z$  292 ( $[M+H]^+$ ).

**2,4-Dichloro-7-iodo-5H-pyrrolo[3,2-d]pyrimidine (148)**



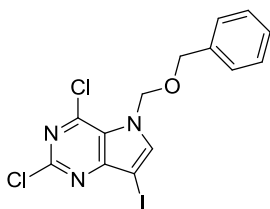
Chemical Formula: C<sub>6</sub>H<sub>2</sub>Cl<sub>2</sub>I<sub>N</sub><sub>3</sub>

Molecular Weight: 313.91

To a stirred solution of 2,4-dichloro-5H-pyrrolo[3,2-d]pyrimidine (**147**) (0.97 g, 5.16 mmol) in anhydrous THF (10 mL) was added *N*-iodosuccinimide (1.28 g, 5.68 mmol). The reaction mixture was stirred at ambient temperature for 1.5 h before being concentrated *in vacuo* and triturated with water (*ca.* 15 mL). The resultant brown solid was collected by filtration and dried *in vacuo* to give the title compound (1.55 g, 96 %).

<sup>1</sup>H NMR (400 MHz, DMSO-*d*<sub>6</sub>) δ 13.18 (br s, 1H), 8.29 (s, 1H); LCMS (System B) R<sub>t</sub> 0.89 min, m/z 314, 316, 318 ([M+H]<sup>+</sup>).

**2,4-Dichloro-7-iodo-5-[(phenylmethyl)oxy]methyl-5H-pyrrolo[3,2-d]pyrimidine (149)**



Chemical Formula: C<sub>14</sub>H<sub>10</sub>Cl<sub>2</sub>I<sub>N</sub><sub>3</sub>O

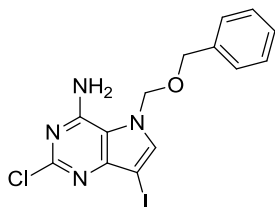
Molecular Weight: 434.06

To a stirred suspension of sodium hydride 60% wt. on mineral oil (0.207 g, 5.18 mmol) in anhydrous THF (10 mL) at 0 °C was added a solution of 2,4-dichloro-7-iodo-5H-pyrrolo[3,2-d]pyrimidine (**148**) (1.55 g, 4.94 mmol) in THF (5 mL) dropwise over 5 min. The resultant mixture was stirred at 0 °C for 15 mins before the addition of a solution of chloromethyl phenylmethyl ether (0.687 mL, 4.94 mmol) in THF (5 mL) dropwise over 5 min. The reaction mixture was stirred at 0 °C for two hours and allowed to warm to ambient temperature. The reaction mixture was then partitioned between EtOAc (200 mL) and water (200 mL). The organic

phase was separated and washed with brine (200 mL), dried (MgSO<sub>4</sub>), filtered and concentrated *in vacuo*. The resulting residue was dissolved in DCM and purified on a silica cartridge (100 g) using a 0-50% EtOAc-cyclohexane gradient over 40 mins. The appropriate fractions were combined and evaporated *in vacuo* to give the title compound (1.63 g, 76 %) as a colourless oil which solidified on standing.

<sup>1</sup>H NMR (400 MHz, CDCl<sub>3</sub>) δ 7.65 (s, 1H), 7.34 - 7.28 (m, 3H), 7.26 - 7.20 (m, 2H), 5.81 (s, 2H), 4.56 (s, 2H); LCMS (System B) R<sub>t</sub> 1.31 min, m/z 434, 436, 438 ([M+H]<sup>+</sup>).

**\*2-Chloro-7-iodo-5-[(phenylmethyl)oxy]methyl}-5H-pyrrolo[3,2-d]pyrimidin-4-amine (150)**



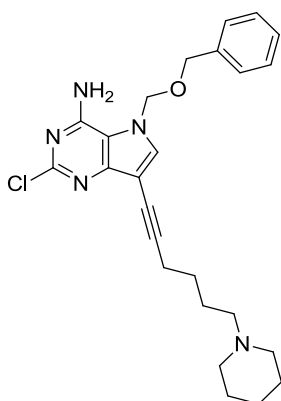
Chemical Formula: C<sub>14</sub>H<sub>12</sub>ClIN<sub>4</sub>O  
Molecular Weight: 414.63

Seven batches of 2,4-dichloro-7-iodo-5-[(phenylmethyl)oxy]methyl-5H-pyrrolo[3,2-d]-pyrimidine (**149**) (1.03 g, 2.37 mmol) were suspended in 0.88 ammonia (0.6 mL, 11 mmol) and IPA (1.4 mL) before being sealed and heated in a Biotage Initiator microwave (absorption setting normal) to 120 °C for 10 min. After cooling, the batches were combined and the solvent was removed *in vacuo*. The residue washed with water (100 mL) then dried *in vacuo* and divided into six batches. Each batch was suspended in 0.88 ammonia (0.8 mL, 14.7 mmol) and IPA (2.4 mL) before being sealed and heated in a Biotage Initiator microwave (absorption setting normal) to 120 °C for 10 min. After cooling, the batches were combined and the solvent was removed *in vacuo*. The residue washed with water (60 mL) then dried *in vacuo* and divided into six batches. Each batch was suspended in 0.88 ammonia (0.8 mL, 14.7 mmol) and IPA (2.4 mL) before being sealed and heated in a Biotage Initiator microwave (absorption setting normal) to 120 °C for 15 min. After cooling, the batches were combined and the solvent was removed *in*

*vacuo*. The residue washed with water (100 mL) then dried *in vacuo* to furnish the title compound (5.07 g, 73 %).

<sup>1</sup>H NMR (400 MHz, DMSO-*d*<sub>6</sub>) δ 7.90 (s, 1H), 7.34 - 7.22 (m, 5H), 7.22 - 7.16 (m, 2H), 5.73 (s, 2H), 4.50 (s, 2H); LCMS (System B) R<sub>t</sub> 1.07 min, m/z 415, 417 ([M+H]<sup>+</sup>).

**\*5-((Benzyloxy)methyl)-2-chloro-7-(6-(piperidin-1-yl)hex-1-yn-1-yl)-5H-pyrrolo[3,2-*d*]pyrimidin-4-amine (151a)**



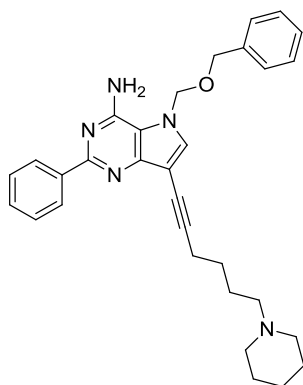
Chemical Formula: C<sub>25</sub>H<sub>30</sub>ClN<sub>5</sub>O  
Molecular Weight: 451.99

To a degassed solution of 2-chloro-7-iodo-5-[[phenylmethyl]oxy]methyl}-5H-pyrrolo[3,2-*d*]pyrimidin-4-amine (**150**) (2.55 g, 6.15 mmol) in anhydrous DMF (50 mL) under nitrogen atmosphere at room temperature was added copper (I) iodide (0.234 g, 1.23 mmol), *bis*(triphenylphosphine)palladium(II)dichloride (0.432 g, 0.615 mmol) and triethylamine (1.28 mL, 9.22 mmol). The mixture was stirred at room temperature under nitrogen atmosphere for 10 min and then a solution of 1-(5-hexyn-1-yl)piperidine (1.32 g, 7.99 mmol) in anhydrous degassed DMF (10 mL) was added. The reaction mixture was stirred at ambient temperature for 16 h before being concentrated *in vacuo* to give a brown oil. The oil was partitioned between water (250 mL) and DCM (250 mL). The organic layer was separated and the aqueous layer extracted with DCM (150 mL). The combined organic extracts were dried (hydrophobic frit) and concentrated *in vacuo* to give a brown oil (5.11 g). The sample was loaded in DCM and purified on aminopropyl functionalised silica

cartridge (100 g) using a 0-100%EtOAc-cyclohexanegradiant over 60 mins. The appropriate fractions were combined and evaporated *in vacuo* to give the title compound (1.60 g, 52%) as a white solid.

<sup>1</sup>H NMR (400 MHz, CDCl<sub>3</sub>) δ 7.42 - 7.35 (m, 3H), 7.31 - 7.23 (m, 3H), 6.11 (br s, 2H), 5.46 (s, 2H), 4.57 (s, 2H), 2.50 (t, *J* = 6.7 Hz, 2H), 2.40 (br s, 4H), 2.37 - 2.31 (m, 2H), 1.71 - 1.63 (m, 4H), 1.63 - 1.56 (m, 4H), 1.49 - 1.39 (m, 2H); <sup>13</sup>C NMR (101 MHz, CDCl<sub>3</sub>) δ 153.6, 152.6, 152.0, 134.8, 134.8, 128.9, 128.8, 128.4, 113.2, 100.1, 93.6, 77.2, 70.2, 59.0, 54.6, 26.9, 26.3, 26.0, 24.5, 19.8; LCMS (System B) R<sub>t</sub> 1.18 min, m/z 452, 454 ([M+H]<sup>+</sup>); HRMS Anal. Calcd. For C<sub>25</sub>H<sub>31</sub>ClN<sub>5</sub>O = 452.2217. Found = 452.2220 ([M+H]<sup>+</sup>); IR (cm<sup>-1</sup>) 3150, 2935, 1648, 1596; Mpt. 164-167 °C.

**5-((Benzyloxy)methyl)-2-phenyl-7-(6-(piperidin-1-yl)hex-1-yn-1-yl)-5H-pyrrolo[3,2-*d*]pyrimidin-4-amine (154a)**



Chemical Formula: C<sub>31</sub>H<sub>35</sub>N<sub>5</sub>O  
Molecular Weight: 493.64

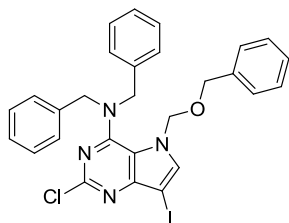
A suspension of 5-((benzyloxy)methyl)-2-chloro-7-(6-(piperidin-1-yl)hex-1-yn-1-yl)-5H-pyrrolo[3,2-*d*]pyrimidin-4-amine (**151a**) (150 mg, 0.33 mmol), potassium carbonate (92 mg, 0.66 mmol), phenylboronic acid (81 mg, 0.66 mmol) and tetrakis(triphenylphosphine)palladium(0) (38 mg, 0.033 mmol) in a mixture of 1,4-dioxane (2 mL) and water (0.5 mL) was sealed and heated in a Biotage Initiator microwave (absorption setting high) to 150 °C for 60 min. After cooling, further phenylboronic acid (81 mg, 0.66 mmol) and further



tetrakis(triphenylphosphine)palladium(0) (38 mg, 0.033 mmol) was added and the reaction vessel was re-sealed and heated in a Biotage Initiator microwave (absorption setting high) to 150 °C for 60 min. After cooling, the reaction mixture was diluted with DCM (10 mL) and filtered through a pad of celite. The filtrate was washed with water (10 mL) and dried (hydrophobic frit) before concentration *in vacuo* to give a brown oil. The oil was dissolved in DCM and purified on a silica cartridge (20 g) using a 0-100% EtOAc-cyclohexane+0-20% MeOH gradient over 40 mins. The appropriate fractions were combined and evaporated *in vacuo* to give the title compound (114 mg, 70 %) as a off-white foam.

<sup>1</sup>H NMR (400 MHz, CDCl<sub>3</sub>) δ 8.46 - 8.42 (m, 2H), 7.52 - 7.33 (m, 5H), 7.32 - 7.24 (m, 4H), 5.72 (s, 2H), 5.51 (s, 2H), 4.56 (s, 2H), 2.93 - 2.71 (m, 6H), 2.58 (t, *J* = 6.8 Hz, 2H), 2.13 - 2.02 (m, 2H), 1.84 - 1.65 (m, 6H), 1.50 - 1.32 (m, 2H); LCMS (System B) R<sub>t</sub> 1.41 min, m/z 494 ([M+H]<sup>+</sup>).

**N,N-Dibenzyl-5-((benzyloxy)methyl)-2-chloro-7-iodo-5H-pyrrolo[3,2-*d*]pyrimidin-4-amine (157)**

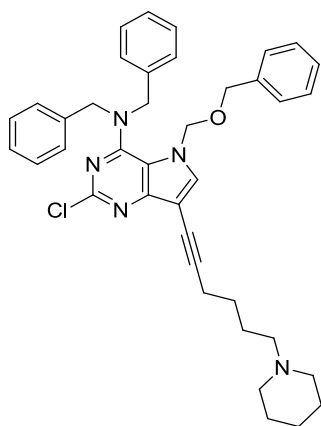


Chemical Formula: C<sub>28</sub>H<sub>24</sub>ClIN<sub>4</sub>O  
Molecular Weight: 594.87

A stirred suspension of 5-((benzyloxy)methyl)-2,4-dichloro-7-iodo-5H-pyrrolo[3,2-*d*]pyrimidine (**149**) (4.1 g, 9.5 mmol) and dibenzylamine (4.0 mL, 20.8 mmol) in EtOH (50 mL) was heated at reflux for 4 h before being concentrated *in vacuo* and the residue partitioned between water (400 mL) and DCM (400 mL). The organic phase was separated and dried (hydrophobic frit) before concentration *in vacuo* and loading in DCM and purification on a silica cartridge (100 g) using a 0-25% EtOAc-cyclohexane gradient over 60 mins. The appropriate fractions were combined and evaporated *in vacuo* to give the title compound (4.92 g, 87 %) as a white foam.

$^1\text{H}$  NMR (400 MHz,  $\text{CDCl}_3$ )  $\delta$  7.52 (s, 1H), 7.32 - 7.22 (m, 8H), 7.12 - 7.02 (m, 7H), 5.59 (s, 2H), 4.56 - 4.50 (m, 4H), 4.29 (s, 2H); LCMS (System B)  $R_t$  1.58 min,  $m/z$  595, 597 ( $[\text{M}+\text{H}]^+$ ), Note: compounds in only 86% pure by UV.

***N,N*-Dibenzyl-5-((benzyloxy)methyl)-2-chloro-7-(6-(piperidin-1-yl)hex-1-yn-1-yl)-5*H*-pyrrolo[3,2-*d*]pyrimidin-4-amine (158a)**

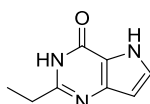


Chemical Formula:  $\text{C}_{39}\text{H}_{42}\text{ClN}_5\text{O}$   
Molecular Weight: 632.24

To a stirred degassed suspension of *N,N*-dibenzyl-5-((benzyloxy)methyl)-2-chloro-7-iodo-5*H*-pyrrolo[3,2-*d*]pyrimidin-4-amine (**157**) (4.91 g, 8.25 mmol), copper(I) iodide (0.314 g, 1.65 mmol) and *bis*(triphenylphosphine)palladium(II)dichloride (0.58 g, 0.83 mmol) in anhydrous DMF (80 mL) was added a solution of 1-(5-hexyn-1-yl)piperidine (1.93 g, 11.7 mmol) and triethylamine (1.86 mL, 13.4 mmol) in DMF (20 mL) dropwise over 15 min. The reaction mixture was stirred at ambient temperature for 18 h before being concentrated *in vacuo* to give a brown oil. The oil was partitioned between EtOAc (500 mL) and water (500 mL). The organic phase was separated, dried ( $\text{MgSO}_4$ ), filtered and concentrated *in vacuo* to give a red foam (4.9 g). This was dissolved in DCM and purified on a silica cartridge (100 g) using a 0-100% EtOAc-DCM+0-20% MeOH gradient over 60 mins. The appropriate fractions were combined and evaporated *in vacuo* to give the title compound (1.79 g, 34%) as an off white foam.

$^1\text{H}$  NMR (400 MHz,  $\text{CDCl}_3$ )  $\delta$  7.69 (s, 1H), 7.35 - 7.24 (m, 10H), 7.21 - 7.13 (m, 2H), 7.12 - 7.04 (m, 3H), 5.60 (s, 2H), 4.57 - 4.47 (m, 4H), 4.33 (s, 2H), 3.69 (br d,  $J = 12$  Hz, 2H), 3.28 - 3.21 (m, 2H), 2.94 - 2.82 (m, 2H), 2.61 (t,  $J = 6.4$  Hz, 2H), 2.36 - 2.20 (m, 6H), 1.96 - 1.87 (m, 2H), 1.82 - 1.72 (m, 2H);  $^{13}\text{C}$  NMR (101 MHz,  $\text{CDCl}_3$ )  $\delta$  155.4, 154.3, 152.1, 138.1, 136.2, 136.1, 128.5, 128.5, 128.4, 128.1, 127.8, 127.6, 116.8, 101.2, 92.7, 72.0, 70.9, 57.0, 53.2, 25.0, 22.5, 21.8, 19.0; LCMS (System A)  $R_t$  1.25 min,  $m/z$  632, 634 ( $[\text{M}+\text{H}]^+$ ); HRMS Anal. Calcd. For  $\text{C}_{39}\text{H}_{43}\text{ClN}_5\text{O} = 632.3156$ . Found = 632.3168 ( $[\text{M}+\text{H}]^+$ ); IR ( $\text{cm}^{-1}$ ) 2930, 1582, 1542, 1522; Mpt. 73-77 °C.

### **2-Ethyl-3H-pyrrolo[3,2-d]pyrimidin-4(5H)-one (164)**



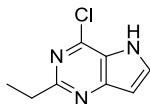
Chemical Formula:  $\text{C}_8\text{H}_9\text{N}_3\text{O}$   
Molecular Weight: 163.18

To a stirred suspension of ethyl 3-amino-1H-pyrrole-2-carboxylate, hydrochloride (3.00 g, 15.7 mmol) in propionitrile (30 mL) was added 4M hydrochloric acid in 1,4-dioxane (20 mL, 80 mmol) and the mixture was heated to 50 °C for 16 h. The reaction mixture was concentrated *in vacuo*. The residue was suspended in EtOH (45 mL) and treated with a solution of NaOH (2.52 g, 62.9 mmol) in water (10 mL) and heated to 80 °C for 4 h. After this time, the reaction mixture was concentrated *in vacuo*. The residue was suspended in water (100 mL) and the pH adjusted to 5 with 2N aqueous hydrochloric acid and extracted with EtOAc (2 x 100 mL). The combined organic extracts were washed with brine (200 mL), dried ( $\text{MgSO}_4$ ), filtered and concentrated *in vacuo* to give a brown solid. The sample was preabsorbed onto Florosil and purified on a silica cartridge (100 g) using a 0-25% MeOH-DCM gradient over 60 mins. The appropriate fractions were combined and evaporated *in vacuo* to give the title compound (827 mg, 32%) as a beige solid.

$^1\text{H}$  NMR (400 MHz,  $\text{DMSO}-d_6$ )  $\delta$  11.89 (br s, 1H), 11.69 (br s, 1H), 7.31 (t,  $J = 2.0$  Hz, 1H), 6.29 (s, 1H), 2.58 (q,  $J = 7.5$  Hz, 2H), 1.21 (t,  $J = 7.5$  Hz, 3H); LCMS

(System B)  $R_t$  0.45 min,  $m/z$  164 ( $[M+H]^+$ ).

#### **4-Chloro-2-ethyl-5H-pyrrolo[3,2-d]pyrimidine (165)**

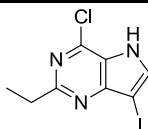


Chemical Formula:  $C_8H_8ClN_3$   
Molecular Weight: 181.62

A stirred suspension of 2-ethyl-3H-pyrrolo[3,2-d]pyrimidin-4(5H)-one (**164**) (820 mg, 5.03 mmol) in phosphorus(V) oxychloride (10.0 mL, 107 mmol) was heated to 100 °C for 2 h. The reaction mixture was concentrated *in vacuo* and azeotroped with toluene. The resultant solid was dissolved in DCM (50 mL) and washed with water (50 mL). The aqueous layer was further extracted with 3:1  $CHCl_3$ :IPA (50 mL). The combined organic extracts were dried (hydrophobic frit) and concentrated *in vacuo* to give the title compound (735 mg, 81%) as a brown gum.

$^1H$  NMR (400 MHz,  $CDCl_3$ )  $\delta$  10.70 (br s, 1H), 7.72 (d,  $J = 2.9$  Hz, 1H), 6.76 (d,  $J = 2.9$  Hz, 1H), 3.11 (q,  $J = 7.6$  Hz, 2H), 1.43 (t,  $J = 7.6$  Hz, 3H); LCMS (System B)  $R_t$  0.64 min,  $m/z$  182,184 ( $[M+H]^+$ ).

#### **4-Chloro-2-ethyl-7-iodo-5H-pyrrolo[3,2-d]pyrimidine (166)**



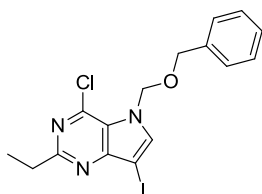
Chemical Formula:  $C_8H_7ClIN_3$   
Molecular Weight: 307.52

To a stirred solution of 4-chloro-2-ethyl-5H-pyrrolo[3,2-d]pyrimidine (**165**) (0.735 g, 4.05 mmol) in anhydrous THF (10 mL) was added solid *N*-iodosuccinimide (1.00 g, 4.45 mmol) in one charge. The reaction mixture was stirred at ambient temperature for 1.5 h. The reaction mixture was concentrated *in vacuo*, and partitioned between water (100 mL) and EtOAc (100 mL). The organic was separated and washed with aqueous sodium thiosulphate (100 mL), dried ( $MgSO_4$ ), filtered and concentrated *in vacuo* to give the title compound (1.05 g, 84 %) as a peach coloured foam.

$^1\text{H}$  NMR (400 MHz,  $\text{CDCl}_3$ )  $\delta$  8.97 (br s, 1H), 7.60 (d,  $J = 2.9$  Hz, 1H), 3.03 (q,  $J = 7.6$  Hz, 2H), 1.35 (t,  $J = 7.6$  Hz, 3H); LCMS (System B)  $R_t$  0.80 min,  $m/z$  308, 310 ( $[\text{M}+\text{H}]^+$ ).

**5-((Benzyloxy)methyl)-4-chloro-2-ethyl-7-iodo-5H-pyrrolo[3,2-d]pyrimidine**

**(167)**

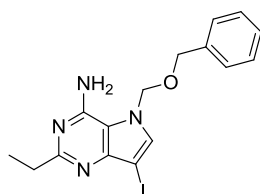


Chemical Formula:  $\text{C}_{16}\text{H}_{15}\text{ClI}\text{N}_3\text{O}$   
Molecular Weight: 427.67

To a stirred slurry of sodium hydride 60% wt. on mineral oil (0.156 g, 3.91 mmol) in anhydrous THF (15 mL) at 0 °C under a nitrogen atmosphere was added a solution of 4-chloro-2-ethyl-7-iodo-5H-pyrrolo[3,2-d]pyrimidine (**166**) (1.045 g, 3.40 mmol) in anhydrous THF (5 mL) dropwise over 10 min. The reaction mixture was stirred at 0 °C for a further 30 min, before addition of a solution of ((chloromethoxy)methyl)benzene (0.612 g, 3.91 mmol) in anhydrous THF (5 mL) dropwise over 10 min. The reaction mixture was then allowed to warm to ambient temperature and stirred for a further 60 min. The reaction mixture was partitioned between water (100 mL) and EtOAc (100 mL). The organic was separated and was washed with brine (100 mL), dried ( $\text{MgSO}_4$ ), filtered and concentrated *in vacuo* to give an orange oil (1.65 g). The oil was dissolved in DCM and purified on a silica cartridge (100 g) using a 0-50% EtOAc-cyclohexane gradient over 60 mins. The appropriate fractions were combined and evaporated *in vacuo* to give the title compound (1.025 g, 71 %) as a yellow oil.

$^1\text{H}$  NMR (400 MHz,  $\text{CDCl}_3$ )  $\delta$  7.58 (s, 1H), 7.22 - 7.35 (m, 5H), 5.81 (s, 2H), 4.53 (s, 2H), 3.08 (q,  $J = 7.6$  Hz, 2H), 1.42 (t, 7.6 Hz, 3H); LCMS (System B)  $R_t$  1.29 min,  $m/z$  428, 430 ( $[\text{M}+\text{H}]^+$ ).

**5-((Benzyloxy)methyl)-2-ethyl-7-iodo-5H-pyrrolo[3,2-d]pyrimidin-4-amine (168)**

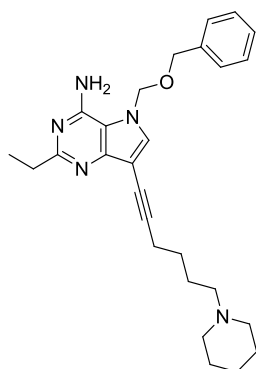


Chemical Formula: C<sub>16</sub>H<sub>17</sub>IN<sub>4</sub>O  
Molecular Weight: 408.24

A suspension of 5-((benzyloxy)methyl)-4-chloro-2-ethyl-7-iodo-5H-pyrrolo[3,2-*d*]pyrimidine (**167**) (1.02 g, 2.39 mmol) in IPA (1 mL) was treated with 880 ammonia (2.00 mL, 36.2 mmol), the reaction vessel was sealed and heated in a Biotage Initiator microwave (using initial absorption setting high) to 135 °C for 90 min. After cooling, further 880 ammonia (1.00 mL, 18.1 mmol) was added and the reaction vessel was sealed and heated in a Biotage Initiator microwave (using initial absorption setting high) to 135 °C for a further 90 min. After cooling, the reaction mixture was concentrated *in vacuo* and was partitioned between water (70 mL) and EtOAc (100 mL). The organic layer was separated, washed with brine (100 mL), dried (MgSO<sub>4</sub>), filtered and concentrated *in vacuo* to give the title compound (834 mg, 86 %) as an off white solid.

<sup>1</sup>H NMR (400 MHz, CDCl<sub>3</sub>) δ 7.43 - 7.34 (m, 3H), 7.31 - 7.24 (m, 2H), 7.20 (s, 1H), 5.71 (br s, 2H), 5.48 (s, 2H), 4.55 (s, 2H), 2.89 (q, *J* = 7.6 Hz, 2H), 1.37 (t, *J* = 7.6 Hz, 3H); <sup>13</sup>C NMR (101 MHz, CDCl<sub>3</sub>) δ 165.9, 151.8, 150.9, 135.2, 135.0, 128.8, 128.7, 128.4, 113.7, 77.0, 70.0, 58.4, 32.5, 13.4; LCMS (System B) R<sub>t</sub> 1.00 min, m/z 409 ([M+H]<sup>+</sup>); HRMS Anal. Calcd. For C<sub>16</sub>H<sub>18</sub>IN<sub>4</sub>O = 409.0520. Found = 409.0515 ([M+H]<sup>+</sup>); IR (cm<sup>-1</sup>) 3391, 3102, 1655, 1594; Mpt. 143-146 °C.

**5-((Benzyloxy)methyl)-2-ethyl-7-(6-(piperidin-1-yl)hex-1-yn-1-yl)-5H-pyrrolo[3,2-d]pyrimidin-4-amine (169a)**

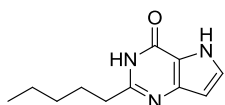


Chemical Formula: C<sub>27</sub>H<sub>35</sub>N<sub>5</sub>O  
Molecular Weight: 445.60

To a degassed stirred suspension of 5-((benzyloxy)methyl)-2-ethyl-7-iodo-5H-pyrrolo[3,2-d]pyrimidin-4-amine (**168**) (300 mg, 0.74 mmol), copper (I) iodide (21 mg, 0.11 mmol) and *bis*(triphenylphosphine)palladium(II) dichloride (39 mg, 0.056 mmol) in anhydrous DMF (8 mL) was added a solution of 1-(5-hexyn-1-yl)piperidine (158 mg, 0.96 mmol) and triethylamine (0.153 mL, 1.10 mmol) in anhydrous DMF (2 mL) dropwise over 2 min. The reaction mixture was stirred at ambient temperature for 22 h. The reaction mixture was concentrated *in vacuo* and the residue partitioned between EtOAc (50 mL) and water (50 mL). The organic layer was separated, washed with brine (50 mL), dried (MgSO<sub>4</sub>), filtered and concentrated *in vacuo* to give a yellow oil. The oil was dissolved in DCM and purified on an aminopropyl functionalised silica cartridge (55 g) using a 0-10% MeOH-DCM gradient over 40 mins. The appropriate fractions were combined and evaporated *in vacuo* to give the title compound (98 mg, 30 %) as a colourless gum.

<sup>1</sup>H NMR (400 MHz, CDCl<sub>3</sub>) δ 7.41 - 7.32 (m, 3H), 7.31 - 7.26 (m, 2H), 7.23 (s, 1H), 5.70 (s, 2H), 5.45 (s, 2H), 4.53 (s, 2H), 2.88 (q, *J* = 7.7 Hz, 2H), 2.54 - 2.49 (m, 2H), 2.43 - 2.28 (m, 6H), 1.74 - 1.63 (m, 4H), 1.62 - 1.55 (m, 4H), 1.48 - 1.40 (m, 2H), 1.36 (t, *J* = 7.7 Hz, 3H); LCMS (System B) R<sub>t</sub> 1.12 min, m/z 446 ([M+H]<sup>+</sup>).

**2-Pentyl-3H-pyrrolo[3,2-d]pyrimidin-4(5H)-one (170)**



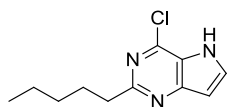
Chemical Formula: C<sub>11</sub>H<sub>15</sub>N<sub>3</sub>O  
Molecular Weight: 205.26

A suspension of ethyl 3-amino-1H-pyrrole-2-carboxylate, hydrochloride (3.00 g, 15.7 mmol), hexanenitrile (30.0 g, 309 mmol) and 4M hydrochloric acid in 1,4-dioxane (20 mL, 80 mmol) was stirred at 50 °C for 20 h. The reaction mixture was allowed to cool to ambient temperature, upon cooling a precipitate formed. To the reaction was added further 4M hydrochloric acid in 1,4-dioxane (10 mL) and the reaction mixture was heated at 50 °C for a further 4 h. The reaction mixture was allowed to cool to ambient temperature and was diluted with TBME (300 mL) and the resultant suspension filtered. The solid cake was washed with TBME (150 mL) and Et<sub>2</sub>O (150 mL) and dried *in vacuo* to give a beige solid (4.4 g). The solid was dissolved in EtOH (45 mL) and treated with a solution of NaOH (2.52 g, 62.9 mmol) in water (10 mL) and the mixture was heated to 80 °C for 4 h. The reaction solvent was removed *in vacuo*. The residue was suspended in water (200 mL) and the pH adjusted to 4 with solid citric acid, and extracted with EtOAc (2 x 200 mL). The combined organic extracts were dried (MgSO<sub>4</sub>), filtered and concentrated *in vacuo* to give a sticky beige solid. The solid was triturated with Et<sub>2</sub>O and the resultant suspension filtered and dried *in vacuo* to give the title compound (1.88 g, 58 %) as an off white solid.

<sup>1</sup>H NMR (400 MHz, DMSO-*d*<sub>6</sub>) δ 11.88 (br s, 1H), 11.68 (br s, 1H), 7.31 (t, *J* = 2.9 Hz, 1H), 6.28 (dd, *J* = 2.9, 0.5 Hz, 1H) 2.58 - 2.49 (m, 2H), 1.73 - 1.64 (m, 2H), 1.36 - 1.23 (m, 4H), 0.87 (t, *J* = 6.9 Hz, 3H); LCMS (System B) R<sub>t</sub> 0.72 min, m/z 206 ([M+H]<sup>+</sup>).



#### **4-Chloro-2-pentyl-5H-pyrrolo[3,2-d]pyrimidine (171)**

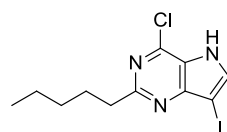


Chemical Formula: C<sub>11</sub>H<sub>14</sub>ClN<sub>3</sub>  
Molecular Weight: 223.70

A stirred suspension of 2-pentyl-3H-pyrrolo[3,2-d]pyrimidin-4(5H)-one (**170**) (1.88 g, 9.16 mmol) in phosphorus(V) oxychloride (20.0 mL, 215 mmol) was heated to 100 °C for 3 h. The reaction mixture was concentrated *in vacuo* and azeotroped with toluene. The resultant gum was dissolved in DCM (100 mL) and washed with water (100 mL) and was dried (hydrophobic frit) before being concentrated *in vacuo* to give a brown solid. The sample was dissolved in DCM and was purified on a silica cartridge (50 g) using a 0-25% MeOH:TBME gradient over 40 mins. The appropriate fractions were combined and evaporated *in vacuo* to give a brown solid, this was triturated with Et<sub>2</sub>O (ca. 100 mL), the resultant suspension was filtered and the solid dried *in vacuo* to give the title compound (1.04 g, 51 %) as a pale brown solid.

<sup>1</sup>H NMR (400 MHz, CDCl<sub>3</sub>) δ 13.63 (br s, 1H), 8.10 (br s, 1H), 7.03 (br s, 1H), 3.31 (t, *J* = 7.6 Hz, 2H), 2.03 - 1.93 (m, 2H), 1.48 - 1.29 (m, 4H), 0.98 - 0.81 (m, 3H); LCMS (System B) R<sub>t</sub> 0.99 min, m/z 224, 226 ([M+H]<sup>+</sup>).

#### **4-Chloro-7-iodo-2-pentyl-5H-pyrrolo[3,2-d]pyrimidine (172)**



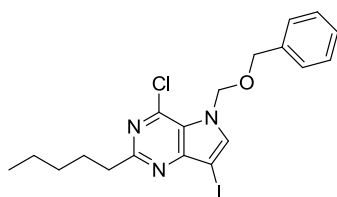
Chemical Formula: C<sub>11</sub>H<sub>13</sub>ClIN<sub>3</sub>  
Molecular Weight: 349.60

To a stirred suspension of 4-chloro-2-pentyl-5H-pyrrolo[3,2-d]pyrimidine (**171**) (1.04 g, 4.65 mmol) in anhydrous THF (15 mL) was added solid *N*-iodosuccinimide (1.15 g, 5.11 mmol) in one charge. The resulting brown solution was stirred at ambient temperature for 1.5 h. The reaction mixture was concentrated *in vacuo*, and partitioned between water (120 mL) and EtOAc (120 mL). The organic was separated and washed with aqueous sodium thiosulphate (120 mL), dried (MgSO<sub>4</sub>),

filtered and concentrated *in vacuo* to give the title compound (1.27 g, 78 %) as a beige solid.

<sup>1</sup>H NMR (400 MHz, CDCl<sub>3</sub>) δ 9.04 (br s, 1H), 7.66 (d, *J* = 2.7 Hz, 1H), 3.11 - 2.99 (m, 2H), 1.95 - 1.81 (m, 2H), 1.44 - 1.29 (m, 4H), 0.95 - 0.85 (m, 3H); LCMS (System B) R<sub>t</sub> 1.21 min, m/z 350, 352 ([M+H]<sup>+</sup>).

**5-((Benzyloxy)methyl)-4-chloro-7-iodo-2-pentyl-5H-pyrrolo[3,2-*d*]pyrimidine (173)**



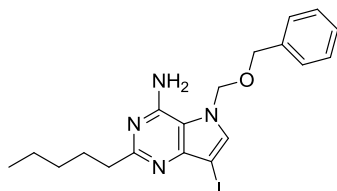
Chemical Formula: C<sub>19</sub>H<sub>21</sub>ClIN<sub>3</sub>O  
Molecular Weight: 469.75

To a stirred slurry of sodium hydride 60% wt. on mineral oil (0.167 g, 4.17 mmol) in anhydrous THF (15 mL) at 0 °C under a nitrogen atmosphere was added a solution of 4-chloro-7-iodo-2-pentyl-5H-pyrrolo[3,2-*d*]pyrimidine (**172**) (1.27 g, 3.63 mmol) in anhydrous THF (10 mL) dropwise over 10 min. The reaction mixture was stirred at 0 °C for a further 30 min before addition of a solution of ((chloromethoxy)methyl)benzene (0.653 g, 4.17 mmol) in anhydrous THF (10 mL) dropwise over 10 min. The reaction mixture was then allowed to warm to ambient temperature and stirred for a further 60 min. To the reaction mixture was added further sodium hydride 60% wt. on mineral oil (30.0 mg, 0.75 mmol) and stirring at ambient temperature was continued for 16 h. The reaction mixture was partitioned between water (120 mL) and EtOAc (120 mL). The organic phase was separated and the aqueous layer back extracted with EtOAc (50 mL). The combined organic extracts were washed with brine (100 mL), dried (MgSO<sub>4</sub>), filtered and concentrated *in vacuo* to give an orange oil. The sample was dissolved in DCM and purified on a silica cartridge (100 g) using a 0-50% EtOAc-cyclohexane gradient over 60 mins. The appropriate fractions were combined and evaporated *in vacuo* to give the title compound (1.48 g, 87 %) as a yellow oil.

$^1\text{H}$  NMR (400 MHz,  $\text{CDCl}_3$ )  $\delta$  7.57 (s, 1H), 7.34 - 7.22 (m, 5H), 5.80 (s, 2H), 4.53 (s, 2H), 3.08 - 3.00 (m, 2H), 1.82 - 1.93 (m, 2H), 1.45 - 1.34 (m, 4H), 0.96 - 0.87 (m, 3H); LCMS (System B)  $R_t$  1.51 min,  $m/z$  470, 472 ( $[\text{M}+\text{H}]^+$ ).

**5-((Benzyloxy)methyl)-7-iodo-2-pentyl-5H-pyrrolo[3,2-*d*]pyrimidin-4-amine**

**(174)**



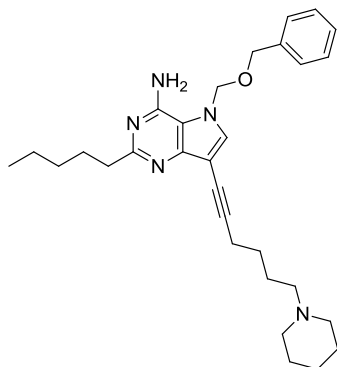
Chemical Formula:  $\text{C}_{19}\text{H}_{23}\text{IN}_4\text{O}$   
Molecular Weight: 450.32

A suspension of 5-((benzyloxy)methyl)-4-chloro-7-iodo-2-pentyl-5H-pyrrolo[3,2-*d*]pyrimidine (**173**) (1.48 g, 3.14 mmol) in IPA (2 mL) was treated with 880 ammonia (2.50 mL, 45.2 mmol), the reaction vessel was sealed and heated in a Biotage Initiator microwave (using initial absorption setting high) to 135 °C for 90 min. After cooling the reaction further 880 ammonia (1 mL) was added and the reaction vessel was re-sealed and heated in a Biotage Initiator microwave (using initial absorption setting high) to 130 °C for 60 min. After cooling, the reaction mixture was concentrated *in vacuo*, the resulting residue was partitioned between water (100 mL) and DCM (100 mL). The organic phase was separated and dried (hydrophobic frit) before concentration *in vacuo* to give a yellow gum. The sample was dissolved in DCM and purified on a silica cartridge (50 g) using a 0-100% EtOAc-cyclohexane gradient over 40 mins. The appropriate fractions were combined and evaporated *in vacuo* to give the title compound (1.03 g, 73 %) as a white foam.

$^1\text{H}$  NMR (400 MHz,  $\text{CDCl}_3$ )  $\delta$  7.44 - 7.36 (m, 3H), 7.34 - 7.26 (m, 2H), 7.22 (s, 1H), 5.74 (br s, 2H), 5.50 (s, 2H), 4.58 (s, 2H), 2.93 - 2.84 (m, 2H), 1.80 - 1.91 (m, 2H), 1.48 - 1.34 (m, 4H), 0.97 - 0.89 (m, 3H);  $^{13}\text{C}$  NMR (101 MHz,  $\text{CDCl}_3$ )  $\delta$  165.2, 151.8, 150.8, 135.2, 135.0, 128.8, 128.7, 128.4, 113.7, 77.0, 70.0, 58.4, 39.5, 31.9, 29.1, 22.7, 14.1; HRMS Anal. Calcd. For  $\text{C}_{19}\text{H}_{24}\text{IN}_4\text{O}$  = 451.0989. Found = 451.0981 ( $[\text{M}+\text{H}]^+$ ); LCMS (System B)  $R_t$  1.26 min,  $m/z$  451 ( $[\text{M}+\text{H}]^+$ ); IR ( $\text{cm}^{-1}$ )

3114, 1645, 1594; Mpt. 99-101 °C.

**5-((Benzyloxy)methyl)-2-pentyl-7-(6-(piperidin-1-yl)hex-1-yn-1-yl)-5H-pyrrolo[3,2-d]pyrimidin-4-amine (175a)**

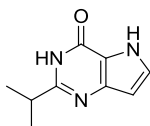


Chemical Formula: C<sub>30</sub>H<sub>41</sub>N<sub>5</sub>O  
Molecular Weight: 487.68

To a degassed stirred suspension of 5-((benzyloxy)methyl)-7-iodo-2-pentyl-5H-pyrrolo[3,2-d]pyrimidin-4-amine (**174**) (300 mg, 0.67 mmol), copper(I) iodide (20 mg, 0.11 mmol) and *bis*(triphenylphosphine)palladium (II)dichloride (36 mg, 0.051 mmol) in anhydrous DMF (8 mL) was added a solution of 1-(5-hexyn-1-yl)piperidine (143 mg, 0.87 mmol) and triethylamine (0.139 mL, 1.00 mmol) in anhydrous DMF (2 mL) dropwise over 2 min. The reaction mixture was stirred at ambient temperature for 16 h. The reaction mixture was concentrated *in vacuo* and the residue partitioned between EtOAc (50 mL) and water (50 mL). The organic layer was separated and was back extracted with EtOAc (25 mL). The combined organic extracts were washed with brine (50 mL), dried (MgSO<sub>4</sub>), filtered and concentrated *in vacuo* to give an orange oil. The oil was dissolved in DCM and purified on an aminopropyl functionalised silica cartridge (20 g) using a 0-10% MeOH-DCM gradient over 40 mins. The appropriate fractions were combined and evaporated *in vacuo* to give a yellow gum. The gum was dissolved in DCM and purified on an aminopropyl functionalised silica cartridge (20 g) using a 0-100% EtOAc-cyclohexane+0-20% EtOH gradient over 60 mins. The appropriate fractions were combined and evaporated *in vacuo* to give the title compound (136 mg, 42 %) as a white gum.

$^1\text{H}$  NMR (400 MHz,  $\text{CDCl}_3$ )  $\delta$  7.43 - 7.34 (m, 3H), 7.31 - 7.22 (m, 3H), 5.63 (s, 2H), 5.45 (s, 2H), 4.53 (s, 2H), 2.88 - 2.79 (m, 2H), 2.51 (t,  $J = 6.7$  Hz, 2H), 2.46 - 2.30 (m, 6H), 1.89 - 1.77 (m, 2H), 1.74 - 1.55 (m, 8H), 1.49 - 1.33 (m, 6H), 0.95 - 0.85 (m, 3H); LCMS (System B)  $R_t$  1.30 min,  $m/z$  488 ( $[\text{M}+\text{H}]^+$ ).

**2-Isopropyl-3H-pyrrolo[3,2-d]pyrimidin-4(5H)-one (176)**



Chemical Formula:  $\text{C}_9\text{H}_{11}\text{N}_3\text{O}$   
Molecular Weight: 177.20

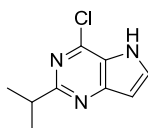
A mixture of isobutyronitrile (40.0 mL, 446 mmol) and ethyl 3-amino-1H-pyrrole-2-carboxylate, hydrochloride (3.00 g, 15.7 mmol) was treated with 4M hydrochloric acid in 1,4-dioxane (20 mL, 80 mmol) and stirred at 50 °C for 72 h. The reaction mixture was allowed to cool to ambient temperature and was diluted with TBME (300 mL) and the resultant sticky gum was agitated until a yellow suspension formed. The suspension was filtered and the cake washed with TBME (50 mL) and dried in air, before being dissolved in EtOH (45 mL) and treated with a solution of NaOH (2.52 g, 62.9 mmol) in water (10 mL) and the mixture being heated to 80 °C for 1.5 h before cooling to ambient temperature. The reaction solvent was removed *in vacuo*. The residue was suspended in water (200 mL) and the pH adjusted to 4 with solid citric acid, and extracted with EtOAc (2 x 200 mL). The combined organic extracts were washed with water then dried ( $\text{MgSO}_4$ ), filtered and concentrated *in vacuo* to give a yellow/brown solid. This solid was triturated with  $\text{Et}_2\text{O}$ , the resulting suspension filtered and the solid dried *in vacuo* to give the title compound (1.05 g, 38%) as a beige solid.

The pH of the combined aqueous washings was adjusted to pH = 6 using saturated aqueous sodium bicarbonate and was then extracted with 3:1 chloroform:IPA (400 mL). The extract was combined with the mother liquor from the trituration (used to isolate batch 1). The resulting organic phase was dried ( $\text{MgSO}_4$ ), filtered and concentrated *in vacuo* to give a brown solid. This solid was triturated with  $\text{Et}_2\text{O}$ , the

resulting suspension filtered and the solid dried *in vacuo* to give a further batch of the title compound (0.80 g, 29%) as a beige solid.

<sup>1</sup>H NMR (400 MHz, DMSO-*d*<sub>6</sub>) δ 11.90 (br s, 1H), 11.65 (br s, 1H), 7.32 (t, *J* = 2.9 Hz, 1H), 6.30 (dd, *J* = 2.9, 0.5 Hz, 1H), 2.87 (sept, *J* = 6.9 Hz, 1H), 1.22 (d, *J* = 6.9 Hz, 6H).; LCMS (System B) R<sub>t</sub> 0.53 min, m/z 178 ([M+H]<sup>+</sup>).

#### **4-Chloro-2-isopropyl-5H-pyrrolo[3,2-*d*]pyrimidine (177)**



Chemical Formula: C<sub>9</sub>H<sub>10</sub>ClN<sub>3</sub>  
Molecular Weight: 195.65

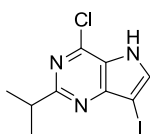
A stirred suspension of 2-isopropyl-3*H*-pyrrolo[3,2-*d*]pyrimidin-4(5*H*)-one (**176**) (1.84 g, 10.4 mmol) in phosphorus(V) oxychloride (25.0 mL, 268 mmol) was heated to 100 °C for 2 h. The reaction mixture was allowed to cool to ambient temperature was concentrated *in vacuo* and azeotroped with toluene. The resultant gum was dissolved in DCM (100 mL) and washed with water (100 mL) and was dried (hydrophobic frit) before being concentrated *in vacuo* to give a brown oil. The oil was dissolved in DCM and purified on a silica cartridge (50 g) using a 0-100% EtOAc-DCM gradient over 40 mins. The column was further eluted with 0-50% MeOH-DCM. The appropriate fractions were combined and concentrated *in vacuo* to give as a sticky brown solid (0.44 g). The residue was dissolved in DCM and purified on a silica cartridge (50 g) using a 0-50% EtOAc-DCM gradient over 40 mins. The appropriate fractions were combined and evaporated *in vacuo* to give the title compound (0.267 g) as an off white solid.

The pH of the original aqueous layer was adjusted to pH = 10 using 10M aqueous NaOH. The aqueous layer was extracted with 3:1 chloroform:IPA (2 x 100 mL). The combined organic extracts were dried (hydrophobic frit) and concentrated *in vacuo* to give a further batch of the title compound as an off white solid (1.288 g).

The two batches of title compound were dissolved in DCM, combined and concentrated *in vacuo* to give a single batch of the title compound (1.48 g, 73%) as an off white solid.

$^1\text{H}$  NMR (400 MHz,  $\text{CDCl}_3$ )  $\delta$  8.68 (br s, 1H), 7.51 (t,  $J = 2.9$  Hz, 1H), 6.68 (dd,  $J = 2.9, 2.0$  Hz, 1H), 3.24 (sept,  $J = 6.9$  Hz, 1H), 1.33 (d,  $J = 6.9$  Hz, 6H); LCMS (System B)  $R_t$  0.78 min,  $m/z$  196, 198 ( $[\text{M}+\text{H}]^+$ ).

#### **4-Chloro-7-iodo-2-isopropyl-5H-pyrrolo[3,2-d]pyrimidine (178)**

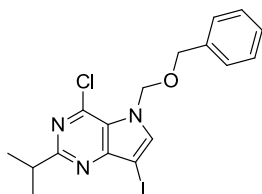


Chemical Formula:  $\text{C}_9\text{H}_9\text{ClIN}_3$   
Molecular Weight: 321.55

To a stirred suspension of 4-chloro-2-isopropyl-5H-pyrrolo[3,2-d]pyrimidine (**177**) (1.48 g, 7.54 mmol) in 2-methyltetrahydrofuran (25 mL) was added solid *N*-iodosuccinimide (1.87 g, 8.29 mmol) in one charge. The resulting brown solution was stirred at ambient temperature for 1 h. The reaction mixture was partitioned between water (100 mL) and EtOAc (100 mL). The organic phase was separated and washed with aqueous sodium thiosulphate (100 mL), dried ( $\text{MgSO}_4$ ), filtered and concentrated *in vacuo* to give the title compound (2.31 g, 95%) as a off-white solid.

$^1\text{H}$  NMR (400 MHz,  $\text{CDCl}_3$ )  $\delta$  8.80 (br s, 1H), 7.58 (d,  $J = 2.7$  Hz, 1H), 3.29 (sept,  $J = 6.9$  Hz, 1H), 1.33 (d,  $J = 6.9$  Hz, 6H); LCMS (System B)  $R_t$  1.06 min,  $m/z$  322, 324 ( $[\text{M}+\text{H}]^+$ ).

**5-((Benzyloxy)methyl)-4-chloro-7-iodo-2-isopropyl-5H-pyrrolo[3,2-*d*]pyrimidine (179)**



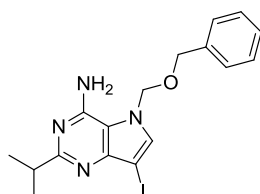
Chemical Formula: C<sub>17</sub>H<sub>17</sub>ClIIN<sub>3</sub>O  
Molecular Weight: 441.69

To a stirred slurry of sodium hydride 60% wt. on mineral oil (0.359 g, 8.98 mmol) in anhydrous THF (40 mL) at 0 °C under a nitrogen atmosphere was added a solution of 4-chloro-7-iodo-2-isopropyl-5H-pyrrolo[3,2-*d*]pyrimidine (**178**) (2.31 g, 7.18 mmol) in anhydrous THF (20 mL) dropwise over 15 min. The reaction was stirred at 0 °C for a further 30 min before addition of a solution of ((chloromethoxy)methyl)benzene (1.18 g, 7.54 mmol) in anhydrous THF (20 mL) dropwise over 20 min. The reaction mixture was then allowed to warm to ambient temperature and stirred for a further 4 h. The reaction mixture was concentrated *in vacuo* and the residue partitioned between water (250 mL) and EtOAc (250 mL). The organic phase was separated and washed with brine (250 mL), dried (MgSO<sub>4</sub>), filtered and concentrated *in vacuo* to give a viscous orange oil (3.21 g). The oil was dissolved in DCM and purified on a silica cartridge (100 g) using a 0-50% DCM-cyclohexane gradient over 40 mins, followed by 0-100% EtOAc-DCM over 30 mins. The appropriate fractions were combined and evaporated *in vacuo* to give the title compound (2.82 g, 89 %) as a yellow oil.

<sup>1</sup>H NMR (400 MHz, CDCl<sub>3</sub>) δ 7.59 (s, 1H), 7.36 - 7.24 (m, 5H), 5.83 (s, 2H), 4.55 (s, 2H), 3.36 (sept, *J* = 6.9 Hz, 1H), 1.43 (d, *J* = 6.9 Hz, 6H); LCMS (System B) R<sub>t</sub> 1.41 min, *m/z* 442, 444 ([M+H]<sup>+</sup>).



**5-((Benzyloxy)methyl)-7-iodo-2-isopropyl-5H-pyrrolo[3,2-d]pyrimidin-4-amine (180)**

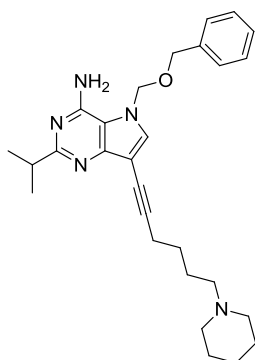


Chemical Formula: C<sub>17</sub>H<sub>19</sub>IN<sub>4</sub>O  
Molecular Weight: 422.26

A suspension of 5-((benzyloxy)methyl)-4-chloro-7-iodo-2-isopropyl-5H-pyrrolo[3,2-d]pyrimidine (**179**) (2.81 g, 6.36 mmol) in IPA (6 mL) was treated with 880 ammonia (5.0 mL, 90 mmol), the reaction vessel was sealed and heated in a Biotage Initiator microwave (using initial absorption setting very high) to 140 °C for 120 min. After cooling the reaction mixture, further 880 ammonia (2.0 mL, 36 mmol) was added and the reaction vessel was sealed and heated in a Biotage Initiator microwave (using initial absorption setting very high) to 140 °C for 60 min. The reaction mixture was diluted with MeOH and concentrated *in vacuo* and partitioned between DCM (100 mL) and water (100 mL), the organic phase was separated and the aqueous phase back extracted with DCM (100 mL). The combined organic extracts were dried (hydrophobic frit) and concentrated *in vacuo* and azeotroped with petroleum ether (40-60) to give the title compound (2.30 g, 85 %) as an off white solid.

<sup>1</sup>H NMR (400 MHz, CDCl<sub>3</sub>) δ 7.43 - 7.36 (m, 3H), 7.34 - 7.27 (m, 2H), 7.22 (s, 1H), 5.75 (br s, 2H), 5.50 (s, 2H), 4.58 (s, 2H), 3.18 (sept, *J* = 6.9 Hz, 1H), 1.37 (d, *J* = 6.9 Hz, 6H); <sup>13</sup>C NMR (101 MHz, CDCl<sub>3</sub>) δ 169.2, 151.7, 151.0, 135.3, 134.9, 128.8, 128.7, 128.4, 113.9, 77.0, 69.9, 58.7, 37.3, 22.1; LCMS (System B) R<sub>t</sub> 1.14 min, m/z 423 ([M+H]<sup>+</sup>); HRMS Anal. Calcd. For C<sub>17</sub>H<sub>20</sub>IN<sub>4</sub>O = 423.0676. Found = 423.0683 ([M+H]<sup>+</sup>); IR (cm<sup>-1</sup>) 3419, 2960, 1646, 1588; Mpt. 120-123 °C.

**5-((Benzyloxy)methyl)-2-isopropyl-7-(6-(piperidin-1-yl)hex-1-yn-1-yl)-5H-pyrrolo[3,2-d]pyrimidin-4-amine (181a)**

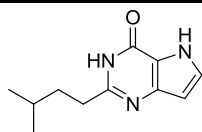


Chemical Formula: C<sub>28</sub>H<sub>37</sub>N<sub>5</sub>O  
Molecular Weight: 459.63

To a degassed stirred suspension of 5-((benzyloxy)methyl)-7-iodo-2-isopropyl-5H-pyrrolo[3,2-d]pyrimidin-4-amine (**180**) (300 mg, 0.71 mmol), copper(I) iodide (20 mg, 0.11 mmol) and *bis*(triphenylphosphine)palladium(II) dichloride (36 mg, 0.051 mmol) in anhydrous DMF (8 mL) was added a solution of 1-(5-hexyn-1-yl)piperidine (153 mg, 0.92 mmol) and triethylamine (0.148 mL, 1.07 mmol) in anhydrous DMF (2 mL) dropwise over 2 min. The reaction mixture was stirred at ambient temperature for 16 h. The reaction mixture was concentrated *in vacuo* and the residue partitioned between EtOAc (50 mL) and water (50 mL). The organic layer was separated and the aqueous phase was back extracted with EtOAc (25 mL). The combined organic extracts were washed with brine (50 mL), dried (MgSO<sub>4</sub>), filtered and concentrated *in vacuo* to give an orange oil. The oil was dissolved in DCM and purified on an aminopropyl functionalised silica cartridge (20 g) using a 0-100% EtOAc-cyclohexane gradient over 40 mins. The appropriate fractions were combined and evaporated *in vacuo* to give the title compound (168 mg, 51%) as a pale yellow gum.

<sup>1</sup>H NMR (400 MHz, CDCl<sub>3</sub>) δ 7.44 - 7.35 (m, 3H), 7.34 - 7.29 (m, 2H), 7.25 (s, 1H), 5.60 (br s, 2H), 5.47 (s, 2H), 4.58 - 4.52 (m, 2H), 3.23 - 3.13 (m, 1H), 2.54 (t, *J* = 6.9 Hz, 2H), 2.47 - 2.32 (m, 6H), 1.78 - 1.58 (m, 8H), 1.49 - 1.42 (m, 2H), 1.36 (d, *J* = 7.1 Hz, 6H); LCMS (System B) R<sub>t</sub> 1.20 min, m/z 460 ([M+H]<sup>+</sup>).

### 2-Isopentyl-3H-pyrrolo[3,2-d]pyrimidin-4(5H)-one (182)



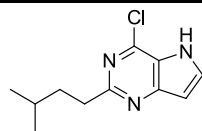
Chemical Formula: C<sub>11</sub>H<sub>15</sub>N<sub>3</sub>O

Molecular Weight: 205.26

A mixture of 4-methylpentanenitrile (40.0 mL, 329 mmol) and ethyl 3-amino-1H-pyrrole-2-carboxylate, hydrochloride (3.00 g, 15.7 mmol) was treated with 4M hydrochloric acid in 1,4-dioxane (20 mL, 80 mmol) and stirred at 50 °C for 16 h. The reaction mixture was allowed to warm to ambient temperature and was diluted with TBME (300 mL) and the resultant suspension filtered. The solid cake was washed with TBME (150 mL) and Et<sub>2</sub>O (150 mL) and dried *in vacuo* to give a beige solid. The solid was dissolved in EtOH (45 mL) and treated with a solution of NaOH (2.52 g, 62.9 mmol) in water (10 mL) and the mixture was heated to 80 °C for 1.5 h. The reaction solvent was removed *in vacuo*. The residue was suspended in water (200 mL) and the pH adjusted to 4 with solid citric acid, and extracted with EtOAc (2 x 200 mL). The combined organic extracts were dried (MgSO<sub>4</sub>), filtered and concentrated *in vacuo* and azeotroped with TBME. The resulting solid was partitioned between water (200 mL) and EtOAc (200 mL) and the pH adjusted to pH 6-7. The organic was separated and dried (MgSO<sub>4</sub>), filtered and concentrated *in vacuo* to give the title compound (2.20 g, 68%) as a pale yellow solid.

<sup>1</sup>H NMR (400 MHz, DMSO-*d*<sub>6</sub>) δ 11.88 (br s, 1H), 11.69 (br s, 1H), 7.31 (t, *J* = 2.6 Hz, 1H), 6.28 (dd, *J* = 2.6, 0.5 Hz, 1H), 2.59 - 2.53 (m, 2H), 1.66 - 1.49 (m, 3H), 0.90 (d, *J* = 6.4 Hz, 6H); LCMS (System B) R<sub>t</sub> 0.71 min, m/z 206 ([M+H]<sup>+</sup>).

### 4-Chloro-2-isopentyl-5H-pyrrolo[3,2-d]pyrimidine (183)



Chemical Formula: C<sub>11</sub>H<sub>14</sub>ClN<sub>3</sub>

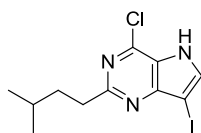
Molecular Weight: 223.70

A stirred suspension of 2-isopentyl-3H-pyrrolo[3,2-d]pyrimidin-4(5H)-one (2.20 g, 10.7 mmol) in phosphorus(V) oxychloride (**182**) (25.0 mL, 268 mmol) was heated to 100 °C for 3 h. The reaction mixture was concentrated *in vacuo* and azeotroped with

toluene. The resultant gum was dissolved in DCM (100 mL) and washed with water (100 mL) and was dried (hydrophobic frit) before being concentrated *in vacuo* to give a brown oil. The oil was dissolved in DCM and purified on a silica cartridge (50 g) using a 0-25% MeOH:TBME gradient over 40 mins. The appropriate fractions were combined and evaporated *in vacuo* to give the title compound (1.98 g, 83 %) as a yellow oil which crystallised on standing.

$^1\text{H}$  NMR (400 MHz,  $\text{CDCl}_3$ )  $\delta$  8.94 (br s, 1H), 7.61 (t,  $J = 3.0$  Hz, 1H), 6.75 (dd,  $J = 3.0, 1.9$  Hz, 1H), 3.10 - 3.01 (m, 2H), 1.85 - 1.73 (m, 2H), 1.68 (sept,  $J = 6.6$  Hz, 1H), 0.98 (d,  $J = 6.6$  Hz, 6H); LCMS (System B)  $R_t$  1.01 min,  $m/z$  224, 226 ( $[\text{M}+\text{H}]^+$ ).

#### **4-Chloro-7-iodo-2-isopentyl-5H-pyrrolo[3,2-d]pyrimidine (184)**



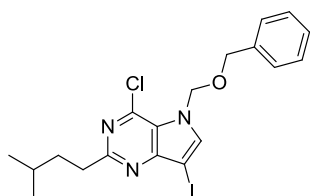
Chemical Formula:  $\text{C}_{11}\text{H}_{13}\text{ClIIN}_3$   
Molecular Weight: 349.60

To a stirred suspension of 4-chloro-2-isopentyl-5H-pyrrolo[3,2-d]pyrimidine (**183**) (1.98 g, 8.86 mmol) in anhydrous THF (30 mL) was added solid *N*-iodosuccinimide (2.19 g, 9.75 mmol) in one charge. The resulting brown solution was stirred at ambient temperature for 1 h. The reaction mixture was partitioned between water (120 mL) and EtOAc (120 mL). The organic phase was separated and washed with aqueous sodium thiosulphate (120 mL), dried ( $\text{MgSO}_4$ ), filtered and concentrated *in vacuo* to give a brown/green gum. The sample was dissolved in DCM and purified on a silica cartridge (100 g) using a 0-50% EtOAc-cyclohexane gradient over 60 mins. The appropriate fractions were combined and evaporated *in vacuo* to give the title compound (2.80 g, 90 %) as a white foam.

$^1\text{H}$  NMR (400 MHz,  $\text{CDCl}_3$ )  $\delta$  9.04 (br s, 1H), 7.69 (d,  $J = 2.7$  Hz, 1H), 3.14 - 3.05 (m, 2H), 1.84 - 1.75 (m, 2H), 1.68 (sept,  $J = 6.6$  Hz, 1H), 0.98 (d,  $J = 6.6$  Hz, 6H); LCMS (System B)  $R_t$  1.21 min,  $m/z$  350, 352 ( $[\text{M}+\text{H}]^+$ ).

**5-((Benzyloxy)methyl)-4-chloro-7-iodo-2-isopentyl-5H-pyrrolo[3,2-d]pyrimidine**

**(185)**

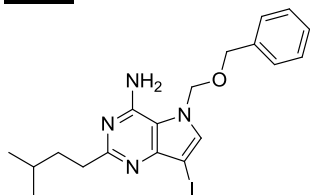


Chemical Formula: C<sub>19</sub>H<sub>21</sub>ClIIN<sub>3</sub>O  
Molecular Weight: 469.75

To a stirred slurry of sodium hydride 60% wt. on mineral oil (0.45 g, 11.2 mmol) in anhydrous THF (30 mL) at 0 °C under a nitrogen atmosphere was added a solution of 4-chloro-7-iodo-2-isopentyl-5H-pyrrolo[3,2-d]pyrimidine (**184**) (2.79 g, 7.98 mmol) in anhydrous THF (20 mL) dropwise over 15 min. The reaction mixture was stirred at 0 °C for a further 30 min before addition of a solution of ((chloromethoxy)methyl)benzene (1.44 g, 9.18 mmol) in anhydrous THF (20 mL) dropwise over 20 min. The reaction mixture was then allowed to warm to ambient temperature and stirred for a further 3.5 h. The reaction mixture was concentrated *in vacuo* and the residue partitioned between EtOAc (250 mL) and water (250 mL). The organic layer was separated and washed with brine (250 mL). The resulting organic layer was dried (MgSO<sub>4</sub>), filtered and concentrated *in vacuo* to give an orange oil. The sample was dissolved in DCM and purified on a silica cartridge (100 g) using a 0-50% EtOAc-cyclohexane gradient over 60 mins. The appropriate fractions were combined and evaporated *in vacuo* to give the title compound (3.37 g, 90 %) as a yellow oil.

<sup>1</sup>H NMR (400 MHz, CDCl<sub>3</sub>) δ 7.57 (s, 1H), 7.33 - 7.21 (m, 5H), 5.80 (s, 2H), 4.53 (s, 2H), 3.09 - 3.01 (m, 2H), 1.82 - 1.73 (m, 2H), 1.68 (sept, *J* = 6.6 Hz, 1H), 0.98 (d, *J* = 6.6 Hz, 6H); LCMS (System B) R<sub>t</sub> 1.53 min, m/z 470, 472 ([M+H]<sup>+</sup>).

**5-((Benzyloxy)methyl)-7-iodo-2-isopentyl-5H-pyrrolo[3,2-d]pyrimidin-4-amine (186)**

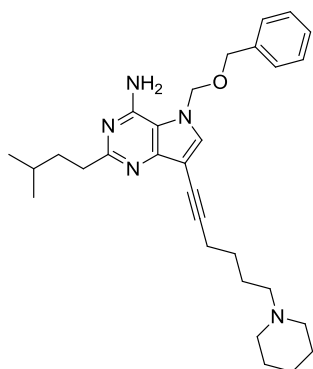


Chemical Formula: C<sub>19</sub>H<sub>23</sub>IN<sub>4</sub>O  
Molecular Weight: 450.32

A suspension of 5-((benzyloxy)methyl)-4-chloro-7-iodo-2-isopentyl-5H-pyrrolo[3,2-d]pyrimidine (**185**) (3.28 g, 6.98 mmol) in IPA (6 mL) was treated with 880 ammonia (5.0 mL, 90 mmol), the reaction vessel was sealed and heated in a Biotage Initiator microwave (using initial absorption setting high) to 140 °C for 120 min. After cooling, the reaction mixture was concentrated *in vacuo* and the residue triturated with water (*ca.* 100 mL). The resulting suspension was filtered and the solid dried *in vacuo* to give the title compound (2.58 g, 82 %) as a white solid.

<sup>1</sup>H NMR (400 MHz, CDCl<sub>3</sub>) δ 7.44 - 7.35 (m, 3H), 7.33 - 7.26 (m, 2H), 7.23 (s, 1H), 5.85 (br s, 2H), 5.50 (s, 2H), 4.58 (s, 2H), 2.94 - 2.86 (m, 2H), 1.81 - 1.65 (m, 3H), 0.99 (d, *J* = 6.4 Hz, 6H); <sup>13</sup>C NMR (101 MHz, CDCl<sub>3</sub>) δ 165.3, 151.8, 150.8, 135.2, 135.0, 128.8, 128.7, 128.4, 113.7, 77.0, 70.0, 58.4, 38.2, 37.6, 28.3, 22.6; LCMS (System B) R<sub>t</sub> 1.24 min, m/z 451 ([M+H]<sup>+</sup>); HRMS Anal. Calcd. For C<sub>19</sub>H<sub>24</sub>IN<sub>4</sub>O = 451.0989. Found = 451.0974 ([M+H]<sup>+</sup>); IR (cm<sup>-1</sup>) 2947, 1645, 1593; Mpt. 132-135 °C.

**5-((Benzyloxy)methyl)-2-isopentyl-7-(6-(piperidin-1-yl)hex-1-yn-1-yl)-5H-pyrrolo[3,2-d]pyrimidin-4-amine (187a)**

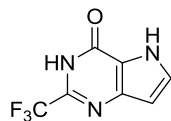


Chemical Formula: C<sub>30</sub>H<sub>41</sub>N<sub>5</sub>O  
Molecular Weight: 487.68

To a degassed stirred suspension of 5-((benzyloxy)methyl)-7-iodo-2-isopentyl-5H-pyrrolo[3,2-d]pyrimidin-4-amine (**186**) (300 mg, 0.67 mmol), copper(I) iodide (20 mg, 0.11 mmol) and *bis*(triphenylphosphine)palladium(II) dichloride (36 mg, 0.051 mmol) in anhydrous DMF (8 mL) was added a solution of 1-(5-hexyn-1-yl)piperidine (143 mg, 0.866 mmol) and triethylamine (0.14 mL, 1.00 mmol) in anhydrous DMF (2 mL) dropwise over 2 min. The reaction mixture was stirred at ambient temperature for 20 h. The reaction mixture was concentrated *in vacuo* and the residue partitioned between EtOAc (50 mL) and water (50 mL). The organic layer was separated and the aqueous phase was back extracted with EtOAc (25 mL). The combined organic extracts were washed with brine (50 mL), dried (MgSO<sub>4</sub>), filtered and concentrated *in vacuo* to give an orange oil. The oil was dissolved in DCM and purified on an aminopropyl functionalised silica cartridge (20 g) using a 0-100% EtOAc-cyclohexane gradient over 40 mins. The appropriate fractions were combined and evaporated *in vacuo* to give the title compound (152 mg, 47 %) as a white gum.

<sup>1</sup>H NMR (400 MHz, CDCl<sub>3</sub>) δ 7.43 - 7.34 (m, 3H), 7.34 - 7.24 (m, 3H), 5.64 (s, 2H), 5.47 (s, 2H), 4.55 (s, 2H), 2.93 - 2.84 (m, 2H), 2.54 (t, *J* = 6.9 Hz, 2H), 2.48 - 2.32 (m, 5H), 1.80 - 1.57 (m, 12H), 1.49 - 1.43 (m, 2H), 0.98 (d, *J* = 6.4 Hz, 6H); LCMS (System B) R<sub>t</sub> 1.28 min, m/z 488 ([M+H]<sup>+</sup>).

**2-(Trifluoromethyl)-3H-pyrrolo[3,2-d]pyrimidin-4(5H)-one (188)**

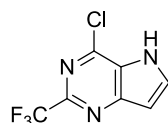


Chemical Formula: C<sub>7</sub>H<sub>4</sub>F<sub>3</sub>N<sub>3</sub>O  
Molecular Weight: 203.12

A stirred mixture of 3-amino-2-ethoxycarbonylpyrrole hydrochloride (2.50 g, 13.1 mmol) and trifluoroacetamide (1.91 g, 17.0 mmol) in *o*-xylene (20 mL) was heated to reflux for 18 h and allowed to cool to ambient temperature. The reaction mixture was diluted with diethyl ether (20 mL), filtered, and the cake washed with diethyl ether (10 mL). The resultant solid was dried *in vacuo* to give the title compound (1.76 g, 66 %) which was used directly in the next step.

LCMS (System B) R<sub>t</sub> 0.34 min, m/z 204 ([M+H]<sup>+</sup>).

**4-Chloro-2-(trifluoromethyl)-5H-pyrrolo[3,2-d]pyrimidine (189)**



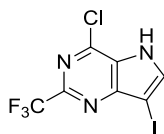
Chemical Formula: C<sub>7</sub>H<sub>3</sub>ClF<sub>3</sub>N<sub>3</sub>  
Molecular Weight: 221.57

A stirred suspension of 2-(trifluoromethyl)-3H-pyrrolo[3,2-d]pyrimidin-4(5H)-one (**188**) (1.76 g, 8.66 mmol) in phosphorus(V) oxychloride (15 mL, 161 mmol) was heated to reflux for 2 h before being allowed to cool to ambient temperature and concentrated *in vacuo*. The resulting residue was triturated with diethyl ether (10 mL), the solid was collected by filtration and dried *in vacuo* to give the title compound (2.05 g, quant.) which was used directly in the next step.

LCMS (System B) R<sub>t</sub> 0.89 min, m/z 220, 222 ([M-H]<sup>-</sup>).



**4-Chloro-7-iodo-2-(trifluoromethyl)-5H-pyrrolo[3,2-d]pyrimidine (190)**

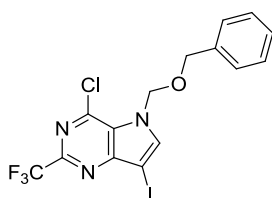


Chemical Formula: C<sub>7</sub>H<sub>2</sub>ClF<sub>3</sub>IN<sub>3</sub>  
Molecular Weight: 347.46

To a stirred solution of 4-chloro-2-(trifluoromethyl)-5H-pyrrolo[3,2-d]pyrimidine (**189**) (2.05 g, 9.25 mmol) in anhydrous THF (20 mL) was added *N*-iodosuccinimide (2.29 g, 10.2 mmol) and the reaction mixture was stirred at ambient temperature for 1.5 h. The reaction mixture was concentrated *in vacuo*, and partitioned between water (200 mL) and EtOAc (200 mL). The organic phase was separated and the aqueous extracted with EtOAc (100 mL). The combined organic extracts were washed with aqueous sodium thiosulfate, dried (MgSO<sub>4</sub>), filtered and concentrated *in vacuo* to give the title compound (1.74 g, 54 %).

<sup>1</sup>H NMR (400 MHz, CDCl<sub>3</sub>) δ 9.39 (br s, 1H), 7.89 (d, *J* = 2.8 Hz, 1H); LCMS (System B) R<sub>t</sub> 1.00 min, m/z 346, 348 ([M-H]<sup>-</sup>).

**5-((Benzyloxy)methyl)-4-chloro-7-iodo-2-(trifluoromethyl)-5H-pyrrolo[3,2-d]pyrimidine (191)**



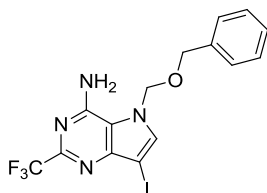
Chemical Formula: C<sub>15</sub>H<sub>10</sub>ClF<sub>3</sub>IN<sub>3</sub>O  
Molecular Weight: 467.61

To a stirred suspension of sodium hydride 60% wt. on mineral oil (0.22 g, 5.50 mmol) in anhydrous THF (10 mL) at 0 °C was added a solution of 4-chloro-7-iodo-2-(trifluoromethyl)-5H-pyrrolo[3,2-d]pyrimidine (**190**) (1.74 g, 5.00 mmol) in THF (10 mL) dropwise over 5 min. The resultant mixture was stirred at 0 °C for 15 mins before the dropwise addition of a solution of chloromethyl phenylmethyl ether (0.70 mL, 5.00 mmol) in THF (5 mL) over 5 min. The reaction mixture was stirred at 0 °C for two hours before being partitioned between EtOAc (200 mL) and water (200

mL). The organic phase was separated and washed with brine (200 mL), dried (MgSO<sub>4</sub>), filtered and concentrated *in vacuo* before being dissolved in DCM and purified on a silica cartridge (100 g) using a 0-50% EtOAc-cyclohexane gradient over 60 mins. The appropriate fractions were combined and evaporated *in vacuo* to give the title compound (1.31 g, 56 %) as a beige solid.

<sup>1</sup>H NMR (400 MHz, CDCl<sub>3</sub>) δ 7.74 (s, 1H), 7.32 - 7.24 (m, 3H), 7.23 - 7.18 (m, 2H), 5.88 (s, 2H), 4.57 (s, 2H); LCMS (System B) R<sub>t</sub> 1.38 min, m/z 468, 470 ([M+H]<sup>+</sup>).

**5-((Benzyloxy)methyl)-7-iodo-2-(trifluoromethyl)-5H-pyrrolo[3,2-d]pyrimidin-4-amine (192)**

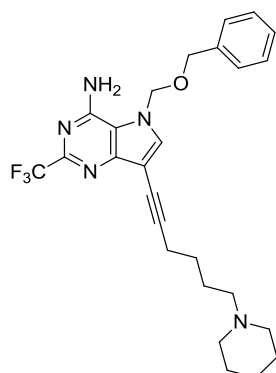


Chemical Formula: C<sub>15</sub>H<sub>12</sub>F<sub>3</sub>IN<sub>4</sub>O  
Molecular Weight: 448.18

A mixture of 5-((benzyloxy)methyl)-4-chloro-7-iodo-2-(trifluoromethyl)-5H-pyrrolo[3,2-d]pyrimidine (1.25 g, 2.67 mmol) and 880 ammonia (2.00 mL, 3.05 mmol) in IPA (10 mL) was sealed and heated in a Biotage Initiator microwave (absorption setting normal) to 150 °C for 60 min. After cooling the reaction mixture was concentrated *in vacuo* and the residue triturated with water (*ca.* 75 mL), the resultant suspension was filtered and the solid dried *in vacuo* to give the title compound (1.04 g, 87%).

<sup>1</sup>H NMR (400 MHz, DMSO-*d*<sub>6</sub>) δ 8.03 (s, 1H), 7.34 - 7.22 (m, 5H), 5.79 (s, 2H), 4.53 (s, 2H) exchangeable protons (NH<sub>2</sub>) not observed; <sup>13</sup>C NMR (101 MHz, DMSO-*d*<sub>6</sub>) δ 159.4, 149.4, 148.4 (m), 138.2, 136.6, 128.2, 127.7, 127.6, 114.3, 77.6, 69.7, 59.7, one carbon (trifluoromethyl) not observed; LCMS (System B) R<sub>t</sub> 1.21 min, m/z 449 ([M+H]<sup>+</sup>); Mpt. 183-185 °C.

**5-((Benzyloxy)methyl)-7-(6-(piperidin-1-yl)hex-1-yn-1-yl)-2-(trifluoromethyl)-5H-pyrrolo[3,2-d]pyrimidin-4-amine (193a)**



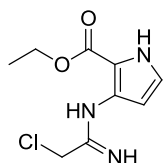
Chemical Formula: C<sub>26</sub>H<sub>30</sub>F<sub>3</sub>N<sub>5</sub>O  
Molecular Weight: 485.54

To a stirred degassed suspension of 5-((benzyloxy)methyl)-7-iodo-2-(trifluoromethyl)-5H-pyrrolo[3,2-d]pyrimidin-4-amine (**192**) (350 mg, 0.78 mmol), copper(I) iodide (30.0 mg, 0.16 mmol) and *bis*(triphenylphosphine)palladium(II) dichloride (55.0 mg, 0.08 mmol) in anhydrous DMF (8 mL) was added dropwise a solution of 1-(5-hexyn-1-yl)piperidine (194 mg, 1.17 mmol) and triethylamine (0.173 mL, 1.25 mmol) in DMF (2 mL) over 5 min. The reaction mixture was stirred at ambient temperature for 18 h before being concentrated *in vacuo* to give a brown oil. The oil was partitioned between EtOAc (100 mL) and water (100 mL), the organic phase was separated, dried (MgSO<sub>4</sub>), filtered and concentrated *in vacuo* before being dissolved in DCM and purified on a silica cartridge (20 g) using a 0-10% MeOH-DCM gradient over 40 mins. The appropriate fractions were combined and evaporated *in vacuo* to give the title compound (143 mg, 38 %) as a peach coloured solid.

<sup>1</sup>H NMR (400 MHz, CDCl<sub>3</sub>) δ 7.76 (s, 1H), 7.40 - 7.33 (m, 3H), 7.31 - 7.28 (m, 2H), 6.10 (s, 2H), 5.59 (s, 2H), 4.62 (s, 2H), 3.40 - 2.60 (m, 6H), 2.57 (t, *J* = 6.4 Hz, 2H), 2.31 - 2.21 (m, 2H), 2.11 (br s, 4H), 1.77 - 1.67 (m, 4H); <sup>13</sup>C NMR (101 MHz, CDCl<sub>3</sub>) δ 151.4, 150.4, 136.2, 134.9, 128.8, 128.8, 128.4, 114.5, 100.2, 92.2, 77.0, 72.2, 70.7, 57.2, 53.3, 25.2, 22.6, 22.5, 21.8, 19.0, two carbons (CF<sub>3</sub> and adjacent quaternary carbon) not observed; <sup>19</sup>F NMR (376 MHz, CDCl<sub>3</sub>) δ -68.83 LCMS

(System B)  $R_t$  1.30 min,  $m/z$  486 ( $[M+H]^+$ ); HRMS Anal. Calcd. For  $C_{26}H_{31}F_3N_5O = 486.2481$ . Found = 486.2475  $[M+H]^+$ ; IR ( $cm^{-1}$ ) 3324, 3183, 2932, 1627, 1598; Mpt. 83-89 °C.

**$\Omega$ Ethyl 3-(2-chloroacetimidamido)-1H-pyrrole-2-carboxylate, hydrochloride (195)**

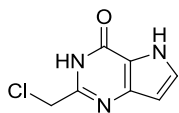


Chemical Formula:  $C_9H_{12}ClN_3O_2$   
Molecular Weight: 229.66

To a suspension of ethyl 3-amino-1H-pyrrole-2-carboxylate hydrochloride (4.99 g, 26.2 mmol) in 1,4-dioxane (75 mL) was added a solution of 4M hydrochloric acid in 1,4-dioxane (25.0 mL, 100 mmol) followed by addition of 2-chloroacetonitrile (6.64 mL, 10.3 mmol) and the resulting mixture heated at 80 °C for 18 hours. The reaction mixture was cooled to room temperature and diluted with TBME (200 mL). The solid material was collected by filtration and washed with TBME and dried *in vacuo* to give title compound (5.63 g, 81%) as an off-white solid which was used directly in the next step.

LCMS (System A)  $R_t$  0.34 min,  $m/z$  230, 232 ( $[M+H]^+$ ).

**2-(Chloromethyl)-3H-pyrrolo[3,2-d]pyrimidin-4(5H)-one (196)**



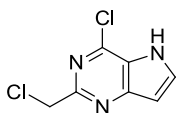
Chemical Formula:  $C_7H_6ClN_3O$   
Molecular Weight: 183.60

To a stirred solution of ethyl 3-(2-chloroacetimidamido)-1H-pyrrole-2-carboxylate, dihydrochloride (**195**) (5.60 g, 21.0 mmol) in water (50 mL) was added 0.1 M aqueous ammonium hydroxide (*ca.* 100 mL) and the mixture stirred at ambient temperature for 30 mins. To the reaction mixture was added further 0.1 M aqueous

ammonium hydroxide (ca. 120 mL) and the reaction mixture was stirred at ambient temperature for a further 30 min at which time the reaction mixture was extracted with EtOAc (2 x 250 mL) and the combined organic extracts were washed with brine (400 mL), dried (MgSO<sub>4</sub>), filtered and concentrated *in vacuo* to give the title compound (2.78 g, 72 %) as a pale brown solid.

<sup>1</sup>H NMR (400 MHz, DMSO-*d*<sub>6</sub>) δ 12.15 (br s, 2H), 7.38 (t, *J* = 2.8 Hz, 1H), 6.40 - 6.37 (m, 1H), 4.53 (s, 2H); LCMS (System B) R<sub>t</sub> 0.58 min, m/z 184, 186 ([M+H]<sup>+</sup>).

#### **4-Chloro-2-(chloromethyl)-5H-pyrrolo[3,2-*d*]pyrimidine (197)**

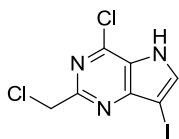


Chemical Formula: C<sub>7</sub>H<sub>5</sub>Cl<sub>2</sub>N<sub>3</sub>  
Molecular Weight: 202.04

A stirred suspension of 2-(chloromethyl)-3*H*-pyrrolo[3,2-*d*]pyrimidin-4(5*H*)-one (**197**) (2.54 g, 13.8 mmol) in phosphorus(V) oxychloride (25.0 mL, 270 mmol) was heated to reflux for 1 h. The reaction mixture was allowed to cool to ambient temperature and concentrated *in vacuo* and azeotroped with toluene. The resulting residue was partitioned between CHCl<sub>3</sub> (250 mL) and water (250 mL). The organic phase was separated and the aqueous phase back extracted with CHCl<sub>3</sub> (250 mL). The combined organic extracts were dried and filtered (hydrophobic frit) before concentration *in vacuo* to give the title compound (2.41 g, 86 %) as a pale brown solid.

<sup>1</sup>H NMR (400 MHz, DMSO-*d*<sub>6</sub>) δ 12.55 (br s, 1H), 8.03 (t, *J* = 2.8 Hz, 1H), 6.75 (dd, *J* = 2.8, 1.8 Hz, 1H), 4.83 (s, 2H); LCMS (System B) R<sub>t</sub> 0.68 min, m/z 202, 204, 206 ([M+H]<sup>+</sup>).

**4-Chloro-2-(chloromethyl)-7-iodo-5H-pyrrolo[3,2-d]pyrimidine (198)**

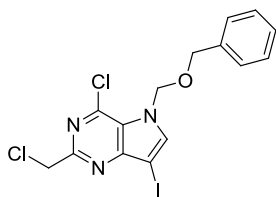


Chemical Formula: C<sub>7</sub>H<sub>4</sub>Cl<sub>2</sub>I<sub>N</sub><sub>3</sub>  
Molecular Weight: 327.94

To a stirred solution of 4-chloro-2-(chloromethyl)-5H-pyrrolo[3,2-d]pyrimidine (**197**) (2.41 g, 11.9 mmol) in THF (25 mL) was added solid *N*-iodosuccinimide (2.95 g, 13.1 mmol) in one charge. The reaction mixture was stirred at ambient temperature for 18 h before being partitioned between water (250 mL) and EtOAc (250 mL). The organic phase was separated and the aqueous phase back extracted with EtOAc (250 mL). The combined organic extracts were washed with aqueous sodium thiosulphate (400 mL), dried (MgSO<sub>4</sub>), filtered and concentrated *in vacuo* to give the title compound (3.89 g, 100 %) which was used directly in the next experiment.

<sup>1</sup>H NMR (400 MHz, CDCl<sub>3</sub>) δ 9.05 (br s, 1H), 7.76 (s, 1H), 4.87 (s, 2H); LCMS (System B) R<sub>t</sub> 0.87 min, m/z 328, 330, 332 ([M+H]<sup>+</sup>).

**5-((Benzyloxy)methyl)-4-chloro-2-(chloromethyl)-7-iodo-5H-pyrrolo[3,2-d]pyrimidine (199)**



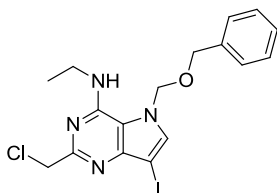
Chemical Formula: C<sub>15</sub>H<sub>12</sub>Cl<sub>2</sub>I<sub>N</sub><sub>3</sub>O  
Molecular Weight: 448.09

To a stirred suspension of sodium hydride 60% dispersion on mineral oil (0.546 g, 13.6 mmol) in anhydrous THF (40 mL) at 0 °C under nitrogen was added a solution of 4-chloro-2-(chloromethyl)-7-iodo-5H-pyrrolo[3,2-d]pyrimidine (**198**) (3.89 g, 11.9 mmol) in anhydrous THF (55 mL) dropwise over 20 min and the reaction mixture stirred for 20 min. To the reaction mixture was added a solution of ((chloromethoxy)methyl)benzene (2.14 g, 13.6 mmol) in anhydrous THF (55 mL)

dropwise over 20 min. The reaction mixture was allowed to warm to ambient temperature and stirred for a further 2 h. The reaction mixture was partitioned between EtOAc (500 mL) and water (500 mL). The organic phase was separated and washed with brine (500 mL), dried (MgSO<sub>4</sub>), filtered and concentrated *in vacuo* to give an orange oil (5.8 g) which solidified on standing. The solid was triturated with diethyl ether (*ca.* 200 mL) and the resultant solid collected by filtration and dried *in vacuo* to give the title compound (4.1 g, 77 %) as an off white solid.

<sup>1</sup>H NMR (400 MHz, CDCl<sub>3</sub>) δ 7.66 (s, 1H), 7.34 - 7.28 (m, 3H), 7.27 - 7.22 (m, 2H), 5.85 (s, 2H), 4.84 (s, 2H), 4.56 (s, 2H); <sup>13</sup>C NMR (101 MHz, CDCl<sub>3</sub>) δ 158.3, 153.7, 143.3, 140.7, 135.9, 128.6, 128.3, 127.6, 123.6, 77.0, 71.0, 59.9, 46.7; LCMS (System B) R<sub>t</sub> 1.29 min, m/z 448, 450, 452 ([M+H]<sup>+</sup>); HRMS Anal. Calcd. For C<sub>15</sub>H<sub>13</sub>Cl<sub>2</sub>IN<sub>3</sub>O = 447.9480. Found = 447.9481 ([M+H]<sup>+</sup>); IR (cm<sup>-1</sup>) 1590, 1511, 1500; Mpt. 125-129 °C.

**5-((Benzyloxy)methyl)-2-(chloromethyl)-N-ethyl-7-iodo-5H-pyrrolo[3,2-d]pyrimidin-4-amine (200)**



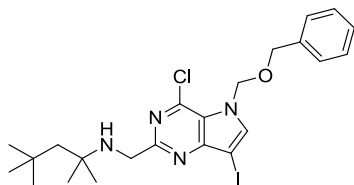
Chemical Formula: C<sub>17</sub>H<sub>18</sub>ClIN<sub>4</sub>O  
Molecular Weight: 456.71

To a stirred suspension of 5-((benzyloxy)methyl)-4-chloro-2-(chloromethyl)-7-iodo-5H-pyrrolo[3,2-d]pyrimidine (**199**) (200 mg, 0.45 mmol) in anhydrous MeOH (10 mL) was added triethylamine (75 μL, 0.54 mmol) and 2M ethylamine in MeOH (245 μL, 0.49 mmol) before heating the reaction mixture to reflux for 2.5 h. The reaction mixture was allowed to cool to ambient temperature before being concentrated *in vacuo* and the residue partitioned between water (50 mL) and DCM (50 mL). The organic phase was separated and the aqueous phase back extracted with DCM (20 mL). The combined organic extracts were washed with brine (50 mL), dried (hydrophobic frit) and concentrated *in vacuo* to give an oil (197 mg). The oil was

dissolved in DCM and purified on a silica cartridge (20 g) using a 0-100% EtOAc-cyclohexane+0-20% MeOH gradient over 40 mins. The appropriate fractions were combined and evaporated *in vacuo* to give the title compound (70 mg, 34%) as a colourless oil.

<sup>1</sup>H NMR (400 MHz, CDCl<sub>3</sub>) δ 7.42 - 7.35 (m, 3H), 7.31 - 7.25 (m, 2H), 7.16 (s, 1H), 6.60 - 6.55 (m, 1H), 5.46 (s, 2H), 4.69 (s, 2H), 4.58 (s, 2H), 3.58 (dq, *J* = 7.3, 5.3 Hz, 2H), 1.18 (t, *J* = 7.3 Hz, 3H); LCMS (System B) R<sub>t</sub> 1.30 min, m/z 457, 459 ([M+H]<sup>+</sup>).

**N-((5-((benzyloxy)methyl)-4-chloro-7-iodo-5H-pyrrolo[3,2-d]pyrimidin-2-yl)methyl)-2,4,4-trimethylpentan-2-amine (201)**



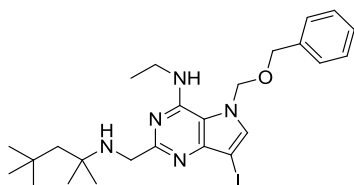
Chemical Formula: C<sub>23</sub>H<sub>30</sub>ClIN<sub>4</sub>O  
Molecular Weight: 540.87

To a stirred suspension of 5-((benzyloxy)methyl)-4-chloro-2-(chloromethyl)-7-iodo-5H-pyrrolo[3,2-d]pyrimidine (**199**) (200 mg, 0.45 mmol) in anhydrous MeCN (5 mL) was added triethylamine (75 μL, 0.54 mmol) and 2,4,4-trimethylpentan-2-amine (82 μL, 0.49 mmol) before heating the reaction mixture to reflux for 1.5 h. The reaction mixture was concentrated *in vacuo* and the resulting residue partitioned between DCM (10 mL) and water (10 mL). The organic phase was separated and dried (hydrophobic frit) before concentrating *in vacuo*. The resultant gum was dissolved in DCM and purified on a silica (Si) cartridge (20 g) using a 0-50% EtOAc-cyclohexane gradient over 40 mins. The appropriate fractions were combined and evaporated *in vacuo* to give the title compound (30 mg, 12 %) as a colourless oil.



$^1\text{H}$  NMR (400 MHz,  $\text{CDCl}_3$ )  $\delta$  7.59 (s, 1H), 7.35 - 7.22 (m, 5H), 5.82 (s, 2H), 4.51 (s, 2H), 4.17 (s, 2H), 1.60 (s, 2H), 1.27 (s, 6H), 1.10 (s, 9H) exchangeable proton (NH) not observed; LCMS (System B)  $R_t$  1.59 min,  $m/z$  541, 543 ( $[\text{M}+\text{H}]^+$ ).

**5-((Benzyloxy)methyl)-N-ethyl-7-iodo-2-(((2,4,4-trimethylpentan-2-yl)amino)methyl)-5H-pyrrolo[3,2-d]pyrimidin-4-amine (202)**

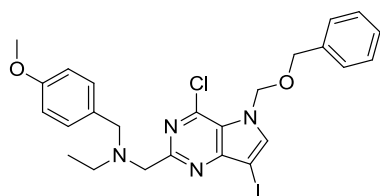


Chemical Formula:  $\text{C}_{25}\text{H}_{36}\text{IN}_5\text{O}$   
Molecular Weight: 549.49

A mixture of *N*-((5-((benzyloxy)methyl)-4-chloro-7-iodo-5*H*-pyrrolo[3,2-*d*]pyrimidin-2-yl)methyl)-2,4,4-trimethylpentan-2-amine (**201**) (30 mg, 0.055 mmol), 2M ethylamine in MeOH (100  $\mu\text{L}$ , 0.20 mmol) and sodium iodide (10 mg, 0.067 mmol) in EtOH (1 mL) was sealed and heated in a Biotage Initiator microwave using initial absorption setting high to 150  $^\circ\text{C}$  for 1 h. After cooling the reaction mixture was concentrated *in vacuo* and partitioned between DCM (10 mL) and water (10 mL). The organic phase was separated and dried (hydrophobic frit) before being concentrated *in vacuo* to give the title compound (23 mg, 75 %) as a yellow gum.

$^1\text{H}$  NMR (400 MHz,  $\text{CDCl}_3$ )  $\delta$  7.41 - 7.34 (m, 3H), 7.30 - 7.25 (m, 2H), 7.19 (s, 1H), 6.73 - 6.66 (m, 1H), 5.48 (s, 2H), 4.60 (s, 2H), 4.21 (s, 2H), 3.52 (dq,  $J = 7.3, 5.3$  Hz, 2H), 1.88 (s, 2H), 1.44 (s, 7H), 1.19 (s, 9H), 1.15 (t,  $J = 7.3$  Hz, 3H) exchangeable proton (NH) not observed;  $^{13}\text{C}$  NMR (101 MHz,  $\text{CDCl}_3$ )  $\delta$  150.9, 135.0, 134.4, 128.8, 128.4, 119.6, 114.6, 77.0, 70.3, 58.1, 52.5, 35.8, 32.0, 31.8, 31.7, 14.5; LCMS (System B)  $R_t$  1.56 min,  $m/z$  550 ( $[\text{M}+\text{H}]^+$ ); HRMS Anal. Calcd. For  $\text{C}_{25}\text{H}_{37}\text{IN}_5\text{O} = 550.2043$ . Found = 550.2045 ( $[\text{M}+\text{H}]^+$ ); IR ( $\text{cm}^{-1}$ ) 3354, 2952, 1608, 1541.

**N-((5-((benzyloxy)methyl)-4-chloro-7-iodo-5H-pyrrolo[3,2-d]pyrimidin-2-yl)methyl)-N-(4-methoxybenzyl)ethanamine (203)**

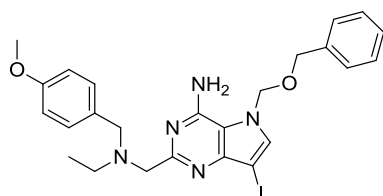


Chemical Formula: C<sub>25</sub>H<sub>26</sub>ClIN<sub>4</sub>O<sub>2</sub>  
Molecular Weight: 576.86

To a stirred suspension of 5-((benzyloxy)methyl)-4-chloro-2-(chloromethyl)-7-iodo-5H-pyrrolo[3,2-d]pyrimidine (**199**) (1.10 g, 2.46 mmol) and N-(4-methoxybenzyl)ethanamine (0.487 g, 2.95 mmol) in anhydrous MeCN (25 mL) was added triethylamine (0.411 mL, 2.95 mmol) and the reaction mixture was heated to reflux for 3 h before allowed to cool to ambient temperature. The solvent was removed *in vacuo* and the resulting residue partitioned between DCM (50 mL) and water (50 mL). The organic phase was separated and the aqueous phase back extracted with DCM (50 mL). The combined organic extracts were dried (hydrophobic frit) and concentrated *in vacuo* before being dissolved in DCM and purified on a silica cartridge (50 g) using a 0-50% EtOAc-cyclohexane gradient over 60 mins. The appropriate fractions were combined and evaporated *in vacuo* to give the title compound (763 mg, 54 %) as a colourless oil.

<sup>1</sup>H NMR (400 MHz, CDCl<sub>3</sub>) δ 7.60 (s, 1H), 7.43 (dt, *J* = 8.8, 2.0 Hz, 2H), 7.36 - 7.22 (m, 5H), 6.86 (dt, *J* = 8.8, 2.0 Hz, 2H), 5.82 (s, 2H), 4.55 (s, 2H), 4.06 (s, 2H), 3.82 - 3.79 (m, 5H), 2.72 (q, *J* = 7.1 Hz, 2H), 1.16 (t, *J* = 7.1 Hz, 3H); LCMS (System B) R<sub>t</sub> 1.49 min, m/z 557, 559 ([M+H]<sup>+</sup>).

**5-((Benzyloxy)methyl)-2-((ethyl(4-methoxybenzyl)amino)methyl)-7-iodo-5H-pyrrolo[3,2-d]pyrimidin-4-amine (204)**

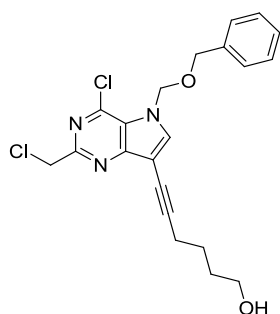


Chemical Formula: C<sub>25</sub>H<sub>28</sub>IN<sub>5</sub>O<sub>2</sub>  
Molecular Weight: 557.43

A solution of *N*-((5-((benzyloxy)methyl)-4-chloro-7-iodo-5*H*-pyrrolo[3,2-*d*]pyrimidin-2-yl)methyl)-*N*-(4-methoxybenzyl)ethanamine (**203**) (750 mg, 1.30 mmol) and 880 ammonia (3.0 mL, 54 mmol) in IPA (1 mL) was sealed and heated in a Biotage Initiator microwave (using initial absorption setting very high) to 150 °C for 60 min. After cooling, the reaction mixture was concentrated *in vacuo* and partitioned between DCM (100 mL) and water (100 mL). The organic phase was separated and dried (hydrophobic frit) before concentration *in vacuo* to give the title compound (606 mg, 84 %) as a white foam.

<sup>1</sup>H NMR (400 MHz, CDCl<sub>3</sub>) δ 7.49 (br d, *J* = 8.5 Hz, 2H), 7.44 - 7.38 (m, 3H), 7.36 - 7.30 (m, 3H), 6.91 - 6.86 (m, 2H), 6.02 (br s, 2H), 5.53 (s, 2H), 4.61 (s, 2H), 3.97 (s, 2H), 3.92 (br s, 2H), 3.83 (s, 3H), 2.83 (m, 2H), 1.24 (t, *J* = 7.0 Hz, 3H); LCMS (System B) R<sub>t</sub> 1.26 min, m/z 558 ([M+H]<sup>+</sup>).

**6-(5-((Benzyloxy)methyl)-4-chloro-2-(chloromethyl)-5H-pyrrolo[3,2-d]pyrimidin-7-yl)hex-5-yn-1-ol (207x)**

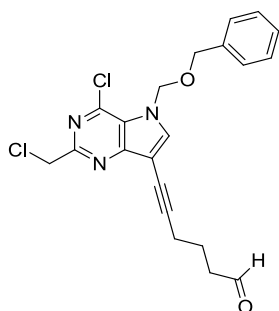


Chemical Formula: C<sub>21</sub>H<sub>21</sub>Cl<sub>2</sub>N<sub>3</sub>O<sub>2</sub>  
Molecular Weight: 418.32

To a degassed, stirred suspension of 5-((benzyloxy)methyl)-4-chloro-2-(chloromethyl)-7-iodo-5*H*-pyrrolo[3,2-*d*]pyrimidine (**199**) (250 mg, 0.558 mmol), copper(I) iodide (20 mg, 0.105 mmol) and *bis*(triphenylphosphine)palladium(II) dichloride (38 mg, 0.054 mmol) in anhydrous DMF (8 mL) at 20 °C was added a solution of hex-5-yn-1-ol (82 mg, 0.84 mmol) and diisopropylethylamine (0.156 mL, 0.893 mmol) in anhydrous DMF (2 mL) dropwise over 10 mins. The reaction mixture was stirred at ambient temperature for 20 h. To the reaction mixture was added further copper(I) iodide (10 mg, 0.052 mmol), further *bis*(triphenylphosphine)palladium(II) dichloride (19 mg, 0.027 mmol) and the reaction was again degassed before addition of a solution of hex-5-yn-1-ol (42 mg, 0.418 mmol) and DIPEA (0.078 mL, 0.446 mmol) in anhydrous DMF (1 mL) dropwise over 1 min. The reaction mixture was stirred at ambient temperature for a further 5.5 h. The reaction mixture was concentrated *in vacuo* and the residue partitioned between water (50 mL) and EtOAc (50 mL). The organic phase was separated and the aqueous phase back extracted with EtOAc (50 mL). The combined organic extracts were washed with brine (50 mL), dried (MgSO<sub>4</sub>), filtered and concentrated *in vacuo* to give a red oil. The oil was dissolved in DCM and purified on a silica cartridge (20 g) using a 0-100% EtOAc-cyclohexane gradient over 40 mins. The appropriate fractions were combined and evaporated *in vacuo* to give the title compound (61 mg, 26%) as a yellow gum.

<sup>1</sup>H NMR (400 MHz, CDCl<sub>3</sub>) δ 7.67 (s, 1H), 7.37 - 7.22 (m, 5H), 5.81 (s, 2H), 4.85 (s, 2H), 4.53 (s, 2H), 3.81 - 3.75 (m, 2H), 2.59 - 2.54 (m, 2H), 2.00 (br s, 1H), 1.85 - 1.74 (m, 4H) LCMS (System B) R<sub>t</sub> 1.15 min, m/z 418, 420, 422 ([M+H]<sup>+</sup>).

**6-(5-((Benzyloxy)methyl)-4-chloro-2-(chloromethyl)-5H-pyrrolo[3,2-d]pyrimidin-7-yl)hex-5-ynal (208y)**

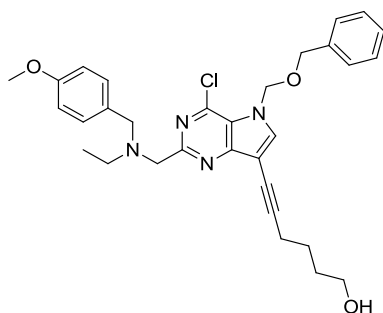


Chemical Formula: C<sub>21</sub>H<sub>19</sub>Cl<sub>2</sub>N<sub>3</sub>O<sub>2</sub>  
Molecular Weight: 416.30

To a stirred suspension of 6-(5-((benzyloxy)methyl)-4-chloro-2-(chloromethyl)-5H-pyrrolo[3,2-d]pyrimidin-7-yl)hex-5-yn-1-ol (**207x**) (48 mg, 0.12 mmol), 4-methylmorpholine *N*-oxide (14 mg, 0.12 mmol) and powdered 4Å molecular sieves in a mixture of anhydrous DCM (2 mL) and anhydrous MeCN (0.2 mL) at ambient temperature was added tetrapropylammonium perruthenate (4 mg, 0.011 mmol), and the reaction was stirred at ambient temperature for 1.5 h. The reaction mixture was filtered through celite and the filtrate concentrated *in vacuo* (water bath temp 20 °C) and the residue dissolved in DCM and purified on a silica cartridge (5 g) using a 0-50% EtOAc-cyclohexane gradient over 20 mins. The appropriate fractions were combined and evaporated *in vacuo* to give the title compound (17 mg, 36 % yield) as a yellow oil.

<sup>1</sup>H NMR (400 MHz, CDCl<sub>3</sub>) δ 9.87 (s, 1H), 7.68 (s, 1H), 7.38 - 7.21 (m, 5H), 5.81 (s, 2H), 4.84 (s, 2H), 4.53 (s, 2H), 2.71 (t, *J* = 7.2 Hz, 2H), 2.60 (t, *J* = 6.9 Hz, 2H), 2.07 - 1.97 (m, 2H); LCMS (System B) R<sub>t</sub> 1.25 min, m/z 416, 418, 420 ([M+H]<sup>+</sup>).

**6-(5-((Benzyloxy)methyl)-4-chloro-2-((ethyl(4-methoxybenzyl)amino)methyl)-5H-pyrrolo[3,2-d]pyrimidin-7-yl)hex-5-yn-1-ol (209x)**

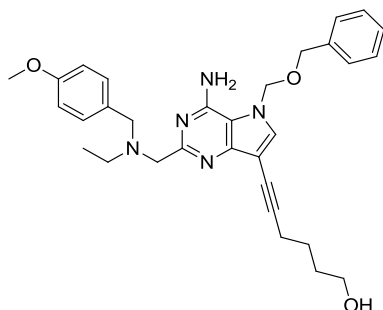


Chemical Formula: C<sub>31</sub>H<sub>35</sub>ClN<sub>4</sub>O<sub>3</sub>  
Molecular Weight: 547.09

To a solution of 6-(5-((benzyloxy)methyl)-4-chloro-2-(chloromethyl)-5H-pyrrolo[3,2-d]pyrimidin-7-yl)hex-5-yn-1-ol (**207x**) (196 mg, 0.47 mmol) in anhydrous MeCN (3 mL) was added a solution of triethylamine (0.078 mL, 0.56 mmol) and *N*-(4-methoxybenzyl)ethanamine (93 mg, 0.56 mmol) in MeCN (2 mL). The reaction mixture was heated to reflux for 16 h. After this time the solvent was removed *in vacuo* and the resulting residue partitioned between DCM (25 mL) and water (25 mL). The organic phase was separated and the aqueous phase back extracted with DCM (10 mL). The combined organic extracts were dried (hydrophobic frit) and concentrated *in vacuo* to give before being dissolved in DCM and purified on a silica cartridge (20 g) using a 0-10% MeOH-DCM gradient over 40 mins. The appropriate fractions were combined and evaporated *in vacuo* to give the title compound (80 mg, 31 %) as a yellow oil.

<sup>1</sup>H NMR (400 MHz, CDCl<sub>3</sub>) δ 7.59 (s, 1H), 7.40 - 7.34 (m, 2H), 7.33 - 7.23 (m, 5H), 6.86 - 6.79 (m, 2H), 5.79 (s, 2H), 4.51 (s, 2H), 4.02 (s, 2H), 3.81 - 3.72 (m, 6H), 2.68 (q, *J* = 7.1 Hz, 2H), 2.56 (t, *J* = 6.5 Hz, 2H), 2.05 (br s, 1H), 1.85 - 1.72 (m, 5H), 1.13 (t, *J* = 7.1 Hz, 3H); <sup>13</sup>C NMR (101 MHz, CDCl<sub>3</sub>) δ 161.3, 158.5, 153.5, 142.8, 138.0, 136.2, 131.2, 130.6, 128.6, 128.2, 127.7, 122.2, 113.4, 101.1, 94.6, 76.6, 70.5, 70.4, 62.0, 58.8, 56.8, 55.2, 47.5, 32.0, 24.7, 19.6, 11.7; LCMS (System B) R<sub>t</sub> 1.34 min, *m/z* 547, 549 ([M+H]<sup>+</sup>); HRMS Anal. Calcd. For C<sub>31</sub>H<sub>36</sub>ClN<sub>3</sub>O<sub>4</sub> = 547.2476. Found = 547.2480 ([M+H]<sup>+</sup>); IR (cm<sup>-1</sup>) 3396, 2933, 1596.

**6-(4-Amino-5-((benzyloxy)methyl)-2-((ethyl(4-methoxybenzyl)amino)methyl)-5H-pyrrolo[3,2-d]pyrimidin-7-yl)hex-5-yn-1-ol (210x)**



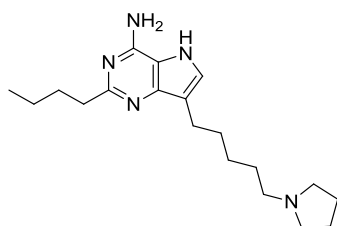
Chemical Formula: C<sub>31</sub>H<sub>37</sub>N<sub>5</sub>O<sub>3</sub>  
Molecular Weight: 527.66

To a solution of 6-(5-((benzyloxy)methyl)-4-chloro-2-((ethyl(4-methoxybenzyl)amino)methyl)-5H-pyrrolo[3,2-d]pyrimidin-7-yl)hex-5-yn-1-ol (**209x**) (80 mg, 0.15 mmol) in IPA (0.5 mL) was added 880 ammonia (0.2 mL, 3.6 mmol). The reaction vessel was sealed and heated in a Biotage Initiator microwave (using initial absorption setting very high) to 150 °C for 1 h. After cooling, the reaction mixture, further 880 ammonia (0.2 mL, 3.62 mmol) was added. The reaction vessel was sealed again and heated in a Biotage Initiator microwave (using initial absorption setting very high) to 150 °C for 1 h. After cooling, the reaction mixture was concentrated *in vacuo* and the residue dissolved in DCM (15 mL), dried (hydrophobic frit) and concentrated *in vacuo* to give the title compound (67 mg, 87 %) as a yellow oil.

<sup>1</sup>H NMR (400 MHz, CDCl<sub>3</sub>) δ 7.39 - 7.32 (m, 5H), 7.29 - 7.25 (m, 2H), 7.20 (s, 1H), 6.84 - 6.80 (m, 2H), 5.89 (br s, 2H), 5.44 (s, 2H), 4.53 (s, 2H), 3.87 (br s, 2H), 3.84 - 3.81 (m, 2H), 3.79 - 3.75 (m, 5H), 2.77 - 2.67 (m, 2H), 2.55 - 2.51 (m 2H), 1.83 - 1.76 (m, 4H), 1.18 - 1.12 (m, 3H) exchangeable proton (OH) not observed; LCMS (System B) R<sub>t</sub> 1.13 min, m/z 528 ([M+H]<sup>+</sup>).

**2-Butyl-7-(5-(pyrrolidin-1-yl)pentyl)-5H-pyrrolo[3,2-d]pyrimidin-4-amine,**

**Formic acid salt (211b)**



Chemical Formula: C<sub>19</sub>H<sub>31</sub>N<sub>5</sub>  
Molecular Weight: 329.48

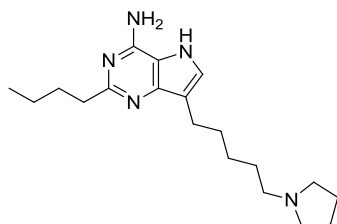
A solution of 5-((benzyloxy)methyl)-2-butyl-7-(5-(pyrrolidin-1-yl)pent-1-yn-1-yl)-5H-pyrrolo[3,2-d]pyrimidin-4-amine (**213b**) (90 mg, 0.20 mmol) in EtOH (10 mL) was hydrogenated using the H-cube (settings: 60 °C, Full H<sub>2</sub>, 1 mL/min flow rate) and a 10% Pd/C CatCart 30 as the catalyst. The reaction mixture was re-hydrogenated using the H-cube (settings: 60 °C, Full H<sub>2</sub>, 1 mL/min flow rate) and 10% Pd/C CatCart 30 as the catalyst and was concentrated *in vacuo*. The sample was dissolved in 1:1 MeOH:DMSO (1 mL) and purified by MDAP on a Sunfire C18 column using MeCN-water with a formic acid modifier. The solvent was removed under a stream of nitrogen in the Radleys<sup>TM</sup> blowdown apparatus to give the title compound as the formic acid salt (16 mg, 21 %) as a white gum.

<sup>1</sup>H NMR (400 MHz, CDCl<sub>3</sub>) δ 13.93 (br s, 1H), 8.78 (s, 2H), 7.22 (s, 1H), 3.13 (br s, 4H), 2.99 (t, *J* = 8.8 Hz, 2H), 2.88 (t, *J* = 7.5 Hz, 2H), 2.67 - 2.61 (m, 2H), 2.10 - 2.04 (m, 4H), 1.87 - 1.74 (m, 4H), 1.64 - 1.54 (m, 2H), 1.55 - 1.46 (m, 2H), 1.45 - 1.36 (m, 2H), 0.94 (t, *J* = 7.4 Hz, 3H) exchangeable protons (NH<sub>2</sub> and OH) not observed; LCMS (System A) R<sub>t</sub> 0.44 min, m/z 330 ([M+H]<sup>+</sup>).



**2-Butyl-7-(5-(pyrrolidin-1-yl)pentyl)-5H-pyrrolo[3,2-d]pyrimidin-4-amine**

**(211b)**



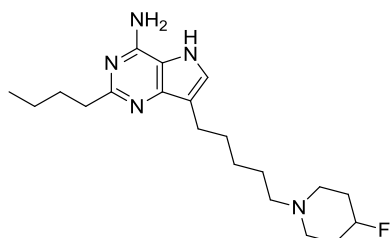
Chemical Formula: C<sub>19</sub>H<sub>31</sub>N<sub>5</sub>  
Molecular Weight: 329.48

A filtered solution of 5-((benzyloxy)methyl)-2-butyl-7-(5-(pyrrolidin-1-yl)pent-1-yn-1-yl)-5H-pyrrolo[3,2-d]pyrimidin-4-amine (**213b**) (535 mg, 1.64 mmol) in EtOH (55 mL) and AcOH (5 mL) was hydrogenated using the H-cube<sup>TM</sup> (settings: 60 °C, Full H<sub>2</sub>, 1mL/min flow rate) and a 10% Pd/C Catcart 30 as the catalyst. The solution was re-hydrogenated using the H-cube<sup>TM</sup> (settings: 60 °C, Full H<sub>2</sub>, 1mL/min flow rate) and a new 10% Pd/C Catcart 30 as the catalyst. To the reaction mixture was added further AcOH (5 mL) and the solution was re-hydrogenated using the H-cube<sup>TM</sup> (settings: 60 °C, Full H<sub>2</sub>, 1mL/min flow rate) and a new 10% Pd/C Catcart 30 as the catalyst. The solution was further hydrogenated using the H-cube<sup>TM</sup> (settings: 60 °C, Full H<sub>2</sub>, 1mL/min flow rate) and a new 10% Pd/C Catcart 30 as the catalyst. The reaction mixture was concentrated *in vacuo*. This residue was partitioned between EtOAc (250 mL) and 0.5 M aqueous NaOH (250 mL). The organic layer was separated the aqueous layer back extracted with EtOAc (100 mL). The combined organic extracts were washed with brine (200 mL), dried (MgSO<sub>4</sub>), filtered and concentrated *in vacuo* to give a solid (444 mg). This solid was triturated with hot EtOAc (20 mL) and filtered. The solid was dried *in vacuo* to give the title compound (325 mg, 61%).

This batch of title compound was blended with six other batches of the title compound. The blended material was triturated with hot EtOAc (40 mL) and filtered. The solid was dried *in vacuo* to give the title compound (754 mg).

$^1\text{H}$  NMR (600 MHz, DMSO- $d_6$ )  $\delta$  10.53 (br s, 1H), 7.19 (s, 1H), 6.49 (br s, 2H), 2.65 - 2.55 (m, 4H), 2.48 (br s, 4H), 2.42 (t,  $J = 7.3$  Hz, 2H), 1.70 - 1.65 (m, 6H), 1.65 - 1.59 (m, 2H), 1.51 - 1.45 (m, 2H), 1.37 - 1.28 (m, 4H), 0.89 (t,  $J = 7.4$  Hz, 3H);  $^{13}\text{C}$  NMR (151 MHz, DMSO- $d_6$ )  $\delta$  160.7, 150.1, 146.6, 124.7, 114.6, 112.4, 55.5, 53.5, 38.4, 30.9, 29.5, 27.8, 26.7, 23.4, 22.9, 22.0, 13.9; LCMS (System B)  $R_t$  0.83 min,  $m/z = 330$  ( $[\text{M}+\text{H}]^+$ ); HRMS Anal. Calcd. For  $\text{C}_{19}\text{H}_{32}\text{N}_5 = 330.2656$ . Found = 330.2658 ( $[\text{M}+\text{H}]^+$ ).

**2-Butyl-7-(5-(4-fluoropiperidin-1-yl)pentyl)-5H-pyrrolo[3,2-*d*]pyrimidin-4-amine (211c)**

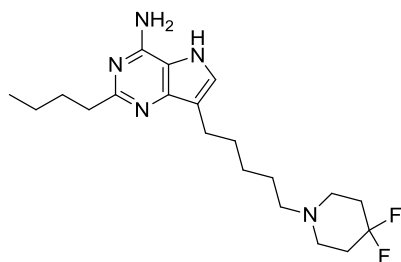


Chemical Formula:  $\text{C}_{20}\text{H}_{32}\text{FN}_5$   
Molecular Weight: 361.50

A solution of 5-((benzyloxy)methyl)-2-butyl-7-(5-(4-fluoropiperidin-1-yl)pent-1-yn-1-yl)-5H-pyrrolo[3,2-*d*]pyrimidin-4-amine (**213c**) (68 mg, 0.14 mmol) in EtOH (7 mL) and AcOH (1 mL) was hydrogenated using the H-cube (settings: 60 °C, Full  $\text{H}_2$ , 1 mL/min flow rate) and a 10% Pd/C CatCart 30 as the catalyst. The reaction mixture was concentrated *in vacuo* and was dissolved in 1:1 MeOH:DMSO (1 mL) and purified by MDAP on an Xbridge column using MeCN-water with an ammonium carbonate modifier. The solvent was removed under a stream of nitrogen in the Radleys<sup>TM</sup> blowdown apparatus to give the title compound (23 mg, 45%) as a white solid.

$^1\text{H}$  NMR (400 MHz, MeOD)  $\delta$  7.22 (s, 1H), 4.65 (dm,  $J = 50$  Hz, 1H), 2.76 - 2.70 (m, 4H), 2.62 - 2.52 (m, 2H), 2.42 - 2.30 (m, 4H), 1.95 - 1.65 (m, 8H), 1.59 - 1.49 (m, 2H), 1.44 - 1.34 (m, 4H), 0.95 (t,  $J = 7.4$  Hz, 3H) exchangeable protons (NH and  $\text{NH}_2$ ) not observed; LCMS (System B)  $R_t$  1.00 min,  $m/z$  362 ( $[\text{M}+\text{H}]^+$ ).

**2-Butyl-7-(5-(4,4-difluoropiperidin-1-yl)pentyl)-5H-pyrrolo[3,2-d]pyrimidin-4-amine (211d)**

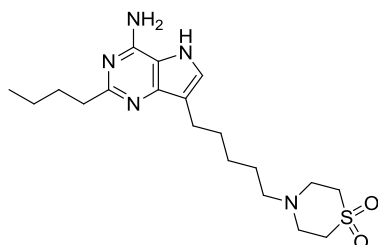


Chemical Formula: C<sub>20</sub>H<sub>31</sub>F<sub>2</sub>N<sub>5</sub>  
Molecular Weight: 379.49

A solution of 5-((benzyloxy)methyl)-2-butyl-7-(5-(4,4-difluoropiperidin-1-yl)pent-1-yn-1-yl)-5H-pyrrolo[3,2-d]pyrimidin-4-amine (**213d**) (77 mg, 0.16 mmol) in EtOH (7 mL) and AcOH (1 mL) was hydrogenated using the H-cube (settings: 60 °C, Full H<sub>2</sub>, 1 mL/min flow rate) and a 10% Pd/C CatCart 30 as the catalyst. The reaction mixture was concentrated *in vacuo* before being dissolved in 1:1 MeOH:DMSO (1 mL) and purified by MDAP on an Xbridge column using MeCN- water with an ammonium carbonate modifier. The solvent was removed under a stream of nitrogen in the Radleys™ blowdown apparatus to give the title compound (20 mg, 33%) as a white solid.

<sup>1</sup>H NMR (400 MHz, MeOD) δ 7.22 (s, 1H), 2.77 - 2.70 (m, 4H), 2.56 - 2.51 (m, 4H), 2.41 - 2.36 (m, 2H), 2.01 - 1.89 (m, 4H), 1.78 - 1.65 (m, 4H), 1.59 - 1.50 (m, 2H), 1.45 - 1.35 (m, 4H), 0.95 (t, *J* = 7.4 Hz, 3H) exchangeable protons (NH and NH<sub>2</sub>) not observed; LCMS (System B) R<sub>t</sub> 1.06 min, *m/z* 380 ([M+H]<sup>+</sup>).

**4-(5-(4-Amino-2-butyl-5H-pyrrolo[3,2-d]pyrimidin-7-yl)pentyl)thiomorpholine 1,1-dioxide (211e)**

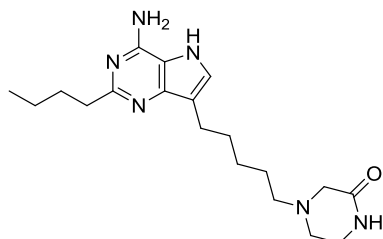


Chemical Formula: C<sub>19</sub>H<sub>31</sub>N<sub>5</sub>O<sub>2</sub>S  
Molecular Weight: 393.55

A solution of 4-(5-(4-amino-5-((benzyloxy)methyl)-2-butyl-5*H*-pyrrolo[3,2-*d*]pyrimidin-7-yl)pent-4-yn-1-yl)thiomorpholine 1,1-dioxide (**213e**) (108 mg, 0.21 mmol) in EtOH (9 mL) and AcOH (1 mL) was hydrogenated using the H-cube (settings: 60 °C, Full H<sub>2</sub>, 1 mL/min flow rate) and a 10% Pd/C CatCart 30 as the catalyst. The reaction mixture was concentrated *in vacuo* and was dissolved in 1:1 MeOH:DMSO (1 mL) and purified by MDAP on an Xbridge column using MeCN-water with an ammonium carbonate modifier. The solvent was removed under a stream of nitrogen in the Radleys™ blowdown apparatus to give the title compound (32 mg, 38%) as a white solid.

<sup>1</sup>H NMR (400 MHz, MeOD) δ 7.22 (s, 1H), 3.07 – 2.99 (m, 4H), 2.97 - 2.90 (m, 4H), 2.77 - 2.69 (m, 4H), 2.53 - 2.46 (m, 2H), 1.78 - 1.65 (m, 4H), 1.58 - 1.48 (m, 2H), 1.46 - 1.33 (m, 4H), 0.95 (t, *J* = 7.4 Hz, 3H) exchangeable protons (NH and NH<sub>2</sub>) not observed; LCMS (System B) R<sub>t</sub> 0.84 min, m/z 394 ([M+H]<sup>+</sup>).

**4-(5-(4-Amino-2-butyl-5*H*-pyrrolo[3,2-*d*]pyrimidin-7-yl)pentyl)piperazin-2-one**  
**(211f)**



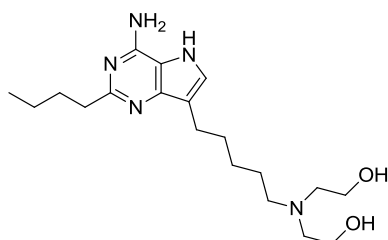
Chemical Formula: C<sub>19</sub>H<sub>30</sub>N<sub>6</sub>O  
Molecular Weight: 358.48

A solution of 4-(5-(4-amino-5-((benzyloxy)methyl)-2-butyl-5*H*-pyrrolo[3,2-*d*]pyrimidin-7-yl)pent-4-yn-1-yl)piperazin-2-one (**213f**) (41 mg, 0.086 mmol) in EtOH (4.5 mL) and AcOH (0.5 mL) was hydrogenated using the H-cube (settings: 60 °C, Full H<sub>2</sub>, 1 mL/min flow rate) and a 10% Pd/C CatCart 30 as the catalyst. The solution was concentrated *in vacuo* and dissolved in 1:1 MeOH:DMSO (1 mL) and purified by MDAP on an Xbridge column using MeCN-water with an ammonium carbonate modifier. The solvent was removed under a stream of nitrogen in the

Radleys<sup>TM</sup> blowdown apparatus to give the title compound (16 mg, 52%) as a white solid.

<sup>1</sup>H NMR (400 MHz, DMSO-d<sub>6</sub>) δ 10.51 (br s, 1H), 7.69 (br s, 1H), 7.22 (s, 1H), 6.54 (br s, 2H), 3.16 - 3.07 (m, 2H), 2.87 (s, 2H), 2.65 - 2.55 (m, 4H), 2.53 - 2.46 (m, 2H), 2.31 (t, *J* = 7.3 Hz, 2H), 1.73 - 1.59 (m, 4H), 1.50 - 1.41 (m, 2H), 1.38 - 1.27 (m, 4H), 0.90 (t, *J* = 7.5 Hz, 3H); <sup>13</sup>C NMR (101 MHz, DMSO-d<sub>6</sub>) δ 167.8, 160.7, 150.1, 146.3, 124.9, 114.6, 112.4, 57.0, 56.8, 48.7, 40.4, 38.4, 30.9, 29.5, 26.5, 25.9, 23.4, 22.1, 13.9; LCMS (System A) R<sub>t</sub> 0.44 min, m/z 359 ([M+H]<sup>+</sup>); HRMS Anal. Calcd. for C<sub>19</sub>H<sub>31</sub>N<sub>6</sub>O = 359.2554. Found = 359.2556 ([M+H]<sup>+</sup>).

**2,2'-((5-(4-Amino-2-butyl-5H-pyrrolo[3,2-*d*]pyrimidin-7-yl)pentyl)azanediyl)diethanol (211g)**

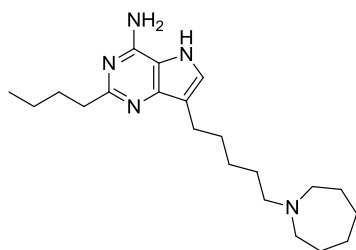


Chemical Formula: C<sub>19</sub>H<sub>33</sub>N<sub>5</sub>O<sub>2</sub>  
Molecular Weight: 363.50

A solution of 2,2'-((5-(4-amino-5-((benzyloxy)methyl)-2-butyl-5H-pyrrolo[3,2-*d*]pyrimidin-7-yl)pent-4-yn-1-yl)azanediyl)diethanol (**213g**) (63 mg, 0.13 mmol) in EtOH (7 mL) was hydrogenated using the H-cube (settings: 60 °C, Full H<sub>2</sub>, 1 mL/min flow rate) and a 10% Pd/C CatCart 30 as the catalyst. The solution was further hydrogenated using the H-cube (settings: 60 °C, Full H<sub>2</sub>, 1 mL/min flow rate) and a 10% Pd/C CatCart 30 as the catalyst. The reaction mixture was concentrated *in vacuo* before being dissolved in 1:1 MeOH:DMSO (1 mL) and purified by MDAP on an Xbridge column using MeCN-water with an ammonium carbonate modifier. The solvent was removed under a stream of nitrogen in the Radleys<sup>TM</sup> blowdown apparatus to give the title compound (23 mg, 48 %) as a white solid.

$^1\text{H}$  NMR (400 MHz, MeOD)  $\delta$  7.21 (s, 1H), 3.58 (t,  $J = 5.9$  Hz, 4H), 2.73 (t,  $J = 7.8$  Hz, 4H), 2.62 (t,  $J = 5.9$  Hz, 4H), 2.56 - 2.49 (m, 2H), 1.78 - 1.64 (m, 4H), 1.57 - 1.47 (m, 2H), 1.44 - 1.33 (m, 4H), 0.95 (t,  $J = 7.4$  Hz, 3H) exchangeable protons (NH,  $\text{NH}_2$  and OHs) not observed; LCMS (System B)  $R_t$  0.75 min,  $m/z$  364 ( $[\text{M}+\text{H}]^+$ ).

**7-(5-(Azepan-1-yl)pentyl)-2-butyl-5H-pyrrolo[3,2-d]pyrimidin-4-amine (211i)**



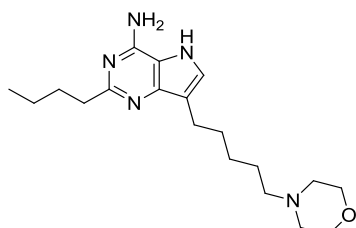
Chemical Formula:  $\text{C}_{21}\text{H}_{35}\text{N}_5$   
Molecular Weight: 357.54

A filtered solution of 7-(5-(azepan-1-yl)pent-1-yn-1-yl)-5-((benzyloxy)methyl)-2-butyl-5H-pyrrolo[3,2-d]pyrimidin-4-amine (**213y**) (500 mg, 1.06 mmol) in EtOH (40 mL) and AcOH (10 mL) was hydrogenated using the H-cube<sup>TM</sup> (settings: 60 °C, Full  $\text{H}_2$ , 1 mL/min flow rate) and a 10% Pd/C CatCart 30 as the catalyst. The solution was re-hydrogenated using the H-cube<sup>TM</sup> (settings: 60 °C, Full  $\text{H}_2$ , 1 mL/min flow rate) and the same 10% Pd/C CatCart 30 as the catalyst. The solution was re-hydrogenated using the H-cube<sup>TM</sup> (settings: 60 °C, Full  $\text{H}_2$ , 1 mL/min flow rate) and a new 10% Pd/C CatCart 30 as the catalyst. The solution was concentrated *in vacuo* and the residue partitioned between EtOAc (200 mL) and 0.2 M aqueous NaOH (200 mL). The organic was separated and washed with brine (100 mL), dried ( $\text{MgSO}_4$ ), filtered and concentrated *in vacuo* to give a sticky white gum. The gum was triturated with hot EtOAc (*ca.* 15 mL) and the resulting suspension filtered (whilst still hot). The solid was dried *in vacuo* to give the title compound (239 mg, 63 %) as a white solid.

$^1\text{H}$  NMR (400 MHz, MeOD)  $\delta$  7.25 (s, 1H), 2.79 - 2.73 (m, 4H), 2.68 - 2.64 (m, 4H), 2.50 - 2.44 (m, 2H), 1.81 - 1.60 (m, 12H), 1.59 - 1.51 (m, 2H), 1.48 - 1.35 (m, 4H), 0.98 (t,  $J = 7.5$  Hz, 3H) exchangeable protons (NH and  $\text{NH}_2$ ) not observed;  $^{13}\text{C}$

NMR (101 MHz, DMSO-d<sub>6</sub>)  $\delta$  160.8, 150.1, 146.8, 124.7, 114.8, 112.4, 57.6, 54.8, 38.5, 31.0, 29.6, 28.0, 27.1, 26.6, 26.5, 23.5, 22.1, 13.9; LCMS (System B)  $R_t$  0.89 min,  $m/z$  358 ( $[M+H]^+$ ); HRMS Anal. Calcd. for C<sub>21</sub>H<sub>36</sub>N<sub>5</sub> = 358.2965. Found = 358.2977 ( $[M+H]^+$ ).

**2-Butyl-7-(5-morpholinopentyl)-5H-pyrrolo[3,2-d]pyrimidin-4-amine (211j)**

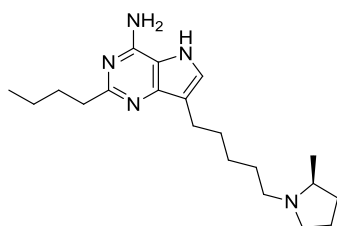


Chemical Formula: C<sub>19</sub>H<sub>31</sub>N<sub>5</sub>O  
Molecular Weight: 345.48

A filtered solution of 5-((benzyloxy)methyl)-2-butyl-7-(5-morpholinopent-1-yn-1-yl)-5H-pyrrolo[3,2-d]pyrimidin-4-amine (**213j**) (130 mg, 0.28 mmol) in EtOH (13 mL) and AcOH (1.5 mL) was hydrogenated using the H-cube<sup>TM</sup> (settings: 60 °C, Full H<sub>2</sub>, 1 mL/min flow rate) and a 10% Pd/C CatCart 30 as the catalyst. The reaction mixture was concentrated *in vacuo* and the residue was dissolved in 1:1 MeOH:DMSO (1 mL) and purified by MDAP on an Xbridge column using MeCN-water with an ammonium carbonate modifier. The solvent was evaporated *in vacuo* to give the title compound (50 mg, 51%) as an off white solid.

<sup>1</sup>H NMR (400 MHz, DMSO-d<sub>6</sub>)  $\delta$  10.52 (br s, 1H), 7.22 (s, 1H), 6.54 (br s, 2H), 3.54 (t,  $J$  = 4.6 Hz, 4H), 2.66 - 2.56 (m, 4H), 2.34 - 2.28 (m, 4H), 2.27 - 2.19 (m, 2H), 1.74 - 1.60 (m, 4H), 1.49 - 1.40 (m, 2H), 1.38 - 1.28 (m, 4H), 0.89 (t,  $J$  = 7.3 Hz, 3H); <sup>13</sup>C NMR (101 MHz, DMSO-d<sub>6</sub>)  $\delta$  160.7, 150.1, 146.3, 124.8, 114.6, 112.4, 66.2, 58.3, 53.4, 38.4, 30.9, 39.6, 26.6, 25.7, 23.4, 22.1, 13.9; LCMS (System B)  $R_t$  0.82 min,  $m/z$  346 ( $[M+H]^+$ ); HRMS Anal. Calcd. for C<sub>19</sub>H<sub>32</sub>N<sub>5</sub>O = 346.2601. Found = 346.2610 ( $[M+H]^+$ ).

**(S)-2-butyl-7-(5-(2-methylpyrrolidin-1-yl)pentyl)-5H-pyrrolo[3,2-d]pyrimidin-4-amine (211k)**



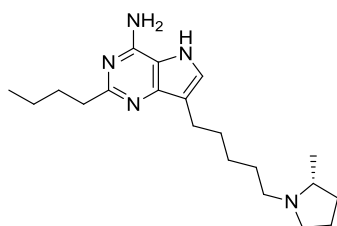
Chemical Formula: C<sub>20</sub>H<sub>33</sub>N<sub>5</sub>  
Molecular Weight: 343.51

A filtered solution of (*S*)-5-((benzyloxy)methyl)-2-butyl-7-(5-(2-methylpyrrolidin-1-yl)pent-1-yn-1-yl)-5*H*-pyrrolo[3,2-*d*]pyrimidin-4-amine (**213k**) (140 mg, 0.31 mmol) in EtOH (12 mL) and AcOH (2 mL) was hydrogenated using the H-cube<sup>TM</sup> (settings: 60 °C, Full H<sub>2</sub>, 1 mL/min flow rate) and a 10% Pd/C CatCart 30 as the catalyst. The reaction mixture was concentrated *in vacuo* and the residue was dissolved in 1:1 MeOH:DMSO (1 mL) and purified by MDAP on an Xbridge column using MeCN-water with an ammonium carbonate modifier. The solvent was evaporated *in vacuo* to give the title compound (40 mg, 38%) as a white solid.

<sup>1</sup>H NMR (400 MHz, DMSO-*d*<sub>6</sub>) δ 10.46 (br s, 1H), 7.20 (d, *J*=2.5 Hz, 1H), 6.45 (s, 2H), 3.07 - 2.95 (m, 1H), 2.73 - 2.65 (m, 1H), 2.64 - 2.55 (m, 4H), 2.23 - 2.12 (m, 1H), 2.01 - 1.90 (m, 2H), 1.89 - 1.77 (m, 1H), 1.74 - 1.53 (m, 6H), 1.52 - 1.20 (m, 7H), 0.98 (d, *J*=6.1 Hz, 3H), 0.90 (t, *J*=7.3 Hz, 3H); <sup>13</sup>C NMR (101 MHz, DMSO-*d*<sub>6</sub>) δ 160.8, 150.1, 146.8, 124.7, 114.8, 112.4, 59.3, 53.3, 53.3, 38.5, 32.5, 31.0, 29.6, 28.1, 26.9, 23.5, 22.1, 21.3, 19.0, 13.9; LCMS (System B) R<sub>t</sub> 0.86 min, m/z 344 ([M+H]<sup>+</sup>); HRMS Anal. Calcd. for C<sub>20</sub>H<sub>34</sub>N<sub>5</sub> = 344.2809. Found = 344.2820 ([M+H]<sup>+</sup>).



**(R)-2-butyl-7-(5-(2-methylpyrrolidin-1-yl)pentyl)-5H-pyrrolo[3,2-d]pyrimidin-4-amine (2111)**

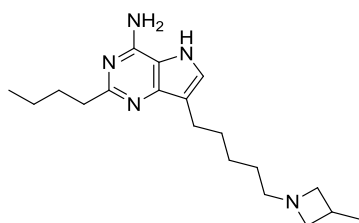


Chemical Formula: C<sub>20</sub>H<sub>33</sub>N<sub>5</sub>  
Molecular Weight: 343.51

A filtered solution of (*R*)-5-((benzyloxy)methyl)-2-butyl-7-(5-(2-methylpyrrolidin-1-yl)pent-1-yn-1-yl)-5*H*-pyrrolo[3,2-*d*]pyrimidin-4-amine (**2131**) (140 mg, 0.31 mmol) in EtOH (12 mL) and AcOH (2 mL) was hydrogenated using the H-cube<sup>TM</sup> (settings: 60 °C, Full H<sub>2</sub>, 1 mL/min flow rate) and a 10% Pd/C CatCart 30 as the catalyst. The reaction mixture was concentrated *in vacuo* and the residue was dissolved in 1:1 MeOH:DMSO (1 mL) and purified by MDAP on an Xbridge column using MeCN-water with an ammonium carbonate modifier. The solvent was evaporated *in vacuo* to give the title compound (47 mg, 62%) as a white solid.

<sup>1</sup>H NMR (400 MHz, DMSO-*d*<sub>6</sub>) δ 10.46 (br s, 1H), 7.20 (d, *J*=2.5 Hz, 1H), 6.45 (s, 2H), 3.07 - 2.95 (m, 1H), 2.73 - 2.65 (m, 1H), 2.64 - 2.55 (m, 4H), 2.23 - 2.12 (m, 1H), 2.01 - 1.90 (m, 2H), 1.89 - 1.77 (m, 1H), 1.74 - 1.53 (m, 6H), 1.52 - 1.20 (m, 7H), 0.98 (d, *J*=6.1 Hz, 3H), 0.90 (t, *J*=7.3 Hz, 3H); <sup>13</sup>C NMR (101 MHz, DMSO-*d*<sub>6</sub>) δ 160.8, 150.1, 146.8, 124.7, 114.8, 112.4, 59.3, 53.3, 53.3, 38.5, 32.5, 31.0, 29.6, 28.1, 26.9, 23.5, 22.1, 21.3, 19.0, 13.9; LCMS (System B) R<sub>t</sub> 0.86 min, *m/z* 345 ([M+H]<sup>+</sup>); HRMS Anal. Calcd. for C<sub>20</sub>H<sub>34</sub>N<sub>5</sub> = 344.2809. Found = 344.2820 ([M+H]<sup>+</sup>).

**2-Butyl-7-(5-(3-methylazetidin-1-yl)pentyl)-5H-pyrrolo[3,2-d]pyrimidin-4-amine (211m)**

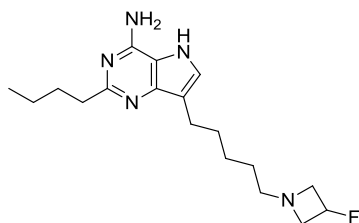


Chemical Formula: C<sub>19</sub>H<sub>31</sub>N<sub>5</sub>  
Molecular Weight: 329.48

A filtered solution of 5-((benzyloxy)methyl)-2-butyl-7-(5-(3-methylazetidin-1-yl)pent-1-yn-1-yl)-5H-pyrrolo[3,2-d]pyrimidin-4-amine (**213m**) (32 mg, 0.072 mmol) in EtOH (16 mL) and AcOH (3 mL) was hydrogenated using the H-cube<sup>TM</sup> (settings: 60 °C, Full H<sub>2</sub>, 1 mL/min flow rate) and a 10% Pd/C CatCart 30 as the catalyst. The reaction mixture was concentrated *in vacuo* and the residue was dissolved in 1:1 MeOH:DMSO (1 mL) and purified by MDAP on an Xbridge column using MeCN-water with an ammonium carbonate modifier. The solvent was evaporated *in vacuo* to give the title compound (7.5 mg, 32%) as a white solid.

<sup>1</sup>H NMR (400 MHz, MeOD) δ 7.24 (s, 1H), 3.52 - 3.46 (m, 2H), 2.82 - 2.71 (m, 6H), 2.63 - 2.52 (m, 1H), 2.48 - 2.42 (m, 2H), 1.81 - 1.64 (m, 4H), 1.48 - 1.36 (m, 6H), 1.15 (d, *J* = 6.6 Hz, 3H), 0.98 (t, *J* = 7.3 Hz, 3H) exchangeable protons (NH and NH<sub>2</sub>) not observed; LCMS (System B) R<sub>t</sub> 0.90 min, m/z 330 ([M+H]<sup>+</sup>).

**2-Butyl-7-(5-(3-fluoroazetidin-1-yl)pentyl)-5H-pyrrolo[3,2-d]pyrimidin-4-amine (211n)**



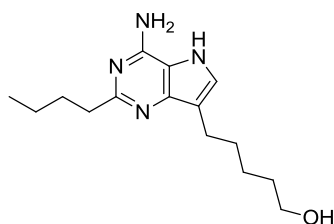
Chemical Formula: C<sub>18</sub>H<sub>28</sub>FN<sub>5</sub>  
Molecular Weight: 333.45

A filtered solution of 5-((benzyloxy)methyl)-2-butyl-7-(5-(3-fluoroazetidin-1-yl)pent-1-yn-1-yl)-5H-pyrrolo[3,2-d]pyrimidin-4-amine (**213n**) (60.0 mg, 0.13

mmol) in EtOH (5 mL) and AcOH (1 mL) was hydrogenated using the H-cube™ (settings: 60 °C, Full H<sub>2</sub>, 1 mL/min flow rate) and a 10% Pd/C CatCart 30 as the catalyst. The solution was re-hydrogenated using the H-cube™ (settings: 60 °C, Full H<sub>2</sub>, 1 mL/min flow rate) and the same 10% Pd/C CatCart 30 as the catalyst. The reaction mixture was concentrated *in vacuo* and the residue was dissolved in 1:1 MeOH:DMSO (1 mL) and purified by MDAP on an Xbridge column using MeCN-water with an ammonium carbonate modifier. The solvent was evaporated *in vacuo* to give the title compound (19.5 mg, 44 %) as a beige solid.

<sup>1</sup>H NMR (400 MHz, MeOD) δ 7.33 (s, 1H), 5.14 (dm, *J* = 19 Hz, 1H), 3.73 - 3.62 (m, 2H), 3.30 - 3.22 (m, 1H), 2.82 - 2.72 (m, 4H), 2.6 - 2.54 (m, 2H), 1.83 - 1.73 (m, 2H), 1.73 - 1.66 (m, 2H), 1.49 - 1.38 (m, 6H), 0.99 (t, *J* = 7.3 Hz, 3H), missing proton signal visible under MeOH signal, exchangeable protons (NH and NH<sub>2</sub>) not observed; LCMS (System B) R<sub>t</sub> 0.89 min, m/z 334 ([M+H]<sup>+</sup>).

**5-(4-Amino-2-butyl-5H-pyrrolo[3,2-d]pyrimidin-7-yl)pentan-1-ol (211x)**



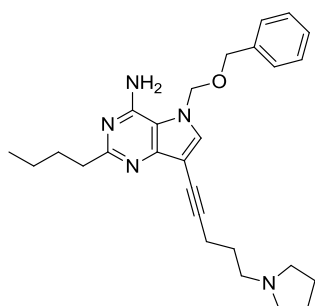
Chemical Formula: C<sub>15</sub>H<sub>24</sub>N<sub>4</sub>O  
Molecular Weight: 276.38

A solution of 5-(4-amino-5-((benzyloxy)methyl)-2-butyl-5H-pyrrolo[3,2-*d*]pyrimidin-7-yl)pent-4-yn-1-ol (**213x**) (90 mg, 0.23 mmol) in EtOH (10 mL) was hydrogenated using the H-cube (settings: 60 °C, Full H<sub>2</sub>, 1 mL/min flow rate) and a 10% Pd/C CatCart 30 as the catalyst. The solution was further hydrogenated using the H-cube (settings: 60 °C, Full H<sub>2</sub>, 1 mL/min flow rate) and a 10% Pd/C CatCart 30 as the catalyst. The reaction mixture was concentrated *in vacuo* and dissolved in 1:1 MeOH:DMSO (1 mL) and purified by MDAP on an Xbridge column using MeCN-water with an ammonium carbonate modifier. The solvent was removed under a

stream of nitrogen in the Radleys™ blowdown apparatus to give the title compound (18 mg, 28 %) as a white solid.

<sup>1</sup>H NMR (400 MHz, MeOD) δ 7.21 (s, 1H), 3.54 (t, *J* = 6.5 Hz, 2H), 3.33 (s, 2H), 2.77 - 2.68 (m, 4H), 1.79 - 1.64 (m, 4H), 1.63 - 1.52 (m, 2H), 1.49 - 1.35 (m, 4H), 0.94 (t, *J* = 7.4 Hz, 3H) exchangeable protons (NH, NH<sub>2</sub> and OH) not observed; LCMS (System B) R<sub>t</sub> 0.75 min, m/z 277 ([M+H]<sup>+</sup>).

**5-((Benzyloxy)methyl)-2-butyl-7-(5-(pyrrolidin-1-yl)pent-1-yn-1-yl)-5H-pyrrolo[3,2-*d*]pyrimidin-4-amine (213b)**



Chemical Formula: C<sub>27</sub>H<sub>35</sub>N<sub>5</sub>O  
Molecular Weight: 445.60

To a stirred solution of 5-((benzyloxy)methyl)-2-butyl-7-(5-chloropent-1-yn-1-yl)-5H-pyrrolo[3,2-*d*]pyrimidin-4-amine (**213y**) (150 mg, 0.37 mmol) and triethylamine (0.061 mL, 0.44 mmol) in anhydrous MeCN (3 mL) at ambient temperature was added neat pyrrolidine (0.033 mL, 0.40 mmol). The reaction mixture was stirred at ambient temperature for 1.5 h before being warmed to 60 °C for 2.5 h and then to 80 °C for 16 h. To the reaction mixture was added further pyrrolidine (0.033 mL, 0.40 mmol) and triethylamine (0.061 mL, 0.44 mmol) and heating at 80 °C continued for 10 h before the reaction mixture was concentrated *in vacuo* and the residue partitioned between DCM (10 mL) and water (10 mL). The organic phase was separated and dried (hydrophobic frit) before concentration *in vacuo* before being dissolved in DCM and purified on an aminopropyl functionalised silica cartridge (11 g) using a 0-100% EtOAc-DCM gradient over 20 mins. The appropriate fractions

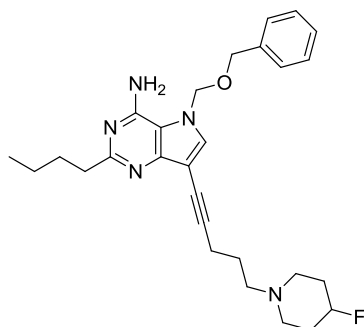
were combined and evaporated *in vacuo* to give the title compound (95 mg, 58%) as an off-white solid.

<sup>1</sup>H NMR (400 MHz, CDCl<sub>3</sub>) δ 7.42 - 7.33 (m, 3H), 7.31 - 7.26 (m, 2H), 7.23 (s, 1H), 5.62 (br s, 2H), 5.45 (s, 2H), 4.54 (s, 2H), 2.90 - 2.82 (m, 2H), 2.65 - 2.59 (m, 2H), 2.58 - 2.51 (m, 6H), 1.93 - 1.76 (m, 8H), 1.50 - 1.39 (m, 2H), 0.96 (t, *J* = 7.4 Hz, 3H); <sup>13</sup>C NMR (126 MHz, CDCl<sub>3</sub>) δ 165.0, 151.7, 150.7, 135.3, 134.1, 128.8, 128.7, 128.4, 113.1, 99.5, 92.7, 76.9, 71.3, 69.8, 55.7, 54.2, 39.4, 31.5, 28.1, 23.5, 22.9, 18.2, 14.1; LCMS (System B) R<sub>t</sub> 1.23 min, m/z 446 ([M+H]<sup>+</sup>); HRMS Anal. Calcd. For C<sub>27</sub>H<sub>35</sub>N<sub>5</sub>O = 446.2914. Found = 446.2930 ([M+H]<sup>+</sup>); IR (cm<sup>-1</sup>) 3407, 2963, 2801, 1652, 1591, 1534; Mpt. 134-136 °C.

**Optimised conditions:** To a stirred solution of 5-((benzyloxy)methyl)-2-butyl-7-(5-chloropent-1-yn-1-yl)-5*H*-pyrrolo[3,2-*d*]pyrimidin-4-amine (**213y**) (1.17 g, 2.85 mmol) in MeCN (20 mL) was added triethylamine (1.191 mL, 8.54 mmol) and pyrrolidine (0.706 mL, 8.54 mmol). The reaction mixture was heated at 60 °C for 16 h. To the reaction mixture was added further aliquots of pyrroline (0.12 mL, 1.45 mmol) and triethylamine (0.2 mL, 1.42 mmol) and heating at 60 °C was continued for a further 1.5 h. To the reaction mixture was added further pyrroline (0.12 mL, 1.45 mmol) and triethylamine (0.2 mL, 1.42 mmol) and heating at 60 °C was continued for a further 1.5 h. The reaction mixture was allowed to cool to ambient temperature, and was partitioned between EtOAc (100 mL) and water (100 mL). The organic layer was separated and back extracted with EtOAc (2 x 50 mL). The combined organic extracts were dried (MgSO<sub>4</sub>), filtered and concentrated *in vacuo* to give a brown solid. The solid was dissolved in DCM and purified on an aminopropyl functionalised silica cartridge (110 g) using a 0-10% MeOH-DCM gradient over 60 mins. The appropriate fractions were combined and evaporated *in vacuo* to give a pale yellow solid. This solid was triturated with Et<sub>2</sub>O and was collected by filtration and dried *in vacuo* to give the title compound (724 mg, 57 % yield) as an off white solid. The filtrate was combined with fractions from the column that were not pure, yet contained product and were concentrated *in vacuo*.

The resultant solid was triturated with Et<sub>2</sub>O and the resulting solid collected by filtration and dried *in vacuo* to give a further batch of title compound (159 mg, 12 %) as a beige solid.

**5-((Benzyloxy)methyl)-2-butyl-7-(5-(4-fluoropiperidin-1-yl)pent-1-yn-1-yl)-5H-pyrrolo[3,2-d]pyrimidin-4-amine (213c)**



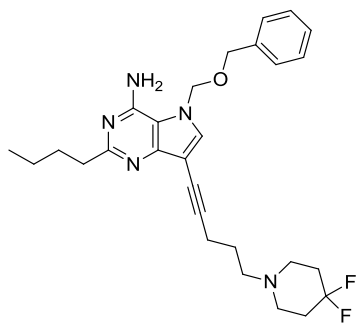
Chemical Formula: C<sub>28</sub>H<sub>36</sub>FN<sub>5</sub>O  
Molecular Weight: 477.62

To a stirred mixture of 5-((benzyloxy)methyl)-2-butyl-7-(5-chloropent-1-yn-1-yl)-5H-pyrrolo[3,2-d]pyrimidin-4-amine (**213y**) (150 mg, 0.37 mmol), triethylamine (0.153 mL, 1.10 mmol) and sodium iodide (55 mg, 0.37 mmol) in MeCN (3 mL) was added solid 4-fluoropiperidine hydrochloride (76 mg, 0.55 mmol) and the reaction mixture was heated at 80 °C for 16 h, before addition of further 4-fluoropiperidine hydrochloride (76 mg, 0.548 mmol) and triethylamine (0.153 mL, 1.10 mmol). The reaction mixture was stirred at 80 °C for a further 21 h. The reaction mixture was concentrated *in vacuo* and the residue partitioned between DCM (10 mL) and water (10 mL), the organic phase was separated and dried (hydrophobic frit) before concentration *in vacuo*. This residue was dissolved in DCM and purified on an aminopropyl functionalised silica cartridge (11 g) using a 0-100% EtOAc-cyclohexane+0-20% MeOH over 40 mins. The appropriate fractions were combined and evaporated *in vacuo* to give the title compound (68 mg, 39 %) as a white solid.

<sup>1</sup>H NMR (400 MHz, CDCl<sub>3</sub>) δ 7.42 - 7.33 (m, 3H), 7.32 - 7.26 (m, 2H), 7.23 (s, 1H), 5.62 (s, 2H), 5.46 (s, 2H), 4.67 (dm, *J* = 49 Hz, 1H), 4.54 (s, 2H), 2.89 - 2.80 (m,

2H), 2.67 - 2.58 (m, 2H), 2.57 - 2.49 (m, 4H), 2.44 - 2.35 (m, 2H), 2.00 - 1.74 (m, 8H), 1.50 - 1.38 (m, 2H), 0.96 (t,  $J = 7.3$  Hz, 3H); LCMS (System B)  $R_t$  1.24 min,  $m/z = 478$  ( $[M+H]^+$ ).

**5-((Benzyloxy)methyl)-2-butyl-7-(5-(4,4-difluoropiperidin-1-yl)pent-1-yn-1-yl)-5H-pyrrolo[3,2-d]pyrimidin-4-amine (213d)**

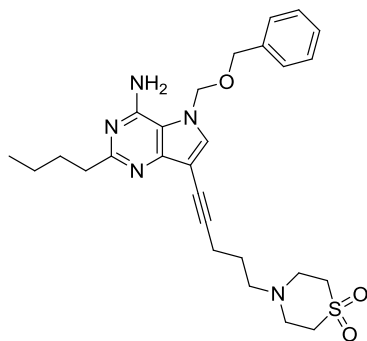


Chemical Formula:  $C_{28}H_{35}F_2N_5O$   
Molecular Weight: 495.61

To a stirred suspension of 5-((benzyloxy)methyl)-2-butyl-7-(5-chloropent-1-yn-1-yl)-5H-pyrrolo[3,2-d]pyrimidin-4-amine (**213y**) (150 mg, 0.37 mmol) and 4,4-difluoropiperidine hydrochloride (86 mg, 0.55 mmol) in anhydrous MeCN (3 mL) at ambient temperature was added triethylamine (0.153 mL, 1.10 mmol) in one charge. The reaction mixture was sealed and heated in a Biotage Initiator microwave (absorption setting normal) to 150 °C for 30 min. The reaction mixture was further heated in a Biotage Initiator microwave (absorption setting normal) to 170 °C for 60 min. After cooling of the reaction mixture further 4,4-difluoropiperidine hydrochloride (86 mg, 0.548 mmol) and triethylamine (0.153 mL, 1.10 mmol) were added and the reaction mixture was re-sealed and heated in a Biotage Initiator microwave (absorption setting normal) to 150 °C for 60 min. The reaction mixture was concentrated *in vacuo* and partitioned between DCM (10 mL) and water (10 mL). The organic phase was separated and dried (hydrophobic frit) and concentrated *in vacuo* before being dissolved in DCM and purified on an aminopropyl functionalised silica cartridge (11 g) using a 0-100 % EtOAc:DCM gradient over 20 mins. The appropriate fractions were concentrated *in vacuo* to give the title compound (77 mg, 43%).

$^1\text{H}$  NMR (400 MHz,  $\text{CDCl}_3$ )  $\delta$  7.42 - 7.33 (m, 3H), 7.32 - 7.25 (m, 2H), 7.23 (s, 1H), 5.62 (s, 2H), 5.46 (s, 2H), 4.54 (s, 2H), 2.89 - 2.81 (m, 2H), 2.63 - 2.52 (m, 6H), 2.07 - 1.95 (m, 4H), 1.88 - 1.77 (m, 4H), 1.66 (br s, 2H), 1.50 - 1.40 (m, 2H), 1.00 - 0.95 (m, 3H); LCMS (System A)  $R_t$  0.62 min,  $m/z$  496 ( $[\text{M}+\text{H}]^+$ ).

**4-(5-(4-Amino-5-((benzyloxy)methyl)-2-butyl-5H-pyrrolo[3,2-d]pyrimidin-7-yl)pent-4-yn-1-yl)thiomorpholine 1,1-dioxide (213e)**



Chemical Formula:  $\text{C}_{27}\text{H}_{35}\text{N}_5\text{O}_3\text{S}$   
Molecular Weight: 509.66

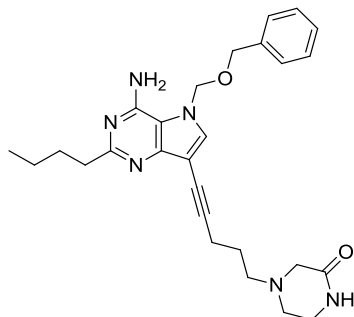
To a stirred mixture of 5-((benzyloxy)methyl)-2-butyl-7-(5-chloropent-1-yn-1-yl)-5H-pyrrolo[3,2-d]pyrimidin-4-amine (**213y**) (150 mg, 0.37 mmol), triethylamine (0.076 mL, 0.55 mmol) and sodium iodide (55 mg, 0.37 mmol) in MeCN (3 mL) was added thiomorpholine 1,1-dioxide (74.0 mg, 0.55 mmol) and the reaction mixture was heated at 80 °C for 16 h. Further thiomorpholine 1,1-dioxide (74.0 mg, 0.55 mmol) and triethylamine (0.076 mL, 0.55 mmol) were added, and stirring at 80 °C was continued for 21 h. The reaction mixture was concentrated *in vacuo* and the residue partitioned between DCM (10 mL) and water (10 mL), the organic phase was separated and dried (hydrophobic frit) before concentration *in vacuo* before being dissolved in DCM and purified on an aminopropyl functionalised silica cartridge (11 g) using a 0-100% EtOAc-cyclohexane + 0-20% MeOH gradient over 40 mins. The appropriate fractions were combined and concentrated *in vacuo* to give the title compound (108 mg, 58%) as an off white foam.

$^1\text{H}$  NMR (400 MHz,  $\text{CDCl}_3$ )  $\delta$  7.41 - 7.33 (m, 3H), 7.31 - 7.25 (m, 2H), 7.22 (s, 1H), 5.64 (br s, 2H), 5.46 (s, 2H), 4.55 (s, 2H), 3.06 (s, 8H), 2.87 - 2.81 (m, 2H), 2.73 (t, J



= 7.0 Hz, 2H), 2.56 (t,  $J = 6.9$  Hz, 2H), 1.87 - 1.77 (m, 4H), 1.49 - 1.39 (m, 2H), 0.96 (t,  $J = 7.3$  Hz, 3H); LCMS (System B)  $R_t$  1.08 min,  $m/z$  510 ( $[M+H]^+$ ).

**4-(5-(4-Amino-5-((benzyloxy)methyl)-2-butyl-5H-pyrrolo[3,2-d]pyrimidin-7-yl)pent-4-yn-1-yl)piperazin-2-one (213f)**

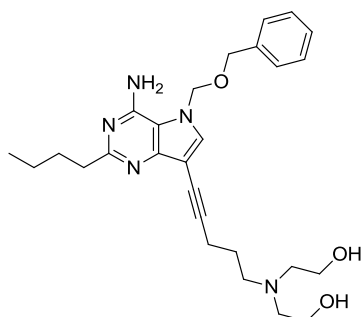


Chemical Formula:  $C_{27}H_{34}N_6O_2$   
Molecular Weight: 474.60

To a stirred solution of 5-((benzyloxy)methyl)-2-butyl-7-(5-chloropent-1-yn-1-yl)-5H-pyrrolo[3,2-d]pyrimidin-4-amine (**213y**) (150 mg, 0.37 mmol) and triethylamine (0.13 mL, 0.92 mmol) in anhydrous MeCN (3 mL) at ambient temperature was added neat piperazin-2-one (91 mg, 0.91 mmol) in one charge. The reaction mixture was heated to 80 °C for 16 h. before further piperazin-2-one (91 mg, 0.91 mmol) and triethylamine (0.13 mL, 0.92 mmol) were added and heating at 80 °C was continued for 16 h. The reaction mixture was concentrated *in vacuo* and the residue dissolved in DCM (10 mL) and washed with water (10 mL). The resulting organic phase was dried (hydrophobic frit) and concentrated *in vacuo* to give a yellow oil which was dissolved in DCM and purified on an aminopropyl functionalised silica cartridge (11 g) using a 0-25% MeOH-DCM gradient over 20 mins. The appropriate fractions were combined and evaporated *in vacuo* to give the title compound (41 mg, 24%) as a yellow foam.

$^1H$  NMR (400 MHz,  $CDCl_3$ )  $\delta$  7.40 - 7.35 (m, 3H), 7.30 - 7.27 (m, 2H), 7.24 (s, 1H), 5.96 (br s, 1H), 5.66 (s, 2H), 5.46 (s, 2H), 4.55 (s, 2H), 3.41 - 3.37 (m, 2H), 3.19 (s, 2H), 2.88 - 2.83 (m, 2H), 2.71 (t,  $J = 5.5$  Hz, 2H), 2.63 (t,  $J = 7.2$  Hz, 2H), 2.57 (t,  $J = 7.2$  Hz, 2H), 1.87 - 1.79 (m, 4H), 1.49 - 1.39 (m, 2H), 0.96 (t,  $J = 7.3$  Hz, 3H); LCMS (System B)  $R_t$  0.98 min,  $m/z$  475 ( $[M+H]^+$ ).

**2,2'-((5-(4-Amino-5-((benzyloxy)methyl)-2-butyl-5H-pyrrolo[3,2-d]pyrimidin-7-yl)pent-4-yn-1-yl)azanediyl)diethanol (213g)**

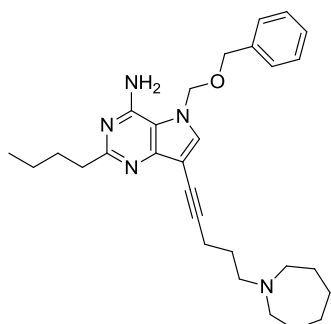


Chemical Formula: C<sub>27</sub>H<sub>37</sub>N<sub>5</sub>O<sub>3</sub>  
Molecular Weight: 479.61

To a stirred solution of 5-((benzyloxy)methyl)-2-butyl-7-(5-chloropent-1-yn-1-yl)-5H-pyrrolo[3,2-d]pyrimidin-4-amine (**213y**) (150 mg, 0.37 mmol) and diethanolamine (60 mg, 0.57 mmol) in anhydrous DMF (3 mL) at ambient temperature was added cesium carbonate (143 mg, 0.44 mmol) in one charge. The reaction mixture was heated at 90 °C for 6 h. The reaction mixture was filtered and to the filtrate was added further diethanolamine (120 mg, 1.4 mmol) and triethylamine (0.10 mL, 0.73 mmol) before heating to 80 °C for 16 h. At this time further diethanolamine (120 mg, 1.40 mmol) was added and heating at 80 °C continued for 5 h. The reaction mixture was concentrated *in vacuo* and the residue partitioned between DCM (10 mL) and water (10 mL). The organic phase was separated and dried (hydrophobic frit) before concentration *in vacuo* and loading in DCM and purification on an aminopropyl functionalised silica cartridge (11 g) using a 0-100% EtOAc-DCM gradient over 20 mins. The cartridge was further eluted with a 0-25% MeOH/DCM gradient over 20 mins. The appropriate fractions were combined and concentrated *in vacuo* to give the title compound (67 mg, 39%) as an off white solid.

<sup>1</sup>H NMR (400 MHz, CDCl<sub>3</sub>) δ 7.40 - 7.35 (m, 3H), 7.32 - 7.28 (m, 2H), 7.25 (s, 1H), 5.67 (br s, 2H), 5.45 (s, 2H), 4.55 (s, 2H), 3.99 - 3.78 (m, 2H), 3.72 (t, *J* = 5.1 Hz, 4H), 2.89 - 2.81 (m, 4H), 2.70 - 2.60 (m, 6H), 1.84 - 1.74 (m, 4H), 1.49 - 1.38 (m, 2H), 0.96 (t, *J* = 7.3 Hz, 3H); LCMS (System B) R<sub>t</sub> 1.02 min, m/z 480 ([M+H]<sup>+</sup>)  
Note: compound only 87% pure by UV.

**7-(5-(Azepan-1-yl)pent-1-yn-1-yl)-5-((benzyloxy)methyl)-2-butyl-5H-pyrrolo[3,2-d]pyrimidin-4-amine (213i)**



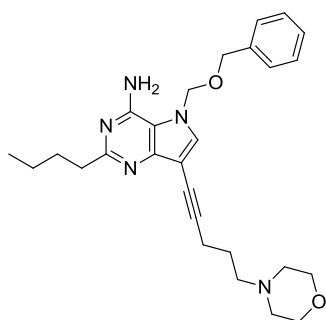
Chemical Formula: C<sub>29</sub>H<sub>39</sub>N<sub>5</sub>O  
Molecular Weight: 473.65

To a stirred solution of 5-((benzyloxy)methyl)-2-butyl-7-(5-chloropent-1-yn-1-yl)-5H-pyrrolo[3,2-d]pyrimidin-4-amine (**213y**) (750 mg, 1.83 mmol) in MeCN (15 mL) was added triethylamine (0.763 mL, 5.48 mmol) and azepane (0.631 mL, 5.48 mmol). The resultant mixture was heated at 60 °C for 16 h. To the reaction mixture was added further azepane (0.42 mL, 3.3 mmol) and further triethylamine (0.51 mL, 3.3 mmol) and the mixture was stirred at 60 °C for a further 16 h. The reaction mixture was concentrated *in vacuo* and the residue partitioned between EtOAc (50 mL) and water (50 mL). The organic phase was separated and the aqueous phase back extracted with EtOAc (50 mL). The combined organic extracts were washed with brine (100 mL), dried (MgSO<sub>4</sub>), filtered and concentrated *in vacuo* to give a brown solid (770 mg). The sample was dissolved in DCM and purified on an aminopropyl functionalised silica cartridge (110 g) using a 0-10% MeOH-DCM gradient over 60 mins. The appropriate fractions were combined and evaporated *in vacuo* to give the title compound (543 mg, 63 %) as an off-white solid.

<sup>1</sup>H NMR (400 MHz, CDCl<sub>3</sub>) δ 7.40 - 7.34 (m, 3H), 7.30 - 7.25 (m, 2H), 7.22 (s, 1H), 5.63 (br s, 2H), 5.45 (s, 2H), 4.53 (s, 2H), 2.88 - 2.81 (m, 2H), 2.70 - 2.59 (m, 6H), 2.52 (t, *J* = 7.3 Hz, 2H), 1.89 - 1.76 (m, 4H), 1.70 - 1.57 (m, 8H), 1.48 - 1.37 (m, 2H), 0.95 (t, *J* = 7.4 Hz, 3H); <sup>13</sup>C NMR (126 MHz, CDCl<sub>3</sub>) δ 165.0, 151.7, 150.8, 135.3, 134.1, 128.8, 128.7, 128.4, 113.1, 99.6, 93.0, 76.9, 71.1, 69.8, 57.3, 55.5, 39.4, 31.5, 28.1, 27.0, 26.9, 22.9, 18.0, 14.1; HRMS Anal. Calcd. For C<sub>29</sub>H<sub>40</sub>N<sub>5</sub>O =

474.3227 . Found = 474.3227 ( $[M+H]^+$ ); LCMS (System B)  $R_t$  1.27 min,  $m/z$  474 ( $[M+H]^+$ ); IR ( $\text{cm}^{-1}$ ) 3425, 3064, 2925, 2868, 1646, 1591, 1533; Mpt. 140-142 °C.

**5-((Benzyloxy)methyl)-2-butyl-7-(5-morpholinopent-1-yn-1-yl)-5H-pyrrolo[3,2-*d*]pyrimidin-4-amine (213j)**

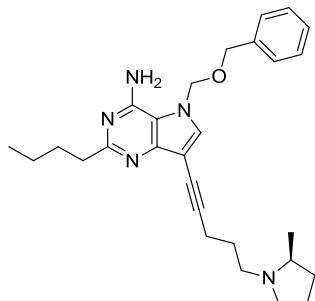


Chemical Formula:  $C_{27}H_{35}N_5O_2$   
Molecular Weight: 461.60

To a stirred solution of 5-((benzyloxy)methyl)-2-butyl-7-(5-chloropent-1-yn-1-yl)-5H-pyrrolo[3,2-*d*]pyrimidin-4-amine (**213y**) (200 mg, 0.49 mmol) in MeCN (4 mL) was added triethylamine (0.20 mL, 1.46 mmol) and morpholine (0.13 mL, 1.46 mmol). The resultant mixture was heated at 60 °C for 22 h. To the reaction mixture was added further morpholine (0.04 mL, 0.49 mmol) and the temperature was increased to 80 °C for a further 7 h. To the reaction mixture was added further morpholine (0.04 mL, 0.49 mmol) and the reaction mixture was stirred at 80 °C for a further 16 h. The reaction mixture was concentrated *in vacuo* and the residue partitioned between DCM (20 mL) and water (20 mL). The organic layer was separated and dried (hydrophobic frit) before concentration *in vacuo* to give a yellow oil. The sample was dissolved in DCM and purified on an aminopropyl functionalised silica cartridge (11 g) using a 0-100% EtOAc-cyclohexane gradient over 40 mins. The appropriate fractions were combined and evaporated *in vacuo* to give the title compound (130 mg, 58 %) as a white solid.

$^1\text{H}$  NMR (400 MHz,  $\text{CDCl}_3$ )  $\delta$  7.32 - 7.26 (m, 3H), 7.22 - 7.18 (m, 2H), 7.15 (s, 1H), 5.56 (br s, 2H), 5.37 (s, 2H), 4.45 (s, 2H), 3.69 - 3.62 (m, 4H), 2.81 - 2.74 (m, 2H), 2.51 - 2.37 (m, 8H), 1.82 - 1.68 (m, 4H), 1.42 - 1.30 (m, 2H), 0.87 (t,  $J = 7.3$  Hz, 3H); LCMS (System B)  $R_t$  1.09 min,  $m/z$  462 ( $[M+H]^+$ ).

**(S)-5-((benzyloxy)methyl)-2-butyl-7-(5-(2-methylpyrrolidin-1-yl)pent-1-yn-1-yl)-5H-pyrrolo[3,2-d]pyrimidin-4-amine (213k)**

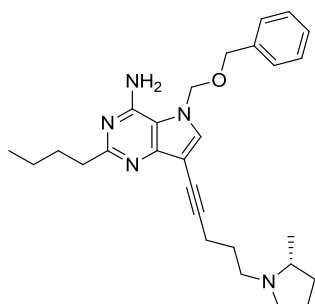


Chemical Formula: C<sub>28</sub>H<sub>37</sub>N<sub>5</sub>O  
Molecular Weight: 459.63

To a stirred solution of 5-((benzyloxy)methyl)-2-butyl-7-(5-chloropent-1-yn-1-yl)-5H-pyrrolo[3,2-d]pyrimidin-4-amine (**213y**) (200 mg, 0.49 mmol) in MeCN (4 mL) was added triethylamine (0.20 mL, 1.46 mmol) and (*S*)-2-methylpyrrolidine (0.15 mL, 1.46 mmol). The resultant mixture was heated at 60 °C for 72 h. To the reaction mixture was added further (*S*)-2-methylpyrrolidine (0.05 mL, 0.49 mmol) and further triethylamine (0.07 mL, 0.49 mmol) and the reaction mixture heated to 80 °C for 5 h. The reaction mixture was concentrated *in vacuo* and the residue partitioned between DCM (20 mL) and water (20 mL). The organic was separated and dried (hydrophobic frit) before concentration *in vacuo* to give a red oil. The oil was dissolved in DCM and purified on an aminopropyl functionalised silica cartridge (11 g) using a 0-50% EtOAc-cyclohexane gradient over 40 mins. The appropriate fractions were combined and evaporated *in vacuo* to give the title compound (142 mg, 64%) as a colourless oil which solidified.

<sup>1</sup>H NMR (400 MHz, CDCl<sub>3</sub>) δ 7.46 - 7.35 (m, 3H), 7.33 - 7.27 (m, 2H), 7.24 (s, 1H), 5.64 (s, 2H), 5.47 (s, 2H), 4.55 (s, 2H), 3.16 - 3.33 (m, 1H), 2.94 - 3.08 (m, 1H), 2.82 - 2.91 (m, 2H), 2.51 - 2.64 (m, 2H), 2.12 - 2.45 (m, 3H), 1.65 - 2.01 (m, 7H), 1.40 - 1.55 (m, 3H), 1.17 (br. s., 3H), 0.97 (t, *J* = 7.3 Hz, 3H); LCMS (System B) R<sub>t</sub> 1.15 min, *m/z* 460 ([M+H]<sup>+</sup>).

**(R)-5-((benzyloxy)methyl)-2-butyl-7-(5-(2-methylpyrrolidin-1-yl)pent-1-yn-1-yl)-5H-pyrrolo[3,2-d]pyrimidin-4-amine (213l)**

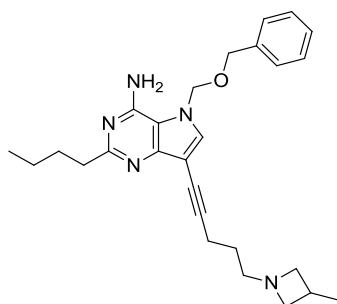


Chemical Formula: C<sub>28</sub>H<sub>37</sub>N<sub>5</sub>O  
Molecular Weight: 459.63

To a stirred solution of 5-((benzyloxy)methyl)-2-butyl-7-(5-chloropent-1-yn-1-yl)-5H-pyrrolo[3,2-d]pyrimidin-4-amine (**213y**) (200 mg, 0.49 mmol) in MeCN (4 mL) was added triethylamine (0.20 mL, 1.46 mmol) and (*R*)-2-methylpyrrolidine (0.149 mL, 1.46 mmol). The resultant mixture was heated at 60 °C for 72 h. To the reaction was added further (*R*)-2-methylpyrrolidine (0.05 mL, 0.49 mmol) and further triethylamine (0.07 mL, 0.49 mmol) and the reaction heated to 80 °C for 5 h. The reaction mixture was concentrated *in vacuo* and the residue partitioned between DCM (20 mL) and water (20 mL). The organic phase was separated and dried (hydrophobic frit) before concentration *in vacuo* to give a red oil. The oil was dissolved in DCM and purified on an aminopropyl functionalised silica cartridge (11 g) using a 0-50% EtOAc-cyclohexane gradient over 40 mins. The appropriate fractions were combined and evaporated *in vacuo* to give the title compound (101 mg, 45%) as a colourless oil which solidified.

<sup>1</sup>H NMR (400 MHz, CDCl<sub>3</sub>) δ 7.32 - 7.27 (m, 3H), 7.23 - 7.18 (m, 2H), 7.24 (s, 1H), 5.69 (br s, 2H), 5.37 (s, 2H), 4.45 (s, 2H), 3.28 - 3.10 (m, 1H), 2.97 - 2.87 (m, 1H), 2.79 - 2.73 (m, 2H), 2.54 - 2.41 (m, 2H), 2.23 - 2.07 (m, 3H), 1.93 - 1.57 (m, 7H), 1.45 - 1.30 (m, 3H), 1.08 (d, *J* = 6.1 Hz, 3H), 0.87 (t, *J* = 7.3 Hz, 3H); LCMS (System B) R<sub>t</sub> 1.12 min, m/z 460 ([M+H]<sup>+</sup>).

**5-((Benzyloxy)methyl)-2-butyl-7-(5-(3-methylazetididin-1-yl)pent-1-yn-1-yl)-5H-pyrrolo[3,2-d]pyrimidin-4-amine (213m)**

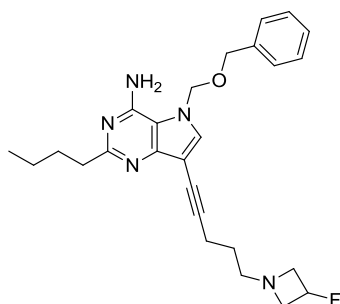


Chemical Formula: C<sub>27</sub>H<sub>35</sub>N<sub>5</sub>O  
Molecular Weight: 445.60

To a stirred suspension of 5-(4-amino-5-((benzyloxy)methyl)-2-butyl-5H-pyrrolo[3,2-d]pyrimidin-7-yl)pent-4-ynal (**213z**) (90 mg, 0.23 mmol) and 4 Å molecular sieves in anhydrous DCM (4 mL) under nitrogen was added a solution of 3-methylazetididine, hydrochloride (28 mg, 0.26 mmol) and triethylamine (0.04 mL, 0.29 mmol) in anhydrous DCM (1 mL). The reaction mixture was stirred at ambient temperature for 1 min. before addition of sodium triacetoxyborohydride (98 mg, 0.46 mmol), stirring at ambient temperature was continued for 4 h. The reaction mixture was diluted with DCM (15 mL) and filtered through celite. The filtrate was washed with saturated aqueous sodium bicarbonate (20 mL), dried (hydrophobic frit) and concentrated *in vacuo* to give a brown oil. The oil was dissolved in DCM and purified on an aminopropyl functionalised silica cartridge (11 g) using a 0-100% EtOAc-cyclohexane gradient over 30 mins. The appropriate fractions were combined and evaporated *in vacuo* to give the title compound (33 mg, 32%) as a colourless oil.

<sup>1</sup>H NMR (400 MHz, CDCl<sub>3</sub>) δ 7.32 - 7.27 (m, 3H), 7.23 - 7.19 (m, 2H), 7.16 (s, 1H), 5.58 (br s, 2H), 5.38 (s, 2H), 4.46 (s, 2H), 3.47 - 3.41 (m, 2H), 2.81 - 2.74 (m, 2H), 2.69 - 2.63 (m, 2H), 2.56 - 2.48 (m, 3H), 2.44 (t, *J* = 7.2 Hz, 2H), 1.80 - 1.69 (m, 2H), 1.66 - 1.57 (m, 2H), 1.42 - 1.31 (m, 2H), 1.08 (d, *J* = 6.9 Hz, 3H), 0.93 - 0.83 (m, 3H); LCMS (System B) R<sub>t</sub> 1.19 min, m/z 446 ([M+H]<sup>+</sup>).

**5-((Benzyloxy)methyl)-2-butyl-7-(5-(3-fluoroazetidin-1-yl)pent-1-yn-1-yl)-5H-pyrrolo[3,2-d]pyrimidin-4-amine (213n)**



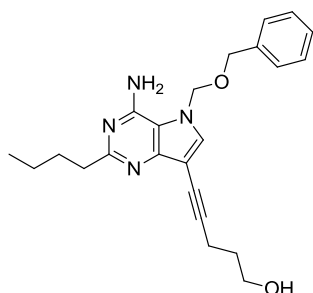
Chemical Formula: C<sub>26</sub>H<sub>32</sub>FN<sub>5</sub>O  
Molecular Weight: 449.56

To a stirred suspension of 5-(4-amino-5-((benzyloxy)methyl)-2-butyl-5H-pyrrolo[3,2-d]pyrimidin-7-yl)pent-4-ynal (**213z**) (100 mg, 0.26 mmol) and 4Å molecular sieves in anhydrous DCM (4 mL) under nitrogen was added a solution of 3-fluoroazetidine, hydrochloride (34 mg, 0.31 mmol) and triethylamine (0.046 mL, 0.33 mmol) in anhydrous DCM (2 mL). The reaction mixture was stirred at ambient temperature for 1 min before addition of sodium triacetoxyborohydride (109 mg, 0.51 mmol), stirring at ambient temperature was continued for 4 h. The reaction mixture was diluted with DCM (15 mL) and filtered through celite. The filtrate was washed with saturated aqueous sodium bicarbonate (20 mL), dried (hydrophobic frit) and concentrated *in vacuo* to give a brown oil. The oil was dissolved in DCM and purified on an aminopropyl functionalised silica cartridge (11 g) using a 0-100% EtOAc-cyclohexane gradient over 30 mins. The appropriate fractions were combined and evaporated *in vacuo* to give the title compound (62 mg, 54 % yield) as a colourless oil.

<sup>1</sup>H NMR (400 MHz, CDCl<sub>3</sub>) δ 7.42 - 7.35 (m, 3H), 7.30 - 7.27 (m, 2H), 7.24 (s, 1H), 5.71 (br s, 2H), 5.46 (s, 2H), 5.26 - 5.05 (dm, *J* = 57 Hz, 1H), 4.54 (s, 2H), 3.79 - 3.70 (m, 2H), 3.24 - 3.19 (m, 1H), 3.18 - 3.13 (m, 1H), 2.87 - 2.83 (m, 2H), 2.73 - 2.68 (m 2H), 2.54 (t, *J* = 7.2 Hz, 2H), 1.87 - 1.77 (m, 2H), 1.77-1.68 (m, 2H), 1.49 - 1.39 (m, 2H), 0.96 (t, *J* = 7.5 Hz, 3H); LCMS (System B) R<sub>t</sub> 1.12 min, m/z 450 ([M+H]<sup>+</sup>).



**5-(4-Amino-5-((benzyloxy)methyl)-2-butyl-5H-pyrrolo[3,2-d]pyrimidin-7-yl)pent-4-yn-1-ol (213x)**

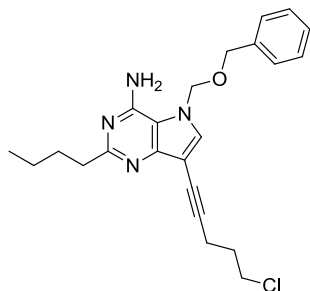


Chemical Formula: C<sub>23</sub>H<sub>28</sub>N<sub>4</sub>O<sub>2</sub>  
Molecular Weight: 392.49

To a degassed suspension of 5-((benzyloxy)methyl)-2-butyl-7-iodo-5H-pyrrolo[3,2-d]pyrimidin-4-amine (**131**) (3.00 g, 6.88 mmol), copper(I) iodide (0.68 g, 1.38 mmol), and *bis*(triphenylphosphine)palladium(II) dichloride (0.48 g, 0.69 mmol) in anhydrous DMF (45 mL) was added a solution of pent-4-yn-1-ol (0.69 g, 8.25 mmol) and triethylamine (1.43 mL, 10.3 mmol) in anhydrous DMF (25 mL) dropwise over 10 min. The reaction mixture was stirred at ambient temperature for 18 h before being concentrated *in vacuo* and the residue being partitioned between EtOAc (500 mL) and water (500 mL). The organic phase was separated and the aqueous phase back extracted with EtOAc (250 mL). The combined organic phases were washed with brine (400 mL), dried (MgSO<sub>4</sub>), filtered and concentrated *in vacuo* to give a red oil (4.2 g). The oil was diluted with DCM and purified on two silica cartridges (2 x 100 g) using a 0-100% EtOAc-DCM+0-20% MeOH gradient over 60 mins. The cleanest fractions (by TLC) were combined and evaporated *in vacuo* to give a yellow gum. Trituration with diethyl ether yielded a yellow solid that was collected by filtration and dried *in vacuo* to give the title compound (723 mg, 27 %) as a pale yellow solid. All remaining column fractions that contain product were combined and concentrated *in vacuo* and were dissolved in DCM and purified on a silica cartridge (100 g) using a 0-10% MeOH-DCM gradient over 60 mins. The appropriate fractions were combined and evaporated *in vacuo* and azeotroped with diethyl ether to give further title compound (867 mg, 32 % yield) as an orange foam.

$^1\text{H}$  NMR (400 MHz,  $\text{CDCl}_3$ )  $\delta$  7.42 - 7.33 (m, 3H), 7.31 - 7.25 (m, 2H), 7.21 (s, 1H), 5.65 (br s, 2H), 5.45 (s, 2H), 4.54 (s, 2H), 3.89 (t,  $J = 5.9$  Hz, 2H), 2.90 - 2.82 (m, 2H), 2.64 (t,  $J = 6.9$  Hz, 2H), 1.96 - 1.87 (m, 2H), 1.86 - 1.77 (m, 2H), 1.49 - 1.39 (m, 2H), 0.96 (t,  $J = 7.4$  Hz, 3H) exchangeable proton (OH) not observed;  $^{13}\text{C}$  NMR (101 MHz,  $\text{CDCl}_3$ )  $\delta$  165.0, 151.9, 150.8, 135.2, 133.6, 128.8, 128.7, 128.4, 113.2, 99.4, 92.9, 76.9, 71.9, 69.9, 61.6, 39.1, 31.4, 31.4, 22.8, 16.8, 14.0; LCMS (System B)  $R_t$  0.93 min,  $m/z$  393 ( $[\text{M}+\text{H}]^+$ ); HRMS Anal. Calcd. For  $\text{C}_{23}\text{H}_{29}\text{N}_4\text{O}_2 = 393.2291$ . Found = 393.2304 ( $[\text{M}+\text{H}]^+$ ); IR ( $\text{cm}^{-1}$ ) 3384, 3094, 2953, 1657, 1600, 1541; Mpt. 123-126  $^\circ\text{C}$ .

**5-((Benzyloxy)methyl)-2-butyl-7-(5-chloropent-1-yn-1-yl)-5H-pyrrolo[3,2-*d*]pyrimidin-4-amine (213v)**



Chemical Formula:  $\text{C}_{23}\text{H}_{27}\text{ClN}_4\text{O}$   
Molecular Weight: 410.94

To a degassed suspension of 5-((benzyloxy)methyl)-2-butyl-7-iodo-5H-pyrrolo[3,2-*d*]pyrimidin-4-amine (**131**) (2.77 g, 6.34 mmol), copper(I) iodide (0.24 g, 1.27 mmol), and *bis*(triphenylphosphine)palladium(II) dichloride (0.45 g, 0.63 mmol) in anhydrous DMF (40 mL) was added a solution of 5-chloropent-1-yne (0.781 g, 7.61 mmol) and triethylamine (1.23 mL, 8.88 mmol) in anhydrous DMF (20 mL) dropwise over 2 min. The reaction mixture was stirred at ambient temperature for 17 h before being concentrated *in vacuo* and the resultant brown oil partitioned between water (500 mL) and EtOAc (500 mL). The organic phase was separated and the aqueous phase back extracted with EtOAc (250 mL). The combined organics were washed with brine (400 mL), dried ( $\text{MgSO}_4$ ), filtered and concentrated *in vacuo* and dissolved in DCM and purified on silica cartridges (2 x 100 g) using a 0-100% EtOAc-cyclohexane gradient over 60 mins. The appropriate fractions were

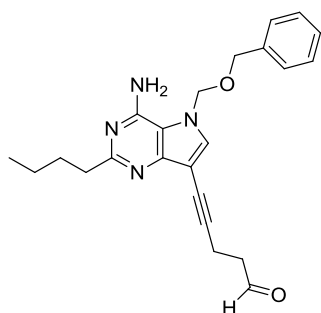
combined and concentrated *in vacuo*, re-dissolved in DCM and purified on a silica cartridge (100 g) using a 0-100% EtOAc-cyclohexane gradient over 80 mins. The appropriate fractions were combined and evaporated *in vacuo* to give the title compound (1.13 g, 43%) as a yellow solid.

$^1\text{H}$  NMR (400 MHz,  $\text{CDCl}_3$ )  $\delta$  7.41 - 7.30 (m, 3H), 7.31 - 7.26 (m, 2H), 7.24 (s, 1H), 5.71 (br s, 2H), 5.46 (s, 2H), 4.54 (s, 2H), 3.75 (t,  $J = 6.5$  Hz, 2H), 2.88 - 2.83 (m, 2H), 2.69 (t,  $J = 6.9$  Hz, 2H), 2.15 - 2.06 (m, 2H), 1.87 - 1.78 (m, 2H), 1.50 - 1.39 (m, 2H), 0.96 (t,  $J = 7.4$  Hz, 3H);  $^{13}\text{C}$  NMR (101 MHz,  $\text{CDCl}_3$ )  $\delta$  165.0, 152.6, 150.8, 135.2, 134.1, 128.8, 128.7, 128.4, 113.1, 99.2, 91.1, 76.9, 72.1, 69.9, 43.9, 39.3, 31.6, 31.4, 22.8, 17.6, 14.0; LCMS (System B)  $R_t$  1.29 min,  $m/z$  411, 413 ( $[\text{M}+\text{H}]^+$ ); HRMS Anal. Calcd. For  $\text{C}_{23}\text{H}_{28}\text{ClN}_4\text{O} = 411.1952$ . Found = 411.1954 ( $[\text{M}+\text{H}]^+$ ); IR ( $\text{cm}^{-1}$ ) 3403, 3123, 1651, 1596, 1540; Mpt. 122-126 °C.

**Optimised conditions:** To a degassed solution of 5-((benzyloxy)methyl)-2-butyl-7-iodo-5*H*-pyrrolo[3,2-*d*]pyrimidin-4-amine (**131**) (5.00 g, 11.5 mmol), *Bis*(triphenylphosphine) palladium(II)dichloride (0.482 g, 0.69 mmol) and copper(I) iodide (0.68 g, 1.38 mmol) in anhydrous DMF (65 mL) was added a solution of 5-chloropent-1-yne (1.528 g, 14.9 mmol) and triethylamine (2.1 mL, 15.1 mmol) in DMF (15 mL) dropwise over 10 min. The reaction mixture was stirred at ambient temperature for 16 h. The majority of the solvent was removed *in vacuo* (water bath max temp 45 °C). The resulting oil was partitioned between EtOAc (300 mL) and Water (300 mL). The organic layer was separated and the aqueous layer back extracted with EtOAc (150 mL). The combined organic extracts were washed with brine (400 mL), dried ( $\text{MgSO}_4$ ), filtered and concentrated *in vacuo* before being dissolved in DCM and purified on a 2 silica cartridges (100 g) using a 0-50% EtOAc-DCM gradient over 60 mins. All product containing fractions were combined and concentrated *in vacuo* and the residue was triturated with  $\text{Et}_2\text{O}$  (ca. 100 mL) and the resultant solid collected by filtration and dried *in vacuo* to give the title compound (2.415 g, 51%) as a yellow solid. The filtrate was concentrated *in vacuo* and triturated again. The solid was collected by filtration and dried *in vacuo*

to give a further batch of title compound (0.742 g, 16%) as a yellow solid. The filtrate was concentrated *in vacuo* and the residue was dissolved in DCM and purified on a silica cartridge (100 g) using a 0-50% EtOAc-cyclohexane gradient over 60 mins. The appropriate fractions were combined and evaporated *in vacuo* to give further title compound (503 mg, 11%) as a yellow oil that solidified on standing.

**5-(4-Amino-5-((benzyloxy)methyl)-2-butyl-5H-pyrrolo[3,2-d]pyrimidin-7-yl)pent-4-ynal (213z)**



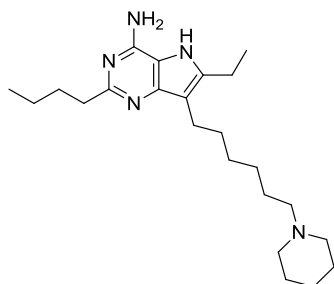
Chemical Formula: C<sub>23</sub>H<sub>26</sub>N<sub>4</sub>O<sub>2</sub>  
Molecular Weight: 390.48

To a stirred suspension of 5-(4-amino-5-((benzyloxy)methyl)-2-butyl-5H-pyrrolo[3,2-d]pyrimidin-7-yl)pent-4-yn-1-ol (**213x**) (200 mg, 0.510 mmol), 4-methylmorpholine *N*-oxide (90 mg, 0.764 mmol) and powdered 4Å molecular sieves in a mixture of anhydrous DCM (10 mL) and anhydrous MeCN (1 mL) at ambient temperature was added tetrapropylammonium perruthenate (18 mg, 0.051 mmol), and the reaction mixture was stirred at ambient temperature for 1.5 h. The reaction mixture was filtered through a pad of celite and was concentrated *in vacuo*. The residue was dissolved in DCM and purified on a silica cartridge (20 g) using a 0-100% EtOAc-dichloromethane gradient over 40 mins. The appropriate fractions were combined and evaporated *in vacuo* to give the title compound (101 mg, 51%) as an off-white foam.

<sup>1</sup>H NMR (400 MHz, CDCl<sub>3</sub>) δ 9.88 (s, 1H), 7.43 - 7.33 (m, 3H), 7.31 - 7.26 (m, 2H), 7.24 (s, 1H), 5.66 (br s, 2H), 5.46 (s, 2H), 4.54 (s, 2H), 2.89 - 2.80 (m, 6H), 1.87 - 1.76 (m, 2H), 1.50 - 1.37 (m, 2H), 0.99 - 0.93 (m, 3H); <sup>13</sup>C NMR (101 MHz, 101

MHz, CDCl<sub>3</sub>) δ 200.8, 165.0, 151.5, 150.8, 135.2, 134.4, 128.8, 128.7, 128.4, 113.1, 99.0, 90.6, 76.9, 72.2, 69.9, 42.7, 39.2, 31.5, 22.8, 14.0, 13.3; LCMS (System B) R<sub>t</sub> 1.08 min, m/z 391 ([M+H]<sup>+</sup>); HRMS Anal. Calcd. For C<sub>23</sub>H<sub>27</sub>N<sub>4</sub>O<sub>2</sub> = 391.2129. Found = 391.2131 ([M+H]<sup>+</sup>); IR (cm<sup>-1</sup>) 3330, 2927, 1722, 1604, 1542; Mpt. 76-80 °C.

**2-Butyl-6-ethyl-7-(6-(piperidin-1-yl)hexyl)-5H-pyrrolo[3,2-d]pyrimidin-4-amine**  
**(216a)**



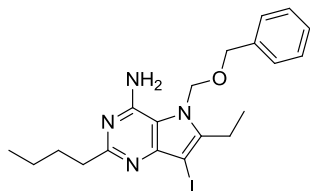
Chemical Formula: C<sub>23</sub>H<sub>39</sub>N<sub>5</sub>  
Molecular Weight: 385.59

A filtered solution of 5-((benzyloxy)methyl)-2-butyl-6-ethyl-7-(6-(piperidin-1-yl)hex-1-yn-1-yl)-5H-pyrrolo[3,2-d]pyrimidin-4-amine (**219a**) (75 mg, 0.15 mmol) in EtOH (6 mL) and AcOH (0.5 mL) was hydrogenated using the H-cube (settings: 60 °C, Full H<sub>2</sub>, 1 mL/min flow rate) and a 5% Pd/C CatCart 30 as the catalyst. The reaction mixture was concentrated *in vacuo* and the residue was dissolved in 1:1 MeOH:DMSO (1 mL) and purified by MDAP on Xbridge column using MeCN-water with an ammonium carbonate modifier. The appropriate fractions were combined and concentrated *in vacuo* to give a black oil. The oil was dissolved in 1:1 MeOH:DMSO (1 mL) and purified by MDAP on an Xbridge column using MeCN-water with an ammonium carbonate modifier. The solvent was dried under a stream of nitrogen in the Radleys blowdown apparatus to give the title compound (20 mg, 35 %) as a beige solid.

<sup>1</sup>H NMR (400 MHz, MeOD) δ 2.81 (q, J = 7.6 Hz, 2H), 2.77 - 2.68 (m, 4H), 2.50 (br s, 4H), 2.40 - 2.34 (m, 2H), 1.80 - 1.71 (m, 2H), 1.67 - 1.58 (m, 6H), 1.58 - 1.47

(m, 4H), 1.46 - 1.31 (m, 9H), 0.98 (t,  $J = 7.3$  Hz, 3H) exchangeable protons (NH and NH<sub>2</sub>) not observed; LCMS (System A) R<sub>t</sub> 0.63 min, m/z 385 ([M-H]).

**5-((Benzyloxy)methyl)-2-butyl-6-ethyl-7-iodo-5H-pyrrolo[3,2-d]pyrimidin-4-amine (218)**

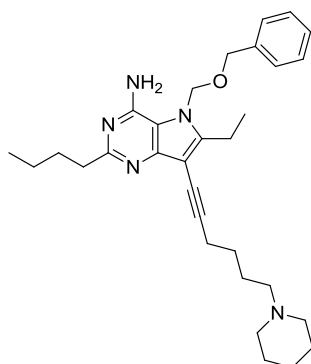


Chemical Formula: C<sub>20</sub>H<sub>25</sub>IN<sub>4</sub>O  
Molecular Weight: 464.34

A suspension of 5-((benzyloxy)methyl)-2-butyl-4-chloro-6-ethyl-7-iodo-5H-pyrrolo[3,2-d]pyrimidine (**217**) (2.40 g, 4.96 mmol) in isopropanol (5 mL) was treated with 880 ammonia (5 mL, 90 mmol), sealed and heated in a Biotage Initiator microwave (using initial absorption setting high) to 140 °C for 120 min. After cooling the reaction mixture, further 880 ammonia (2 mL, 36 mmol) was added and the reaction vessel was re-sealed and heated in a Biotage Initiator microwave (using initial absorption setting high) to 140 °C for 90 min. After cooling the reaction mixture was concentrated *in vacuo* to give a off white solid. The solid was partitioned between DCM (50 mL) and water (50 mL). The organic extract was separated and dried (hydrophobic frit) before being concentrated *in vacuo* and triturated with petroleum ether (40-60). The resultant suspension was filtered and the solid dried *in vacuo* to give the title compound (1.67 g, 73 %) as an off white solid.

<sup>1</sup>H NMR (400 MHz, CDCl<sub>3</sub>) δ 7.41 - 7.36 (m, 3H), 7.32 - 7.26 (m, 2H), 5.65 (br. s., 2H), 5.60 (br s, 2H), 4.59 (s, 2H), 2.90 - 2.83 (m, 4H), 1.88 - 1.78 (m, 2H), 1.51 - 1.41 (m, 2H), 1.19 (t,  $J = 7.6$  Hz, 3H), 0.97 (t,  $J = 7.3$  Hz, 3H); <sup>13</sup>C NMR (101 MHz, DMSO-d<sub>6</sub>) δ 162.9, 150.3, 150.1, 146.4, 137.0, 128.3, 127.8, 127.6, 113.5, 74.0, 69.1, 62.0, 38.1, 30.8, 22.1, 20.0, 13.9, 13.7; LCMS (System B) R<sub>t</sub> 1.27 min, m/z 465 ([M+H]<sup>+</sup>); HRMS Anal. Calcd. For C<sub>20</sub>H<sub>25</sub>IN<sub>4</sub>O = 465.1146. Found = 465.1162 ([M+H]<sup>+</sup>); IR (cm<sup>-1</sup>) 2963, 1647, 1588, 1537; Mpt. 115-116 °C.

**5-((Benzyloxy)methyl)-2-butyl-6-ethyl-7-(6-(piperidin-1-yl)hex-1-yn-1-yl)-5H-pyrrolo[3,2-d]pyrimidin-4-amine (219a)**

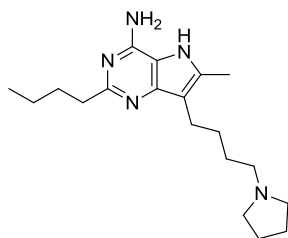


Chemical Formula: C<sub>31</sub>H<sub>43</sub>N<sub>5</sub>O  
Molecular Weight: 501.71

To a degassed stirred suspension of 5-((benzyloxy)methyl)-2-butyl-6-ethyl-7-iodo-5H-pyrrolo[3,2-d]pyrimidin-4-amine (**218**) (300 mg, 0.65 mmol), copper (I) iodide (20 mg, 0.11 mmol) and *bis*(triphenylphosphine)palladium(II)dichloride (36 mg, 0.05 mmol) in anhydrous DMF (8 mL) was added a solution of 1-(5-hexyn-1-yl)piperidine (139 mg, 0.84 mmol) and triethylamine (0.13 mL, 0.96 mmol) in anhydrous DMF (2 mL) dropwise over 2 min before being stirred at 50 °C for 20 h. To the reaction mixture was added a solution of 1-(5-hexyn-1-yl)piperidine (139 mg, 0.84 mmol) and triethylamine (0.13 mL, 0.96 mmol) in anhydrous DMF (2 mL) dropwise over 2 min. The reaction mixture was stirred at 50 °C for a further 4 h before being concentrated *in vacuo* and the residue partitioned between EtOAc (50 mL) and water (50 mL). The organic layer was separated and was back extracted with EtOAc (25 mL). The combined organic extracts were washed with brine (50 mL), dried (MgSO<sub>4</sub>), filtered and concentrated *in vacuo* to give an orange oil (432 mg). The oil was dissolved in DCM and purified on a aminopropyl functionalised silica cartridge (20 g) using a 0-100% EtOAc-cyclohexane gradient over 40 mins. The appropriate fractions were combined and evaporated *in vacuo* to give a yellow oil (184 mg). The oil was dissolved in DCM and purified on a silica cartridge (20 g) using a 0-10% MeOH-DCM gradient over 40 mins. The appropriate fractions were combined and evaporated *in vacuo* and azeotroped with petroleum ether (40-60) to give the title compound (77 mg, 24 %) as a off-white solid.

$^1\text{H}$  NMR (400 MHz,  $\text{CDCl}_3$ )  $\delta$  7.43 - 7.34 (m, 3H), 7.32 - 7.26 (m, 2H), 5.58 (s, 2H), 5.55 (br s, 2H), 4.56 (s, 2H), 2.90 - 2.81 (m, 4H), 2.80 - 2.62 (m, 2H), 2.58 (t,  $J = 7.0$  Hz, 2H), 2.00 - 1.66 (m, 14H), 1.60 - 1.40 (m, 4H), 1.24 (t,  $J = 7.6$  Hz, 3H), 0.97 (t,  $J = 7.5$  Hz, 3H); LCMS (System A)  $R_t$  0.76 min,  $m/z$  503 ( $[\text{M}+\text{H}]^+$ ).

**2-Butyl-6-methyl-7-(4-(pyrrolidin-1-yl)butyl)-5H-pyrrolo[3,2-*d*]pyrimidin-4-amine (220b)**



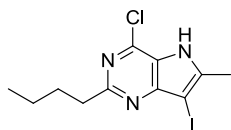
Chemical Formula:  $\text{C}_{19}\text{H}_{31}\text{N}_5$   
Molecular Weight: 329.48

A filtered solution of 5-((benzyloxy)methyl)-2-butyl-6-methyl-7-(4-(pyrrolidin-1-yl)butyl)-5H-pyrrolo[3,2-*d*]pyrimidin-4-amine (**228b**) (100 mg, 0.61 mmol) in EtOH (9 mL) and AcOH (1 mL) was hydrogenated using the H-cube<sup>TM</sup> (settings: 60 °C, Full  $\text{H}_2$ , 1 mL/min flow rate) and a 10% Pd/C CatCart 30 as the catalyst. The reaction mixture was dried under a stream of nitrogen in the Radleys<sup>TM</sup> blowdown apparatus and the residue was dissolved in 1:1 MeOH:DMSO 1 mL and purified by MDAP on an Xbridge column using MeCN-water with an ammonium carbonate modifier. The solvent was dried under a stream of nitrogen in the Radleys<sup>TM</sup> blowdown apparatus to give the title compound (39 mg, 53%) as a white solid.

$^1\text{H}$  NMR (400 MHz, MeOD)  $\delta$  2.78 - 2.70 (m, 4H), 2.57 - 2.46 (m, 6H), 2.41 (s, 3H), 1.69 - 1.84 (m, 6H), 1.68 - 1.54 (m, 4H), 1.48 - 1.37 (m, 2H), 0.97 (t,  $J = 7.5$  Hz, 3H) exchangeable protons (NH and  $\text{NH}_2$ ) not observed.; LCMS (System B)  $R_t$  1.00 min,  $m/z$  330 ( $[\text{M}+\text{H}]^+$ ).



**2-Butyl-4-chloro-7-iodo-6-methyl-5H-pyrrolo[3,2-d]pyrimidine (222)**

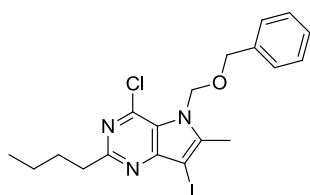


Chemical Formula: C<sub>11</sub>H<sub>13</sub>ClIN<sub>3</sub>  
Molecular Weight: 349.60

To a stirred solution of 2-butyl-4-chloro-6-methyl-5H-pyrrolo[3,2-d]pyrimidine (**221**) (8.0 g, 35.8 mmol) in anhydrous THF (100 mL) was added solid *N*-iodosuccinimide (8.85 g, 39.3 mmol) portionwise. The reaction mixture was stirred at ambient temperature for 2 h before being concentrated *in vacuo*. The resulting residue was triturated with water (ca. 400 mL), and the resultant pale yellow solid collected by filtration and dried *in vacuo* to give the title compound (12.25 g, 98%).

<sup>1</sup>H NMR (400 MHz, CDCl<sub>3</sub>) δ 8.82 (br. s., 1H), 3.07 - 3.00 (m, 2H), 2.61 (s, 3H), 1.90 - 1.81 (m, 2H), 1.49 - 1.37 (m, 2H), 0.95 (t, *J* = 7.4 Hz, 3H); <sup>13</sup>C NMR (101 MHz, CDCl<sub>3</sub>) δ 164.5, 152.9, 145.1, 141.3, 123.5, 60.4, 38.9, 31.5, 22.6, 15.3, 13.9; LCMS (System B) R<sub>t</sub> 1.19 min, *m/z* 350, 352 ([M+H]<sup>+</sup>); HRMS Anal. Calcd. For C<sub>11</sub>H<sub>13</sub>ClIN<sub>3</sub> = 349.9932. Found = 349.9915 ([M+H]<sup>+</sup>); IR (cm<sup>-1</sup>) 2958, 1614, 1534, 1519; Mpt. 184-186 °C.

**5-((Benzyloxy)methyl)-2-butyl-4-chloro-7-iodo-6-methyl-5H-pyrrolo[3,2-d]pyrimidine (223)**



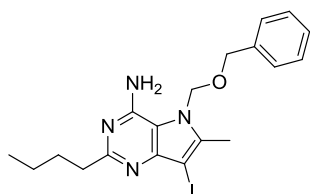
Chemical Formula: C<sub>19</sub>H<sub>21</sub>ClIN<sub>3</sub>O  
Molecular Weight: 469.75

To a stirred slurry of sodium hydride 60% wt. on mineral oil (1.41 g, 35.1 mmol) in anhydrous THF (100 mL) at 0 °C under a nitrogen atmosphere was added a solution of 2-butyl-4-chloro-7-iodo-6-methyl-5H-pyrrolo[3,2-d]pyrimidine (**222**) (10.7 g, 30.5 mmol) in anhydrous THF (75 mL) dropwise over 15 min. The reaction mixture was stirred at 0 °C for a further 60 min before addition of a solution of

((chloromethoxy)methyl)benzene (5.50 g, 35.1 mmol) in anhydrous THF (75 mL) dropwise over 20 min. The reaction mixture was then allowed to warm to ambient temperature and stirred for a further 60 min. The reaction mixture was concentrated *in vacuo* and the residue partitioned between water (500 mL) and EtOAc (500 mL). The organic phase was separated and the aqueous phase back extracted with EtOAc (250 mL). The combined organic extracts were washed with brine (500 mL), dried (MgSO<sub>4</sub>), filtered and concentrated *in vacuo* and the residue was dissolved in DCM and purified on 2 silica cartridges (2 x 100 g) using a 0-50% EtOAc-cyclohexane gradient over 60 mins. The appropriate fractions were combined and evaporated *in vacuo*, and triturated with petroleum ether (40-60). The solid was collected and dried *in vacuo* to give the title compound (9.87 g, 69 %) as a white solid.

<sup>1</sup>H NMR (400 MHz, CDCl<sub>3</sub>) δ 7.32 - 7.25 (m, 3H), 7.25 - 7.21 (m, 2H), 5.95 (s, 2H), 4.59 (s, 2H), 3.05 – 2.99 (m, 2H), 2.63 (s, 3H), 1.91 - 1.81 (m, 2H), 1.50 - 1.40 (m, 2H), 0.97 (t, *J* = 7.40 Hz, 3H); LCMS (System B) R<sub>t</sub> 1.52 min, m/z 470, 472 ([M+H]<sup>+</sup>).

**5-((Benzyloxy)methyl)-2-butyl-7-iodo-6-methyl-5H-pyrrolo[3,2-*d*]pyrimidin-4-amine (224)**



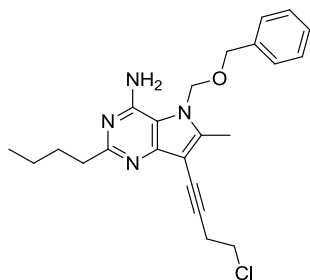
Chemical Formula: C<sub>19</sub>H<sub>23</sub>IN<sub>4</sub>O  
Molecular Weight: 450.32

In three identical batches: 5-((benzyloxy)methyl)-2-butyl-4-chloro-7-iodo-6-methyl-5H-pyrrolo[3,2-*d*]pyrimidine (**223**) (1.00 g, 2.13 mmol) was dissolved in IPA (10 mL) and treated with 880 ammonia (2.00 mL, 103 mmol), the reaction vessels were sealed and heated in a Biotage Initiator microwave (absorption setting high) to 150 °C for 1 h. To each of the reactions was added a further aliquot of 880 ammonia (2.00 mL, 103 mmol), the reaction vessels were sealed and heated in a Biotage Initiator microwave (absorption setting high) to 150 °C for 4 h. After cooling, the

reaction mixtures (now thick slurries) were mobilised with IPA and combined prior to concentration *in vacuo* to give a white solid. The solid was triturated with water (ca. 250 mL), and the resultant solid collected by filtration and dried *in vacuo* the title compound (2.59 g, 90%) as a fluffy white solid.

$^1\text{H}$  NMR (400 MHz,  $\text{CDCl}_3$ )  $\delta$  7.40 - 7.34 (m, 3H), 7.30 - 7.26 (m, 2H), 5.61 (br. s., 2H), 5.58 (br s, 2H), 4.58 (s, 2H), 2.88 - 2.82 (m, 2H), 2.44 (s, 3H), 1.87 - 1.76 (m, 2H), 1.50 - 1.38 (m, 2H), 0.99 - 0.93 (m, 3H);  $^{13}\text{C}$  NMR (101 MHz,  $\text{CDCl}_3$ )  $\delta$  164.9, 151.4, 150.1, 140.9, 135.7, 128.8, 128.6, 127.9, 114.4, 73.6, 69.6, 63.0, 39.2, 31.6, 22.8, 14.1, 13.7; LCMS (System B)  $R_t$  1.24 min,  $m/z$  451 ( $[\text{M}+\text{H}]^+$ ); HRMS Anal. Calcd. For  $\text{C}_{19}\text{H}_{24}\text{N}_4\text{O}$  = 451.0989. Found = 451.0981 ( $[\text{M}+\text{H}]^+$ ); IR ( $\text{cm}^{-1}$ ) 3407, 3112, 1646, 1592; Mpt. 163-164 °C.

**5-((Benzyloxy)methyl)-2-butyl-7-(4-chlorobut-1-yn-1-yl)-6-methyl-5H-pyrrolo[3,2-*d*]pyrimidin-4-amine (225)**



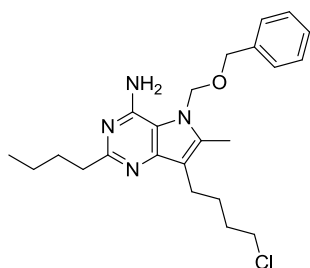
Chemical Formula:  $\text{C}_{23}\text{H}_{27}\text{ClN}_4\text{O}$   
Molecular Weight: 410.94

To a degassed suspension of 5-((benzyloxy)methyl)-2-butyl-7-iodo-6-methyl-5H-pyrrolo[3,2-*d*]pyrimidin-4-amine (**224**) (2.57 g, 5.71 mmol), copper(I) iodide (0.22 g, 1.14 mmol), and *bis*(triphenylphosphine)palladium(II) dichloride (0.40 g, 0.57 mmol) in anhydrous DMF (40 mL) was added a solution of 4-chlorobut-1-yne (0.657 g, 7.42 mmol) and triethylamine (1.19 mL, 8.56 mmol) in anhydrous DMF (20 mL) dropwise over 10 min. The reaction mixture was stirred at ambient temperature for 18 h. To the reaction was added further *bis*(triphenylphosphine)palladium(II)dichloride (100 mg, 0.11 mmol), copper (I) iodide (40 mg, 0.21 mmol) and the reaction mixture was degassed prior to the addition of a solution of 4-

chlorobut-1-yne (165 mg, 1.86 mmol) and triethylamine (0.30 mL, 2.16 mmol) in anhydrous DMF (5 mL) dropwise over 2 min. The reaction mixture was stirred for a further 6 h. The reaction mixture was concentrated *in vacuo* and the residue partitioned between EtOAc (500 mL) and water (500 mL). The organic phase was separated and the aqueous phase back extracted with EtOAc (2 x 150 mL). The combined organic extracts were washed with brine (500 mL) and dried (MgSO<sub>4</sub>), filtered and concentrated *in vacuo* to give an orange gum. The sample was dissolved in DCM and purified on 2 silica cartridges (2 x 100 g) using a 0-50% EtOAc-DCM gradient over 60 mins. The appropriate fractions were combined and evaporated *in vacuo* to give two batches of the title compound: (755 mg, 32%) a pale yellow solid and (456 mg, 19%) an orange solid.

<sup>1</sup>H NMR (400 MHz, CDCl<sub>3</sub>) δ 7.40 - 7.33 (m, 3H), 7.30 - 7.25 (m, 2H), 5.55 (br s, 2H), 5.52 (s, 2H), 4.56 (s, 2H), 3.74 (t, *J* = 7.2 Hz, 2H), 3.00 (t, *J* = 7.3 Hz, 2H), 2.87 - 2.81 (m, 2H), 2.43 (s, 3H), 1.86 - 1.76 (m, 2H), 1.50 - 1.38 (m, 2H), 0.96 (t, *J* = 7.4 Hz, 3H); <sup>13</sup>C NMR (126 MHz, CDCl<sub>3</sub>) δ 164.9, 150.9, 149.9, 144.2, 135.6, 128.8, 128.6, 127.9, 113.1, 98.4, 73.9, 73.0, 69.6, 42.6, 39.3, 31.6, 24.5, 22.8, 14.0, 13.7, 11.6; LCMS (System B) R<sub>t</sub> 1.24 min, m/z 411, 413 ([M+H]<sup>+</sup>); HRMS Anal. Calcd. For C<sub>23</sub>H<sub>28</sub>ClN<sub>4</sub>O = 411.1946. Found = 411.1950 ([M+H]<sup>+</sup>); IR (cm<sup>-1</sup>) 3415, 3311, 3112, 2961, 2926, 1648, 1597, 1542; Mpt. 155-159 °C.

**5-((Benzyloxy)methyl)-2-butyl-7-(4-chlorobutyl)-6-methyl-5H-pyrrolo[3,2-*d*]pyrimidin-4-amine (227)**



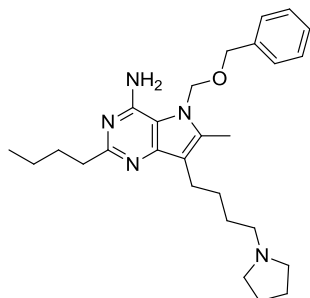
Chemical Formula: C<sub>23</sub>H<sub>31</sub>ClN<sub>4</sub>O  
Molecular Weight: 414.97

A solution of 5-((benzyloxy)methyl)-2-butyl-7-(4-chlorobut-1-yn-1-yl)-6-methyl-5H-pyrrolo[3,2-*d*]pyrimidin-4-amine (**225**) (460 mg, 1.12 mmol) in EtOH (50 mL)

was hydrogenated using the H-cube<sup>TM</sup> (settings: 20 °C, Full H<sub>2</sub>, 1mL/min flow rate) and 5% Pd/C CatCart 30 as the catalyst. The reaction mixture was concentrated *in vacuo* to give the title compound (348 mg, 73%) as an off white solid.

<sup>1</sup>H NMR (400 MHz, CDCl<sub>3</sub>) δ 7.40 - 7.33 (m, 3H), 7.32 - 7.25 (m, 2H), 5.78 (br s., 2H), 5.52 (s, 2H), 4.57 (s, 2H), 3.60 (t, *J* = 6.4 Hz, 2H), 2.89 - 2.82 (m, 2H), 2.76 (t, *J* = 7.0 Hz, 2H), 2.28 (s, 3H), 1.89 - 1.74 (m, 6H), 1.49 - 1.38 (m, 2H), 0.96 (t, *J* = 7.3 Hz, 3H); LCMS (System B) R<sub>t</sub> 1.32 min, m/z 415, 417 ([M+H]<sup>+</sup>), Note: compound is only 82% pure by UV.

**5-((Benzyloxy)methyl)-2-butyl-6-methyl-7-(4-(pyrrolidin-1-yl)butyl)-5H-pyrrolo[3,2-*d*]pyrimidin-4-amine (228b)**

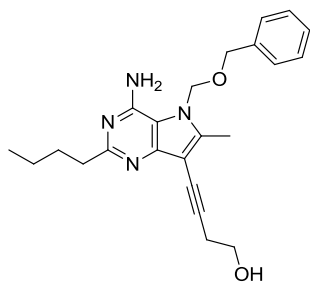


Chemical Formula: C<sub>27</sub>H<sub>39</sub>N<sub>5</sub>O  
Molecular Weight: 449.63

To a stirred suspension of 4-(4-amino-5-((benzyloxy)methyl)-2-butyl-6-methyl-5H-pyrrolo[3,2-*d*]pyrimidin-7-yl)butanal (**231**) (230 mg, 0.58 mmol) and 4Å mol sieves in anhydrous DCM (10 mL) was added pyrrolidine (0.1 mL, 1.21 mmol) followed by sodium triacetoxyborohydride (250 mg, 1.18 mmol). The resultant mixture was stirred at ambient temperature under an atmosphere of nitrogen for 2.5 h. The reaction mixture was filtered through a pad of celite, and the cake washed with DCM (40 mL). The combined filtrates were washed with saturated aqueous sodium bicarbonate (50 mL) and dried (hydrophobic frit) before concentration *in vacuo* to give a yellow solid (209 mg). The sample was dissolved in DCM and purified on a silica cartridge (20 g) using a 0-10% MeOH-DCM gradient over 40 mins. The appropriate fractions were combined and evaporated *in vacuo* to give the title compound (124 mg, 47 %) as a white solid.

$^1\text{H}$  NMR (400 MHz,  $\text{CDCl}_3$ )  $\delta$  7.41 - 7.33 (m, 3H), 7.26 - 7.33 (m, 2H), 5.53 - 5.48 (m, 4H), 4.56 (s, 2H), 2.84 - 2.78 (m, 2H), 2.73 (t,  $J = 7.2$  Hz, 2H), 2.53 - 2.44 (m, 6H), 2.28 (s, 3H), 1.86 - 1.73 (m, 6H), 1.72 - 1.63 (m, 2H), 1.63 - 1.53 (m, 2H), 1.50 - 1.38 (m, 2H), 0.96 (t,  $J = 7.5$  Hz, 3H);  $^{13}\text{C}$  NMR (101 MHz,  $\text{CDCl}_3$ )  $\delta$  163.3, 150.7, 149.7, 136.7, 136.2, 128.7, 128.4, 127.9, 113.9, 113.5, 72.7, 69.2, 56.4, 54.2, 39.3, 31.7, 28.5, 23.4, 22.9, 22.8, 14.1, 10.4; LCMS (System B)  $R_t$  1.19 min,  $m/z$  450 ( $[\text{M}+\text{H}]^+$ ); HRMS Anal. Calcd. For  $\text{C}_{27}\text{H}_{40}\text{N}_5\text{O} = 450.3227$ . Found = 450.3225 ( $[\text{M}+\text{H}]^+$ ); IR ( $\text{cm}^{-1}$ ) 3098, 2928, 1653, 1654, 1570, 1539; Mpt. 99-101 °C.

**4-(4-Amino-5-((benzyloxy)methyl)-2-butyl-6-methyl-5H-pyrrolo[3,2-d]pyrimidin-7-yl)but-3-yn-1-ol (229)**



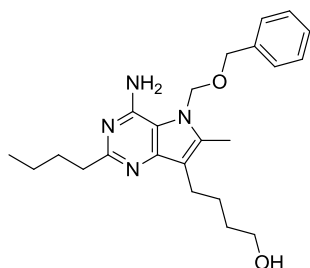
Chemical Formula:  $\text{C}_{23}\text{H}_{28}\text{N}_4\text{O}_2$   
Molecular Weight: 392.49

To a stirred, degassed solution of 5-((benzyloxy)methyl)-2-butyl-7-iodo-6-methyl-5H-pyrrolo[3,2-d]pyrimidin-4-amine (**224**) (1.65 g, 3.66 mmol), *bis*(triphenylphosphine)-palladium(II)dichloride (0.15 g, 0.22 mmol) and copper(I) iodide (0.08 g, 0.44 mmol) in anhydrous DMF (20 mL) was added a solution of but-3-yn-1-ol (0.39 g, 5.50 mmol) and triethylamine (0.77 mL, 5.50 mmol) in anhydrous DMF (5 mL) dropwise over 3 mins. The resultant mixture was stirred at ambient temperature for 16 h. The reaction mixture was concentrated *in vacuo* and the resultant gum partitioned between EtOAc (250 mL) and water (250 mL). The organic layer was separated and the aqueous layer extracted further with EtOAc (80 mL). The combined organic extracts were washed with brine (200 mL), dried ( $\text{MgSO}_4$ ), filtered and concentrated *in vacuo* to give a red gum (1.65 g). The sample was dissolved in DCM and purified on a silica cartridge (100 g) using a 0-25%

MeOH-DCM gradient over 60 mins. The appropriate fractions were combined and evaporated *in vacuo*. The resultant orange sticky solid was triturated with Et<sub>2</sub>O and the solid collected by filtration and dried *in vacuo* to give the title compound (552 mg, 38%) as an off-white solid. The filtrate was concentrated *in vacuo* and the residue was dissolved in DCM and purified on a silica cartridge (50 g) using a 0-10% MeOH-DCM gradient over 60 mins. The appropriate fractions were combined and evaporated *in vacuo* to give an orange oil. The oil was triturated with Et<sub>2</sub>O. The resultant solid was collected by filtration and dried *in vacuo* to give a further batch of the title compound (303 mg, 21%)

<sup>1</sup>H NMR (400 MHz, CDCl<sub>3</sub>) δ 7.43 - 7.32 (m, 3H), 7.31 - 7.23 (m, 2H), 5.65 (br s., 2H), 5.51 (s, 2H), 4.54 (s, 2H), 3.86 (t, *J* = 6.1 Hz, 2H), 2.88 - 2.75 (m, 4H), 2.41 (s, 3H), 1.85 - 1.74 (m, 2H), 1.48 - 1.36 (m, 2H), 0.94 (t, *J* = 7.3 Hz, 3H) exchangeable proton (OH) not observed; LCMS (System B) R<sub>t</sub> 1.06 min, m/z 393 ([M+H]<sup>+</sup>).

**4-(4-Amino-5-((benzyloxy)methyl)-2-butyl-6-methyl-5H-pyrrolo[3,2-*d*]pyrimidin-7-yl)butan-1-ol (230)**



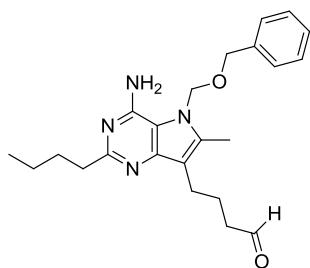
Chemical Formula: C<sub>23</sub>H<sub>32</sub>N<sub>4</sub>O<sub>2</sub>  
Molecular Weight: 396.53

A filtered solution of 4-(4-amino-5-((benzyloxy)methyl)-2-butyl-6-methyl-5H-pyrrolo[3,2-*d*]pyrimidin-7-yl)but-3-yn-1-ol (**229**) (853 mg, 2.17 mmol) in EtOH (80 mL) was hydrogenated using the H-cube<sup>TM</sup> (settings: 20 °C, Full H<sub>2</sub>, 1 mL/min flow rate) and a 10% Pd/C CatCart 30 as the catalyst. The solution was re-hydrogenated using the H-cube<sup>TM</sup> (settings: 20 °C, Full H<sub>2</sub>, 1 mL/min flow rate) and a new 10% Pd/C CatCart 30 as the catalyst. The reaction mixture was concentrated *in vacuo* and the residue was dissolved in DCM and purified on a silica cartridge (100 g) using a 0-25% MeOH-DCM gradient over 60 mins. The appropriate fractions were

combined and evaporated *in vacuo* to give the title compound (543 mg, 63%) as a off-white solid.

$^1\text{H}$  NMR (400 MHz,  $\text{CDCl}_3$ )  $\delta$  7.39 - 7.32 (m, 3H), 7.31 - 7.23 (m, 2H), 5.76 (br s, 2H), 5.52 (s, 2H), 4.57 (s, 2H), 3.81 (t,  $J = 5.9$  Hz, 2H), 2.87 - 2.80 (m, 4H), 2.27 (s, 3H), 1.83 - 1.71 (m, 4H), 1.63 - 1.55 (m, 2H), 1.47 - 1.35 (m, 2H), 0.94 (t,  $J = 7.3$  Hz, 3H) exchangeable proton (OH) not observed;  $^{13}\text{C}$  NMR (126 MHz,  $\text{CDCl}_3$ )  $\delta$  162.6, 149.7, 149.2, 137.6, 135.9, 128.8, 128.5, 127.9, 113.8, 113.2, 72.8, 69.6, 62.7, 38.3, 31.4, 30.6, 27.6, 22.6, 22.0, 14.0, 10.3; LCMS (System A)  $R_t$  0.83 min,  $m/z$  397 ( $[\text{M}+\text{H}]^+$ ); HRMS Anal. Calcd. For  $\text{C}_{23}\text{H}_{33}\text{N}_4\text{O}_2 = 397.2598$ . Found = 397.2588 ( $[\text{M}+\text{H}]^+$ ); IR ( $\text{cm}^{-1}$ ) 3325, 3115, 2957, 2928, 2870, 1602, 1542; Mpt. 120-121 °C.

**4-(4-Amino-5-((benzyloxy)methyl)-2-butyl-6-methyl-5H-pyrrolo[3,2-*d*]pyrimidin-7-yl)butanal (231)**



Chemical Formula:  $\text{C}_{23}\text{H}_{30}\text{N}_4\text{O}_2$   
Molecular Weight: 394.51

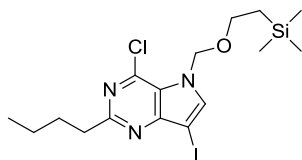
To a stirred suspension of 4-(4-amino-5-((benzyloxy)methyl)-2-butyl-6-methyl-5H-pyrrolo[3,2-*d*]pyrimidin-7-yl)butan-1-ol (**230**) (230 mg, 0.58 mmol), 4-methylmorpholine *N*-oxide (82 mg, 0.70 mmol) and powdered 4Å molecular sieves in a mixture of anhydrous DCM (10 mL) and anhydrous MeCN (1 mL) at ambient temperature was added tetrapropylammonium perruthenate (22 mg, 0.063 mmol), and the reaction was stirred at ambient temperature for 2 h. The reaction mixture was concentrated *in vacuo* (water bath 20 °C). The resultant residue was slurried with DCM (10 mL) and filtered through a pad of celite. The resultant filtrate was concentrated *in vacuo* and re-dissolved in DCM and purified on a silica cartridge (20 g) using a 0-10% MeOH-DCM gradient over 40 mins. The appropriate fractions



were combined and evaporated *in vacuo* to give the title compound (114 mg, 50%) as a yellow gum.

<sup>1</sup>H NMR (400 MHz, CDCl<sub>3</sub>) δ 9.66 (t, *J* = 1.7 Hz, 1H), 7.39 - 7.23 (m, 5H), 5.62 - 5.44 (m, 4H), 4.55 (s, 2H), 2.84 - 2.72 (m, 4H), 2.46 (dt, *J* = 7.1, 1.7 Hz, 2H), 2.26 (s, 3H), 2.07 - 1.97 (m, 2H), 1.84 - 1.74 (m, 2H), 1.48 - 1.37 (m, 2H), 0.95 (t, *J* = 7.3 Hz, 3H); LCMS (System B) R<sub>t</sub> 1.13 min, m/z 395 ([M+H]<sup>+</sup>).

**\*2-Butyl-4-chloro-7-iodo-5-((2-(trimethylsilyl)ethoxy)methyl)-5H-pyrrolo[3,2-*d*]pyrimidine (234)**

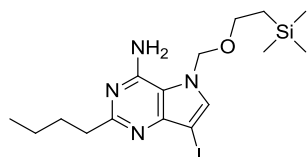


Chemical Formula: C<sub>16</sub>H<sub>25</sub>ClIIN<sub>3</sub>OSi  
Molecular Weight: 465.83

To a stirred suspension of sodium hydride 60% wt. on mineral oil (20 mg, 0.50 mmol) in anhydrous THF (3 mL) at 0 °C was added a solution of 2-butyl-4-chloro-7-iodo-5H-pyrrolo[3,2-*d*]pyrimidine (**129**) (100 mg, 0.30 mmol) in THF (3 mL) dropwise over 5 min. The resultant mixture was stirred at 0 °C for 15 mins before the addition of a solution of (2-(chloromethoxy)ethyl)trimethylsilane (0.06 mL, 0.33 mmol) in THF (2 mL) dropwise over 5 min. The reaction mixture was at stirred ambient temperature for two hours before being quenched with water. The reaction mixture was partitioned between EtOAc (20 mL) and water (20 mL). The organic phase was separated and washed with brine (20 mL), dried, filtered and concentrated *in vacuo*. The resulting residue was dissolved in DCM and purified on a silica cartridge (10 g) using a 0-100% DCM-cyclohexane gradient over 30 mins. The appropriate fractions were combined and evaporated *in vacuo* to give the title compound (125 mg, 90%) as an orange oil.

$^1\text{H}$  NMR (400 MHz,  $\text{CDCl}_3$ )  $\delta$  7.64 (s, 1H), 5.75 (s, 2H), 3.59 - 3.52 (m, 2H), 3.09 - 3.02 (m, 2H), 1.92 - 1.82 (m, 2H), 1.50 - 1.40 (m, 2H), 1.00 - 0.88 (m, 5H), -0.04 - -0.06 (m, 9H); LCMS (System B)  $R_t$  1.66 min,  $m/z$  = 466, 468 ( $[\text{M}+\text{H}]^+$ ).

**\*2-Butyl-7-iodo-5-((2-(trimethylsilyl)ethoxy)methyl)-5H-pyrrolo[3,2-*d*]pyrimidin-4-amine (235)**

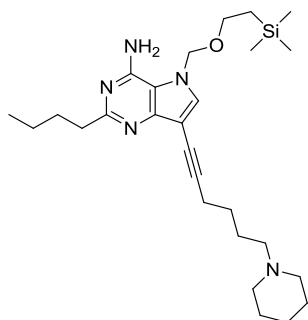


Chemical Formula:  $\text{C}_{16}\text{H}_{27}\text{IN}_4\text{OSi}$   
Molecular Weight: 446.40

2-butyl-4-chloro-7-iodo-5-((2-(trimethylsilyl)ethoxy)methyl)-5H-pyrrolo[3,2-*d*]pyrimidine (**234**) (150 mg, 0.32 mmol) was suspended in 0.88 ammonia (1.0 mL, 18.2 mmol) and IPA (3 mL) and was sealed and heated in a Biotage Initiator microwave using initial absorption setting normal to 150 °C for 2 h. After cooling, the solvent was removed *in vacuo* and the residue was partitioned between water (20 mL) and EtOAc (25 mL). The organic phase was separated and concentrated *in vacuo* to give the title compound (126 mg, 75 %) as a white solid.

$^1\text{H}$  NMR (400 MHz,  $\text{CDCl}_3$ )  $\delta$  7.26 (s, 1H), 5.70 (br s, 2H), 5.44 (s, 2H), 3.65 - 3.58 (m, 2H), 2.89 - 2.83 (m, 2H), 1.85 - 1.78 (m, 2H), 1.50 - 1.40 (m, 2H), 1.27 (t,  $J$  = 7.2 Hz, 2H), 1.00 - 0.92 (m, 3H), -0.03 - -0.04 (m, 9H); LCMS (System A)  $R_t$  1.38 min,  $m/z$  447 ( $[\text{M}+\text{H}]^+$ ).

**2-Butyl-7-(6-(piperidin-1-yl)hex-1-yn-1-yl)-5-((2-(trimethylsilyl)ethoxy)methyl)-5H-pyrrolo[3,2-d]pyrimidin-4-amine (236a)**

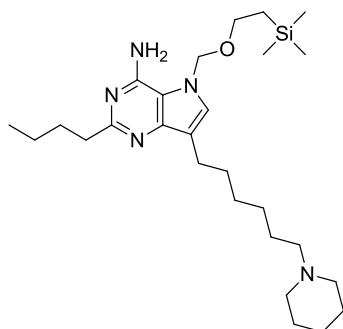


Chemical Formula: C<sub>27</sub>H<sub>45</sub>N<sub>5</sub>OSi  
Molecular Weight: 483.76

To a degassed stirred solution of 2-butyl-7-iodo-5-((2-(trimethylsilyl)ethoxy)methyl)-5H-pyrrolo[3,2-d]pyrimidin-4-amine (**235**) (400 mg, 0.90 mmol), copper(I) iodide (34 mg, 0.18 mmol) and *bis*(triphenylphosphine)palladium(II) dichloride (63 mg, 0.09 mmol) in anhydrous DMF (6 mL) was added a solution of 1-(hex-5-yn-1-yl)piperidine (193 mg, 1.17 mmol) and triethylamine (0.19 mL, 1.34 mmol) in anhydrous DMF (3 mL) dropwise over 5 mins. The reaction mixture was stirred at ambient temperature under a nitrogen atmosphere for 20 h. The reaction mixture was concentrated *in vacuo* and the residue partitioned between EtOAc (50 mL) and water (50 mL), the organic phase was separated and the aqueous phase back extracted with EtOAc (50 mL). The combined organic phases were washed with brine (50 mL), dried (MgSO<sub>4</sub>), filtered and concentrated *in vacuo* to give an orange gum which was dissolved in DCM and purified on a silica cartridge (50 g) using a 0-10% MeOH-DCM gradient over 40 mins. The appropriate fractions were combined and evaporated *in vacuo* to give the title compound (87 mg, 20 %) as a yellow foam.

<sup>1</sup>H NMR (400 MHz, CDCl<sub>3</sub>) δ 7.65 (s, 1H), 5.70 (br s, 2H), 5.47 (s, 2H), 3.66 - 3.60 (m, 2H), 3.15 (br s., 2H), 3.09 - 3.01 (m, 2H), 2.86 - 2.80 (m, 2H), 2.58 - 2.52 (m, 2H), 2.23 - 2.00 (m, 6H), 1.85 - 1.75 (m, 2H), 1.74 - 1.63 (m, 4H), 1.49 - 1.38 (m, 2H), 1.01 - 0.92 (m, 4H), 0.91 - 0.81 (m, 3H), -0.06 - -0.07 (m, 9H); LCMS (System A) R<sub>t</sub> 0.71 min, m/z 484 ([M+H]<sup>+</sup>).

**2-Butyl-7-(6-(piperidin-1-yl)hexyl)-5-((2-(trimethylsilyl)ethoxy)methyl)-5H-pyrrolo[3,2-d]pyrimidin-4-amine (237a)**

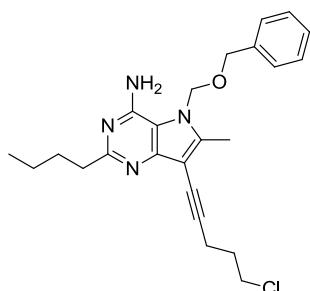


Chemical Formula: C<sub>27</sub>H<sub>49</sub>N<sub>5</sub>OSi  
Molecular Weight: 487.80

A solution of 2-butyl-7-(6-(piperidin-1-yl)hex-1-yn-1-yl)-5-((2-(trimethylsilyl)ethoxy)methyl)-5H-pyrrolo[3,2-d]pyrimidin-4-amine (**236a**) (87 mg, 0.18 mmol) in EtOH (8 mL) and AcOH (1 mL) was hydrogenated using the H-cube (settings: 60 °C, Full H<sub>2</sub>, 1 mL/min flow rate) and a 10% Pd/C CatCart 30 as the catalyst. The reaction mixture was concentrated *in vacuo* and the residue partitioned between DCM (20 mL) and 2N aqueous sodium hydroxide (20 mL). The organic phase was separated and dried (hydrophobic frit) before concentration *in vacuo* to give the title compound (50 mg, 57%)

<sup>1</sup>H NMR (400 MHz, CDCl<sub>3</sub>) δ 6.90 (s, 1H), 5.59 (br s, 2H), 5.40 (s, 2H), 3.62 - 3.55 (m, 2H), 2.84 - 2.78 (m, 2H), 2.76 - 2.70 (s, 2H), 2.39 - 2.32 (m, 4H), 2.30 - 2.24 (m, 2H), 1.85 - 1.76 (m, 2H), 1.75 - 1.65 (m, 2H), 1.63 - 1.55 (m, 4H), 1.53 - 1.31 (m, 10H), 0.98 - 0.92 (m, 5H), 0.03 - -0.04 (m, 9H); LCMS (System A) R<sub>t</sub> 0.86 min, m/z 489 ([M+H]<sup>+</sup>).

**5-((Benzyloxy)methyl)-2-butyl-7-(5-chloropent-1-yn-1-yl)-6-methyl-5H-pyrrolo[3,2-d]pyrimidin-4-amine (238y)**



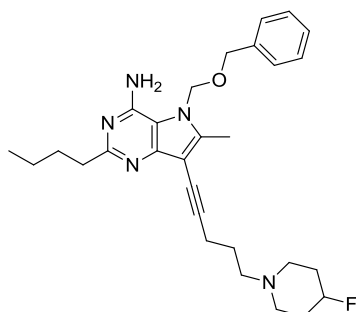
Chemical Formula: C<sub>24</sub>H<sub>29</sub>ClN<sub>4</sub>O  
Molecular Weight: 424.97

To a stirred degassed suspension of 5-((benzyloxy)methyl)-2-butyl-7-iodo-6-methyl-5H-pyrrolo[3,2-d]pyrimidin-4-amine (**221**) (1.10 g, 2.44 mmol), *bis*(triphenylphosphine) palladium(II) dichloride (0.10 g, 0.15 mmol) and copper(I) iodide (0.06 g, 0.29 mmol) in anhydrous DMF (12 mL) at 50 °C was added a solution of 5-chloropent-1-yne (0.33 g, 3.18 mmol) and triethylamine (0.51 mL, 3.66 mmol) in anhydrous DMF (3 mL) dropwise over 5 mins. The resulting solution was stirred at 50 °C for 18 h. The reaction mixture was degassed and further *bis*(triphenylphosphine)palladium(II) dichloride (40 mg, 0.057 mmol), further copper(I) iodide (20 mg, 0.1 mmol) and a solution of 5-chloropent-1-yne (100 mg, 0.97 mmol) in anhydrous DMF (2 mL) were added and the reaction mixture stirred at 50 °C for a further 78.5 h. The reaction mixture was concentrated *in vacuo* and the residue partitioned between EtOAc (200 mL) and water (200 mL). The organic layer was separated and the aqueous layer back extracted with EtOAc (50 mL). The combined organics were washed with brine (250 mL), dried (hydrophobic frit) and concentrated *in vacuo* to give an orange gum (1.35 g). The gum was dissolved in DCM and purified on an aminopropyl functionalised silica cartridge (110 g) using a 0-50% EtOAc-cyclohexane gradient over 60 mins. The appropriate fractions were combined and evaporated *in vacuo* to give a sticky yellow solid. This residue was triturated with Et<sub>2</sub>O, the suspension filtered and the solid dried *in vacuo* to give the title compound (457 mg, 44%) as a off-white solid.

<sup>1</sup>H NMR (400 MHz, CDCl<sub>3</sub>) δ 7.43 - 7.34 (m, 3H), 7.32 - 7.27 (m, 2H), 5.65 (br s,

2H), 5.54 (s, 2H), 4.57 (s, 2H), 3.78 (t,  $J = 6.5$  Hz, 2H), 2.89 - 2.83 (m, 2H), 2.74 (t,  $J = 6.9$  Hz, 2H), 2.43 (s, 3H), 2.17 - 2.09 (m, 2H), 1.89 - 1.78 (m, 2H), 1.52 - 1.40 (m, 2H), 0.97 (t,  $J = 7.5$  Hz, 3H);  $^{13}\text{C}$  NMR (126 MHz,  $\text{CDCl}_3$ )  $\delta$  164.5, 151.0, 149.7, 143.8, 135.6, 128.8, 128.6, 128.0, 113.0, 99.0, 92.7, 73.0, 72.7, 69.6, 43.9, 39.1, 31.7, 31.4, 22.8, 17.6, 14.0, 11.6; LCMS (System B)  $R_t$  1.29 min,  $m/z$  425, 427 ( $[\text{M}+\text{H}]^+$ ); HRMS Anal. Calcd. For  $\text{C}_{24}\text{H}_{30}\text{ClN}_4\text{O} = 425.2108$ . Found = 425.2093 ( $[\text{M}+\text{H}]^+$ ); IR ( $\text{cm}^{-1}$ ) 3438, 3306, 3132, 2961, 2932, 1644, 1598, 1543; Mpt. 140-142 °C.

**5-((Benzyloxy)methyl)-2-butyl-7-(5-(4-fluoropiperidin-1-yl)pent-1-yn-1-yl)-6-methyl-5H-pyrrolo[3,2-*d*]pyrimidin-4-amine (239c)**

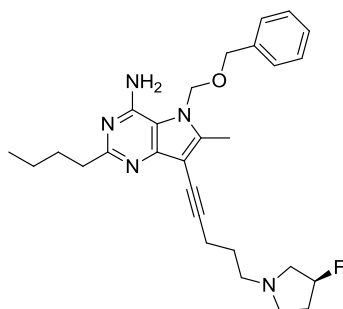


Chemical Formula:  $\text{C}_{29}\text{H}_{38}\text{FN}_5\text{O}$   
Molecular Weight: 491.64

To a stirred solution of 5-((benzyloxy)methyl)-2-butyl-7-(5-chloropent-1-yn-1-yl)-6-methyl-5H-pyrrolo[3,2-*d*]pyrimidin-4-amine (**238y**) (140 mg, 0.33 mmol) in MeCN (3 mL) was added triethylamine (0.28 mL, 1.98 mmol) and 4-fluoropiperidine hydrochloride (138 mg, 0.99 mmol). The resultant mixture was heated at 60 °C for 18 h. To the reaction was added further 4-fluoropiperidine hydrochloride (50 mg, 0.36 mmol) and further triethylamine (0.10 mL, 0.72 mmol) and heating at 60 °C continued for 20 h. To the reaction mixture was added further triethylamine (0.10 mL, 0.72 mmol) and the reaction was heated to 80 °C for 4 h. The reaction mixture was concentrated *in vacuo* and the residue partitioned between DCM (20 mL) and water (20 mL). The organic phase was separated and dried (hydrophobic frit) before concentration *in vacuo* to give a red oil. The oil was dissolved in DCM and purified on an aminopropyl functionalised silica cartridge (11 g) using a 0-100% EtOAc-cyclohexane gradient over 30 mins. The appropriate fractions were combined and evaporated *in vacuo* to give the title compound (85 mg, 53%) as a colourless gum.

$^1\text{H}$  NMR (400 MHz,  $\text{CDCl}_3$ )  $\delta$  7.41 - 7.32 (m, 3H), 7.31 - 7.24 (m, 2H), 5.54 (br s, 2H), 5.51 (s, 2H), 4.79 - 4.58 (m, 1H), 4.54 (s, 2H), 2.88 - 2.79 (m, 2H), 2.67 - 2.49 (m, 6H), 2.40 - 2.36 (s, 5H), 1.99 - 1.75 (m, 8H), 1.48 - 1.37 (m, 2H), 0.94 (t,  $J = 7.3$  Hz, 3H); LCMS (System B)  $R_t$  1.24 min,  $m/z$  492 ( $[\text{M}+\text{H}]^+$ ).

**(S)-5-((benzyloxy)methyl)-2-butyl-7-(5-(3-fluoropyrrolidin-1-yl)pent-1-yn-1-yl)-6-methyl-5H-pyrrolo[3,2-d]pyrimidin-4-amine (239o)**

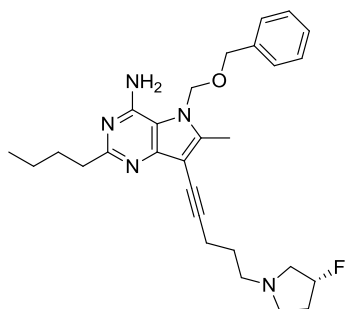


Chemical Formula:  $\text{C}_{28}\text{H}_{36}\text{FN}_5\text{O}$   
Molecular Weight: 477.62

To a stirred solution of 5-((benzyloxy)methyl)-2-butyl-7-(5-chloropent-1-yn-1-yl)-6-methyl-5H-pyrrolo[3,2-d]pyrimidin-4-amine (**238y**) (140 mg, 0.33 mmol) in MeCN (3 mL) was added triethylamine (0.28 mL, 1.98 mmol) and (S)-3-fluoropyrrolidine hydrochloride (124 mg, 0.99 mmol). The resultant mixture was heated at 60 °C for 22 h. To the reaction mixture was added further (S)-3-fluoropyrrolidine hydrochloride (35 mg, 0.28 mmol) and further triethylamine (0.10 mL, 0.72 mmol) and heating at 60 °C continued for 20 h. To the reaction mixture was added further triethylamine (0.10 mL, 0.72 mmol) and the reaction mixture heated to 80 °C for 4 h. The reaction mixture was concentrated *in vacuo* and the residue partitioned between DCM (20 mL) and water (20 mL). The organic phase was separated and dried (hydrophobic frit) before concentration *in vacuo* to give a red oil. The sample was dissolved in DCM and purified on an aminopropyl functionalised silica cartridge (11 g) using a 0-100% EtOAc-cyclohexane gradient over 30 mins. The appropriate fractions were combined and evaporated *in vacuo* to give the title compound (86 mg, 55%) as a colourless oil which solidified.

$^1\text{H}$  NMR (400 MHz,  $\text{CDCl}_3$ )  $\delta$  7.43 - 7.35 (m, 3H), 7.32 - 7.27 (m, 2H), 5.79 (br s, 2H), 5.53 (s, 2H), 5.34 - 5.14 (m, 1H), 4.57 (s, 2H), 3.07 - 2.93 (m, 2H), 2.92 - 2.76 (m, 6H), 2.63 (t,  $J = 7.0$  Hz, 2H), 2.43 (s, 3H), 2.33 - 2.11 (m, 2H), 2.04 - 1.93 (m, 2H), 1.88 - 1.77 (m, 2H), 1.50 - 1.39 (m, 2H), 1.00 - 0.93 (m, 3H); LCMS (System B)  $R_t$  1.20 min,  $m/z$  478 ( $[\text{M}+\text{H}]^+$ ).

**(R)-5-((benzyloxy)methyl)-2-butyl-7-(5-(3-fluoropyrrolidin-1-yl)pent-1-yn-1-yl)-6-methyl-5H-pyrrolo[3,2-d]pyrimidin-4-amine (239p)**



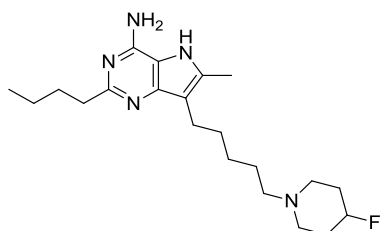
Chemical Formula:  $\text{C}_{28}\text{H}_{36}\text{FN}_5\text{O}$   
Molecular Weight: 477.62

To a stirred solution of 5-((benzyloxy)methyl)-2-butyl-7-(5-chloropent-1-yn-1-yl)-6-methyl-5H-pyrrolo[3,2-d]pyrimidin-4-amine (**238y**) (140 mg, 0.33 mmol) in MeCN (3 mL) was added triethylamine (0.28 mL, 1.98 mmol) and (*S*)-3-fluoropyrrolidine, hydrochloride (124 mg, 0.99 mmol). The resultant mixture was heated at 60 °C for 22 h. To the reaction mixture was added further (*R*)-3-fluoropyrrolidine, hydrochloride (35 mg, 0.28 mmol) and further triethylamine (0.10 mL, 0.72 mmol) and heating at 60 °C continued for 20 h. To the reaction mixture was added further triethylamine (0.10 mL, 0.72 mmol) and the reaction mixture heated to 80 °C for 4 h. The reaction mixture was concentrated *in vacuo* and the residue partitioned between DCM (20 mL) and water (20 mL). The organic phase was separated and dried (hydrophobic frit) before concentration *in vacuo* to give a red oil. The sample was dissolved in DCM and purified on an aminopropyl functionalised silica cartridge (11 g) using a 0-100% EtOAc-cyclohexane gradient over 30 mins. The appropriate fractions were combined and evaporated *in vacuo* to give the title compound (74 mg, 46%) as a colourless oil which solidified.



$^1\text{H}$  NMR (400 MHz,  $\text{CDCl}_3$ )  $\delta$  7.43 - 7.35 (m, 3H), 7.32 - 7.27 (m, 2H), 5.79 (br s, 2H), 5.53 (s, 2H), 5.34 - 5.14 (m, 1H), 4.57 (s, 2H), 3.07 - 2.93 (m, 2H), 2.92 - 2.76 (m, 6H), 2.63 (t,  $J = 7.0$  Hz, 2H), 2.43 (s, 3H), 2.33 - 2.11 (m, 2H), 2.04 - 1.93 (m, 2H), 1.88 - 1.77 (m, 2H), 1.50 - 1.39 (m, 2H), 1.00 - 0.93 (m, 3H); LCMS (System B)  $R_t$  1.20 min,  $m/z$  478 ( $[\text{M}+\text{H}]^+$ ).

**2-Butyl-7-(5-(4-fluoropiperidin-1-yl)pentyl)-6-methyl-5H-pyrrolo[3,2-*d*]pyrimidin-4-amine (240c)**

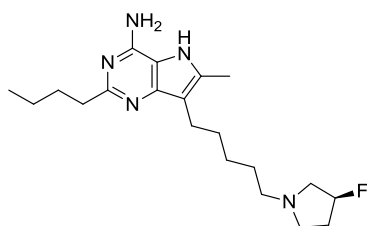


Chemical Formula:  $\text{C}_{21}\text{H}_{34}\text{FN}_5$   
Molecular Weight: 375.53

A filtered solution of 5-((benzyloxy)methyl)-2-butyl-7-(5-(4-fluoropiperidin-1-yl)pent-1-yn-1-yl)-6-methyl-5H-pyrrolo[3,2-*d*]pyrimidin-4-amine (**239c**) (84 mg, 0.17 mmol) in EtOH (16 mL) and AcOH (3 mL) was hydrogenated using the H-cube<sup>TM</sup> (settings: 60 °C, Full  $\text{H}_2$ , 1 mL/min flow rate) and a 10% Pd/C CatCart 30 as the catalyst. The reaction mixture was concentrated *in vacuo* and the residue was dissolved in 1:1 MeOH:DMSO (1 mL) and purified by MDAP on an Xbridge column using MeCN-water with an ammonium carbonate modifier. The solvent was evaporated *in vacuo* to give a sticky colourless gum (47 mg). The residue was dissolved in DCM (10 mL) and washed with saturated aqueous sodium bicarbonate (10 mL). The organic was separated and the aqueous back extracted with 1:1 EtOAc: $\text{CHCl}_3$  (3 x 10 mL). The combined organic extracts were dried (hydrophobic frit) and concentrated *in vacuo* to give the title compound (19 mg, 30 %) as a white solid.

$^1\text{H}$  NMR (400 MHz, MeOD)  $\delta$  4.75 - 4.55 (m, 1H), 2.78 - 2.68 (m, 4H), 2.65 - 2.54 (m, 2H), 2.40 (s, 3H), 2.38 - 2.32 (m, 2H), 1.98 - 1.70 (m, 6H), 1.67 - 1.50 (m, 4H), 1.47 - 1.29 (m, 6H), 0.97 (t,  $J = 7.5$  Hz, 3H); LCMS (System B)  $R_t$  1.01 min,  $m/z$  376 ( $[\text{M}+\text{H}]^+$ ).

**(S)-2-butyl-7-(5-(3-fluoropyrrolidin-1-yl)pentyl)-6-methyl-5H-pyrrolo[3,2-  
d]pyrimidin-4-amine (240o)**

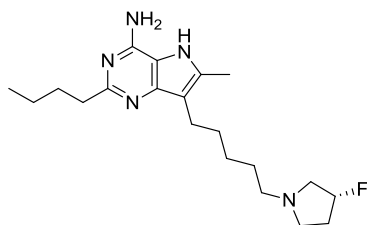


Chemical Formula: C<sub>20</sub>H<sub>32</sub>FN<sub>5</sub>  
Molecular Weight: 361.50

A filtered solution of (S)-5-((benzyloxy)methyl)-2-butyl-7-(5-(3-fluoropyrrolidin-1-yl)pent-1-yn-1-yl)-6-methyl-5H-pyrrolo[3,2-*d*]pyrimidin-4-amine (**239o**) (85 mg, 0.18 mmol) in EtOH (16 mL) and AcOH (3 mL) was hydrogenated using the H-cube<sup>TM</sup> (settings: 60 °C, Full H<sub>2</sub>, 1 mL/min flow rate) and a 10% Pd/C CatCart 30 as the catalyst. The reaction mixture was concentrated *in vacuo* and the residue was dissolved in 1:1 MeOH:DMSO (1 mL) and purified by MDAP on an Xbridge column using MeCN-water with an ammonium carbonate modifier. The solvent was evaporated *in vacuo* to give the title compound (32 mg, 50% yield) as a white solid.

<sup>1</sup>H NMR (400 MHz, MeOD) δ 5.26 - 5.03 (dm, *J* = 55.5 Hz, 1H), 2.98 - 2.84 (m, 2H), 2.76 - 2.69 (m, 4H), 2.69 - 2.55 (m, 1H), 2.51 - 2.43 (m, 2H), 2.43 - 3.56 (m, 4H), 2.27 - 2.10 (m, 1H), 2.08 - 1.92 (m, 1H), 1.79 - 1.70 (m, 2H), 1.68 - 1.51 (m, 4H), 1.48 - 1.34 (m, 4H), 0.97 (t, *J* = 7.3 Hz, 3H); LCMS (System B) R<sub>t</sub> 0.96 min, m/z 362 ([M+H]<sup>+</sup>).

**(R)-2-butyl-7-(5-(3-fluoropyrrolidin-1-yl)pentyl)-6-methyl-5H-pyrrolo[3,2-  
d]pyrimidin-4-amine (240p)**



Chemical Formula: C<sub>20</sub>H<sub>32</sub>FN<sub>5</sub>  
Molecular Weight: 361.50

A filtered solution of (*R*)-5-((benzyloxy)methyl)-2-butyl-7-(5-(3-fluoropyrrolidin-1-yl)pent-1-yn-1-yl)-6-methyl-5*H*-pyrrolo[3,2-*d*]pyrimidin-4-amine (**239p**) (73 mg, 0.153 mmol) in EtOH (16 mL) and AcOH (3 mL) was hydrogenated using the H-cube<sup>TM</sup> (settings: 60 °C, Full H<sub>2</sub>, 1 mL/min flow rate) and a 10% Pd/C CatCart 30 as the catalyst. The reaction mixture was concentrated *in vacuo* and the residue was dissolved in 1:1 MeOH:DMSO (1 mL) and purified by MDAP on an Xbridge column using MeCN/H<sub>2</sub>O with an ammonium carbonate modifier. The solvent was evaporated *in vacuo* to give the title compound (25 mg, 45% yield) as a white solid.

<sup>1</sup>H NMR (400 MHz, MeOD) δ 5.26 - 5.03 (dm, *J* = 55.5 Hz, 1H), 2.98 - 2.84 (m, 2H), 2.76 - 2.69 (m, 4H), 2.69 - 2.55 (m, 1H), 2.51 - 2.43 (m, 2H), 2.43 - 3.56 (m, 4H), 2.27 - 2.10 (m, 1H), 2.08 - 1.92 (m, 1H), 1.79 - 1.79 (m, 2H), 1.68 - 1.51 (m, 4H), 1.48 - 1.34 (m, 4H), 0.97 (t, *J* = 7.3 Hz, 3H); LCMS (System B) R<sub>t</sub> 0.96 min, m/z 362 ([M+H]<sup>+</sup>).

## 5 Appendix

### 5.1 Spectral analysis of compound **211b**

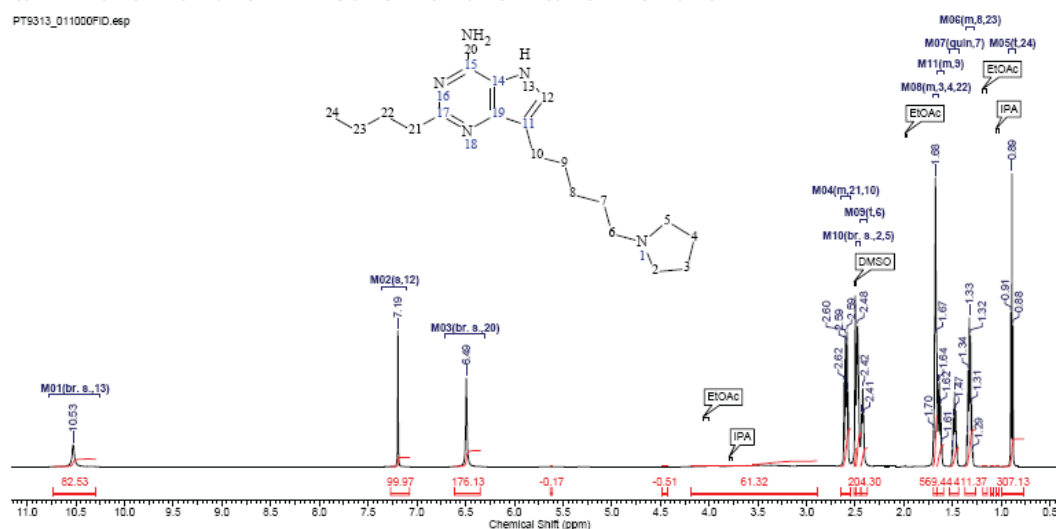
#### 5.1.1 NMR of compound **211b**

28/02/2012 17:06:43

Formula	C <sub>18</sub> H <sub>21</sub> N <sub>5</sub>	FW	329.4829
Acquisition Time (sec)	1.9999	Comment	PT9313 N22278-72-1 DT35268 DMSO- <i>d</i> <sub>6</sub> 1H Tape_Daniel T
Date Stamp	28 Feb 2012 10:12:16	File Name	C:\DATA\CHEMIST\NMR\PT9313\11\FID
Frequency (MHz)	600.40	Nucleus	<sup>1</sup> H
Original Points Count	21644	Owner	chemist
Receiver Gain	8.00	SW (cyclical) (Hz)	10822.51
Spectrum Type	STANDARD	Sweep Width (Hz)	10822.18
		Solvent	DMSO- <i>d</i> <sub>6</sub>
		Temperature (degree C)	30.000
		Points Count	32768
		Pulse Sequence	zgpg30
		Spectrum Offset (Hz)	4495.6501

<sup>1</sup>H NMR (600 MHz, DMSO-*d*<sub>6</sub>) δ ppm 0.89 (t, *J*=7.43 Hz, 3 H) 1.28 - 1.37 (m, 4 H) 1.48 (quin, *J*=7.43 Hz, 2 H) 1.59 - 1.66 (m, 2 H) 1.65 - 1.70 (m, 6 H) 2.42 (t, *J*=7.27 Hz, 2 H) 2.48 (br. s., 4 H) 2.55 - 2.65 (m, 4 H) 6.49 (br. s., 2 H) 7.19 (s, 1 H) 10.53 (br. s., 1 H)

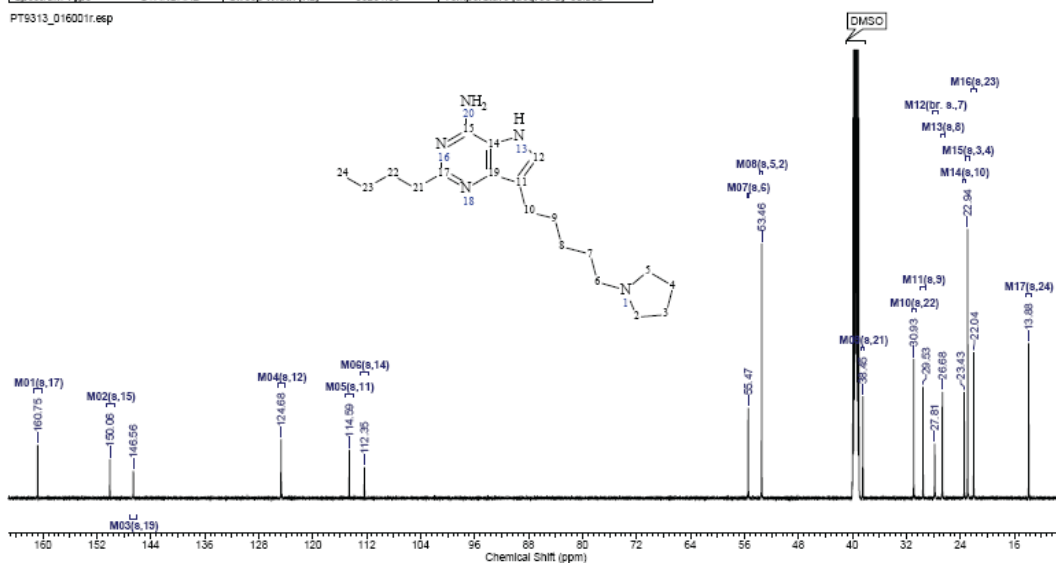
PT9313\_011000FID.esp



28/02/2012 17:09:25

CNMR Match Factor	0.25	CNMR Reliability	35.00	CNMR RMS of Assignment	2.73	CNMR Structure Purity	80.36
Formula	C <sub>18</sub> H <sub>21</sub> N <sub>5</sub>	FW	329.4829				
Acquisition Time (sec)	0.9044	Comment	PT9313 N22278-72-1 DT35268 DMSO- <i>d</i> <sub>6</sub> 13C Tape_Daniel T				
Date Stamp	28 Feb 2012 11:50:24	File Name	C:\DATA\CHEMIST\NMR\PT9313\16\pdata\11r				
Frequency (MHz)	150.97	Nucleus	<sup>13</sup> C				
Original Points Count	32768	Owner	chemist				
Receiver Gain	2050.00	SW (cyclical) (Hz)	36231.88				
Spectrum Type	STANDARD	Sweep Width (Hz)	36231.33				
		Solvent	DMSO- <i>d</i> <sub>6</sub>				
		Temperature (degree C)	30.000				
		Points Count	65536				
		Pulse Sequence	zgpg32bo				
		Spectrum Offset (Hz)	16524.5560				

PT9313\_016001r.esp



## 5.1.2 HRMS of compound 211b

### Single Mass Analysis (displaying only valid results)

Tolerance = 2.0 PPM / DBE: min = -1.5, max = 50.0

Selected filters: Carbon; Cl & Br; Sulphur;

Monoisotopic Mass, Even Electron Ions

396 formula(e) evaluated with 1 results within limits (up to 10 best isotopic matches for each mass)

Elements Used:

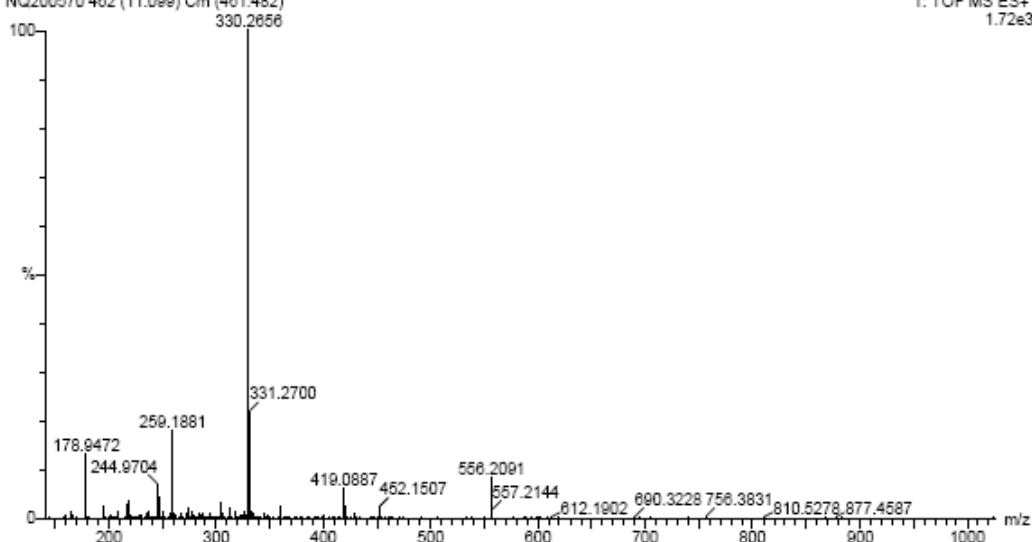
C: 1-100 H: 1-1000 N: 0-10 O: 0-10

N22278-72-1 [2]

Daniel Tape

NQ200570 462 (11.099) Cm (461:462)

28-Feb-2012  
Kinetix C18 2.6µm (2.1 x 100mm)  
1: TOF MS ES+  
1.72e3



Minimum: -1.5  
Maximum: 5.0 2.0 50.0

Mass	Calc. Mass	mDa	PPM	DBE	i-FIT	Formula
330.2656	330.2656	-0.2	-0.6	6.5	9.1	C19 H32 N5

## 6 References

1. Holgate, S. T.; Holloway, J.; Wilson, S.; Howarth, P. H.; Haitchi, H. M.; Babu, S.; Davies, D. E. Understanding the pathophysiology of severe asthma to generate new therapeutic opportunities. *J. Allergy Clin. Immunol.* **2006**, *117*, 496-506.
2. Smit, J.J.; Lukacs, N.W. A closer look at chemokines and their role in asthmatic responses; *Eur. J. Pharmacol.* **2006**, *533*, 277-288.
3. Image sourced online from: <http://shsgdp.wikispaces.com/Period+2+Asthma> (31/12/2011).
4. World Health Organization Fact Sheet, Fact sheet No 307: Asthma". 2011. <http://web.archive.org/web/20110629035454/http://www.who.int/mediacentre/factsheets/fs307/en/>. Retrieved Jan 17th, 2013
5. Akinbami, L. J.; Moorman, J. E.; Bailey, C.; zahran, H. S.; King, M.; Johnson, C. A.; Liu, X. Trends in asthma prevalence, health care use, and mortality in the United States, 2001-2010. NCHS data brief, no 94. Hyattsville, MD: national Centre for Health Statistics. **2012**
6. Asthma UK news centre, facts for journalists. <http://www.asthma.org.uk/news-centre/facts-for-journalists/> Retrieved 19 April 2012.
7. Bahadori, K.; Doyle-Walters, M. M.; Marra, C.; Lynd, L.; Alasaly, K.; Swiston, J.; FitzGerald, J. M. Economic burden of asthma, a systematic review. *BMC Pulmonary Medicine* **2009**, *9*, 24-40.
8. Yawn, B. P. Factors accounting for asthma variability: achieving optimal symptom control for individual patients; *Prim Care Respir J.* **2008**, *17*, 138-147.
9. (a) Kim, H. Y.; DeKruyff, R. H.; Umetsu, D. T. The many paths to asthma: phenotype shaped by adaptive immunity; *Nat. Immunol.* **2010**, *11*, 577-584. (b) Bhakta, N. R.; Woodruff, P. G. Human asthma phenotypes: from the clinic, to cytokines, and back again; *Immunol. Rev.* **2011**, *242*, 220-232. (c) Wenzel, S. A. Asthma phenotypes: the evolution from clinical to molecular approaches. *Nat. Medicine* **2012**, *18*, 716-725.
10. (a) Agache, I.; Akdis, C.; Jutel, M; Virchow, J. C. Untangling asthma phenotypes and endotypes. *Allergy* **2012**, *67*, 835-846. (b) Fahy, J. V. Type 2 inflammation in asthma – present in most, absent in many. *Nat. Rev. Immunol.* **2015**, *15*, 57-65.
11. Sompayrac, L. *How the immune system works*, 4<sup>th</sup> edition, Wiley-Blackwell, N.J. **2012**.
12. Galli, S. J.; Tsai, M. IgE and mast cells in allergic disease. *Nat. Medicine* **2012**, *18*, 693-704.
13. Holgate, S. T.; Polosa, R. Treatment strategies for allergy and asthma. *Nat. Rev. Immunol.* **2008**, *8*, 218-230.
14. Kalinski, P.; Hilkens, C.M.; Wierenga, E. A; Kapensberg, M. L. T-cell priming by type-1 and type-2 polarized dendritic cells: the concept of a third signal. *Immunol. Today.* **1999**, *20*, 561-567.

15. Waldeck, B.  $\beta$ -Adrenoceptor agonists and asthma – 100 years of development. *Eur. J. Pharmacol.* **2002**, *445*, 1-12.
16. Glossop, P. A.; Price, D. A. Progress in the development of inhaled, long-acting  $\beta_2$ -adrenoceptor agonists. *Ann. Rep. Med. Chem.* **2006**, *41*, 237-248.
17. Cazzola, M.; Calzetta, L.; Matera, M. G.  $\beta_2$  adrenoceptor agonist: current and future direction. *Br. J. Pharmacol.* **2011**, *163*, 4-17.
18. Gibbons, I. L. Peripheral autonomic nervous system. In Paxinos, G (ed). *The human nervous system*. Academic Press, San Diego. **1990**.
19. Rang, H. P.; Dale, M. M.; Ritter, J. M.; Flower, R. J. Noradrenergic transmission. In *Rang and Dale's Pharmacology, 6<sup>th</sup> edition*. Churchill Livingstone **2007**, 168-188.
20. Bullock, J. G. M.; Kaplan, D. M. On the hypodermic use of adrenalin chloride in the treatment of asthma attacks. *Med. News* **1903**, *83*, 787-790.
21. Boushey, H. A.; Drugs used in asthma. In: Katzung, B. G.; Masters, S. B.; Trevor, A. J. eds. *Basic & Clinical Pharmacology*. 12th ed. New York: McGraw-Hill; **2012**.
22. Bennett, J. A.; Harrison, T. W.; Tattersfield, A. The contribution of the swallowed fraction of an inhaled dose of salmeterol to its systemic effects. *Eur. Respir. J.* **1999**, *13*, 445-448.
23. Bodor, N.; Bachwald, P. Drug targeting *via* retrometabolic approaches. *Pharmacol. Ther.* **1997**, *76*, 1-27.
24. Lee, H.; Ko, D.-H.; McLean, H. M. Recent advances in prodrugs and antedugs. *Curr. Opin. Drug Discovery Dev.* **1998**, *1*, 235-244.
25. Coleman, R. A.; Johnson, M.; Nials, A. T.; Vardey, C. J. Exosites: their current status, and their relevance to the duration of action of long-acting  $\beta_2$ -adrenoceptor agonists. *Trends Pharmacol. Sci.* **1996**, *17*, 324-330.
26. (a) Collin, D. T.; Hartley, D.; Jack, D.; Lunts, L. H. C.; Press, J. C.; Ritchie, A. C.; Toon, P. Saligenin analogues of sympathomimetic catecholamines. *J. Med. Chem.* **1970**, *13*, 674-680.  
(b) Tattersfield, A. E.; McNicol, M. W. Salbutamol and Isoproterol. Double blind trial to compare bronchodilator and cardiovascular activity. *N. Eng. J. Med.* **1969**, *281*, 1323-1326.
27. (a) Sackner, M. A.; Silva, G. Effects of terbutaline aerosol in reversible airway obstruction. *Chest* **1978**, *73*, 802-806. (b) Schwender, C. F.; Sunday, B. R.; Shavel Jr. J.; Giles, R. E. 3-( $\alpha$ -(*tert*-butylamino)methyl)-5-hydroxy-*m*-xylene- $\alpha$ ,  $\alpha'$ -diol, a selective bronchodilator. *J. Med. Chem.* **1974**, *17*, 1112-1115.
28. (a) Ullman, A.; Svedmyr, N. Salmeterol, a new long-acting inhaled  $\beta_2$ -adrenoceptor agonist: comparison with salbutamol in adult asthmatic patients. *Thorax* **1988**, *43*, 674-678. (b) Johnson, M. The pharmacology of salmeterol. *Lung* **1990**, *168*, 115-119.
29. (a) Tattersfield, A. Clinical pharmacology of long acting beta agonists. *Life Sci.* **1993**, *52*, 2161-2169. (b) Faulds, D.; Hollingshed, L. M.; Goa, K. L. Formoterol: a

- review of its pharmacology and therapeutic potential in reversible obstructive airway disease. *Drugs* **1991**, *42*, 115-137. (c) Murase, K.; Mase, T.; Ida, H.; Takahashi, K.; Murakami, M. New  $\beta$ -adrenoreceptor stimulants. Studies on 3-acylamino-4-hydroxy- $\alpha$ -(*N*-substituted aminomethyl)benzyl alcohols. *Chem. Pharm. Bull.* **1977**, *25*, 1368-1377. (d) Alikhani, V.; Beer, D.; Bently, D.; Bruce, I.; Cuenound, B. M.; Fairhurst, R. A.; Gedeck, P.; Haberthuer, S.; Hayden, C.; Janus, D.; Jordan, L.; Lewis, C.; Smithies, K.; Wissler, E. Long-chain formoterol analogues: an investigation into the effect of increasing amino-substituent length on the  $\beta_2$ -adrenoceptor activity. *Bioorg. Med. Chem. Lett.* **2004**, *14*, 4705-4710.
30. (a) Procopiou, P. A.; Barrett, V. J.; Bevan, N. J.; Biggadike, K.; Box, P. C.; Butchers, P. R.; Coe, D. M.; Conroy, R.; Emmons, A.; Ford, A. J.; Holmes, D. S.; Horsley, H.; Kerr, F.; Li-Kwai-Cheung, A.-M.; Looker, B. E.; Mann, I. S.; McLay, I. M.; Morrison, V. S.; Mutch, P. J.; Smith, C. E.; Tomlin, P. Synthesis and structure activity relationships of long-acting  $\beta_2$  adrenergic receptor agonists incorporating metabolic inactivation: an antedrug approach. *J. Med. Chem.* **2010**, *53*, 4522–4530. (b) Barrett, V. J.; Morrison, V.; Sturton, R. G.; Ford, A. J.; Knowles, R. Pharmacological characterisation of GW642444, a long-acting  $\beta_2$ -agonist (LABA) with rapid onset and long duration, on isolated large and small human airways. *Am. J. Respir. Crit. Care Med.* **2010**, *181*, A4453. (c) Lötval, J.; Bateman, E. D.; Bleecker, E. R.; Busse, W.; Woodcock, A.; Follows, R.; Lim, J.; Stone, S.; Jaques, L.; Haumann, B. 24-h duration of the novel LABA vilanterol trifenate in asthma patients treated with inhaled corticosteroids. *Eur. Respir. J.* **2012**, *40*, 570-579.
31. Gupta, R.; Jindal, D. P.; Kumar, G. Corticosteroids: the mainstay in asthma therapy. *Bioorg. Med. Chem.* **2004**, *12*, 6331-6342.
32. Barnes, P. J. Efficacy of inhaled corticosteroids in asthma. *J. Allergy Clin. Immunol.* **1998**, *102*, 531-538.
33. Hatipoglu, B. A. Cushing's syndrome. *J. Surg. Oncol.* **2012**, *106*, 565-571.
34. Chang, K. C.; Miklich, D. R.; Barwise, G.; Chai, H.; Miles-Lawrence, R. Linear growth of chronic asthmatic children: the effects of the disease and various forms of steroid therapy. *Clin. Allergy* **1982**, *12*, 369-378.
35. Harris, M. S. Cortisone in treatment of bronchial asthma. *Calif. Med.* **1951**, *75*, 85–88.
36. (a) Frey, F. J.; Escher, G.; Frey, B. M. Pharmacology of 11beta-hydroxysteroid dehydrogenase. *Steroids* **1994**, *59*, 74-79. (b) Aaronson, A. L.; Kaplan, M. A.; Taub, S. J.; Prednisone (meticorten) in the treatment of bronchial asthma; a clinical study. *J. Allergy* **1956**, *276*, 514-22.
37. (a) Bodor, N.; Harget, A. J.; Phillips, E. W. Structure activity relationships in the anti-inflammatory steroids, a pattern recognition approach. *J. Med. Chem.* **1983**, *26*, 318-328. (b) Cameron, S. J.; Cooper, E. J.; Crompton, G. K.; Hoare, M. V.; Grant, I. W. Substitution of



- beclomethasone aerosol for oral prednisolone in the treatment of chronic asthma. *Br. Med. J.* **1973**, 5886, 205-7.
38. (a) Edsbaecker, S.; Joensson, S.; Lindberg, C.; Ryrfeldt, A.; Thalen, A. Metabolic pathways of the topical glucocorticoid budesonide in man. *Drug Metab. Dispos.* **1983**, 11, 590-596. (b) Derendorf, H.; Hochhaus, G.; Meibohm, B.; Möllmann, H.; Barth, J. Pharmacokinetics and pharmacodynamics of inhaled corticosteroids. *J. Allergy Clin. Immunol.* **1998**, 101, S440-S446. (c) Ashton, M. J.; Lawrence, C.; Karlsson, J.-A.; Stuttle, K. A. J.; Newton, C. G.; Vacher, B. Y. J.; Webber, S.; Withnall, M. J. Anti-inflammatory 17 $\beta$ -Thioalkyl-16 $\alpha$ ,17 $\alpha$ -ketal and -acetal androstanes: a new class of airway selective steroids for the treatment of asthma. *J. Med. Chem.* **1996**, 39, 4888–4896.
39. (a) McGrath, N. A.; Brichacek, M.; Njardason, J. T. A graphical journey of innovative organic architectures that have improved our lives. *J. Chem. Educ.* **2010**, 87, 1348-1349. (b) Barnes, P. J.; Pedersen, S.; Busse, W. W. Efficacy and safety of inhaled corticosteroids. New developments. *Am. Rev. Respir. Crit. Care Med.* **1998**, 157, S1-S53. (c) Harding, S. M. The human pharmacology of fluticasone propionate. *Respir. Med.* **1990**, 84, 25-29. (d) Philipps, G. H.; Bailey, E. J.; Bain, B. M.; Borella, R. A.; Buckton, J. B.; Clark, J. C.; Doherty, A. E.; English, A. F.; Fazakerley, H.; Laing, S. B.; Lane-Allman, E.; Robinson, J. D.; Sandford, P. E.; Sharratt, P. J.; Steeples, I. P.; Stonehouse, R. D.; Williamson, C. Synthesis and structure-activity relationships in a series of anti-inflammatory corticosteroid analogues, halomethyl androstane-17 $\beta$ -carbothioates and -17 $\beta$ -carboselenoates. *J. Med. Chem.* **1994**, 37, 3717-3729.
40. (a) McCormack, P. L.; Plosker, G. L.; Inhaled mometasone furoate: a review of its use in persistent asthma in adults and adolescents. *Drugs* **2006**, 66, 1151-1168. (b) Sandham, D. A.; Barker, L.; Beattie, D.; Beer, D.; Bidlake, L.; Bentley, D.; Butler, K. D.; Craid, S.; Farr, D.; Foulkes-Jones, C.; Fozard, J. R.; Habberthuer, S.; Howes, C.; Hynx, D.; Jeffers, S.; Keller, T. H.; Kirkham, P. A.; Maas, J. C.; Mazzoni, L.; Nicholls, A.; Pilgrim, G. E.; Schaeublin E.; Spooner, G. M.; Stringer, R.; Tranter, P.; Turner, K. L.; Tweed, M. F.; Walker, C.; Watson, S. J.; Cuenoud, B. M. Synthesis and biological properties of novel glucocorticoid androstene C-17 furoate esters. *Bioorg. Med. Chem. Lett.* **2004**, 12, 5213-5224.
41. Sobera, L. A.; Serradell, N.; Bolos, J. Fluticasone furoate. *Drugs Future*, **2007**, 32, 12-16.
42. (a) Ratner, P. H.; van Bavel, J. H.; Hampel, F.; Wingertzahn, M. A.; Darken, P. F.; Shah, T.; Hellbardt, S.; Brookman, S. Dose-dependent effectiveness of ciclesonide nasal spray in the treatment of seasonal allergic rhinitis (SAR). *J. Allergy Clin. Immunol.* **2004**, 113, S28. (b) Taylor, D. A.; Jensen, M. W.; Kanabar, V.; Engelstatter, R.; Steinijans, V. W.; Barnes, P. J.; O'Connor, B. J. A dose-dependent effect of the novel inhaled corticosteroid ciclesonide on

- airway responsiveness to adenosine-5'-monophosphate in asthmatic patients. *Am. J. Respir. Crit. Care Med.* **1999**, *160*, 237-43.
43. Singh, R. K.; Gupta, S.; Dastidar, S.; Ray, A. Cysteinyl Leukotrienes and Their Receptors: Molecular and Functional Characteristics. *Pharmacology* **2010**, *85*, 336-349.
44. Hallstrand, T. S.; Henderson, Jr., W. R. An update on the role of leukotrienes in asthma. *Curr. Opin. Allergy Clin. Immunol.* **2010**, *10*, 60-66.
45. Schliemer, R. P.; MacGlashan, D. W.; Peters, S. P.; Pinckard, R. N.; Adkinson, N. F. Jr.; Lichtenstein, L. M. Characterization of inflammatory mediator release from purified human lung mast cells. *Am. Rev. Respir. Dis.* **1986**, *133*, 614–617.
46. Weller, P. F.; Lee, C. W.; Foeter, D. W.; Corey, E. J.; Austen, K. F.; Lewis, R. A. Generation and metabolism of 5-lipoxygenase pathway leukotrienes by human eosinophils: Predominant production of leukotriene C<sub>4</sub>. *Proc. Natl. Acad. Sci. USA.* **1983**, *80*, 7626–7630.
47. Lynch, K. R.; O'Neill, G. P.; Liu, Q.; Im, D. S.; Sawyer, N.; Metters, K. M. Coulombe, N.; Abramovitz, M.; Figuero, D. J.; Zeng, Z.; Connolly, B. M.; Bai, C.; Austin, C. P.; Chateauneuf, A.; Stocco, R.; Greig, G. M.; Kargman, S.; Hooks, S. B.; Hosfield, E.; Williams, D. L. Jnr.; Ford-Hutchinson, A. W.; Caskey, T.; Evans, J. F. Characterization of the human cysteinyl leukotriene CysLT<sub>1</sub> receptor. *Nature* **1999**, *399*, 789–793.
48. (a) Bernstein, P. R.; Snyder, D. W.; Adams, E. J.; Krell, R. D.; Vacek, E. P.; Willard, A. K. Chemically stable homocinnamyl analogues of the leukotrienes: synthesis and preliminary biological evaluation. *J. Med. Chem.* **1986**, *29*, 2477-2482. (b) Bernstein, P. R.; Vacek, E. P.; Adams, E. J.; Snyder, D. W.; Krell, R. D. Synthesis and pharmacological characterisation of a series of leukotriene analogues with antagonist and agonist activities. *J. Med. Chem.* **1988**, *31*, 692-696. (c) Bernstein, P. R. Chemistry and structure activity relationships of leukotriene receptor antagonists. *Am. J. Respir. Crit. Care Med.* **1998**, *157*, S220-S226. (d) Jones, T. R.; Labelle, M.; Belley, M.; Champion, E.; Charette, L.; Evans, J.; Ford-Hutchinson, A. W.; Gauthier, J.-Y.; Lord, A.; Masson, M.; McAuliffe, M.; McFarlane, C. S.; Metters, K. M.; Pickett, C.; Piechuta, H.; Rochette, C.; Rodger, I. W.; Sawyer, N.; Young, R.N.; Zamboni, R.; Abraham, W. M. Pharmacology of montelukast sodium (singulair<sup>TM</sup>), a potent and selective leukotriene D<sub>4</sub> receptor antagonist. *Can. J. Physiol. Pharmacol.* **1995**, *73*, 191-201.
49. (a) Nakai, H.; Konno, M.; Kosuge, S.; Sakuyama, S.; Toda, M.; Arai, Y.; Obata, T.; Katsube, N.; Miyamoto, T.; Okegawa, T.; Kwasaki, A. New potent antagonists of leukotriene C<sub>4</sub> and D<sub>4</sub>. 1. Synthesis and structure-activity relationships. *J. Med. Chem.* **1988**, *31*, 84-91. (b) Gozalo-Requez, F.; Estrada-Rodriguez, J. L. Tolerability of leukotriene modifiers in asthma. *Biodrugs* **1999**, *11*, 385-394. (c) Taniguchi, Y.; Tamura, G.; Honma, M.; Aizawa, T.; Maruyama, N.; Shiarto, K.; Takishima, T. The effect of an oral leukotriene antagonist,

- ONO-1078, on allergen-induced immediate bronchoconstriction in asthmatic subjects. *J. Allergy Clin. Immunol.* **1993**, *92*, 507-512.
50. (a) Matassa, V. G.; Maduskuie, T. P.; Shapiro, H. S.; Hesp, B.; Synder, D. W.; Aharony, D.; Krell, R. D.; Keith, R. A. Evolution of a series of peptidoleukotriene antagonists: synthesis and structure/activity relationships of 1,3,5-substituted indoles and indazoles. *J. Med. Chem.* **1990**, *33*, 1781-1790. (b) Brown, F. J.; Yee, Y. K.; Cronk, L. A.; Hebbel, K. C.; Krell, R. D.; Synder, D. W. Evolution of a series of peptidoleukotriene antagonists: synthesis and structure/activity relationships of 1,6-disubstituted indoles and indazoles. *J. Med. Chem.* **1990**, *33*, 1771-1781. (c) Yee, Y. K.; Bernstein, P. R.; Adams, E. J.; Brown, F. J.; Cronk, L. A.; Hebbel, K. C.; Vacek, E. P.; Krell, R. D.; Synder, D. W. A novel series of selective leukotriene antagonists: exploration and optimisation of the acidic region in 1,6-disubstituted indoles and indazoles. *J. Med. Chem.* **1990**, *33*, 2437-2451.
51. Bernstein, P. R. Chemistry and structure activity relationships of leukotriene receptor antagonists. *Am. J. Respir. Crit. Care Med.* **1998**, *157*, S220-S226.
52. Montuschi, P.; Leukotrienes, antileukotrienes and asthma. *Mini-Rev. Med. Chem.* **2008**, *8*, 647-656.
53. McMillan, R. M.; Cysteinyl leukotriene antagonists. *Prog. Respir. Res.* **2001**, *31*, 111-114.
54. (a) Schulman, S. Development of a monoclonal anti-immunoglobulin E antibody (omalizumab) for the treatment of allergic respiratory disorders. *Am. J. Respir. Crit. Care Med.* **2001**, *164*, s6-s11. (b) Busse, W.; Corren, J.; Lanier, B.Q.; McAlary, M.; Fowler-Taylor, A.; Cioppa, G.D.; As, A.V.; Gupta, N. Omalizumab, anti-IgE recombinant humanized monoclonal antibody, for the treatment of severe allergic asthma. *J. Allergy Clin. Immunol.* **2001**, *108*, 184-190.
55. Boushey, H. A. Experiences with monoclonal antibody therapy for allergic asthma. *J. Allergy Clin Immunol.* **2001**, *108*, s77-s83.
56. Barnes, P. J. Immunology of asthma and chronic obstructive pulmonary disease. *Nat. Rev. Immunol.* **2008**, *8*, 183-192.
57. Lloyd, C. M.; Hessel, E. M. Functions of T-cells in asthma: more than just T<sub>H</sub>2 cells. *Nat. Rev. Immunol.* **2010**, *10*, 838-848.
58. Larché, M.; Akdis, C. A.; Valenta, R. Immunological mechanisms of allergen-specific immunotherapy. *Nat. Rev. Immunol.* **2006**, *6*, 761-771.
59. Akdis, C. A. Therapies for allergic inflammation: refining strategies to induce tolerance. *Nat. Med.* **2012**, *18*, 736-749.
60. Ciprandi, G.; Alesina, R.; Ariano, R.; Aurnia, P.; Borrelli, P.; Cadario, G.; Capristo, A.; Carosso, A.; Casino, G.; Castiglioni, G.; Cesinaro Di Rocco, P.; Colangelolo, C.; Di Gioacchino, M.; Di Paola, M.G.; Errico, G.; Fiorina, A.; Gambuzza, F.; Gangemi, S.;

- Gasparini, A.; Giugno, R.; Iemoli, E.; Isola, S.; Maniero, G.; Marengo, F.; Mazzali, P.; Minelli, M.; Mosca, M.; Pellegrino, R.; Piconi, S.; Pravettoni, V.; Quaglio, L.; Ricciardi, L.; Ridolo, E.; Sillano, V.; Valle, C.; Varin, E.; Verini, M.; Zambito, M.; Riario-Sforza, G. G.; Incorvaia, C.; Puccinelli, P.; Scurati, S.; Frati, F. Characteristics of patients with allergic polysensitization: the POLISMAIL study. *Eur. Ann. Allergy Clin. Immunol.* **2008**, *40*, 77-83.
61. (a) Creagh, E. M.; O'Neill, L. A. J. TLRs, NLRs and RLRs: a trinity of pathogen sensors that co-operate in innate immunity. *Trends Immunol.* **2006**, *27*, 352-357. (b) Kawai, T.; Akira, S. The roles of TLRs, RLRs and NLRs in pathogen recognition. *Int. Immunol.* **2009**, *21*, 317-337.
62. (a) Werling, D.; Jungi, T. W. Toll-like receptors linking innate and adaptive immune response. *Vet. Immunol. Immunopath.* **2003**, *91*, 1-12. (b) Iwasaki, A.; Medzhitov, R. Toll-like receptor control of the adaptive immune responses. *Nat. Immunol.* **2004**, *5*, 987-995. (c) Tipping, P. G. Toll-like receptors: the interface between innate and adaptive immunity. *J. Am. Soc. Nephrol.* **2006**, *17*, 1769-1771.
63. (a) Corry, D. B. Emerging immune targets for the therapy of allergic asthma. *Nat. Rev. Drug Disc.* **2002**, *1*, 55-64. (b) Gangloff, S. C.; Guenounou, M. Toll-like receptors and immune response in allergic disease. *Clin. Rev. Allergy Immunol.* **2004**, *26*, 115-125. (c) Heine, H. TLRs, NLRs and RLRs: Innate sensors and their impact on allergic diseases – a current view. *Immunol. Lett.* **2011**, *139*, 14-24. (d) Aryan, Z.; Holgate, S. T.; Radzioch, D.; Rezaei, N. A new era of targeting the ancient gatekeepers of the immune system: toll-like agonists in the treatment of allergic rhinitis and asthma. *Int. Arch. Allergy Immunol.* **2014**, *164*, 46-63.
64. Hoffman, J.A. The immune response of *Drosophila*. *Nature* **2003**, *426*, 33-38.
65. Gay, N. J.; Gangloff, M. Structure and function of Toll receptors and their ligands. *Annu. Rev. Biochem.* **2007**, *76*, 141-165.
66. Gay, N. J.; Gangloff, M.; Weber, A. N. R. Toll-like receptors as molecular switches. *Nat. Rev. Immunol.* **2006**, *6*, 693-698.
67. Kanzler, H.; Barrat, F. J.; Hessel, E. M.; Coffman, R. L. Therapeutic targeting of innate immunity with toll-like receptor agonists and antagonists. *Nat. Med.* **2007**, *13*, 552-559.
68. (a) Ranoa, D. R.; Kelley, S. L.; Tapping, R. I. Human Lipopolysaccharide-binding Protein (LBP) and CD14 Independently Deliver Triacylated Lipoproteins to Toll-like Receptor 1 (TLR1) and TLR2 and Enhance Formation of the Ternary Signaling Complex. *J. Biol. Chem.* **2013**, *288*, 9729-9741. (b) Schumann, R. R.; Tapping, R. I. Genomic variants of TLR1 - it takes (TLR-)two to tango. *Eur. J. Immunol.* **2007**, *37*, 2059-2062.
69. (a) Lien, E.; Sellati, T. J.; Yoshimura, A.; Flo, T. H.; Rawadhi, G.; Finberg, R. W.; Carroll, D.; Espevik, T.; Ingalls, R. R.; Radolf, J. D.; Golenbock, D. T. Toll-like receptor 2 functions as a pattern recognition receptor for diverse bacterial products. *J. Biol. Chem.* **1999**, *274*,

- 33419-33425. (b) Wetzler, L. M. The role of Toll-like receptor 2 in microbial disease and immunity. *Vaccine* **2003**, *21*, S2/55-S2/60.
70. (a) Takeuchi, O.; Kawai, T.; Sanjo, H.; Copeland, N. G.; Gilbert, D. J.; Jenkins, N. A.; Takeda, K.; Akira, S. TLR6: a novel member of an expanding Toll-like receptor family. *Gene* **1999**, *231*, 59-65. (b) Nakao, Y.; Funami, K.; Kikkawa, S.; Taniguchi, M.; Nishiguchi, M.; Fukumori, Y.; Seya, T.; Matsumoto, M. Surface-Expressed TLR6 Participates in the Recognition of Diacylated Lipopeptide and Peptidoglycan in Human Cells. *J. Immunol.* **2005**, *174*, 1566-1573.
71. (a) Sen, G. C.; Sarkar, S. N. Transcriptional signaling by double-stranded RNA: role of TLR3. *Cytokine Growth Factor Rev.* **2005**, *16*, 1-14. (b) Matsumoto, M.; Seya, T. TLR3: interferon induction by double-stranded RNA including poly(I:C). *Adv. Drug Delivery Rev.* **2008**, *60*, 805-812.
72. (a) Miller, S. I.; Ernst, R. K.; Bader, M. W. LPS, TLR4 and infectious disease diversity. *Nat. Rev. Microbiol.* **2005**, *3*, 36-46. (b) Sabroe, I. Toll-like receptor 4. *Prog. Respir. Res.* **2010**, *39*, 81-86.
73. Stewart, C. R.; Stuart, L. M.; Wilkinson, K.; van Gils, J. M.; Deng, J.; Halle, A.; Rayner, K. J.; Boyer, L.; Zhong, R.; Frazier, W. A.; Lacy-Hulbert, A.; El Khoury, J.; Golenbock, D. T.; Moore, K. J. CD36 ligands promote sterile inflammation through assembly of a Toll-like receptor 4 and 6 heterodimer. *Nat. Immunol.* **2010**, *11*, 155-162.
74. (a) Smith, K. D.; Ozinsky, A. Toll-like receptor-5 and the innate immune response to bacterial flagellin. *Curr. Top. Microbiol. Immunol.* **2002**, *270*, 93-108. (b) Liaudet, L.; Deb, A.; Pacher, P.; Mabley, J. G.; Murthy, K. G. K.; Salzman, A. L.; Szabo, C. The flagellin-TLR5 axis: therapeutic opportunities. *Drug News Persp.* **2002**, *15*, 397-409.
75. (a) Diebold, S. S. Recognition of viral single-stranded RNA by Toll-like receptors. *Adv. Drug Delivery Rev.* **2008**, *60*, 813-823. (b) Diebold, S. S.; Kaisho, T.; Hemmi, H.; Akira, S.; Reis e Sousa, C. Innate antiviral responses by means of TLR7-mediated recognition of single-stranded RNA. *Science* **2004**, *303*, 1529-1532.
76. Cervantes, J. L.; Weinerman, B.; Basole, C.; Salazar, J. C. TLR8: the forgotten relative revindicated. *Cell. Mol. Immunol.* **2012**, *9*, 434-438.
77. (a) Bauer, S.; Wagner, H. Bacterial CpG-DNA licenses TLR9. *Curr. Top. Microbiol. Immunol.* **2002**, *270*, 145-154. (b) Kumagai, Y.; Takeuchi, O.; Akira, S. TLR9 as a key receptor for the recognition of DNA. *Adv. Drug Del. Rev.* **2008**, *60*, 795-804.
78. Hasan, U.; Chaffois, C.; Gaillard, C.; Saulnier, V.; Merck, E.; Tancredi, S.; Guet, C.; Briere, F.; Vlach, J.; Lebecque, S.; Trinchieri, G.; Bates, E. E. M. Human TLR10 is a functional receptor, expressed by B cells and plasmacytoid dendritic cells, which activates gene transcription through MyD88. *J. Immunol.* **2005**, *174*, 2942-2950.

79. Lee, C. C.; Avalos, A. M.; Ploegh, H. L. Accessory molecules for Toll-like receptors and their function. *Nat. Rev. Immunol.* **2012**, *12*, 168-179.
80. (a) Czarniecki, M. Small molecule modulators of Toll-like receptors. *J. Med. Chem.* **2008**, *51*, 6621-6626. (b) Spyvee, M.; Hawkins, L. D.; Ishixaka, S. T. Modulators of Toll-like receptor (TLR) signalling. *Annu. Rep. Med. Chem.* **2010**, *45*, 191-207. (c) Mancini, R. J.; Stutts, L.; Ryu, K. A.; Tom, J. K.; Esser-Kahn, A. P. Directing the immune system with chemical compounds. *ACS Chem. Biol.* **2014**, *9*, 1075-1085.
81. Baxevanis, C. N.; Voutsas, I. F.; Tsitsilonis, O. E. Toll-like receptor agonists: current status and future perspective on their utility as adjuvants in improving anticancer vaccination strategies. *Immunotherapy* **2013**, *5*, 497-511.
82. Holldack, J.; Toll-like receptors as therapeutic targets for cancer. *Drug Disc. Today.* **2014**, *19*, 379-382.
83. Mills, K. H. G. TLR-dependent T-cell activation in autoimmunity. *Nat. Rev. Immunol.* **2011**, *11*, 807-822.
84. (a) Romagne, F. Current and future drugs targeting one class of innate immunity receptors: the Toll-like receptors. *Drug Disc. Today* **2007**, *12*, 80-87. (b) Gearing, A. J. H. Targeting toll-like receptors for drug development: a summary of commercial approaches. *Immunol. Cell Biol.* **2007**, *85*, 490-494. (c) Hennessy, E. J.; Parker, A. E.; O'Neill, L. A. J. Targeting Toll-like receptors: emerging therapeutics. *Nat. Rev. Drug Disc.* **2010**, *9*, 293-307. (d) Connolly, D. J.; O'Neill, L. A. J. New developments in Toll-like receptor targeted therapeutics. *Curr. Opin. Pharmacol.* **2012**, *11*, 510-518.
85. Hussein, W. H.; Liu, T. Y.; Skwarczynski, M.; Toth, I. Toll-like receptor agonists: a patent review 2011-2013. *Expert Opin. Ther. Patents* **2014**, *24*, 453-470.
86. Ohto, U.; Tanji, H.; Shimizu, T. Structure and function of toll-like receptor 8. *Microb. Infect.* **2014**, *16*, 273-282.
87. Moynagh, P. N. TLR signalling and activation of IRFs: revisiting old friends from the NF- $\kappa$ B pathway. *Trends. Immunol.* **2005**, *26*, 469-476.
88. Kuźnik, A.; Panter, G.; Jerala, R. Recognition of nucleic acids by Toll-Like receptors and development of immunomodulatory drugs. *Curr. Med. Chem.* **2010**, *17*, 1899-1914.
89. Gorden, K. B.; Gorski, K. S.; Gibson, S. J.; Kedl, R. M.; Kieper, W. C.; Qui, X.; Tomai, M. A.; Alkan, S. S.; Vasilakos, J. P. Synthetic TLR agonists reveal functional differences between human TLR7 and TLR8. *J. Immunol.* **2005**, *174*, 1259-1268.
90. Fitzgerald-Bocarsly, P.; Dai, J.; Singh, S. Plasmacytoid dendritic cells and type 1 IFN: 50 years of convergent history. *Cytokine Growth Factor Rev.* **2008**, *19*, 3-19.
91. Vignali, D. A. A.; Kuchroo, V. K. IL-12 family cytokines: immunological playmakers. *Nat. Immunol.* **2012**, *13*, 722-728.

92. Muzio, M.; Bosisio, D.; Polentarutti, N.; D'amico, G.; Stoppacciaro, A.; Mancinelli, R.; Van't Veer, C.; Penton-Rol, G.; Ruco, L. P.; Allavena, P.; Mantovani, A. Differential expression and regulation of toll-like receptors (TLR) in human leukocytes: selective expression of TLR3 in dendritic cells. *J. Immunol.* **2000**, *164*, 5998-6005.
93. Han, X.; Li, X.; Yue, S. C.; Anandaiah, A.; Hashem, F.; Reinach, P. S.; Koziel, H.; Tachado, S. D. Epigenetic regulation of tumour necrosis factor  $\alpha$  (TNF $\alpha$ ) release in human macrophages by HIV-1 single stranded RNA (ssRNA) is dependent on TLR8 signalling. *J. Biol. Soc.* **2012**, *287*, 13778-13786.
94. Brinkmann, V.; Geiger, T.; Alkan, S.; Heusser, C. H. Interferon alpha increases the frequency of interferon-gamma producing human CD4+ T cells. *J. Exp. Med.* **1993**, *178*, 1655-1663.
95. Hervas-Stubbs, S.; Perez-Gracia, J. L.; Rouzaut, A.; Sanmamed, M. F.; Le Bon, A.; Melero, I. Direct effects of type 1 interferons on cells of the immune system. *Clin. Cancer. Res.* **2011**, *17*, 669-687.
96. Villadangos, J. A.; Young, L. Antigen-presentation properties of plasmacytoid dendritic cells. *Immunity* **2008**, *29*, 352-361.
97. Hervas-Stubbs, S.; Perez-Gracia, J. L.; Rouzaut, A.; Sanmamed, M. F.; Le Bon, A.; Melero, I. Direct effects of type 1 interferons on cells of the immune system. *Clin. Cancer. Res.* **2011**, *17*, 669-687.
98. Ito, T.; Amakawa, R.; Inaba, M.; Ikehara, S.; Inaba, K.; Fukuhara, S. Differential regulation of human blood dendritic cell subsets by IFNs. *J. Immunol.* **2001**, *166*, 2961-2969.
99. Corssmit, E. P. M.; De Metz, J.; Sauerwein, H. P.; Romijn, J. A. Biologic responses to IFN- $\alpha$  administration in humans. *J. Interferon & Cytokine Res.* **2000**, *20*, 1039-1047.
100. Belardelli, F.; Ferrantini, M.; Proietti, E.; Kirkwood, J. N. Interferon-alpha in tumour immunity and immunotherapy. *Cytokine & Growth Factor Rev.* **2002**, *13*, 119-134.
101. (a) Rawling, D. J.; Schwartz, M. A.; Jackson, S. W.; Meyer-Bahlburg, A. Integration of B cell responses through Toll-like receptors and antigen receptors. *Nat. Rev. Immunol.* **2012**, *12*, 282-294. (b) Khan, A. R.; Amu, S.; Saunders, S. P.; Hams, E.; Blackshields, G.; Leonard, M. O.; Weaver, C. T.; Sparwasser, T.; Sheils, O.; Fallon, P. G. Ligation of TLR7 on CD19(+) CD1d(hi) B cells suppresses allergic lung inflammation via regulatory T cells. *Eur. J. Immunol.* **2015**, *45*, 1842-1854.
102. Kulkarni, R.; Behboudi, S.; Shariff, S. Insights into the role of Toll-like receptors in modulation of T-cell responses. *Cell Tissue Res.* **2011**, *343*, 141-152.
103. Krieg, A. M.; Vollmer, J. Toll like receptors 7, 8, and 9: linking innate immunity to autoimmunity. *Immunol. Rev.* **2007**, *220*, 251-269.

104. Jarnicki, A. G.; Conroy, H.; Brereton, C.; Donnelly, G.; Toomey, D.; Walsh, K.; Sweeney, C.; Leavy, O.; Fletcher, J.; Lavelle, E. C.; Dunne, P.; Mills, K. H. G. Tenuating Regulatory T Cell Induction by TLR Agonists through Inhibition of p38 MAPK Signaling in Dendritic Cells Enhances Their Efficacy as Vaccine Adjuvants and Cancer Immunotherapeutics. *J. Immunol.* **2008**, *180*, 3797-3806.
105. Peng, G.; Guo, Z.; Kiniwa, Y.; Voo, K. S.; Peng, W.; Fu, T.; Wang, D. Y.; Li, Y.; Wang, H. W.; Wang, R. F. Toll-Like Receptor 8-Mediated Reversal of CD4<sup>+</sup> Regulatory T Cell Function. *Science* **2005**, *309*, 1380-1384.
106. Matesic, D.; Lenert, A.; Lenart, P. Modulating Toll-like Receptor 7 and 9 responses as therapy for allergy and autoimmunity. *Curr. Allergy Asthma Rep.* **2012**, *12*, 8-17.
107. (a) Drake, M. G.; Kaufmann, E. H.; Fryer, A. D.; Jacoby, D. B. The therapeutic potential of toll-like receptor 7 stimulation in asthma. *Inflammation & Allergy – Drug Targets.* **2012**, *11*, 484-491. (b) Hayashi, T. TLR-9 based immunotherapy for allergic disease. *Am. J. Med.* **2006**, *119*, 897.e1-897.e6.
108. Beeh, K.M.; Kanniss, F.; Wagner, F.; Schilder, C.; Naudts, I.; Hammann-Haenni, A.; Willers, J.; Stocker, H.; Mueller, P.; Bachmann, M.F.; Renner, W.A. The novel TLR-9 agonist QbG10 shows clinical efficacy in persistent allergic asthma. *J. Allergy Clin. Immunol.* **2013**, *131*, 866–874.
109. Casale, T.B.; Cole, J.; Beck, E.; Vogelmeier, C. F.; Willers, J.; Lassen, C.; Hammann-Haenni, A.; Trokan, L.; Saudan, P.; Wechsler, M.E. CYT003, a TLR9 agonist, in persistent allergic asthma – a randomized placebo-controlled Phase 2b study. *Allergy* **2015**, *70*, 1160–1168.
108. Adner, M.; Strakhammer, M.; Kumlien-Georén, S.; Dahlen, S.V.; Cardell, L. O. Toll-like receptor (TLR) 7 decreases and TLR9 increases the airway responses in mice with established allergic inflammation. *Eur. J. Pharmacol.* **2013**, *718*, 541-551.
109. (a) Ekman, A.K.; Adner, M.; Cardell, L. O. Toll-like receptor 7 activation reduces the contractile response of airway smooth muscle. *Eur. J. Pharmacol.* **2011**, *652*, 145-151. (b) Drake, M. G.; Scott, G. D.; Proskocil, B. J.; Fryer, A. D.; Jacoby, D. B. Toll-like receptor 7 rapidly relaxes human airways. *Am. J. Resp. Crit. Care Med.* **2013**, *188*, 664-672.
110. (a) Goodchild, G. Therapeutic oligonucleotides. *Methods Mol. Biol.* **2011**, *764*, 1-15. (b) Verma, S.; Eckstein, F.; Modified oligonucleotides: synthesis and strategy for users. *Annu. Rev. Biochem.* **1998**, *67*, 99-134. (c) Geary, R. S.; Antisense oligonucleotide pharmacokinetics and metabolism. *Exp. Opin. Drug Metabol. Toxicol.* **2009**, *5*, 381-391.
111. Hemmi, H.; Kaisho, T.; Takeuchi, O.; Sato, S.; Sanjo, H.; Hoshino, K.; Horiuchi, T.; Tomizawa, H.; Takeda, K. Akira, S. Small anti-viral compounds activate immune cells via the TLR7 MyD88-dependent signalling pathway. *Nat. Immunol.* **2002**, *3*, 196-200.



112. De Clercq, E.; Descamps, J.; De Somer, P. (S)-9-(2,3-Dihydroxypropyl)adenine: An aliphatic nucleoside analogue with broad spectrum antiviral activity. *Science* **1978**, *200* 563-565.
113. Weeks, C. E.; Gibson, S. J.; Induction of interferon and other cytokines by imiquimod and its hydroxylated metabolite R-842 in human blood cells *in vitro*. *J. Interferon Res.* **1994**, *14*, 81-85.
114. Gerster, J. F.; Lindstrom, K. J.; Miller, R. L.; Tomai, M. A.; Birmachu, W.; Bomersine, S. N.; Gibson, S. J.; Imbertson, L. M.; Jacobson, J. R.; Knafla, R. T.; Maye, P. V.; Nikolaides, N.; Oneyemi, F. Y.; Parkhurst, G. J.; Pecore, S. E.; Reiter, M. J.; Scribner, L. S.; Testerman, T. L.; Thompson, N. J.; Wagner, T. L.; Weeks, C. E.; Andre, J. D.; Lagain, D.; Bastard, Y.; Lupu, M. Synthesis and structure-activity relationships of 1*H*-imidazo[4,5-*c*]quinolines that induce interferon production. *J. Med. Chem.* **2005**, *48*, 3481–3491.
115. Harrison, C. J.; Jenks, L.; Voychehovski, T.; Bemslein, D. I. Modification of immunological responses and clinical disease during topical R-837 treatment of genital HSV-2 infection. *Antiviral Res.* **1988**, *10*, 209-224.
116. Ryu, J.; Yang, F. C.; A review of topical imiquimod in the management of basal cell carcinoma, actinic keratosis, and other skin lesions. *Clin. Med. Ther.* **2009**, *1*, 1557-1575.
117. Vidal, D.; Alomar, A. Mode of action and clinical use of imiquimod. *Expert Rev. Dermatol.* **2008**, *3*, 151-159.
118. Witt, P. L.; Ritch, P. S.; Reding, D.; McAuliffe, T. L.; Westrick, L.; Grossberg, S. E.; Borden, E. C. Phase I trial of an oral immunomodulator and interferon inducer in cancer patients. *Cancer Res.* **1993**, *53*, 5176-5180.
119. Savage, P.; Horton, V, Moore, J.; Owens, M.; Witt.; Gore, M. E. A phase 1 clinical trial of imiquimod, an oral interferon inducer, administered daily. *Br. J. Cancer.* **1996**, *74*, 1482-1486.
120. Shukla, N. M.; Malladi, S. S.; Mutz, C. A.; Balakrishma, R.; David, S. A. Structure – activity relationships in human Toll-like receptor 7-active imidazoquinoline analogues. *J. Med. Chem.* **2010**, *53*, 4450-4465.
121. Hood, J. D.; Warshakoon, H. J.; Kimbrell M. R.; Shukla, N. M.; Malladi, S. S.; Wang, X.; David, S. A. Immunoprofilling toll-like receptor ligands comparison of immunostimulatory and proinflammatory profiles in ex vivo human blood models. *Hum. Vaccines* **2010**, *6*, 322–335.
122. (a) Ma, F.; Zhang, J.; Zhang, J.; Zhang, C. The TLR7 agonists imiquimod and gardiquimod improve DC-based immunotherapy for melanoma in mice. *Cell. Mol. Immunol.* **2010**, *7*, 381-388. (b) Buitendijk, M.; Eszterhas, S. K.; Howell, A. L. Gardiquimod: A toll-like receptor-7

- agonist that inhibits HIV type 1 infection of human macrophages and activated T cells. *AIDS Res. Hum. Retroviruses* **2013**, *29*, 907-918. (b)
123. Drake, M. G.; Kaufman, E. H.; Fryer, A. D.; Jacoby, D. B. The therapeutic potential of Toll-like receptor 7 stimulation in asthma. *Inflammation & Allergy Drug Tar.* **2012**, *11*, 484-491.
124. Frotscher, B.; Anton, K.; Worm, M. Inhibition of IgE production by the imidazolquinoline Resiquimod in non-allergic and allergic donors. *J. Invest. Dermatol.* **2002**, *119*, 1059-1064.
125. Shi, C.; Xiong, Z.; Chittepu, P.; Aldrich, C. C.; Ohlfest, J. R.; Ferguson, D. M. Discovery of imidazoquinolines with Toll-Like Receptor 7/8 independent cytokine induction. *ACS Med. Chem. Lett.* **2012**, *3*, 501-504.
126. Tanji, H.; Ohto, U.; Shibata, T.; Miyake, K.; Shimiziu, T. Structural reorganisation of the Toll-like receptor 8 dimer induced by agonistic ligands. *Science* **2013**, *339*, 1426-1429.
127. (a) Jurk, M.; Heil, F.; Vollmer, J.; Schetter, C.; Krieg, A. M.; Wagner, H.; Lipford, G.; Bauer, S. Human TLR7 or TLR8 independently confer responsiveness to the antiviral compound R-848. *Nat. Immunol.* **2002**, *3*, 499-500. (b) Brown, J. N.; Kohler, J. J.; Coberley, C. R.; Sleasman, J. W.; Goodenow, M. M. HIV-1 activates macrophages independent of Toll-like receptors. *PLoS ONE* 2008, *3*, e3664.
128. Gibbard, R. J.; Morley, P. J.; Gay, N. J.; Conserved features in the extracellular domain of human toll-like receptor8 are essential for pH-dependent signaling. *J. Biol. Chem.* **2006**, *281*, 27503–27511.
129. (a) Kokatla, H. P.; Sil, D.; Malladi, S.S.; Balakrishna, R.; Hermanson, A. R.; Fox, L. M.; Wang, X.; Dixit, A.; David, S. A. Exquisite selectivity for human Toll-like receptor 8 in substituted furo[2,3-c]quinolines. *J. Med. Chem.* **2013**, *56*, 6871–6885. (b) Yoo, E.; Salunke, D. B.; Sil, D.; Guo, X.; Salyer, A. C.; Hermanson, A. R.; Kumar, M.; Malladi, S. S.; Balakrishna, R.; Thompson, W. H.; Tanji, H.; Ohto, U.; Shimizu, T.; David, S. A. Determinants of activity at human Toll-like receptors 7 and 8: quantitative structure-activity relationship (QSAR) of diverse heterocyclic scaffolds. *J. Med. Chem.* **2013**, *57*, 7955-7970. (c) Kokatla, H. P.; Sil, D.; Tanji, H.; Ohto, U.; Malladi, S.S.; Fox, L. M.; Shimizu, T.; David, S. A. Structure-based design of novel human Toll-like receptor 8 agonists. *ChemMedChem* **2014**, *9*, 719-723.
130. (a) Shi, C.; Xiong, Z.; Chittepu, P.; Aldrich, C. C.; Ohlfest, J. R.; Ferguson, D. M. Discovery of imidazoquinolines with Toll-Like Receptor 7/8 independent cytokine induction. *ACS Med. Chem. Lett.* **2012**, *3*, 501-504. (b) Schiaffo, C. E.; Shi, C.; Xiong, Z.; Olin, M.; Ohlfest, J. R.; Aldrich, C. C.; Ohlfest, J. R.; Ferguson, D. M. Structure-activity relationship analysis of imidazoquinolines with Toll-like receptors 7 and 8 and enhanced cytokine induction. *J. Med. Chem.* **2014**, *57*, 339-347.

131. Kužnik, A.; Panter, G.; Jerala, R. Recognition of nucleic acids by Toll-Like receptors and development of immunomodulatory drugs. *Curr. Med. Chem.* **2010**, *17*, 1899-1914.
132. Harrison, L. I.; Astry, C.; Kumar, S.; Yunis, C. Pharmacokinetics of 852A, an imidazoquinoline Toll-Like Receptor 7-specific agonist, following intravenous, subcutaneous and oral administrations in humans. *J. Clin. Pharmacol.* **2007**, *47*, 962-969.
133. Fidock, M. D.; Souberbielle, B. E.; Laxton, C.; Rawal, J.; Delpuech-Adams.; Corey, T. P.; Colman, P.; Kumar, V.; Cheng, J. B.; Wright, K.; Srinivasan, S.; Rana, K.; Craid, C.; Horscroft, N.; Perros, M.; Westby, M.; Webster, R.; van der Ryst, E. The innate immune response, clinical outcomes and *ex vivo* HCV antiviral activity of a TLR7 agonist (PF-4878691). *Clin. Pharm. Ther.* **2011**, *89*, 821-829.
134. Tanji, H.; Ohto, U.; Shibata, T.; Taoka, M.; Yamauchi, Y.; Isobe, T.; Miyake, K.; Shimizu, T. Toll-like receptor 8 senses degradation products of single stranded RNA. *Nat. Struct. Mol. Biol.* **2015**, *22*, 109-115.
135. Diebold, S. S.; Kaisho, T.; Hemmi, H.; Akira, S.; Reis e Sousa, C. Innate antiviral responses by means of TLR7-mediated recognition of single-stranded RNA. *Science* **2004**, *303*, 1529-1531.
136. Lee, J.; Chuang, T. H.; Redecke, V.; She, L.; Pitha, P. M.; Carson, D. A.; Raz, E.; Cottam, H. B.; Molecular basis for the immunostimulatory activity of guanine nucleoside analogs: Activation of Toll-like receptor 7. *PNAS* **2003**, *100*, 6646-6651.
137. Horsmans, Y.; Berg, T.; Desager, J.-P.; Mueller, T.; Schott, E.; Fletcher, S.P.; Steffy, K.R.; Bauman, L.A.; Kerr, B.M.; Averett, D.R. Isatoribine, an agonist of TLR7, reduces plasma virus concentration in chronic hepatitis C infection. *Hepatology* **2005**, *42*, 724-731.
138. Xiang, A. X.; Webber, S. E.; Kerr, B. M.; Rueden, E. J.; Lennox, J. R.; Haley, G. J.; Wang, T.; Ng, J. S.; Herbert, M. R.; Clark, D. L.; Banh, V. N.; Li, W.; Fletcher, S. P.; Steffy, K. R.; Bartkowski, D. M.; Kirkovsky, L. I.; Bauman, L. A.; Averett, D. R. Discovery of ANA975: An oral prodrug of the TLR-7 agonist Isatoribine. *Nucleosides, Nucleotides and Nucleic Acids* **2007**, *26*, 635-640.
139. <http://ir.anadyspharma.com/phoenix.zhtml?c=148908&p=irol-newsArticle&ID=1032389&highlight> Retrieved Aug 2nd, 2013
140. Boonstra, A.; Liu, B.; Groothuisink, Z. M. A.; Bergmann, J. F.; de Bruijne, J.; Hotho, D. M.; Hansen, B. E.; van Vliet, A.A.; van de Wetering de Rooij, J.; Fletcher, S. P.; Bauman, L. A.; Rahimy, M.; Appleman, J. R.; J. L. Freddo, J. L.; Janssen, H. L. A.; Reesink, H. Potent immune activation in chronic hepatitis C patients upon administration of an oral inducer of endogenous interferons that acts *via* Toll-like receptor 7. *Antiviral Ther.* **2012**, *17*, 657-667.
141. Bergmann, J. F.; de Bruijne, J.; Hotho, D. M.; de Knecht, R. J.; Boonstra, A.; Weegink, C. J.; van Vliet, A. A.; van de Wetering, J.; Fletcher, S. P.; Bauman, L. A.; Rahimy, M.;

- Appleman, J. R.; J. L. Freddo, J. L.; Janssen, H. L. A.; Reesink, H. W. Randomised clinical trial: anti-viral activity of ANA773, an oral inducer of endogenous interferons acting via TLR7, in chronic HCV. *Aliment Pharmacol Ther.* **2011**, *34*, 443-453.
142. Isobe, Y.; Tobe, M.; Ogita, H.; Kurimoto, A.; Ogino, T.; Kawakami, H.; Takaku, H.; Sajiki, H.; Hirotab, K.; Hayashia, H. Synthesis and structure–activity relationships of 2-Substituted-8-hydroxyadenine derivatives as orally available interferon inducers without emetic side effects. *Bioorg. Med. Chem.* **2003**, *11*, 3641-3647.
143. Kurimoto, A.; Ogino, T.; Ichii, S.; Isobe, Y.; Tobe, M.; Ogita, H.; Takaku, H.; Sajiki, H.; Hirotab, K.; Kawakamia, H. Synthesis and evaluation of 2-substituted 8-hydroxyadenines as potent interferon inducers with improved oral bioavailabilities. *Bioorg. Med. Chem.* **2004**, *12*, 1091-1099.
144. Kurimoto, A.; Ogino, T.; Ichii, S.; Isobe, Y.; Tobe, M.; Ogita, H.; Takaku, H.; Sajiki, H.; Hirotab, K.; Kawakamia, H. Synthesis and structure–activity relationships of 2-amino-8-hydroxyadenines as orally active interferon inducing agents. *Bioorg. Med. Chem.* **2003**, *11*, 5501-5508.
145. Hirota, K.; Kazaoka, K.; Sajiki, H. Synthesis and biological evaluation of 2,8-disubstituted 9-benzyladenines: discovery of 8-mercaptoadenines as potent interferon-inducers. *Bioorg. Med. Chem.* **2003**, *11*, 2715-2722.
146. Jin, G.; Wu, C. C. N.; Tawatao, R. I.; Chan, M.; Carson, D. A.; Cottam, H. B. Synthesis and immunostimulatory activity of 8-substituted amino 9-benzyladenines as potent Toll-like receptor 7 agonists. *Bioorg. Med. Chem. Lett.* **2006**, *16*, 4559-4563.
147. Isobe, Y.; Kurimoto, A.; Tobe, M.; Hashimoto, K.; Nakamura, T.; Norimura, K.; Ogita, H.; Takaku, H. Synthesis and biological evaluation of novel 9-substituted-8-hydroxyadenine derivatives as potent interferon inducers. *J. Med. Chem.* **2006**, *49*, 2088-2095.
148. Nakamura, T.; Wada, H.; Kurebayashi, H.; McNally, T.; Bonnert, R.; Isobe, Y. Synthesis and evaluation of 8-oxoadenine derivatives as potent Toll-like receptor 7 agonists with high water solubility. *Bioorg. Med. Chem. Lett.* **2013**, *23*, 669-672.
149. Adlard, A. L.; Dovedi, S. J.; Telfer, B. A.; Koga-Yamakawa, E.; Pollard, C.; Honeychurch, J.; Illidge, T. M.; Murata, M.; Robinson, D. T.; Jewsbury, P. J.; Wilkinson, R. W.; Stratford, I. J. A novel systemically administered Toll-like receptor 7 agonist potentiates the effect of ionizing radiation in murine solid tumor models. *Int. J. Cancer* **2014**, *135*, 820-829.
150. Kurimoto, A.; Hashimoto, K.; Nakamura, T.; Norimura, K.; Ogita, H.; Bonnert, R.; McNally, T.; Wada, H.; Isobe, Y. Synthesis and biological evaluation of 8-oxoadenine derivatives as Toll-like receptor 7 agonists introducing the antedrug concept. *J. Med. Chem.* **2010**, *53*, 2964-2972.

151. (a) Kaufman, E. H.; Jacoby, D. B. Upping the antedrug: is a novel anti-inflammatory Toll-like receptor 7 agonist also a bronchodilator? *Br. J. Pharmacol.* **2012**, *166*, 569-572. (b) Biffen, M.; Matsui, H.; Edwards, S.; Leishman, A. J.; Eiho, K.; Holness, E.; Satterthwaite, G.; Doyle, I.; Wada, H.; Fraser, N. J.; Hawkins, S. L.; Aoki, M.; Tomizawa, H.; Benjamin, A. D.; Takaku, H.; McNally, T.; Murray, C. M. Biological characterisation of a novel class of toll-like receptor 7 (TLR7) agonists designed to have reduced systemic activity. *Br. J. Pharmacol.*, **2012**, *166*, 573-586.
152. (a) Greiff, L.; Cervin, A.; Ahlström-Emanuelsson, C.; Almqvist, G.; Andersson, M.; Dolata, J.; Eriksson, L.; Högestatt, E.; Källén, A.; Norlén, P.; Sjölin, I. L.; Widegren, H. Repeated intranasal TLR7 stimulation reduces allergen responsiveness in allergic rhinitis. *Respir. Res.* **2012**, *13*, 53. (b) Leaker, B.; Singh, D.; Lindgren, S.; Almqvist, J.; Young, B.; O'Connor, B. Effects of the novel toll-like receptor 7 (TLR7) agonist AZD8848 on allergen-induced responses in patients with mild asthma. *Eur. Resp. J.* **2012**, *40* (Supp. 56), 3086.
153. Bazin, H. G.; Li, Y.; Khalaf, J. K.; Mwakwari, S.; Livesay, M. T.; Evans, J. T.; Johnson D. Structural requirements for TLR7-selective signaling by 9-(4-piperidinylalkyl)-8-oxoadenine derivatives. *Bioorg. Med. Chem. Lett.* **2015**, *25*, 1318-1823.
154. Pryde, D. C.; Tran, T. D.; Jones, P.; Parsons, G. C.; Bish, G.; Adam, F. M.; Smith, M. C.; Middleton, D. S.; Smith, N. N.; Calo, F.; Hay, D.; Paradowski, M.; Proctor, K. J. W.; Parkinson, T.; Laxton, C.; Fox, D. N. A.; Horscroft, N. J.; Ciaramella, G.; Jones, H. M.; Duckworth, J.; Benson, N.; Harrison, A.; Webster, R. The discovery of a novel prototype small molecule TLR7 agonist for the treatment of hepatitis C virus infection. *Med. Chem. Commun.* **2011**, *2*, 185-189.
155. Jones, P.; Pryde, D. C.; Tran, T. D.; Adam, F. M.; Bish, G.; Calo, F.; Ciaramella, G.; Dixon, R.; Duckworth, J.; Fox, D. N. A.; Hay, D.; Hitchin, J.; Horscroft, N. J.; Howard, M.; Laxton, C.; Parkinson, T.; Parsons, G. C.; Proctor, K. J. W.; Smith, M. C.; Smith, N.; Thomas, A. Discovery of a highly potent series of TLR7 agonists. *Bioorg. Med. Chem. Lett.* **2011**, *21*, 5939-5943.
156. Tran, T. D.; Pryde, D. C.; Jones, P.; Adam, F. M.; Benson, M.; Bish, G.; Calo, F.; Ciaramella, G.; Dixon, R.; Duckworth, J.; Fox, D. N. A.; Hay, D.; Hitchin, J.; Horscroft, N. J.; Howard, M.; Gardner, I.; Jones, H. M.; Laxton, C.; Parkinson, T.; Parsons, G. C.; Proctor, K. J. W.; Smith, M. C.; Smith, N.; Thomas, A. Design and optimisation of orally active TLR7 agonists for the treatment of hepatitis C virus infection. *Bioorg. Med. Chem. Lett.* **2011**, *21*, 2389-2393.
157. Roethle, P. A.; McFadden, R. M.; Yang, H.; Hrvatin, P.; Hui, H.; Graupe, M.; Gallagher, B.; Chao, J.; Hesselgesser, J.; Duatschek, P.; Zheng, J.; Lu, B.; Tumas, D. B.; Perry, J.;

- Halcomb, R. L. Identification and optimization of pteridinone Toll-like receptor 7 (TLR7) agonists for the oral treatment of viral hepatitis. *J. Med. Chem.* **2013**, *56*, 7324-33.
158. Lanford, R. E.; Guerra, B.; Chavez, D.; Giavedoni, L.; Hodara, V. L.; Brasky, K. M.; Fosdick, A.; Frey, C. R.; Zheng, J.; Wolfgang, G.; Halcomb, R. L.; Tumas, D. B. GS-9620, an oral agonist of Toll-Like Receptor 7, induces prolonged suppression of hepatitis B in chronically infection chimpanzees. *Gastroenterology* **2013**, *144*, 1508-1517.
159. (a) Lapatin, U.; Wolfgang, G.; tumas, D.; Frey, C. R.; Ohmstede, C.; Hesselgesser, J.; Kearney, B.; Moorehead, L.; Subramanian, G. M.; McHutchinson, J. G. Safety, pharmacokinetics and pharmacodynamics of GS-9620, an oral Toll-like receptor 7 agonist. *Antiviral Ther.* **2013**, *18*, 409-418. (b) Fosdick, A.; Zheng, J.; Pflanz, S.; Frey, C. R.; Hesselgesser, J.; Halcomb, R. L.; Wolfgang, G.; Tumas, D. B. Pharmacokinetic and pharmacodynamic properties of GS-9620, a novel Toll-like receptor 7 agonist, demonstrate interferon-stimulated gene induction without detectable serum interferon at low oral doses. *J. Pharmacol. Exp. Ther.* **2013**, *348*, 96-105.
160. Yoo, E.; Crall, B. M.; Balakrishna, R.; Malladi, S. S.; Fox, L. M.; Hermanson, A. R.; David, S. A. Structure-activity relationships in Toll-like receptor 7 agonistic 1H-imidazo[4,5-c]pyridines. *Org. Biomol. Chem.* **2013**, *11*, 6526-6545.
161. (a): Bennett, N. J.; McInally, T.; Mochel, T.; Thom, S.; Tíden, A. K. Pyrimidine deravitive for the treatment of asthma, COPD, allergic rhinitis, allergic conjunntivitus, atopic dermatisis, cancer, hepatitis B, hepatitis C, HIV, HPV, bacterial infections and dermatitis. WO 2009/067081A. (b): Bennett, N. J.; McInally, T.; Thom, S. Novel pyrimidines and their treatment in cancer and other diseases. WO 2010/113885 A1. (c): Bailey, A.; Highton, A. J.; McInally, T.; Mochel, T.; Daisuke, U. Phenol compounds as Toll-Like Receptor 7 agonists. WO 2012/066335 A1. (d): McInally, T.; Mochel, T.; Hasegawa, F.; Hori, S. Benzylamine compounds as Toll-Like Receptor 7 agonists. WO 2012/066336 A1. (e): Tosaki, S.; Hori, S.; Tanaka, M. Cyclic amide compounds and their use in the treatment of disease. WO 2012/067268 A1. (f): Hori, S.; McInally, T.; Daisuke, U.; Tanaka, M. Aminoalkoxyphenyl compounds and their use in the treatment of disease. WO 2012/067269 A1.
162. Damm, J.; Wiegand, F.; Harden, L. M.; Gerstberger, R.; Rummel, C.; Roth, J. Fever, sickness behaviour and expression of inflammatory genes in the hypothalamus after systemic and localized subcutaneous stimulation of rats with the Toll-like receptor 7 agonist Imiquimod. *Neuroscience* **2012**, *201*, 166-183.
163. Krieg, A. M.; Vollmer, J. Toll like receptors 7, 8, and 9: linking innate immunity to autoimmunity. *Immunol. Rev.* **2007**, *220*, 251-269.
164. (a) Lehmann, S. M.; Krüger, C.; Park, B.; Derkow, K.; Rosenberger, K.; Baumgart, J.; Trimbuch, T.; Eom, G.; Hinz, M.; Kaul, D.; Habel, P.; Kälin, R.; Franzoni, E.; Rybak, A.;

- Nguyen, D.; Veh, R.; Ninnemann, O.; Peters, O.; Nitsch, R.; Heppner, F. L.; Golenbock, D.; Schott, E.; Ploegh, H. L.; Wulczyn, G.; Lehnardt, S. An unconventional role for miRNA: let-7 activates Toll-like receptor 7 and causes neurodegeneration. *Nat. Neurosci.* **2012**, *15*, 827-835. (b) Drouin-Ouellet, J.; Cicchetti, F. Inflammation and neurodegeneration: the story 'retolled' *Trends Pharmacol. Sci.* **2012**, *33*, 542-551.
165. Lipinski, C.A.; Lombardo, F.; Dominy, B.W.; Feeney, P.J. Experimental and computational approaches to estimate solubility and permeability in drug discovery and development settings. *Adv. Drug Deliv. Rev.* **1997**, *23*, 3-25.
166. Gleeson, M. P.; Generation of a set of simple ADMET rules of thumb. *J. Med. Chem.* **2008**, *51*, 817-834.
167. Keserü, G. M.; Makara, G. M. The influence of lead discovery strategies on the properties of drug candidates. *Nat. Rev. Drug Disc.* **2009**, *8*, 203-212.
168. Hill, A. P.; Young, R. J. Getting physical in drug discovery: a contemporary perspective on solubility and hydrophobicity. *Drug Disc. Today* **2010**, *15*, 648-655.
169. Leeson, P. D.; Springthorpe, B. The influence of drug-like concepts on decision-making in medicinal chemistry. *Nat. Rev. Drug Disc.* **2007**, *6*, 881-890.
170. Southall, N. T.; Dill, K. A.; A view of the hydrophobic effect. *J. Phys. Chem. B.* **2002**, *106*, 521-533.
171. Hughes, J. D.; Blagg, J.; Price, D.A.; Bailey, S.; DeCrescenzo, G. A.; Devraj, R. V.; Ellsworth, E.; Fobian, Y. M.; Gibbs, M. E.; Gilles, R.W.; Greene, N.; Huang, E.; Krieger-Burke, T.; Loesel, J.; Wager, T.; Whitely, L.; Zhang, Y. Physicochemical drug properties associated with *in vivo* toxicological outcomes. *Bioorg. Med. Chem. Lett.* **2008**, *18*, 4872-4875.
172. Young, R. J.; Green, D. V. S.; Luscombe, C. N.; Hill, A. P. Getting physical in drug discovery II: the impact of chromatographic hydrophobicity measurements and aromaticity. *Drug Disc. Today* **2011**, *16*, 822-830.
173. The exact details of the dosing regime will be determined as a result of data obtained from clinical trials.
174. Bowes, J.; Brown, A. J.; Hamon, J.; Jarolimek, W.; Sridhar, A.; Waldron, G.; Whitebread, S. Reducing safety-related drug attrition: the use of *in vitro* pharmacological profiling. *Nat. Rev. Drug. Discov.* **2012**, *11*, 909-922.
175. Dunne, A.; Jowett, M.; Rees, S. Use of primary human cells in high-throughput screens. *Methods Mol. Biol.* **2009**, *565*, 239-257.
176. Ertl, P.; Rohde, B.; Selzer, P. Fast calculation of molecular polar surface area as a sum of fragment based contributions and its application to the prediction of drug transport properties. *J. Med. Chem.* **2000**, *43*, 3714-3717.

177. BioByte software from BioByte, 201 W. 4<sup>th</sup> St. 204 Claremont, California, CA91711, USA. www.biobyte.com.
178. Forsbach, A.; Müller, C.; Montino, C.; Kritzler, A.; Nguyen, T.; Weeratna, R.; Jurk, M.; Vollmer, J. Negative regulation of the type 1 interferon signalling pathway by synthetic Toll-Like Receptor 7 ligands. *J. Interferon Cytokine Res.* **2011**, *32*, 254-268.
179. (a) Qi, S.; Yu, H.; Jin, H.; Wang, Z. Three dimensional common-feature hypotheses for Toll-like receptor 7 agonists. *J. Chin. Pharm. Sci.* **2013**, *22*, 148-153. (b) Yu, H.; Jin, H.; Sun, L.; Zhang, L.; Sun, G.; Wang, Z.; Yu, Y. Toll-Like receptor 7 agonists: chemical feature based pharmacophore identification and molecular docking studies. *PLOS ONE* **2013**, *8*, e56514.
180. MOE 2014 software available from Chemical Computing Group, St John's Innovation Centre, Cowley Road, Cambridge, United Kingdom, CB4 0WS.
181. Sorkin, A.; von Zastrow, M. Signal transduction and endocytosis: close encounters of many kinds. *Nat. Rev. Mol. Cell Biol.* **2002**, *3*, 600-614.
182. JChem for office software available from ChemAxon Kft. Záhony u. 7, Building HX 1031 Budapest, Hungary.
183. Jana, R.; Pathak, T. P.; Sigman, M. S. Advances in transition metal (Pd,Ni,Fe)-catalyzed cross-coupling reactions using alkyl-organometallics as reaction partners. *Chem. Rev.* **2011**, *111*, 1417-1492.
184. Fürstner, A.; Leitner, A.; Méndez, M.; Krause, H. Iron-catalysed cross-coupling reactions. *J. Am. Chem. Soc.* **2002**, *124*, 13856-13863.
185. Zhang, C. P.; Wang, Z. L.; Chen, Q. Y.; Zhang, C. T.; Gu, Y. C.; Xiao, J. C.; Copper-mediated trifluoromethylation of heteroaromatic compounds by trifluoromethyl sulfonium salts. *Angew. Chem. Int. Ed.* **2011**, *50*, 1896-1900.
186. Chen, M.; Buchwald, S. L. Rapid and efficient trifluoromethylation of aromatic and heteroaromatic compounds using potassium trifluoroacetate enabled by a flow system. *Angew. Chem. Int. Ed.* **2013**, *52*, 11628–11631
187. Cho, E. J.; Senecal, T. D.; Kinzel, T.; Zhang, Y.; Watson, D. A.; Buchwald, S. L. The palladium-catalyzed trifluoromethylation of aryl chlorides. *Science* **2010**, *328*, 1679-1681.
188. Njoroge, F. G.; Arasappan, A.; Bennett, F.; Piwinski, J. J.; Shih, N. Y.; Kwong, C. D.; Ananthan, S.; Clark, J.; Fowler, A.T.; Geng, F.; Kezar, H. S.; Maddry, J. A.; Reynolds, R. C.; Roychowdhury, A.; Secrist, J. A. Ethynyl-substituted pyridine and pyrimidine derivatives and their use in treating viral infections. WO 2010/22125.
189. Gelin, R.; Hablot, J. C.; Synthesis of  $\gamma$ - or  $\delta$ -acetylenic amines and of a derivative of pentynal. *Bull. Soc. Chim. Fr.* 1966, *10*, 3079-3082.
190. Baldwin, J.E.; Rules for ring closure. *J. Chem. Soc. Chem. Commun.* **1976**, 734-736.



191. (a) Olomucki, M. and Marszak, I. Cyclization of some acetylenic amines. *Compt. Rend.* **1962**, 255, 1409-1411. (b) Ziv, D. Amino acids and their derivatives. VII. Acetylenic diisopropylamino and phenyl(methyl)amino compounds. *Bull. Soc. Chim. Fr.* **1970**, 1, 150-154. (c) Baker, M.V. Intramolecular hydroamination of 1,4,7-tri(pent-4'-yn-1'-yl)-1,4,7-triazacyclononane: formation of an azoniaspiro[4.8]tridecane. *Aus. J. Chem.* **2000**, 53, 791-797.
192. Meier, G.; Ligneau, X.; Pertz, H. H.; Ganellin, R.; Schwartz, J. C.; Shunack, W.; Stark, H.; Piperidino-hydrocarbon compounds as novel non-imidazole histamine H<sub>3</sub>-receptor antagonists. *Bioorg. Med. Chem.* **2002**, 10, 2535-2542.
193. Bradbury, R. H.; Breault, G. A.; Jewbury, P. J.; Pease, J. E.; 2,4-Diamino pyrimidine compounds having anti-cell proliferative activity. US2003/6593326.
194. (a) Gangjee, A.; Yu, J.; Kisliuk, R. L.; 2-Amino-4-oxo-6-substituted-pyrrolo[2,3-d]pyrimidines as potential inhibitors of thymidylate synthase. *J. Het. Chem.* **2002**, 39, 833-840. (b) Steffan, R. J.; Matelam, E. M.; Bowen, S. M.; Ullrich, J. W.; Wrobel, J. E.; Zamaratski, E.; Kruger, L.; Olsen Hedemyr, A. L.; Cheng, A.; Hansson, T.; Unwalla, R. J.; Miller, C. P.; Rhonnstad, P. P.; Imidazoles useful in treating cardiovascular disease. US2006/0030612. (c) Gijssen, H. J. M.; De Cleyn, M. A. J.; Surkyn, M.; Verbist, B. M. P.; Preparation of benzimidazole derivatives as cannabinoid CB2 agonists. WO2008/003665.
195. Appel, R. Tertiary phosphane/tetrachloromethane, a versatile reagent for chlorination, dehydration, and P-N linkage. *Angew. Chem. Int. Ed.* **1975**, 14, 801-811.
196. van Kalker, H. A.; van Delft, F. L.; Rutjes, F. P. J. T.; Catalytic Appel reactions. *Pure Appl. Chem.* **2013**, 85, 817-828.
197. Byrne, P. A.; Rajendran, K. V.; Muldoon, J.; Gilheany, D. G. A convenient and mild chromatography-free method for the purification of the products of Wittig and Appel reactions. *Org. Biomol. Chem.* **2012**, 10, 3531-3537.
198. Schnyder, A.; Indolese, A.F.; Studer, M.; Blaser, H.U.; A New Generation of Air Stable, Highly Active Pd Complexes for C-C and C-N Coupling Reactions with Aryl Chlorides. *Angew. Chem. Int. Ed.* **2002**, 41, 3668-3671.
199. Hanan, E. J.; Fucini, R. V.; Romanowski, M. J.; Elling, R. A.; Lew, W.; Purkey, H. E.; Van der Porten, E. C.; Yang, W.; Design and synthesis of 2-amino-isoxazolopyridines as Polo-like kinase inhibitors. *Bioorg. Med. Chem. Lett.* **2008**, 18, 5186-5189.
200. Morgentiu, R.; Pasquet, G.; Boutron, P.; Jung, F.; Lamorlette, M.; Maudet, M.; Plé, P.; Strategic studies in the syntheses of novel 6,7-substituted quinolones and 7- or 6-substituted 1,6- and 1,7-naphthyridones. *Tetrahedron* **2008**, 64, 2772-2782.

201. Kim, B. R.; Won, J. Eun.; Park, S. E.; Lee, H. G.; Kim, M. J.; Jung, K. J.; Kim, J. J.; Yoon, Y. J. Efficient synthesis of 4,5,6-trisubstituted-2-aminopyrimidines. *Bull. Kor. Chem. Soc.* **2009**, *30*, 2107-2110.
202. Cocco, M. T.; Congiu, C.; Onnis, V. Transformation of 6-methylthiopyrimidines. Preparation of new pyrimidine derivatives and fused azolopyrimidines. *J. Heterocycl. Chem.* **2000**, *37*, 707-710.
203. Epp, J. B.; Schmitzer, P. R.; Balko, T. W.; Ruiz, J. M.; Yerkes, C. N.; Siddall, T. L.; Lo, W. C.; 2-Substituted-6-amino-5-alkyl, alkenyl or alkynyl-4-pyrimidinecarboxylic acids and 6-substituted-4-amino-3-alkyl, alkenyl or alkynyl picolinic acids and their use as herbicides. US 2009/0088322.
204. Blackburn, C.; Guan, B.; A novel dealkylation affording 3-aminoimidazo[1,2-a]pyridines: access to new substitution patterns by solid-phase synthesis. *Tetrahedron Lett.* **2000**, *41*, 1495.
205. (a) Chen, Y.; Cushing, T. D.; Xialin, H.; Xiao, H.; Reichelt, A.; Rzasa, R. M.; Seganish, J.; Youngsook, S.; Zhang, D.; 3-Substituted quinoline or quinoxaline derivatives and their use as phosphatidyl-nositol 3-kinase (PI3K) inhibitors. WO 2008/118455. (b) Halsall, C.T.; Rudge, D. A.; Simpson, I.; Ward, R. A.; Pyrimidinodiazepane derivatives as PIK1 inhibitors and their preparation, pharmaceutical compositions, and use in the treatment of cancer. WO 2008/003958.
206. Lagerlund, O.; Larhed, M.; Microwave-Promoted Aminocarbonylations of Aryl Chlorides Using Mo(CO)<sub>6</sub> as a Solid Carbon Monoxide Source. *J. Comb. Chem.* **2006**, *8*, 4-6.
207. Huth, J.R.; Park, C.; Petros, A.M.; Kunzer, A.R.; Wendt, M.D.; Wang, X.; Lynch, C.L.; Mack, J.C.; Swift, K.M.; Judge, R.A.; Chen, J.; Richardson, P.L.; Jin, S.; Tahir, S.K.; Matayoshi, E.D.; Dorwin, S.A.; Lador, U.S.; Severin, J.M.; Walter, K.A.; Bartley, D.M.; Fesik, S.W.; Elmore, S.W.; Hajduk, P.J.; Discovery and Design of Novel HSP90 Inhibitors Using Multiple Fragment-based Design Strategies. *Chem. Biol. Drug Des.* **2007**, *70*, 1-12.
208. Doláková, P.; Masojídková, M.; Holý, A.; Efficient synthesis of pyrimidine carbonitriles and their derivatives. *Heterocycles* **2007**, *71*, 1107-1114.
209. Ghosh, A. K.; Liu, C.; Devasamudram, T.; Lei, H.; Swanson, L. M.; Ankala, S. V.; Lilly, J. C.; Bilcer, G. M. Isophthalamide compounds which inhibit beta-secretase activity and their preparation, pharmaceutical compositions and use in the treatment of Alzheimer's disease. WO 2009/015369.
210. (a) Dobbs, K. D.; Marshall, W. J.; Grushin, V. V. Why excess cyanide can be detrimental to Pd-catalyzed cyanation of haloarenes. Facile formation and characterization of [Pd(CN)<sub>3</sub>(H)]<sub>2</sub><sup>-</sup> and [Pd(CN)<sub>3</sub>(Ph)]<sub>2</sub><sup>-</sup>. *J. Am. Chem. Soc.* **2007**, *129*, 30-31. (b) Erhardt, S.; Grushin, V.V.; Kilpatrick, A. H.; Macgregor, S. A.; Marshall, W. J.; Roe, C. D. Mechanisms

- of catalyst poisoning in palladium-catalyzed cyanation of haloarenes. Remarkably facile C–N bond activation in the [(Ph<sub>3</sub>P)<sub>4</sub>Pd]/[Bu<sub>4</sub>N]<sup>+</sup> CN<sup>-</sup> system. *J. Am. Chem. Soc.* **2008**, *130*, 4828-4845.
211. Beaulieu, F.; Beauregard, L. P.; Courchesne, G.; Couturir, M.; LaFlamme, F.; L'Heureux, A. Aminodifluorosulfonium tetrafluoroborate salts as stable and crystalline deoxofluorinating reagents. *Org. Lett.* **2009**, *11*, 5050-5053.
212. L'Heureux, A.; Beaulieu, F.; Beauregard, L. P.; Bennett, C.; Bill, D. R.; Clayton, S.; LaFlamme, F.; Mirmehrabi, M.; Tadayon, S.; Tovell, D.; Couturir, M. Aminodifluorosulfonium salts: selective fluorination reagents with enhanced thermal stability and ease of handling. *J. Org. Chem.* **2010**, *75*, 3401-3411.
213. (a) Howard, J. A. K.; Hoy, V. J.; O'Hagan, D.; Smith, G. T. How good is fluorine as a hydrogen bond acceptor? *Tetrahedron* **1996**, *52*, 1663-1682. (b) Dunitz, J. D.; Taylor, R. Organic fluorine hardly ever accepts hydrogen bonds. *Chem. Eur. J.* **1997**, *3*, 89-98. (c) Restorp, P.; Berryman, O. B.; Sather, A. C.; Ajamia, D.; Rebek Jr. J. A synthetic receptor for hydrogen-bonding to fluorines of trifluoroborates. *Chem. Commun.* **2009**, 5692-5694.
214. Laube, T. Interactions between carbocations and anions in crystals. *Chem. Rev.* **1998**, *98*, 1277-1312.
215. (a) Iwatmbo, T.; Hirota, N.; Ooie, T.; Suzuki, H.; Shimada, N.; Chiba, K.; Ishizaki, T.; Green, C. E.; Tyson, C. P. Sugiyama, Y.; Prediction of *in vivo* drug metabolism in the human liver from *in vitro* metabolism data. *Pharmacol. Ther.* **1997**, *73*, 147-171. (b) Scaling factors and values for liver blood flow were sourced from SimCyp, part of Certara USA, Inc. 100 Overlook Center, Suite 101, Princeton, NJ 08540 USA, www.simcyp.com.
216. Norman, M. H.; Chen, N.; Chen, Z.; Fotsch, C.; Hale, C.; Han, N.; Hurt, R.; Jenkins, T.; Kincaid, J.; Liu, Y.; Moreno, O.; Santora, V. J.; Sonnenberg, J. D.; Karbon, W. Structure-activity relationships of a series of pyrrolo[3,2-*d*]pyrimidine derivatives and related compounds as neuropeptide Y5 receptor antagonists. *J. Med. Chem.* **2000**, *43*, 4288-4312.
217. Bambuch, V.; Otmar, M.; Pohl, R.; Masojídková, M.; Holý, A. C-Functionalization of 9-deazapurines by cross-coupling reactions. *Tetrahedron*. **2007**, *63*, 1589-1601.
218. Bartoccini, F.; Cabri, W.; Celona, D.; Minetti, P.; Piersanti, G.; Tarzia, G. Direct  $\beta$ -alkyl Suzuki-Miyaura cross coupling of 2-halopurines. Practical synthesis of ST1535, a potent adenosine A<sub>2A</sub> receptor agonist. *J. Org. Chem.* **2010**, *75*, 5398-5401.
219. Kotha, S.; Lahiri, K.; Kashinath, D. Recent applications of the Suzuki–Miyaura cross-coupling reaction in organic synthesis. *Tetrahedron* **2002**, *58*, 9633-9695.
220. Miyaura, N.; Suzuki, A. Palladium-Catalyzed Cross-Coupling Reactions of Organoboron Compounds. *Chem. Rev.* **1995**, *95*, 2456-2482.

221. (a) Molander, G. A.; Sandrock, D. L.; Aminomethylations *via* cross-coupling of potassium organotrifluoroborates with aryl bromides. *Org. Lett.* **2007**, *9*, 1597-1600. (b) Molander, G. A.; Gormisky, P. E.; Sandrock, D. L.; Scope of aminomethylations *via* Suzuki-Miyaura cross-couplings of organotrifluoroborates. *J. Org. Chem.* **2008**, *73*, 2052-2057. (c) Raushel, J.; Sandrock, D. L.; Josyula, K. V.; Pakyz, D.; Molander, G. A.; Reinvestigation of aminomethyltrifluoroborates and their application in Suzuki-Miyaura cross-coupling reactions. *J. Org. Chem.* **2011**, *76*, 2762-2769.
222. Kinzel, T.; Zhang, Y.; Buchwald, S. L. A new palladium precatalyst allows for the fast Suzuki-Miyaura coupling reactions of unstable polyfluorophenyl and 2-heteroaryl boronic acids. *J. Am. Chem. Soc.* **2010**, *132*, 14073-14075.
223. Zou, D.; Cui, X.; Qin, L.; Li, J.; Wu, Y.; Wu, Y. Aminomethylation *via* cyclopalladated-ferrocenylimine-complexes-catalysed Suzuki-Miyaura coupling of aryl halides with potassium *N,N*-dialkyaminomethyltrifluoroborates. *Synlett* **2011**, *3*, 349-356.
224. Dreher, S. D.; Lim, S. E.; Sandrock, D. L.; Molander, G. A. Suzuki-Miyaura cross-coupling reactions of primary alkyltrifluoroborates with aryl chlorides. *J. Org. Chem.* **2009**, *74*, 3626-3631.
225. Wang, L.; Li, J.; Cui, X.; Wu, Y.; Zhu, Z.; Wu, Y. Cyclopalladated ferrocenylimine as efficient catalysts for the synthesis of arylboronate esters. *Adv. Synth. Catal.* **2010**, *352*, 2002-2010.
226. Merino, I.; Monge, A.; Font, M.; Martinez de Irujo, J. J.; Alberdi, E.; Santiago, E.; Prieto, I.; Lasarte, J. J.; Sarobe, P.; Borrás, F. Synthesis and anti-HIV-1 activities of new pyrimido[5,4-*b*]indole. *Il Farmaco* **1999**, *54*, 255-264.
227. Tolman, C. A.; Steric effects of phosphorus ligands in organometallic chemistry and homogeneous catalysis. *Chem. Rev.* **1977**, *77*, 313-348.
228. Hundertmark, T.; Littke, A. F.; Buchwald, S. L.; Fu, G. C. Pd(PhCN)<sub>2</sub>Cl<sub>2</sub>/P(*t*-Bu)<sub>3</sub>: A versatile catalyst for Sonogashira reactions of aryl bromides at room temperature. *Org. Lett.* **2000**, *2*, 1729-1731.
229. Böhm, V. P. W.; Herrmann, W. A. Coordination chemistry and mechanisms of metal-catalyzed C-C coupling reactions. A copper-free procedure for the palladium-catalysed Sonogashira reaction of aryl bromides with terminal alkynes at room temperature. *Eur. J. Org. Chem.* **2000**, 3679-3681.
230. Soheili, A.; Albaneze-Walker, J.; Murry, J. A.; Dormer, P. G. Hughes, D. L. Efficient and general protocol for the copper-free Sonogashira coupling of aryl bromides at room temperature. *Org. Lett.* **2003**, *22*, 4191-4194.

231. Netherton, M. R.; Fu, G. C. Air-stable trialkylphosphonium salts: simple, practical, and versatile replacements for air-sensitive trialkylphosphines. Applications in stoichiometric and catalytic processes. *Org. Lett.* **2001**, *3*, 4295-4298.
232. Griffith, W.P.; Ley, S.V.; Whitcombe, G.P.; White, A.D. Preparation and use of tetra-n-butylammonium per-ruthenate (TBAP reagent) and tetra-n-propylammonium per-ruthenate (TPAP reagent) as new catalytic oxidants for alcohols. *J. Chem. Soc., Chem. Commun.* **1987**, 1625-1627.
233. Cruciani, G.; Carosati, E.; De Boeck, B.; Ethirajulu, K.; Mackie, C.; Howe, T.; Vianello, R. MetaSite: understanding metabolism in human cytochromes from the perspective of the chemist. *J. Med. Chem.* **2005**, *48*, 6970-6979.
234. Rose, J.; Castagnoli, N. The metabolism of tertiary amines. *Med. Res. Rev.* **1983**, *3*, 73-88.
235. Burka, L. T. F.; Guengerich, P.; Willard, R. J.; Macdonald, T. L. Mechanism of cytochrome P-450 catalysis. Mechanism of *N*-dealkylation and amine oxide deoxygenation. *J. Am. Chem. Soc.* **1985**, *107*, 2549-2551.
236. Hollenburg, P. F.; Mechanisms of cytochrome P450 and peroxidase catalysed xenobiotic metabolism. *FASEB* **1992**, *6*, 686-694.
237. Morgenthaler, M.; Schweizer, E.; Hoffamn-Röder, A.; Benini, F.; Martin, R. E.; Jaeschke, G.; Wagner, B.; Fischer, H.; Bendels, S.; Zimmerli, D.; Schneider, J.; Diederich, F.; Kansy, M.; Müller, K. Predicting and tuning physiochemical properties in lead optimization: amine basicities. *ChemMedChem* **2007**, *2*, 1100-1115.
238. Myers, R. C.; Ballantyne, B. Comparative acute toxicity and primary irritancy of various classes of amines. *Toxic Subs, Mech.* 1997, *16*, 151-194.
239. Sun, H.; Scott, D. O. Metabolism of 4-Aminopiperidine drugs by cytochrome p450s: molecular and quantum mechanical insights into drug design. *ACS Med. Chem. Lett.* **2011**, *2*, 638-643.
240. Klečka, M.; Pohl, R.; Klepetářová, B.; Hocek, M. Direct C–H borylation and C–H arylation of pyrrolo[2,3-*d*]pyrimidines: synthesis of 6,8-disubstituted 7-deazapurines. *Org. Biomol. Chem.* **2009**, *7*, 866-868.
241. Khoje, A. D.; Kulendrn, A.; Charnock, C.; Wan, B.; Franzblau, S.; Gunderson, L. L.; Synthesis of non-purine analogs of 6-aryl-9-benzylpurines, and their antimycobacterial activities. Compounds modified in the imidazole ring. *Biorg. Med. Chem.* **2010**, *18*, 7274-7282.
242. Stadlweiser, J.; Schmidt, B.; Bernsmann, H.; Dunkern, T.; Benediktus, E.; Pahl, A.; Hussong, R.; Minz, O.; Müller, M.; Viertelhaus, M.; Methylpyrrolopyrimidinecarboxamides. WO2011023693.

243. Muchowski, J. M.; Solas, D. R.; Protecting groups for the pyrrole and indole nitrogen atom. The [2-(trimethylsilyl)ethoxy]methyl moiety. Lithiation of 1-{{2-(trimethylsilyl)ethoxy}methyl}pyrrole. *J. Org. Chem.* **1984**, *49*, 203-205.
244. Ames, B.; McCann, J. Yamasaki, E. Methods for detecting carcinogens and mutagens with the Salmonella/mammalian-microsome mutagenicity test. *Mutat. Res.* **1975**, *31*, 347-364.
245. Clive, D.; Flamm, W. G.; Machesko, M. R.; Bernheim, N. J. A mutational assay system using the thymidine kinase locus in mouse lymphoma cells. *Mutat. Res.* **1972**, *16*, 77-87.
246. Chen, X.; Cordes, J. S.; Bradley, J. A.; Sun, Z.; Zhou, J.; Use of arterially perfused rabbit ventricular wedge in predicting arrhythmogenic potentials of drugs. *J. Pharmacol. Toxicol. Methods* **2006**, *54*, 66-272.
247. Duffus, J. H.; Nordberg, M.; Templeton, D. M. Glossary of terms used in toxicology, 2<sup>nd</sup> Ed. *Pure Appl. Chem.* **2007**, *79*, 1153-1344.
248. Lasser, K. E.; Allen, P. D.; Woolhandle, S. J.; Himmelstein, D. U.; Wolfe, S. M. Bor, D. H.; Timing of new black box warnings and withdrawals for prescription medications. *J. Am. Med. Assoc.* **2002**, *287*, 2215-2220.
249. Dessertenne, F.; La tachycardia ventriculaire à deux foyes opposes variables. *Arch. Mal. Coeur. Vaiss.* **1966**, *59*, 66-272.
250. Roden, D. M.; Drug induced prolongation of the QT interval. *N. Engl. J. Med.* **2004**, *350*, 1013-1022.
251. Klabunde, R. E.; Electrical activity of the heart, In *Cardiovascular physiology concepts* 2<sup>nd</sup> Ed., Lippincott Williams & Wilkins Baltimore. **2012**, 9-40.
252. Wang, D.; Patel, C.; Cui, C.; Yan, G.X.; Preclinical assessment of drug-induced proarrhythmias: Role of the arterially perfused rabbit left ventricular wedge preparation. *Pharmacol. Ther.* **2008**, *119*, 141-151.
253. Abriel, H.; Roles and regulation of the sodium channel Nav1.5: Recent insights from experimental studies. *Cardiovasc. Res.* **2007**, *76*, 381-389.
254. (a) Thomas, D.; Karle, C.A.; Kiehn, J. The cardiac hERG/IKr potassium channel as pharmacological target: structure, function, regulation, and clinical applications. *Curr Pharm Des.* **2006**, *12*, 2271-2283. (b) Ritter, J. M.; Cardiac safety, drug induced QT prolongation and torsade de pointes (TdP). *Br. J. Pharmacol.* **2012**, *73*, 331-334.
255. Towart, R.; Linders, J. T. M.; Hermans, A. N.; Rohrbacher, J.; Van Der Linde, H. J.; Ercken, M.; Cik, M.; Roevens, P.; Teisman, A.; Gallacher, D. J. Blockade of the I<sub>Ks</sub> potassium channel: An overlooked cardiovascular liability in drug safety screening? *J. Pharmacol. Toxicol. Methods* **2009**, *60*, 1-10.
256. Schroeder, K.; Neagle, B.; Trezise, D. J.; Worley, J.; IonWorks HT: A new high throughput electrophysiology measurement platform. *J. Biomol. Screen.* **2003**, *8*, 50-64.

257. Gillie, D. J.; Novick, S. J.; Donovan, B. T.; Payne, L. A.; Townsend, C. Development of a high-throughput electrophysiological assay for the human ether-à-go-go related potassium channel hERG. *J. Pharmacol. Toxicol. Methods* **2013**, *67*, 33-44.
258. Jone, K. A.; Garbati, N.; Khang, H.; Large, C. H.; Automated patch clamping using the QPatch. *Methods Mol. Biol.* **2009**, *565*, 209-62.
259. Bass, A. S.; Darpo, B.; Breidenbach, A.; Bruse, K.; Feldman, H. S.; Garnes, D.; Hammond, T.; Haverkamp, W.; January, C.; Koerner, J.; Lawrence, C.; Leishman, D.; Roden, D.; Valentin, J. P.; Vos, M. A.; Zhou, Y-Y.; Karluss, T.; Sager, P. International Life Sciences Institute (Health and Environmental Sciences Institute, HESI) initiative on moving towards better predictors of drug-induced torsades de pointes. *Br. J. Pharmacol.* **2008**, *154*, 1491-1501.
260. Chevalier, P.; Ruffly, F.; Danilo, P.; Rosen, M. R. Interaction between *Alpha*-1 adrenergic and vagal effects on cardiac rate and repolarization. *Pharmacol. Exp. Ther.* **1998**, *284*, 832-837.
261. Raj, K.; Goyal, M. D. Muscarinic receptor subtypes. *N. Engl. J. Med.* **1989**, *321*, 1022-1029.
262. McFadden, E. P.; Clarke, J. G.; Davies, G. J.; Kaski, J. C.; Haider, A. W.; Maseri, A. Effect of intracoronary serotonin on coronary vessels in patients with stable angina and patients with variant angina. *N. Engl. J. Med.* **1991**, *324*, 648-654.
263. Gao, Z. G.; Jacobsen, K. A. Emerging adenosine receptor agonists. *Expert Opin. Emerging Ther.* **2007**, *12*, 479-492.
264. Rose, T.; Grützkau, A.; Hirseland, H.; Huscher, D.; Dähnrich, C.; Dzionek, A.; Ozimkowski, T.; Schlumberger, W.; Enghard, P.; Radbruch, A.; Riemekasten, G.; Burmester, G. R.; Hiepe, F.; Biesen, R. IFN $\alpha$  and its response proteins, IP-10 and SIGLEC-1, are biomarkers of disease activity in systemic lupus erythematosus. *Ann. Rheum. Dis.* **2012**, *0*, 1–7.
265. Vidal, V.; Alomar, A. Mode of action and clinical use of imiquimod. *Expert Rev. Dermatol.* **2008**, *3*, 151-159.
266. Ryu, J.; Yang, F. C. A review of topical imiquimod in the management of basal cell carcinoma, actinic keratosis and other skin lesions. *Clin. Med. Therapeutics* **2009**, *1*, 1557-1575.
267. Wiechers, J. W. The barrier function of the skin in relation to percutaneous absorption of drugs. *Pharm. Weekblad Scientific Ed.* **1989**, *11*, 185-198.
268. Windsor, T.; Burch, G. E. Differential roles of layers of human epigastric skin on diffusion rate of water. *Arch. Intern. Med.* **1944**, *74*, 428-436.
269. Potts, R. O.; Guy, R. H. Predicting skin permeability. *Pharm. Res.* **1992**, *9*, 663-669.
270. ACD software from Advanced Chemistry Development, Inc. Toronto, On, Canada. [www.acdlabs.com](http://www.acdlabs.com).

271. Abad-Zapatero, C.; Metz, J. T. Ligand efficiency indices as guideposts for drug discovery. *Drug. Disc. Today*, **2005**, *10*, 464-469.
272. Ruoho, A. E.; Kiefer, H.; Roeder, P. E.; Singer, S. J. The mechanism of photoaffinity labeling. *Proc. Natl. Acad. Sci. U.S.A.* **1973**, *70*, 2567–2571.